UNIVERSITY OF CALIFORNIA, SAN DIEGO

Structural and electronic studies of complexes relevant to the electrocatalyic reduction of carbon dioxide.

A dissertation submitted in partial satisfaction of the requirements for the degree of

Doctor of Philosophy

in

Chemistry

by

Eric Edward Benson

Committee in charge:

Professor Clifford P. Kubiak, Chair
Professor Andrew G. Dickson
Professor Joshua S. Figueroa
Professor Arnold L. Rheingold
Professor Michael J. Tauber

2012

The dissertation of Eric Edward Benson is approved, and it is acceptable in quality and form for publication on microfilm and electronically.

Chair

University of California, San Diego

2012

DEDICATION

to my family

EPIGRAPH

The further one goes, the less one knows.

–Lao Tzu

TABLE OF CONTENTS

LIST OF FIGURES

LIST OF SCHEMES

LIST OF TABLES

ACKNOWLEDGEMENTS

As I look back on the curious series of events that ultimately ended with receiving a PhD in chemistry, I must thank those instrumental in making it possible. There are many people who have influenced and helped me over the years, and while I have tried to include everyone, there are not enough words to properly thank everyone.

First and foremost, I must acknowledge the support and encouragement from my parents, Anne and Nathan. From a very early age my parents were supportive of my quest for knowledge, even if it meant destroying old computers, making potato cannons, or setting off dry-ice bombs. I owe an incredible amount of debt to my parents for their constant encouragement and instilling the idea that I can accomplish anything if I work hard enough. I attribute who I am as a person to the upbringing that my parents provided and would certainly not be here without their support. My dad would often say, “Anything worth doing is worth doing to excess,” and this PhD is a small tribute.

My brother Andrew has been an incredible source of support and guidance whether he knows it or not. His carefree attitude, artistic abilities and devotion to his craft have been a major source of inspiration on how I should live my life. He has taught me to do what I enjoy and where my priorities should lie. The many adventures we shared as a kid, as well as college and graduate school are some of my fondest memories. I look forward to the many adventures we will share in the future.

Of course none of this would be possible without my advisor Cliff. He has been supportive in letting me do the research that I am interested in, while guiding me

through the process of academic research. He involves his graduate students in every aspect of the academic life, writing your own papers, grant writing, grant and paper submission and revision, and this has been an incredibly valuable experience that will forever shape my professional career. While working for Cliff, I have had the opportunity to share my research numerous times and thank him for the chance to travel, while pushing me to collect my thoughts and data into coherent presentations.

There are also those within the department that have helped me along the way. Arnie Rheingold, Antonio DiPasquale and Curtis Moore have all helped to teach me X-Ray crystallography, which is still my favorite technique. Hannah Shaffat, Mike Tauber, and Maria Angelella helped with the EPR experiments. Daniel Friebel has patiently guided me through the more physical aspects of X-Ray absorption. Josh Figueroa helped teach me computational chemistry as well as generously allowing me to run them on his cluster. I also must thank Anthony Mrse and Yongxuan Su for their help with NMR and MS respectively.

I would not have been able to get anything accomplished without the help and support of the Kubiak group, past and present. I must thank those who were senior to me in their role in shaping me as a scientist, and getting me to join the group in the first place. Ben, Johnny, Caballero, Goeltz, Starla, Aaron, and Kristina made the lab an enjoyable place to work and I hope that I was able to do the same for the next generation. I must acknowledge Goeltz, Smieja, Frank, Starla, Gabe, Canadace, Kyle, Julia and Shayak for their innumerable contributions; I would not have survived without their help and support.

While I had much help in lab, there were many people outside of lab who made my life in San Diego much more enjoyable. Goeltz, while also being a co-member of the Kubiak lab, was also a great companion for beer festivals, DJ shows and Caturday brewing sessions. Smieja has always been my partner in crime in the Kubiak Lab. He got me into running, somehow convinced me to compete in a triathlon, and has made graduate school a much more enjoyable experience. Michael started me brewing, got me back into snow-sports and has been an amazing roommate for the past few years. Beer and Pizza night will never be the same without Jon, Lacey and Michael, but the tradition will live on. Noah, while not technically in San Diego, has been a great influence and constant supporter of my graduate school decision.

While the support from friends and family has been instrumental in obtaining this degree, I must acknowledge the places where I spent my time that made graduate life a little more bearable. I do not know how I would have survived without the Art of Espresso. Not only was the caffeination necessary on long days, but just taking a break in the day to sit outside and enjoy a double Americano put the days problems in perspective. I must thank Kevin Song and The Spirits of St. Germain for their beer selection that was available when I wanted to celebrate a good result, or for when I wanted to forget a bad one. Along those lines, I must also thank O'Briens Pub, as it was a great place to hang out and enjoy some beer(s) at the end of the week.

SPECIFIC CHAPTER ACKNOWLEDGMENTS

Chapter 1: Much of the material for this chapter comes directly from a manuscript entitled "Electrocatalyic and homogeneous approaches to conversion of CO_2 to liquid fuels." by Eric E. Benson, Clifford P. Kubiak, Aaron J. Sathrum, and Jonathan M. Smieja, which has been published in *Chemical Society Reviews*, **2009**, *38*, 89-99. http://dx.doi.org/10.1039/b804323j.

Chapter 2: Much of the material for this chapter comes directly from a manuscript entitled "Synthesis and characterization of 6,6'-(2,4,6-triisopropylphenyl)-2,2'-bipyridine (tripbipy) and its complexes of the late first row transition metals." by Eric E. Benson, Arnold L. Rheingold, and Clifford P. Kubiak, which has been published in *Inorganic Chemistry*, **2010**, *49* (4), 1458-1464. http://dx.doi.org/10.1021/ic9016382.

Chapter 4: Much of the material for this chapter comes directly from a manuscript entitled "Structural investigations into the deactivation pathway of the CO_2 reduction electrocatalyst $Re(bipy)(CO)_3Cl$." by Eric E. Benson and Clifford P. Kubiak, which has been submitted to *Chemical Communications.*

Chapter 5: Part of the material for this chapter comes directly from a manuscript entitled "Kinetic and structural studies, origins of selectivity, and interfacial charge transfer in the artificial photosynthesis of CO" by Jonathan M. Smieja, Eric E. Benson, Bhupendra Kumar, Kyle A. Grice, Candace S. Seu, Alexander J. M. Miller, James M.

Mayer and Clifford P. Kubiak, which has been published in *Proceedings of the National Academy Science USA,* **2012**, *Accepted*.

Chapter 6: The material in this chapter is unpublished work and was performed in collaboration with Prof. Anders Nilsson, Dr. Daniel Friebel, Matthew Sampson, Dr. Jonathan Smieja, and Dr. Kyle Grice.

Chapter 7: The material in this chapter is unpublished work and was performed in collaboration with Frank Mariskal.

VITA

2012	Doctor of Philosophy, University of California, San Diego
2008	Master of Science, University of California, San Diego
2005	Bachelor of Science, University of Arizona

PUBLICATIONS

Smieja, J.M., Sharp, I.D., Benson, E.E., Kubiak, C.P., *Stopped-flow infrared spectroscopy studies of the kinetics of the reactions of* $[Re(bipy\text{-}tBu)(CO)_3]^{-1}$ *and* $[Re(bipy)(CO)_3]^{-1}$ *with* CO_2. Energy & Environmental Science (2012), *Submitted.*

Benson, E.E. and Kubiak, C.P., *Structural investigations into the deactivation pathway of the* CO_2 *reduction electrocatalyst* $Re(bipy)(CO)_3Cl$. Chemical Communications (2012) *Submitted.*

Smieja, J.M., Benson, E.E, Kumar, B., Grice, K.A., Seu, C.S., Miller, A.J.M, Mayer, J. M., and Kubiak C.P., *Kinetic and structural studies, origins of selectivity, and interfacial charge transfer in the artificial photosynthesis of CO.* Proceedings of the National Academy of Sciences (2012), *Accepted.*

Goeltz, J.C., Benson, E.E., Kubiak, C.P., *Electronic Structural Effects in Self-Exchange Reactions.* Journal of Physical Chemistry B (2010), *114* (45), 14729–14734.

Benson, E.E., Rheingold, A.L., Kubiak, C.P., *Synthesis and Characterization of 6,6′-(2,4,6-Triisopropylphenyl)-2,2′-bipyridine (tripbipy) and Its Complexes of the Late First Row Transition Metals.* Inorganic Chemistry (2010), *49* (4), 1458-1464.

Benson, E.E., Kubiak, C.P., Sathrum, A. J., Smieja, J. M., *Electrocatalytic and homogeneous approaches to conversion of* CO_2 *to liquid fuels.* Chemical Society Reviews (2009), *38*, 89-99.

ABSTRACT OF THE DISSERTATION

Structural and electronic studies of complexes relevant to the electrocatalyic reduction of carbon dioxide.

by

Eric Edward Benson

Doctor of Philosophy in Chemistry

University of California, San Diego, 2012

Professor Clifford P. Kubiak, Chair

Herein we report the synthesis and characterization of transition metal complexes with modified 2,2'-bipyridines. Bipyridines with different substitutions at the 4,4' and 6,6' position were synthesized and their complexes with several transition metals were investigated to elucidate the electronics and steric requirements for the electrochemical reduction of CO_2 to CO.

The synthesis of tripbipy (6,6'-(2,4,6-triisopropylphenyl)-2,2'-bipyridine), a new substituted bipyridine ligand, and the syntheses, structures, and magnetic properties of the first coordination compounds based on this ligand are described. Reported here are the tripbipy complexes of five late first row transition metal

chlorides (MCl_2; M = Fe, Co, Ni, Cu, Zn). All MCl_2tripbipy complexes are four coordinate and contain a distorted tetrahedral metal center.

The synthesis and X-ray crystallographic characterization of several reduced complexes from the chemical reduction of Re(tripbipy)$(CO)_3Cl$ are reported. The one-electron reduction of this complex results in the loss of the halide to form the neutral 5-coordinate complex. The two-electron reduction of the starting material with KC_8 results in the loss of the halide, and reduction of the bipyridine ligand. Bond alternation can be seen in the XRD as well as the DFT calculations using ADF 2007.1.

We report a series of complexes synthesized from the chemical reduction of the fac-tricarbonyl complex Re(bpy)$(CO)_3Cl$. Reduction of the parent complex with one equivalent of KC_8 results in the formation of the dimer $[Re(bpy)(CO)_3]_2$. The one-electron reduction of this dimer does not result in cleavage of the metal-metal bond, but leads to the formation of the anionic dimer $[Re(bpy)(CO)_3]_2^-$. The reduction of the parent compound with 2.1 equivalents of KC_8 results in the formation of the anionic species $Re(bpy)(CO)_3^-$, which has long been postulated as the active species that reacts with carbon dioxide in the electrochemical reduction of CO_2 to CO.

Modification of the 6,6' position of 2,2'-bipyridine for the addition of proton relays to the electrocatalyst Re(bipy)$(CO)_3Cl$ is reported. Synthesis and electrochemistry of Re(bipy-CH_2OH)$(CO)_3Cl$ and Re(6,6'-dmb)$(CO)_3Cl$ (6,6'-dmb = 6,6'-dimethyl-2,2'-bipyridine) are reported. Addition of substituents at the 6,6' position inhibits catalysis when compared to the complexes with the functional groups at the 4,4' position.

Chapter 1

Electrocatalytic and homogenous approaches to conversion of CO_2 to liquid fuels.

1.1 Introduction

The catalytic conversion of CO_2 to liquid fuels is a critical goal that would positively impact the global carbon balance by recycling CO_2 into usable fuels. The challenges presented here are great, but the potential rewards are enormous. CO_2 is an extremely stable molecule generally produced by fossil fuel combustion and respiration. Returning CO_2 to a useful state by activation/reduction is a scientifically challenging problem, requiring appropriate catalysts and energy input. This poses several fundamental challenges in chemical catalysis, electrochemistry, photochemistry, and semiconductor physics and engineering.

1.1.1 The challenge of CO_2 reduction, thermodynamic considerations.

With respect to CO_2 reduction to liquid fuels or fuel precursors such as CO/H_2 (synthesis gas), proton-coupled multi-electron steps are generally more favorable than single electron reductions, as thermodynamically more stable molecules are produced. This is summarized in equations 1.1-1.5 (pH 7 in aqueous solution versus NHE, 25 °C, 1 atmosphere gas pressure, and 1 M for the other solutes).[1, 2] In contrast, the single electron reduction of CO_2 to $CO_2^{\bullet -}$ occurs at E° = – 1.90 V, equation 1.6, due to a large reorganizational energy between the linear molecule and bent radical anion.

$$CO_2 + 2H^+ + 2e^- \rightarrow CO + H_2O \qquad E° = – 0.53 \text{ V} \qquad \text{(E1.1)}$$

$$CO_2 + 2H^+ + 2e^- \rightarrow HCO_2H \qquad E° = – 0.61 \text{ V} \qquad \text{(E1.2)}$$

$$CO_2 + 4H^+ + 4e^- \rightarrow HCHO + H_2O \qquad E° = – 0.48 \text{ V} \qquad \text{(E1.3)}$$

$$CO_2 + 6H^+ + 6e^- \rightarrow CH_3OH + H_2O \qquad E° = – 0.38 \text{ V} \qquad \text{(E1.4)}$$

$$CO_2 + 8H^+ + 8e^- \rightarrow CH_4 + 2H_2O \qquad E° = – 0.24 \text{ V} \qquad \text{(E1.5)}$$

$$CO_2 + e^- \rightarrow CO_2^{\bullet -} \qquad E° = – 1.90 \text{ V} \qquad \text{(E1.6)}$$

1.1.2 The challenge of CO_2 reduction, kinetic considerations.

One key problem in the conversion of CO_2 to liquid fuels is the assembly of the nuclei and formation of chemical bonds to convert the relatively simple CO_2 molecule into more complex and energetic molecules. Strategically, there are two primary ways that this can be accomplished. The first is to convert CO_2 and H_2O into CO and H_2 (synthesis gas), and then to use well proven Fischer-Tröpsch technologies to convert the synthesis gas to liquid fuels, including gasoline. The advantage here is

that it is considerably easier to convert CO_2 to CO and H_2O to H_2 than it is to make even a simple liquid fuel such as methanol by electrocatalytic processes. The second primary option, then, is to attempt to "do it the hard way" by converting CO_2 directly to liquid fuels by electrocatalytic processes. Here, the kinetic challenges are great. One possibility is to identify a single catalyst that can direct the complete sequence of steps necessary for converting CO_2 to CO, then to H_2CO, then to hydrocarbons or alcohols, *all* with low kinetic barriers. Catalysts that bring required functionalities into the proper position at the proper time will be required. A second possibility is to identify catalyst "panels", where each panel contains optimal catalysts for each of the steps in the overall transformation of CO_2 to a liquid fuel. An advantage of the parallel approach is that the catalysts for each step can be optimized independently using combinatorial or traditional ligand tuning methods, and then the catalyst panel can be assembled from the proven catalyst components.

1.2 Tutorial on electrocatalysis

If the reduction of carbon dioxide to liquid fuels is to be accomplished through photovoltaic or other electrochemical means, the deployment of efficient *electrocatalysts* will be essential for the development of practical industrial processes. An electrocatalyst both participates in an electron transfer reaction (at an electrode) and facilitates acceleration of a chemical reaction. The electron transfer and chemical kinetics both must be fast for an efficient electrocatalyst. Additionally, an *optimal* electrocatalyst must display a good thermodynamic match between the redox potential (E^0) for the electron transfer reaction and the chemical reaction that is being catalyzed

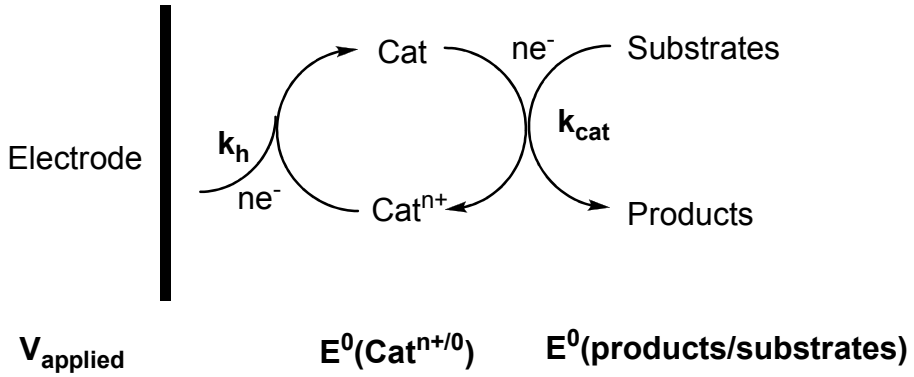

Scheme 1.1 Electrocatalysis with electron source.

(*e.g.* reduction of CO_2 to CO). These factors can be optimized by chemical tuning of the electrocatalyst metal centers via appropriate ligand design. Electrocatalysts are typically screened for their redox potentials, current efficiencies, electron transfer rate and chemical kinetics in order to determine the best overall catalysts.

In the general sense, electrocatalysts are electron transfer agents that ideally operate near the thermodynamic potential of the reaction to be driven, E^0(products/substrates). Direct electrochemical reduction of carbon dioxide on most electrode surfaces requires large overvoltages which consequently lowers the conversion efficiency. The overvoltage can be considered to be the difference between the applied electrode potential, $V_{applied}$, and E^0(products/substrates), at a given current density. Both thermodynamic and kinetic considerations are important here. Clearly, in order to minimize overvoltages, catalysts need to be developed that have formal potentials, $E^0(Cat^{n+/0})$ well matched to E^0(products/substrates), and appreciable rate constants, k_{cat}, for the chemical reduction of substrates to products at this potential. In addition, the heterogeneous rate constant, k_h, for reduction of the

electrocatalyst at the electrode must be high for $V_{applied}$ near $E^0(Cat^{n+/0})$. A general approach for an electrocatalytic system is given in scheme 1.1.

Reaction rates for these processes can be estimated from the steady-state limiting current in cyclic voltammetry, or by rotating disk voltammetry studies of the heterogeneous electron transfer kinetics. Identification of electrocatalytic activity can be seen easily in cyclic voltammetry (CV) (Figure 1.1). In a CV under a dry inert atmosphere, an electrocatalyst should show a reversible redox couple. Upon addition of CO_2, the diffusion limited current should increase significantly, while the potential shifts anodically, and the reversibility in the return oxidation wave is lost due to the chemical reaction between CO_2 and the electrocatalyst. Electrocatalysts offer critical solutions to lowering the overpotentials, improving selectivity, and increasing the reaction kinetics of carbon dioxide conversion.

1.3 A review of CO_2 reduction catalysts to date

The efficient electrochemical reduction of carbon dioxide to useful molecules such as carbon monoxide, formic acid, methanol, ethanol, and methane, presents an important challenge and a great opportunity for chemistry today. The field of transition metal catalyzed reduction of CO_2 is relatively new, its origins tracing back to the 1970s, but the field has gained in breadth and intensity over the last 30 years.

Before we review the important studies in the electrocatalytic reduction of CO_2, we must consider several molecular chemistry studies of the reactivity of CO_2 toward transition metal complexes that provide important insights concerning the activation and reduction of CO_2. Aresta and Nobile first published the crystal

structure of CO_2 bound to a transition metal complex in 1975 and reported an η^2-bidentate binding mode involving the carbon atom and one oxygen atom, with significant bending in the CO_2 structure.[3] Another important study came in 1981 when Darensbourg and co-workers reported that anionic group 6B metal hydrides would react readily with CO_2 to form the metal formats.[4] This reaction proceeds according to equation 1.7.

$$HM(CO)_5^- + CO_2 \leftrightarrow HC(O)OM(CO)_5^- \qquad \text{(E1.7)}$$

Work on the homogeneous transition metal catalyzed electrochemical reductions of CO_2 was preceded by studies of the reduction of CO_2 at various types of

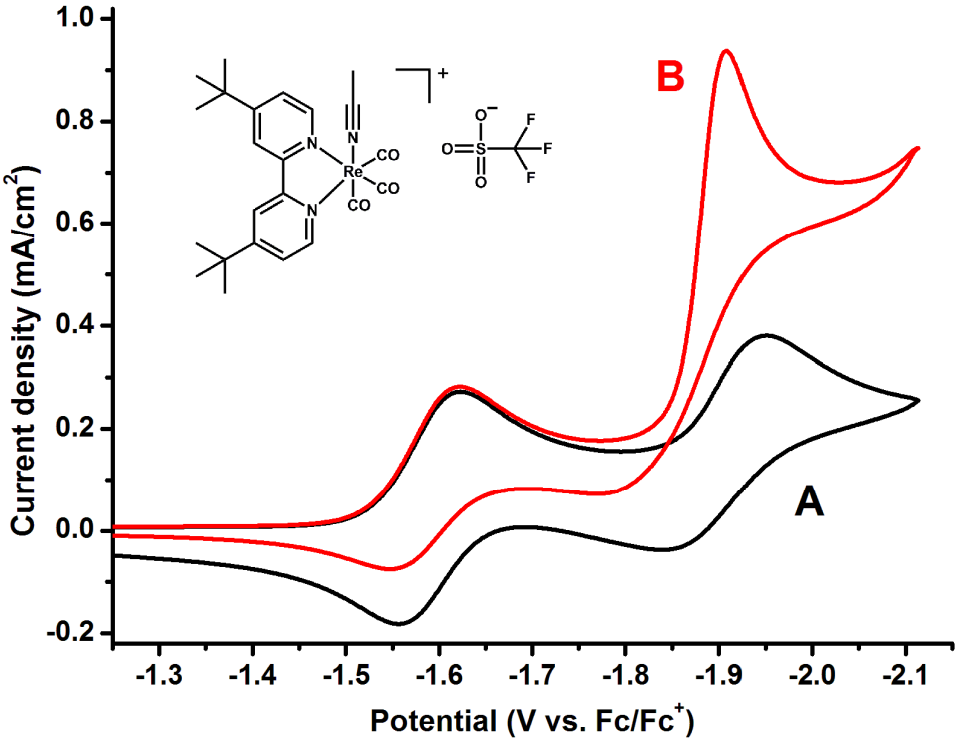

Figure 1.1 Example cyclic voltammogram (CV) under (a) N_2 and (b) CO_2. Under a CO_2 environment is readily observed (1) anodic potential shift (2) large increase in current (3) non-reversible waveform.

electrode materials. The most successful electrode for the reduction of CO_2 to formic acid was found to be a mercury drop electrode. Although several groups had studied this reaction previously, Eyring and co-workers published a paper in 1969 with an in-depth study of the mechanism and kinetics of the reaction. They were able to obtain current efficiencies of 100% in pH 6.7 solutions with a lithium bicarbonate supporting electrolyte.[5]

In subsequent years, many reports of apparently homogeneous electrocatalysts for the reduction of CO_2 appeared in the literature. We have divided the catalysts into three major categories that depend on ligand type: (1) metal catalysts with macrocyclic ligands, (2) metal catalysts with bipyridine ligands, and (3) metal catalysts with phosphine ligands. These seminal studies are summarized in the following subsections. It is important to note that this review is concerned with the electrocatalytic and homogenous reduction of carbon dioxide and therefore may omit other types of carbon dioxide activation such as photocatalytic reduction, heterogeneous catalysis, and various others.

1.3.1 Metal complexes with macrocyclic ligands.

Important early work in this area of electrocatalysis was done by Meshitsuka and Eisenberg. In 1974 Meshitsuka and co-workers reported the first electrocatalysis of CO_2 using cobalt and nickel phthalocyanines.[6] This communication did not report turnover numbers or current efficiencies and it was not clear what products were formed, but the research represented a first step in the understanding the types of

transition metal complexes that could display activity for the electrocatalytic reduction of CO_2.

The first reported transition metal catalysts with high current efficiencies and turnover numbers were demonstrated by Eisenberg and co-workers in 1980.[7] In this work, tetraazomacrocyclic complexes of cobalt and nickel were employed as shown in Figure 1.2. These complexes were able to reduce carbon dioxide to carbon monoxide or a combination of CO and molecular hydrogen at potentials ranging from -1.3 to -1.6V vs. SCE. These catalysts were also able to provide high current efficiencies, up to 98% (complex **3**), but displayed low turnover frequencies between 2 and 9 per hour

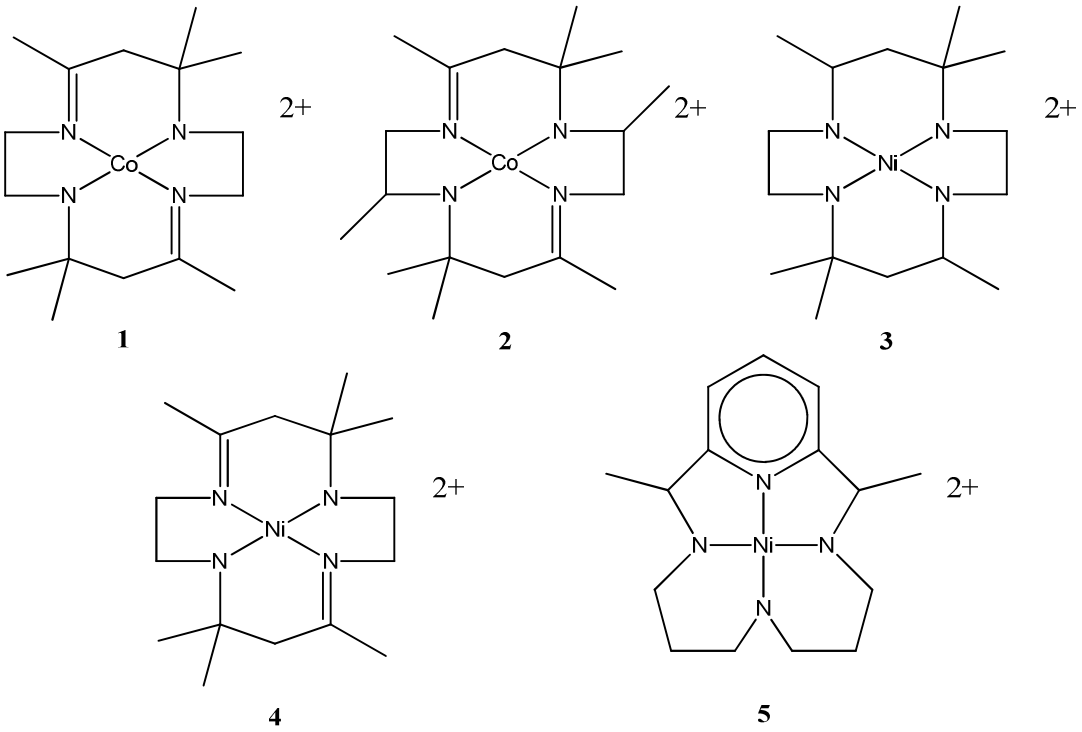

Figure 1.2 Eisenberg catalysts for the reduction of CO_2 to CO.[7] All complexes (1-5) were effective for the reduction with varying degrees of success. System suffered from a requirement of high overpotentials for the reduction as well as the coincidental and competing production of H_2.

at 23 °C.

Sauvage and co-workers have extensively studied the reaction of CO_2 with Ni^{II}(cyclam) complexes.[8-10] The Sauvage complexes are extremely stable, highly selective, and can show faradaic efficiencies up to 96% in the production of CO at –0.86 V vs. SCE, even under aqueous conditions. The ligand geometry allows for a highly accessible metal center. It was noted that unsaturated or open chain complexes of similar moieties showed poor catalytic activity. The nickel macrocycle complexes were shown to be very sensitive to the pH and required an Hg electrode surface to turnover. The anion in the supporting electrolyte was shown to affect the selectivity, with KNO_3 and $KClO_4$ showing the fastest observed rates. A subsequent study on a binuclear transition-metal centered nickel complex using bicyclam showed similar reactivity towards CO_2 but no coupling products were observed. As shown in later studies by Balazs the high electrocatalytic activity originates with $Ni(cyclam)^+$ strongly absorbed on a mercury electrode surface.[11] It was also found that CO limits the long-term stability of the catalyst in an unstirred solution by the deposition of an insoluble precipitate believed to be Ni(cyclam)(CO).

Iron(0) porphyrins were reported by the Savéant group in 1991 to reduce CO_2 to CO at -1.8V vs. SCE in DMF.[12] However the porphyrins were unstable and degraded after a few catalytic cycles. With the addition of a hard electrophile, such as Mg^{2+}, the stability and reactivity of the catalyst improved noticeably. It is believed through mechanistic studies that the Mg^{2+} ion assists in the breaking of the CO_2 bound to iron creating Fe(II)CO and $MgCO_3$. This is an example where the electron rich iron

center initiates the reduction while the Lewis acidic Mg^{2+} helps complete the process, by sequestering an oxygen atom in $MgCO_3$.

Later Savéant found that iron(0) porphyrins (Figure 1.3) were able to catalyze the reduction of CO_2 to CO in the presence of weak Brönsted acids.[13] For the system where weak Brönsted acids such as 1-propanol, 2-pyrrolidine, and CF_3CH_2OH were added, Savéant found that catalysis was significantly improved in terms of both the efficiency and lifetime, without significant formation of H_2. They were also able to reach turnover numbers as high as 350 h^{-1} at a catalyst decay rate of 1% per catalytic cycle. This system does, however, require reduction potentials that are still too

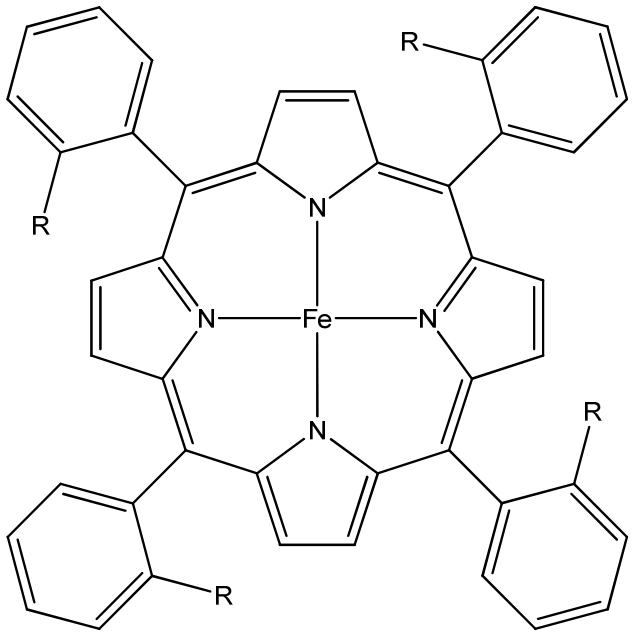

6

Figure 1.3 Savéant Iron(0) porphyrin catalyst structure shown to reduce CO_2 to CO in the presence of weak Brönsted acids at a potential of -1.5 V vs. SCE.[12] Porphyrins of this nature reduce CO_2 to CO with at with high turnover frequency and low catalyst degradation, but require potentials too high for practical applications.

negative for practical use (approximately -1.5 V vs. SCE) and the necessity of a mercury electrode, which we have noted above can display significant activity in the reduction of CO_2 sans catalyst.

In 2002 Fujita and co-workers published their findings on cobalt and iron corroles and their ability to catalyze the reduction of CO_2 to CO.[14] These complexes of the structure shown in Figure 1.4 displayed a catalytic current with onset at approximately -1.7 V vs. SCE in the presence of CO_2. The majority of analytical studies of the products for this reaction were done during photochemical reduction, but it was found that the major product of reduction was CO. Photochemical reduction of the complexes was acheived in deoxygenated solvents containing "sacrificial"

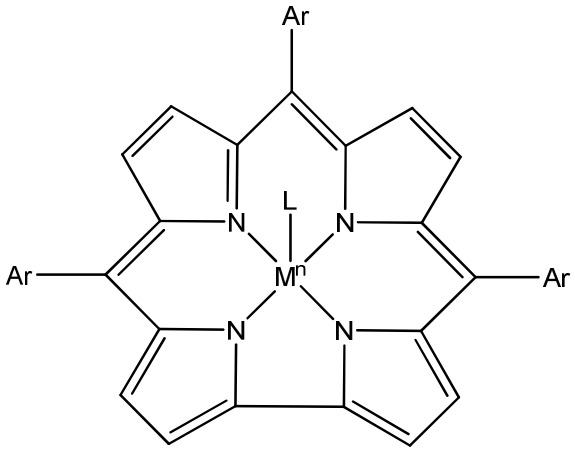

M	n	Ar	L	Abbreviation	Complex #
Co	III	C_6F_5	Ph_3P	$Ph_3PCo(tpfc)$	**7**
Fe	IV	C_6F_5	Cl	ClFe(tpfc)	**8**
Fe	IV	2,6-$C_6H_3Cl_2$	Cl	ClFe(tdcc)	**9**

Figure 1.4 Fujita metal corrole complexes for the photochemical reduction of CO_2 to CO.

triethylamine (Et_3N) reducing agent and *p*-terphenyl (TP) as a sensitizer. The catalysts would produce varying amounts of CO and H_2 (depending on catalyst) for up to 10 hours. Problems with this catalyst system include high overpotentials for reduction of CO and catalyst breakdown after long periods of irradiation.

1.3.2 Metal complexes with bipyridine ligands.

In 1984 the Lehn group reported the electrocatalytic reduction of CO_2 by the use of a $Re(bipy)(CO)_3Cl$ (bipy = 2,2'-bipyridine) complex.[15] Using this rhenium bipyridine complex they were able to show the selective reduction of CO_2 to CO at a potential of -1.49 V vs. SCE using a 9:1 DMF-H_2O solution. It was also noted that as the percentage of water was increased the selectivity for CO was diminished, and when the reduction was run under an atmosphere of argon, only molecular hydrogen was produced. While this system had high current efficiencies (98%), and excellent selectivity for carbon monoxide over hydrogen production, the limiting factor was the low TOF of 21.4 h^{-1}.

It was later reported by Tanaka and co-workers that bipyridine complexes of ruthenium could catalyze the reduction of CO_2.[16] $Ru(bipy)(CO)_2^{2+}$ and $Ru(bipy)(CO)Cl^{+}$ were found to electrocatalytically reduce CO_2 to CO, H_2, and $HCOO^-$. Both complexes were shown to reduce CO_2 at -1.40 V vs. SCE. Following a two electron reduction of the complex, CO is lost to form a five coordinate neutral complex. In the presence of CO_2 the complex forms an η^1-CO_2 adduct of Ru(0). This species can also be formed by addition of two equivalents of OH^- to $Ru(bipy)(CO)_2^{2+}$. Addition of a proton forms the LRu(CO)(COOH) species which under acidic

conditions (pH 6.0) gains another proton to lose water and regenerate the catalyst as shown in scheme 1.2. Under basic conditions (pH 9.5) the catalyst may undergo a two electron reduction with the participation of a proton to create $HCOO^-$ and regenerate the five coordinate Ru(0) complex. Even with the limitations of this system, such as low turnover numbers and low selectivity, it helped to elucidate several of the key intermediates in the reduction of CO_2.

In a similar system studied by the Meyer group, it was found that 2,2'-Bipyridine complexes of Rhodium and Iridium act as electrocatalysts for the reduction of CO_2.[17] They found that *cis*-$[Rh(bpy)_2X_2]^+$ (X is Cl or TFMS) reduces CO_2 at -1.55

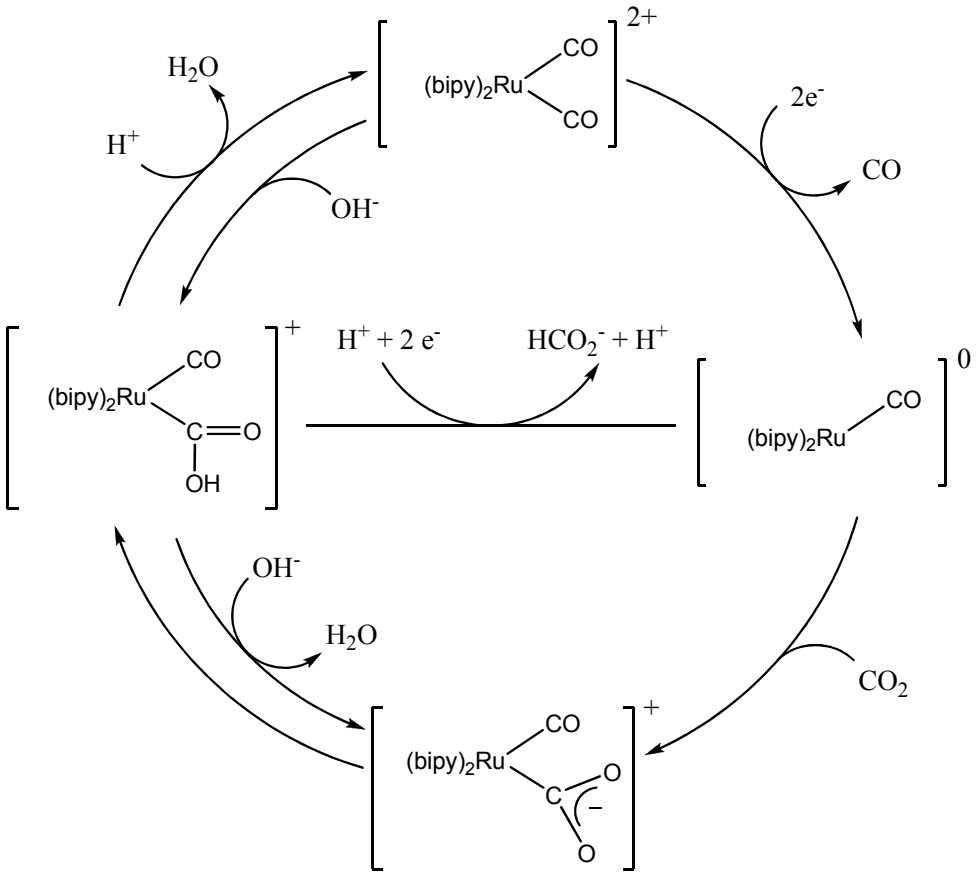

Scheme 1.2 Proposed mechanism for Tanaka catalyst.

V vs. SCE to predominantly form formate. It is interesting to note that no CO was detected in any of the electrolysis experiments; however, H_2 was formed presumably by the degradation of the supporting electrolyte. This system was found to have both low turnovers (6.8 to 12.3) and poor current efficiencies (64% for formate, and 12% for H_2). Meyer and co-workers also found that $[M(bpy)_2(CO)H]^+$ (M = Os, Ru) were electrocatalysts for the reduction of CO_2.[18] Under anhydrous conditions the major product was CO, and with the addition of H_2O up to 25% formate was observed.

1.3.3 CO_2 reduction by transition metal phosphine complexes.

The first reported transition metal electrocatalyst containing phosphine ligands was the $Rh(dppe)_2Cl$ (dppe = 1,2-bis(diphenylphosphino)ethane) complex reported in 1984 by the Wagenknecht group.[19] In this system the products upon reduction of CO_2 were found to be the formate anion with small percentages of cyanoacetate. Current efficiencies for the generation of the formate anion were approximately 42% for short electrolysis runs and down to 22% for longer runs. While mechanistic studies were not undertaken, it was hypothesized that the reduction of the complex resulted in either hydrogen abstraction from acetonitrile to form the transition metal hydride followed by insertion of CO_2 to form the formate complex, or through the formation of a CO_2 adduct followed by abstraction of the proton from acetonitrile. While the reduction of CO_2 will occur at -2.21 V vs. SCE in neat DMF, the reported reduction of CO_2 was nearly 700mV lower at -1.55 V vs. SCE using the $Rh(dppe)_2Cl$ complexes.

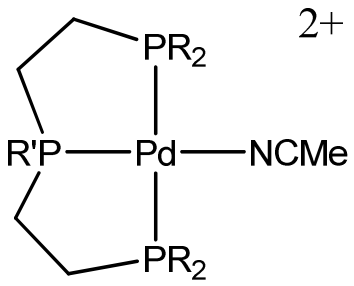

10

Figure 1.5 DuBois tridentate phosphine catalyst.

Palladium complexes using polydentate phosphine ligands represent some of the most extensively studied CO_2 reduction catalysts to date. First reported in 1991 by the Dubois group[20] these systems have shown significant development over the last 15 years.[21, 22] The typical catalyst system is based on a tridentate phosphine ligand that was initially coordinated to Co, Fe, or Ni. While the iron system showed catalysis of CO_2 reduction, the overpotentials were high and the rates were slow. However, the Ni system displayed two one-electron reductions in the area of interest for CO_2 reduction. This observation ultimately led this group to study the palladium triphos complexes as catalysts. The first reported complex, $[Pd(triphos)(PR_3)](BF_4)_2$ (Figure 1.5), would catalyze the reduction of CO_2 to CO in acidic acetonitrile solutions. The active species was later found to be the phosphine-dissociated solvent complex $[Pd(triphos)(solvent)](BF_4)_2$.

In later mechanistic studies it was determined that as the Pd(II) complex gained an electron to form a Pd(I) intermediate, a reaction with CO_2 occurred to form a five-coordinate CO_2 adduct. Upon transfer of the second electron, the Pd(0) intermediate dissociated the solvent. Protonation of one of the oxygen atoms of coordinated CO_2 affords a metallocarboxylic acid intermediate, Pd-COOH. It is believed that the metallocarboxylic acid is protonated again to form a "dihydroxy carbene", and that CO is then formed by dehydration of the dihydroxy carbene. CO dissociation and solvent association regenerates the initial complex. This proposed catalytic cycle is shown in scheme 1.3. In solutions of high acid concentration the rate

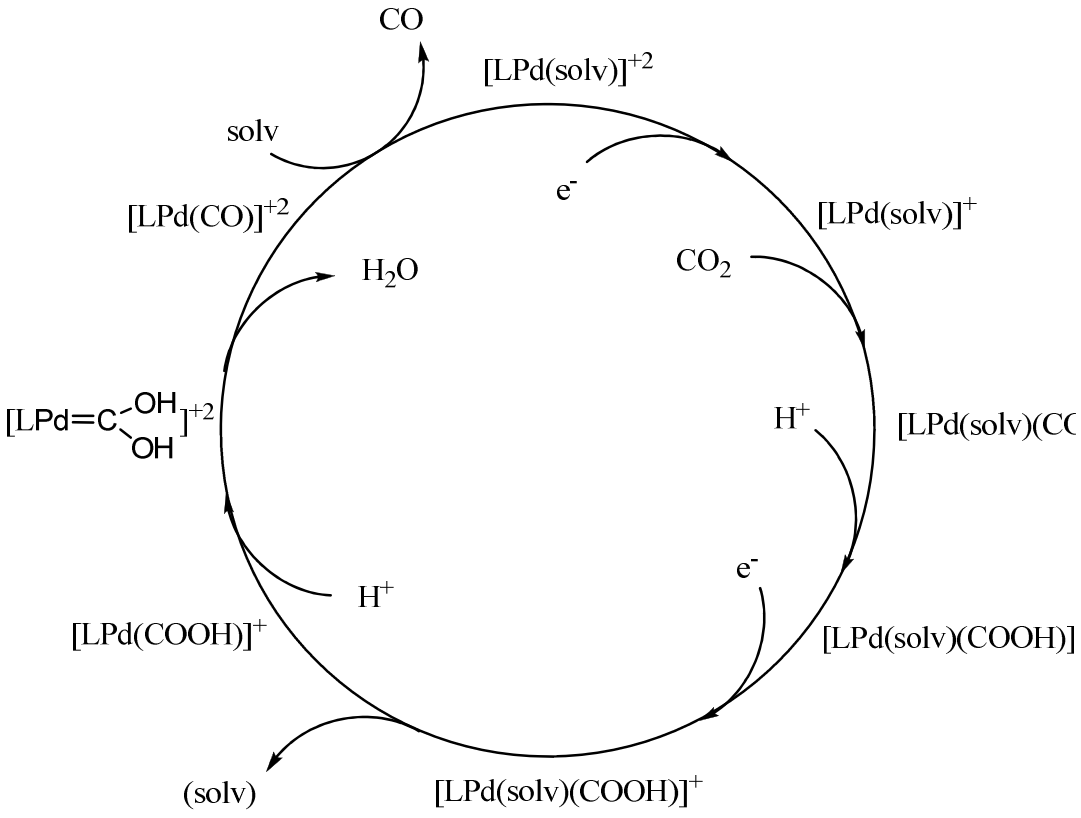

Scheme 1.3 Proposed catalytic cycle for DuBois Pd catalyst.

determining step was found to be the reaction of the Pd(I) intermediate with CO_2. However, in solutions of low acid concentrations the cleavage of the C-O bond to form carbon monoxide and water limits the rate of the catalytic cycle.

The triphosphine ligand system allows for variation of both electronic and steric effects. Changing the substituent on the central phosphorus to a mesityl group effectively blocked one of the open coordination sites cutting the rate of reaction in half, excluding the possibility of a six-coordinate intermediate that has been proposed for some Ni(I) macrocyclic complexes.[11, 23] The central donating atom of the tridentate ligand was varied from P to C, N, S, and As as shown in Figure 1.6. None was as effective as the original triphosphine ligand, however mechanistic insight into the production of molecular hydrogen was gained. With the $[Pd(PCP)(CH_3CN)](BF_4)_2$ (**11**) complex CO_2 was found to be a cofactor in the production of hydrogen suggesting that H_2 production goes through the same intermediate that produces CO. From these studies DuBois hypothesized that the preference for forming hydrogen or carbon monoxide depends on the basicity/redox potential of the catalyst. The more negative redox potential favors the protonation of the Pd to form a hydride, the less negative redox potential favors protonation of the coordinated CO_2 oxygen to form

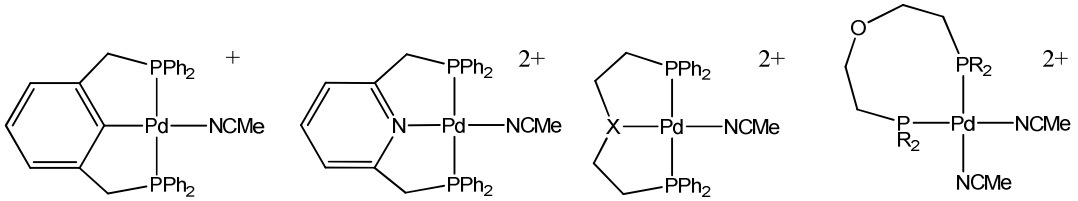

Figure 1.6 Varied tridentate phosphine ligands.

CO and H_2O.

Recent studies have focused on complexes incorporating two or more independent Pd triphosphine units.[21] Early studies with dendrimers of the Pd catalyst showed decreased activity and selectivity, however with the methylene bridged monomers of the catalysts, rates were found to increase by three orders of magnitude, suggesting a cooperative binding of CO_2. Along with this increase in catalytic activity came an increase in the formation of Pd(I)-Pd(I) bonds, thus decreasing catalyst lifetimes.

These classes of Pd phosphine complexes have shown catalytic rates in the range of 10 to 300 M^{-1} s^{-1} and with >90% current efficiencies for CO production. Overpotentials were in the range of 100-300 mV, yet turnover numbers were low (*ca.*10-100) and the decomposition to Pd(I) dimers and hydrides eventually causes cessation of catalytic activity.

Catalytic CO_2 reduction has been reported by our group as early as 1987 with a binuclear Ni(0) "cradle" complex, $[Ni_2(CNMe)_3(dppm)_2][PF_6]_2$ operating around –0.87 V vs. SCE.[24] However over extended time periods the complete carbonylation of the complex occurs to give $Ni_2(CO)_3(dppm)_2$. More recently, we have returned to a binuclear $[Ni_2(\mu\text{-dppa})_2(\mu\text{-CNR})(CNR)_2]$ system.[25] This system also suffers from the CO produced being trapped by the catalyst.

Table 1.1 Spectroscopic Data for $[Ni_3(\mu_2\text{-dppm})_3(\mu_3\text{-L})(\mu_3\text{-I})][PF_6]$ Clusters

	L	$E_{1/2}(+/0)$[a] (V*vs.* SCE)	FT-Ir[b] ν(C≡N)	^{31}P NMR[c] δ (ppm)	UV-vis[d] λ_{max} (ε)
15	$CNCH_3$	-1.18	1927, 1871	0.4 s	527.0 (3.8)
16	CN(*i*-C_3H_7)	-1.18	1876, 1815	-0.2 s	534.4 (4.5)
17	CNC_6H_{11}	-1.17	1885, 1832	0.3 s	536.5 (5.0)
18	$CNCH_2C_6H_5$	-1.11	1887, 1801	0.4 s	529.3 (4.3)
19	CN(*t*-C_4H_9)	-1.12	1780[e]	-1.4 s	539.2 (3.8)
20	CN(2,6-$Me_2C_6H_3$)	-1.08	1849, 1822	-1.9 s	542.2 (3.4)
21	CO	-1.12	1726[f]	3.1 s	520.0 (6.3)

[a]Cyclic voltammograms recorded in CH_3CN. [b]Recorded as KBr pellets. [c]Recorded at 121.6 MHz in CD_3CN. [d]Recorded in CH_3CN, λ_{max} in nm, ε ($M^{-1}\cdot cm^{-1} \times 10^3$) given in parentheses. [e]Broad. [f]ν(C≡O).

A key finding was made in 1992 when a new trinuclear nickel cluster $[Ni_3(\mu_3\text{-I})(\mu_3\text{-CNMe})(\mu_2\text{-dppm})_3]^+$ (dppm = bis(diphenylphosphino)methane) (**15**) was found to be an eletrocatalyst for the reduction of CO_2. We have extended this class of nickel cluster electrocatalysts significantly over the past several years to include other isocyanide capped clusters (**16–20**),[26, 27] the CO capped cluster **21** (Table 1.1),[26] and chalcogenide capped clusters.[28] Results of studies of the electrochemical kinetics of the reduction of CO_2 by clusters **15–21** have been reported.[27] These results are summarized here briefly. Under an atmosphere of CO_2 in dry acetonitrile, the reduction of **15** affords CO and CO_3^{2-} as the only products observed by GC, HPLC, and IR spectroscopy. The use of $^{13}CO_2$ results in ^{13}CO and $^{13}CO_3^{2-}$, and no oxalate was observed. The relative rates of reaction of the alkyl or aryl substituted isocyanide or carbonyl capped clusters with CO_2 follow the order: $CNCH_3$ (**15**) ~ CN(*i*-C_3H_7) (**16**) > CNC_6H_{11} (**17**) > $CNCH_2C_6H_5$ (**18**) > CO (**21**) > CN(*t*-C_4H_9) (**19**) ~ CN(2,6-

$Me_2C_6H_3$) (**20**) (Table 1.2). It is important to note that although the values of $E_{1/2}(+/0)$ fall into a relatively narrow range of -1.18 (**15**) to -1.08 V (**20**) *vs*. SCE, small differences in $E_{1/2}(+/0)$ dramatically affect the rates of the reaction with CO_2. The data indicate that the reaction rates of the isocyanide capped nickel clusters **16-20** with CO_2 are primarily influenced by the reduction potentials of the clusters and that the size and geometry of the substituents of the capping ligand play a secondary role. The interaction of CO_2 with the reduced forms of **16-20** can occur either at the isocyanide ligand or at the nickel core. In these clusters, we have favored a metal-based mechanism as molecular orbital studies have shown that the LUMO which becomes singly occupied in the reduction of this class of clusters is almost entirely metal-centered.[26] The electrochemical studies also suggest that the energy of this orbital correlates with reactivity toward CO_2. The secondary steric effect observed in the electrochemical kinetics study further suggests that CO_2 activation is occurring on the isocyanide capped face of the clusters.

Table 1.2 Rate Data for the Homogeneous Rate of Reaction Between CO_2 and $[Ni_3(\mu_2\text{-dppm})_3(\mu_3\text{-L})(\mu_3\text{-I})][PF_6]$ Clusters

	L	$E_{1/2}(+/0)$[a] (V*vs.* SCE)	k_{CO2}[b] ($M^{-1}s^{-1}$)
15	$CNCH_3$	-1.18	1.6 ± 0.3
16	CN(*i*-C_3H_7)	-1.18	1.4 ± 0.3
17	CNC_6H_{11}	-1.17	0.5 ± 0.1
18	$CNCH_2C_6H_5$	-1.11	0.2 ± 0.05
19	CN(*t*-C_4H_9)	-1.12	0.0 ± 0.05
20	CN(2,6-$Me_2C_6H_3$)	-1.08	0.0 ± 0.05
21	CO	-1.12	0.1 ± 0.1

[a]Cyclic voltammograms recorded in CH_3CN. [b]Rates determined by rotating disk voltammetry.

The binuclear copper complex, $[Cu_2(\mu\text{-}PPh_2bipy)_2(MeCN)_2][PF_6]_2$, **22**, ($PPh_2bipy$ = 6-diphenylphosphino-2,2'-bipyridyl), and its pyridine analog, $[Cu_2(\mu\text{-}PPh_2bipy)_2(py)_2][PF_6]_2$, **23** (Figure 1.7), were also found to be efficient electrocatalysts for the reduction of CO_2.[29] Two sequential single electron transfers to **22** are observed at $E_{1/2}(2+/+)$ = -1.35 V and $E_{1/2}(+/0)$ = -1.53 V vs SCE in MeCN. Both are required to effect CO_2 reduction. Again, the CO_2 derived products correspond mainly to the reductive disproportionation to CO and CO_3^{2-}. The only gaseous product was found to be CO. A turn-over frequency of >2 h^{-1} was maintained over the course of a 24 hour experiment. The catalyst was still active at the end of this experiment, and **22** was recovered quantitatively in its original form. The homogeneous electron transfer kinetics for the reduction of CO_2 by complex **22**

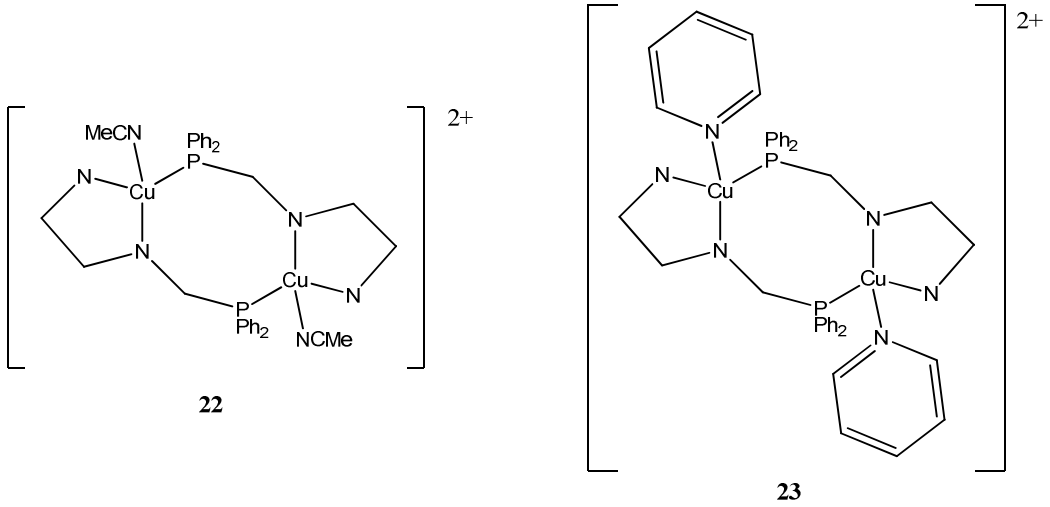

Figure 1.7 Kubiak dinuclear copper complexes that reduce CO_2 to CO and CO_3^{2-}at -1.53 V vs. SCE. Catalyst shows turnover numbers of greater than 2 h^{-1} over 24 hour periods and is still intact after catalytic period. Catalysts are effective, but suffer from low tunrover and high overpotentials.

were studied by chronoamperometry. The limiting rate constant, k_{CO2}, for the reaction of the doubly reduced state of **22** with CO_2, was determined to be 0.7 $M^{-1}s^{-1}$ in acetonitrile. The rate constant, k_{CO2}, for **22** in methylene chloride solvent is comparable, 0.6 M^{-1} s^{-1}. However, the rate constant, k_{CO2}, for the pyridine adduct, **23**, in methylene chloride solvent is significantly less, 0.1 $M^{-1}s^{-1}$. These data suggest that substitution of the labile acetonitrile or pyridine ligands of **22** and **23** respectively is required for CO_2 reduction. Significantly, **22** is a $2e^-$ electrocatalyst for the reduction of carbon dioxide. The $2e^-$ redox cycle of **22** appears to lead to at least an order of magnitude increase of the steady state catalytic currents for CO_2 reduction compared to our nickel cluster electrocatalysts described above. The difference in overall rates is significant since the limiting [CO_2] dependent derived rate constants are comparable. This suggests that the nickel cluster catalysts are slow because they operate via a single electron redox cycle while the overall reduction of CO_2 is a $2e^-$ process. On the other hand, the potentials required by the copper catalysts to reduce CO_2 are between 350 and 450 mV, more negative than those of the trinuclear nickel catalysts.

1.4 Lessons from nature

Of all of the synthetic systems reported for the electrochemical reduction of carbon dioxide[3-29] none are as efficient and selective as the systems found in nature. The classes of enzymes that catalyze the oxidation of carbon monoxide are designated as carbon monoxide dehydrogenases (CODHs). They are the only catalysts

kinetically and thermodynamically optimized to equilibrate CO_2 and CO at room temperature. CODHs reversibly catalyze the reaction of carbon monoxide with water to form carbon dioxide, protons and electrons (equation 8).

$$CO + H_2O \leftrightarrow CO_2 + 2H^+ + 2e^- \qquad (E8)$$

There are two basic classes of CODHs. The first class is derived from anaerobic bacteria and archae that use oxygen sensitive Fe and Ni active sites. The second class comes from aerobic and carboxydotrophic bacteria that use Cu, Mo, and Fe active sites.[30]

1.4.1 Ni-Fe-S.

The crystal structure of CO dehydrogenase from the anaerobic bacteria *Carboxydothermus hydrogenoformans* reveals an active site containing a complex $NiFe_4S_4$ center.[30] The structure was recently solved in three different reduced states, one held at a potential of -320 mV, another at -600 mV, and a third at -600 mV in combination with CO_2. In both of its reduced states the nickel is coordinated by three sulfur ligands forming a distorted T-shaped geometry.

Upon addition of CO_2 to the reduced state, CO_2 binds to both the Ni and Fe. This binding causes minimal geometry changes and occupies the forth position around Ni completing the square planar geometry. In the coordination of CO_2 nickel acts as the Lewis base, while the iron acts as the Lewis acid, and the partial negative charge on the oxygen is stabilized through hydrogen bonding provided by the protein surroundings. The positions of the Ni and Fe are held in place by the Fe_3S_4 framework and are essentially unchanged by the presence or absence of CO_2. The cluster also serves to act as an electronic buffer stabilizing the electronic charges on Fe and Ni during the catalytic cycle (scheme 1.4). It is this low reorganization energy that

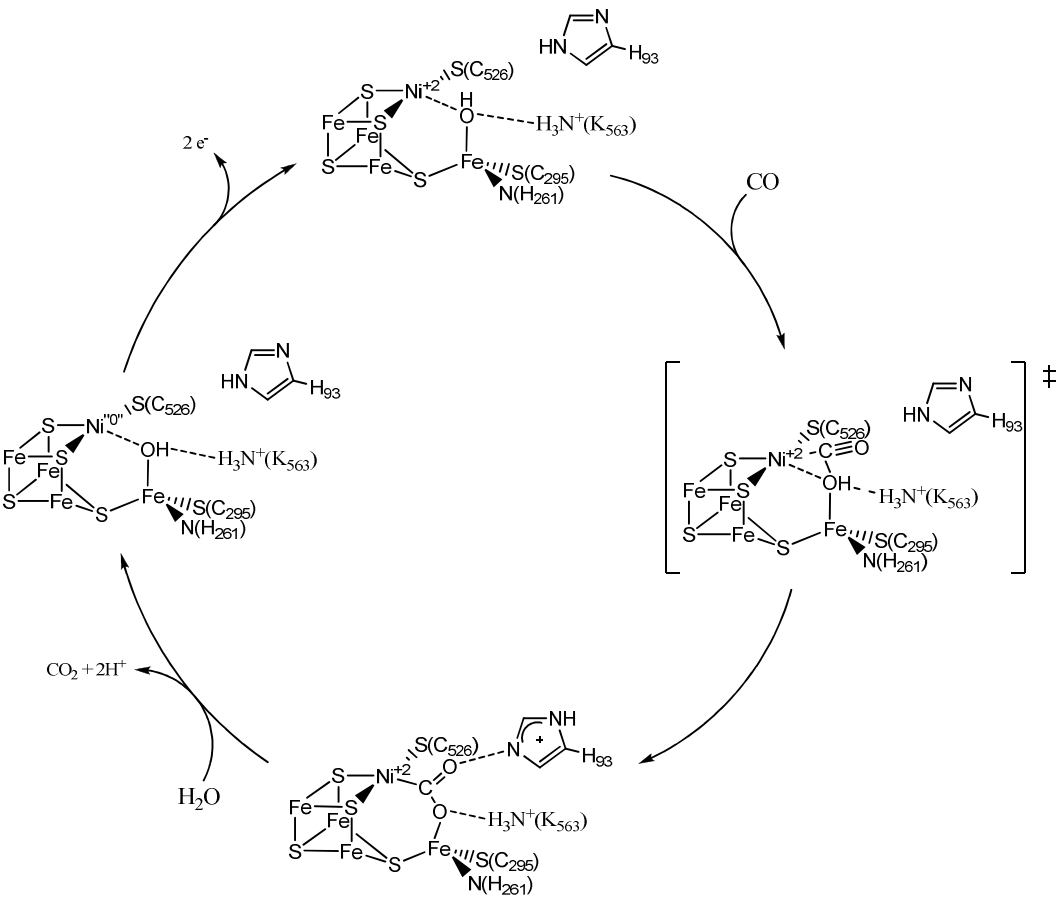

Scheme 1.4 Proposed catalytic cycle for anaerobic CO dehydrogenases

allows for a catalyst with a turnover rate of 31,000 s^{-1}.[30]

1.4.2 Mo-S-Cu.

The first crystal structure of the Mo-S-Cu active site isolated from the aerobic bacteria *Oligotropha Carboxidovorans* was reported in 1999 by Dobbek and co-workers.[31] The structure was reported to contain an active site consisting of molybdenum with three oxo ligands, molybdopterin-cytosine and *S*-selanylcysteine. Upon further review the active site was reported to be a Mo(=O)SCu active site, while the presence of selenium could not be confirmed (Figure 1.8).[32]

The active site consists of distorted square pyramidal molybdenum with an apical oxo ligand, a hydroxyl group, bridging sulfur to the copper and bound to the protein through molybdopterin cytosine dinucleotide cofactor. The copper is attached to the protein through the Sγ atom of Cys-388. Within the second coordination sphere of the active site there are several groups within hydrogen bonding distance, allowing for stabilization of charges. In the CO reduced, air oxidized, cyanide inactivated, and n-butyl isocyanide bound states the hydrogen bonding distances remain essentially the same. The active site lies 17Å deep within the protein with a hydrophobic channel

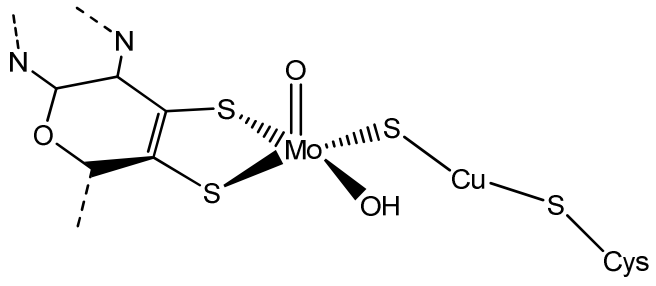

Figure 1.8 Active site of aerobic CO dehydrogenase

that averages 7Å in diameter.

In the refined structures of the reduced state, the active site remains structurally similar to the air oxidized state. Several of the bond lengths increase (Mo--Cu 3.74Å to 3.93Å and Mo--OH 1.87Å to 2.03Å) yet the overall geometry remains the same. The enzyme has a catalytic rate of 107 s^{-1}. The active site of *O. Carboxidovorans* can be inhibited by the use of isocyanides. When inhibited by n-butyl isocyanide, an "intermediate" in the reduction of CO_2 can be observed.

From the crystal structures reported to date the requirements for efficient reduction of carbon dioxide are becoming evident. Each of these structures exhibit late first row transition metals in low oxidation states, Cu(I) and Ni(0), and a redox

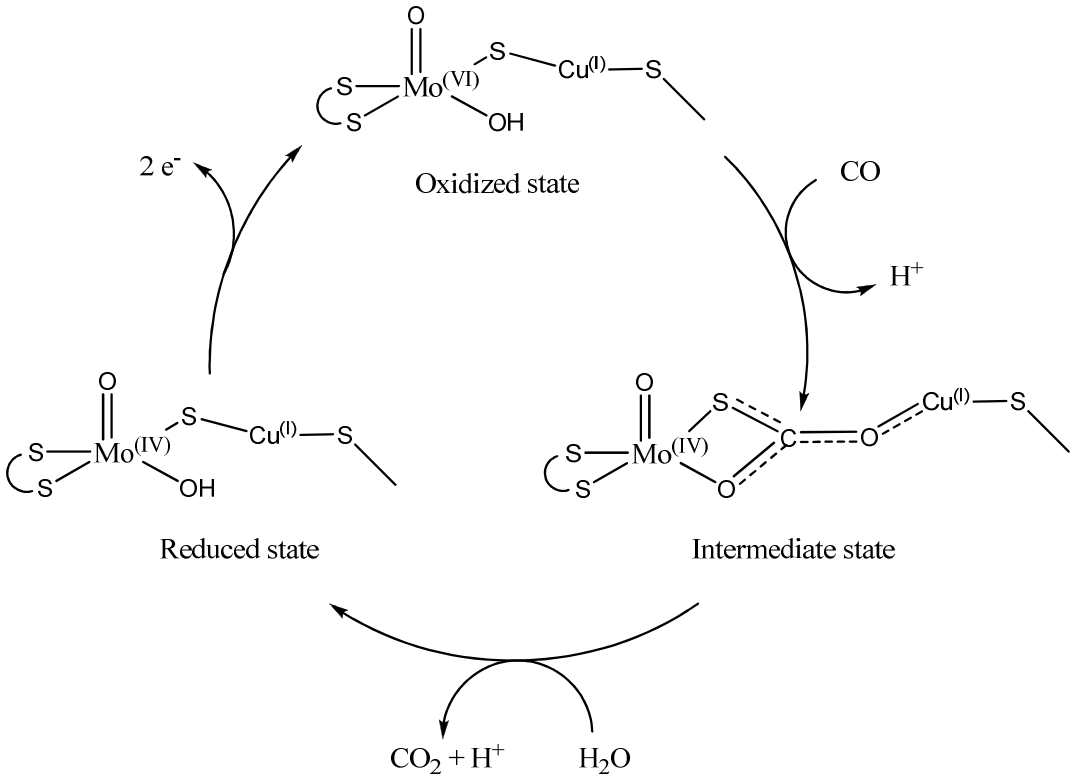

Scheme 1.5 Proposed catalytic cycle for aerobic CO dehydrogenases.

reservoir (Mo(IV) and Fe_3S_4) to supply electrons for the reduction of carbon dioxide. A key feature of both enzymes is the minimal change in energy between the reduced and oxidized states.

Although most of the work mimicking active sites of proteins has focused on the hydrogenases,[33] some research has been done on "bio-inspired" reduction of CO_2. Tezuka and co-workers first reported the reduction of CO_2 by using a $Fe_4S_4(SR)_4^{2-}$ cluster in DMF.[34] With this cluster they showed that they were able to reduce CO_2 to formate at a potential of -1.7 V vs. SCE. They also report considerable amounts of C_3 hydrocarbons in the gas analyses after controlled potential electrolysis, however this may be due to the reduction of the electrolyte.

More recently, Tatsumi and co-workers reported the synthesis of sulfide bridged molybdenum-copper complexes related to the active site of *O. Carboxidovorans*.[35] Several compounds were synthesized mimicking the active site, however none exhibited reactivity towards either carbon monoxide or t-butyl isocyanide. This emphasizes the difficulty in creating a working mimic of biological systems.

1.5 *De Novo* synthetic catalysts.

In the previous section the operating principles of the biological and biologically inspired catalysts were reviewed as they provide important leads for the future of CO_2 reduction at low potentials. At this stage of development, however, it is not clear whether the best catalysts will be developed based on lessons learned from nature, or whether *de novo* synthetic catalysts will be superior for the production of

synthetic fuels from carbon dioxide. Synthetic catalysts for the reduction of CO_2 reported to date do not possess the efficiencies or stabilities needed for useful large-scale technology. The major obstacle preventing efficient conversion of carbon dioxide into energy-bearing products is the high potential at which carbon dioxide is reduced coupled with the lack of a catalyst that can use an abundant renewable energy source to perform the reaction (e.g., electricity from solar, wind, or geothermal sources). The difficulties in synthesizing a legitimate electrocatalyst for the reduction of CO_2 arise from a variety of sources, including, but not limited to, gaps in understanding about what types of complexes will make the best catalysts, the fact that carbon dioxide is a relatively inert molecule, and the problem of performing multi-electron reductions to produce a usable end product. Currently, a literature search of the best catalysts reported to date yields some that have good current efficiencies, some that are robust, and some that give reasonable turnover numbers, but none that accomplish all of these goals. There are also many catalysts with high efficiencies and good activity towards CO_2 reduction, but they require the use of sacrificial reducing agents. Another of the notable absences from the current literature is a catalyst that can fix and transform CO_2 at low overpotentials, specifically at less than 0.1V.

In the case of CO_2, slow kinetics and high overpotentials for electrochemical reduction result from a large nuclear reorganization energy. The winning strategy for efficient reduction of CO_2 must involve simultaneous multi-electron transfers and catalytic sites that direct nuclear configurations of reactants favorably for product

formation. The development of catalysts to enable two-electron transfer from the *same* molecule will allow for kinetically more efficient reduction of CO_2.

Past examples of carbon dioxide reduction catalysts have cleared some paths for understanding what remains be done in order to solve the problems summarized above. In most of these past studies the major products have been carbon monoxide and formic acid, and on relatively small scales. In only a few studies has methane or methanol been the primary product of the reductions.

In order to do a multi-electron reduction of CO_2 to a usable liquid fuel we will have to develop new methods for activating the carbon dioxide molecule and it will probably be necessary to develop a catalyst that can perform several different kinds of reduction or a series of catalysts that can each work together to perform the required steps.

As an example, consider the first logical step in a CO_2 reduction scheme; the hydrogenation of CO_2 to formic acid, HCOOH. CO_2 is an "amphoteric" molecule

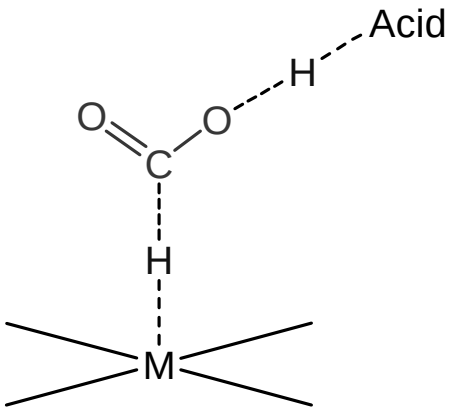

Figure 1.9 One way to envision proton-couple electron transfer to CO_2 is from a metal hydride and a neighboring acid.

(possessing both acidic and basic properties). The carbon atom is susceptible to attack by nucleophiles and the oxygen atoms are susceptible to attack by electrophiles. In the hydrogenation of CO_2, therefore, one can think of activation of CO_2 being initiated by attack of a nucleophilic metal hydride (H^-) at the CO_2 carbon atom. The transfer of charge from the hydride to the carbon atom in turn causes negative charge to develop on the oxygen atoms. This charge can be stabilized by a Brönsted acid (H^+). In the limit of these interactions, one can consider the hydrogenation of CO_2 to result from a heterolytic process that adds H^- to the carbon and H^+ to the oxygen as shown in Figure 1.9. The next logical step in the reduction of CO_2 is the deoxygenation of formic acid (HCOOH) to formaldehyde (H_2CO). In photosynthesis, for example, CO_2 is reduced to H_2CO equivalents that are combined to form saccharides $(H_2CO)_6$. The reduction of formic acid to a formaldehyde equivalent can again be thought to proceed by H^- addition to the carbon atom and H^+ addition to the OH group. However, it is important to note that the details of how this next step in the reduction (strength of hydride and proton equivalents, geometry of addition, etc.) can be expected to be quite different from those required in the production of formic acid in the first place. Similarly, the third step, namely reduction of formaldehyde to methanol (CH_3OH), may proceed by a completely different mechanism such as the direct addition of H_2 across the C=O double bond of formaldehyde. This illustrates the need for detailed mechanistic and theoretical knowledge in the development of catalysts for the conversion of CO_2 to liquid fuels.

1.6 Conclusions and Future Directions

In this discussion, we have attempted to review the prior art in the field of electrocatalytic and homogenous approaches to the reduction of CO_2. We also covered its conversion to molecules that are precursors to, or are directly usable as fuels. At this stage, it is useful to draw conclusions from past work, and try to identify concepts that will provide a framework for research leading to the next major advances in the field.

One important lesson from previous work is that the fundamental reorganization energies of both the CO_2 molecule and the catalysts that reduce CO_2 are extremely important considerations. An important distinction between the biological CODHs and the synthetic transition metal complex catalysts for CO_2 reduction is that the CODHs can equilibrate CO_2 and CO. In other words; they can catalyze the reduction of CO_2 in both directions. This implies that the CODHs function at the thermodynamic potential for CO_2 reduction. It further implies that the CODHs operate at low barriers that result from active sites that direct the linear CO_2 molecular substrate toward a necessarily bent CO_2 configuration in the reduction intermediates.

A second feature which prior studies also suggest to be important in guiding future work is a multi-electron transfer capacity of the electrocatalysts. For example, of all of the known synthetic electrocatalysts for CO_2 reduction, only the $[Ni_3(\mu_3\text{-}I)(\mu_3\text{-}CNR)(\mu_2\text{-}dppm)_3]^+$ can equilibrate CO_2 with CO and CO_3^{2-}. The rates, however, are quite slow and this has been attributed to the fact that the $[Ni_3(\mu_3\text{-}I)(\mu_3\text{-}CNMe)(\mu_2\text{-}dppm)_3]^+$ catalysts function only by a single-electron redox cycle, while

the reduction of CO_2 to CO and CO_3^{2-} is a two-electron process. The development of CO_2 reduction catalysts that have highly reversible electrochemistry, indicative of low catalyst reorganization energies, but that also possess multiple electron redox capacities appears to be a very promising area of research.

A third point which has been largely overlooked in previous work, but should figure importantly in future work is proton coupled electron transfer. Proton coupled electron transfer (PCET) is frequently discussed in mechanisms for water splitting. PCET may well be even more important in CO_2 reduction catalysis. The redox potentials summarized in equations 1-5 show that the coupling of C-H bond forming reactions with CO_2 reduction can lead to very reasonable overall thermodynamics. The key challenge here then is not just one proton coupled electron transfer, but

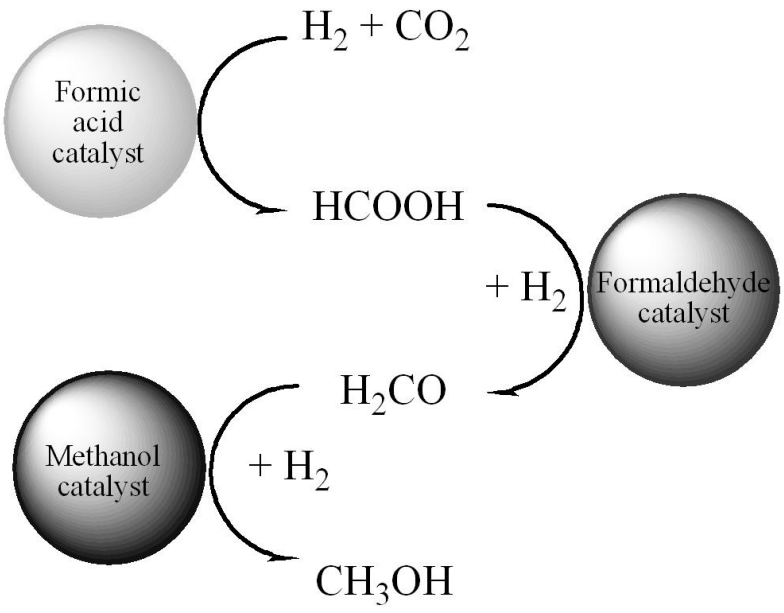

Scheme 1.6 Proposed path for the tandem catalytic reduction of CO_2 to methanol. A series of three catalysts that each contributes to the overall reduction of CO_2 to methanol in optimized single steps.

multiple proton coupled electron transfers to produce molecules such as methanol or methane. One observation that we make from this is that it is difficult to imagine *one* catalyst that can do it all. As we noted in the previous section, in the hydrogenation of CO_2, it appears that the most effective initial hydrogenation of CO_2 to formic acid would occur by the heterolytic hydride (H^-)/proton (H^+) addition of H_2. The second step in the reduction of CO_2 is the deoxygenation of formic acid (HCOOH) to formaldehyde (H_2CO). The reduction of formic acid to a formaldehyde equivalent may again be thought to proceed by H^- addition to the carbon atom and H^+ addition to the OH group, but by a mechanism that could be quite different from that which led to the production of formic acid in the first place.

Finally, the fact that the reduction of formaldehyde to methanol (CH_3OH) – may proceed by a completely different mechanism still illustrates that either a multi-functional single catalyst or panel of catalysts would be needed for efficient conversion of CO_2 to methanol. Presently, we favor the second approach as shown in scheme 1.6. This approach includes a panel of three catalysts that each contributes to the overall reduction of CO_2 to methanol in optimized single steps. There are various platforms for such catalysts to be developed. These include immobilization on beads, anchoring to separate or single supports or surfaces, etc.

Note: Much of the material for this chapter comes directly from a manuscript entitled “Electrocatalyic and homogeneous approaches to conversion of CO_2 to liquid fuels.” by Eric E. Benson, Clifford P. Kubiak, Aaron J. Sathrum, and Jonathan M. Smieja, which has been published in *Chemical Society Reviews*, **2009**, *38*, 89-99. http://dx.doi.org/10.1039/b804323j. The dissertation author is an equal author of this manuscript.

1.7 References

1. Halmann MM & Steinberg M (1999) *Greenhouse Gas Carbon Dioxide Mitigation Science and Technology* (Lewis Publishers, Boca Raton, FL).

2. Sutin N, Creutz C, & Fujita E (1997) Photo-induced generation of dihydrogen and reduction of carbon dioxide using transition metal complexes. *Comment. Inorg. Chem.* 19(2):67-92.

3. Aresta M, Nobile CF, Albano VG, Forni E, & Manassero M (1975) New Nickel-Carbon Dioxide Complex - Synthesis, Properties, and Crystallographic Characterization of (Carbon Dioxide)-Bis(Tricyclohexylphosphine)Nickel. *J. Chem. Soc.-Chem. Commun.* (15):636-637.

4. Darensbourg DJ, Rokicki A, & Darensbourg MY (1981) Facile reduction of carbon dioxide by anionic Group 6b metal hydrides. Chemistry relevant to catalysis of the water-gas shift reaction. *J. Am. Chem. Soc.* 103(11):3223-3224.

5. Paik W, Andersen TN, & Eyring H (1969) Kinetic Studies of Electrolytic Reduction of Carbon Dioxide on Mercury Electrode. *Electrochim. Acta* 14(12):1217-&.

6. Meshitsuka S, Ichikawa M, & Tamaru K (1974) Electrocatalysis by Metal Phthalocyanines in Reduction of Carbon-Dioxide. *J. Chem. Soc.-Chem. Commun.* (5):158-159.

7. Fisher B & Eisenberg R (1980) Electrocatalytic Reduction of Carbon-Dioxide by Using Macrocycles of Nickel and Cobalt. *J. Am. Chem. Soc.* 102(24):7361-7363.

8. Collin JP, Jouaiti A, & Sauvage JP (1988) Electrocatalytic Properties of Ni(Cyclam)2+ and Ni2(Biscyclam)4+ with Respect to Co2 and H2o Reduction. *Inorg. Chem.* 27(11):1986-1990.

9. Beley M, Collin JP, Ruppert R, & Sauvage JP (1986) Electrocatalytic Reduction of Co2 by Ni Cyclam2+ in Water - Study of the Factors Affecting the Efficiency and the Selectivity of the Process. *J. Am. Chem. Soc.* 108(24):7461-7467.

10. Beley M, Collin JP, Ruppert R, & Sauvage JP (1984) Nickel(Ii) Cyclam - an Extremely Selective Electrocatalyst for Reduction of CO_2 in Water. *J. Chem. Soc.-Chem. Commun.* (19):1315-1316.

11. Balazs GB & Anson FC (1993) Effects of Co on the Electrocatalytic Activity of Ni (Cyclam)(2+) toward the Reduction of Co2. *J. Electroanal. Chem.* 361(1-2):149-157.

12. Hammouche M, Lexa D, Momenteau M, & Saveant JM (1991) Chemical catalysis of electrochemical reactions. Homogeneous catalysis of the electrochemical reduction of carbon dioxide by iron("0") porphyrins. Role of the addition of magnesium cations. *J. Am. Chem. Soc.* 113(22):8455-8466.

13. Bhugun I, Lexa D, & Saveant JM (1996) Catalysis of the electrochemical reduction of carbon dioxide by iron(O) porphyrins: Synergystic effect of weak Bronsted acids. *J. Am. Chem. Soc.* 118(7):1769-1776.

14. Grodkowski J, *et al.* (2002) Reduction of Cobalt and Iron Corroles and Catalyzed Reduction of CO_2. *J. Phys. Chem. A* 106(18):4772-4778.

15. Hawecker J, Lehn JM, & Ziessel R (1984) Electrocatalytic reduction of carbon dioxide mediated by $Re(bipy)(CO)_3Cl$ (bipy = 2,2'-bipyridine). *J. Chem. Soc.-Chem. Commun.* (6):328-330.

16. Ishida H, Tanaka K, & Tanaka T (1987) Electrochemical CO2 reduction catalyzed by ruthenium complexes [Ru(bpy)2(CO)2]2+ and [Ru(bpy)2(CO)Cl]+. Effect of pH on the formation of CO and HCOO. *Organometallics* 6(1):181-186.

17. Bolinger CM, Story N, Sullivan BP, & Meyer TJ (1988) Electrocatalytic reduction of carbon dioxide by 2,2'-bipyridine complexes of rhodium and iridium. *Inorg. Chem.* 27(25):4582-4587.

18. Bruce MRM, *et al.* (1988) Electrocatalytic reduction of carbon dioxide by associative activation. *Organometallics* 7(1):238-240.

19. Slater S & Wagenknecht JH (1984) Electrochemical reduction of carbon dioxide catalyzed by $Rh(diphos)_2Cl$. *J. Am. Chem. Soc.* 106(18):5367-5368.

20. DuBois DL, Miedaner A, & Haltiwanger RC (1991) Electrochemical reduction of carbon dioxide catalyzed by [Pd(triphosphine)(solvent)](BF4)2 complexes: synthetic and mechanistic studies. *J. Am. Chem. Soc.* 113(23):8753-8764.

21. Raebiger JW, *et al.* (2006) Electrochemical Reduction of CO_2 to CO Catalyzed by a Bimetallic Palladium Complex. *Organometallics* 25(14):3345-3351.

22. Dubois DL (1997) Development of transition metal phosphine complexes as electrocatalysts for CO_2 and CO reduction. *Comment. Inorg. Chem.* 19(5):307-325.

23. Sakaki S (1992) An ab initio MO/SD-CI study of model complexes of intermediates in electrochemical reduction of carbon dioxide catalyzed by NiCl2(cyclam). *J. Am. Chem. Soc.* 114(6):2055-2062.

24. Delaet DL, Delrosario R, Fanwick PE, & Kubiak CP (1987) Carbon-Dioxide Chemistry and Electrochemistry of a Binuclear Cradle Complex of Ni(0), Ni2(Mu-Cnme)(Cnme)2(Pph2ch2pph2)2. *J. Am. Chem. Soc.* 109(3):754-758.

25. Simon-Manso E & Kubiak CP (2005) Dinuclear nickel complexes as catalysts for electrochemical reduction of carbon dioxide. *Organometallics* 24(1):96-102.

26. Morgenstern DA, *et al.* (1996) A Class of Halide-Supported Trinuclear Nickel Clusters $[Ni_3(\mu_3\text{-}L)(\mu_3\text{-}X)(\mu_2\text{-}dppm)_3]^{n+}$ (L = I^-, Br^-, CO, CNR; X = I^-, Br^-; n = 0,1; dppm = $Ph_2PCH_2PPh_2$): Novel Physical Properties and the Fermi Resonance of Symmetric μ_3-η^1 Bound Isocyanide Ligands. *J. Am. Chem. Soc.* 118:2198-2207.

27. Wittrig RE, Washington J, Ferrence GM, & Kubiak CP (1998) IR Spectroelectrochemical and Electrochem. Kinetics of the Electrocatalytic Reduction of CO_2... *Comment. Inorg. Chem.* 270:111-117.

28. Ferrence GM, Fanwick PE, & Kubiak CP (1996) A Telluride Capped Trinuclear Nickel Cluster, $[Ni_3(\mu_3\text{-}Te)_2(\mu_2\text{-}dppm)_3]^n$ with Four Accessible Redox States (n = 1^-, 0, 1^+, 2^+). *J. Chem. Soc.-Chem. Commun.*:1575.

29. Haines RJ, Wittrig RE, & Kubiak CP (1994) Electrocatalytic Reduction of Carbon-Dioxide by the Binuclear Copper Complex [Cu-2(6-(Diphenylphosphino)-2,2'-Bipyridyl)(2)(Mecn)(2)][Pf6](2). *Inorg. Chem.* 33(21):4723-4728.

30. Jeoung JH & Dobbek H (2007) Carbon dioxide activation at the Ni,Fe-cluster of anaerobic carbon monoxide dehydrogenase. *Science* 318:1461-1464.

31. Dobbek H, Gremer L, Meyer O, & Huber R (1999) Crystal structure and mechanism of CO dehydrogenase, a molybdo iron-sulfur flavoprotein containing S-selanylcysteine. *P. Nat. Acad. Sci. USA* 96(16):8884-8889.

32. Dobbek H, Gremer L, Kiefersauer R, Huber R, & Meyer O (2002) Catalysis at a dinuclear [CuSMo(==O)OH] cluster in a CO dehydrogenase resolved at 1.1-angstrom resolution. *P. Nat. Acad. Sci. USA* 99(25):15971-15976.

33. Pickett CJ & Best SP (2005) Special issue on Hydrogenases. *Coordin. Chem. Rev.* 249(15-16):1517–1690.

34. Tezuka M, *et al.* (1982) Electroreduction of carbon dioxide catalyzed by iron-sulfur cluster compounds $[Fe_4S_4(SR)_4]_2$. *J. Am. Chem. Soc.* 104(24):6834-6836.

35. Takuma M, Ohki Y, & Tatsumi K (2005) Sulfido-Bridged Dinuclear Molybdenum-Copper Complexes Related to the Active Site of CO Dehydrogenase: $[(dithiolate)Mo(O)S_2Cu(SAr)]^{2-}$ (dithiolate = 1,2-$S_2C_6H_4$, 1,2-$S_2C_6H_2$-3,6-Cl_2, 1,2-$S_2C_2H_4$). *Inorg. Chem.* 44(17):6034-6043.

Chapter 2

Synthesis and characterization of 6,6'-(2,4,6-triisopropylphenyl)-2,2'-bipyridine (tripbipy) and its complexes of the late first row transition metals.

2.1 Introduction

Bipyridines are one of the most ubiquitous classes of ligands in coordination chemistry. Their ability to bind to a wide range of metal ions and stabilize different oxidation states has been extensively studied. The ability to tune both the electronics and sterics of bipyridine ligands *via* manipulation of substituents around the pyridyl rings has been a crucial foundation for their widespread applicability. Besides their abundant use in supramolecular,[1] nano materials,[2] macromolecular,[3] and photo-

physical chemistry[4], bipyridine ligands have been of interest because of their potential for ligand centered redox chemistry and metal-to-ligand-charge-transfer (MLCT) interactions.[5] Herein we report the synthesis of tripbipy (6,6'-(2,4,6-triisopropylphenyl)-2,2'-bipyridine), a new substituted bipyridine ligand, and the properties of the first coordination compounds based on this ligand.

Low coordinate metal centers are often invoked as catalytically active sites in a number of important catalytic systems, from enzymes to small molecule activation in organometallic complexes. In order to access a low coordinate active site, steric protection of the metal site is often necessary. The use of large substituents (mes = 2,4,6-trimethylphenyl, dipp = 2,6-diisopropylphenyl, trip = 2,4,6-triisopropylphenyl), in various blocking positions of carbenes,[6] arenes, and various other ligand frameworks have shown interesting structural motifs and reactivity.

Inspired by the work of Robinson,[7, 8] Power[9-12] and others using 2,4,6-triisopropylphenyl (trip) groups as large blocking groups, we have developed a synthesis of a chelating bipyridine with sterically encumbering trip groups in the 6,6' positions. Our first foray into the coordination chemistry of tripbipy is described

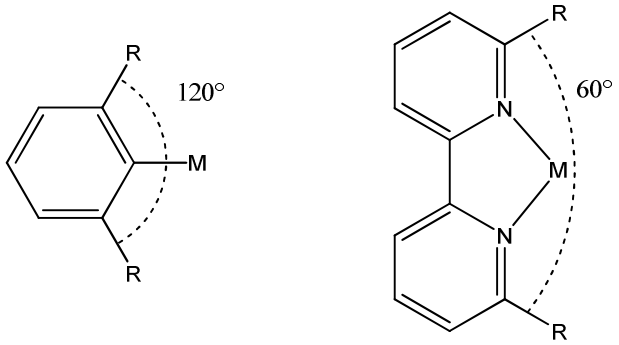

Figure 2.1 Idealized angles for steric protection of metal centers.

herein.

2.2 Results and discussion

The synthesis of 6,6'-(2,4,6-triisopropylphenyl)-2,2'-bipyridine (tripbipy) is summarized in Scheme 1. Tripbipy was readily synthesized by the Suzuki coupling of 2,4,6-triisopropyphenyl (trip) boronic acid and 6, 6'-dibromo-2, 2'-bipyridine in good yields (>75%). The resulting white solid was characterized by ^{1}H and ^{13}C NMR, combustion analysis, and mass spectrometry. The coupling proceeds in high yield despite the steric bulk of the isopropyl groups flanking the boronic acid. Tripbipy is sparingly soluble in chlorinated solvents (CH_2CL_2, $CHCl_3$), toluene, and THF.

Tripbipy functions as a sterically encumbering ligand for the late transition metal chlorides, (MCl_2; M = Fe, Co, Ni, Cu, Zn). The syntheses of all five complexes MCl_2tripbipy (M = Fe, Co, Ni, Cu, Zn) are accomplished by slow addition of ethanol solutions of the metal chloride hydrates to toluene solutions of tripbipy. The overall synthetic plan is depicted in Scheme 2. The subsequent heating and removal of water

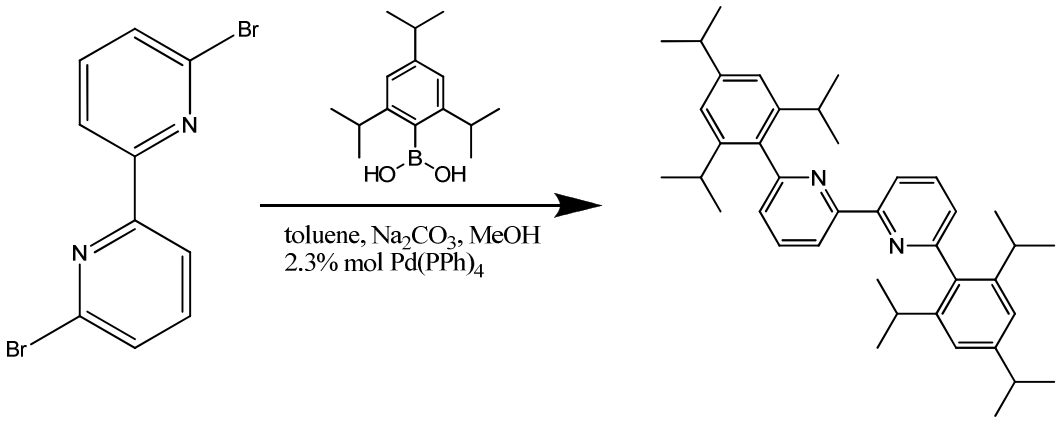

Scheme 2.1 Synthesis of tripbipy

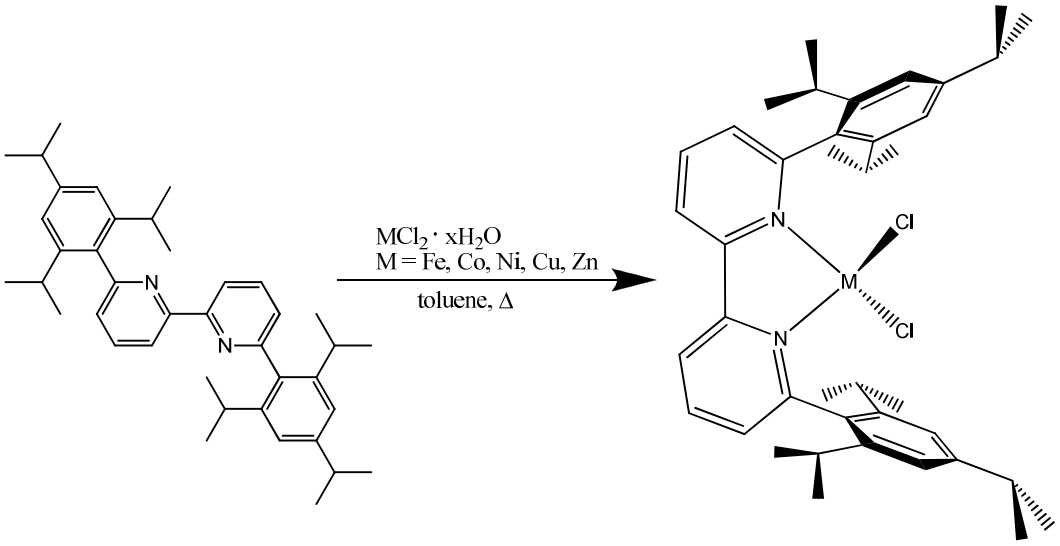

Scheme 2.2 Synthesis of MCl_2tripbipy

from the reaction resulted in the complex MCl_2tripbipy in high yields. MCl_2tripbipy complexes are stable to atmosphere; however, in solution they are susceptible to attack from nucleophiles (H_2O, ACN, THF, pyridine), resulting in varying degrees of ligand dissociation from the metal as verified by ^{1}H NMR, color change, and recovery of free ligand.

2.2.1 X-ray Crystallography

The MCl_2tripbipy complexes (M = Fe, Co, Ni, Cu, Zn) were readily crystallized by vapor diffusion of pentane or diethyl ether into solutions of the complex in chloroform.

FeCl2tripbipy. The molecular structure of $FeCl_2$tripbipy was determined by single crystal X-ray diffraction and crystallizes in the space group P $2_1/c$ with one solvent molecule ($CHCl_3$). The structure shows a distorted tetrahedral coordination environment around the iron center (Figure 2.2). Calculation of Houser's τ_4 four-

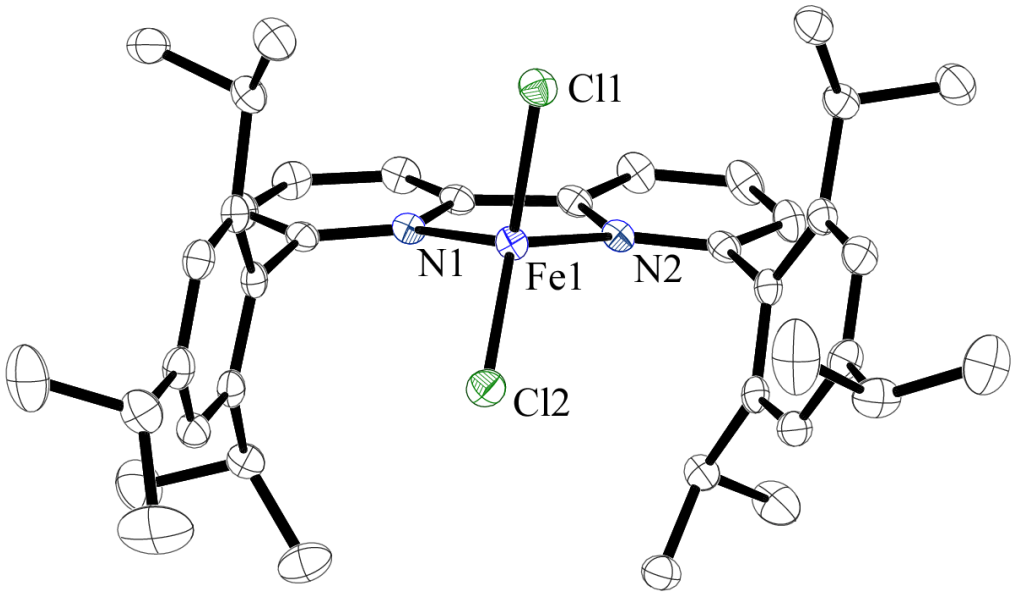

Figure 2.2 Molecular structure of $FeCl_2$tripbipy, hydrogen atoms and solvent of crystallization removed for clarity.

coordinate geometry index[13] gives a value of 0.83 which suggests that the four coordinate geometry present is closely related to a distorted trigonal pyramidal structure (idealized trigonal pyramid = 0.85). One of the triisopropylphenyl groups is nearly orthogonal to the bipyridine plane, with a torsion angle of 86.69(4)°. The other trip group is inclined at an angle of 69.49(4)° relative to the plane of the bipy ring. This is most likely caused by crystal packing effects, and a C-H – π interaction between the solvent of crystallization and three of the carbons in the benzene ring of the trip group (C15 - H41, 2.772Å). The bite angle of the bipyridine is 77.24(6)° which is similar to the reported structures of $FeCl_2$(6,6'dimethyl-2,2'bipyidine) which are 77.50(10)° and 78.12(8)° for the two polymorphs.[14] The difference in Fe-Cl distances (Fe1-Cl1 = 2.2526(5) Å, Fe1-Cl2 = 2.2154(5) Å) and Fe-N (Fe1-N1 = 2.1217(15), Fe1-N2 = 2.1318(14) Å) are also believed to be indicative of crystal

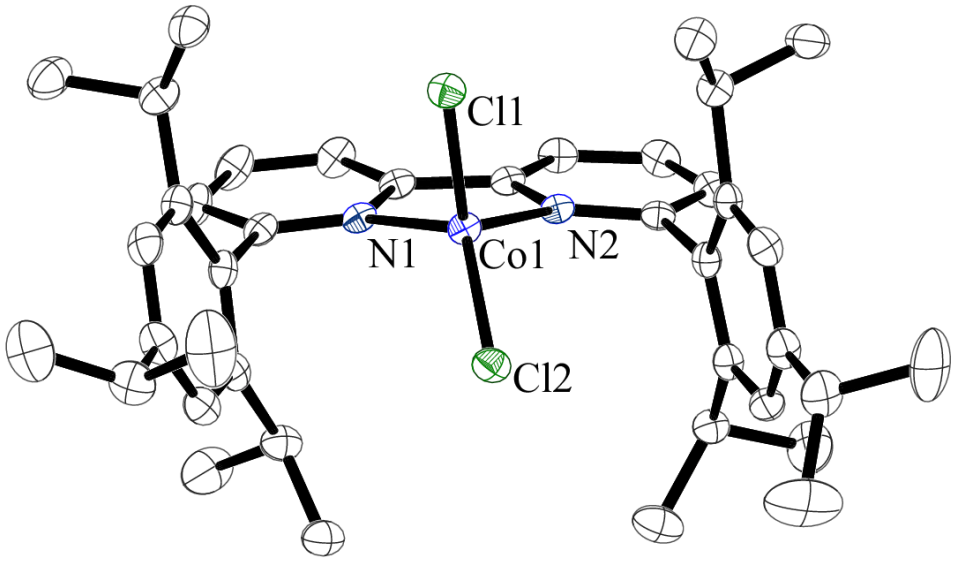

Figure 2.3 Molecular structure of $CoCl_2$tripbipy, hydrogen atoms and solvent of crystallization removed for clarity.

packing effects rather than a Jahn-Teller distortion, as comparable distortions are seen with the structurally similar diamagnetic $ZnCl_2$tripbipy complex (*vide infra*).

$CoCl_2$tripbipy. The cobalt complex was prepared in similar manner to $FeCl_2$tripbipy and crystallizes in the same space group P $2_1/c$ and an isomorphous unit cell with one solvent molecule of chloroform. The complex is structurally similar to $FeCl_2$tripbipy (Figure 2.3), in that there is one trip group close to orthogonal (87.01(7)°) to the plane of the bipyridine, and the other that is distorted (71.65(8)°) again, presumably from a C-H – π interaction from the chloroform (C15 – H41 = 2.771Å). The bite angle of the chelating pyridine is (N1-Co1-N2) 80.64(10)° and is smaller than most Co^{2+} structures reported,[15] but is larger than typical Co^{3+} bipyridine complexes. Again, due to crystal packing effects, we see a slight difference in bond lengths for the Co-Cl and Co-N bonds (Table 1), similar to the trend observed for

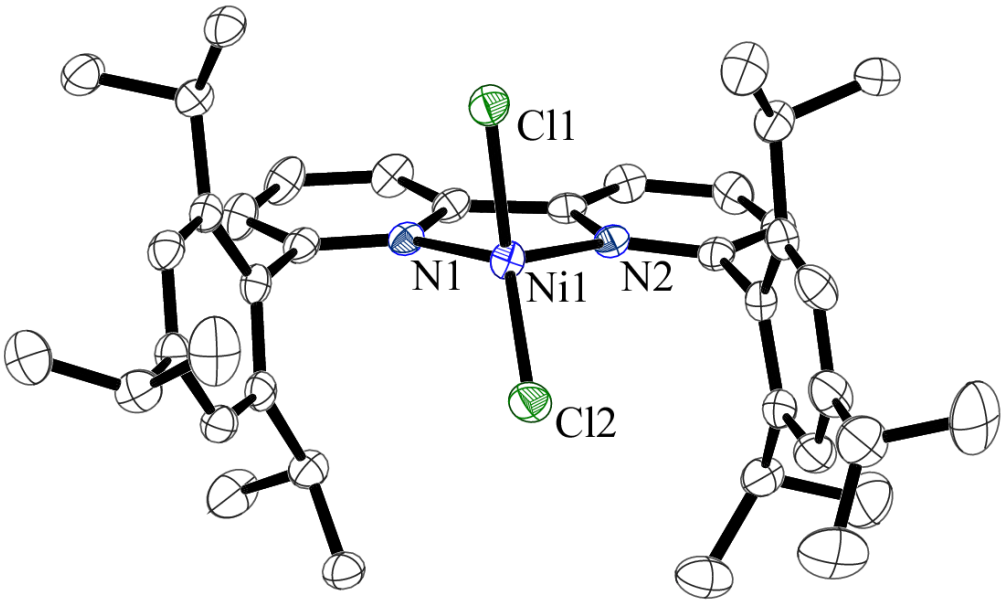

Figure 2.4 Molecular structure of $NiCl_2$tripbipy, hydrogen atoms and solvent of crystallization removed for clarity.

$FeCl_2$tripbipy. Using the Houser τ_4 parameter we obtain a value of 0.86 again suggesting a distorted trigonal pyramid geometry in the solid state.

$NiCl_2$tripbipy. The nickel complex crystallizes in the same space group, P $2_1/c$, as the homologous iron (II) and cobalt (II) complexes, in an isomorphous unit cell that contains one solvent molecule ($CHCl_3$). As with the previous two compounds, one of the triispropylphenyl groups is nearly orthogonal to the bipyridine plane, and the other significantly distorted (86.96(7)° vs. 71.20(7)°). The bite angle of the bipyridine is 81.60(9) °, which is smaller than most four-coordinate bipyridine structures found in the Cambridge database. This may arise from the torsion of the complex toward a square planar geometry or a pseudo Jahn-Teller distortion. The τ_4

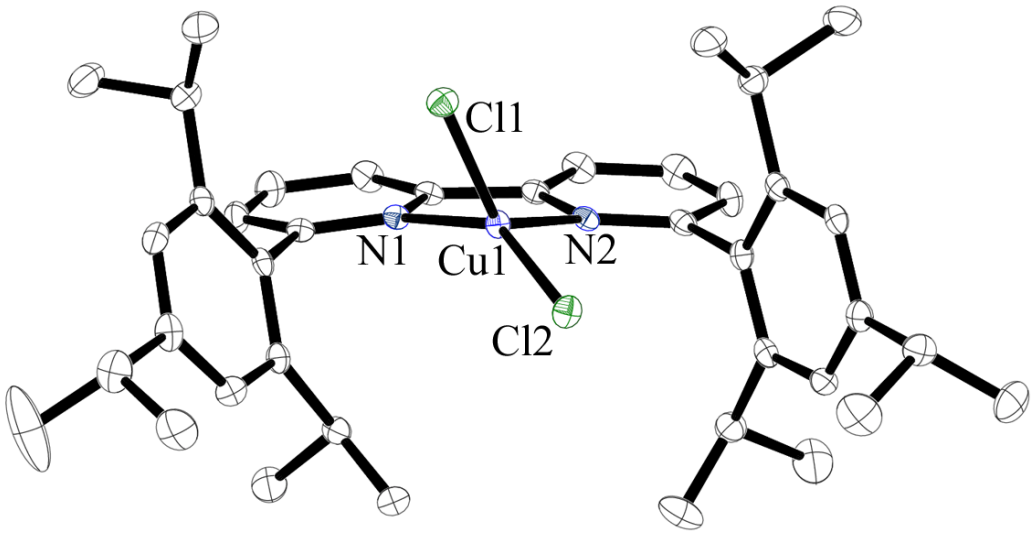

Figure 2.5 Molecular structure of $CuCl_2$tripbipy, hydrogen atoms and solvents of crystallization removed for clarity.

value of 0.79 shows a stronger distortion from the tetrahedral geometry than is seen in $FeCl_2$tripbipy, $CoCl_2$tripBipy and $ZnCl_2$tripbipy (Table 2.1).

$CuCl_2$tripbipy. The copper complex is the only compound in this series that did not crystallize in the space group P 2_1/c. Rather it crystallized in the space group P 2_1 2_1 2_1 with two independent solvent molecules ($CHCl_3$). The geometry around the metal center is severely distorted, τ_4 = 0.60. We attribute this distortion away from tetrahedral geometry to a strong pseudo Jahn-Teller distortion which is not uncommon with Cu^{2+} d^9 complexes.[16] We still see the orthogonal and canted dispositions of the two trip groups that are seen in the structures of the iron, cobalt, and nickel complexes, however, there is no solvent molecule within close contact of the trip group to be the sole cause of the distortion. This can be attributed to crystal packing effects, and the

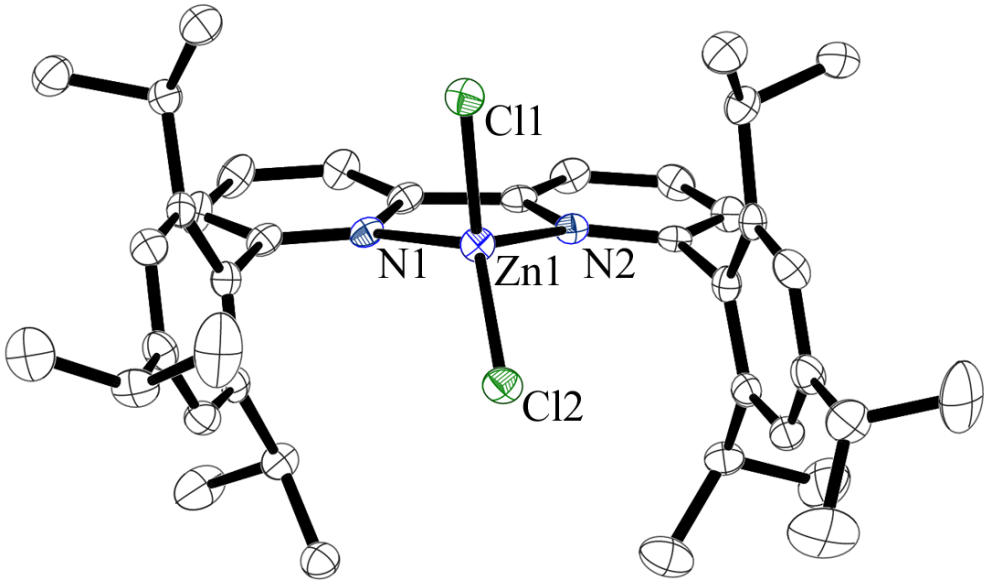

Figure 2.6 Molecular structure of $ZnCl_2$tripbipy, hydrogen atoms and solvent of crystallization removed for clarity.

steric repulsion of the chloride due to an elongation of the Cu – Cl bond arising from the pseudo Jahn-Teller distortion. A Houser τ_4 value of 0.60 is severely distorted from the traditional four-coordinate geometries, and its value lies closer to that of a seesaw (0.65). However, close inspection of the geometry suggests that the structure most closely resembles an intermediate geometry between tetrahedral and square planar, where the steric bulk of the trip groups impedes the transition to square planar (Figure 2.5).

$ZnCl_2$tripbipy. The zinc complex crystallizes in same space group P $2_1/c$ and isomorphous unit cell with one solvent of crystallization as the iron, cobalt, and nickel complexes. As with the previous metals we see a distortion in one of the trip groups while the other is nearly normal to the bipyridine ligand plane (70.96(8)° vs.

Table 2.1 Selected Bond Distances (Å), Angles (deg) and τ_4 geometry index[13] for MCl_2tripbipy complexes

	Fe	Co	Ni	Cu	Zn
M - N1	2.1318(14)	2.0558(25)	2.0173(21)	1.9811(23)	2.0798(26)
M - N2	2.1217(15)	2.0638(25)	2.0287(21)	2.0590(24)	2.0932(27)
M - Cl1	2.2526(5)	2.2348(9)	2.2419(11)	2.2380(9)	2.2298(9)
M - Cl2	2.2154(5)	2.1992(9)	2.1836(11)	2.1738(9)	2.1833(9)
N1 - M - N2	77.24(6)	80.64(10)	81.60(9)	81.73(10)	79.72(10)
Cl1 - M - N1	112.31(4)	105.55(7)	98.34(7)	96.36(7)	104.10(8)
Cl1 - M - N2	103.13(4)	113.28(7)	107.17(7)	128.66(7)	111.54(8)
Cl1 - M - Cl2	119.19(2)	114.55(3)	121.31(5)	100.22(4)	117.71(4)
Cl2 - M - N1	114.23(4)	123.47(8)	126.76(7)	146.60(7)	122.92(8)
Cl2 - M - N2	123.41(4)	114.95(7)	114.06(7)	109.02(7)	114.79(8)
τ_4	0.83	0.86	0.79	0.60	0.85

86.94(7)°). As in the related complexes, this is attributed to the solvent C-H bond being within 2.777Å (C15-H41) of the π system of the distorted trip group, which is within the range for a C-H – π interaction.[17] However, in solution the molecule shows C_{2v} symmetry from the ^{13}C and ^{1}H NMR, suggesting that the distortion from tetrahedral geometry arises from crystal packing effects rather than an intrinsic electronic or steric property.

Summary of Structures. The tripbipy complexes of iron, cobalt, nickel, and zinc all crystallize in the same space group (P 2_1/c) and in an almost identical unit cell ($\boldsymbol{a}$ = 8.96(5), $\boldsymbol{b}$ = 28.14(7), $\boldsymbol{c}$ = 16.78(8), $\boldsymbol{\alpha}$ = 90, $\boldsymbol{\beta}$ = 99.8(3), $\boldsymbol{\gamma}$ = 90), where the standard deviations are those for the mean cell constants for the four structures. These four complexes are nearly isostructural, with only minimal changes around the metal core. The $CuCl_2$tripbipy complex, on the other hand, crystallized in the space group (P 2_1 2_1 2_1) with two solvent molecules of crystallization, and its structure is quite different from the iron, cobalt, nickel, and zinc members of the series. The bulk of the trip groups has effectively controlled the coordination environment around the metal

center in both coordination number, and geometry. This is in contrast to the more prevalent metal halide complexes in which there is coordination of two or three bipyridines to the metal center. Previously the MCl_2bipy (M=Fe, Co, Ni) complexes have been obtained through thermal decomposition of the parent tris-bipyridine complex, and have been shown to consist of polymeric chains containing six-coordinate metal centers.[18, 19]

In our case, the tripbipy ligand appears to be an enforcer of tetrahedral coordination geometries, precluding six-coordination in the cases of iron (II) and cobalt (II), and a square planar geometry in the cases of nickel (II) and copper (II). By far the majority of nickel (II) bipy four-coordinate complexes are square planar.[20] By using bipyridine as a backbone to rigidly hold the trip groups near the metal center we are able to narrow the open space between the trip groups. This can be quantified as the angle defined between the two trip groups and the metal center. In the $ZnCl_2$tripbipy complex, this angle is 42.72(12)°. In comparison, substituted 2,6-bisphenylbenzene (*m*-terphenyl) complexes present an angle between the two flanking phenyl group planes of nearly 120°.[7, 9-12] A comparison of the angles between the substituents of a 2, 6 - phenyl type ligand vs. a 6, 6'- bipy ligand is presented in Figure 2.1. This protection of the metal center by tripbipy may allow for the stabilization of geometries and coordination environments unseen with substituted terphenyl groups.

2.2.2 Electronic Spectra

The electronic spectra of the title compounds in dichloromethane are shown in Figure 2.7. All compounds show a ligand based $\pi \rightarrow \pi^*$ transition centered near

310nm (= 11000-17000 $M^{-1}cm^{-1}$). The Fe complex shows a single d-d transition at 505nm (= 260 $M^{-1}cm^{-1}$) which we assign to the $^5E_2 \rightarrow {}^5T_2$ transition, consistent with a monomeric tetrahedral iron center. Here, the irreducible representations and states are taken from Td symmetry, not the structurally more precise C_{2v} symmetry as an approximation. This is in contrast to what is seen in $FeCl_2$bipy which shows transitions corresponding to polymeric chains in C_{2v} symmetry.[19]

The $CoCl_2$tripbipy complex shows three distinct bands at 690, 640, 580nm (= 310, 210, 230 $M^{-1}cm^{-1}$) and are assigned to the $^4A_2 \rightarrow {}^4T_1$ transition. The fine structure of this transition is attributed to spin-orbit coupling of the *T* state. $NiCl_2$tripbipy shows a number of peaks in the regions of 480-610nm and 845-1280nm (Figure 2.8). These are attributed to the $^3T_1 \rightarrow {}^3A_2$ and $^3T_1 \rightarrow {}^3T_2$ transitions respectively. Again these are the transitions are taken from Td symmetry and compare favorably to the spectra of tetrahedral $NiCl_4^{2-}$.[21]

The copper complex shows a MLCT band at 450nm (= 860 $M^{-1}cm^{-1}$) and a broad d-d transition centered at 890nm (= 100 $M^{-1}cm^{-1}$) and contains the transitions expected for $^2E_2 \rightarrow {}^2T_2$. This matches well with the literature for monomeric Cu^{II} complexes.[22-24] As expected $ZnCl_2$tripbipy shows no d-d transitions, only a ligand based $\pi - \pi^*$ transition at 310nm (= 17000 $M^{-1}cm^{-1}$)

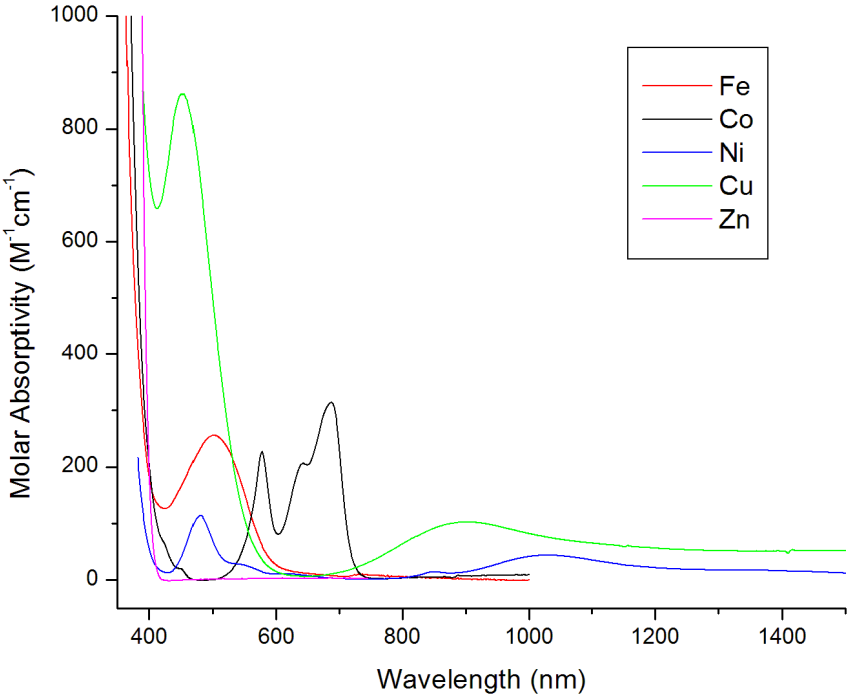

Figure 2.7 Near-infrared-visible spectra of MCl_2tripbipy complexes

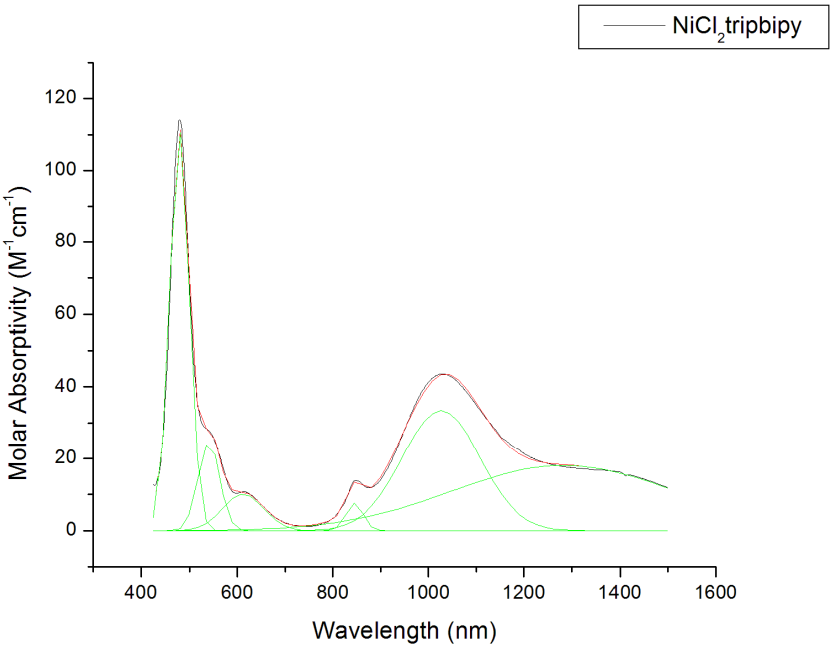

Figure 2.8 Near-infrared-visible spectra of $NiCl_2$tripbipy and Gaussian fit.

2.2.3 Magnetic Studies:

To further characterize the properties of the new tripbipy complexes, magnetic data were used to confirm the number of unpaired spins within each complex. Magnetic data of the MCl_2tripbipy complexes at 4T is shown in Figure 2.9. For $FeCl_2$tripbipy the $\chi_M T$ at 300K (3.56 cm^3 mol^{-1} K) is consistent with a tetrahedral Fe^{2+} center with an S = 2 ground state. This value is nearly constant through the range of 300-100 K and increases upon cooling to reach a maximum value of 4.27 cm^3 mol^{-1} K, and then decreases below 18 K. This behavior suggests weak intermolecular coupling at lower temperatures, with the decrease of $\chi_M T$ below 18 K being attributed to zero-

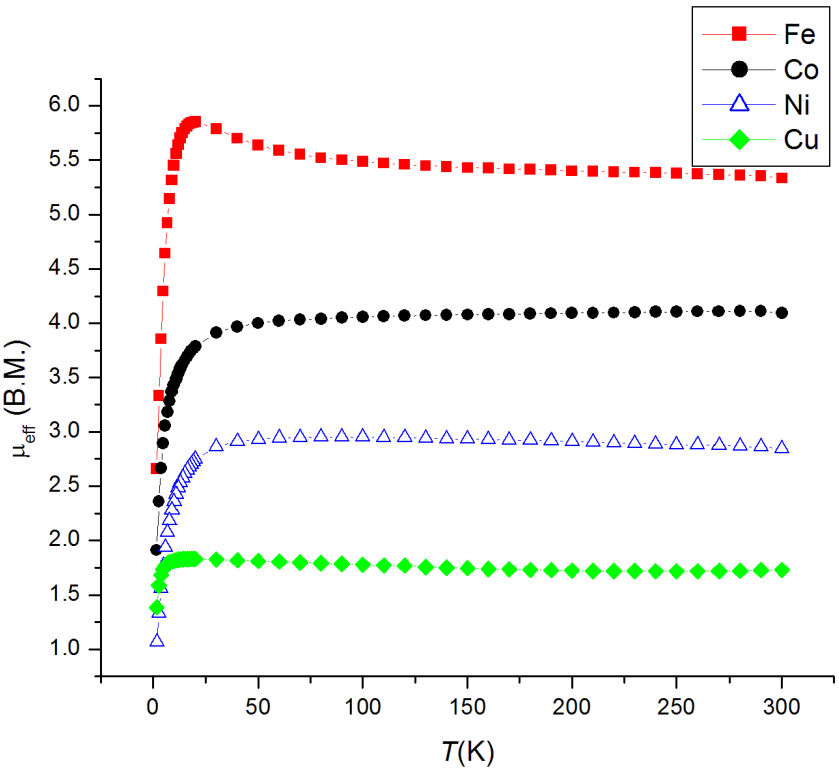

Figure 2.9 Plot of μ_{eff} vs. T for MCl_2tripbipy, M = Fe, Co, Ni, Cu.

field splitting.

The $\chi_M T$ of $CoCl_2$tripbipy at 300K (2.10 cm^3 mol^{-1} K) supports the assignment of a high spin tetrahedral Co^{2+} center (S = 3/2). Unlike the $FeCl_2$tripbipy complex, we do not see any long range coupling at lower temperatures. The $\chi_M T$ stays nearly constant from 300-40 K and then below 40K starts decreasing presumably from the zero-field splitting. The $\chi_M T$ at 300 K for $NiCl_2$tripbipy at 4T is 1.01 cm^3 mol^{-1} K and is consistent with a Ni^{2+} center with 2 unpaired electrons giving a S=1 ground state. As with the $CoCl_2$tripbipy system we do not see magnetic coupling at lower temperatures and similarly we see $\chi_M T$ staying relatively constant until the temperature is below 40 K. The magnetic response of $CuCl_2$tripbipy gives a $\chi_M T$ at 300K of 0.37 cm^3 mol^{-1} K and stays relatively constant over the entire temperature range; it is not until below 5K that we begin to see the value decrease.

The μ_{eff} of the MCl_2tripbipy complexes compare favorably with the spin only values and due to the C_{2v} symmetry of the complexes we do not see affects due to spin-orbit coupling. The magnetics differ from reported values of MCl_2bipy complexes. $FeCl_2$bipy has been shown to be a ferromagnet with a curie temp of ~4K,[19] while in the case of $FeCl_2$tripbipy, the metal centers are magnetically dilute from the large separation in the lattice (*d*(Fe – Fe) 8.6Å) imposed by the bulky bipyridyl ligand. With the nickel and cobalt MCl_2bipy analogs, a high μ_{eff} value has been reported (α-Co - 5.10 B.M., Ni - 3.38 B.M.), consistent with octahedral chloro-bridged chains.[18] In a similar system $NiI_2(PPh_3)$shows values close to the spin only value (2.9 B.M.) arising from distortion of the molecule away from tetrahedral symmetry.[25]

2.2.4 Electrochemistry

Electrochemistry of $FeCl_2$tripbipy in CH_2Cl_2 shows a reversible $1e^-$ oxidation at 0.48V vs. Fc/Fc^+ corresponding to the Fe^{II}/Fe^{III} couple and an irreversible $2e^-$ reduction at -1.87V vs. Fc/Fc^+ that is tentatively assigned to the Fe^{II}/Fe^0 couple. The number of electrons transferred was determined by differential pulse voltametry with a known concentration of an internal standard (Fc). Controlled potential electrolysis experiments were inconclusive due to fouling of the electrode presumably from decomposition of the complex. Sample voltamograms can be found in the appendix. $CoCl_2$tripbipy shows an irreversible $2e^-$ reduction at -1.68V vs. Fc/Fc^+. No oxidation to Co^{III} was observed out to +1.2V vs. Fc/Fc^+ in CH_2CL_2. As with $FeCl_2$tripbipy, we assign this as a metal-based reduction. Similarly $NiCl_2$tripbipy shows an irreversible reduction at -1.43 vs. Fc/Fc^+. This is tentatively assigned to the Ni^{II}/Ni^0 couple.

Electrochemistry of $CuCl_2$tripbipy in CH_2Cl_2 at slow scan rates (0.025V/s) shows a single reversible reduction at 0.05V vs Fc/Fc^+. At faster scan rates (>0.05V/s) the voltamograms become more convoluted, which may be due to a coupled chemical reaction with the solvent and or electrolyte or a disproportionation. $CuCl_2$tripbipy will oxidize Fc to Fc^+ as evident in the CV's and the color change of the solution upon addition of ferrocene.

Electrochemistry of $ZnCl_2$tripbipy in CH_2CL_2 shows a reversible ligand based reduction at -1.94V vs. Fc/Fc^+. Due to the filled d orbitals of zinc, and the reversibility of the reduction, it suggests that the reduction is ligand-based. This also lends credence to the assignment of the reductions seen in the previous Fe, Co, and Ni complexes as metal, not ligand based.

2.2.5 EPR

In order to further probe the electronic structure of $CuCl_2$tripbipy, EPR was performed in a toluene solution at room temperature and in a frozen glass at X band frequencies. The isotropic g value in fluid solution is 2.044 with an apparent A value of 222 MHz, which is consistent with coupling to ^{65,63}Cu nuclei with S=3/2. In a frozen glass at 110K, the spectrum becomes more convoluted, however, it gives $g_{\perp}$, and $g_{\parallel}$ values near 2.2 and 2.1 respectively which suggests a tetrahedral compression resulting in the free electron residing in a d_{xy} orbital. This is consistent with the shorter than average Cu-Cl bonds and strongly distorted tetrahedral molecular geometry seen in the X-ray diffraction study. The hyperfine coupling to the Cu nucleus was unresolved due to overlap of the $g_{\perp}$, and $g_{\parallel}$ transitions. EPR spectra and simulations can be found in the appendix.

2.3 Conclusions

Tripbipy has been shown to be an effective ligand for control of the coordination number and geometry of five late first row transition metals. Coordination to metal chlorides (M=Fe, Co, Ni, Cu, Zn) gives pseudo-tetrahedral coordination environments. Tripbipy can be regarded as an “enforcer” of tetrahedral geometries when alternate octahedral or square planar geometries are available. Tripbipy, through its large flanking arms and narrow coordination region between them is able to protect the metal centers to which it is attached. Tripbipy does show a tendency to be labilized in the presence of other nucleophilic ligands. We anticipate

that tripbipy will find important applications in stabilizing coordinativly unsaturated species in low oxidation states.

Acknowledgment. The authors wish to thank Dr. Antonio DiPasquale at the UCSD Crystallography Facility as well as Prof. Michael Tauber and Hannah Shafaat for their assistance with the EPR measurements.

2.4 Experimental

General Considerations.

6,6'-dibromo-2,2'-bipyridine was synthesized according to literature procedures,[26] all other chemicals were purchased from commercial sources and used as received. Toluene and methylene chloride were sparged with argon and dried over basic alumina with a custom dry solvent system. $CHCl_3$ was filtered through activated basic alumina and distilled over P_2O_5. Magnetic measurements were collected on a Quantum Design MPMS 5 SQUID magnetometer. The susceptibility measurements were performed in the 1.8-300 K temperature range with an applied field of 4 Tesla. Data were corrected for diamagnetic contributions from both the sample holder and the tripbipy ligand using Pascal's constants. Electrochemistry was carried out using a BAS epsilon workstation using a glassy carbon working electrode, Pt wire counter, and Ag/AgCl pseudo-reference electrode using tetrabutylammonium hexafluorophosphate (TBAH) as the supporting electrolyte. All solutions were referenced to Fc/Fc^+ using an internal standard. ^1H NMR were obtained using a Jeol ECA-500 spectrometer. ^{13}C NMR were obtained using Varian Mercury 400 and 500 spectrometers. All NMR spectra were referenced to internal solvent peaks.

UV/VIS/NIR spectra were collected on a Shimadzu UV-3600 in dichloromethane. Combustion analysis was performed by Midwest MicroLab, LLC, Indianapolis, IN.

Crystallographic Structure Determinations. Single-crystal X-ray structure determinations were carried out at 150(2) K on either a Bruker P4 or Platform Diffractometer using Mo Kα radiation (λ = 0.71073 Å) in conjunction with a Bruker APEX detector. All structures were solved by direct methods using SHELXS-97 and refined with full-matrix least-squares procedures using SHELXL-97.[27] Crystallographic data collection and refinement information can be found in the appendix.

Synthesis of tripbipy (1). To a toluene (250ml) solution of 6,6'-dibromo-2,2'-bipyridine (2g, 6.37 mmol) an excess of 2,4,6-triisopropylbenzene boronic acid (4g, 16.1 mmol) suspended in 30ml of methanol was added. 30ml of 2M sodium carbonate and 175mg of $Pd(PPh_3)_4$ (2.3% mol cat.) were added and refluxed for 72h in air. After cooling the layers were separated and the organic layer was washed with brine (2x100 ml), and the aqueous layer washed with chloroform (2x 100ml). The organic fractions were combined, and dried under rotary evaporation. The crude solid was then dissolved in minimal amount of hot chloroform, filtered, and crashed out with methanol. The white precipitate was filtered and dried in vacuo at 80°C. Yield: 2.78g, 4.97 mmol, 78.0%. ^{1}H NMR (500 MHz, CH_2Cl_2, 20°C): δ = 8.41 (d, 2H, J = 8 Hz), 7.81 (t, 2H, J = 8 Hz), 7.27 (d, 2H, J = 8 Hz), 7.13 (s, 4H), 2.97 (sep., 2H, J = 7 Hz), 2.60 (sep., 4H, J = 7 Hz), 1.32 (d, 12H, J = 7 Hz), 1.14 (d, 12H, J = 6 Hz), 1.12 (d, 12H, J = 6 Hz). ^{13}C NMR (125.1 MHz, $CHCl_3$, 20°C): δ = 159.3, 156.0, 148.7, 146.5,

136.9, 136.4, 125.1, 120.9, 119.2, 34.6, 30.5, 24.5, 24.3, 24.2 ppm. Anal. Calcd for $C_{40}H_{52}N_2$: C, 85.66; H, 9.35; N, 4.99. Found: C, 85.41; H, 9.44; N, 5.04.

Synthesis of MCl_2tripbipy. To a solution of tripbipy in toluene (200mg, 0.357mmol, 25ml), 1 eq. of the corresponding metal chloride or chloride hydrate in 3ml EtOH was added slowly and refluxed for 3 hours. The condenser was then removed and the solution was reduced to 10ml under heat and N_2. After cooling, 50 ml of pentane was added to the solution and cooled to -20°C overnight. Crystals were filtered and washed with pentane and dried in vacuo.

$FeCl_2$tripbipy: 70.9mg $FeCl_2 \cdot 4H_2O$, 0.357mmol. Yield 218mg, 0.318mmol, 89.1%. Anal. Calcd for $C_{40}H_{52}N_2Cl_2Fe$: C, 69.87; H, 7.62; N, 4.07. Found: C, 68.68; H, 7.75; N, 3.82. Crystals suitable for X-ray diffraction were grown from vapor diffusion of pentane into chloroform.

$CoCl_2$tripbipy: 46.3mg $CoCl_2$, 0.357mmol. Yield 202mg, 0.292mmol, 82.0%. Anal. Calcd for $C_{40}H_{52}N_2Cl_2Co$: C, 69.56; H, 7.59; N, 4.06. Found: C, 68.73; H, 7.53; N, 4.04. Crystals suitable for X-ray diffraction were grown from the vapor diffusion of Et_2O into chloroform.

$NiCl_2$tripbipy: 84.8mg $NiCl_2 \cdot 6H_2O$, 0.357mmol. Yield 198mg, 0.287mmol, 80.4%. Recrystalized from $CHCl_3$/Pentane as the chloroform solvate. Anal. Calcd for $C_{40}H_{52}N_2Cl_2Ni \cdot CHCl_3$: C, 60.81; H, 6.60; N, 3.46. Found: C, 61.23; H, 6.76; N, 3.48. Crystals suitable for X-ray diffraction were grown from the vapor diffusion of pentane into chloroform.

$CuCl_2$tripbipy: 60.8mg $CuCl_2 \cdot 2H_2O$, 0.357mmol. Yield 247mg, 0.348mmol, 97.5%. Orange-red crystals, Anal. Calcd for $C_{40}H_{52}N_2Cl_2Cu$: C, 69.10; H, 7.54; N, 4.03. Found: C, 68.19; H, 7.52; N, 3.99. Crystals suitable for X-ray diffraction were grown from the vapor diffusion of Et_2O into chloroform.

$ZnCl_2$tripbipy: 48.6mg $ZnCl_2$, 0.357mmol. Yield 235mg, 0.337mmol, 94.5%. ^1H NMR (500.2 MHz, CH_2Cl_2, 20°C): δ = 8.31 (d, 2H, J = 7 Hz), 8.16 (t, 2H, J = 8 Hz), 7.66 (d, 2H, J = 7 Hz), 7.03 (s, 4H), 2.86 (sep., 2H, J = 7 Hz), 2.39 (sep., 4H, J = 7 Hz), 1.29 (d, 12H, J = 7 Hz), 1.22 (d, 12H, J = 7 Hz), 0.95 (d, 12H, J = 7 Hz). ^{13}C NMR (100.6 MHz, $CHCl_3$, 20°C): δ = 162.0, 150.7, 149.6, 146.7, 139.8, 131.6, 129.7, 121.0, 120.5, 34.5, 26.1, 24.1, 22.7 ppm. Anal. Calcd for $C_{40}H_{52}N_2Cl_2Zn$: C, 68.91; H, 7.52; N, 4.02. Found: C, 68.80; H, 7.49; N, 4.07. Crystals suitable for X-ray diffraction were grown from the vapor diffusion of Et_2O into chloroform.

Note: Much of the material for this chapter comes directly from a manuscript entitled “Synthesis and characterization of 6,6’-(2,4,6-triisopropylphenyl)-2,2’-bipyridine (tripbipy) and its complexes of the late first row transition metals.” by Eric E. Benson, Arnold L. Rheingold, and Clifford P. Kubiak, which has been published in *Inorganic Chemistry*, **2010**, *49* (4), 1458-1464. http://dx.doi.org/10.1021/ic9016382. The dissertation author is the primary author of this manuscript.

2.5 References

1. Ye B-H, Tong M-L, & Chen X-M (2005) Metal-organic molecular architectures with 2,2'-bipyridyl-like and carboxylate ligands. *Coordin. Chem. Rev.* 249(5-6):545-565.

2. Fletcher AJ, *et al.* (2001) Adsorption Dynamics of Gases and Vapors on the Nanoporous Metal Organic Framework Material Ni_2(4,4'-Bipyridine)$_3$(NO_3)$_4$: Guest Modification of Host Sorption Behavior. *J. Am. Chem. Soc.* 123(41):10001-10011.

3. Ulrich S. Schubert CE (2002) Macromolecules Containing Bipyridine and Terpyridine Metal Complexes: Towards Metallosupramolecular Polymers. *Angew. Chem. Int. Edit.* 41(16):2892-2926.

4. Shan BZ, Zhao Q, Goswami N, Eichhorn* DM, & Rillema* DP (2001) Structure, NMR and other physical and photophysical properties of ruthenium(II) complexes containing the 3,3'-dicarboxyl-2,2'-bipyridine ligand. *Coordin. Chem. Rev.* 211(1):117-144.

5. Sullivan BP, Bolinger CM, Conrad D, Vining WJ, & Meyer TJ (1985) One-Electron and 2-Electron Pathways in the Electrocatalytic Reduction of CO_2 by Fac-Re(2,2'-Bipyridine)(CO)$_3$Cl. *J. Chem. Soc.-Chem. Commun.* (20):1414-1415.

6. Wang YZ, *et al.* (2008) Carbene-Stabilized Diphosphorus. *J. Am. Chem. Soc.* 130(45):14970-+.

7. Wang Y & Robinson GH (2007) Organometallics of the Group 13 M-M Bond (M = Al, Ga, In) and the Concept of Metalloaromaticity. *Organometallics* 26(1):2-11.

8. Su J, Li X-W, Crittendon RC, & Robinson GH (1997) How Short is a -Ga-Ga- Triple Bond? Synthesis and Molecular Structure of Na_2[Mes*$_2$$C_6H_3$-Ga-Ga-$C_6H_3$Mes*$_2$] (Mes* = 2,4,6-i-Pr$_3$$C_6H_2$): The First Gallyne. *J. Am. Chem. Soc.* 119(23):5471-5472.

9. Ni C, Ellis BD, Fettinger JC, Long GJ, & Power PP (2008) Univalent transition metal complexes of arenes stabilized by a bulky terphenyl ligand: differences in the stability of Cr(I), Mn(I) or Fe(I) complexes. *Chem. Commun.* (8):1014-1016.

10. Wolf R, *et al.* (2007) Substituent effects in formally quintuple-bonded ArCrCrAr compounds (Ar = terphenyl) and related species. *Inorg. Chem.* 46(26):11277-11290.

11. Hardman NJ, Wright RJ, Phillips AD, & Power PP (2003) Structures, bonding, and reaction chemistry of the neutral organogallium(I) compounds (GaAr)(n) (n=1 or 2) (Ar = terphenyl or related ligand): An experimental investigation of Ga-Ga multiple bonding. *J. Am. Chem. Soc.* 125(9):2667-2679.

12. Twamley B, Sofield CD, Olmstead MM, & Power PP (1999) Homologous Series of Heavier Element Dipnictenes 2,6-$Ar_2H_3C_6E$=EC_6H_3-2,6-Ar_2 (E = P, As, Sb, Bi; Ar = Mes = C_6H_2-2,4,6-Me_3; or Trip = C_6H_2-2,4,6-iPr_3) Stabilized by m-Terphenyl Ligands. *J. Am. Chem. Soc.* 121(14):3357-3367.

13. Yang L, Powell DR, & Houser RP (2007) Structural variation in copper(I) complexes with pyridylmethylamide ligands: structural analysis with a new four-coordinate geometry index, tau(4). *Dalton T.*:955-964.

14. Chan BCK & Baird MC (2004) Reactions of 6,6'-dimethyl-2,2'-bipyridyl with iron(II) in aqueous and non-aqueous media. *Inorg. Chim. Acta* 357(9):2776-2782.

15. Carsten B, Margareta Z, & Daniel B (1990) Optically Active Bipyridines in Asymmetric Catalysis. *Angew. Chem. Int. Edit.* 29(2):205-207.

16. Reinen D, Atanasov M, Nikolov G, & Steffens F (1988) Local and cooperative Jahn-Teller distortions of nickel(2+) and copper (2+) in tetrahedral coordination. *Inorg. Chem.* 27(10):1678-1686.

17. 1999) *The Weak Hydrogen Bond* (Oxford Science Publications).

18. Lee RH, Griswold E, & Kleinberg J (1964) Studies on Stepwise Controlled Decomposition of 2,2-Bipyridine Complexes of Cobalt(2) + Nickel)2) Chlorides. (Translated from English) *Inorg. Chem.* 3(9):1278-& (in English).

19. Reiff WM, Dockum B, Weber MA, & Frankel RB (1975) Magnetic ordering of mono(diimine)iron(II)chlorides. (2,2'-Bipyridine)dichloroiron and (5,5'-dimethyl-2,2'-bipyridine)dichloroiron. *Inorg. Chem.* 14(4):800-806.

20. Matsunaga PT, Hillhouse GL, & Rheingold AL (2002) Oxygen-atom transfer from nitrous oxide to a nickel metallacycle. Synthesis, structure, and reactions of [cyclic] (2,2'-bipyridine)Ni(OCH2CH2CH2CH2). *J. Am. Chem. Soc.* 115(5):2075-2077.

21. Donoghue JT & Drago RS (1962) Non-aqueous Coordination Phenomena-Complexes of Hexamethylphosphoramide. Preparation and Properties of Tetrahedral $[Zn\{PO[N(CH_3)_2]_3\}_4]^{+2}$, $[Co\{PO[N(CH_3)_2]_3\}_4]^{+2}$,and $[Ni\{PO[N(CH_3)_2]_3\}_4]^{+2}$ Compounds. *Inorg. Chem.* 1(4):866-872.

22. Davis WM, Zask A, Nakanishi K, & Lippard SJ (1985) Copper(II) tropocoronands: synthesis, structure, and properties of mononuclear complexes. *Inorg. Chem.* 24(23):3737-3743.

23. Hathaway BJ & Billing DE (1970) The electronic properties and stereochemistry of mono-nuclear complexes of the copper(II) ion. *Coordin. Chem. Rev.* 5(2):143-207.

24. Kwong HL, Lee WS, Ng HF, Chiu WH, & Wong WT (1998) Chiral bipyridine-copper(II) complex. Crystal structure and catalytic activity in asymmetric cyclopropanation. (Translated from English) *J Chem Soc Dalton* (6):1043-1046 (in English).

25. Venanzi LM (1958) Tetrahedral Nickel(II) Complexes and the Factors Determing Their Formation. (Translated from English) *J Chem Soc* (Feb):719-724 (in English).

26. Parks JE, Wagner BE, & Holm RH (1973) Syntheses Employing Pyridyllithium Reagents - New Routes to 2,6-Disubstituted Pyridines and 6,6'-Disubstituted 2,2'-Bipyridyls. *J. Organomet. Chem.* 56(AUG1):53-66.

27. Sheldrick G (2008) A short history of SHELX. *Acta Crystall. A* 64(1):112-122.

2.6 Appendix

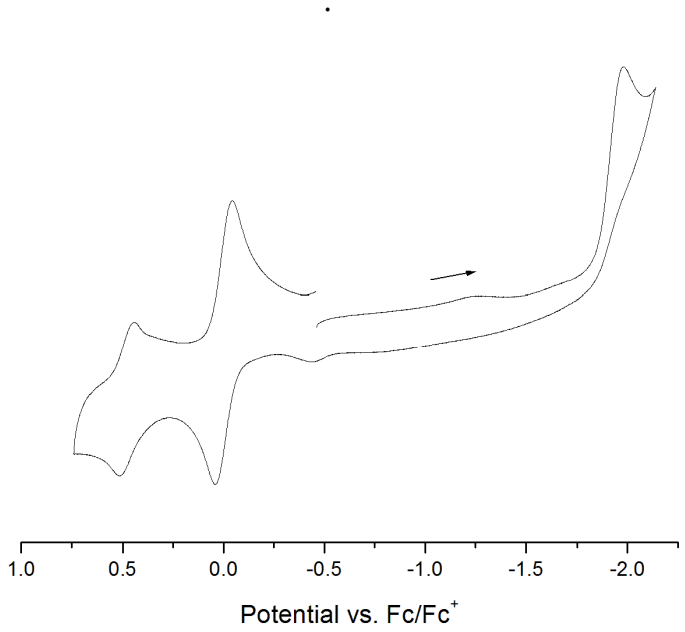

Figure 2.10 Cyclic voltammetry of $FeCl_2$tripbipy in CH_2Cl_2 with Fc/Fc^+ internal standard at 100mV/s.

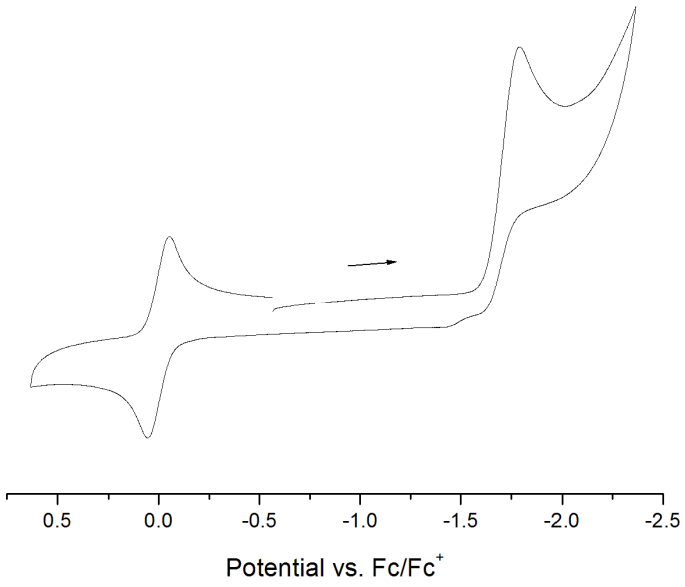

Figure 2.11 Cyclic voltammetry of $CoCl_2$tripbipy in CH_2Cl_2 with Fc/Fc^+ internal standard at 100mV/s.

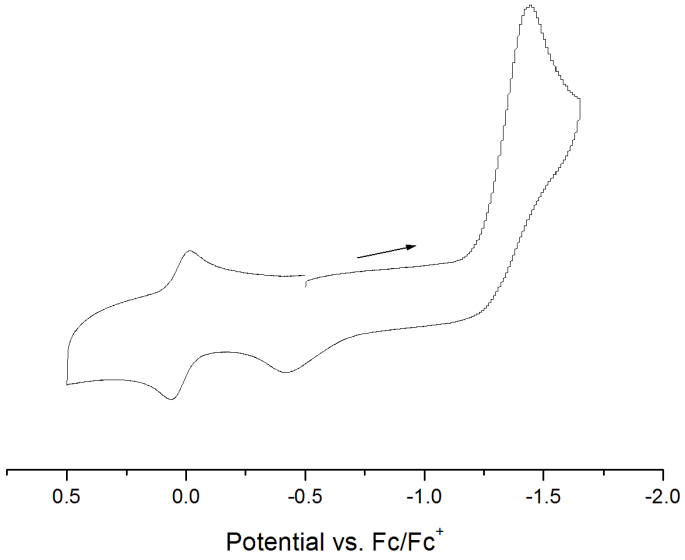

Figure 2.12 Cyclic voltammetry of $NiCl_2$tripbipy in CH_2Cl_2 at 100mV/s with Fc/Fc^+ internal standard.

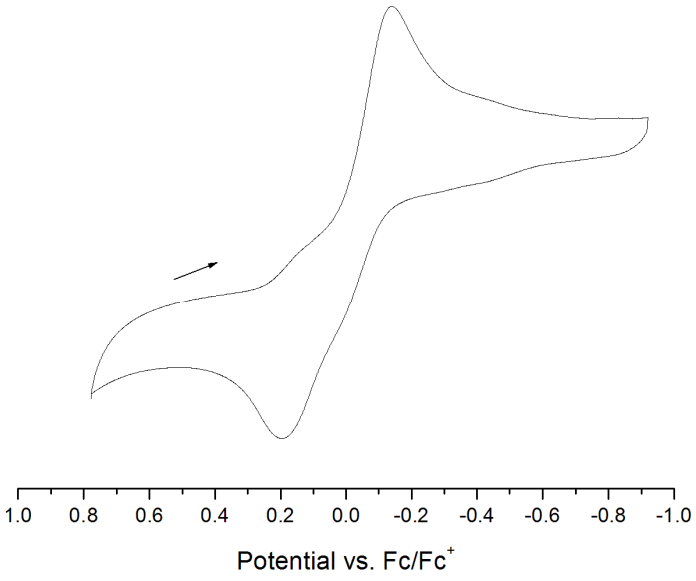

Figure 2.13 Cyclic voltammetry of $CuCl_2$tripbipy in CH_2Cl_2 at 25mV/s.

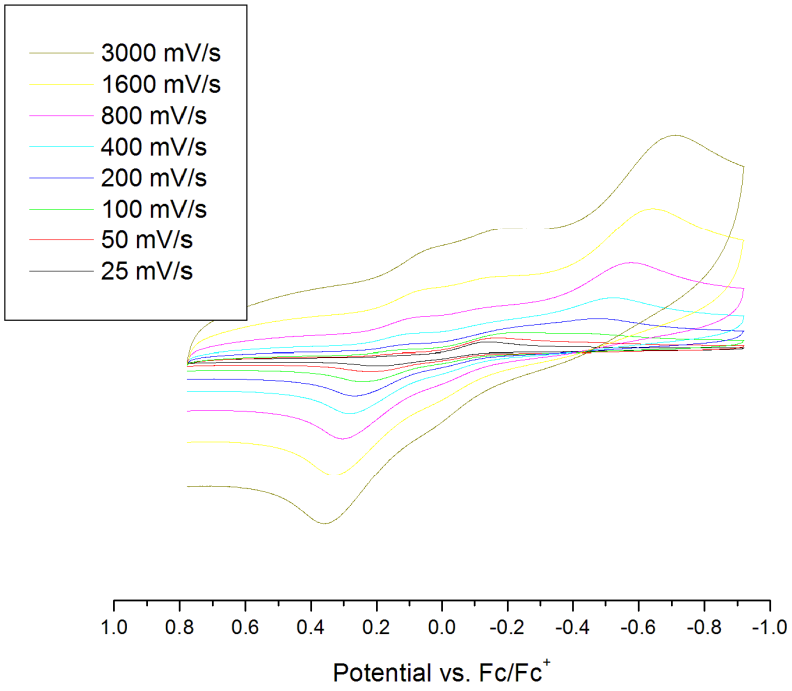

Figure 2.14 Scan rate dependence of $CuCl_2$tripbipy in CH_2Cl_2.

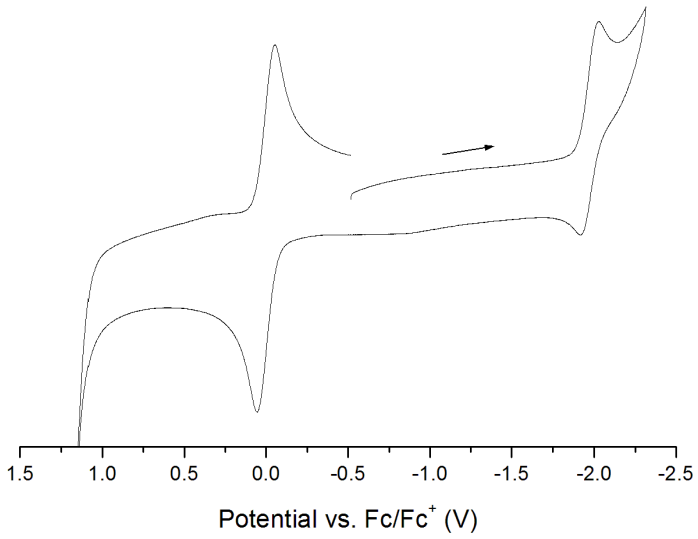

Figure 2.15 Cyclic voltammetry of $ZnCl_2$tripbipy in CH_2Cl_2 with Fc/Fc^+ internal standard at 100mV/s.

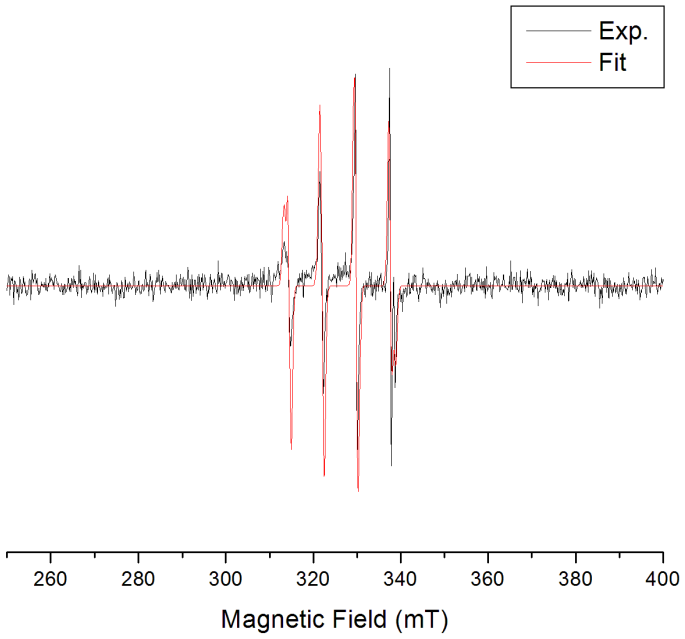

Figure 2.16 Room temperature EPR spectrum and fit of $CuCl_2$tripbipy.

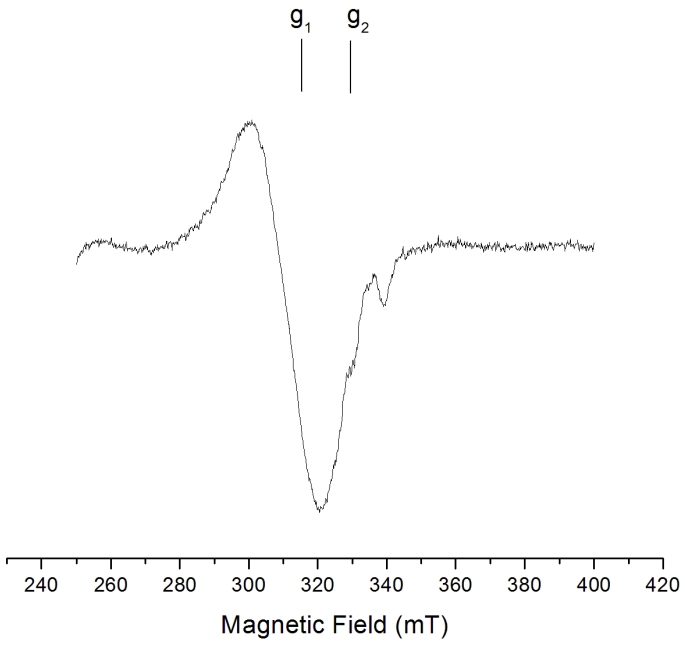

Figure 2.17 EPR spectrum of $CuCl_2$tripbipy at 110K.

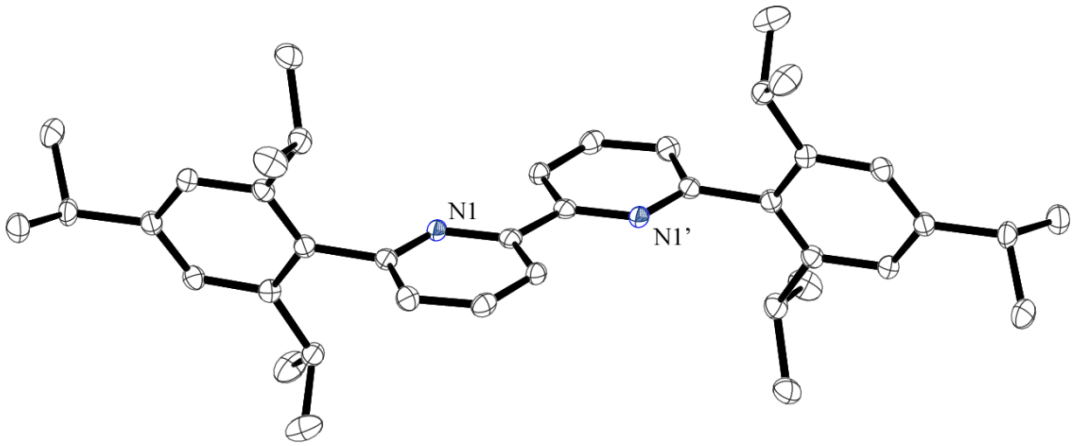

Figure 2.18 Molecular structure of tripbipy, hydrogen atoms omitted for clarity and ellipsoids are set at 50% probability.

Table 2.2 Crystal data and structure refinement for $FeCl_2$tripbipy

Identification code	fecl2tripbipy	
Empirical formula	C41 H53 Cl5 Fe N2	
Formula weight	806.95	
Temperature	150(2) K	
Wavelength	0.71073 Å	
Crystal system	Monoclinic	
Space group	P2(1)/c	
Unit cell dimensions	a = 8.9257(5) Å	α= 90°.
	b = 28.1409(17) Å	β= 100.1670(10)°.
	c = 16.8549(10) Å	γ = 90°.
Volume	4167.1(4) $Å^3$	
Z	4	
Density (calculated)	1.286 Mg/m^3	
Absorption coefficient	0.713 mm^{-1}	
F(000)	1696	
Crystal size	0.40 x 0.20 x 0.20 mm^3	
Theta range for data collection	1.42 to 25.47°.	
Index ranges	-10<=h<=10, -34<=k<=34, -20<=l<=20	
Reflections collected	60122	
Independent reflections	7713 [R(int) = 0.0412]	
Completeness to theta = 25.00°	100.0 %	
Absorption correction	Semi-empirical from equivalents	
Max. and min. transmission	0.8706 and 0.7636	
Refinement method	Full-matrix least-squares on F^2	
Data / restraints / parameters	7713 / 0 / 454	
Goodness-of-fit on F^2	1.041	
Final R indices [I>2sigma(I)]	R1 = 0.0309, wR2 = 0.0711	
R indices (all data)	R1 = 0.0403, wR2 = 0.0751	
Largest diff. peak and hole	0.435 and -0.456 e.$Å^{-3}$	

Table 2.3 Bond lengths [Å] and angles [°] for $FeCl_2$tripbipy

C(1)-C(2)	1.389(2)	C(16)-C(29)	1.527(3)
C(1)-C(17)	1.498(2)	C(17)-C(18)	1.408(2)
C(1)-N(1)	1.353(2)	C(17)-C(22)	1.403(2)
C(2)-H(2)	0.9500	C(18)-C(19)	1.385(3)
C(2)-C(3)	1.382(3)	C(18)-C(32)	1.522(2)
C(3)-H(3)	0.9500	C(19)-H(19)	0.9500
C(3)-C(4)	1.384(3)	C(19)-C(20)	1.393(3)
C(4)-H(4)	0.9500	C(20)-C(21)	1.385(3)
C(4)-C(5)	1.386(2)	C(20)-C(35)	1.524(3)
C(5)-C(6)	1.488(3)	C(21)-H(21)	0.9500
C(5)-N(1)	1.357(2)	C(21)-C(22)	1.398(3)
C(6)-C(7)	1.383(3)	C(22)-C(38)	1.523(3)
C(6)-N(2)	1.360(2)	C(23)-H(23)	1.0000
C(7)-H(7)	0.9500	C(23)-C(24)	1.534(3)
C(7)-C(8)	1.385(3)	C(23)-C(25)	1.529(3)
C(8)-H(8)	0.9500	C(24)-H(24A)	0.9800
C(8)-C(9)	1.381(3)	C(24)-H(24B)	0.9800
C(9)-H(9)	0.9500	C(24)-H(24C)	0.9800
C(9)-C(10)	1.393(3)	C(25)-H(25A)	0.9800
C(10)-C(11)	1.498(2)	C(25)-H(25B)	0.9800
C(10)-N(2)	1.349(2)	C(25)-H(25C)	0.9800
C(11)-C(12)	1.410(3)	C(26)-H(26)	1.0000
C(11)-C(16)	1.410(2)	C(26)-C(27)	1.534(3)
C(12)-C(13)	1.394(3)	C(26)-C(28)	1.511(3)
C(12)-C(23)	1.520(2)	C(27)-H(27A)	0.9800
C(13)-H(13)	0.9500	C(27)-H(27B)	0.9800
C(13)-C(14)	1.386(3)	C(27)-H(27C)	0.9800
C(14)-C(15)	1.390(3)	C(28)-H(28A)	0.9800
C(14)-C(26)	1.526(3)	C(28)-H(28B)	0.9800
C(15)-H(15)	0.9500	C(28)-H(28C)	0.9800
C(15)-C(16)	1.394(3)	C(29)-H(29)	1.0000
C(15)-H(41)#1	2.7721	C(29)-C(30)	1.525(3)

Table 2.3 Cont.

C(29)-C(31)	1.531(3)	C(40)-H(40B)	0.9800
C(30)-H(30A)	0.9800	C(40)-H(40C)	0.9800
C(30)-H(30B)	0.9800	C(41)-H(41)	1.0000
C(30)-H(30C)	0.9800	C(41)-Cl(3)	1.761(2)
C(31)-H(31A)	0.9800	C(41)-Cl(4)	1.759(2)
C(31)-H(31B)	0.9800	C(41)-Cl(5)	1.745(2)
C(31)-H(31C)	0.9800	N(1)-Fe(1)	2.1318(14)
C(32)-H(32)	1.0000	N(2)-Fe(1)	2.1217(15)
C(32)-C(33)	1.522(3)	Cl(1)-Fe(1)	2.2526(5)
C(32)-C(34)	1.533(3)	Cl(2)-Fe(1)	2.2154(5)
C(33)-H(33A)	0.9800		
C(33)-H(33B)	0.9800	C(2)-C(1)-C(17)	122.26(16)
C(33)-H(33C)	0.9800	N(1)-C(1)-C(2)	120.77(16)
C(34)-H(34A)	0.9800	N(1)-C(1)-C(17)	116.86(15)
C(34)-H(34B)	0.9800	C(1)-C(2)-H(2)	120.2
C(34)-H(34C)	0.9800	C(3)-C(2)-C(1)	119.61(17)
C(35)-H(35)	1.0000	C(3)-C(2)-H(2)	120.2
C(35)-C(36)	1.508(3)	C(2)-C(3)-H(3)	120.2
C(35)-C(37)	1.529(3)	C(2)-C(3)-C(4)	119.63(17)
C(36)-H(36A)	0.9800	C(4)-C(3)-H(3)	120.2
C(36)-H(36B)	0.9800	C(3)-C(4)-H(4)	120.7
C(36)-H(36C)	0.9800	C(3)-C(4)-C(5)	118.66(17)
C(37)-H(37A)	0.9800	C(5)-C(4)-H(4)	120.7
C(37)-H(37B)	0.9800	C(4)-C(5)-C(6)	122.48(16)
C(37)-H(37C)	0.9800	N(1)-C(5)-C(4)	121.78(16)
C(38)-H(38)	1.0000	N(1)-C(5)-C(6)	115.68(15)
C(38)-C(39)	1.530(3)	C(7)-C(6)-C(5)	122.88(16)
C(38)-C(40)	1.525(3)	N(2)-C(6)-C(5)	115.19(15)
C(39)-H(39A)	0.9800	N(2)-C(6)-C(7)	121.90(16)
C(39)-H(39B)	0.9800	C(6)-C(7)-H(7)	120.6
C(39)-H(39C)	0.9800	C(6)-C(7)-C(8)	118.75(17)
C(40)-H(40A)	0.9800	C(8)-C(7)-H(7)	120.6

Table 2.3 Cont.

C(7)-C(8)-H(8)	120.3	C(22)-C(17)-C(18)	120.66(16)
C(9)-C(8)-C(7)	119.43(18)	C(17)-C(18)-C(32)	120.40(16)
C(9)-C(8)-H(8)	120.3	C(19)-C(18)-C(17)	118.53(16)
C(8)-C(9)-H(9)	120.1	C(19)-C(18)-C(32)	121.00(16)
C(8)-C(9)-C(10)	119.76(18)	C(18)-C(19)-H(19)	119.0
C(10)-C(9)-H(9)	120.1	C(18)-C(19)-C(20)	122.09(17)
C(9)-C(10)-C(11)	121.78(16)	C(20)-C(19)-H(19)	119.0
N(2)-C(10)-C(9)	120.76(16)	C(19)-C(20)-C(35)	118.44(17)
N(2)-C(10)-C(11)	117.47(15)	C(21)-C(20)-C(19)	118.23(17)
C(12)-C(11)-C(10)	119.19(16)	C(21)-C(20)-C(35)	123.33(17)
C(16)-C(11)-C(10)	120.08(16)	C(20)-C(21)-H(21)	119.0
C(16)-C(11)-C(12)	120.73(17)	C(20)-C(21)-C(22)	122.04(17)
C(11)-C(12)-C(23)	122.22(16)	C(22)-C(21)-H(21)	119.0
C(13)-C(12)-C(11)	118.21(17)	C(17)-C(22)-C(38)	121.89(16)
C(13)-C(12)-C(23)	119.57(16)	C(21)-C(22)-C(17)	118.34(17)
C(12)-C(13)-H(13)	118.9	C(21)-C(22)-C(38)	119.77(16)
C(14)-C(13)-C(12)	122.20(17)	C(12)-C(23)-H(23)	107.9
C(14)-C(13)-H(13)	118.9	C(12)-C(23)-C(24)	112.70(16)
C(13)-C(14)-C(15)	118.47(17)	C(12)-C(23)-C(25)	110.70(15)
C(13)-C(14)-C(26)	121.35(17)	C(24)-C(23)-H(23)	107.9
C(15)-C(14)-C(26)	120.05(17)	C(25)-C(23)-H(23)	107.9
C(14)-C(15)-H(15)	119.0	C(25)-C(23)-C(24)	109.70(16)
C(14)-C(15)-C(16)	122.00(17)	C(23)-C(24)-H(24A)	109.5
C(14)-C(15)-H(41)#1	78.6	C(23)-C(24)-H(24B)	109.5
C(16)-C(15)-H(15)	119.0	C(23)-C(24)-H(24C)	109.5
C(16)-C(15)-H(41)#1	79.0	H(24A)-C(24)-H(24B)	109.5
H(41)#1-C(15)-H(15)	113.6	H(24A)-C(24)-H(24C)	109.5
C(11)-C(16)-C(29)	120.96(16)	H(24B)-C(24)-H(24C)	109.5
C(15)-C(16)-C(11)	118.33(16)	C(23)-C(25)-H(25A)	109.5
C(15)-C(16)-C(29)	120.70(16)	C(23)-C(25)-H(25B)	109.5
C(18)-C(17)-C(1)	120.96(15)	C(23)-C(25)-H(25C)	109.5
C(22)-C(17)-C(1)	118.36(15)	H(25A)-C(25)-H(25B)	109.5

Table 2.3 Cont.

H(25A)-C(25)-H(25C)	109.5	C(29)-C(31)-H(31A)	109.5
H(25B)-C(25)-H(25C)	109.5	C(29)-C(31)-H(31B)	109.5
C(14)-C(26)-H(26)	107.9	C(29)-C(31)-H(31C)	109.5
C(14)-C(26)-C(27)	109.38(17)	H(31A)-C(31)-H(31B)	109.5
C(27)-C(26)-H(26)	107.9	H(31A)-C(31)-H(31C)	109.5
C(28)-C(26)-C(14)	113.77(18)	H(31B)-C(31)-H(31C)	109.5
C(28)-C(26)-H(26)	107.9	C(18)-C(32)-H(32)	107.9
C(28)-C(26)-C(27)	109.73(19)	C(18)-C(32)-C(34)	109.38(15)
C(26)-C(27)-H(27A)	109.5	C(33)-C(32)-C(18)	114.38(16)
C(26)-C(27)-H(27B)	109.5	C(33)-C(32)-H(32)	107.9
C(26)-C(27)-H(27C)	109.5	C(33)-C(32)-C(34)	109.23(16)
H(27A)-C(27)-H(27B)	109.5	C(34)-C(32)-H(32)	107.9
H(27A)-C(27)-H(27C)	109.5	C(32)-C(33)-H(33A)	109.5
H(27B)-C(27)-H(27C)	109.5	C(32)-C(33)-H(33B)	109.5
C(26)-C(28)-H(28A)	109.5	C(32)-C(33)-H(33C)	109.5
C(26)-C(28)-H(28B)	109.5	H(33A)-C(33)-H(33B)	109.5
C(26)-C(28)-H(28C)	109.5	H(33A)-C(33)-H(33C)	109.5
H(28A)-C(28)-H(28B)	109.5	H(33B)-C(33)-H(33C)	109.5
H(28A)-C(28)-H(28C)	109.5	C(32)-C(34)-H(34A)	109.5
H(28B)-C(28)-H(28C)	109.5	C(32)-C(34)-H(34B)	109.5
C(16)-C(29)-H(29)	107.5	C(32)-C(34)-H(34C)	109.5
C(16)-C(29)-C(31)	110.76(15)	H(34A)-C(34)-H(34B)	109.5
C(30)-C(29)-C(16)	113.83(16)	H(34A)-C(34)-H(34C)	109.5
C(30)-C(29)-H(29)	107.5	H(34B)-C(34)-H(34C)	109.5
C(30)-C(29)-C(31)	109.48(15)	C(20)-C(35)-H(35)	106.7
C(31)-C(29)-H(29)	107.5	C(20)-C(35)-C(37)	110.69(17)
C(29)-C(30)-H(30A)	109.5	C(36)-C(35)-C(20)	114.23(18)
C(29)-C(30)-H(30B)	109.5	C(36)-C(35)-H(35)	106.7
C(29)-C(30)-H(30C)	109.5	C(36)-C(35)-C(37)	111.5(2)
H(30A)-C(30)-H(30B)	109.5	C(37)-C(35)-H(35)	106.7
H(30A)-C(30)-H(30C)	109.5	C(35)-C(36)-H(36A)	109.5
H(30B)-C(30)-H(30C)	109.5	C(35)-C(36)-H(36B)	109.5

Table 2.3 Cont.

C(35)-C(36)-H(36C)	109.5	C(38)-C(40)-H(40B)	109.5
H(36A)-C(36)-H(36B)	109.5	C(38)-C(40)-H(40C)	109.5
H(36A)-C(36)-H(36C)	109.5	H(40A)-C(40)-H(40B)	109.5
H(36B)-C(36)-H(36C)	109.5	H(40A)-C(40)-H(40C)	109.5
C(35)-C(37)-H(37A)	109.5	H(40B)-C(40)-H(40C)	109.5
C(35)-C(37)-H(37B)	109.5	Cl(3)-C(41)-H(41)	108.6
C(35)-C(37)-H(37C)	109.5	Cl(4)-C(41)-H(41)	108.6
H(37A)-C(37)-H(37B)	109.5	Cl(4)-C(41)-Cl(3)	109.98(12)
H(37A)-C(37)-H(37C)	109.5	Cl(5)-C(41)-H(41)	108.6
H(37B)-C(37)-H(37C)	109.5	Cl(5)-C(41)-Cl(3)	110.20(12)
C(22)-C(38)-H(38)	107.8	Cl(5)-C(41)-Cl(4)	110.73(12)
C(22)-C(38)-C(39)	112.41(16)	C(1)-N(1)-C(5)	119.50(15)
C(22)-C(38)-C(40)	110.19(16)	C(1)-N(1)-Fe(1)	125.80(12)
C(39)-C(38)-H(38)	107.8	C(5)-N(1)-Fe(1)	114.46(11)
C(40)-C(38)-H(38)	107.8	C(6)-N(2)-Fe(1)	114.65(11)
C(40)-C(38)-C(39)	110.71(17)	C(10)-N(2)-C(6)	119.35(15)
C(38)-C(39)-H(39A)	109.5	C(10)-N(2)-Fe(1)	125.20(12)
C(38)-C(39)-H(39B)	109.5	N(1)-Fe(1)-Cl(1)	112.31(4)
C(38)-C(39)-H(39C)	109.5	N(1)-Fe(1)-Cl(2)	114.23(4)
H(39A)-C(39)-H(39B)	109.5	N(2)-Fe(1)-N(1)	77.24(6)
H(39A)-C(39)-H(39C)	109.5	N(2)-Fe(1)-Cl(1)	103.13(4)
H(39B)-C(39)-H(39C)	109.5	N(2)-Fe(1)-Cl(2)	123.41(4)
C(38)-C(40)-H(40A)	109.5	Cl(2)-Fe(1)-Cl(1)	119.19(2)

Symmetry transformations used to generate equivalent atoms:
#1 -x,y-1/2,-z+1/2

Table 2.4 Crystal data and structure refinement for $CoCl_2$tripbipy

Identification code	cocl2tripbipy	
Empirical formula	C41 H53 Cl5 Co N2	
Formula weight	810.03	
Temperature	150(2) K	
Wavelength	0.71073 Å	
Crystal system	Monoclinic	
Space group	P2(1)/c	
Unit cell dimensions	a = 8.9196(7) Å	α= 90°.
	b = 28.052(2) Å	β= 100.069(2)°.
	c = 16.8310(14) Å	γ = 90°.
Volume	4146.4(6) $Å^3$	
Z	4	
Density (calculated)	1.298 Mg/m^3	
Absorption coefficient	0.766 mm^{-1}	
F(000)	1700	
Crystal size	0.35 x 0.25 x 0.25 mm^3	
Theta range for data collection	1.43 to 25.44°.	
Index ranges	-9<=h<=10, -33<=k<=33, -20<=l<=20	
Reflections collected	35788	
Independent reflections	7645 [R(int) = 0.0491]	
Completeness to theta = 25.00°	100.0 %	
Absorption correction	Semi-empirical from equivalents	
Max. and min. transmission	0.8315 and 0.7753	
Refinement method	Full-matrix least-squares on F^2	
Data / restraints / parameters	7645 / 0 / 454	
Goodness-of-fit on F^2	1.064	
Final R indices [I>2sigma(I)]	R1 = 0.0497, wR2 = 0.1303	
R indices (all data)	R1 = 0.0597, wR2 = 0.1371	
Largest diff. peak and hole	0.595 and -0.893 $e.Å^{-3}$	

Table 2.5 Bond lengths [Å] and angles [°] for $CoCl_2$tripbipy

C(1)-N(1)	1.341(4)	C(17)-C(18)	1.396(5)
C(1)-C(2)	1.400(4)	C(17)-C(22)	1.409(5)
C(1)-C(17)	1.503(4)	C(18)-C(19)	1.403(5)
C(2)-C(3)	1.380(5)	C(18)-C(32)	1.519(5)
C(2)-H(2)	0.9500	C(19)-C(20)	1.381(5)
C(3)-C(4)	1.381(5)	C(19)-H(19)	0.9500
C(3)-H(3)	0.9500	C(20)-C(21)	1.382(5)
C(4)-C(5)	1.387(4)	C(20)-C(35)	1.530(5)
C(4)-H(4)	0.9500	C(21)-C(22)	1.394(5)
C(5)-N(1)	1.360(4)	C(21)-H(21)	0.9500
C(5)-C(6)	1.489(4)	C(22)-C(38)	1.524(5)
C(6)-N(2)	1.360(4)	C(23)-C(24)	1.526(4)
C(6)-C(7)	1.385(4)	C(23)-C(25)	1.530(5)
C(7)-C(8)	1.380(5)	C(23)-H(23)	1.0000
C(7)-H(7)	0.9500	C(24)-H(24A)	0.9800
C(8)-C(9)	1.387(5)	C(24)-H(24B)	0.9800
C(8)-H(8)	0.9500	C(24)-H(24C)	0.9800
C(9)-C(10)	1.388(4)	C(25)-H(25A)	0.9800
C(9)-H(9)	0.9500	C(25)-H(25B)	0.9800
C(10)-N(2)	1.354(4)	C(25)-H(25C)	0.9800
C(10)-C(11)	1.495(4)	C(26)-C(27)	1.486(6)
C(11)-C(16)	1.401(5)	C(26)-C(28)	1.523(6)
C(11)-C(12)	1.408(4)	C(26)-H(26)	1.0000
C(12)-C(13)	1.383(4)	C(27)-H(27A)	0.9800
C(12)-C(23)	1.517(4)	C(27)-H(27B)	0.9800
C(13)-C(14)	1.387(5)	C(27)-H(27C)	0.9800
C(13)-H(13)	0.9500	C(28)-H(28A)	0.9800
C(14)-C(15)	1.387(5)	C(28)-H(28B)	0.9800
C(14)-C(26)	1.528(5)	C(28)-H(28C)	0.9800
C(15)-C(16)	1.396(4)	C(29)-C(30)	1.527(5)
C(15)-H(41)#1	9.9978	C(29)-C(31)	1.530(5)
C(15)-H(15)	0.9500	C(29)-H(29)	1.0000
C(16)-C(29)	1.523(4)	C(30)-H(30A)	0.9800

Table 2.5 Cont.

C(30)-H(30B)	0.9800	C(41)-Cl(3)	1.740(4)
C(30)-H(30C)	0.9800	C(41)-Cl(5)	1.751(4)
C(31)-H(31A)	0.9800	C(41)-Cl(4)	1.771(5)
C(31)-H(31B)	0.9800	C(41)-H(41)	1.0000
C(31)-H(31C)	0.9800	N(1)-Co(1)	2.056(3)
C(32)-C(33)	1.526(5)	N(2)-Co(1)	2.064(3)
C(32)-C(34)	1.535(5)	Cl(1)-Co(1)	2.2348(9)
C(32)-H(32)	1.0000	Cl(2)-Co(1)	2.1992(9)
C(33)-H(33A)	0.9800		
C(33)-H(33B)	0.9800	N(1)-C(1)-C(2)	120.6(3)
C(33)-H(33C)	0.9800	N(1)-C(1)-C(17)	117.5(3)
C(34)-H(34A)	0.9800	C(2)-C(1)-C(17)	121.9(3)
C(34)-H(34B)	0.9800	C(3)-C(2)-C(1)	119.6(3)
C(34)-H(34C)	0.9800	C(3)-C(2)-H(2)	120.2
C(35)-C(37)	1.508(6)	C(1)-C(2)-H(2)	120.2
C(35)-C(36)	1.527(6)	C(2)-C(3)-C(4)	119.6(3)
C(35)-H(35)	1.0000	C(2)-C(3)-H(3)	120.2
C(36)-H(36A)	0.9800	C(4)-C(3)-H(3)	120.2
C(36)-H(36B)	0.9800	C(3)-C(4)-C(5)	118.7(3)
C(36)-H(36C)	0.9800	C(3)-C(4)-H(4)	120.7
C(37)-H(37A)	0.9800	C(5)-C(4)-H(4)	120.7
C(37)-H(37B)	0.9800	N(1)-C(5)-C(4)	121.7(3)
C(37)-H(37C)	0.9800	N(1)-C(5)-C(6)	115.6(3)
C(38)-C(39)	1.523(5)	C(4)-C(5)-C(6)	122.7(3)
C(38)-C(40)	1.527(5)	N(2)-C(6)-C(7)	121.6(3)
C(38)-H(38)	1.0000	N(2)-C(6)-C(5)	115.7(3)
C(39)-H(39A)	0.9800	C(7)-C(6)-C(5)	122.7(3)
C(39)-H(39B)	0.9800	C(8)-C(7)-C(6)	118.8(3)
C(39)-H(39C)	0.9800	C(8)-C(7)-H(7)	120.6
C(40)-H(40A)	0.9800	C(6)-C(7)-H(7)	120.6
C(40)-H(40B)	0.9800	C(7)-C(8)-C(9)	119.6(3)
C(40)-H(40C)	0.9800	C(7)-C(8)-H(8)	120.2

Table 2.5 Cont.

C(9)-C(8)-H(8)	120.2	C(17)-C(18)-C(32)	121.9(3)
C(8)-C(9)-C(10)	119.7(3)	C(19)-C(18)-C(32)	119.9(3)
C(8)-C(9)-H(9)	120.1	C(20)-C(19)-C(18)	121.9(3)
C(10)-C(9)-H(9)	120.1	C(20)-C(19)-H(19)	119.0
N(2)-C(10)-C(9)	120.5(3)	C(18)-C(19)-H(19)	119.0
N(2)-C(10)-C(11)	116.8(3)	C(19)-C(20)-C(21)	118.7(3)
C(9)-C(10)-C(11)	122.5(3)	C(19)-C(20)-C(35)	121.3(3)
C(16)-C(11)-C(12)	120.6(3)	C(21)-C(20)-C(35)	119.9(3)
C(16)-C(11)-C(10)	118.3(3)	C(20)-C(21)-C(22)	122.0(3)
C(12)-C(11)-C(10)	121.0(3)	C(20)-C(21)-H(21)	119.0
C(13)-C(12)-C(11)	118.6(3)	C(22)-C(21)-H(21)	119.0
C(13)-C(12)-C(23)	121.0(3)	C(21)-C(22)-C(17)	118.3(3)
C(11)-C(12)-C(23)	120.3(3)	C(21)-C(22)-C(38)	120.6(3)
C(12)-C(13)-C(14)	122.0(3)	C(17)-C(22)-C(38)	121.1(3)
C(12)-C(13)-H(13)	119.0	C(12)-C(23)-C(24)	114.6(3)
C(14)-C(13)-H(13)	119.0	C(12)-C(23)-C(25)	109.5(3)
C(13)-C(14)-C(15)	118.4(3)	C(24)-C(23)-C(25)	109.2(3)
C(13)-C(14)-C(26)	118.6(3)	C(12)-C(23)-H(23)	107.8
C(15)-C(14)-C(26)	123.0(3)	C(24)-C(23)-H(23)	107.8
C(14)-C(15)-C(16)	121.9(3)	C(25)-C(23)-H(23)	107.8
C(14)-C(15)-H(41)#1	99.8	C(23)-C(24)-H(24A)	109.5
C(16)-C(15)-H(41)#1	64.0	C(23)-C(24)-H(24B)	109.5
C(14)-C(15)-H(15)	119.1	H(24A)-C(24)-H(24B)	109.5
C(16)-C(15)-H(15)	119.1	C(23)-C(24)-H(24C)	109.5
H(41)#1-C(15)-H(15)	106.1	H(24A)-C(24)-H(24C)	109.5
C(15)-C(16)-C(11)	118.3(3)	H(24B)-C(24)-H(24C)	109.5
C(15)-C(16)-C(29)	119.8(3)	C(23)-C(25)-H(25A)	109.5
C(11)-C(16)-C(29)	121.9(3)	C(23)-C(25)-H(25B)	109.5
C(18)-C(17)-C(22)	120.9(3)	H(25A)-C(25)-H(25B)	109.5
C(18)-C(17)-C(1)	119.5(3)	C(23)-C(25)-H(25C)	109.5
C(22)-C(17)-C(1)	119.6(3)	H(25A)-C(25)-H(25C)	109.5
C(17)-C(18)-C(19)	118.2(3)	H(25B)-C(25)-H(25C)	109.5

Table 2.5 Cont.

C(27)-C(26)-C(28)	113.3(4)	H(31A)-C(31)-H(31B)	109.5
C(27)-C(26)-C(14)	114.3(3)	C(29)-C(31)-H(31C)	109.5
C(28)-C(26)-C(14)	110.5(3)	H(31A)-C(31)-H(31C)	109.5
C(27)-C(26)-H(26)	106.0	H(31B)-C(31)-H(31C)	109.5
C(28)-C(26)-H(26)	106.0	C(18)-C(32)-C(33)	112.8(3)
C(14)-C(26)-H(26)	106.0	C(18)-C(32)-C(34)	110.5(3)
C(26)-C(27)-H(27A)	109.5	C(33)-C(32)-C(34)	109.8(3)
C(26)-C(27)-H(27B)	109.5	C(18)-C(32)-H(32)	107.9
H(27A)-C(27)-H(27B)	109.5	C(33)-C(32)-H(32)	107.9
C(26)-C(27)-H(27C)	109.5	C(34)-C(32)-H(32)	107.9
H(27A)-C(27)-H(27C)	109.5	C(32)-C(33)-H(33A)	109.5
H(27B)-C(27)-H(27C)	109.5	C(32)-C(33)-H(33B)	109.5
C(26)-C(28)-H(28A)	109.5	H(33A)-C(33)-H(33B)	109.5
C(26)-C(28)-H(28B)	109.5	C(32)-C(33)-H(33C)	109.5
H(28A)-C(28)-H(28B)	109.5	H(33A)-C(33)-H(33C)	109.5
C(26)-C(28)-H(28C)	109.5	H(33B)-C(33)-H(33C)	109.5
H(28A)-C(28)-H(28C)	109.5	C(32)-C(34)-H(34A)	109.5
H(28B)-C(28)-H(28C)	109.5	C(32)-C(34)-H(34B)	109.5
C(16)-C(29)-C(30)	112.4(3)	H(34A)-C(34)-H(34B)	109.5
C(16)-C(29)-C(31)	110.1(3)	C(32)-C(34)-H(34C)	109.5
C(30)-C(29)-C(31)	110.6(3)	H(34A)-C(34)-H(34C)	109.5
C(16)-C(29)-H(29)	107.8	H(34B)-C(34)-H(34C)	109.5
C(30)-C(29)-H(29)	107.8	C(37)-C(35)-C(36)	109.6(4)
C(31)-C(29)-H(29)	107.8	C(37)-C(35)-C(20)	113.4(3)
C(29)-C(30)-H(30A)	109.5	C(36)-C(35)-C(20)	109.4(3)
C(29)-C(30)-H(30B)	109.5	C(37)-C(35)-H(35)	108.1
H(30A)-C(30)-H(30B)	109.5	C(36)-C(35)-H(35)	108.1
C(29)-C(30)-H(30C)	109.5	C(20)-C(35)-H(35)	108.1
H(30A)-C(30)-H(30C)	109.5	C(35)-C(36)-H(36A)	109.5
H(30B)-C(30)-H(30C)	109.5	C(35)-C(36)-H(36B)	109.5
C(29)-C(31)-H(31A)	109.5	H(36A)-C(36)-H(36B)	109.5
C(29)-C(31)-H(31B)	109.5	C(35)-C(36)-H(36C)	109.5

Table 2.5 Cont.

H(36A)-C(36)-H(36C)	109.5	H(40A)-C(40)-H(40B)	109.5
H(36B)-C(36)-H(36C)	109.5	C(38)-C(40)-H(40C)	109.5
C(35)-C(37)-H(37A)	109.5	H(40A)-C(40)-H(40C)	109.5
C(35)-C(37)-H(37B)	109.5	H(40B)-C(40)-H(40C)	109.5
H(37A)-C(37)-H(37B)	109.5	Cl(3)-C(41)-Cl(5)	110.6(2)
C(35)-C(37)-H(37C)	109.5	Cl(3)-C(41)-Cl(4)	110.4(2)
H(37A)-C(37)-H(37C)	109.5	Cl(5)-C(41)-Cl(4)	109.7(2)
H(37B)-C(37)-H(37C)	109.5	Cl(3)-C(41)-H(41)	108.7
C(39)-C(38)-C(22)	114.0(3)	Cl(5)-C(41)-H(41)	108.7
C(39)-C(38)-C(40)	109.2(3)	Cl(4)-C(41)-H(41)	108.7
C(22)-C(38)-C(40)	111.0(3)	C(1)-N(1)-C(5)	119.8(3)
C(39)-C(38)-H(38)	107.5	C(1)-N(1)-Co(1)	126.6(2)
C(22)-C(38)-H(38)	107.5	C(5)-N(1)-Co(1)	113.1(2)
C(40)-C(38)-H(38)	107.5	C(10)-N(2)-C(6)	119.8(3)
C(38)-C(39)-H(39A)	109.5	C(10)-N(2)-Co(1)	127.2(2)
C(38)-C(39)-H(39B)	109.5	C(6)-N(2)-Co(1)	112.9(2)
H(39A)-C(39)-H(39B)	109.5	N(1)-Co(1)-N(2)	80.64(10)
C(38)-C(39)-H(39C)	109.5	N(1)-Co(1)-Cl(2)	123.47(8)
H(39A)-C(39)-H(39C)	109.5	N(2)-Co(1)-Cl(2)	114.95(7)
H(39B)-C(39)-H(39C)	109.5	N(1)-Co(1)-Cl(1)	105.55(7)
C(38)-C(40)-H(40A)	109.5	N(2)-Co(1)-Cl(1)	113.28(7)
C(38)-C(40)-H(40B)	109.5	Cl(2)-Co(1)-Cl(1)	114.55(3

Symmetry transformations used to generate equivalent atoms:

#1 x+1,y,z

Table 2.6 Crystal data and structure refinement for $NiCl_2$tripbipy

Identification code	nicl2tripbipy	
Empirical formula	C41 H53 Cl5 N2 Ni	
Formula weight	809.81	
Temperature	150(2) K	
Wavelength	0.71073 Å	
Crystal system	Monoclinic	
Space group	P2(1)/c	
Unit cell dimensions	a = 9.036(6) Å	α= 90°.
	b = 28.218(18) Å	β= 99.386(9)°.
	c = 16.666(11) Å	γ = 90°.
Volume	4192(5) $Å^3$	
Z	4	
Density (calculated)	1.283 Mg/m^3	
Absorption coefficient	0.811 mm^{-1}	
F(000)	1704	
Crystal size	0.40 x 0.20 x 0.20 mm^3	
Theta range for data collection	1.43 to 25.71°.	
Index ranges	-10<=h<=10, -34<=k<=33, -20<=l<=20	
Reflections collected	46656	
Independent reflections	7858 [R(int) = 0.0533]	
Completeness to theta = 25.00°	100.0 %	
Absorption correction	Semi-empirical from equivalents	
Max. and min. transmission	0.8546 and 0.7373	
Refinement method	Full-matrix least-squares on F^2	
Data / restraints / parameters	7858 / 0 / 454	
Goodness-of-fit on F^2	1.064	
Final R indices [I>2sigma(I)]	R1 = 0.0423, wR2 = 0.0963	
R indices (all data)	R1 = 0.0513, wR2 = 0.1020	
Largest diff. peak and hole	1.016 and -0.672 $e.Å^{-3}$	

Table 2.7 Bond lengths [Å] and angles [°] for $NiCl_2$tripbipy

C(1)-N(1)	1.352(3)	C(17)-C(18)	1.414(3)
C(1)-C(2)	1.398(3)	C(17)-C(22)	1.416(4)
C(1)-C(17)	1.499(4)	C(18)-C(19)	1.395(4)
C(2)-C(3)	1.378(4)	C(18)-C(32)	1.525(4)
C(2)-H(2)	0.9500	C(19)-C(20)	1.389(4)
C(3)-C(4)	1.388(4)	C(19)-H(19)	0.9500
C(3)-H(3)	0.9500	C(20)-C(21)	1.395(4)
C(4)-C(5)	1.389(3)	C(20)-C(35)	1.525(4)
C(4)-H(4)	0.9500	C(21)-C(22)	1.396(4)
C(5)-N(1)	1.356(3)	C(21)-H(21)	0.9500
C(5)-C(6)	1.490(3)	C(22)-C(38)	1.530(3)
C(6)-N(2)	1.362(3)	C(23)-C(24)	1.529(4)
C(6)-C(7)	1.385(3)	C(23)-C(25)	1.532(4)
C(7)-C(8)	1.394(4)	C(23)-H(23)	1.0000
C(7)-H(7)	0.9500	C(24)-H(24A)	0.9800
C(8)-C(9)	1.382(4)	C(24)-H(24B)	0.9800
C(8)-H(8)	0.9500	C(24)-H(24C)	0.9800
C(9)-C(10)	1.391(3)	C(25)-H(25A)	0.9800
C(9)-H(9)	0.9500	C(25)-H(25B)	0.9800
C(10)-N(2)	1.361(3)	C(25)-H(25C)	0.9800
C(10)-C(11)	1.498(3)	C(26)-C(27)	1.492(5)
C(11)-C(16)	1.407(4)	C(26)-C(28)	1.514(5)
C(11)-C(12)	1.411(4)	C(26)-H(26)	1.0000
C(12)-C(13)	1.382(4)	C(27)-H(27A)	0.9800
C(12)-C(23)	1.519(4)	C(27)-H(27B)	0.9800
C(13)-C(14)	1.382(4)	C(27)-H(27C)	0.9800
C(13)-H(13)	0.9500	C(28)-H(28A)	0.9800
C(14)-C(15)	1.400(4)	C(28)-H(28B)	0.9800
C(14)-C(26)	1.530(4)	C(28)-H(28C)	0.9800
C(15)-C(16)	1.397(4)	C(29)-C(30)	1.526(4)
C(15)-H(15)	0.9500	C(29)-C(31)	1.535(4)
C(16)-C(29)	1.522(4)	C(29)-H(29)	1.0000

Table 2.7 Cont.

C(30)-H(30A)	0.9800	C(40)-H(40C)	0.9800
C(30)-H(30B)	0.9800	C(41)-Cl(3)	1.747(3)
C(30)-H(30C)	0.9800	C(41)-Cl(5)	1.757(3)
C(31)-H(31A)	0.9800	C(41)-Cl(4)	1.763(4)
C(31)-H(31B)	0.9800	C(41)-H(41)	1.0000
C(31)-H(31C)	0.9800	N(1)-Ni(1)	2.017(2)
C(32)-C(34)	1.533(4)	N(2)-Ni(1)	2.029(2)
C(32)-C(33)	1.535(4)	Cl(1)-Ni(1)	2.2419(11)
C(32)-H(32)	1.0000	Cl(2)-Ni(1)	2.1836(11)
C(33)-H(33A)	0.9800		
C(33)-H(33B)	0.9800	N(1)-C(1)-C(2)	120.2(2)
C(33)-H(33C)	0.9800	N(1)-C(1)-C(17)	117.8(2)
C(34)-H(34A)	0.9800	C(2)-C(1)-C(17)	122.1(2)
C(34)-H(34B)	0.9800	C(3)-C(2)-C(1)	120.2(2)
C(34)-H(34C)	0.9800	C(3)-C(2)-H(2)	119.9
C(35)-C(37)	1.524(4)	C(1)-C(2)-H(2)	119.9
C(35)-C(36)	1.538(4)	C(2)-C(3)-C(4)	119.2(2)
C(35)-H(35)	1.0000	C(2)-C(3)-H(3)	120.4
C(36)-H(36A)	0.9800	C(4)-C(3)-H(3)	120.4
C(36)-H(36B)	0.9800	C(3)-C(4)-C(5)	118.9(2)
C(36)-H(36C)	0.9800	C(3)-C(4)-H(4)	120.6
C(37)-H(37A)	0.9800	C(5)-C(4)-H(4)	120.6
C(37)-H(37B)	0.9800	N(1)-C(5)-C(4)	121.6(2)
C(37)-H(37C)	0.9800	N(1)-C(5)-C(6)	115.0(2)
C(38)-C(40)	1.528(4)	C(4)-C(5)-C(6)	123.3(2)
C(38)-C(39)	1.533(4)	N(2)-C(6)-C(7)	121.9(2)
C(38)-H(38)	1.0000	N(2)-C(6)-C(5)	115.3(2)
C(39)-H(39A)	0.9800	C(7)-C(6)-C(5)	122.7(2)
C(39)-H(39B)	0.9800	C(6)-C(7)-C(8)	118.5(2)
C(39)-H(39C)	0.9800	C(6)-C(7)-H(7)	120.8
C(40)-H(40A)	0.9800	C(8)-C(7)-H(7)	120.8
C(40)-H(40B)	0.9800	C(9)-C(8)-C(7)	119.5(2)

Table 2.7 Cont.

C(9)-C(8)-H(8)	120.3	C(20)-C(19)-C(18)	122.2(2)
C(7)-C(8)-H(8)	120.3	C(20)-C(19)-H(19)	118.9
C(8)-C(9)-C(10)	120.2(2)	C(18)-C(19)-H(19)	118.9
C(8)-C(9)-H(9)	119.9	C(19)-C(20)-C(21)	118.5(2)
C(10)-C(9)-H(9)	119.9	C(19)-C(20)-C(35)	121.0(2)
N(2)-C(10)-C(9)	120.2(2)	C(21)-C(20)-C(35)	120.4(2)
N(2)-C(10)-C(11)	117.8(2)	C(20)-C(21)-C(22)	121.9(2)
C(9)-C(10)-C(11)	121.9(2)	C(20)-C(21)-H(21)	119.0
C(16)-C(11)-C(12)	120.7(2)	C(22)-C(21)-H(21)	119.0
C(16)-C(11)-C(10)	118.4(2)	C(21)-C(22)-C(17)	118.3(2)
C(12)-C(11)-C(10)	120.9(2)	C(21)-C(22)-C(38)	121.1(2)
C(13)-C(12)-C(11)	118.7(2)	C(17)-C(22)-C(38)	120.6(2)
C(13)-C(12)-C(23)	120.8(2)	C(12)-C(23)-C(24)	114.6(2)
C(11)-C(12)-C(23)	120.3(2)	C(12)-C(23)-C(25)	109.4(2)
C(12)-C(13)-C(14)	122.4(3)	C(24)-C(23)-C(25)	109.6(2)
C(12)-C(13)-H(13)	118.8	C(12)-C(23)-H(23)	107.7
C(14)-C(13)-H(13)	118.8	C(24)-C(23)-H(23)	107.7
C(13)-C(14)-C(15)	117.9(3)	C(25)-C(23)-H(23)	107.7
C(13)-C(14)-C(26)	118.7(3)	C(23)-C(24)-H(24A)	109.5
C(15)-C(14)-C(26)	123.4(3)	C(23)-C(24)-H(24B)	109.5
C(16)-C(15)-C(14)	122.3(3)	H(24A)-C(24)-H(24B)	109.5
C(16)-C(15)-H(15)	118.8	C(23)-C(24)-H(24C)	109.5
C(14)-C(15)-H(15)	118.8	H(24A)-C(24)-H(24C)	109.5
C(15)-C(16)-C(11)	117.8(2)	H(24B)-C(24)-H(24C)	109.5
C(15)-C(16)-C(29)	120.3(2)	C(23)-C(25)-H(25A)	109.5
C(11)-C(16)-C(29)	122.0(2)	C(23)-C(25)-H(25B)	109.5
C(18)-C(17)-C(22)	120.7(2)	H(25A)-C(25)-H(25B)	109.5
C(18)-C(17)-C(1)	119.2(2)	C(23)-C(25)-H(25C)	109.5
C(22)-C(17)-C(1)	120.1(2)	H(25A)-C(25)-H(25C)	109.5
C(19)-C(18)-C(17)	118.3(2)	H(25B)-C(25)-H(25C)	109.5
C(19)-C(18)-C(32)	119.6(2)	C(27)-C(26)-C(28)	114.1(3)
C(17)-C(18)-C(32)	122.1(2)	C(27)-C(26)-C(14)	114.2(3)

Table 2.7 Cont.

C(28)-C(26)-C(14)	111.0(3)	H(31A)-C(31)-H(31C)	109.5
C(27)-C(26)-H(26)	105.5	H(31B)-C(31)-H(31C)	109.5
C(28)-C(26)-H(26)	105.5	C(18)-C(32)-C(34)	110.5(2)
C(14)-C(26)-H(26)	105.5	C(18)-C(32)-C(33)	112.5(2)
C(26)-C(27)-H(27A)	109.5	C(34)-C(32)-C(33)	110.0(2)
C(26)-C(27)-H(27B)	109.5	C(18)-C(32)-H(32)	107.9
H(27A)-C(27)-H(27B)	109.5	C(34)-C(32)-H(32)	107.9
C(26)-C(27)-H(27C)	109.5	C(33)-C(32)-H(32)	107.9
H(27A)-C(27)-H(27C)	109.5	C(32)-C(33)-H(33A)	109.5
H(27B)-C(27)-H(27C)	109.5	C(32)-C(33)-H(33B)	109.5
C(26)-C(28)-H(28A)	109.5	H(33A)-C(33)-H(33B)	109.5
C(26)-C(28)-H(28B)	109.5	C(32)-C(33)-H(33C)	109.5
H(28A)-C(28)-H(28B)	109.5	H(33A)-C(33)-H(33C)	109.5
C(26)-C(28)-H(28C)	109.5	H(33B)-C(33)-H(33C)	109.5
H(28A)-C(28)-H(28C)	109.5	C(32)-C(34)-H(34A)	109.5
H(28B)-C(28)-H(28C)	109.5	C(32)-C(34)-H(34B)	109.5
C(16)-C(29)-C(30)	112.7(2)	H(34A)-C(34)-H(34B)	109.5
C(16)-C(29)-C(31)	109.9(2)	C(32)-C(34)-H(34C)	109.5
C(30)-C(29)-C(31)	111.0(3)	H(34A)-C(34)-H(34C)	109.5
C(16)-C(29)-H(29)	107.7	H(34B)-C(34)-H(34C)	109.5
C(30)-C(29)-H(29)	107.7	C(37)-C(35)-C(20)	113.1(2)
C(31)-C(29)-H(29)	107.7	C(37)-C(35)-C(36)	109.8(2)
C(29)-C(30)-H(30A)	109.5	C(20)-C(35)-C(36)	109.9(2)
C(29)-C(30)-H(30B)	109.5	C(37)-C(35)-H(35)	108.0
H(30A)-C(30)-H(30B)	109.5	C(20)-C(35)-H(35)	108.0
C(29)-C(30)-H(30C)	109.5	C(36)-C(35)-H(35)	108.0
H(30A)-C(30)-H(30C)	109.5	C(35)-C(36)-H(36A)	109.5
H(30B)-C(30)-H(30C)	109.5	C(35)-C(36)-H(36B)	109.5
C(29)-C(31)-H(31A)	109.5	H(36A)-C(36)-H(36B)	109.5
C(29)-C(31)-H(31B)	109.5	C(35)-C(36)-H(36C)	109.5
H(31A)-C(31)-H(31B)	109.5	H(36A)-C(36)-H(36C)	109.5
C(29)-C(31)-H(31C)	109.5	H(36B)-C(36)-H(36C)	109.5

Table 2.7 Cont.

C(35)-C(37)-H(37A)	109.5	C(38)-C(40)-H(40C)	109.5
C(35)-C(37)-H(37B)	109.5	H(40A)-C(40)-H(40C)	109.5
H(37A)-C(37)-H(37B)	109.5	H(40B)-C(40)-H(40C)	109.5
C(35)-C(37)-H(37C)	109.5	Cl(3)-C(41)-Cl(5)	110.08(19)
H(37A)-C(37)-H(37C)	109.5	Cl(3)-C(41)-Cl(4)	111.37(19)
H(37B)-C(37)-H(37C)	109.5	Cl(5)-C(41)-Cl(4)	109.73(18)
C(40)-C(38)-C(22)	113.7(2)	Cl(3)-C(41)-H(41)	108.5
C(40)-C(38)-C(39)	109.5(2)	Cl(5)-C(41)-H(41)	108.5
C(22)-C(38)-C(39)	110.7(2)	Cl(4)-C(41)-H(41)	108.5
C(40)-C(38)-H(38)	107.6	C(1)-N(1)-C(5)	119.9(2)
C(22)-C(38)-H(38)	107.6	C(1)-N(1)-Ni(1)	126.12(16)
C(39)-C(38)-H(38)	107.6	C(5)-N(1)-Ni(1)	113.69(16)
C(38)-C(39)-H(39A)	109.5	C(10)-N(2)-C(6)	119.6(2)
C(38)-C(39)-H(39B)	109.5	C(10)-N(2)-Ni(1)	127.28(16)
H(39A)-C(39)-H(39B)	109.5	C(6)-N(2)-Ni(1)	113.02(16)
C(38)-C(39)-H(39C)	109.5	N(1)-Ni(1)-N(2)	81.60(9)
H(39A)-C(39)-H(39C)	109.5	N(1)-Ni(1)-Cl(2)	126.76(7)
H(39B)-C(39)-H(39C)	109.5	N(2)-Ni(1)-Cl(2)	114.06(7)
C(38)-C(40)-H(40A)	109.5	N(1)-Ni(1)-Cl(1)	98.34(7)
C(38)-C(40)-H(40B)	109.5	N(2)-Ni(1)-Cl(1)	107.17(7)
H(40A)-C(40)-H(40B)	109.5	Cl(2)-Ni(1)-Cl(1)	121.31(5)

Table 2.8 Crystal data and structure refinement for CuCl2tripbipy

Identification code	cucl2tripbipy	
Empirical formula	C42 H54 Cl8 Cu N2	
Formula weight	934.01	
Temperature	150(2) K	
Wavelength	0.71073 Å	
Crystal system	Orthorhombic	
Space group	P2(1)2(1)2(1)	
Unit cell dimensions	a = 13.785(5) Å	α= 90°.
	b = 16.968(6) Å	β= 90°.
	c = 19.525(7) Å	γ = 90°.
Volume	4567(3) $Å^3$	
Z	4	
Density (calculated)	1.358 Mg/m^3	
Absorption coefficient	0.977 mm^{-1}	
F(000)	1940	
Crystal size	0.30 x 0.25 x 0.25 mm^3	
Theta range for data collection	1.59 to 25.53°.	
Index ranges	-16<=h<=16, -20<=k<=20, -22<=l<=23	
Reflections collected	58105	
Independent reflections	8485 [R(int) = 0.0670]	
Completeness to theta = 25.00°	100.0 %	
Absorption correction	Semi-empirical from equivalents	
Max. and min. transmission	0.7922 and 0.7581	
Refinement method	Full-matrix least-squares on F^2	
Data / restraints / parameters	8485 / 0 / 490	
Goodness-of-fit on F^2	0.955	
Final R indices [I>2sigma(I)]	R1 = 0.0317, wR2 = 0.0732	
R indices (all data)	R1 = 0.0345, wR2 = 0.0753	
Absolute structure parameter	0.00	
Largest diff. peak and hole	0.303 and -0.345 e.$Å^{-3}$	

Table 2.9 Bond lengths [Å] and angles [°] for $CuCl_2$tripbipy

C(1)-N(1)	1.353(3)	C(17)-C(22)	1.405(4)
C(1)-C(2)	1.386(4)	C(17)-C(18)	1.401(4)
C(1)-C(17)	1.493(4)	C(18)-C(19)	1.389(4)
C(2)-C(3)	1.373(4)	C(18)-C(32)	1.524(4)
C(2)-H(2)	0.9500	C(19)-C(20)	1.380(4)
C(3)-C(4)	1.379(4)	C(19)-H(19)	0.9500
C(3)-H(3)	0.9500	C(20)-C(21)	1.389(4)
C(4)-C(5)	1.382(4)	C(20)-C(35)	1.515(4)
C(4)-H(4)	0.9500	C(21)-C(22)	1.388(4)
C(5)-N(1)	1.349(3)	C(21)-H(21)	0.9500
C(5)-C(6)	1.479(4)	C(22)-C(38)	1.526(4)
C(6)-N(2)	1.359(3)	C(23)-C(24)	1.523(4)
C(6)-C(7)	1.381(4)	C(23)-C(25)	1.533(4)
C(7)-C(8)	1.382(4)	C(23)-H(23)	1.0000
C(7)-H(7)	0.9500	C(24)-H(24A)	0.9800
C(8)-C(9)	1.375(4)	C(24)-H(24B)	0.9800
C(8)-H(8)	0.9500	C(24)-H(24C)	0.9800
C(9)-C(10)	1.395(4)	C(25)-H(25A)	0.9800
C(9)-H(9)	0.9500	C(25)-H(25B)	0.9800
C(10)-N(2)	1.350(3)	C(25)-H(25C)	0.9800
C(10)-C(11)	1.489(4)	C(26)-C(28)	1.524(4)
C(11)-C(16)	1.401(4)	C(26)-C(27)	1.532(4)
C(11)-C(12)	1.405(4)	C(26)-H(26)	1.0000
C(12)-C(13)	1.385(4)	C(27)-H(27A)	0.9800
C(12)-C(23)	1.517(4)	C(27)-H(27B)	0.9800
C(13)-C(14)	1.383(4)	C(27)-H(27C)	0.9800
C(13)-H(13)	0.9500	C(28)-H(28A)	0.9800
C(14)-C(15)	1.390(4)	C(28)-H(28B)	0.9800
C(14)-C(26)	1.516(4)	C(28)-H(28C)	0.9800
C(15)-C(16)	1.378(4)	C(29)-C(31)	1.522(4)
C(15)-H(15)	0.9500	C(29)-C(30)	1.526(4)
C(16)-C(29)	1.520(4)	C(29)-H(29)	1.0000

Table 2.9 Cont.

C(30)-H(30A)	0.9800	C(40)-H(40C)	0.9800
C(30)-H(30B)	0.9800	C(41)-Cl(5)	1.752(3)
C(30)-H(30C)	0.9800	C(41)-Cl(4)	1.759(4)
C(31)-H(31A)	0.9800	C(41)-Cl(3)	1.757(3)
C(31)-H(31B)	0.9800	C(41)-H(41)	1.0000
C(31)-H(31C)	0.9800	C(42)-Cl(6)	1.751(3)
C(32)-C(33)	1.529(4)	C(42)-Cl(8)	1.758(3)
C(32)-C(34)	1.533(4)	C(42)-Cl(7)	1.753(3)
C(32)-H(32)	1.0000	C(42)-H(42)	1.0000
C(33)-H(33A)	0.9800	N(1)-Cu(1)	1.980(2)
C(33)-H(33B)	0.9800	N(2)-Cu(1)	2.059(2)
C(33)-H(33C)	0.9800	Cl(1)-Cu(1)	2.2382(9)
C(34)-H(34A)	0.9800	Cl(2)-Cu(1)	2.1741(9)
C(34)-H(34B)	0.9800		
C(34)-H(34C)	0.9800	N(1)-C(1)-C(2)	120.1(2)
C(35)-C(37)	1.508(5)	N(1)-C(1)-C(17)	120.8(2)
C(35)-C(36)	1.504(5)	C(2)-C(1)-C(17)	119.1(2)
C(35)-H(35)	1.0000	C(3)-C(2)-C(1)	120.0(3)
C(36)-H(36A)	0.9800	C(3)-C(2)-H(2)	120.0
C(36)-H(36B)	0.9800	C(1)-C(2)-H(2)	120.0
C(36)-H(36C)	0.9800	C(2)-C(3)-C(4)	119.8(3)
C(37)-H(37A)	0.9800	C(2)-C(3)-H(3)	120.1
C(37)-H(37B)	0.9800	C(4)-C(3)-H(3)	120.1
C(37)-H(37C)	0.9800	C(3)-C(4)-C(5)	118.3(3)
C(38)-C(39)	1.517(4)	C(3)-C(4)-H(4)	120.9
C(38)-C(40)	1.534(4)	C(5)-C(4)-H(4)	120.9
C(38)-H(38)	1.0000	N(1)-C(5)-C(4)	122.0(2)
C(39)-H(39A)	0.9800	N(1)-C(5)-C(6)	115.4(2)
C(39)-H(39B)	0.9800	C(4)-C(5)-C(6)	122.5(2)
C(39)-H(39C)	0.9800	N(2)-C(6)-C(7)	123.0(2)
C(40)-H(40A)	0.9800	N(2)-C(6)-C(5)	115.5(2)
C(40)-H(40B)	0.9800	C(7)-C(6)-C(5)	121.4(2)

Table 2.9 Cont.

C(8)-C(7)-C(6)	118.5(3)	C(18)-C(17)-C(1)	119.7(2)
C(8)-C(7)-H(7)	120.8	C(19)-C(18)-C(17)	118.5(2)
C(6)-C(7)-H(7)	120.8	C(19)-C(18)-C(32)	119.6(3)
C(9)-C(8)-C(7)	118.9(3)	C(17)-C(18)-C(32)	121.8(2)
C(9)-C(8)-H(8)	120.5	C(20)-C(19)-C(18)	122.4(3)
C(7)-C(8)-H(8)	120.5	C(20)-C(19)-H(19)	118.8
C(8)-C(9)-C(10)	120.6(3)	C(18)-C(19)-H(19)	118.8
C(8)-C(9)-H(9)	119.7	C(19)-C(20)-C(21)	118.2(3)
C(10)-C(9)-H(9)	119.7	C(19)-C(20)-C(35)	120.9(3)
N(2)-C(10)-C(9)	120.5(2)	C(21)-C(20)-C(35)	120.9(3)
N(2)-C(10)-C(11)	120.6(2)	C(20)-C(21)-C(22)	121.8(3)
C(9)-C(10)-C(11)	118.8(2)	C(20)-C(21)-H(21)	119.1
C(16)-C(11)-C(12)	120.4(3)	C(22)-C(21)-H(21)	119.1
C(16)-C(11)-C(10)	119.4(2)	C(21)-C(22)-C(17)	118.8(2)
C(12)-C(11)-C(10)	120.0(2)	C(21)-C(22)-C(38)	118.5(2)
C(13)-C(12)-C(11)	118.1(2)	C(17)-C(22)-C(38)	122.4(2)
C(13)-C(12)-C(23)	120.3(2)	C(12)-C(23)-C(24)	111.7(2)
C(11)-C(12)-C(23)	121.7(2)	C(12)-C(23)-C(25)	110.9(2)
C(12)-C(13)-C(14)	122.7(3)	C(24)-C(23)-C(25)	110.2(2)
C(12)-C(13)-H(13)	118.6	C(12)-C(23)-H(23)	108.0
C(14)-C(13)-H(13)	118.6	C(24)-C(23)-H(23)	108.0
C(13)-C(14)-C(15)	117.7(3)	C(25)-C(23)-H(23)	108.0
C(13)-C(14)-C(26)	121.3(3)	C(23)-C(24)-H(24A)	109.5
C(15)-C(14)-C(26)	121.0(3)	C(23)-C(24)-H(24B)	109.5
C(16)-C(15)-C(14)	122.1(3)	H(24A)-C(24)-H(24B)	109.5
C(16)-C(15)-H(15)	118.9	C(23)-C(24)-H(24C)	109.5
C(14)-C(15)-H(15)	118.9	H(24A)-C(24)-H(24C)	109.5
C(15)-C(16)-C(11)	118.9(2)	H(24B)-C(24)-H(24C)	109.5
C(15)-C(16)-C(29)	120.1(2)	C(23)-C(25)-H(25A)	109.5
C(11)-C(16)-C(29)	121.0(2)	C(23)-C(25)-H(25B)	109.5
C(22)-C(17)-C(18)	120.3(2)	H(25A)-C(25)-H(25B)	109.5
C(22)-C(17)-C(1)	119.4(2)	C(23)-C(25)-H(25C)	109.5

Table 2.9 Cont.

H(25A)-C(25)-H(25C)	109.5	C(29)-C(31)-H(31B)	109.5
H(25B)-C(25)-H(25C)	109.5	H(31A)-C(31)-H(31B)	109.5
C(14)-C(26)-C(28)	112.6(3)	C(29)-C(31)-H(31C)	109.5
C(14)-C(26)-C(27)	110.7(2)	H(31A)-C(31)-H(31C)	109.5
C(28)-C(26)-C(27)	110.5(3)	H(31B)-C(31)-H(31C)	109.5
C(14)-C(26)-H(26)	107.7	C(18)-C(32)-C(33)	112.0(3)
C(28)-C(26)-H(26)	107.7	C(18)-C(32)-C(34)	111.7(2)
C(27)-C(26)-H(26)	107.7	C(33)-C(32)-C(34)	109.8(2)
C(26)-C(27)-H(27A)	109.5	C(18)-C(32)-H(32)	107.7
C(26)-C(27)-H(27B)	109.5	C(33)-C(32)-H(32)	107.7
H(27A)-C(27)-H(27B)	109.5	C(34)-C(32)-H(32)	107.7
C(26)-C(27)-H(27C)	109.5	C(32)-C(33)-H(33A)	109.5
H(27A)-C(27)-H(27C)	109.5	C(32)-C(33)-H(33B)	109.5
H(27B)-C(27)-H(27C)	109.5	H(33A)-C(33)-H(33B)	109.5
C(26)-C(28)-H(28A)	109.5	C(32)-C(33)-H(33C)	109.5
C(26)-C(28)-H(28B)	109.5	H(33A)-C(33)-H(33C)	109.5
H(28A)-C(28)-H(28B)	109.5	H(33B)-C(33)-H(33C)	109.5
C(26)-C(28)-H(28C)	109.5	C(32)-C(34)-H(34A)	109.5
H(28A)-C(28)-H(28C)	109.5	C(32)-C(34)-H(34B)	109.5
H(28B)-C(28)-H(28C)	109.5	H(34A)-C(34)-H(34B)	109.5
C(16)-C(29)-C(31)	110.8(2)	C(32)-C(34)-H(34C)	109.5
C(16)-C(29)-C(30)	112.1(2)	H(34A)-C(34)-H(34C)	109.5
C(31)-C(29)-C(30)	111.1(3)	H(34B)-C(34)-H(34C)	109.5
C(16)-C(29)-H(29)	107.5	C(37)-C(35)-C(36)	111.1(3)
C(31)-C(29)-H(29)	107.5	C(37)-C(35)-C(20)	110.2(3)
C(30)-C(29)-H(29)	107.5	C(36)-C(35)-C(20)	113.4(3)
C(29)-C(30)-H(30A)	109.5	C(37)-C(35)-H(35)	107.3
C(29)-C(30)-H(30B)	109.5	C(36)-C(35)-H(35)	107.3
H(30A)-C(30)-H(30B)	109.5	C(20)-C(35)-H(35)	107.3
C(29)-C(30)-H(30C)	109.5	C(35)-C(36)-H(36A)	109.5
H(30A)-C(30)-H(30C)	109.5	C(35)-C(36)-H(36B)	109.5
H(30B)-C(30)-H(30C)	109.5	H(36A)-C(36)-H(36B)	109.5
C(29)-C(31)-H(31A)	109.5	C(35)-C(36)-H(36C)	109.5

Table 2.9 Cont.

H(36A)-C(36)-H(36C)	109.5	H(40B)-C(40)-H(40C)	109.5
H(36B)-C(36)-H(36C)	109.5	Cl(5)-C(41)-Cl(4)	110.53(17)
C(35)-C(37)-H(37A)	109.5	Cl(5)-C(41)-Cl(3)	110.05(18)
C(35)-C(37)-H(37B)	109.5	Cl(4)-C(41)-Cl(3)	109.72(18)
H(37A)-C(37)-H(37B)	109.5	Cl(5)-C(41)-H(41)	108.8
C(35)-C(37)-H(37C)	109.5	Cl(4)-C(41)-H(41)	108.8
H(37A)-C(37)-H(37C)	109.5	Cl(3)-C(41)-H(41)	108.8
H(37B)-C(37)-H(37C)	109.5	Cl(6)-C(42)-Cl(8)	110.18(17)
C(39)-C(38)-C(22)	113.4(2)	Cl(6)-C(42)-Cl(7)	110.82(18)
C(39)-C(38)-C(40)	110.4(2)	Cl(8)-C(42)-Cl(7)	110.21(17)
C(22)-C(38)-C(40)	109.4(2)	Cl(6)-C(42)-H(42)	108.5
C(39)-C(38)-H(38)	107.8	Cl(8)-C(42)-H(42)	108.5
C(22)-C(38)-H(38)	107.8	Cl(7)-C(42)-H(42)	108.5
C(40)-C(38)-H(38)	107.8	C(5)-N(1)-C(1)	119.7(2)
C(38)-C(39)-H(39A)	109.5	C(5)-N(1)-Cu(1)	114.11(17)
C(38)-C(39)-H(39B)	109.5	C(1)-N(1)-Cu(1)	126.18(18)
H(39A)-C(39)-H(39B)	109.5	C(10)-N(2)-C(6)	118.4(2)
C(38)-C(39)-H(39C)	109.5	C(10)-N(2)-Cu(1)	129.80(18)
H(39A)-C(39)-H(39C)	109.5	C(6)-N(2)-Cu(1)	110.92(16)
H(39B)-C(39)-H(39C)	109.5	N(1)-Cu(1)-N(2)	81.75(9)
C(38)-C(40)-H(40A)	109.5	N(1)-Cu(1)-Cl(2)	146.60(7)
C(38)-C(40)-H(40B)	109.5	N(2)-Cu(1)-Cl(2)	109.02(7)
H(40A)-C(40)-H(40B)	109.5	N(1)-Cu(1)-Cl(1)	96.37(7)
C(38)-C(40)-H(40C)	109.5	N(2)-Cu(1)-Cl(1)	128.64(6)
H(40A)-C(40)-H(40C)	109.5	Cl(2)-Cu(1)-Cl(1)	100.21(4)

Table 2.10 Crystal data and structure refinement for $ZnCl_2$tripbipy

Identification code	zncl2tripbipy	
Empirical formula	C41 H53 Cl5 N2 Zn	
Formula weight	816.47	
Temperature	150(2) K	
Wavelength	0.71073 Å	
Crystal system	Monoclinic	
Space group	P2(1)/c	
Unit cell dimensions	a = 8.9639(8) Å	α= 90°.
	b = 28.157(2) Å	β= 99.8660(10)°.
	c = 16.7861(14) Å	γ = 90°.
Volume	4174.0(6) $Å^3$	
Z	4	
Density (calculated)	1.299 Mg/m^3	
Absorption coefficient	0.939 mm^{-1}	
F(000)	1712	
Crystal size	0.30 x 0.30 x 0.10 mm^3	
Theta range for data collection	1.43 to 25.50°.	
Index ranges	-10<=h<=10, -34<=k<=33, -20<=l<=20	
Reflections collected	56541	
Independent reflections	7721 [R(int) = 0.0936]	
Completeness to theta = 25.00°	100.0 %	
Absorption correction	Semi-empirical from equivalents	
Max. and min. transmission	0.9120 and 0.7660	
Refinement method	Full-matrix least-squares on F^2	
Data / restraints / parameters	7721 / 0 / 454	
Goodness-of-fit on F^2	1.013	
Final R indices [I>2sigma(I)]	R1 = 0.0491, wR2 = 0.0999	
R indices (all data)	R1 = 0.0851, wR2 = 0.1135	
Largest diff. peak and hole	0.732 and -0.469 $e.Å^{-3}$	

Table 2.11 Bond lengths [Å] and angles [°] for $ZnCl_2$tripbipy

C(1)-N(1)	1.344(4)	C(17)-C(18)	1.401(4)
C(1)-C(2)	1.391(5)	C(17)-C(22)	1.414(5)
C(1)-C(17)	1.503(4)	C(18)-C(19)	1.403(5)
C(2)-C(3)	1.383(5)	C(18)-C(32)	1.515(5)
C(2)-H(2)	0.9500	C(19)-C(20)	1.394(5)
C(3)-C(4)	1.383(5)	C(19)-H(19)	0.9500
C(3)-H(3)	0.9500	C(20)-C(21)	1.381(5)
C(4)-C(5)	1.385(5)	C(20)-C(35)	1.527(5)
C(4)-H(4)	0.9500	C(21)-C(22)	1.394(5)
C(5)-N(1)	1.368(4)	C(21)-H(21)	0.9500
C(5)-C(6)	1.480(5)	C(22)-C(38)	1.529(5)
C(6)-N(2)	1.360(4)	C(23)-C(24)	1.520(5)
C(6)-C(7)	1.394(5)	C(23)-C(25)	1.529(5)
C(7)-C(8)	1.377(5)	C(23)-H(23)	1.0000
C(7)-H(7)	0.9500	C(24)-H(24A)	0.9800
C(8)-C(9)	1.376(5)	C(24)-H(24B)	0.9800
C(8)-H(8)	0.9500	C(24)-H(24C)	0.9800
C(9)-C(10)	1.390(5)	C(25)-H(25A)	0.9800
C(9)-H(9)	0.9500	C(25)-H(25B)	0.9800
C(10)-N(2)	1.347(4)	C(25)-H(25C)	0.9800
C(10)-C(11)	1.506(4)	C(26)-C(27)	1.497(6)
C(11)-C(16)	1.400(5)	C(26)-C(28)	1.515(6)
C(11)-C(12)	1.411(4)	C(26)-H(26)	1.0000
C(12)-C(13)	1.387(4)	C(27)-H(27A)	0.9800
C(12)-C(23)	1.517(5)	C(27)-H(27B)	0.9800
C(13)-C(14)	1.385(5)	C(27)-H(27C)	0.9800
C(13)-H(13)	0.9500	C(28)-H(28A)	0.9800
C(14)-C(15)	1.387(5)	C(28)-H(28B)	0.9800
C(14)-C(26)	1.533(5)	C(28)-H(28C)	0.9800
C(15)-C(16)	1.398(5)	C(29)-C(31)	1.526(5)
C(15)-H(15)	0.9500	C(29)-C(30)	1.527(5)
C(16)-C(29)	1.524(5)	C(29)-H(29)	1.0000

Table 2.11 Cont.

C(30)-H(30A)	0.9800	C(40)-H(40C)	0.9800
C(30)-H(30B)	0.9800	C(41)-Cl(4)	1.749(4)
C(30)-H(30C)	0.9800	C(41)-Cl(3)	1.758(4)
C(31)-H(31A)	0.9800	C(41)-Cl(5)	1.760(4)
C(31)-H(31B)	0.9800	C(41)-H(41)	1.0000
C(31)-H(31C)	0.9800	N(1)-Zn(1)	2.080(3)
C(32)-C(34)	1.527(5)	N(2)-Zn(1)	2.093(3)
C(32)-C(33)	1.533(5)	Cl(1)-Zn(1)	2.2298(9)
C(32)-H(32)	1.0000	Cl(2)-Zn(1)	2.1833(9)
C(33)-H(33A)	0.9800		
C(33)-H(33B)	0.9800	N(1)-C(1)-C(2)	121.1(3)
C(33)-H(33C)	0.9800	N(1)-C(1)-C(17)	117.4(3)
C(34)-H(34A)	0.9800	C(2)-C(1)-C(17)	121.5(3)
C(34)-H(34B)	0.9800	C(3)-C(2)-C(1)	119.3(3)
C(34)-H(34C)	0.9800	C(3)-C(2)-H(2)	120.3
C(35)-C(37)	1.513(5)	C(1)-C(2)-H(2)	120.3
C(35)-C(36)	1.535(6)	C(2)-C(3)-C(4)	119.8(3)
C(35)-H(35)	1.0000	C(2)-C(3)-H(3)	120.1
C(36)-H(36A)	0.9800	C(4)-C(3)-H(3)	120.1
C(36)-H(36B)	0.9800	C(3)-C(4)-C(5)	118.8(3)
C(36)-H(36C)	0.9800	C(3)-C(4)-H(4)	120.6
C(37)-H(37A)	0.9800	C(5)-C(4)-H(4)	120.6
C(37)-H(37B)	0.9800	N(1)-C(5)-C(4)	121.4(3)
C(37)-H(37C)	0.9800	N(1)-C(5)-C(6)	115.5(3)
C(38)-C(39)	1.523(5)	C(4)-C(5)-C(6)	123.1(3)
C(38)-C(40)	1.536(5)	N(2)-C(6)-C(7)	120.9(3)
C(38)-H(38)	1.0000	N(2)-C(6)-C(5)	116.4(3)
C(39)-H(39A)	0.9800	C(7)-C(6)-C(5)	122.6(3)
C(39)-H(39B)	0.9800	C(8)-C(7)-C(6)	118.8(3)
C(39)-H(39C)	0.9800	C(8)-C(7)-H(7)	120.6
C(40)-H(40A)	0.9800	C(6)-C(7)-H(7)	120.6
C(40)-H(40B)	0.9800	C(9)-C(8)-C(7)	120.1(3)

Table 2.11 Cont.

C(9)-C(8)-H(8)	120.0	C(20)-C(19)-C(18)	121.4(3)
C(7)-C(8)-H(8)	120.0	C(20)-C(19)-H(19)	119.3
C(8)-C(9)-C(10)	119.3(3)	C(18)-C(19)-H(19)	119.3
C(8)-C(9)-H(9)	120.3	C(21)-C(20)-C(19)	119.0(3)
C(10)-C(9)-H(9)	120.3	C(21)-C(20)-C(35)	120.1(3)
N(2)-C(10)-C(9)	120.9(3)	C(19)-C(20)-C(35)	120.7(3)
N(2)-C(10)-C(11)	116.8(3)	C(20)-C(21)-C(22)	122.0(3)
C(9)-C(10)-C(11)	122.1(3)	C(20)-C(21)-H(21)	119.0
C(16)-C(11)-C(12)	121.2(3)	C(22)-C(21)-H(21)	119.0
C(16)-C(11)-C(10)	117.9(3)	C(21)-C(22)-C(17)	118.2(3)
C(12)-C(11)-C(10)	120.9(3)	C(21)-C(22)-C(38)	120.8(3)
C(13)-C(12)-C(11)	118.2(3)	C(17)-C(22)-C(38)	120.9(3)
C(13)-C(12)-C(23)	121.1(3)	C(12)-C(23)-C(24)	114.7(3)
C(11)-C(12)-C(23)	120.6(3)	C(12)-C(23)-C(25)	109.4(3)
C(14)-C(13)-C(12)	121.9(3)	C(24)-C(23)-C(25)	109.2(3)
C(14)-C(13)-H(13)	119.0	C(12)-C(23)-H(23)	107.8
C(12)-C(13)-H(13)	119.0	C(24)-C(23)-H(23)	107.8
C(13)-C(14)-C(15)	118.7(3)	C(25)-C(23)-H(23)	107.8
C(13)-C(14)-C(26)	118.4(3)	C(23)-C(24)-H(24A)	109.5
C(15)-C(14)-C(26)	122.9(3)	C(23)-C(24)-H(24B)	109.5
C(14)-C(15)-C(16)	122.0(3)	H(24A)-C(24)-H(24B)	109.5
C(14)-C(15)-H(15)	119.0	C(23)-C(24)-H(24C)	109.5
C(16)-C(15)-H(15)	119.0	H(24A)-C(24)-H(24C)	109.5
C(15)-C(16)-C(11)	117.9(3)	H(24B)-C(24)-H(24C)	109.5
C(15)-C(16)-C(29)	119.8(3)	C(23)-C(25)-H(25A)	109.5
C(11)-C(16)-C(29)	122.4(3)	C(23)-C(25)-H(25B)	109.5
C(18)-C(17)-C(22)	120.9(3)	H(25A)-C(25)-H(25B)	109.5
C(18)-C(17)-C(1)	119.1(3)	C(23)-C(25)-H(25C)	109.5
C(22)-C(17)-C(1)	120.0(3)	H(25A)-C(25)-H(25C)	109.5
C(17)-C(18)-C(19)	118.4(3)	H(25B)-C(25)-H(25C)	109.5
C(17)-C(18)-C(32)	122.4(3)	C(27)-C(26)-C(28)	113.4(4)
C(19)-C(18)-C(32)	119.2(3)	C(27)-C(26)-C(14)	114.2(3)

Table 2.11 Cont.

C(28)-C(26)-C(14)	110.8(3)	H(31B)-C(31)-H(31C)	109.5
C(27)-C(26)-H(26)	105.9	C(18)-C(32)-C(34)	110.7(3)
C(28)-C(26)-H(26)	105.9	C(18)-C(32)-C(33)	113.0(3)
C(14)-C(26)-H(26)	105.9	C(34)-C(32)-C(33)	109.7(3)
C(26)-C(27)-H(27A)	109.5	C(18)-C(32)-H(32)	107.7
C(26)-C(27)-H(27B)	109.5	C(34)-C(32)-H(32)	107.7
H(27A)-C(27)-H(27B)	109.5	C(33)-C(32)-H(32)	107.7
C(26)-C(27)-H(27C)	109.5	C(32)-C(33)-H(33A)	109.5
H(27A)-C(27)-H(27C)	109.5	C(32)-C(33)-H(33B)	109.5
H(27B)-C(27)-H(27C)	109.5	H(33A)-C(33)-H(33B)	109.5
C(26)-C(28)-H(28A)	109.5	C(32)-C(33)-H(33C)	109.5
C(26)-C(28)-H(28B)	109.5	H(33A)-C(33)-H(33C)	109.5
H(28A)-C(28)-H(28B)	109.5	H(33B)-C(33)-H(33C)	109.5
C(26)-C(28)-H(28C)	109.5	C(32)-C(34)-H(34A)	109.5
H(28A)-C(28)-H(28C)	109.5	C(32)-C(34)-H(34B)	109.5
H(28B)-C(28)-H(28C)	109.5	H(34A)-C(34)-H(34B)	109.5
C(16)-C(29)-C(31)	110.0(3)	C(32)-C(34)-H(34C)	109.5
C(16)-C(29)-C(30)	112.5(3)	H(34A)-C(34)-H(34C)	109.5
C(31)-C(29)-C(30)	111.1(3)	H(34B)-C(34)-H(34C)	109.5
C(16)-C(29)-H(29)	107.7	C(37)-C(35)-C(20)	113.3(3)
C(31)-C(29)-H(29)	107.7	C(37)-C(35)-C(36)	109.8(3)
C(30)-C(29)-H(29)	107.7	C(20)-C(35)-C(36)	109.6(3)
C(29)-C(30)-H(30A)	109.5	C(37)-C(35)-H(35)	108.0
C(29)-C(30)-H(30B)	109.5	C(20)-C(35)-H(35)	108.0
H(30A)-C(30)-H(30B)	109.5	C(36)-C(35)-H(35)	108.0
C(29)-C(30)-H(30C)	109.5	C(35)-C(36)-H(36A)	109.5
H(30A)-C(30)-H(30C)	109.5	C(35)-C(36)-H(36B)	109.5
H(30B)-C(30)-H(30C)	109.5	H(36A)-C(36)-H(36B)	109.5
C(29)-C(31)-H(31A)	109.5	C(35)-C(36)-H(36C)	109.5
C(29)-C(31)-H(31B)	109.5	H(36A)-C(36)-H(36C)	109.5
H(31A)-C(31)-H(31B)	109.5	H(36B)-C(36)-H(36C)	109.5
C(29)-C(31)-H(31C)	109.5	C(35)-C(37)-H(37A)	109.5
H(31A)-C(31)-H(31C)	109.5	C(35)-C(37)-H(37B)	109.5

Table 2.11 Cont.

H(37A)-C(37)-H(37B)	109.5	H(40A)-C(40)-H(40C)	109.5
C(35)-C(37)-H(37C)	109.5	H(40B)-C(40)-H(40C)	109.5
H(37A)-C(37)-H(37C)	109.5	Cl(4)-C(41)-Cl(3)	110.9(2)
H(37B)-C(37)-H(37C)	109.5	Cl(4)-C(41)-Cl(5)	109.8(2)
C(39)-C(38)-C(22)	113.8(3)	Cl(3)-C(41)-Cl(5)	110.1(2)
C(39)-C(38)-C(40)	109.5(3)	Cl(4)-C(41)-H(41)	108.7
C(22)-C(38)-C(40)	110.7(3)	Cl(3)-C(41)-H(41)	108.7
C(39)-C(38)-H(38)	107.5	Cl(5)-C(41)-H(41)	108.7
C(22)-C(38)-H(38)	107.5	C(1)-N(1)-C(5)	119.6(3)
C(40)-C(38)-H(38)	107.5	C(1)-N(1)-Zn(1)	126.5(2)
C(38)-C(39)-H(39A)	109.5	C(5)-N(1)-Zn(1)	113.2(2)
C(38)-C(39)-H(39B)	109.5	C(10)-N(2)-C(6)	119.9(3)
H(39A)-C(39)-H(39B)	109.5	C(10)-N(2)-Zn(1)	127.1(2)
C(38)-C(39)-H(39C)	109.5	C(6)-N(2)-Zn(1)	112.9(2)
H(39A)-C(39)-H(39C)	109.5	N(1)-Zn(1)-N(2)	79.72(10)
H(39B)-C(39)-H(39C)	109.5	N(1)-Zn(1)-Cl(2)	122.92(8)
C(38)-C(40)-H(40A)	109.5	N(2)-Zn(1)-Cl(2)	114.79(8)
C(38)-C(40)-H(40B)	109.5	N(1)-Zn(1)-Cl(1)	104.10(8)
H(40A)-C(40)-H(40B)	109.5	N(2)-Zn(1)-Cl(1)	111.54(8)
C(38)-C(40)-H(40C)	109.5	Cl(2)-Zn(1)-Cl(1)	117.71(4)

Table 2.12 Crystal data and structure refinement for tripbipy

Identification code	eb_091124_0m	
Empirical formula	C40 H52 N2	
Formula weight	560.84	
Temperature	100(2) K	
Wavelength	0.71073 Å	
Crystal system	Triclinic	
Space group	P-1	
Unit cell dimensions	a = 6.172(3) Å	α= 80.360(6)°.
	b = 8.333(4) Å	β= 85.552(7)°.
	c = 16.679(7) Å	γ = 83.180(6)°.
Volume	838.2(6) $Å^3$	
Z	1	
Density (calculated)	1.111 Mg/m^3	
Absorption coefficient	0.063 mm^{-1}	
F(000)	306	
Crystal size	0.50 x 0.40 x 0.05 mm^3	
Theta range for data collection	2.48 to 27.48°.	
Index ranges	-7<=h<=7, -10<=k<=10, 0<=l<=21	
Reflections collected	5713	
Independent reflections	5713 [R(int) = 0.0000]	
Completeness to theta = 25.00°	99.8 %	
Absorption correction	None	
Max. and min. transmission	0.9968 and 0.9690	
Refinement method	Full-matrix least-squares on F^2	
Data / restraints / parameters	5713 / 0 / 197	
Goodness-of-fit on F^2	1.131	
Final R indices [I>2sigma(I)]	R1 = 0.0793, wR2 = 0.1724	
R indices (all data)	R1 = 0.1008, wR2 = 0.1823	
Largest diff. peak and hole	0.291 and -0.296 $e.Å^{-3}$	

Table 2.13 Bond lengths [Å] and angles [°] for tripbipy

N(1)-C(1)	1.346(3)	C(15)-H(15)	1.0000
N(1)-C(5)	1.350(3)	C(16)-H(16A)	0.9800
C(1)-C(2)	1.400(3)	C(16)-H(16B)	0.9800
C(1)-C(1)#1	1.490(5)	C(16)-H(16C)	0.9800
C(2)-C(3)	1.383(4)	C(17)-H(17A)	0.9800
C(2)-H(2)	0.9500	C(17)-H(17B)	0.9800
C(3)-C(4)	1.387(4)	C(17)-H(17C)	0.9800
C(3)-H(3)	0.9500	C(18)-C(19)	1.522(3)
C(4)-C(5)	1.397(3)	C(18)-C(20)	1.539(4)
C(4)-H(4)	0.9500	C(18)-H(18)	1.0000
C(5)-C(6)	1.502(3)	C(19)-H(19A)	0.9800
C(6)-C(7)	1.404(3)	C(19)-H(19B)	0.9800
C(6)-C(11)	1.415(3)	C(19)-H(19C)	0.9800
C(7)-C(8)	1.397(3)	C(20)-H(20A)	0.9800
C(7)-C(12)	1.532(3)	C(20)-H(20B)	0.9800
C(8)-C(9)	1.397(3)	C(20)-H(20C)	0.9800
C(8)-H(8)	0.9500		
C(9)-C(10)	1.396(3)	C(1)-N(1)-C(5)	118.0(2)
C(9)-C(15)	1.525(3)	N(1)-C(1)-C(2)	122.5(2)
C(10)-C(11)	1.395(3)	N(1)-C(1)-C(1)#1	116.9(3)
C(10)-H(10)	0.9500	C(2)-C(1)-C(1)#1	120.5(3)
C(11)-C(18)	1.523(3)	C(3)-C(2)-C(1)	118.7(2)
C(12)-C(14)	1.536(4)	C(3)-C(2)-H(2)	120.6
C(12)-C(13)	1.536(4)	C(1)-C(2)-H(2)	120.6
C(12)-H(12)	1.0000	C(2)-C(3)-C(4)	119.3(2)
C(13)-H(13A)	0.9800	C(2)-C(3)-H(3)	120.3
C(13)-H(13B)	0.9800	C(4)-C(3)-H(3)	120.3
C(13)-H(13C)	0.9800	C(3)-C(4)-C(5)	118.6(2)
C(14)-H(14A)	0.9800	C(3)-C(4)-H(4)	120.7
C(14)-H(14B)	0.9800	C(5)-C(4)-H(4)	120.7
C(14)-H(14C)	0.9800	N(1)-C(5)-C(4)	122.6(2)
C(15)-C(17)	1.529(4)	N(1)-C(5)-C(6)	116.0(2)
C(15)-C(16)	1.536(4)	C(4)-C(5)-C(6)	121.4(2)

Table 2.13 Cont.

C(7)-C(6)-C(11)	120.3(2)	H(14A)-C(14)-H(14B)	109.5
C(7)-C(6)-C(5)	120.2(2)	C(12)-C(14)-H(14C)	109.5
C(11)-C(6)-C(5)	119.4(2)	H(14A)-C(14)-H(14C)	109.5
C(8)-C(7)-C(6)	119.0(2)	H(14B)-C(14)-H(14C)	109.5
C(8)-C(7)-C(12)	119.6(2)	C(9)-C(15)-C(17)	111.6(2)
C(6)-C(7)-C(12)	121.4(2)	C(9)-C(15)-C(16)	111.9(2)
C(7)-C(8)-C(9)	122.0(2)	C(17)-C(15)-C(16)	110.3(2)
C(7)-C(8)-H(8)	119.0	C(9)-C(15)-H(15)	107.6
C(9)-C(8)-H(8)	119.0	C(17)-C(15)-H(15)	107.6
C(10)-C(9)-C(8)	117.8(2)	C(16)-C(15)-H(15)	107.6
C(10)-C(9)-C(15)	120.4(2)	C(15)-C(16)-H(16A)	109.5
C(8)-C(9)-C(15)	121.8(2)	C(15)-C(16)-H(16B)	109.5
C(11)-C(10)-C(9)	122.5(2)	H(16A)-C(16)-H(16B)	109.5
C(11)-C(10)-H(10)	118.8	C(15)-C(16)-H(16C)	109.5
C(9)-C(10)-H(10)	118.8	H(16A)-C(16)-H(16C)	109.5
C(10)-C(11)-C(6)	118.4(2)	H(16B)-C(16)-H(16C)	109.5
C(10)-C(11)-C(18)	120.8(2)	C(15)-C(17)-H(17A)	109.5
C(6)-C(11)-C(18)	120.7(2)	C(15)-C(17)-H(17B)	109.5
C(7)-C(12)-C(14)	112.4(2)	H(17A)-C(17)-H(17B)	109.5
C(7)-C(12)-C(13)	110.8(2)	C(15)-C(17)-H(17C)	109.5
C(14)-C(12)-C(13)	110.7(2)	H(17A)-C(17)-H(17C)	109.5
C(7)-C(12)-H(12)	107.6	H(17B)-C(17)-H(17C)	109.5
C(14)-C(12)-H(12)	107.6	C(19)-C(18)-C(11)	113.7(2)
C(13)-C(12)-H(12)	107.6	C(19)-C(18)-C(20)	110.2(2)
C(12)-C(13)-H(13A)	109.5	C(11)-C(18)-C(20)	110.1(2)
C(12)-C(13)-H(13B)	109.5	C(19)-C(18)-H(18)	107.5
H(13A)-C(13)-H(13B)	109.5	C(11)-C(18)-H(18)	107.5
C(12)-C(13)-H(13C)	109.5	C(20)-C(18)-H(18)	107.5
H(13A)-C(13)-H(13C)	109.5	C(18)-C(19)-H(19A)	109.5
H(13B)-C(13)-H(13C)	109.5	C(18)-C(19)-H(19B)	109.5
C(12)-C(14)-H(14A)	109.5	H(19A)-C(19)-H(19B)	109.5
C(12)-C(14)-H(14B)	109.5	C(18)-C(19)-H(19C)	109.5

Table 2.13 Cont.

H(19A)-C(19)-H(19C)	109.5	H(20A)-C(20)-H(20B)	109.5
H(19B)-C(19)-H(19C)	109.5	C(18)-C(20)-H(20C)	109.5
C(18)-C(20)-H(20A)	109.5	H(20A)-C(20)-H(20C)	109.5
C(18)-C(20)-H(20B)	109.5	H(20B)-C(20)-H(20C)	109.5

Symmetry transformations used to generate equivalent atoms:
#1 -x+2,-y+1,-z+

Chapter 3

Stabilization of intermediates through the use of a bulky bipyridine, 6,6'-(2,4,6-triisopropylphenyl)-2,2'-bipyridine, in the reduction of CO_2 by rhenium polypyridyl complexes.

3.1 Introduction

Of the known electrocatalysts for the reduction of CO_2, Re(bipy)$(CO)_3$Cl, originally studied by Lehn,[1, 2] is one of the most robust and well-characterized systems. Many groups have studied the electrocatalytic, photocatalyic, and photophysical properties of this system and its analogs. Through all this study, however, there has been a lack of structural data for various proposed mechanisms.

Therefore, we set out to study the structural properties of the catalyst and its intermediates.

In previous studies by Meyer,[3] others,[4-6] and ourselves,[7] it was proposed that the first reduction of the complex is a bipyrine-based reduction followed by electron transfer to the metal with subsequent halide loss (Scheme 3.1). Further reduction of this complex results in the formation of the catalytically active Re(-1) species, which can then react with CO_2. However, some of these reduced intermediates have been shown to dimerize and form M–M bonds.[3-5] In order to prevent this unproductive side reaction we sought to add steric bulk to the bipyridine. With our previous success using 6,6'-(2,4,6-triisopropylphenyl)-2,2'-bipyridine (tripbipy) to crystalize the series

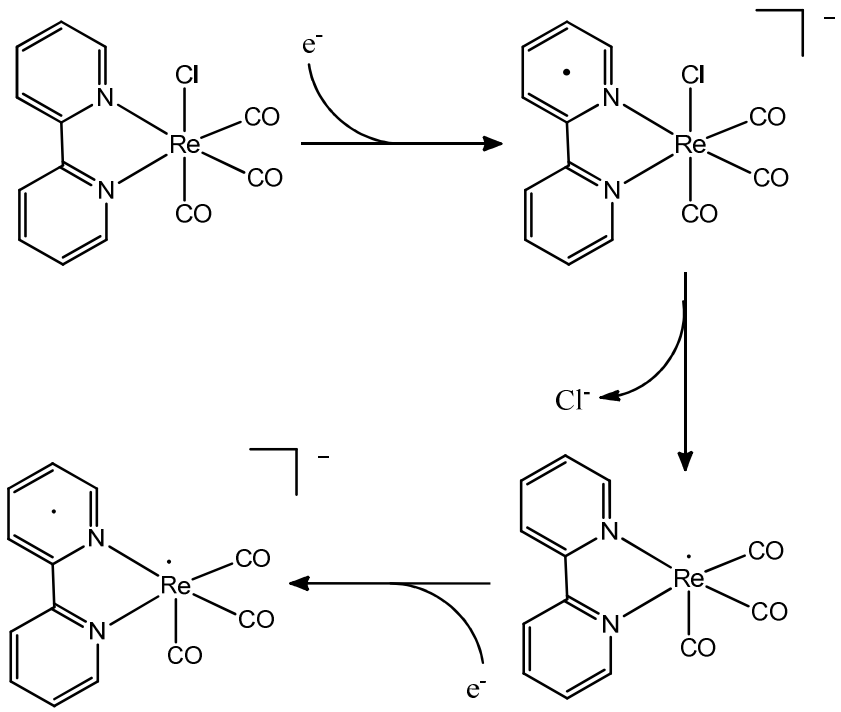

Scheme 3.1 Proposed precatalytic mechanism for the formation of the active Re(-1) anion.

of M(tripbipy)Cl_2 (M=Fe, Co, Ni, Cu, Zn) complexes,[8] we thought to extended this work to the rhenium tricarbonyl bipyrine system.

3.2 Results and discussion

3.2.1 Synthesis and FTIR spectroscopy

Re(tripbipy)$(CO)_3Cl$ (**1**) was synthesized by the reflux of $Re(CO)_5Cl$ and tripbipy in toluene, proceeding with yields in excess of 76%. Complex (**1**) exists as a yellow powder and is soluble in ACN, THF, and halogenated solvents. Reduction of the starting halide complex using 1.1 equivalents of KC_8 or Na/Hg amalgam in THF results in a red solution of the neutral species, Re(tripbipy)$(CO)_3$ (**2**). Reduction of (**1**) using 2.5 equivalents of KC_8 results in the clean (FTIR) formation of the deep purple anionic species, [Re(tripbipy)$(CO)_3$][$K(THF)_2$] (**3**).

One of the advantages of these *fac*-tricarbonyl complexes is the ability to follow the reductions by their characteristic IR stretching frequencies. Backbonding from the metal center into the π^* orbitals results in a decreased ν(CO) stretching frequency of the carbonyls, giving a good marker for the electron density at the metal center. After the first reduction of the complex the high energy band shifts 25 cm^{-1} lower in energy. The two electron reduction shifts the high energy band a total of 61 cm^{-1} to 1955 cm^{-1}. Complex (**3**) displays additional bands in the ν(CO) region assigned to coordination from the potassium counterion (*vide infra*). When 18-crown-6 ether is added to the solution of (**3**), formation of the encapsulated potassium complex can be seen, resulting in the formation of [Re(tripbipy)$(CO)_3$][K(18-crown-

6)] (**4**) which has three distinct peaks in the ν(CO) region. ν(CO) stretching frequencies for (**1**)-(**4**) can be found in Table 3.1.

In previous studies,[4, 5, 7] the one-electron reduction of the bipyridine ligand resulted in a shift of the high energy band of ~20 cm^{-1} to form the $[Re(bpy)(CO)_3Cl]^{-1}$ species, which then shuttles the electron to the metal center and shifts another 20 cm^{-1}. The first shift is consistent with a ligand-based reduction and the total shift of *ca*. 40 cm^{-1} is consistent with the oxidation state of the metal changing to form the bpy^0Re^0 species. The transfer of another electron to the complex results in another shift of ~40 cm^{-1} to between 1940-1950 cm^{-1}. From the IR spectra of (**2**) we see an intermediate shift that falls roughly in between the two previously reported species. This could be attributed to the change in solvent, lack of supporting electrolyte, or difference in ligand properties (sterics and electronics). Complexes (**3**) and (**4**) have similar high energy stretches near 1955 cm^{-1} and, again, are slightly higher than previously reported anions where ν(CO) stretches are observed at 1943 cm^{-1} and 1947cm^{-1} for $[Re(bpy\text{-}tBu)(CO)_3]^{-1}$ and $[Re(bpy)(CO)_3]^{-1}$ respectively. Attempts to obtain FTIR-

Table 3.1 IR stretching frequencies for compounds **1-4**

Compound	ν(CO) (cm^{-1})
$Re(tripbipy)(CO)_3Cl$ (**1**)	2017, 1913, 1890
$Re(tripbipy)(CO)_3$ (**2**)	1992, 1895, 1870
$[Re(tripbipy)(CO)_3][K(THF)_2]$ (**3**)	1955, 1927, 1854, 1838, 1801
[Re(tripbipy)(CO)$_3$][K(18-crown-6)(THF)] (**4**)	1956, 1855, 1839

SEC data for Re(tripbipy)$(CO)_3$Cl have been unsuccessful thus far due too prohibitively negative reduction potentials.

3.2.2 Electrochemistry

Electrochemistry of (**1**) in THF is shown in Figure 3.1. There are two reductions, one at -2.03 V and a second at -2.69 V vs Fc/Fc^+. The first reduction is reversible and attributed to a ligand-based reduction, while the second is an irreversible metal-based reduction. The electrochemistry is similar to Re(bpy)$(CO)_3$Cl, but the potentials are shifted significantly more cathodic, possibly due to the added reorganization energy from the large triisopropylphenyl groups.

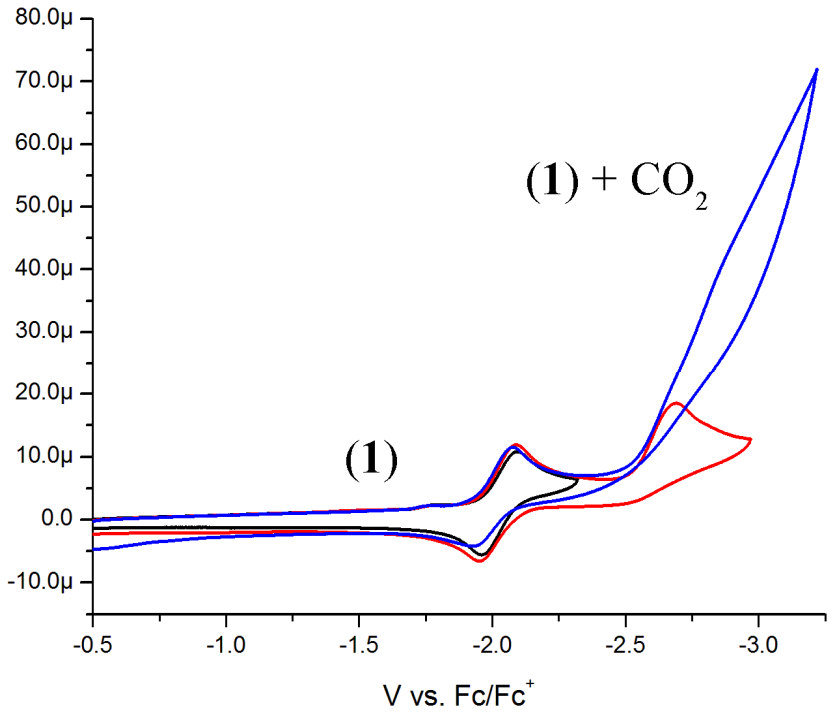

Figure 3.1 Cyclic voltammetry of 1mM Re(tripbipy)$(CO)_3$Cl in THF at 100mV/s using a glassy carbon working electrode, Pt counter, and silver wire reference with Fc as an internal standard**.**

Under an atmosphere of CO_2 an increase in current is observed at the second reduction, however with potentials this negative we appear to be on the edge of the solvent window. It is inferred from similar studies, as well as the presence of CO in the headspace after bulk electrolysis, that this complex is a CO_2 reduction electrocatalyst, albeit not a very good one.

3.2.3 X-Ray crystallography

Single crystals of (**1**) were grown from the vapor diffusion of Et_2O into an ACN solution of the complex. The complex crystallizes in the space group C 2/c and the rhenium atom lies on a special position. The rhenium center is coordinated by three facial carbonyls, the chelating tripbipy, and a chloride in the axial position (Figure 3.2). Due to the crystal having higher symmetry than the molecule, the axial

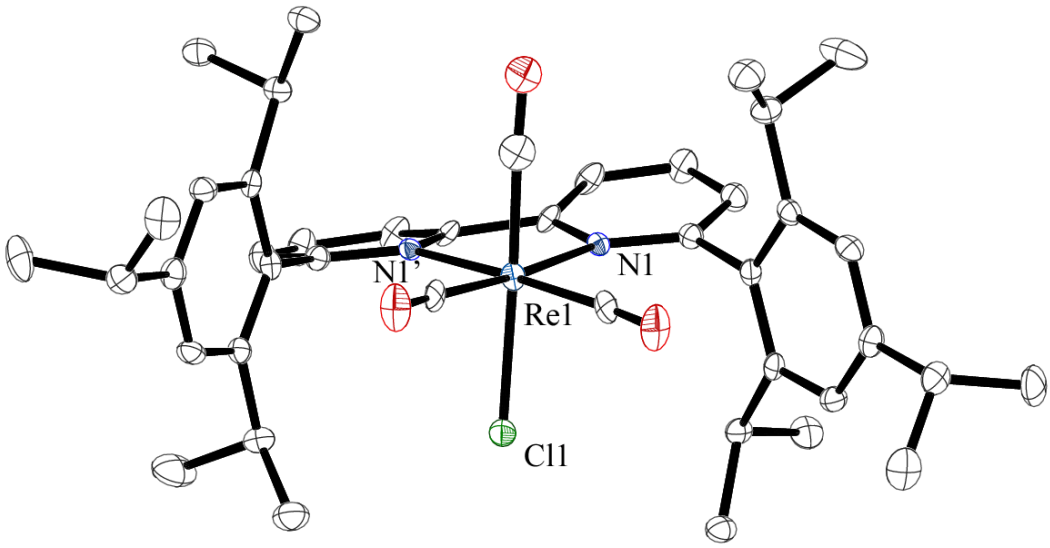

Figure 3.2 Molecular structure of Re(tripbipy)$(CO)_3$Cl, hydrogen atoms removed for clarity. Ellipsoids are set at the 50% probability level.

chloride and carbonyls are disordered within the crystal. The triispropylphenyl group is nearly orthogonal to the pyridyl group (80.46°) and there is significant distortion of the bipyridine as the two pyridyl planes have a twist of 19.17°. The bite angle of the bipyridine is 51.68°, which is similar to what is seen with the unsubstituted bipyridine complex (52.51°).[9]

Crystals of complexes (**2-4**) suitable for diffraction were grown from the vapor diffusion of pentane into a solution of the respective complex in THF. Complex (**2**) crystalizes in the same space group as (**1**) and is structurally similar with the notable exception of the loss of chloride (Figure 3.3). While no electron density was found suitable for a chloride, there is the possibility that a hydride could have been formed that was not observed in the XRD structure. To address this concern, the remaining crystals from the crystallization vial were placed in a mortar and pestle with mineral

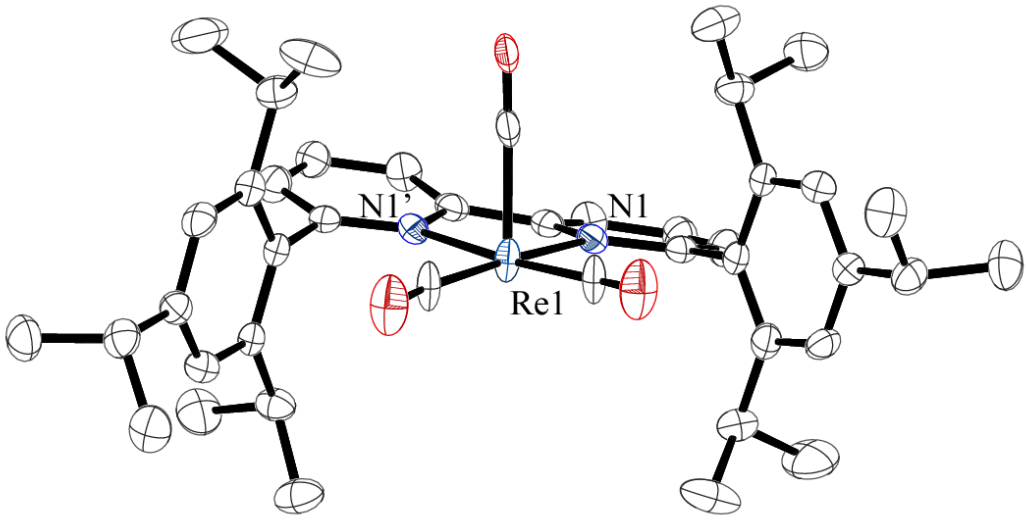

Figure 3.3 Molecular structure of Re(tripbipy)$(CO)_3$, hydrogen atoms removed for clarity. Ellipsoids are set at the 50% probability level.

oil to form a mull. While the ν(CO) stretching frequencies (1992, 1895, 1870 cm^{-1}) are close to what is seen with the $Re(bpy)(CO)_3H$ we do not see a peak assignable to a Re-H stretch, reported at 2018 cm^{-1} for $Re(bpy)(CO)_3H$.[10]

The anion (**3**) crystalizes in the space group Pnma with one disordered THF solvent of crystallization, and again the rhenium atom lies on a special position. The rhenium adopts a pseudo-square planar geometry with a τ_5 value of 0.24, where 0 represents a perfect square planar complex and 1 represents that of an ideal trigonal bipyrimid.[11] The potassium cation is coordinated by two disordered THF solvent molecules, two equatorial carbonyls of one $[Re(tripbipy)(CO)_3]^{-1}$ anion and an axial carbonyl from an adjacent anion (Figure 3.4). After reduction, the bipyridine

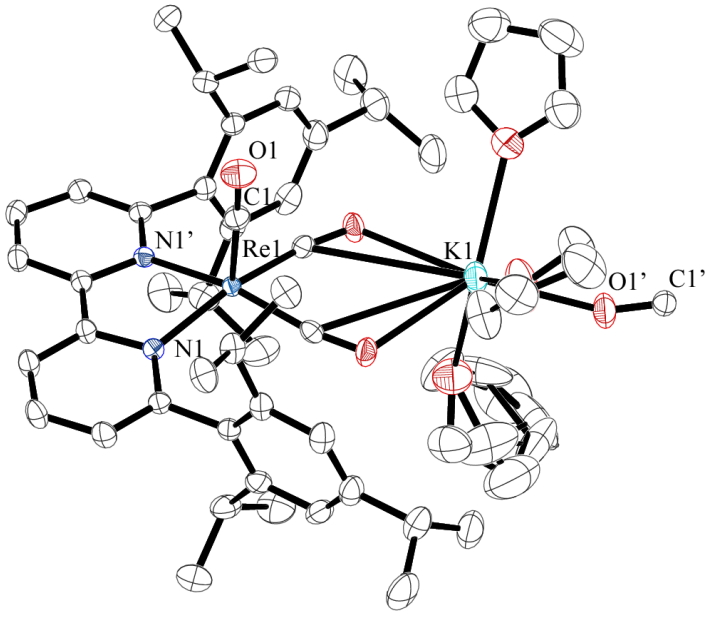

Figure 3.4 Molecular structure of $[Re(tripbipy)(CO)_3][K(THF)2]\cdot THF$, hydrogen atoms and disordered THF molecule removed for clarity. Ellipsoids are set at the 50% probability level.

backbone increases in planarity (twist angle = 0.00°, fold angle = 8.03°, for the two pyridyl groups), and bond alternation can be seen (Table 3.3, appendix), suggesting that there is significant electron density in the bipyridine π* orbital. A structural overlay of compound's **1-3** can be found in the appendix (Figure 3.7).

We were successful in growing crystals of (**4**) and show that, upon encapsulation of the potassium with the crown ether, the local coordination environment around the rhenium center does not change. In the asymmetric unit the $[K(18\text{-crown-6})(THF]^+$ lies on a special position and was disordered around the site of symmetry, and we were unsuccessful in modeling the disorder. While this could be partially modeled (R1~0.11), the geometry around the rhenium center did not significantly change from (**3**) so the electron density from the $K(18\text{-crown-6})(THF)^+$ counterion was removed using PLATON/SQUEEZE[12] so the geometry around the rhenium center could be modeled better (Figure 3.6, appendix).

A useful marker for the occupancy of the bipyridine π* orbital is the bridging

Table 3.2 Distance between bridging carbons for compounds **1-3**. 2,2'-bipridine distances from Goicoechea *et al.*[13]

2,2'-bipyridine	1.490(3)
2,2'-bipyridine $^-$	1.431(3)
2,2'-bipyridine $^{2-}$	1.399(6)
$Re(tripbipy)(CO)_3Cl$	1.478(8)
$Re(tripbipy)(CO)_3$	1.469(14)
$Re(tripbipy)(CO)_3^-$	1.403(4)

2,2' carbon distance,[13] Table 3.2 gives the bridging bond lengths for compounds **1-3** and three bipyridine ligands in different formal oxidation states. As expected, the bond distance does not change significantly for compounds (**1**) and (**2**), leading us to believe that the additional electron is centered on the metal. It is not until we start populating the π* orbital of the ligand with the second electron that we start to see more of a double bond character between the two bridging carbons.

Since the bond distance was close to that of bpy^{2-}, we employed the use of DFT (using ADF 2007.1) to aid in understanding the electronic ground state. The calculated HOMO is a hybrid involving both the ligand and the metal center, containing substantial π* character (Figure 3.5, xyz coordinates in Table 3.12). This is consistent with the observed bond length alternation and suggests that the complex is a reduced bipyridine coordinated to a Re(0) atom. The difference in bond lengths is then attributed to the coordination of the transition metal atom. The 2,2' bridging bond distance of (**1**) is smaller for the coordinated bipyridine than is seen in the free bipyridine. Since these early studies we have employed X-Ray absorption near edge structure (XANES) to better understand the electronics of the ground state (Chapter 6).

3.3 Conclusions

Tripbipy has shown its ability to stabilize compounds of relevance to the electrocatalytic reduction of carbon dioxide. We have been able to crystalize and characterize a set of compounds in three different formal oxidation states. The five coordinate $[Re(tripbipy)(CO)_3]^{-1}$ anion is one of the first crystal structures reported that is relevant to an active site of an electrocatalyst. From the X-Ray diffraction and

computational studies we believe that the anionic state is mainly Re(0) in nature with a reduced bipyridine storing the charge for the two electron reduction of carbon dioxide to carbon monoxide.

3.4 Experimental

General Considerations: Tripbipy and KC_8 were synthesized by previously reported methods.[8, 14] THF and Pentane were sparged with argon and dried over basic alumina with a custom dry solvent system and then stored over activated molecular sieves under an inert atmosphere in a dry box. 18-crown-6 was recrystallized from acetonitrile, tetrabutylammonium hexafluorophosphate (TBAH) was recrystallized twice from methanol, and both were dried in vacuo. All other chemicals were purchased from commercial sources and used as received. Elemental analysis was performed by Midwest MicroLab, LLC, Indianapolis, IN.

Crystallographic Structure Determinations. Single-crystal X-ray structure determinations were carried out at 150(2) K on either a Bruker P4 or Platform Diffractometer using Mo Kα radiation (λ = 0.71073 Å) in conjunction with a Bruker APEX detector. All structures were solved by direct methods using SHELXS-97 and refined with full-matrix least-squares procedures using SHELXL-97.[15] Crystallographic data collection and refinement information can be found in the appendix.

Computational methods. The DFT calculations were performed with the Amsterdam Density Functional (ADF) program suite [16, 17], version 2007.1 using the triple-ζ Slater-type orbital basis set. Zero-order regular approximation (ZORA) [18, 19] was included

for relativistic effects in conjunction with the local density approximation of Vosko *et al.* (VWN).[20] Generalized gradient approximations for electron exchange and correlation were used as described by Becke[21] and Perdew [22, 23]. Molecular orbitals and final geometries were visualized with ADF-GUI.

Synthesis of Re(tripbipy)(CO)$_3$Cl. To a solution of Re(CO)$_5$Cl in 25 mL toluene (100.0 mg, 0.276 mmol) 155.0 mg of tripbipy (0.276 mmol) was added and the solution was refluxed for one hour. The deep orange solution was evaporated to a powder, brought up in chloroform, filtered and recrystallized to yield 183 mg (0.211 mmol, 76.4%) of Re(tripbipy)(CO)$_3$Cl. ^{1}H NMR (400 MHz, CD_2CL_2, 20 °C): δ 0.91 (d, 3H, J = 7 Hz), δ 0.97 (d, 3H, J = 7 Hz), δ 1.23 (d, 9H, J = 7 Hz), δ 1.30 (d, 3H, J = 7 Hz), δ 2.57 (sep., 2H, J = 7 Hz), δ 2.90 (sep., 1H, J = 7 Hz), δ 7.10 (d, 4H, J = 6 Hz), δ 7.52 (d, 2H, J = 7 Hz), δ 8.02 (t, 2H, J = 8 Hz), δ 8.27 (d, 2H, J = 7 Hz). IR(THF) ν(CO): 1990, 1952, 1986, 1862 cm-1. Anal. Calcd for **1**, $C_{42}H_{52}ClN_4O_3Re$: C, 59.60; H, 6.05; N, 3.23. Found: C, 61.94; H, 6.41; N, 3.47.

Synthesis of Re(tripbipy)(CO)$_3$. 25 mg (0.029 mmol) of Re(tripbipy)(CO)$_3$Cl was dissolved in 10 mL of THF and cooled to -35°C in the freezer of the glove box. 1.1 eq of KC_8 (4.3 mg, 0.032 mmol) was then added to the solution and it was allowed to warm to room temperature for an hour. The solution was then filtered through a short plug of silica gel and evaporated to dryness. X-ray quality crystals were grown by the vapor diffusion of pentane in to a THF solution of the complex. IR(nujol) ν(CO): 1992, 1895, 1870 cm^{-1}

Reduction of Re(tripbipy)(CO)$_3$Cl with KC$_8$. 1-10 mM solutions of Re(tripbipy)(CO)$_3$Cl were prepared in THF in an inert atmosphere and cooled to -35 °C. For complex (**4**), 18-crown-6 (2.5 eq) was added to the solution. 2.5 equivalents of KC_8 were added to the cooled solution and allowed to warm to room temperature over a period of 30 minutes. The solution was then filtered, affording a deep purple solution of the anion. The solution was concentrated from 10 mL to approximately 3 mL and 15 mL of pentane was added. That solution was stored in the freezer for two hours. The solution was then decanted and the purple solid was dried under vacuum. X-ray quality crystals were grown by the vapor diffusion of pentane in to a THF solution of the complex. A typical yield of 78% was observed. IR(THF) ν(CO) (**3**): 1955, 1927, 1854, 1838, 1801 cm^{-1}, IR(THF) ν(CO) (**4**): 1956, 1855, 1839 cm^{-1}

3.5 References

1. Hawecker J, Lehn JM, & Ziessel R (1986) Photochemical and Electrochemical Reduction of Carbon-Dioxide to Carbon-Monoxide Mediated by (2,2'-Bipyridine)Tricarbonylchlororhenium(I) and Related Complexes as Homogeneous Catalysts. *Helv. Chim. Acta* 69(8):1990-2012.

2. Hawecker J, Lehn JM, & Ziessel R (1984) Electrocatalytic Reduction of Carbon-Dioxide Mediated by Re(bipy)$(CO)_3$Cl (Bipy=2,2'-Bipyridine). *J. Chem. Soc.-Chem. Commun.* (6):328-330.

3. Sullivan BP, Bolinger CM, Conrad D, Vining WJ, & Meyer TJ (1985) One-Electron and 2-Electron Pathways in the Electrocatalytic Reduction of CO_2 by Fac-Re(2,2'-Bipyridine)$(CO)_3$Cl. *J. Chem. Soc.-Chem. Commun.* (20):1414-1415.

4. Johnson FPA, George MW, Hartl F, & Turner JJ (1996) Electrocatalytic Reduction of CO_2 Using the Complexes [Re(bpy)$(CO)_3$L]n (n = +1, L = $P(OEt)_3$, CH_3CN; n = 0, L = Cl-, Otf-; bpy = 2,2‘-Bipyridine; Otf- = CF_3SO_3) as Catalyst Precursors: Infrared Spectroelectrochemical Investigation. *Organometallics* 15(15):3374-3387.

5. Stor GJ, Hartl F, van Outersterp JWM, & Stufkens DJ (1995) Spectroelectrochemical (IR, UV/Vis) Determination of the Reduction Pathways for a Series of $[Re(CO)_3(.alpha.\text{-diimine})L']^{0/+}$ (L' = Halide, OTf-, THF, MeCN, n-PrCN, PPh_3, $P(OMe)_3$) Complexes. *Organometallics* 14(3):1115-1131.

6. Breikss AI & Abruña HD (1986) Electrochemical and mechanistic studies of Re(CO)3(dmbpy)CI] and their relation to the catalytic reduction of CO2. *Journal of Electroanalytical Chemistry and Interfacial Electrochemistry* 201(2):347-358.

7. Smieja JM & Kubiak CP (2010) Re(bipy-tBu)$(CO)_3$Cl−improved Catalytic Activity for Reduction of Carbon Dioxide: IR-Spectroelectrochemical and Mechanistic Studies. *Inorg. Chem.* 49(20):9283-9289.

8. Benson EE, Rheingold AL, & Kubiak CP (2010) Synthesis and Characterization of 6,6′-(2,4,6-Triisopropylphenyl)-2,2′-bipyridine (tripbipy) and Its Complexes of the Late First Row Transition Metals. *Inorg. Chem.* 49(4):1458-1464.

9. Kurz P, Probst B, Spingler B, & Alberto R (2006) Ligand Variations in [ReX(diimine)$(CO)_3$] Complexes: Effects on Photocatalytic CO_2 Reduction. *Eur. J. Inorg. Chem.* 2006(15):2966-2974.

10. Sullivan BP & Meyer TJ (1984) Photoinduced irreversible insertion of CO_2 into a metal-hydride bond. *J. Chem. Soc.-Chem. Commun.* (18):1244-1245.

11. Addison AW, Rao TN, Reedijk J, van Rijn J, & Verschoor GC (1984) Synthesis, structure, and spectroscopic properties of copper(II) compounds containing nitrogen-sulphur donor ligands; the crystal and molecular structure of aqua[1,7-bis(N-methylbenzimidazol-2'-yl)-2,6-dithiaheptane]copper(II) perchlorate. *J. Chem. Soc. Dalton* (7):1349-1356.

12. Spek A (2009) Structure validation in chemical crystallography. *Acta Crystallographica Section D* 65(2):148-155.

13. Gore-Randall E, Irwin M, Denning MS, & Goicoechea JM (2009) Synthesis and Characterization of Alkali-Metal Salts of 2,2′- and 2,4′-Bipyridyl Radicals and Dianions. *Inorg. Chem.* 48(17):8304-8316.

14. Schwindt MA, Lejon T, & Hegedus LS (1990) Improved synthesis of (aminocarbene)chromium(0) complexes with use of C8K-generated Cr(CO)52-. Multivariant optimization of an organometallic reaction. *Organometallics* 9(10):2814-2819.

15. Sheldrick G (2008) A short history of SHELX. *Acta Crystall. A* 64(1):112-122.

16. te Velde G, *et al.* (2001) Chemistry with ADF. *Journal of Computational Chemistry* 22(9):931-967.

17. Fonseca Guerra C, Snijders JG, te Velde G, & Baerends EJ (1998) Towards an order-N DFT method. *Theoretical Chemistry Accounts: Theory, Computation, and Modeling (Theoretica Chimica Acta)* 99(6):391-403.

18. van Lenthe E, Snijders JG, & Baerends EJ (1996) The zero-order regular approximation for relativistic effects: The effect of spin--orbit coupling in closed shell molecules. *The Journal of Chemical Physics* 105(15):6505-6516.

19. van Lenthe E, Baerends EJ, & Snijders JG (1993) Relativistic regular two-component Hamiltonians. *The Journal of Chemical Physics* 99(6):4597-4610.

20. Vosko SH, Wilk L, & Nusair M (1980) Accurate spin-dependent electron liquid correlation energies for local spin density calculations: a critical analysis. *Canadian Journal of Physics* 58(8):1200-1211.

21. Becke AD (1988) Density-functional exchange-energy approximation with correct asymptotic behavior. *Physical Review A* 38(6):3098-3100.

22. Perdew JP (1986) Density-functional approximation for the correlation energy of the inhomogeneous electron gas. *Physical Review B* 33(12):8822-8824.

23. Perdew JP (1986) Erratum: Density-functional approximation for the correlation energy of the inhomogeneous electron gas. *Physical Review B* 34(10):7406-7406.

3.6 Appendix

Table 3.3 Bond alternation in Re(tripbipy)(CO)3^{-} (**3**)

N1 – C3	1.394(3)
C3 – C4	1.367(3)
C4 – C5	1.415(3)
C5 – C6	1.353(3)
C6 – C7	1.421(3)
C7 – N1	1.405(3)
C7 – C7’	1.403(4)

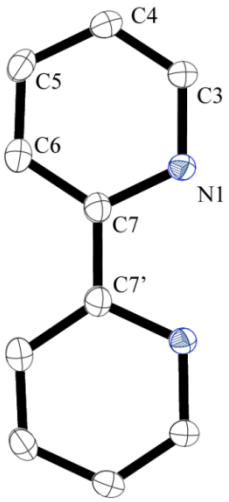

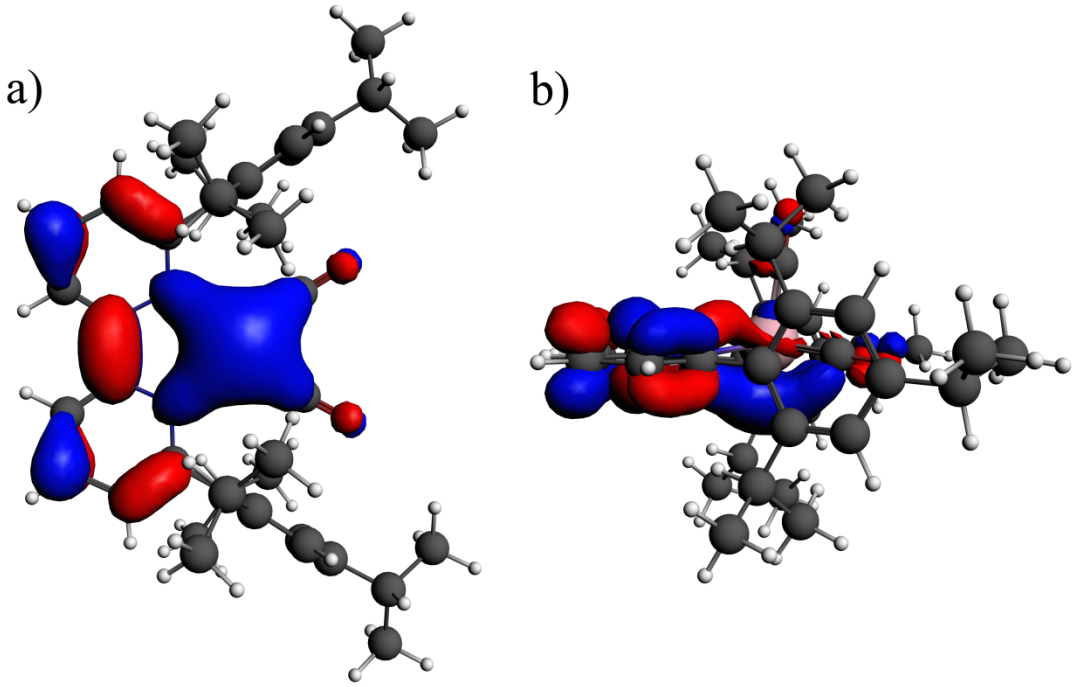

Figure 3.5 HOMO of Re(tripbipy)$(CO)_3^-$ anion calculated using ADF 2007.1

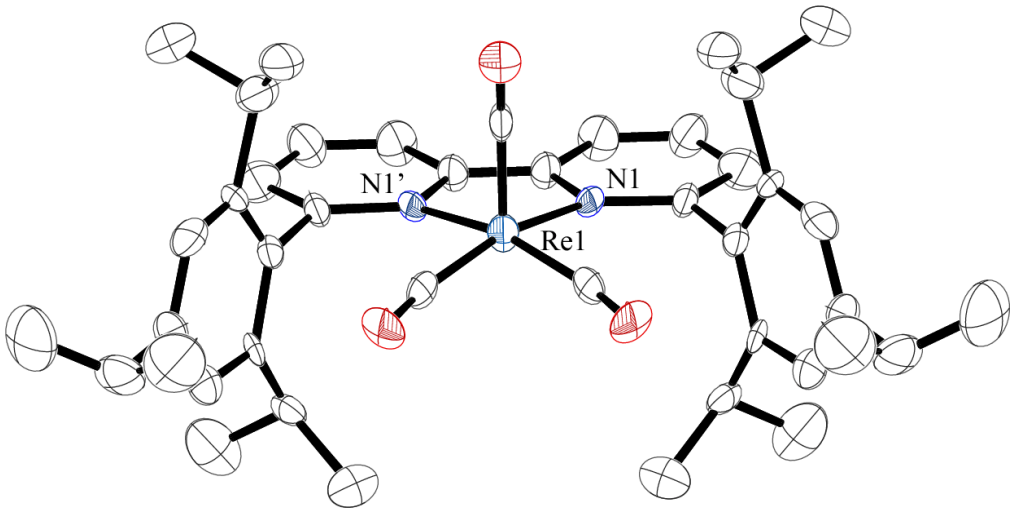

Figure 3.6 Molecular structure of [Re(tripbipy)$(CO)_3$]$^-$, hydrogen atoms and disordered [K(18-crown-6)(THF)] cation removed for clarity. Ellipsoids are set at the 50% probability level.

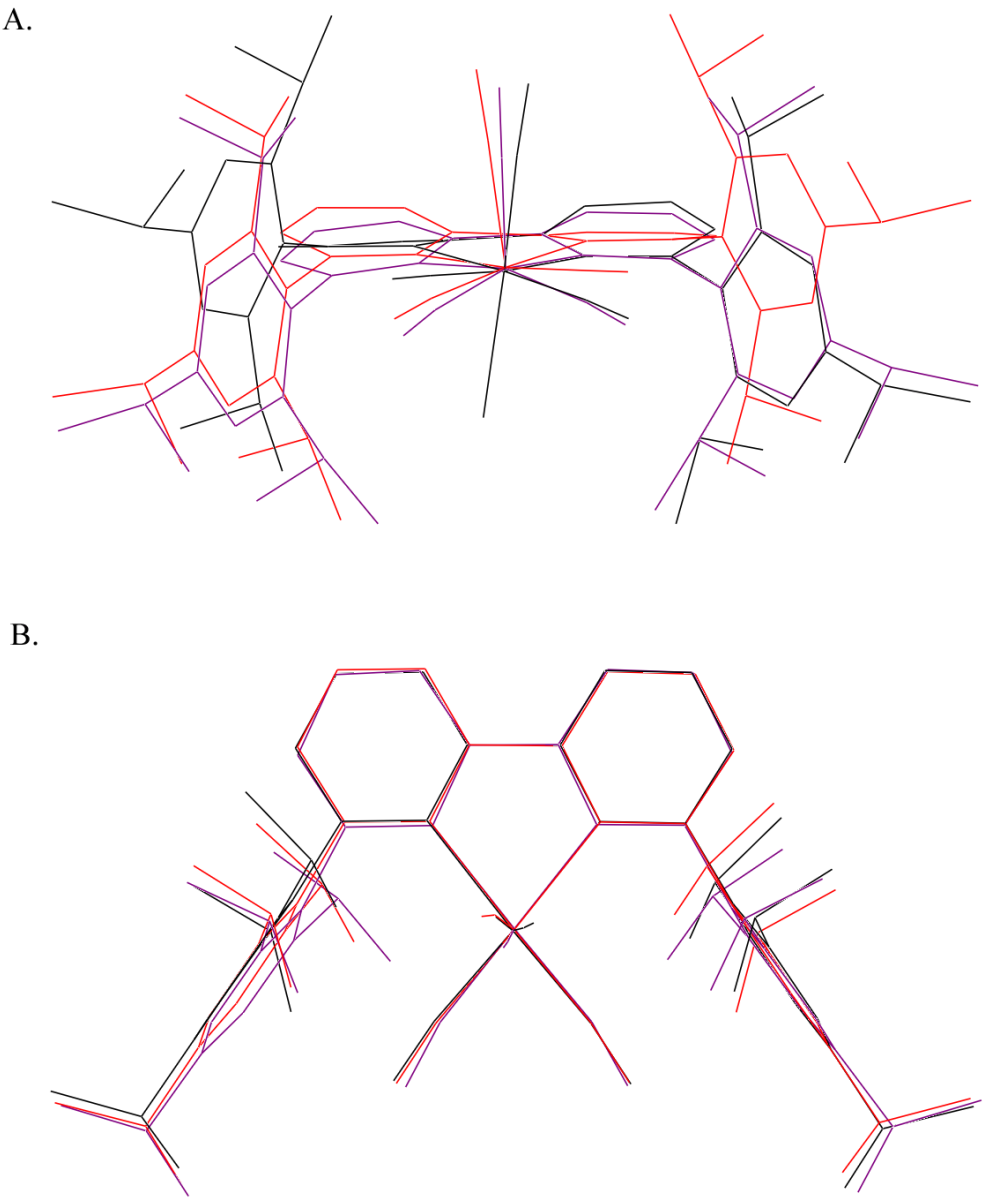

Figure 3.7 Structural overlay for compounds Re(tripbipy)(CO)3Cl (black), Re(tripbipy)(CO)3 (red), and Re(tripbipy)(CO)3- (purple)**.**

Table 3.4 Crystal data and structure refinement for $Re(tripbipy)(CO)_3Cl$

Identification code	eb_091119_0ma	
Empirical formula	C43 H52 Cl N2 O3 Re	
Formula weight	866.52	
Temperature	100(2) K	
Wavelength	0.71073 Å	
Crystal system	Monoclinic	
Space group	C2/c	
Unit cell dimensions	a = 29.332(2) Å	α= 90°.
	b = 9.5788(6) Å	β= 110.2880(10)°.
	c = 14.7284(9) Å	γ = 90°.
Volume	3881.5(4) $Å^3$	
Z	4	
Density (calculated)	1.483 Mg/m^3	
Absorption coefficient	3.240 mm^{-1}	
F(000)	1760	
Crystal size	0.50 x 0.20 x 0.10 mm^3	
Theta range for data collection	1.48 to 28.12°.	
Index ranges	-38<=h<=38, -12<=k<=12, -19<=l<=19	
Reflections collected	24954	
Independent reflections	4498 [R(int) = 0.0784]	
Completeness to theta = 25.00°	100.0 %	
Absorption correction	None	
Max. and min. transmission	0.7376 and 0.2942	
Refinement method	Full-matrix least-squares on F^2	
Data / restraints / parameters	4498 / 0 / 240	
Goodness-of-fit on F^2	0.997	
Final R indices [I>2sigma(I)]	R1 = 0.0311, wR2 = 0.0601	
R indices (all data)	R1 = 0.0422, wR2 = 0.0821	
Largest diff. peak and hole	1.376 and -1.680 $e.Å^{-3}$	

Table 3.5 Bond lengths [Å] and angles [°] for Re(tripbipy)$(CO)_3$Cl

Re(1)-C(2)#1	1.885(13)	C(13)-C(20)	1.525(6)
Re(1)-C(2)	1.885(13)	C(14)-C(16)	1.530(6)
Re(1)-C(1)#1	1.916(4)	C(14)-C(15)	1.531(6)
Re(1)-C(1)	1.916(4)	C(14)-H(14)	1.0000
Re(1)-N(1)#1	2.216(3)	C(15)-H(15A)	0.9800
Re(1)-N(1)	2.216(3)	C(15)-H(15B)	0.9800
Re(1)-Cl(1)	2.466(3)	C(15)-H(15C)	0.9800
Re(1)-Cl(1)#1	2.466(3)	C(16)-H(16A)	0.9800
Cl(1)-C(2)	0.699(11)	C(16)-H(16B)	0.9800
Cl(1)-O(2)	0.732(7)	C(16)-H(16C)	0.9800
O(1)-C(1)	1.153(5)	C(17)-C(19)	1.523(6)
O(2)-C(2)	1.163(15)	C(17)-C(18)	1.525(6)
N(1)-C(3)	1.352(5)	C(17)-H(17)	1.0000
N(1)-C(7)	1.366(5)	C(18)-H(18A)	0.9800
C(3)-C(4)	1.399(5)	C(18)-H(18B)	0.9800
C(3)-C(8)	1.498(5)	C(18)-H(18C)	0.9800
C(4)-C(5)	1.374(6)	C(19)-H(19A)	0.9800
C(4)-H(4)	0.9500	C(19)-H(19B)	0.9800
C(5)-C(6)	1.374(6)	C(19)-H(19C)	0.9800
C(5)-H(5)	0.9500	C(20)-C(22)	1.532(6)
C(6)-C(7)	1.385(5)	C(20)-C(21)	1.533(6)
C(6)-H(6)	0.9500	C(20)-H(20)	1.0000
C(7)-C(7)#1	1.478(8)	C(21)-H(21A)	0.9800
C(8)-C(9)	1.408(6)	C(21)-H(21B)	0.9800
C(8)-C(13)	1.410(6)	C(21)-H(21C)	0.9800
C(9)-C(10)	1.394(6)	C(22)-H(22A)	0.9800
C(9)-C(14)	1.523(6)	C(22)-H(22B)	0.9800
C(10)-C(11)	1.389(6)	C(22)-H(22C)	0.9800
C(10)-H(10)	0.9500		
C(11)-C(12)	1.395(6)	C(2)#1-Re(1)-C(2)	176.2(6)
C(11)-C(17)	1.517(6)	C(2)#1-Re(1)-C(1)#1	86.4(4)
C(12)-C(13)	1.387(5)	C(2)-Re(1)-C(1)#1	90.7(4)
C(12)-H(12)	0.9500	C(2)#1-Re(1)-C(1)	90.7(4)

Table 3.5 Cont.

C(2)-Re(1)-C(1)	86.4(4)	Cl(1)-C(2)-Re(1)	140.6(13)
C(1)#1-Re(1)-C(1)	81.7(2)	O(2)-C(2)-Re(1)	176.2(10)
C(2)#1-Re(1)-N(1)#1	92.9(3)	N(1)-C(3)-C(4)	120.9(4)
C(2)-Re(1)-N(1)#1	90.1(3)	N(1)-C(3)-C(8)	121.3(3)
C(1)#1-Re(1)-N(1)#1	100.95(14)	C(4)-C(3)-C(8)	117.7(4)
C(1)-Re(1)-N(1)#1	175.66(17)	C(5)-C(4)-C(3)	120.3(4)
C(2)#1-Re(1)-N(1)	90.1(3)	C(5)-C(4)-H(4)	119.9
C(2)-Re(1)-N(1)	92.9(3)	C(3)-C(4)-H(4)	119.9
C(1)#1-Re(1)-N(1)	175.66(17)	C(6)-C(5)-C(4)	118.5(4)
C(1)-Re(1)-N(1)	100.95(14)	C(6)-C(5)-H(5)	120.7
N(1)#1-Re(1)-N(1)	76.64(17)	C(4)-C(5)-H(5)	120.7
C(2)#1-Re(1)-Cl(1)	173.4(3)	C(5)-C(6)-C(7)	120.0(4)
C(2)-Re(1)-Cl(1)	10.4(3)	C(5)-C(6)-H(6)	120.0
C(1)#1-Re(1)-Cl(1)	97.62(15)	C(7)-C(6)-H(6)	120.0
C(1)-Re(1)-Cl(1)	95.00(15)	N(1)-C(7)-C(6)	121.5(4)
N(1)#1-Re(1)-Cl(1)	81.27(11)	N(1)-C(7)-C(7)#1	117.2(2)
N(1)-Re(1)-Cl(1)	85.63(11)	C(6)-C(7)-C(7)#1	121.3(3)
C(2)#1-Re(1)-Cl(1)#1	10.4(3)	C(9)-C(8)-C(13)	120.4(4)
C(2)-Re(1)-Cl(1)#1	173.4(3)	C(9)-C(8)-C(3)	120.6(4)
C(1)#1-Re(1)-Cl(1)#1	95.00(15)	C(13)-C(8)-C(3)	118.7(4)
C(1)-Re(1)-Cl(1)#1	97.62(15)	C(10)-C(9)-C(8)	118.2(4)
N(1)#1-Re(1)-Cl(1)#1	85.63(11)	C(10)-C(9)-C(14)	120.1(4)
N(1)-Re(1)-Cl(1)#1	81.27(11)	C(8)-C(9)-C(14)	121.7(4)
Cl(1)-Re(1)-Cl(1)#1	163.30(14)	C(11)-C(10)-C(9)	122.5(4)
C(2)-Cl(1)-O(2)	108.8(14)	C(11)-C(10)-H(10)	118.8
C(2)-Cl(1)-Re(1)	29.0(10)	C(9)-C(10)-H(10)	118.8
O(2)-Cl(1)-Re(1)	137.7(7)	C(10)-C(11)-C(12)	118.0(4)
Cl(1)-O(2)-C(2)	34.7(8)	C(10)-C(11)-C(17)	120.6(4)
C(3)-N(1)-C(7)	118.5(3)	C(12)-C(11)-C(17)	121.5(4)
C(3)-N(1)-Re(1)	127.3(2)	C(13)-C(12)-C(11)	122.0(4)
C(7)-N(1)-Re(1)	113.6(3)	C(13)-C(12)-H(12)	119.0
O(1)-C(1)-Re(1)	173.4(3)	C(11)-C(12)-H(12)	119.0
Cl(1)-C(2)-O(2)	36.6(9)	C(12)-C(13)-C(8)	118.8(4)

Table 3.5 Cont.

C(12)-C(13)-C(20)	120.0(4)	H(18A)-C(18)-H(18B)	109.5
C(8)-C(13)-C(20)	121.1(3)	C(17)-C(18)-H(18C)	109.5
C(9)-C(14)-C(16)	111.9(3)	H(18A)-C(18)-H(18C)	109.5
C(9)-C(14)-C(15)	110.5(4)	H(18B)-C(18)-H(18C)	109.5
C(16)-C(14)-C(15)	110.5(4)	C(17)-C(19)-H(19A)	109.5
C(9)-C(14)-H(14)	107.9	C(17)-C(19)-H(19B)	109.5
C(16)-C(14)-H(14)	107.9	H(19A)-C(19)-H(19B)	109.5
C(15)-C(14)-H(14)	107.9	C(17)-C(19)-H(19C)	109.5
C(14)-C(15)-H(15A)	109.5	H(19A)-C(19)-H(19C)	109.5
C(14)-C(15)-H(15B)	109.5	H(19B)-C(19)-H(19C)	109.5
H(15A)-C(15)-H(15B)	109.5	C(13)-C(20)-C(22)	109.6(3)
C(14)-C(15)-H(15C)	109.5	C(13)-C(20)-C(21)	113.5(3)
H(15A)-C(15)-H(15C)	109.5	C(22)-C(20)-C(21)	110.2(4)
H(15B)-C(15)-H(15C)	109.5	C(13)-C(20)-H(20)	107.8
C(14)-C(16)-H(16A)	109.5	C(22)-C(20)-H(20)	107.8
C(14)-C(16)-H(16B)	109.5	C(21)-C(20)-H(20)	107.8
H(16A)-C(16)-H(16B)	109.5	C(20)-C(21)-H(21A)	109.5
C(14)-C(16)-H(16C)	109.5	C(20)-C(21)-H(21B)	109.5
H(16A)-C(16)-H(16C)	109.5	H(21A)-C(21)-H(21B)	109.5
H(16B)-C(16)-H(16C)	109.5	C(20)-C(21)-H(21C)	109.5
C(11)-C(17)-C(19)	110.8(4)	H(21A)-C(21)-H(21C)	109.5
C(11)-C(17)-C(18)	113.4(4)	H(21B)-C(21)-H(21C)	109.5
C(19)-C(17)-C(18)	110.9(4)	C(20)-C(22)-H(22A)	109.5
C(11)-C(17)-H(17)	107.1	C(20)-C(22)-H(22B)	109.5
C(19)-C(17)-H(17)	107.1	H(22A)-C(22)-H(22B)	109.5
C(18)-C(17)-H(17)	107.1	C(20)-C(22)-H(22C)	109.5
C(17)-C(18)-H(18A)	109.5	H(22A)-C(22)-H(22C)	109.5
C(17)-C(18)-H(18B)	109.5	H(22B)-C(22)-H(22C)	109.5

Symmetry transformations used to generate equivalent atoms:

#1 -x,y,-z+1/2

Table 3.6 Crystal data and structure refinement for $Re(tripbipy)(CO)_3$

Identification code	eb_100202_0m	
Empirical formula	C43 H52 N2 O3 Re	
Formula weight	831.07	
Temperature	100(2) K	
Wavelength	0.71073 Å	
Crystal system	Monoclinic	
Space group	C2/c	
Unit cell dimensions	a = 29.201(6) Å	α= 90°.
	b = 9.5417(19) Å	β= 109.843(2)°.
	c = 14.835(3) Å	γ = 90°.
Volume	3887.9(14) $Å^3$	
Z	4	
Density (calculated)	1.420 Mg/m^3	
Absorption coefficient	3.165 mm^{-1}	
F(000)	1692	
Crystal size	0.30 x 0.30 x 0.20 mm^3	
Theta range for data collection	1.48 to 25.53°.	
Index ranges	-35<=h<=35, -11<=k<=11, -17<=l<=17	
Reflections collected	26300	
Independent reflections	3621 [R(int) = 0.0358]	
Completeness to theta = 25.00°	100.0 %	
Absorption correction	None	
Max. and min. transmission	0.5701 and 0.4502	
Refinement method	Full-matrix least-squares on F^2	
Data / restraints / parameters	3621 / 0 / 168	
Goodness-of-fit on F^2	1.265	
Final R indices [I>2sigma(I)]	R1 = 0.0570, wR2 = 0.1611	
R indices (all data)	R1 = 0.0589, wR2 = 0.1660	
Largest diff. peak and hole	4.462 and -1.802 $e.Å^{-3}$	

Table 3.7 Bond lengths [Å] and angles [°] for Re(tripbipy)$(CO)_3$

Re(1)-C(1)#1	1.9364(18)	C(11)-C(10)	1.3791
Re(1)-C(1)	1.936(2)	C(11)-C(12)	1.4009
Re(1)-C(2)	2.041(3)	C(11)-C(17)	1.5205
Re(1)-C(2)#1	2.041(2)	C(8)-C(13)	1.4026
Re(1)-N(1)	2.183(6)	C(10)-H(10)	0.9500
Re(1)-N(1)#1	2.183(6)	C(5)-H(5)	0.9500
N(1)-C(3)	1.350(6)	C(12)-C(13)	1.3964
N(1)-C(7)	1.364(9)	C(12)-H(12)	0.9500
C(7)-C(6)	1.396(8)	C(20)-C(13)	1.5163
C(7)-C(7)#1	1.469(14)	C(20)-H(20)	1.0000
C(14)-C(9)	1.510(9)	C(16)-H(16A)	0.9800
C(14)-C(15)	1.522(9)	C(16)-H(16B)	0.9800
C(14)-C(16)	1.531(8)	C(16)-H(16C)	0.9800
C(14)-H(14)	1.0000	O(1)-C(1)	1.1429
C(21)-C(20)	1.5282	O(2)-C(2)	1.1839
C(21)-H(21A)	0.9800	C(17)-C(18)	1.5188
C(21)-H(21B)	0.9800	C(17)-C(19)	1.5322
C(21)-H(21C)	0.9800	C(17)-H(17)	1.0000
C(15)-H(15A)	0.9800	C(19)-H(19A)	0.9800
C(15)-H(15B)	0.9800	C(19)-H(19B)	0.9800
C(15)-H(15C)	0.9800	C(19)-H(19C)	0.9800
C(4)-C(5)	1.3773	C(18)-H(18A)	0.9800
C(4)-C(3)	1.4052	C(18)-H(18B)	0.9800
C(4)-H(4)	0.9500	C(18)-H(18C)	0.9800
C(3)-C(8)	1.5127		
C(6)-C(5)	1.3901	C(1)#1-Re(1)-C(1)	80.51(11)
C(6)-H(6)	0.9500	C(1)#1-Re(1)-C(2)	93.95(8)
C(22)-C(20)	1.5172	C(1)-Re(1)-C(2)	90.99(9)
C(22)-H(22A)	0.9800	C(1)#1-Re(1)-C(2)#1	90.99(8)
C(22)-H(22B)	0.9800	C(1)-Re(1)-C(2)#1	93.95(7)
C(22)-H(22C)	0.9800	C(2)-Re(1)-C(2)#1	173.52(11)
C(9)-C(8)	1.4017	C(1)#1-Re(1)-N(1)	175.94(16)
C(9)-C(10)	1.4071	C(1)-Re(1)-N(1)	101.47(16)

Table 3.7 Cont.

C(2)-Re(1)-N(1)	89.57(15)	C(3)-C(4)-H(4)	119.7
C(2)#1-Re(1)-N(1)	85.35(15)	N(1)-C(3)-C(4)	121.6(3)
C(1)#1-Re(1)-N(1)#1	101.47(16)	N(1)-C(3)-C(8)	120.6(3)
C(1)-Re(1)-N(1)#1	175.94(15)	C(4)-C(3)-C(8)	117.8
C(2)-Re(1)-N(1)#1	85.35(16)	C(5)-C(6)-C(7)	119.4(3)
C(2)#1-Re(1)-N(1)#1	89.57(15)	C(5)-C(6)-H(6)	120.3
N(1)-Re(1)-N(1)#1	76.8(3)	C(7)-C(6)-H(6)	120.3
C(3)-N(1)-C(7)	117.8(5)	C(20)-C(22)-H(22A)	109.5
C(3)-N(1)-Re(1)	127.6(4)	C(20)-C(22)-H(22B)	109.5
C(7)-N(1)-Re(1)	114.2(4)	H(22A)-C(22)-H(22B)	109.5
N(1)-C(7)-C(6)	122.5(6)	C(20)-C(22)-H(22C)	109.5
N(1)-C(7)-C(7)#1	116.6(4)	H(22A)-C(22)-H(22C)	109.5
C(6)-C(7)-C(7)#1	120.8(3)	H(22B)-C(22)-H(22C)	109.5
C(9)-C(14)-C(15)	110.8(6)	C(8)-C(9)-C(10)	117.1
C(9)-C(14)-C(16)	111.5(5)	C(8)-C(9)-C(14)	122.0(3)
C(15)-C(14)-C(16)	110.4(5)	C(10)-C(9)-C(14)	120.9(3)
C(9)-C(14)-H(14)	108.0	C(10)-C(11)-C(12)	118.2
C(15)-C(14)-H(14)	108.0	C(10)-C(11)-C(17)	120.4
C(16)-C(14)-H(14)	108.0	C(12)-C(11)-C(17)	121.4
C(20)-C(21)-H(21A)	109.5	C(9)-C(8)-C(13)	122.1
C(20)-C(21)-H(21B)	109.5	C(9)-C(8)-C(3)	119.8
H(21A)-C(21)-H(21B)	109.5	C(13)-C(8)-C(3)	117.7
C(20)-C(21)-H(21C)	109.5	C(11)-C(10)-C(9)	122.8
H(21A)-C(21)-H(21C)	109.5	C(11)-C(10)-H(10)	118.6
H(21B)-C(21)-H(21C)	109.5	C(9)-C(10)-H(10)	118.6
C(14)-C(15)-H(15A)	109.5	C(4)-C(5)-C(6)	118.0
C(14)-C(15)-H(15B)	109.5	C(4)-C(5)-H(5)	121.0
H(15A)-C(15)-H(15B)	109.5	C(6)-C(5)-H(5)	121.0
C(14)-C(15)-H(15C)	109.5	C(13)-C(12)-C(11)	121.9
H(15A)-C(15)-H(15C)	109.5	C(13)-C(12)-H(12)	119.1
H(15B)-C(15)-H(15C)	109.5	C(11)-C(12)-H(12)	119.1
C(5)-C(4)-C(3)	120.6	C(13)-C(20)-C(22)	114.0
C(5)-C(4)-H(4)	119.7	C(13)-C(20)-C(21)	109.0

Table 3.7 Cont.

C(22)-C(20)-C(21)	109.5	C(19)-C(17)-H(17)	107.1
C(13)-C(20)-H(20)	108.0	C(17)-C(19)-H(19A)	109.5
C(22)-C(20)-H(20)	108.0	C(17)-C(19)-H(19B)	109.5
C(21)-C(20)-H(20)	108.0	H(19A)-C(19)-H(19B)	109.5
C(14)-C(16)-H(16A)	109.5	C(17)-C(19)-H(19C)	109.5
C(14)-C(16)-H(16B)	109.5	H(19A)-C(19)-H(19C)	109.5
H(16A)-C(16)-H(16B)	109.5	H(19B)-C(19)-H(19C)	109.5
C(14)-C(16)-H(16C)	109.5	C(17)-C(18)-H(18A)	109.5
H(16A)-C(16)-H(16C)	109.5	C(17)-C(18)-H(18B)	109.5
H(16B)-C(16)-H(16C)	109.5	H(18A)-C(18)-H(18B)	109.5
O(1)-C(1)-Re(1)	173.27(6)	C(17)-C(18)-H(18C)	109.5
O(2)-C(2)-Re(1)	172.14(5)	H(18A)-C(18)-H(18C)	109.5
C(18)-C(17)-C(11)	110.8	H(18B)-C(18)-H(18C)	109.5
C(18)-C(17)-C(19)	110.6	C(12)-C(13)-C(8)	117.9
C(11)-C(17)-C(19)	113.7	C(12)-C(13)-C(20)	119.98(6)
C(18)-C(17)-H(17)	107.1	C(8)-C(13)-C(20)	122.13(6)
C(11)-C(17)-H(17)	107.1		

Symmetry transformations used to generate equivalent atoms:

#1 -x+1,y,-z+1/2

Table 3.8 Crystal data and structure refinement for $[Re(tripbipy)(CO)_3][K(THF)_2]\cdot THF$

Identification code	eb_091002_0ma	
Empirical formula	C59 H84 K N2 O7 Re	
Formula weight	1158.58	
Temperature	293(2) K	
Wavelength	0.71073 Å	
Crystal system	Orthorhombic	
Space group	Pnma	
Unit cell dimensions	a = 16.198(2) Å	α= 90°.
	b = 22.670(3) Å	β= 90°.
	c = 15.347(2) Å	γ = 90°.
Volume	5635.6(13) $Å^3$	
Z	4	
Density (calculated)	1.366 Mg/m^3	
Absorption coefficient	2.282 mm^{-1}	
F(000)	2408	
Crystal size	0.10 x 0.10 x 0.05 mm^3	
Theta range for data collection	1.60 to 28.36°.	
Index ranges	-21<=h<=21, -29<=k<=29, -20<=l<=20	
Reflections collected	64378	
Independent reflections	6972 [R(int) = 0.0374]	
Completeness to theta = 25.00°	100.0 %	
Absorption correction	None	
Max. and min. transmission	0.8945 and 0.8040	
Refinement method	Full-matrix least-squares on F^2	
Data / restraints / parameters	6972 / 1 / 326	
Goodness-of-fit on F^2	1.131	
Final R indices [I>2sigma(I)]	R1 = 0.0236, wR2 = 0.0630	
R indices (all data)	R1 = 0.0285, wR2 = 0.0646	
Extinction coefficient	0.00015(6)	
Largest diff. peak and hole	1.388 and -0.574 $e.Å^{-3}$	

Table 3.9 Bond lengths [Å] and angles [°] for [Re(tripbipy)$(CO)_3$][K$(THF)_2$]·THF

Re(1)-C(1)	1.863(3)	C(3S)-C(4S)	1.42(2)
Re(1)-C(2)#1	1.920(2)	C(3S)-H(3SA)	0.9700
Re(1)-C(2)	1.920(2)	C(3S)-H(3SB)	0.9700
Re(1)-N(1)	2.1085(17)	C(4)-C(5)	1.415(3)
Re(1)-N(1)#1	2.1085(17)	C(4)-H(4)	0.9300
K(2)-O(1S)	2.678(3)	C(4S)-H(4SA)	0.9700
K(2)-O(2S)	2.716(2)	C(4S)-H(4SB)	0.9700
K(2)-O(2S)#1	2.716(2)	C(5)-C(6)	1.353(3)
K(2)-O(1)#2	2.734(3)	C(5)-H(5)	0.9300
K(2)-O(2)#1	2.8767(17)	C(5S)-C(6S)	1.472(5)
K(2)-O(2)	2.8768(17)	C(5S)-H(5SA)	0.9700
K(2)-C(2)	3.506(2)	C(5S)-H(5SB)	0.9700
K(2)-C(2)#1	3.506(2)	C(6)-C(7)	1.421(3)
O(1)-C(1)	1.178(4)	C(6)-H(6)	0.9300
O(1)-K(2)#3	2.734(3)	C(6S)-C(7S)	1.486(6)
O(1S)-C(1S)#1	1.337(13)	C(6S)-H(6SA)	0.9700
O(1S)-C(1S)	1.337(13)	C(6S)-H(6SB)	0.9700
O(1S)-C(4S)#1	1.473(13)	C(7)-C(7)#1	1.403(4)
O(1S)-C(4S)	1.473(13)	C(7S)-C(8S)	1.460(5)
O(2)-C(2)	1.170(3)	C(7S)-H(7SA)	0.9700
O(2S)-C(8S)	1.408(4)	C(7S)-H(7SB)	0.9700
O(2S)-C(5S)	1.419(4)	C(8)-C(9)	1.399(3)
N(1)-C(3)	1.394(3)	C(8)-C(13)	1.409(3)
N(1)-C(7)	1.405(3)	C(8S)-H(8SA)	0.9700
C(1S)-C(2S)	1.486(9)	C(8S)-H(8SB)	0.9700
C(1S)-H(1SA)	0.9700	C(9)-C(10)	1.407(3)
C(1S)-H(1SB)	0.9700	C(9)-C(14)	1.516(3)
C(2S)-C(3S)	1.59(3)	C(10)-C(11)	1.388(4)
C(2S)-H(2SA)	0.9700	C(10)-H(10)	0.9300
C(2S)-H(2SB)	0.9700	C(11)-C(12)	1.379(3)
C(3)-C(4)	1.367(3)	C(11)-C(17)	1.524(3)
C(3)-C(8)	1.501(3)	C(12)-C(13)	1.393(3)

Table 3.9 Cont.

C(12)-H(12)	0.9300	C(1)-Re(1)-N(1)	101.89(9)
C(13)-C(20)	1.512(3)	C(2)#1-Re(1)-N(1)	101.23(8)
C(14)-C(15)	1.529(4)	C(2)-Re(1)-N(1)	165.45(8)
C(14)-C(16)	1.534(4)	C(1)-Re(1)-N(1)#1	101.89(9)
C(14)-H(14)	0.9800	C(2)#1-Re(1)-N(1)#1	165.45(8)
C(15)-H(15A)	0.9600	C(2)-Re(1)-N(1)#1	101.23(8)
C(15)-H(15B)	0.9600	N(1)-Re(1)-N(1)#1	76.25(9)
C(15)-H(15C)	0.9600	O(1S)-K(2)-O(2S)	130.48(6)
C(16)-H(16A)	0.9600	O(1S)-K(2)-O(2S)#1	130.48(6)
C(16)-H(16B)	0.9600	O(2S)-K(2)-O(2S)#1	95.62(12)
C(16)-H(16C)	0.9600	O(1S)-K(2)-O(1)#2	77.14(9)
C(17)-C(18)	1.486(4)	O(2S)-K(2)-O(1)#2	88.67(6)
C(17)-C(19)	1.512(4)	O(2S)#1-K(2)-O(1)#2	88.67(6)
C(17)-H(17)	0.9800	O(1S)-K(2)-O(2)#1	78.78(7)
C(18)-H(18A)	0.9600	O(2S)-K(2)-O(2)#1	135.38(7)
C(18)-H(18B)	0.9600	O(2S)#1-K(2)-O(2)#1	78.72(6)
C(18)-H(18C)	0.9600	O(1)#2-K(2)-O(2)#1	134.73(5)
C(19)-H(19A)	0.9600	O(1S)-K(2)-O(2)	78.78(7)
C(19)-H(19B)	0.9600	O(2S)-K(2)-O(2)	78.72(6)
C(19)-H(19C)	0.9600	O(2S)#1-K(2)-O(2)	135.38(7)
C(20)-C(22)	1.529(3)	O(1)#2-K(2)-O(2)	134.74(5)
C(20)-C(21)	1.538(3)	O(2)#1-K(2)-O(2)	75.51(6)
C(20)-H(20)	0.9800	O(1S)-K(2)-C(2)	79.28(8)
C(21)-H(21A)	0.9600	O(2S)-K(2)-C(2)	91.43(6)
C(21)-H(21B)	0.9600	O(2S)#1-K(2)-C(2)	122.23(6)
C(21)-H(21C)	0.9600	O(1)#2-K(2)-C(2)	148.90(6)
C(22)-H(22A)	0.9600	O(2)#1-K(2)-C(2)	57.87(5)
C(22)-H(22B)	0.9600	O(2)-K(2)-C(2)	17.87(5)
C(22)-H(22C)	0.9600	O(1S)-K(2)-C(2)#1	79.28(8)
		O(2S)-K(2)-C(2)#1	122.23(6)
C(1)-Re(1)-C(2)#1	92.66(10)	O(2S)#1-K(2)-C(2)#1	91.43(6)
C(1)-Re(1)-C(2)	92.66(10)	O(1)#2-K(2)-C(2)#1	148.90(6)
C(2)#1-Re(1)-C(2)	77.54(12)	O(2)#1-K(2)-C(2)#1	17.87(5)

Table 3.9 Cont.

O(2)-K(2)-C(2)#1	57.87(5)	C(1S)-C(2S)-H(2SB)	111.8
C(2)-K(2)-C(2)#1	40.12(7)	C(3S)-C(2S)-H(2SB)	111.8
C(1)-O(1)-K(2)#3	151.4(2)	H(2SA)-C(2S)-H(2SB)	109.5
C(1S)#1-O(1S)-C(1S)	104.5(12)	C(4)-C(3)-N(1)	122.67(19)
C(1S)#1-O(1S)-C(4S)#1	103.0(5)	C(4)-C(3)-C(8)	117.36(19)
C(1S)-O(1S)-C(4S)#1	29.4(7)	N(1)-C(3)-C(8)	119.94(18)
C(1S)#1-O(1S)-C(4S)	29.4(7)	C(4S)-C(3S)-C(2S)	104.0(10)
C(1S)-O(1S)-C(4S)	103.0(5)	C(4S)-C(3S)-H(3SA)	111.0
C(4S)#1-O(1S)-C(4S)	87.7(10)	C(2S)-C(3S)-H(3SA)	111.0
C(1S)#1-O(1S)-K(2)	127.7(6)	C(4S)-C(3S)-H(3SB)	111.0
C(1S)-O(1S)-K(2)	127.7(6)	C(2S)-C(3S)-H(3SB)	111.0
C(4S)#1-O(1S)-K(2)	121.1(5)	H(3SA)-C(3S)-H(3SB)	109.0
C(4S)-O(1S)-K(2)	121.1(5)	C(3)-C(4)-C(5)	120.9(2)
C(2)-O(2)-K(2)	113.17(14)	C(3)-C(4)-H(4)	119.5
C(8S)-O(2S)-C(5S)	109.3(3)	C(5)-C(4)-H(4)	119.5
C(8S)-O(2S)-K(2)	125.0(2)	C(3S)-C(4S)-O(1S)	104.9(11)
C(5S)-O(2S)-K(2)	123.89(19)	C(3S)-C(4S)-H(4SA)	110.8
C(3)-N(1)-C(7)	116.16(17)	O(1S)-C(4S)-H(4SA)	110.8
C(3)-N(1)-Re(1)	128.03(13)	C(3S)-C(4S)-H(4SB)	110.8
C(7)-N(1)-Re(1)	115.63(13)	O(1S)-C(4S)-H(4SB)	110.8
O(1)-C(1)-Re(1)	178.1(3)	H(4SA)-C(4S)-H(4SB)	108.8
O(1S)-C(1S)-C(2S)	109.8(9)	C(6)-C(5)-C(4)	117.9(2)
O(1S)-C(1S)-H(1SA)	109.7	C(6)-C(5)-H(5)	121.0
C(2S)-C(1S)-H(1SA)	109.7	C(4)-C(5)-H(5)	121.0
O(1S)-C(1S)-H(1SB)	109.7	O(2S)-C(5S)-C(6S)	108.2(3)
C(2S)-C(1S)-H(1SB)	109.7	O(2S)-C(5S)-H(5SA)	110.1
H(1SA)-C(1S)-H(1SB)	108.2	C(6S)-C(5S)-H(5SA)	110.1
O(2)-C(2)-Re(1)	169.64(18)	O(2S)-C(5S)-H(5SB)	110.1
O(2)-C(2)-K(2)	48.97(11)	C(6S)-C(5S)-H(5SB)	110.1
Re(1)-C(2)-K(2)	120.67(8)	H(5SA)-C(5S)-H(5SB)	108.4
C(1S)-C(2S)-C(3S)	99.9(12)	C(5)-C(6)-C(7)	121.3(2)
C(1S)-C(2S)-H(2SA)	111.8	C(5)-C(6)-H(6)	119.4
C(3S)-C(2S)-H(2SA)	111.8	C(7)-C(6)-H(6)	119.4

Table 3.9 Cont.

C(5S)-C(6S)-C(7S)	104.6(3)	C(11)-C(12)-C(13)	121.9(2)
C(5S)-C(6S)-H(6SA)	110.8	C(11)-C(12)-H(12)	119.0
C(7S)-C(6S)-H(6SA)	110.8	C(13)-C(12)-H(12)	119.0
C(5S)-C(6S)-H(6SB)	110.8	C(12)-C(13)-C(8)	119.1(2)
C(7S)-C(6S)-H(6SB)	110.8	C(12)-C(13)-C(20)	119.1(2)
H(6SA)-C(6S)-H(6SB)	108.9	C(8)-C(13)-C(20)	121.79(19)
C(7)#1-C(7)-N(1)	115.30(11)	C(9)-C(14)-C(15)	111.9(2)
C(7)#1-C(7)-C(6)	123.73(12)	C(9)-C(14)-C(16)	110.3(2)
N(1)-C(7)-C(6)	120.94(19)	C(15)-C(14)-C(16)	111.3(2)
C(8S)-C(7S)-C(6S)	105.5(3)	C(9)-C(14)-H(14)	107.7
C(8S)-C(7S)-H(7SA)	110.6	C(15)-C(14)-H(14)	107.7
C(6S)-C(7S)-H(7SA)	110.6	C(16)-C(14)-H(14)	107.7
C(8S)-C(7S)-H(7SB)	110.6	C(14)-C(15)-H(15A)	109.5
C(6S)-C(7S)-H(7SB)	110.6	C(14)-C(15)-H(15B)	109.5
H(7SA)-C(7S)-H(7SB)	108.8	H(15A)-C(15)-H(15B)	109.5
C(9)-C(8)-C(13)	120.2(2)	C(14)-C(15)-H(15C)	109.5
C(9)-C(8)-C(3)	119.3(2)	H(15A)-C(15)-H(15C)	109.5
C(13)-C(8)-C(3)	120.15(19)	H(15B)-C(15)-H(15C)	109.5
O(2S)-C(8S)-C(7S)	107.5(3)	C(14)-C(16)-H(16A)	109.5
O(2S)-C(8S)-H(8SA)	110.2	C(14)-C(16)-H(16B)	109.5
C(7S)-C(8S)-H(8SA)	110.2	H(16A)-C(16)-H(16B)	109.5
O(2S)-C(8S)-H(8SB)	110.2	C(14)-C(16)-H(16C)	109.5
C(7S)-C(8S)-H(8SB)	110.2	H(16A)-C(16)-H(16C)	109.5
H(8SA)-C(8S)-H(8SB)	108.5	H(16B)-C(16)-H(16C)	109.5
C(8)-C(9)-C(10)	118.3(2)	C(18)-C(17)-C(19)	112.5(2)
C(8)-C(9)-C(14)	121.4(2)	C(18)-C(17)-C(11)	112.7(2)
C(10)-C(9)-C(14)	120.3(2)	C(19)-C(17)-C(11)	110.9(2)
C(11)-C(10)-C(9)	122.1(2)	C(18)-C(17)-H(17)	106.8
C(11)-C(10)-H(10)	118.9	C(19)-C(17)-H(17)	106.8
C(9)-C(10)-H(10)	118.9	C(11)-C(17)-H(17)	106.8
C(12)-C(11)-C(10)	118.3(2)	C(17)-C(18)-H(18A)	109.5
C(12)-C(11)-C(17)	119.8(2)	C(17)-C(18)-H(18B)	109.5
C(10)-C(11)-C(17)	121.9(2)	H(18A)-C(18)-H(18B)	109.5

Table 3.9 Cont.

C(17)-C(18)-H(18C)	109.5	C(21)-C(20)-H(20)	108.0
H(18A)-C(18)-H(18C)	109.5	C(20)-C(21)-H(21A)	109.5
H(18B)-C(18)-H(18C)	109.5	C(20)-C(21)-H(21B)	109.5
C(17)-C(19)-H(19A)	109.5	H(21A)-C(21)-H(21B)	109.5
C(17)-C(19)-H(19B)	109.5	C(20)-C(21)-H(21C)	109.5
H(19A)-C(19)-H(19B)	109.5	H(21A)-C(21)-H(21C)	109.5
C(17)-C(19)-H(19C)	109.5	H(21B)-C(21)-H(21C)	109.5
H(19A)-C(19)-H(19C)	109.5	C(20)-C(22)-H(22A)	109.5
H(19B)-C(19)-H(19C)	109.5	C(20)-C(22)-H(22B)	109.5
C(13)-C(20)-C(22)	110.8(2)	H(22A)-C(22)-H(22B)	109.5
C(13)-C(20)-C(21)	112.01(19)	C(20)-C(22)-H(22C)	109.5
C(22)-C(20)-C(21)	110.00(19)	H(22A)-C(22)-H(22C)	109.5
C(13)-C(20)-H(20)	108.0	H(22B)-C(22)-H(22C)	109.
C(22)-C(20)-H(20)	108.0		

Symmetry transformations used to generate equivalent atoms:

#1 x,-y+1/2,z #2 x+1/2,-y+1/2,-z+1/2 #3 x-1/2,-y+1/2,-z+1/2

Table 3.10 Crystal data and structure refinement for [Re(tripbipy)$(CO)_3$] [K(18-crown-6)(THF)]

Identification code	eb_090810_0ma	
Empirical formula	C59 H84 K N2 O10 Re	
Formula weight	1206.58	
Temperature	100(2) K	
Wavelength	0.71073 Å	
Crystal system	Orthorhombic	
Space group	Pnma	
Unit cell dimensions	a = 16.477(3) Å	α= 90°.
	b = 22.345(4) Å	β= 90°.
	c = 16.820(3) Å	γ = 90°.
Volume	6192.6(18) $Å^3$	
Z	4	
Density (calculated)	1.294 Mg/m^3	
Absorption coefficient	2.083 mm^{-1}	
F(000)	2504	
Crystal size	0.20 x 0.20 x 0.10 mm^3	
Theta range for data collection	1.52 to 25.37°.	
Index ranges	-19<=h<=19, -26<=k<=21, -19<=l<=20	
Reflections collected	39124	
Independent reflections	5834 [R(int) = 0.0658]	
Completeness to theta = 25.00°	99.9 %	
Max. and min. transmission	0.8188 and 0.6808	
Refinement method	Full-matrix least-squares on F^2	
Data / restraints / parameters	5834 / 0 / 232	
Goodness-of-fit on F^2	1.057	
Final R indices [I>2sigma(I)]	R1 = 0.0704, wR2 = 0.1743	
R indices (all data)	R1 = 0.0847, wR2 = 0.1807	
Largest diff. peak and hole	6.741 and -2.564 $e.Å^{-3}$	

Table 3.11 Bond lengths [Å] and angles [°] for [Re(tripbipy)$(CO)_3$] [K(18-crown-6)(THF)]

C(1)-C(1)#1	1.359(14)	C(15)-C(16)	1.532(19)
C(1)-N(1)	1.419(9)	C(15)-H(15)	1.0000
C(1)-C(2)	1.438(10)	C(16)-H(16A)	0.9800
C(2)-C(3)	1.326(12)	C(16)-H(16B)	0.9800
C(2)-H(2)	0.9500	C(16)-H(16C)	0.9800
C(3)-C(4)	1.469(13)	C(17)-H(17A)	0.9800
C(3)-H(3)	0.9500	C(17)-H(17B)	0.9800
C(4)-C(5)	1.424(11)	C(17)-H(17C)	0.9800
C(4)-H(4)	0.9500	C(18)-C(20)	1.516(13)
C(5)-N(1)	1.407(9)	C(18)-C(19)	1.565(11)
C(5)-C(6)	1.474(10)	C(18)-H(18)	1.0000
C(6)-C(7)	1.427(12)	C(19)-H(19A)	0.9800
C(6)-C(11)	1.452(10)	C(19)-H(19B)	0.9800
C(7)-C(8)	1.353(12)	C(19)-H(19C)	0.9800
C(7)-C(12)	1.562(11)	C(20)-H(20A)	0.9800
C(8)-C(9)	1.393(12)	C(20)-H(20B)	0.9800
C(8)-H(8)	0.9500	C(20)-H(20C)	0.9800
C(9)-C(10)	1.387(12)	C(21)-O(1)	1.157(9)
C(9)-C(15)	1.563(12)	C(21)-Re(1)	1.915(8)
C(10)-C(11)	1.388(11)	N(1)-Re(1)	2.104(6)
C(10)-H(10)	0.9500	Re(1)-C(21)#1	1.915(8)
C(11)-C(18)	1.486(11)	Re(1)-C(22)	1.916(10)
C(12)-C(13)	1.502(15)	Re(1)-N(1)#1	2.104(6)
C(12)-C(14)	1.584(15)	O(2)-C(22)	1.084(12)
C(12)-H(12)	1.0000		
C(13)-H(13A)	0.9800	C(1)#1-C(1)-N(1)	116.1(4)
C(13)-H(13B)	0.9800	C(1)#1-C(1)-C(2)	124.1(5)
C(13)-H(13C)	0.9800	N(1)-C(1)-C(2)	119.7(7)
C(14)-H(14A)	0.9800	C(3)-C(2)-C(1)	121.3(8)
C(14)-H(14B)	0.9800	C(3)-C(2)-H(2)	119.4
C(14)-H(14C)	0.9800	C(1)-C(2)-H(2)	119.4
C(15)-C(17)	1.423(15)	C(2)-C(3)-C(4)	123.0(8)

Table 3.11 Cont.

C(2)-C(3)-H(3)	118.5	C(12)-C(13)-H(13B)	109.5
C(4)-C(3)-H(3)	118.5	H(13A)-C(13)-H(13B)	109.5
C(5)-C(4)-C(3)	113.6(8)	C(12)-C(13)-H(13C)	109.5
C(5)-C(4)-H(4)	123.2	H(13A)-C(13)-H(13C)	109.5
C(3)-C(4)-H(4)	123.2	H(13B)-C(13)-H(13C)	109.5
N(1)-C(5)-C(4)	125.3(7)	C(12)-C(14)-H(14A)	109.5
N(1)-C(5)-C(6)	119.6(6)	C(12)-C(14)-H(14B)	109.5
C(4)-C(5)-C(6)	115.0(7)	H(14A)-C(14)-H(14B)	109.5
C(7)-C(6)-C(11)	118.2(7)	C(12)-C(14)-H(14C)	109.5
C(7)-C(6)-C(5)	121.2(6)	H(14A)-C(14)-H(14C)	109.5
C(11)-C(6)-C(5)	120.4(7)	H(14B)-C(14)-H(14C)	109.5
C(8)-C(7)-C(6)	120.1(7)	C(17)-C(15)-C(16)	110.4(11)
C(8)-C(7)-C(12)	121.1(8)	C(17)-C(15)-C(9)	111.1(10)
C(6)-C(7)-C(12)	118.6(7)	C(16)-C(15)-C(9)	110.8(9)
C(7)-C(8)-C(9)	122.8(9)	C(17)-C(15)-H(15)	108.1
C(7)-C(8)-H(8)	118.6	C(16)-C(15)-H(15)	108.1
C(9)-C(8)-H(8)	118.6	C(9)-C(15)-H(15)	108.1
C(10)-C(9)-C(8)	118.1(8)	C(15)-C(16)-H(16A)	109.5
C(10)-C(9)-C(15)	120.4(8)	C(15)-C(16)-H(16B)	109.5
C(8)-C(9)-C(15)	121.4(8)	H(16A)-C(16)-H(16B)	109.5
C(9)-C(10)-C(11)	122.8(8)	C(15)-C(16)-H(16C)	109.5
C(9)-C(10)-H(10)	118.6	H(16A)-C(16)-H(16C)	109.5
C(11)-C(10)-H(10)	118.6	H(16B)-C(16)-H(16C)	109.5
C(10)-C(11)-C(6)	118.1(7)	C(15)-C(17)-H(17A)	109.5
C(10)-C(11)-C(18)	120.9(7)	C(15)-C(17)-H(17B)	109.5
C(6)-C(11)-C(18)	121.0(6)	H(17A)-C(17)-H(17B)	109.5
C(13)-C(12)-C(7)	111.7(8)	C(15)-C(17)-H(17C)	109.5
C(13)-C(12)-C(14)	112.4(9)	H(17A)-C(17)-H(17C)	109.5
C(7)-C(12)-C(14)	106.3(8)	H(17B)-C(17)-H(17C)	109.5
C(13)-C(12)-H(12)	108.8	C(11)-C(18)-C(20)	112.4(7)
C(7)-C(12)-H(12)	108.8	C(11)-C(18)-C(19)	111.7(7)
C(14)-C(12)-H(12)	108.8	C(20)-C(18)-C(19)	113.3(8)
C(12)-C(13)-H(13A)	109.5	C(11)-C(18)-H(18)	106.3

Table 3.11 Cont.

C(20)-C(18)-H(18)	106.3	C(5)-N(1)-C(1)	116.9(6)
C(19)-C(18)-H(18)	106.3	C(5)-N(1)-Re(1)	127.5(5)
C(18)-C(19)-H(19A)	109.5	C(1)-N(1)-Re(1)	115.3(4)
C(18)-C(19)-H(19B)	109.5	C(21)-Re(1)-C(21)#1	79.9(4)
H(19A)-C(19)-H(19B)	109.5	C(21)-Re(1)-C(22)	91.4(4)
C(18)-C(19)-H(19C)	109.5	C(21)#1-Re(1)-C(22)	91.4(4)
H(19A)-C(19)-H(19C)	109.5	C(21)-Re(1)-N(1)#1	165.7(3)
H(19B)-C(19)-H(19C)	109.5	C(21)#1-Re(1)-N(1)#1	100.0(3)
C(18)-C(20)-H(20A)	109.5	C(22)-Re(1)-N(1)#1	102.9(3)
C(18)-C(20)-H(20B)	109.5	C(21)-Re(1)-N(1)	100.0(3)
H(20A)-C(20)-H(20B)	109.5	C(21)#1-Re(1)-N(1)	165.7(3)
C(18)-C(20)-H(20C)	109.5	C(22)-Re(1)-N(1)	102.9(3)
H(20A)-C(20)-H(20C)	109.5	N(1)#1-Re(1)-N(1)	76.6(3)
H(20B)-C(20)-H(20C)	109.5	O(2)-C(22)-Re(1)	175.1(11)
O(1)-C(21)-Re(1)	170.8(6)		

Symmetry transformations used to generate equivalent atoms:

#1 x,-y+1/2,z

Table 3.12 XYZ coordinates of Re(tripbipy)$(CO)_3^-$ from ADF 2007.1

Atom	X	Y	Z				
C	1.717	6.292	14.840	H	4.594	8.116	14.174
C	0.857	7.065	14.022	C	6.701	7.996	14.535
H	0.134	6.553	13.392	H	7.559	8.633	14.798
C	0.919	8.434	14.009	H	6.903	7.555	13.547
H	0.257	9.027	13.380	H	6.642	7.183	15.270
C	1.896	9.054	14.836	C	5.480	9.935	13.460
H	2.021	10.136	14.839	H	4.526	10.473	13.372
C	2.717	8.302	15.644	H	5.740	9.532	12.469
C	3.736	9.052	16.445	H	6.255	10.665	13.742
C	3.399	9.582	17.711	C	4.969	6.808	17.833
C	4.342	10.360	18.390	N	2.654	6.912	15.705
H	4.089	10.740	19.382	O	5.825	7.388	18.391
C	5.607	10.627	17.858	Re	3.695	5.587	17.037
C	5.904	10.119	16.593	O	1.994	5.591	19.588
H	6.890	10.319	16.167	C	2.658	5.588	18.612
C	4.995	9.334	15.873	C	1.717	4.880	14.840
C	2.038	9.313	18.347	C	0.858	4.107	14.021
H	1.609	8.442	17.831	H	0.137	4.619	13.387
C	2.133	8.963	19.842	C	0.920	2.738	14.009
H	2.854	8.157	20.020	H	0.260	2.146	13.377
H	1.155	8.625	20.212	C	1.894	2.118	14.838
H	2.431	9.836	20.444	H	2.019	1.037	14.842
C	1.076	10.500	18.146	C	2.715	2.870	15.647
H	1.470	11.404	18.635	C	3.734	2.120	16.447
H	0.092	10.275	18.587	C	3.400	1.591	17.714
H	0.930	10.723	17.080	C	4.344	0.811	18.390
C	6.667	11.368	18.661	H	4.093	0.431	19.382
H	7.534	11.501	17.994	C	5.608	0.543	17.854
C	7.130	10.525	19.866	C	5.901	1.051	16.588
H	7.972	11.009	20.386	H	6.886	0.850	16.160
H	7.434	9.519	19.550	C	4.991	1.837	15.871
H	6.309	10.404	20.588	C	2.041	1.861	18.353
C	6.210	12.764	19.118	H	1.611	2.731	17.838
H	5.925	13.392	18.264	C	2.141	2.212	19.848
H	7.012	13.274	19.673	H	2.862	3.019	20.022
H	5.339	12.691	19.786	H	1.163	2.550	20.220
C	5.389	8.800	14.499	H	2.441	1.340	20.449
				C	1.078	0.673	18.157

Table 3.12 Cont.

H	1.474	-0.230	18.647	C	5.382	2.370	14.496
H	0.096	0.898	18.601	H	4.588	3.055	14.172
H	0.929	0.449	17.092	C	6.695	3.173	14.528
C	6.671	-0.199	18.653	H	7.553	2.535	14.787
H	7.532	-0.339	17.980	H	6.895	3.613	13.539
C	7.146	0.650	19.849	H	6.639	3.986	15.263
H	7.989	0.165	20.366	C	5.470	1.234	13.458
H	7.454	1.652	19.525	H	4.515	0.697	13.372
H	6.331	0.780	20.576	H	5.728	1.636	12.466
C	6.211	-1.590	19.121	H	6.245	0.504	13.739
H	5.917	-2.222	18.273	N	2.652	4.260	15.706
H	7.016	-2.100	19.672	C	4.966	4.364	17.836
H	5.347	-1.510	19.796	O	5.821	3.783	18.394

Chapter 4

Structural investigations into the deactivation pathway of the CO_2 reduction electrocatalyst $Re(bpy)(CO)_3Cl$

4.1 Introduction

Carbon dioxide (CO_2) is an increasingly important molecule on the global stage, particularly with regard to its role in climate change. Efficient transformation of this stable molecule into an energy dense state is a technically demanding challenge that offers many potential rewards. The activation/reduction of CO_2 to higher energy products requires catalysts that are robust, selective, and ideally operate close to the thermodynamic potential for the transformation of interest. Coupling these catalysts to

a renewable source of energy represents a large step towards a carbon neutral economy.

Of the few reported catalysts that can electrochemically reduce CO_2, the $Re(bpy)(CO)_3Cl$ complex, originally reported by Lehn, is one of the most robust and well characterized systems.[1, 2] Since the original report, many researchers have studied the electrocatalytic,[3, 4] photophysical,[5, 6] and photocatalytic[7-9] properties of this system and its analogs. The Re catalyst has been shown to have high turnover numbers, some of the highest reported rates of catalysis, and to be highly selective for the reduction CO_2 to CO in the presence of protons. These high rates, however, are still modest in comparison to natural enzymes, which can operate near the thermodynamic potential and equilibrate the reduced and oxidized species.[10] To improve the rates and the overall function of the $Re(bpy)(CO)_3Cl$ system, it is important to understand the catalytic intermediates and degradation products.

In many electrocatalytic systems the degradation of the active catalyst is a common dead end in catalyst development. One common degradation pathway is the formation of thermodynamically stable and often catalytically inactive dimers.[11, 12] Prevention of dimer formation relies on the compromise between increasing catalyst bulk and maintaining activity. In previous studies of the Re complexes, spectroelectrochemical (SEC) reductions of the parent compound $Re(bpy)(CO)_3Cl$ resulted in the formation of the anion, with partial formation of the dimer $[Re(bpy)(CO)_3]_2$.[4, 13] It was also suggested that the subsequent two electron reduction of the dimer led to cleavage of the metal-metal bond giving the catalytically active

Re(-1) species. Recently, we have observed increased catalytic activity for CO_2 reduction from Re(*t*Bu-bpy)$(CO)_3Cl$, where steric bulk is added at the 4,4' positions of the 2,2'-bipyridine ligand.[14] However, it is unclear whether this increased catalytic activity is derived from steric or electronic effects. To further elucidate the improved catalysis, we sought to isolate and characterize the reduced species that are related to the catalytic mechanism.

4.2 Results and discussion

One of the proposed degradation pathways for Re bipyridine catalysts is dimer formation. To probe this pathway we reduced the parent compound, Re(bpy)$(CO)_3Cl$ (**1**), and independently synthesized the $[Re(bpy)(CO)_3]_2$ dimer (**2**). The dimer was synthesized by the addition of one equivalent of KC_8 to a solution of Re(bpy)$(CO)_3Cl$

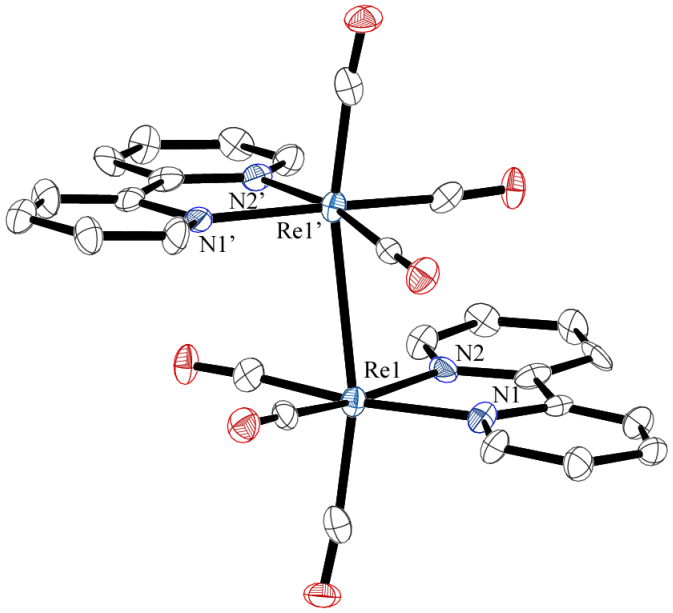

Figure 4.1 Molecular structure of $[Re(bpy)(CO_3]_2$ (2), with hydrogen atoms omitted for clarity. Ellipsoids are shown at the 50% probability level.

in THF and was characterized by FTIR, X-ray crystallography, and ^{1}H NMR. The infrared ν(CO) band of the isolated dimer matches closely with that reported in SEC studies.[4] Dark green crystals of **2** were grown from the vapor diffusion of pentane into THF under an inert atmosphere. The complex exists as two octahedral Re centers containing three facially coordinated carbonyls, a chelating bipyridine, and a Re-Re bond (Figure 4.1). The two Re atoms are separated by 3.0791(13) Å. For comparison, in the well-known $Re_2(CO)_{10}$ dimer the reported Re-Re distance is 3.0413(11) Å.[15]

The electrochemistry of **2** in acetonitrile reveals two quasi-reversible one electron reductions, with cathodic peaks at –2.07 and –2.25 V vs. Fc/Fc^{+}, and one quasi-reversible oxidation and one irreversible oxidation located at –0.56 V and –0.21 V (Figure 4.2). The irreversibility of the second oxidation suggests an EC mechanism

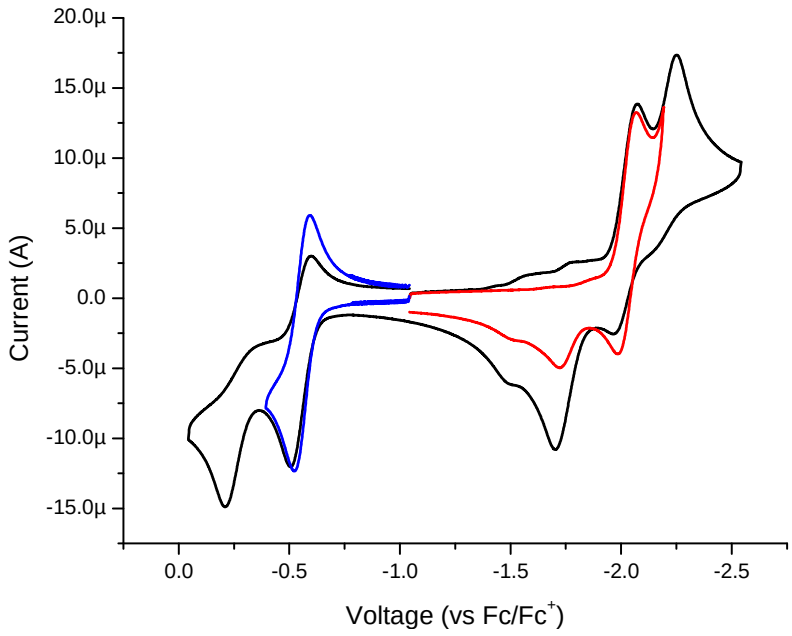

Figure 4.2 Electrochemistry of $[Re(bpy)(CO)_3]_2$ (**2**) 1mM in THF with a 3 mm glassy counter working electrode, silver wire reference, and Pt counter. A scan with added Fc provided an internal standard (not shown).

in which the oxidation results in the cleavage of the dimer to form two independent Re(I) fragments. While there are two distinct one electron reductions, the re-oxidation wave is convoluted by coupled chemical transformations such as dimer cleavage and reorganization. In the classical $M_2(CO)_{10}$ system (M = Mn, Re), the reduction of the dimer results in the formation of two distinct $[M(CO)_5]^-$ fragments that can be reoxidized to reform $M_2(CO)_{10}$.[16] However, in the presence of electro-active bipyridine ligands, the additional electrons may not occupy the σ* orbital of the metal-metal bond, but rather the π* orbitals of the bipy ligand.

To isolate the proposed active state of the catalyst, $[Re(bpy)(CO)_3]^-$, we reduced both the dimer **2** and the starting Re(I) chloride **1**. The addition of 2.1 equivalents of both KC_8 and 18-crown-6 to $Re(bpy)(CO)_3Cl$ results in the clean formation (evidenced by FTIR) of the anion, $[Re(bpy)(CO)_3]^-$, (**3**). The anion can also be formed by the addition of 2.1 equivalents of KC_8 and 18-crown-6 to a solution/suspension of **2** in THF. Complex **3** was characterized by FTIR, X-ray crystallography and ^1H NMR. The carbonyl stretching frequencies of **3** are shifted to 1945 and 1839 cm^{-1} (from 2020, 1917 and 1893 cm^{-1} for **1**), suggesting significant back bonding to the carbonyls. This corresponds favorably with previous reports from IR-SEC experiments.[4] Dark purple crystals were grown from the vapor diffusion of pentane into a solution of **3** in THF. The complex crystalizes in the space group P2(1)/c with two independent molecules in the unit cell. The potassium cation is encapsulated by the crown ether with one of the axial sites coordinated by a disordered THF molecule, and the opposite axial position is associated with the axial carbonyl of

the rhenium (K – O, 2.760(av) Å) (Figure 4.3). The rhenium anion adopts a distorted square pyramidal geometry with an average τ_5 of 0.17 (where 0 = square pyramidal, 1 = trigonal bipyramidal).[17] This is significantly less distorted from square planar than what is seen with the [Re(bpy-*t*Bu)$(CO)_3]^-$, where the metal center adopts a geometry closer to trigonal bipyramidal (τ_5 = 0.46).[18]

Bond alternation in the bipyridine ligand of **3** can be seen clearly in the crystal structure (Table 4.1). This bond alternation is similar to what is seen in the structures of isolated reduced bipyridines,[19] This suggests that the ability of bipyrine to act as a non-innocent ligand is crucial not only for the complex to deliver two electrons to

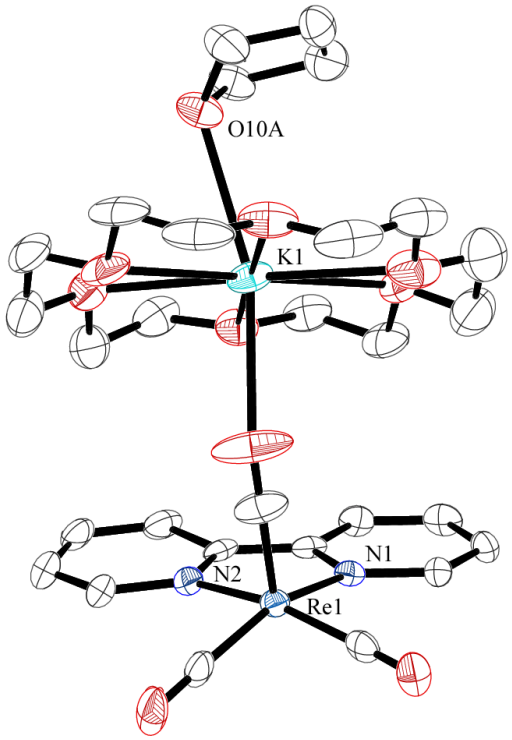

Figure 4.3 Molecular structure of one of the Re(bpy)(CO3)$^-$ (**3**) molecules found in the unit cell (Z=2), showing position 1 of 2 for the disordered THF molecule. The hydrogen atoms are omitted for clarity, and the ellipsoids are shown at the 50% probability level**.**

carbon dioxide but also to impart selectivity over proton reduction.[18] The shortened Re-N distances and increased bipyridine bite angle suggest better orbital overlap with the bipyridine in **3** compared with the halide starting material **1**. A table of selected bond distances and angles can be found in Table 4.3.

Originally, crystals of the reduced dimer $[Re(bpy)(CO)_3]_2^-$ (**4**) were grown (repeatedly) as an impurity during attempts to isolate the anionic Re(-1) species. The complex was later characterized by FTIR and could be obtained through either the direct reduction of $Re(bpy)(CO)_3Cl$ or the oxidation of $[Re(bpy)(CO)_3]^-$ by $[FeCp_2][PF_6]$. Dark purple crystals of **4** were grown from the vapor diffusion of Et_2O into THF. The complex is similar to **2** in that it contains two octahedral rhenium

Table 4.1 Bond alternation in one of the molecules of $Re(bipy)(CO)_3^-$ (**3**) in the asymmetric unit, Z' = 2.

N1 – C3	1.385(5)
C3 – C4	1.351(6)
C4 – C5	1.414(6)
C5 – C6	1.355(6)
C6 – C7	1.408(6)
C7 – N1	1.397(5)
C7 – C8	1.391(6)
C8 – N2	1.394(6)
C8 – C9	1.427(6)
C9 – C10	1.350(7)
C10 – C11	1.415(7)
C11 – C12	1.346(7)
C12 – N2	1.382(6)

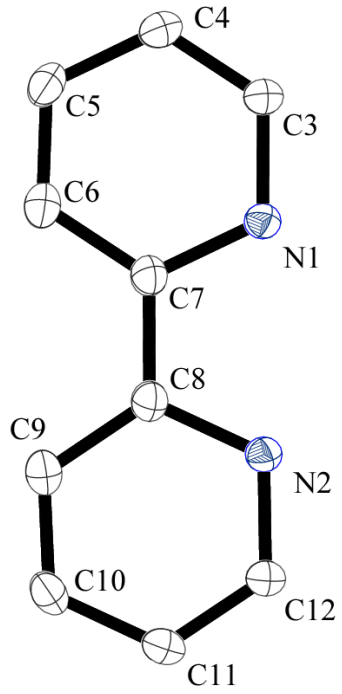

centers each with three facial carbonyls and a bipyridine ligand. The potassium cation is encapsulated by the crown ether and is within a short distance of one of the carbonyl oxygen atoms (K1 – O5, 2.659(8)). The potassium is also coordinated by a disordered Et_2O molecule.

Crystals of **4** have also been grown without the crown ether, and no significant structural differences are observed (Figure 4.5). The rhenium centers in **4** are separated by 3.1574(6) Å, which is a slightly longer rhenium-rhenium bond that is seen in **2**. This is longer than the typical Re–Re bonds found in the Cambridge Structural Database, with only two other reported structures exhibiting longer Re–Re bonds (3.179 Å and 3.284 Å).[20, 21]

In the structure of **2**, the bipyidine ligands are found in a pseudo-trans geometry, but upon the transfer of an additional electron the bipyridine ligands shift to

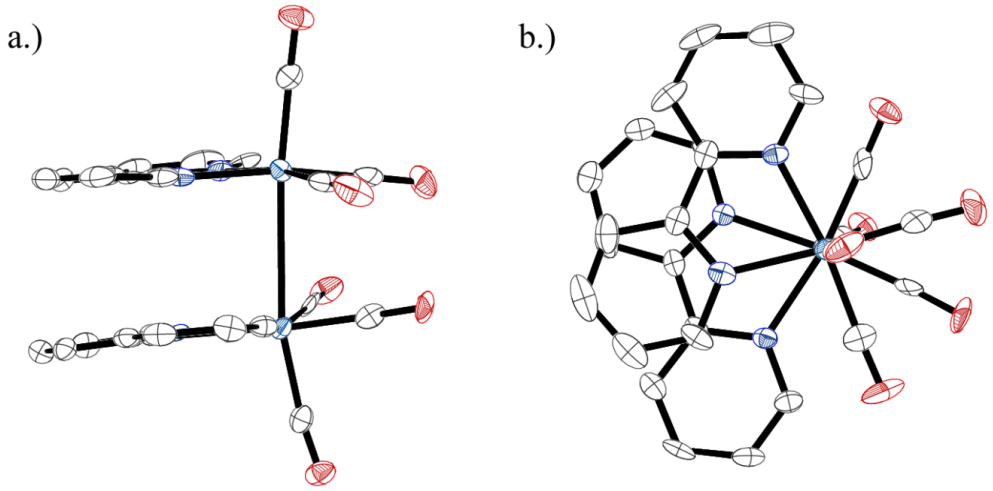

Figure 4.4 Molecular structure of [Re(bpy)(CO3]2- (4) a.) along the M-M bond and b.) along the M-M bond. The hydrogen atoms, cation, and solvents are omitted for clarity. The ellipsoids are shown at the 50% probability level. A full structure (Figure 4.5) and a table of bond lengths and angles can be found in the appendix.

form a π-stacked conformation (Figure 4.6). The bipyridine ligands are 3.24(4) Å apart, which is shorter than expected for traditional π-stacking (e.g., 3.4-3.6 for π-stacked porphyrins).[22] Although bond alternation (arising from π* occupancy) can be seen in the bipyridine ligand on both metal centers, we speculate from the FTIR spectrum that this is due to positional crystallographic disorder between the reduced and neutral ligands in the unit cell.

While the solid state structures of the anions of the bipyridine and 4,4'-di-*tert*-butyl substituted bipyridine complexes are similar, it is still unclear which underlying property (i.e., electronic or steric) results in the large difference observed in the electrocatalytic rates. With the support of the data presented here, we can postulate that the formation of the dimer and the subsequent reduction to cleave the metal-metal bond is an unproductive side reaction that decreases the total available active species in the electrocatalytic double-layer. We are currently investigating the relationship between the structures of several anionic species and their corresponding electrocatalytic rates using a range of substituted bipyridine ligands.

4.3 Conclusions

Here we have reported the structures of the Re-Re dimer $[Re(bpy)(CO)_3]_2$ (**2**), the reduced dimer $[Re(bpy)(CO)_3]_2^-$ (**4**), and the anionic monomer $Re(bpy)(CO)_3^-$ (**3**), which were synthesized by the addition of 1, 1.5, and 2 equivalents of KC_8 to $Re(bpy)(CO)_3Cl$, respectively. Interestingly the first reduction of the dimer does not result in the cleavage of the metal-metal bond; rather, due to the electro-active bipyridines, the dimeric structure is maintained until a second electron is introduced.

Acknowledgment. Financial support was provided by DARPA (Surface Catalysis for Energy Program). We thank Prof. Arnold Rheingold and Dr. Curtis Moore at the UCSD Crystallography Facility.

4.4 Experimental

General Considerations: $Re(bpy)(CO)_3Cl$ and KC_8 were synthesized by previously reported methods.[14, 23] THF and Pentane were sparged with argon and dried over basic alumina with a custom dry solvent system and then stored over activated molecular sieves. 18-crown-6 was recrystallized from acetonitrile, tetrabutylammonium hexafluorophosphate (TBAH) was recrystallized twice from methanol, and both were dried in vacuo. All other chemicals were purchased from commercial sources and used as received. Elemental analysis was performed by Midwest MicroLab, LLC, Indianapolis, IN.

Synthesis of $[Re(bpy)(CO)_3]_2$ (2). $Re(bpy)(CO)_3Cl$ (0.100 g, 0.217 mmol) was added to ~20 mL THF under an inert atmosphere. The solution was then cooled to –35 °C and 1.1 eq (0.032 g, 0.238 mmol) of KC_8 was added to the solution and allowed to warm to room temperature. After an hour, the solution was filtered through a plug of silica gel, and the column was washed with an additional 20 mL of THF. The solvent was removed *in vacuo* to afford the sparingly soluble (**2**) with a total yield of 54% (0.050 g, 0.117 mmol). ^{1}H NMR (500 MHz, THF-d_8, 20 °C): δ 7.08 (dt, 4H, J = 6 Hz, 1 Hz), δ 7.66 (dt, 4H, J = 8 Hz, 2 Hz), δ 8.25 (d, 4H, J = 6 Hz), δ 8.36 (d, 4H, J = 8 Hz). IR(THF) ν(CO): 1990, 1952, 1986, 1862 cm^{-1}. Anal. Calcd for **1**, $C_{26}H_{16}N_4O_6Re_2$: C, 36.63; H, 1.89; N, 6.57. Found: C, 36.68; H, 2.06; N, 6.43.

Synthesis of [Re(bpy)(CO)$_3$] [K(18-crown-6)] (3). To 20 mL of THF, Re(bpy)(CO)$_3$Cl (0.100 g, 0.217 mmol) and 18-crown-6 ether (0.120 mg, 0.455 mmol) were added under an inert atmosphere. The solution was then cooled to –35 °C, and 2.1 eq (0.061 g, 0.455 mmol) of KC_8 was added to the solution and allowed to warm to room temperature. After warming to room temperature for an hour, the solution was filtered, affording a spectroscopically pure deep purple solution. The solution was concentrated under vacuum, and then ~15 mL of pentane was added to the solution before placing the vial in a freezer. After 2 hours the product was obtained by decanting the supernatant and dried *in vacuo* to yield 0.116 mg of **(3)** (0.159 mmol, 73% yield). An analogous procedure using **2** as the starting material yields **3** quantitatively as shown by FTIR. ^{1}H NMR (500 MHz, THF-d$_8$, 20 °C): δ 3.55 (s, 24H), δ 5.26 (dt, 2H, *J* = 7 Hz, 1 Hz), δ 5.92 (ddd, 2H, *J* = 9 Hz, 6 Hz, 1 Hz), δ 7.23 (d, 2H, *J* = 9 Hz), δ 8.88 (d, 2H, *J* = 6 Hz). IR(THF) ν(CO): 1945, 1839 cm^{-1}. Anal. Calcd for **1**, $C_{25}H_{32}KN_2O_9Re$: C, 41.14; H, 4.42; N, 3.84. Found: C, 42.20; H, 4.23; N, 3.62

X-ray structure determination. The single crystal X-ray diffraction studies were carried out on either a Bruker Kappa APEX-II CCD diffractometer or Bruker Platform APEX CCD diffractometer, and both instruments were equipped with Mo Kα radiation (λ = 0.71073 Å). The crystals were mounted on a Cryoloop with Paratone oil, and data was collected under a nitrogen gas stream at 100(2) K using ω and ϕ scans. Data was integrated using the Bruker SAINT software program and scaled using the SADABS software program. Solution by direct methods (SHELXS)

produced a complete phasing model consistent with the proposed structure. All nonhydrogen atoms were refined anisotropically by full-matrix least-squares methods (SHELXL-97).[24] All hydrogen atoms were placed using a riding model. Their positions were constrained relative to their parent atom using the appropriate HFIX command in SHELXL-97. Crystallographic data are summarized in the appendix.

Note: Much of the material for this chapter comes directly from a manuscript entitled "Structural investigations into the deactivation pathway of the CO_2 reduction electrocatalyst Re(bipy)$(CO)_3$Cl" by Eric E. Benson, and Clifford P. Kubiak, which has been submitted to *Chemical Communications,* **2012.** The dissertation author is the primary author of this manuscript.

4.5 References

1. Benson EE, Kubiak CP, Sathrum AJ, & Smieja JM (2009) Electrocatalytic and homogeneous approaches to conversion of CO_2 to liquid fuels. *Chem. Soc. Rev.* 38(1):89-99.

2. Savéant J-M (2008) Molecular Catalysis of Electrochemical Reactions. Mechanistic Aspects. *Chem. Rev.* 108(7):2348-2378.

3. Sullivan BP, Bolinger CM, Conrad D, Vining WJ, & Meyer TJ (1985) One-Electron and 2-Electron Pathways in the Electrocatalytic Reduction of CO_2 by Fac-Re(2,2'-Bipyridine)$(CO)_3$Cl. *J. Chem. Soc.-Chem. Commun.* (20):1414-1415.

4. Johnson FPA, George MW, Hartl F, & Turner JJ (1996) Electrocatalytic Reduction of CO_2 Using the Complexes [Re(bpy)$(CO)_3$L]n (n = +1, L = $P(OEt)_3$, CH_3CN; n = 0, L = Cl-, Otf-; bpy = 2,2‘-Bipyridine; Otf- = CF_3SO_3) as Catalyst Precursors: Infrared Spectroelectrochemical Investigation. *Organometallics* 15(15):3374-3387.

5. Fujita E & Muckerman JT (2004) Why Is Re−Re Bond Formation/Cleavage in [Re(bpy)$(CO)_3]_2$ Different from That in [Re$(CO)_5]_2$? Experimental and Theoretical Studies on the Dimers and Fragments. *Inorg. Chem.* 43(24):7636-7647.

6. Vlček A (2010) Ultrafast Excited-State Processes in Re(I) Carbonyl-Diimine Complexes: From Excitation to Photochemistry Photophysics of Organometallics. Topics in Organometallic Chemistry, ed Lees AJ (Springer Berlin / Heidelberg), Vol 29, pp 115-158.

7. Hawecker J, Lehn JM, & Ziessel R (1983) Efficient photochemical reduction of CO_2 to CO by visible-light irradiation of systemes containgin Re(bipy)$(CO)_3$X or Ru$(bipy)_3^{2+}$ -Co^{2+} combination as homogeneous catalysts. *J. Chem. Soc.-Chem. Commun.* (9):536-538.

8. Takeda H, Koike K, Inoue H, & Ishitani O (2008) Development of an Efficient Photocatalytic System for CO_2 Reduction Using Rhenium(I) Complexes Based on Mechanistic Studies. *J. Am. Chem. Soc.* 130(6):2023-2031.

9. Hayashi Y, Kita S, Brunschwig BS, & Fujita E (2003) Involvement of a Binuclear Species with the Re−C(O)O−Re Moiety in CO_2 Reduction Catalyzed by Tricarbonyl Rhenium(I) Complexes with Diimine Ligands: Strikingly Slow Formation of the Re−Re and Re−C(O)O−Re Species from Re(dmb)(CO)3S (dmb = 4,4‘-Dimethyl-2,2‘-bipyridine, S = Solvent). *J. Am. Chem. Soc.* 125(39):11976-11987.

10. Armstrong FA & Hirst J (2011) Reversibility and efficiency in electrocatalytic energy conversion and lessons from enzymes. *P. Nat. Acad. Sci. USA* 108(34):14049-14054.

11. Thoi VS & Chang CJ (2011) Nickel N-heterocyclic carbene-pyridine complexes that exhibit selectivity for electrocatalytic reduction of carbon dioxide over water. *Chem. Commun.* 47(23):6578-6580.

12. DuBois DL, Miedaner A, & Haltiwanger RC (1991) Electrochemical reduction of carbon dioxide catalyzed by [Pd(triphosphine)(solvent)](BF4)2 complexes: synthetic and mechanistic studies. *J. Am. Chem. Soc.* 113(23):8753-8764.

13. Stor GJ, Hartl F, van Outersterp JWM, & Stufkens DJ (1995) Spectroelectrochemical (IR, UV/Vis) Determination of the Reduction Pathways for a Series of $[Re(CO)_3(.alpha.\text{-}diimine)L']^{0/+}$ (L' = Halide, OTf-, THF, MeCN, n-PrCN, PPh_3, $P(OMe)_3$) Complexes. *Organometallics* 14(3):1115-1131.

14. Smieja JM & Kubiak CP (2010) $Re(bipy\text{-}tBu)(CO)_3Cl$−improved Catalytic Activity for Reduction of Carbon Dioxide: IR-Spectroelectrochemical and Mechanistic Studies. *Inorg. Chem.* 49(20):9283-9289.

15. Churchill MR, Amoh KN, & Wasserman HJ (1981) Redetermination of the crystal structure of dimanganese decacarbonyl and determination of the crystal structure of dirhenium decacarbonyl. Revised values for the manganese-manganese and rhenium-rhenium bond lengths in dimanganese decacarbonyl and dirhenium decacarbonyl. *Inorg. Chem.* 20(5):1609-1611.

16. Lee KY, Kuchynka DJ, & Kochi JK (1987) Formation of metal-metal bonds by ion-pair annihilation. Dimanganese carbonyls from manganate(I-) anions and manganese(I) cations. *Organometallics* 6(9):1886-1897.

17. Addison AW, Rao TN, Reedijk J, van Rijn J, & Verschoor GC (1984) Synthesis, structure, and spectroscopic properties of copper(II) compounds containing nitrogen-sulphur donor ligands; the crystal and molecular structure of aqua[1,7-bis(N-methylbenzimidazol-2'-yl)-2,6-dithiaheptane]copper(II) perchlorate. *J. Chem. Soc. Dalton* (7):1349-1356.

18. Smieja JM, *et al.* (2012) Kinetic and structural studies, origins of selectivity, and interfacial charge transfer in the artificial photosynthesis of CO. *P. Nat. Acad. Sci. USA*:Accepted.

19. Gore-Randall E, Irwin M, Denning MS, & Goicoechea JM (2009) Synthesis and Characterization of Alkali-Metal Salts of 2,2′- and 2,4′-Bipyridyl Radicals and Dianions. *Inorg. Chem.* 48(17):8304-8316.

20. Fan W, Zhang R, Leong WK, & Yan YK (2004) Reactions of the complexes [$Re_2(CO)_9$([eta]1-P-P)] (P-P=$Ph_2P(CH_2)nPPh_2$, n=1-6) with Me_3NO: formation of close-bridged complexes [$Re_2(CO)_8$([mu]-P-P)] and phosphine oxide complexes [$Re_2(CO)_9${P-P(O)}]. *Inorg. Chim. Acta* 357(9):2441-2450.

21. Narayanan BA & Kochi JK (1986) Transient formyl derivatives of rhenium carbonyls. The facile ligand dissociation of halorhenate species. *Inorg. Chim. Acta* 122(1):85-90.

22. Hunter CA & Sanders JKM (1990) The nature of .pi.-.pi. interactions. *J. Am. Chem. Soc.* 112(14):5525-5534.

23. Schwindt MA, Lejon T, & Hegedus LS (1990) Improved synthesis of (aminocarbene)chromium(0) complexes with use of C8K-generated Cr(CO)52-. Multivariant optimization of an organometallic reaction. *Organometallics* 9(10):2814-2819.

24. Sheldrick G (2008) A short history of SHELX. *Acta Crystall. A* 64(1):112-122.

4.6 Appendix

Table 4.2 Crystallographic Data and Refinement Information

Compound	**$[Re(bpy)(CO)_3]_2$**	**$[Re(bpy)(CO)_3]_2$ [K(18-crown-6)•Et_2O]**	**$[Re(bpy)(CO)_3]_2$ [K$(THF)_2$]**	**$Re(bpy)(CO)_3$ [K(18-crown-6)THF]**
empirical formula	$C_{26}H_{16}N_4O_6Re_2$	$C_{42}H_{50}KN_4O_{13}Re_2$	$C_{34}H_{32}KN_4O_8Re_2$	$C_{29}H_{40}KN_2O_{10}Re$
formula weight	852.83	1305.50	1036.14	801.93
crystal system	Monoclinic	Monoclinic	Monoclinic	Monoclinic
lattice parameters				
a (Å)	9.620(3)	8.9201(8)	8.8574(5)	23.3023(13)
b (Å)	19.620(6)	12.4212(12)	11.5882(7)	18.0705(9)
c (Å)	12.933(4)	38.087(4)	32.4500(18)	16.0034(8)
α (deg)	90	90	90	90.00
β (deg)	103.710(4)	95.7410(10)	95.504(3)	73.240(3)
γ (deg)	90	90	90	90.00
V (Å3)	2371.5(13)	4198.8(7)	3315.4(3)	6452.5(6)
space group	C 2/c	P 2_1/n	P 2_1/n	P 2_1/c
Z value	4	4	4	8
ρcalc (g/cm3)	2.389	1.829	2.076	1.651
μ (Mo Kα) (mm-1)	0.71073	0.71073	0.71073	0.71073
temperature (K)	100(2)	100(2)	100(2)	100(2)
2Θ max (deg)	56.52	50.88	50.7	51.12
no. obs. ($I > 2\alpha(I)$)	2666	7756	6067	11977
no. parameters	173	508	441	798
goodness of fit	1.006	1.165	1.137	1.079
max. shift in cycle	0.001	0.001	0.001	0.027
residuals: R1; wR2	0.0489; 0.1094	0.0512; 0.1050	0.0207; 0.0412	0.0331; 0.0578
largest peak	2.355	1.960	0.625	1.705
deepest hole	-2.666	-2.675	-0.789	-0.756

Table 4.3 Selected bond lengths and angles for complexes presented.

Compound	$[Re(bpy)(CO)_3]_2$	$[Re(bpy)(CO)_3]_2[K(18\text{-crown-}6)\bullet Et_2O]$	$[Re(bpy)(CO)_3]_2[K(THF)_2]$	$Re(bpy)(CO)_3[K(18\text{-crown-}6)THF]$[a]
Re1 – N1	2.165(8)	2.142(7)	2.136(3)	2.074(3)
Re1 – N2	2.141(8)	2.133(8)	2.131(4)	2.085(4)
N1 – Re1 – N2	76.2(3)	75.2(3)	74.96(13)	75.04(14)
Re1 – C1	1.909(11)	1.897(12)	1.906(5)	1.915(5)
Re1 – C2	1.939(11)	1.906(10)	1.911(5)	1.894(5)
Re1 – C3	1.935(11)	1.883(10)	1.895(5)	1.855(5)
C1 – O1	1.150(12)	1.188(13)	1.159(5)	1.167(5)
C2 – O2	1.129(12)	1.177(12)	1.161(5)	1.166(6)
C3 – O3	1.116(13)	1.185(12)	1.161(6)	1.166(6)
N1 – Re1 – C1	97.2(4)	100.9(4)	97.90(15)	98.64(17)
N1 – Re1 – C3	95.8(4)	94.5(4)	94.07(16)	110.33(18)
N2 – Re1 – C3	97.4(4)	98.1(4)	97.25(18)	102.8(2)
N2 – Re1 – C2	95.0(4)	97.3(4)	97.46(16)	95.23(18)
C1 – Re1 – C2	91.0(4)	85.5(5)	88.60(18)	85.78(19)
Re1 – Re1	3.0791(13)			
Re1 – Re2		3.1574(6)	3.1348(3)	
Re2 – N3		2.124(7)	2.131(3)	
Re2 – N4		2.140(8)	2.129(3)	
N3 – Re1 – N4		75.5(3)	75.20(13)	
Re1 – C14		1.906(11)	1.907(5)	
Re1 – C15		1.881(10)	1.901(4)	
Re1 – C16		1.891(10)	1.900(5)	
C14 – O4		1.176(12)	1.155(5)	
C15 – O5		1.187(12)	1.172(5)	
C16 – O6		1.189(12)	1.159(6)	
N3 – Re1 – C14		95.7(4)	98.13(16)	
N3 – Re1 – C16		97.0(3)	95.89(16)	
N4 – Re1 – C15		98.8(3)	98.70(16)	
N4 – Re1 – C16		103.7(4)	97.07(17)	
C14 – Re1 – C15		88.7(4)	86.82(18)	

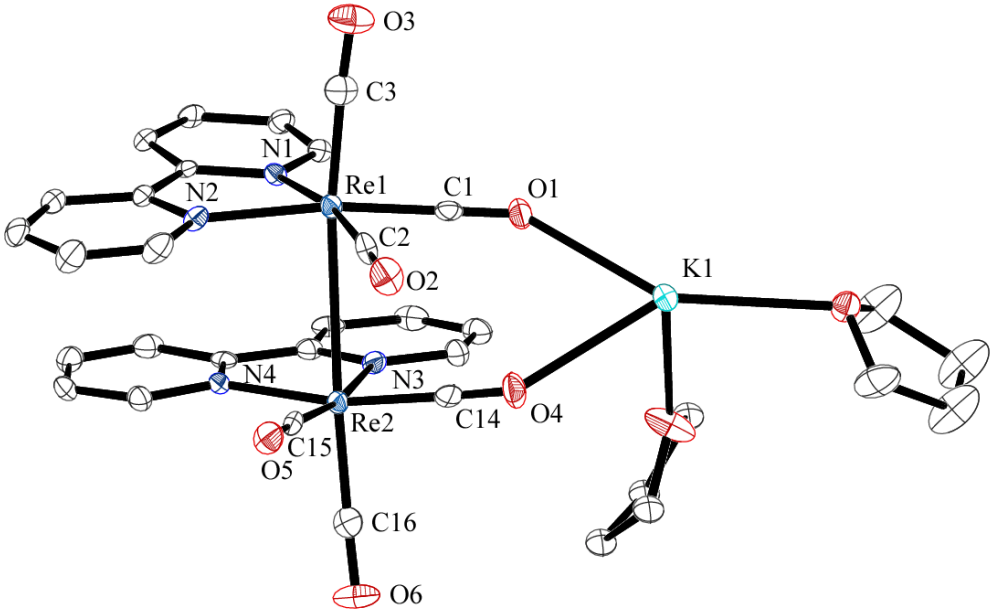

Figure 4.5 Molecular structure of [[Re(bpy)(CO)3]2][K(THF)2], with hydrogen atoms omitted for clarity. Position 1 of 2 is shown for the disordered THF molecules, and the ellipsoids are set at the 50% probability level.

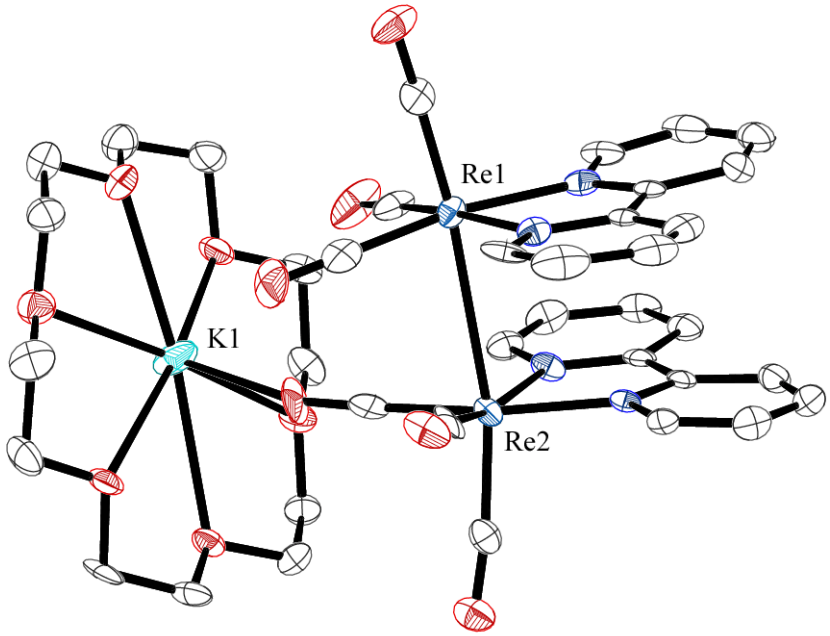

Figure 4.6 Molecular structure of $[[Re(bpy)(CO)_3]_2][K(18\text{-crown-6})]$, with hydrogen atoms and disordered Et_2O molecule removed for clarity. The ellipsoids are set at the 50% level.

Table 4.4 Crystal data and structure refinement for $[Re(bpy)(CO)_3]_2$

Identification code	eb_100412_0ma	
Empirical formula	C26 H16 N4 O6 Re2	
Formula weight	852.83	
Temperature	100(2) K	
Wavelength	0.71073 Å	
Crystal system	Monoclinic	
Space group	C2/c	
Unit cell dimensions	a = 9.620(3) Å	α= 90°.
	b = 19.620(6) Å	β= 103.710(4)°.
	c = 12.933(4) Å	γ = 90°.
Volume	2371.5(13) $Å^3$	
Z	4	
Density (calculated)	2.389 Mg/m^3	
Absorption coefficient	10.252 mm^{-1}	
F(000)	1592	
Crystal size	0.38 x 0.21 x 0.09 mm^3	
Theta range for data collection	2.08 to 28.63°.	
Index ranges	-12<=h<=12, 0<=k<=25, 0<=l<=17	
Reflections collected	2666	
Independent reflections	2666 [R(int) = 0.0638]	
Completeness to theta = 25.00°	96.0 %	
Absorption correction	Semi-empirical from equivalents	
Max. and min. transmission	0.4589 and 0.1119	
Refinement method	Full-matrix least-squares on F^2	
Data / restraints / parameters	2666 / 0 / 173	
Goodness-of-fit on F^2	1.006	
Final R indices [I>2sigma(I)]	R1 = 0.0489, wR2 = 0.1094	
R indices (all data)	R1 = 0.0755, wR2 = 0.1197	
Largest diff. peak and hole	2.355 and -2.666 e.$Å^{-3}$	

Table 4.5 Bond lengths [Å] and angles [°] for $[Re(bpy)(CO)_3]_2$

Re(1)-Re(1)#1	3.0791(13)	N(2)-Re(1)-Re(1)#1	92.2(2)
Re(1)-N(1)	2.165(8)	N(2)-Re(1)-N(1)	76.2(3)
Re(1)-N(2)	2.141(8)	C(1)-Re(1)-Re(1)#1	80.4(3)
Re(1)-C(1)	1.909(11)	C(1)-Re(1)-N(1)	97.2(4)
Re(1)-C(2)	1.939(11)	C(1)-Re(1)-N(2)	169.7(4)
Re(1)-C(3)	1.935(11)	C(1)-Re(1)-C(2)	91.0(4)
O(1)-C(1)	1.150(12)	C(1)-Re(1)-C(3)	91.1(4)
O(2)-C(2)	1.129(12)	C(2)-Re(1)-Re(1)#1	81.9(3)
O(3)-C(3)	1.116(13)	C(2)-Re(1)-N(1)	170.6(4)
N(1)-C(4)	1.319(15)	C(2)-Re(1)-N(2)	95.0(4)
N(1)-C(8)	1.424(13)	C(3)-Re(1)-Re(1)#1	167.1(3)
N(2)-C(9)	1.387(13)	C(3)-Re(1)-N(1)	95.8(4)
N(2)-C(13)	1.333(13)	C(3)-Re(1)-N(2)	97.4(4)
C(4)-H(4)	0.9500	C(3)-Re(1)-C(2)	88.6(4)
C(4)-C(5)	1.389(14)	C(4)-N(1)-Re(1)	124.2(7)
C(5)-H(5)	0.9500	C(4)-N(1)-C(8)	117.4(9)
C(5)-C(6)	1.394(15)	C(8)-N(1)-Re(1)	118.1(7)
C(6)-H(6)	0.9500	C(9)-N(2)-Re(1)	116.3(7)
C(6)-C(7)	1.355(15)	C(13)-N(2)-Re(1)	126.0(7)
C(7)-H(7)	0.9500	C(13)-N(2)-C(9)	117.6(9)
C(7)-C(8)	1.335(14)	O(1)-C(1)-Re(1)	178.6(9)
C(8)-C(9)	1.484(14)	O(2)-C(2)-Re(1)	176.2(9)
C(9)-C(10)	1.412(15)	O(3)-C(3)-Re(1)	174.8(9)
C(10)-H(10)	0.9500	N(1)-C(4)-H(4)	118.7
C(10)-C(11)	1.374(15)	N(1)-C(4)-C(5)	122.5(11)
C(11)-H(11)	0.9500	C(5)-C(4)-H(4)	118.7
C(11)-C(12)	1.397(15)	C(4)-C(5)-H(5)	120.1
C(12)-H(12)	0.9500	C(4)-C(5)-C(6)	119.8(11)
C(12)-C(13)	1.378(14)	C(6)-C(5)-H(5)	120.1
C(13)-H(13)	0.9500	C(5)-C(6)-H(6)	121.5
		C(7)-C(6)-C(5)	117.0(10)
N(1)-Re(1)-Re(1)#1	94.9(2)	C(7)-C(6)-H(6)	121.5

Table 4.5 Cont.

C(6)-C(7)-H(7)	118.4	C(11)-C(10)-H(10)	119.5
C(8)-C(7)-C(6)	123.2(12)	C(10)-C(11)-H(11)	121.3
C(8)-C(7)-H(7)	118.4	C(10)-C(11)-C(12)	117.3(9)
N(1)-C(8)-C(9)	111.0(9)	C(12)-C(11)-H(11)	121.3
C(7)-C(8)-N(1)	120.1(10)	C(11)-C(12)-H(12)	120.0
C(7)-C(8)-C(9)	128.9(11)	C(13)-C(12)-C(11)	120.0(9)
N(2)-C(9)-C(8)	118.3(9)	C(13)-C(12)-H(12)	120.0
N(2)-C(9)-C(10)	120.2(9)	N(2)-C(13)-C(12)	123.8(10)
C(10)-C(9)-C(8)	121.5(10)	N(2)-C(13)-H(13)	118.1
C(9)-C(10)-H(10)	119.5	C(12)-C(13)-H(13)	118.1
C(11)-C(10)-C(9)	121.1(10)		

Symmetry transformations used to generate equivalent atoms:
#1 -x+1,y,-z+3/2

Table 4.6 Crystal data and structure refinement for $[(Re(bpy)(CO)_3)_2]$ $[K(18\text{-crown-}6)(Et_2O)]$

Identification code	eb_100923_0m	
Empirical formula	C42 H50 K N4 O13 Re2	
Formula weight	1304.50	
Temperature	100(2) K	
Wavelength	0.71073 Å	
Crystal system	Monoclinic	
Space group	P2(1)/n	
Unit cell dimensions	a = 8.9201(8) Å	α= 90°.
	b = 12.4212(12) Å	β= 95.7410(10)°.
	c = 38.087(4) Å	γ = 90°.
Volume	4198.8(7) $Å^3$	
Z	4	
Density (calculated)	1.829 Mg/m^3	
Absorption coefficient	5.924 mm^{-1}	
F(000)	2244	
Crystal size	0.10 x 0.05 x 0.03 mm^3	
Theta range for data collection	1.73 to 25.44°.	
Index ranges	-9<=h<=10, -12<=k<=15, -45<=l<=45	
Reflections collected	32169	
Independent reflections	7756 [R(int) = 0.0585]	
Completeness to theta = 25.00°	100.0 %	
Absorption correction	Semi-empirical from equivalents	
Max. and min. transmission	0.8660 and 0.5888	
Refinement method	Full-matrix least-squares on F^2	
Data / restraints / parameters	7756 / 0 / 508	
Goodness-of-fit on F^2	1.165	
Final R indices [I>2sigma(I)]	R1 = 0.0512, wR2 = 0.1050	
R indices (all data)	R1 = 0.0612, wR2 = 0.1083	
Largest diff. peak and hole	1.960 and -2.675 e.$Å^{-3}$	

Table 4.7 Bond lengths [Å] and angles [°] for $[(Re(bpy)(CO)_3)_2]$ $[K(18\text{-crown-}6)(Et_2O)]$

Re(1)-C(3)	1.883(10)	O(11)-C(35)	1.419(11)
Re(1)-C(1)	1.897(12)	O(11)-C(34)	1.435(11)
Re(1)-C(2)	1.906(10)	O(12)-C(36)	1.418(11)
Re(1)-N(2)	2.133(8)	O(12)-C(37)	1.430(11)
Re(1)-N(1)	2.142(7)	N(1)-C(4)	1.354(12)
Re(1)-Re(2)	3.1574(6)	N(1)-C(8)	1.385(12)
Re(2)-C(15)	1.881(10)	N(2)-C(13)	1.367(12)
Re(2)-C(16)	1.891(10)	N(2)-C(9)	1.382(12)
Re(2)-C(14)	1.906(11)	N(3)-C(17)	1.375(11)
Re(2)-N(3)	2.124(7)	N(3)-C(21)	1.385(12)
Re(2)-N(4)	2.140(8)	N(4)-C(26)	1.361(11)
K(1)-O(5)	2.659(8)	N(4)-C(22)	1.387(12)
K(1)-O(8)	2.775(7)	C(4)-C(5)	1.382(15)
K(1)-O(12)	2.810(7)	C(4)-H(4)	0.9500
K(1)-O(7)	2.811(7)	C(5)-C(6)	1.428(18)
K(1)-O(10)	2.814(7)	C(5)-H(5)	0.9500
K(1)-O(9)	2.820(8)	C(6)-C(7)	1.330(17)
K(1)-O(11)	2.846(7)	C(6)-H(6)	0.9500
O(1)-C(1)	1.188(13)	C(7)-C(8)	1.395(13)
O(2)-C(2)	1.177(12)	C(7)-H(7)	0.9500
O(3)-C(3)	1.185(12)	C(8)-C(9)	1.441(14)
O(4)-C(14)	1.176(12)	C(9)-C(10)	1.424(14)
O(5)-C(15)	1.187(12)	C(10)-C(11)	1.369(17)
O(6)-C(16)	1.189(12)	C(10)-H(10)	0.9500
O(7)-C(38)	1.422(12)	C(11)-C(12)	1.401(18)
O(7)-C(27)	1.450(12)	C(11)-H(11)	0.9500
O(8)-C(29)	1.425(12)	C(12)-C(13)	1.367(15)
O(8)-C(28)	1.433(13)	C(12)-H(12)	0.9500
O(9)-C(31)	1.416(13)	C(13)-H(13)	0.9500
O(9)-C(30)	1.430(12)	C(17)-C(18)	1.358(13)
O(10)-C(32)	1.431(12)	C(17)-H(17)	0.9500
O(10)-C(33)	1.439(11)	C(18)-C(19)	1.381(14)

Table 4.7 Cont.

C(18)-H(18)	0.9500	C(34)-H(34B)	0.9900
C(19)-C(20)	1.379(14)	C(35)-C(36)	1.512(13)
C(19)-H(19)	0.9500	C(35)-H(35A)	0.9900
C(20)-C(21)	1.416(13)	C(35)-H(35B)	0.9900
C(20)-H(20)	0.9500	C(36)-H(36A)	0.9900
C(21)-C(22)	1.414(13)	C(36)-H(36B)	0.9900
C(22)-C(23)	1.426(13)	C(37)-C(38)	1.518(14)
C(23)-C(24)	1.369(13)	C(37)-H(37A)	0.9900
C(23)-H(23)	0.9500	C(37)-H(37B)	0.9900
C(24)-C(25)	1.400(15)	C(38)-H(38A)	0.9900
C(24)-H(24)	0.9500	C(38)-H(38B)	0.9900
C(25)-C(26)	1.364(14)		
C(25)-H(25)	0.9500	C(3)-Re(1)-C(1)	89.8(4)
C(26)-H(26)	0.9500	C(3)-Re(1)-C(2)	93.2(4)
C(27)-C(28)	1.493(15)	C(1)-Re(1)-C(2)	85.5(5)
C(27)-H(27A)	0.9900	C(3)-Re(1)-N(2)	98.1(4)
C(27)-H(27B)	0.9900	C(1)-Re(1)-N(2)	171.4(4)
C(28)-H(28A)	0.9900	C(2)-Re(1)-N(2)	97.3(4)
C(28)-H(28B)	0.9900	C(3)-Re(1)-N(1)	94.5(4)
C(29)-C(30)	1.506(15)	C(1)-Re(1)-N(1)	100.9(4)
C(29)-H(29A)	0.9900	C(2)-Re(1)-N(1)	169.9(4)
C(29)-H(29B)	0.9900	N(2)-Re(1)-N(1)	75.2(3)
C(30)-H(30A)	0.9900	C(3)-Re(1)-Re(2)	174.3(3)
C(30)-H(30B)	0.9900	C(1)-Re(1)-Re(2)	84.7(3)
C(31)-C(32)	1.503(15)	C(2)-Re(1)-Re(2)	85.0(3)
C(31)-H(31A)	0.9900	N(2)-Re(1)-Re(2)	87.5(2)
C(31)-H(31B)	0.9900	N(1)-Re(1)-Re(2)	87.9(2)
C(32)-H(32A)	0.9900	C(15)-Re(2)-C(16)	89.1(4)
C(32)-H(32B)	0.9900	C(15)-Re(2)-C(14)	88.7(4)
C(33)-C(34)	1.471(14)	C(16)-Re(2)-C(14)	90.2(4)
C(33)-H(33A)	0.9900	C(15)-Re(2)-N(3)	172.4(3)
C(33)-H(33B)	0.9900	C(16)-Re(2)-N(3)	97.0(3)
C(34)-H(34A)	0.9900	C(14)-Re(2)-N(3)	95.7(4)

Table 4.7 Cont.

C(15)-Re(2)-N(4)	98.8(3)	C(27)-O(7)-K(1)	113.4(6)
C(16)-Re(2)-N(4)	103.7(4)	C(29)-O(8)-C(28)	112.2(7)
C(14)-Re(2)-N(4)	164.2(4)	C(29)-O(8)-K(1)	116.8(6)
N(3)-Re(2)-N(4)	75.5(3)	C(28)-O(8)-K(1)	113.1(6)
C(15)-Re(2)-Re(1)	82.1(3)	C(31)-O(9)-C(30)	111.9(8)
C(16)-Re(2)-Re(1)	165.6(3)	C(31)-O(9)-K(1)	112.2(6)
C(14)-Re(2)-Re(1)	78.2(3)	C(30)-O(9)-K(1)	109.5(6)
N(3)-Re(2)-Re(1)	92.69(19)	C(32)-O(10)-C(33)	112.4(7)
N(4)-Re(2)-Re(1)	89.0(2)	C(32)-O(10)-K(1)	115.4(6)
O(5)-K(1)-O(8)	115.1(2)	C(33)-O(10)-K(1)	114.7(6)
O(5)-K(1)-O(12)	87.0(2)	C(35)-O(11)-C(34)	111.3(7)
O(8)-K(1)-O(12)	120.2(2)	C(35)-O(11)-K(1)	112.1(5)
O(5)-K(1)-O(7)	122.2(2)	C(34)-O(11)-K(1)	113.4(5)
O(8)-K(1)-O(7)	61.4(2)	C(36)-O(12)-C(37)	111.9(7)
O(12)-K(1)-O(7)	60.04(19)	C(36)-O(12)-K(1)	118.2(5)
O(5)-K(1)-O(10)	69.0(2)	C(37)-O(12)-K(1)	117.4(5)
O(8)-K(1)-O(10)	121.2(2)	C(4)-N(1)-C(8)	117.1(8)
O(12)-K(1)-O(10)	118.6(2)	C(4)-N(1)-Re(1)	125.0(7)
O(7)-K(1)-O(10)	167.4(2)	C(8)-N(1)-Re(1)	117.8(6)
O(5)-K(1)-O(9)	98.5(2)	C(13)-N(2)-C(9)	117.9(9)
O(8)-K(1)-O(9)	60.9(2)	C(13)-N(2)-Re(1)	124.8(7)
O(12)-K(1)-O(9)	173.2(2)	C(9)-N(2)-Re(1)	117.2(6)
O(7)-K(1)-O(9)	119.2(2)	C(17)-N(3)-C(21)	117.6(8)
O(10)-K(1)-O(9)	60.5(2)	C(17)-N(3)-Re(2)	125.2(6)
O(5)-K(1)-O(11)	74.3(2)	C(21)-N(3)-Re(2)	116.9(6)
O(8)-K(1)-O(11)	170.6(2)	C(26)-N(4)-C(22)	117.5(8)
O(12)-K(1)-O(11)	59.22(19)	C(26)-N(4)-Re(2)	126.2(7)
O(7)-K(1)-O(11)	115.2(2)	C(22)-N(4)-Re(2)	116.3(6)
O(10)-K(1)-O(11)	60.00(19)	O(1)-C(1)-Re(1)	177.0(9)
O(9)-K(1)-O(11)	118.4(2)	O(2)-C(2)-Re(1)	177.3(11)
C(15)-O(5)-K(1)	152.6(7)	O(3)-C(3)-Re(1)	178.1(10)
C(38)-O(7)-C(27)	110.0(7)	N(1)-C(4)-C(5)	123.2(11)
C(38)-O(7)-K(1)	112.6(5)	N(1)-C(4)-H(4)	118.4

Table 4.7 Cont.

C(5)-C(4)-H(4)	118.4	N(3)-C(17)-H(17)	118.4
C(4)-C(5)-C(6)	117.7(11)	C(17)-C(18)-C(19)	119.8(9)
C(4)-C(5)-H(5)	121.2	C(17)-C(18)-H(18)	120.1
C(6)-C(5)-H(5)	121.2	C(19)-C(18)-H(18)	120.1
C(7)-C(6)-C(5)	120.3(10)	C(20)-C(19)-C(18)	119.3(10)
C(7)-C(6)-H(6)	119.9	C(20)-C(19)-H(19)	120.3
C(5)-C(6)-H(6)	119.8	C(18)-C(19)-H(19)	120.3
C(6)-C(7)-C(8)	119.7(11)	C(19)-C(20)-C(21)	120.0(9)
C(6)-C(7)-H(7)	120.1	C(19)-C(20)-H(20)	120.0
C(8)-C(7)-H(7)	120.1	C(21)-C(20)-H(20)	120.0
N(1)-C(8)-C(7)	122.0(10)	N(3)-C(21)-C(22)	115.4(8)
N(1)-C(8)-C(9)	114.0(8)	N(3)-C(21)-C(20)	120.1(8)
C(7)-C(8)-C(9)	124.0(10)	C(22)-C(21)-C(20)	124.6(9)
N(2)-C(9)-C(10)	120.0(10)	N(4)-C(22)-C(21)	115.7(8)
N(2)-C(9)-C(8)	115.9(8)	N(4)-C(22)-C(23)	120.3(8)
C(10)-C(9)-C(8)	124.2(9)	C(21)-C(22)-C(23)	124.0(9)
C(11)-C(10)-C(9)	120.3(11)	C(24)-C(23)-C(22)	120.1(9)
C(11)-C(10)-H(10)	119.9	C(24)-C(23)-H(23)	120.0
C(9)-C(10)-H(10)	119.9	C(22)-C(23)-H(23)	120.0
C(10)-C(11)-C(12)	119.2(11)	C(23)-C(24)-C(25)	118.8(9)
C(10)-C(11)-H(11)	120.4	C(23)-C(24)-H(24)	120.6
C(12)-C(11)-H(11)	120.4	C(25)-C(24)-H(24)	120.6
C(13)-C(12)-C(11)	119.2(11)	C(26)-C(25)-C(24)	119.7(9)
C(13)-C(12)-H(12)	120.4	C(26)-C(25)-H(25)	120.1
C(11)-C(12)-H(12)	120.4	C(24)-C(25)-H(25)	120.1
C(12)-C(13)-N(2)	123.4(11)	N(4)-C(26)-C(25)	123.6(10)
C(12)-C(13)-H(13)	118.3	N(4)-C(26)-H(26)	118.2
N(2)-C(13)-H(13)	118.3	C(25)-C(26)-H(26)	118.2
O(4)-C(14)-Re(2)	179.1(9)	O(7)-C(27)-C(28)	107.7(8)
O(5)-C(15)-Re(2)	176.2(8)	O(7)-C(27)-H(27A)	110.2
O(6)-C(16)-Re(2)	172.0(8)	C(28)-C(27)-H(27A)	110.2
C(18)-C(17)-N(3)	123.3(9)	O(7)-C(27)-H(27B)	110.2
C(18)-C(17)-H(17)	118.4	C(28)-C(27)-H(27B)	110.2

Table 4.7 Cont.

H(27A)-C(27)-H(27B)	108.5	C(34)-C(33)-H(33A)	110.1
O(8)-C(28)-C(27)	109.4(8)	O(10)-C(33)-H(33B)	110.1
O(8)-C(28)-H(28A)	109.8	C(34)-C(33)-H(33B)	110.1
C(27)-C(28)-H(28A)	109.8	H(33A)-C(33)-H(33B)	108.4
O(8)-C(28)-H(28B)	109.8	O(11)-C(34)-C(33)	109.3(8)
C(27)-C(28)-H(28B)	109.8	O(11)-C(34)-H(34A)	109.8
H(28A)-C(28)-H(28B)	108.2	C(33)-C(34)-H(34A)	109.8
O(8)-C(29)-C(30)	108.4(8)	O(11)-C(34)-H(34B)	109.8
O(8)-C(29)-H(29A)	110.0	C(33)-C(34)-H(34B)	109.8
C(30)-C(29)-H(29A)	110.0	H(34A)-C(34)-H(34B)	108.3
O(8)-C(29)-H(29B)	110.0	O(11)-C(35)-C(36)	107.5(7)
C(30)-C(29)-H(29B)	110.0	O(11)-C(35)-H(35A)	110.2
H(29A)-C(29)-H(29B)	108.4	C(36)-C(35)-H(35A)	110.2
O(9)-C(30)-C(29)	108.6(9)	O(11)-C(35)-H(35B)	110.2
O(9)-C(30)-H(30A)	110.0	C(36)-C(35)-H(35B)	110.2
C(29)-C(30)-H(30A)	110.0	H(35A)-C(35)-H(35B)	108.5
O(9)-C(30)-H(30B)	110.0	O(12)-C(36)-C(35)	108.5(8)
C(29)-C(30)-H(30B)	110.0	O(12)-C(36)-H(36A)	110.0
H(30A)-C(30)-H(30B)	108.4	C(35)-C(36)-H(36A)	110.0
O(9)-C(31)-C(32)	109.1(9)	O(12)-C(36)-H(36B)	110.0
O(9)-C(31)-H(31A)	109.9	C(35)-C(36)-H(36B)	110.0
C(32)-C(31)-H(31A)	109.9	H(36A)-C(36)-H(36B)	108.4
O(9)-C(31)-H(31B)	109.9	O(12)-C(37)-C(38)	108.3(8)
C(32)-C(31)-H(31B)	109.9	O(12)-C(37)-H(37A)	110.0
H(31A)-C(31)-H(31B)	108.3	C(38)-C(37)-H(37A)	110.0
O(10)-C(32)-C(31)	108.7(9)	O(12)-C(37)-H(37B)	110.0
O(10)-C(32)-H(32A)	110.0	C(38)-C(37)-H(37B)	110.0
C(31)-C(32)-H(32A)	110.0	H(37A)-C(37)-H(37B)	108.4
O(10)-C(32)-H(32B)	110.0	O(7)-C(38)-C(37)	108.5(8)
C(31)-C(32)-H(32B)	110.0	O(7)-C(38)-H(38A)	110.0
H(32A)-C(32)-H(32B)	108.3	C(37)-C(38)-H(38A)	110.0
O(10)-C(33)-C(34)	108.2(8)	O(7)-C(38)-H(38B)	110.0
O(10)-C(33)-H(33A)	110.1	C(37)-C(38)-H(38B)	110.0

Table 4.7 Cont.

H(38A)-C(38)-H(38B)	108.

Table 4.8 Crystal data and structure refinement for $[(Re(bpy)(CO)_3)_2][K(THF)_2]$

Identification code	eb_111014_0m	
Empirical formula	C34 H32 K N4 O8 Re2	
Formula weight	1036.14	
Temperature	100(2) K	
Wavelength	0.71073 Å	
Crystal system	Monoclinic	
Space group	P2(1)/n	
Unit cell dimensions	a = 8.8574(5) Å	α= 90°.
	b = 11.5882(7) Å	β= 95.504(3)°.
	c = 32.4500(18) Å	γ = 90°.
Volume	3315.4(3) $Å^3$	
Z	4	
Density (calculated)	2.076 Mg/m^3	
Absorption coefficient	7.480 mm^{-1}	
F(000)	1988	
Crystal size	0.10 x 0.05 x 0.01 mm^3	
Theta range for data collection	1.26 to 25.38°.	
Index ranges	-10<=h<=10, -13<=k<=9, -36<=l<=39	
Reflections collected	23718	
Independent reflections	6067 [R(int) = 0.0280]	
Completeness to theta = 25.00°	99.9 %	
Absorption correction	Semi-empirical from equivalents	
Max. and min. transmission	0.9290 and 0.5217	
Refinement method	Full-matrix least-squares on F^2	
Data / restraints / parameters	6067 / 3 / 441	
Goodness-of-fit on F^2	1.140	
Final R indices [I>2sigma(I)]	R1 = 0.0207, wR2 = 0.0429	
R indices (all data)	R1 = 0.0247, wR2 = 0.0508	
Largest diff. peak and hole	0.639 and -0.791 $e.Å^{-3}$	

Table 4.9 Bond lengths [Å] and angles [°] for $[(Re(bpy)(CO)_3)_2][K(THF)_2]$

Re(1)-C(3)	1.895(5)	O(7)-C(30B)	1.471(19)
Re(1)-C(1)	1.906(5)	O(7)-K(1)#1	2.771(3)
Re(1)-C(2)	1.911(5)	O(8)-C(31A)	1.342(10)
Re(1)-N(2)	2.131(4)	O(8)-C(34A)	1.391(13)
Re(1)-N(1)	2.136(3)	O(8)-C(34B)	1.479(14)
Re(1)-Re(2)	3.1348(3)	O(8)-C(31B)	1.549(13)
Re(2)-C(16)	1.900(5)	N(1)-C(13)	1.360(5)
Re(2)-C(15)	1.901(4)	N(1)-C(9)	1.385(5)
Re(2)-C(14)	1.907(5)	N(2)-C(4)	1.357(6)
Re(2)-N(4)	2.129(3)	N(2)-C(8)	1.379(5)
Re(2)-N(3)	2.131(3)	N(3)-C(17)	1.363(5)
K(1)-O(8)	2.622(4)	N(3)-C(21)	1.377(5)
K(1)-O(4)	2.758(3)	N(4)-C(26)	1.362(5)
K(1)-O(7)#1	2.771(3)	N(4)-C(22)	1.378(5)
K(1)-O(7)	2.876(3)	C(4)-C(5)	1.362(7)
K(1)-O(1)	2.912(3)	C(4)-H(4)	0.9500
K(1)-O(2)#2	2.924(3)	C(5)-C(6)	1.397(7)
K(1)-O(5)#3	2.932(3)	C(5)-H(5)	0.9500
K(1)-C(30A)#1	3.346(17)	C(6)-C(7)	1.365(6)
K(1)-C(34B)	3.515(13)	C(6)-H(6)	0.9500
K(1)-C(27)	3.539(6)	C(7)-C(8)	1.402(6)
K(1)-K(1)#1	3.7553(19)	C(7)-H(7)	0.9500
O(1)-C(1)	1.159(5)	C(8)-C(9)	1.425(6)
O(2)-C(2)	1.161(5)	C(9)-C(10)	1.405(6)
O(2)-K(1)#2	2.924(3)	C(10)-C(11)	1.362(6)
O(3)-C(3)	1.161(6)	C(10)-H(10)	0.9500
O(4)-C(14)	1.155(5)	C(11)-C(12)	1.397(6)
O(5)-C(15)	1.172(5)	C(11)-H(11)	0.9500
O(5)-K(1)#4	2.932(3)	C(12)-C(13)	1.367(6)
O(6)-C(16)	1.159(6)	C(12)-H(12)	0.9500
O(7)-C(30A)	1.41(2)	C(13)-H(13)	0.9500
O(7)-C(27)	1.424(6)	C(17)-C(18)	1.363(6)

Table 4.9 Cont.

C(17)-H(17)	0.9500	C(30A)-H(30A)	0.9900
C(18)-C(19)	1.396(7)	C(30A)-H(30B)	0.9900
C(18)-H(18)	0.9500	C(30B)-H(30C)	0.9900
C(19)-C(20)	1.361(6)	C(30B)-H(30D)	0.9900
C(19)-H(19)	0.9500	C(31A)-C(32A)	1.547(10)
C(20)-C(21)	1.410(6)	C(31A)-H(31A)	0.9900
C(20)-H(20)	0.9500	C(31A)-H(31B)	0.9900
C(21)-C(22)	1.427(6)	C(31B)-C(32B)	1.501(18)
C(22)-C(23)	1.409(6)	C(31B)-H(31C)	0.9900
C(23)-C(24)	1.357(7)	C(31B)-H(31D)	0.9900
C(23)-H(23)	0.9500	C(32A)-C(33A)	1.523(13)
C(24)-C(25)	1.407(7)	C(32A)-H(32A)	0.9900
C(24)-H(24)	0.9500	C(32A)-H(32B)	0.9900
C(25)-C(26)	1.352(6)	C(32B)-C(33B)	1.450(18)
C(25)-H(25)	0.9500	C(32B)-H(32C)	0.9900
C(26)-H(26)	0.9500	C(32B)-H(32D)	0.9900
C(27)-C(28A)	1.338(16)	C(33A)-C(34A)	1.501(13)
C(27)-C(28B)	1.574(14)	C(33A)-H(33A)	0.9900
C(27)-H(27A)	0.9900	C(33A)-H(33B)	0.9900
C(27)-H(27B)	0.9900	C(33B)-C(34B)	1.468(17)
C(28A)-C(29A)	1.792(19)	C(33B)-H(33C)	0.9900
C(28A)-H(28A)	0.9900	C(33B)-H(33D)	0.9900
C(28A)-H(28B)	0.9900	C(34A)-H(34A)	0.9900
C(28B)-C(29B)	1.10(2)	C(34A)-H(34B)	0.9900
C(28B)-H(28C)	0.9900	C(34B)-H(34C)	0.9900
C(28B)-H(28D)	0.9900	C(34B)-H(34D)	0.9900
C(29A)-C(30A)	1.58(3)		
C(29A)-H(29A)	0.9900	C(3)-Re(1)-C(1)	92.57(19)
C(29A)-H(29B)	0.9900	C(3)-Re(1)-C(2)	92.49(19)
C(29B)-C(30B)	1.63(3)	C(1)-Re(1)-C(2)	88.60(18)
C(29B)-H(29C)	0.9900	C(3)-Re(1)-N(2)	97.25(18)
C(29B)-H(29D)	0.9900	C(1)-Re(1)-N(2)	168.20(16)
C(30A)-K(1)#1	3.346(17)	C(2)-Re(1)-N(2)	97.46(16)

Table 4.9 Cont.

C(3)-Re(1)-N(1)	94.07(16)	O(7)-K(1)-O(1)	132.36(9)
C(1)-Re(1)-N(1)	97.90(15)	O(8)-K(1)-O(2)#2	84.18(11)
C(2)-Re(1)-N(1)	170.54(16)	O(4)-K(1)-O(2)#2	70.56(10)
N(2)-Re(1)-N(1)	74.96(13)	O(7)#1-K(1)-O(2)#2	109.56(10)
C(3)-Re(1)-Re(2)	172.85(14)	O(7)-K(1)-O(2)#2	91.02(9)
C(1)-Re(1)-Re(2)	82.06(13)	O(1)-K(1)-O(2)#2	135.18(10)
C(2)-Re(1)-Re(2)	82.70(14)	O(8)-K(1)-O(5)#3	91.68(10)
N(2)-Re(1)-Re(2)	88.64(9)	O(4)-K(1)-O(5)#3	127.26(10)
N(1)-Re(1)-Re(2)	91.36(9)	O(7)#1-K(1)-O(5)#3	73.74(9)
C(16)-Re(2)-C(15)	91.03(18)	O(7)-K(1)-O(5)#3	68.06(9)
C(16)-Re(2)-C(14)	92.71(19)	O(1)-K(1)-O(5)#3	65.45(9)
C(15)-Re(2)-C(14)	86.82(18)	O(2)#2-K(1)-O(5)#3	159.06(10)
C(16)-Re(2)-N(4)	97.07(17)	O(8)-K(1)-C(30A)#1	167.5(3)
C(15)-Re(2)-N(4)	98.70(16)	O(4)-K(1)-C(30A)#1	96.8(3)
C(14)-Re(2)-N(4)	168.65(16)	O(7)#1-K(1)-C(30A)#1	24.4(4)
C(16)-Re(2)-N(3)	95.89(16)	O(7)-K(1)-C(30A)#1	114.2(3)
C(15)-Re(2)-N(3)	171.27(16)	O(1)-K(1)-C(30A)#1	81.0(3)
C(14)-Re(2)-N(3)	98.13(16)	O(2)#2-K(1)-C(30A)#1	91.6(3)
N(4)-Re(2)-N(3)	75.20(13)	O(5)#3-K(1)-C(30A)#1	96.3(4)
C(16)-Re(2)-Re(1)	174.99(14)	O(8)-K(1)-C(34B)	22.4(2)
C(15)-Re(2)-Re(1)	86.27(13)	O(4)-K(1)-C(34B)	65.1(2)
C(14)-Re(2)-Re(1)	82.94(14)	O(7)#1-K(1)-C(34B)	170.2(2)
N(4)-Re(2)-Re(1)	87.51(9)	O(7)-K(1)-C(34B)	79.6(2)
N(3)-Re(2)-Re(1)	87.21(9)	O(1)-K(1)-C(34B)	109.1(2)
O(8)-K(1)-O(4)	70.69(12)	O(2)#2-K(1)-C(34B)	61.8(2)
O(8)-K(1)-O(7)#1	165.41(11)	O(5)#3-K(1)-C(34B)	112.6(2)
O(4)-K(1)-O(7)#1	117.73(11)	C(30A)#1-K(1)-C(34B)	151.1(4)
O(8)-K(1)-O(7)	77.72(11)	O(8)-K(1)-C(27)	72.50(14)
O(4)-K(1)-O(7)	144.58(11)	O(4)-K(1)-C(27)	126.72(12)
O(7)#1-K(1)-O(7)	96.65(9)	O(7)#1-K(1)-C(27)	107.30(12)
O(8)-K(1)-O(1)	93.64(12)	O(7)-K(1)-C(27)	22.77(10)
O(4)-K(1)-O(1)	66.61(9)	O(1)-K(1)-C(27)	152.33(11)
O(7)#1-K(1)-O(1)	80.13(10)	O(2)#2-K(1)-C(27)	68.60(11)

Table 4.9 Cont.

O(5)#3-K(1)-C(27)	90.56(11)	C(31A)-O(8)-K(1)	124.6(5)
C(30A)#1-K(1)-C(27)	116.9(3)	C(34A)-O(8)-K(1)	123.0(5)
C(34B)-K(1)-C(27)	66.1(2)	C(34B)-O(8)-K(1)	115.1(5)
O(8)-K(1)-K(1)#1	123.45(10)	C(31B)-O(8)-K(1)	147.3(5)
O(4)-K(1)-K(1)#1	165.35(10)	C(13)-N(1)-C(9)	117.2(3)
O(7)#1-K(1)-K(1)#1	49.53(7)	C(13)-N(1)-Re(1)	125.6(3)
O(7)-K(1)-K(1)#1	47.13(7)	C(9)-N(1)-Re(1)	116.9(3)
O(1)-K(1)-K(1)#1	112.93(7)	C(4)-N(2)-C(8)	117.4(4)
O(2)#2-K(1)-K(1)#1	105.11(8)	C(4)-N(2)-Re(1)	125.1(3)
O(5)#3-K(1)-K(1)#1	60.48(7)	C(8)-N(2)-Re(1)	117.5(3)
C(30A)#1-K(1)-K(1)#1	69.1(3)	C(17)-N(3)-C(21)	117.4(4)
C(34B)-K(1)-K(1)#1	126.1(2)	C(17)-N(3)-Re(2)	125.3(3)
C(27)-K(1)-K(1)#1	60.87(10)	C(21)-N(3)-Re(2)	117.2(3)
C(1)-O(1)-K(1)	129.3(3)	C(26)-N(4)-C(22)	117.7(4)
C(2)-O(2)-K(1)#2	154.5(3)	C(26)-N(4)-Re(2)	125.0(3)
C(14)-O(4)-K(1)	139.8(3)	C(22)-N(4)-Re(2)	117.1(3)
C(15)-O(5)-K(1)#4	149.7(3)	O(1)-C(1)-Re(1)	179.3(4)
C(30A)-O(7)-C(27)	107.0(8)	O(2)-C(2)-Re(1)	178.2(4)
C(30A)-O(7)-C(30B)	20.6(10)	O(3)-C(3)-Re(1)	176.8(4)
C(27)-O(7)-C(30B)	107.9(8)	N(2)-C(4)-C(5)	123.8(4)
C(30A)-O(7)-K(1)#1	101.3(7)	N(2)-C(4)-H(4)	118.1
C(27)-O(7)-K(1)#1	120.3(3)	C(5)-C(4)-H(4)	118.1
C(30B)-O(7)-K(1)#1	115.9(8)	C(4)-C(5)-C(6)	118.9(4)
C(30A)-O(7)-K(1)	138.3(7)	C(4)-C(5)-H(5)	120.5
C(27)-O(7)-K(1)	105.8(3)	C(6)-C(5)-H(5)	120.5
C(30B)-O(7)-K(1)	122.1(7)	C(7)-C(6)-C(5)	118.9(4)
K(1)#1-O(7)-K(1)	83.35(9)	C(7)-C(6)-H(6)	120.6
C(31A)-O(8)-C(34A)	112.3(7)	C(5)-C(6)-H(6)	120.6
C(31A)-O(8)-C(34B)	117.5(7)	C(6)-C(7)-C(8)	120.5(4)
C(34A)-O(8)-C(34B)	21.9(6)	C(6)-C(7)-H(7)	119.8
C(31A)-O(8)-C(31B)	26.4(5)	C(8)-C(7)-H(7)	119.8
C(34A)-O(8)-C(31B)	87.5(7)	N(2)-C(8)-C(7)	120.5(4)
C(34B)-O(8)-C(31B)	97.6(7)	N(2)-C(8)-C(9)	115.1(4)

Table 4.9 Cont.

C(7)-C(8)-C(9)	124.4(4)	C(20)-C(21)-C(22)	124.2(4)
N(1)-C(9)-C(10)	120.5(4)	N(4)-C(22)-C(23)	120.1(4)
N(1)-C(9)-C(8)	115.0(4)	N(4)-C(22)-C(21)	115.3(4)
C(10)-C(9)-C(8)	124.5(4)	C(23)-C(22)-C(21)	124.6(4)
C(11)-C(10)-C(9)	120.8(4)	C(24)-C(23)-C(22)	120.4(4)
C(11)-C(10)-H(10)	119.6	C(24)-C(23)-H(23)	119.8
C(9)-C(10)-H(10)	119.6	C(22)-C(23)-H(23)	119.8
C(10)-C(11)-C(12)	118.6(4)	C(23)-C(24)-C(25)	119.2(4)
C(10)-C(11)-H(11)	120.7	C(23)-C(24)-H(24)	120.4
C(12)-C(11)-H(11)	120.7	C(25)-C(24)-H(24)	120.4
C(13)-C(12)-C(11)	119.3(4)	C(26)-C(25)-C(24)	118.7(4)
C(13)-C(12)-H(12)	120.4	C(26)-C(25)-H(25)	120.7
C(11)-C(12)-H(12)	120.4	C(24)-C(25)-H(25)	120.7
N(1)-C(13)-C(12)	123.6(4)	C(25)-C(26)-N(4)	123.8(4)
N(1)-C(13)-H(13)	118.2	C(25)-C(26)-H(26)	118.1
C(12)-C(13)-H(13)	118.2	N(4)-C(26)-H(26)	118.1
O(4)-C(14)-Re(2)	177.7(4)	C(28A)-C(27)-O(7)	114.5(7)
O(5)-C(15)-Re(2)	177.4(4)	C(28A)-C(27)-C(28B)	16.3(9)
O(6)-C(16)-Re(2)	175.2(4)	O(7)-C(27)-C(28B)	102.2(6)
C(18)-C(17)-N(3)	123.4(4)	C(28A)-C(27)-K(1)	159.5(6)
C(18)-C(17)-H(17)	118.3	O(7)-C(27)-K(1)	51.4(2)
N(3)-C(17)-H(17)	118.3	C(28B)-C(27)-K(1)	143.2(6)
C(17)-C(18)-C(19)	119.2(4)	C(28A)-C(27)-H(27A)	113.4
C(17)-C(18)-H(18)	120.4	O(7)-C(27)-H(27A)	111.3
C(19)-C(18)-H(18)	120.4	C(28B)-C(27)-H(27A)	111.3
C(20)-C(19)-C(18)	119.1(4)	K(1)-C(27)-H(27A)	67.1
C(20)-C(19)-H(19)	120.4	C(28A)-C(27)-H(27B)	96.1
C(18)-C(19)-H(19)	120.4	O(7)-C(27)-H(27B)	111.3
C(19)-C(20)-C(21)	120.1(4)	C(28B)-C(27)-H(27B)	111.3
C(19)-C(20)-H(20)	119.9	K(1)-C(27)-H(27B)	103.0
C(21)-C(20)-H(20)	119.9	H(27A)-C(27)-H(27B)	109.2
N(3)-C(21)-C(20)	120.7(4)	C(27)-C(28A)-C(29A)	99.0(11)
N(3)-C(21)-C(22)	115.1(4)	C(27)-C(28A)-H(28A)	112.0

Table 4.9 Cont.

C(29A)-C(28A)-H(28A)	112.0	O(7)-C(30B)-H(30C)	112.4
C(27)-C(28A)-H(28B)	112.0	C(29B)-C(30B)-H(30C)	112.4
C(29A)-C(28A)-H(28B)	112.0	O(7)-C(30B)-H(30D)	112.4
H(28A)-C(28A)-H(28B)	109.6	C(29B)-C(30B)-H(30D)	112.4
C(29B)-C(28B)-C(27)	112.3(16)	H(30C)-C(30B)-H(30D)	109.9
C(29B)-C(28B)-H(28C)	109.1	O(8)-C(31A)-C(32A)	105.6(7)
C(27)-C(28B)-H(28C)	109.1	O(8)-C(31A)-H(31A)	110.6
C(29B)-C(28B)-H(28D)	109.1	C(32A)-C(31A)-H(31A)	110.6
C(27)-C(28B)-H(28D)	109.1	O(8)-C(31A)-H(31B)	110.6
H(28C)-C(28B)-H(28D)	107.9	C(32A)-C(31A)-H(31B)	110.6
C(30A)-C(29A)-C(28A)	90.5(12)	H(31A)-C(31A)-H(31B)	108.8
C(30A)-C(29A)-H(29A)	113.6	C(32B)-C(31B)-O(8)	103.1(9)
C(28A)-C(29A)-H(29A)	113.6	C(32B)-C(31B)-H(31C)	111.1
C(30A)-C(29A)-H(29B)	113.6	O(8)-C(31B)-H(31C)	111.1
C(28A)-C(29A)-H(29B)	113.6	C(32B)-C(31B)-H(31D)	111.1
H(29A)-C(29A)-H(29B)	110.8	O(8)-C(31B)-H(31D)	111.1
C(28B)-C(29B)-C(30B)	110.3(17)	H(31C)-C(31B)-H(31D)	109.1
C(28B)-C(29B)-H(29C)	109.6	C(33A)-C(32A)-C(31A)	104.1(8)
C(30B)-C(29B)-H(29C)	109.6	C(33A)-C(32A)-H(32A)	110.9
C(28B)-C(29B)-H(29D)	109.6	C(31A)-C(32A)-H(32A)	110.9
C(30B)-C(29B)-H(29D)	109.6	C(33A)-C(32A)-H(32B)	110.9
H(29C)-C(29B)-H(29D)	108.1	C(31A)-C(32A)-H(32B)	110.9
O(7)-C(30A)-C(29A)	107.8(16)	H(32A)-C(32A)-H(32B)	109.0
O(7)-C(30A)-K(1)#1	54.3(6)	C(33B)-C(32B)-C(31B)	105.0(10)
C(29A)-C(30A)-K(1)#1	149.7(12)	C(33B)-C(32B)-H(32C)	110.8
O(7)-C(30A)-H(30A)	110.1	C(31B)-C(32B)-H(32C)	110.8
C(29A)-C(30A)-H(30A)	110.1	C(33B)-C(32B)-H(32D)	110.8
K(1)#1-C(30A)-H(30A)	63.6	C(31B)-C(32B)-H(32D)	110.8
O(7)-C(30A)-H(30B)	110.1	H(32C)-C(32B)-H(32D)	108.8
C(29A)-C(30A)-H(30B)	110.1	C(34A)-C(33A)-C(32A)	102.2(8)
K(1)#1-C(30A)-H(30B)	99.6	C(34A)-C(33A)-H(33A)	111.3
H(30A)-C(30A)-H(30B)	108.5	C(32A)-C(33A)-H(33A)	111.3
O(7)-C(30B)-C(29B)	96.9(12)	C(34A)-C(33A)-H(33B)	111.3

Table 4.9 Cont.

C(32A)-C(33A)-H(33B)	111.3	C(33A)-C(34A)-H(34B)	110.9
H(33A)-C(33A)-H(33B)	109.2	H(34A)-C(34A)-H(34B)	108.9
C(32B)-C(33B)-C(34B)	107.4(11)	C(33B)-C(34B)-O(8)	105.6(10)
C(32B)-C(33B)-H(33C)	110.2	C(33B)-C(34B)-K(1)	132.4(8)
C(34B)-C(33B)-H(33C)	110.2	O(8)-C(34B)-K(1)	42.5(4)
C(32B)-C(33B)-H(33D)	110.2	C(33B)-C(34B)-H(34C)	110.6
C(34B)-C(33B)-H(33D)	110.2	O(8)-C(34B)-H(34C)	110.6
H(33C)-C(33B)-H(33D)	108.5	K(1)-C(34B)-H(34C)	113.8
O(8)-C(34A)-C(33A)	104.4(9)	C(33B)-C(34B)-H(34D)	110.6
O(8)-C(34A)-H(34A)	110.9	O(8)-C(34B)-H(34D)	110.6
C(33A)-C(34A)-H(34A)	110.9	K(1)-C(34B)-H(34D)	69.9
O(8)-C(34A)-H(34B)	110.9	H(34C)-C(34B)-H(34D)	108.7

Symmetry transformations used to generate equivalent atoms:

#1 -x-1,-y,-z #2 -x,-y,-z #3 x-1,y,z #4 x+1,y,z

Table 4.10 Crystal data and structure refinement for $[Re(bpy)(CO)_3][K(18\text{-crown-6})(THF)]$

Identification code	eb_111101b	
Empirical formula	C19 H40 K N2 O30 Re	
Formula weight	801.93	
Temperature	100(2) K	
Wavelength	0.71073 Å	
Crystal system	Monoclinic	
Space group	P2(1)/c	
Unit cell dimensions	a = 23.3023(13) Å	α= 90°.
	b = 18.0705(9) Å	β= 73.240(3)°.
	c = 16.0034(8) Å	γ = 90°.
Volume	6452.5(6) $Å^3$	
Z	8	
Density (calculated)	1.651 Mg/m^3	
Absorption coefficient	3.952 mm^{-1}	
F(000)	3216	
Crystal size	0.20 x 0.10 x 0.10 mm^3	
Theta range for data collection	1.74 to 25.56°.	
Index ranges	-28<=h<=28, -21<=k<=21, -19<=l<=18	
Reflections collected	44779	
Independent reflections	11977 [R(int) = 0.0311]	
Completeness to theta = 25.00°	99.9 %	
Absorption correction	Semi-empirical from equivalents	
Max. and min. transmission	0.6933 and 0.5054	
Refinement method	Full-matrix least-squares on F^2	
Data / restraints / parameters	11977 / 0 / 798	
Goodness-of-fit on F^2	1.079	
Final R indices [I>2sigma(I)]	R1 = 0.0331, wR2 = 0.0578	
R indices (all data)	R1 = 0.0537, wR2 = 0.0636	
Largest diff. peak and hole	1.705 and -0.756 $e.Å^{-3}$	

Table 4.11 Bond lengths [Å] and angles [°] for [Re(bpy)$(CO)_3$] [K(18-crown-6)(THF)]

Re(1)-C(3)	1.866(5)	O(4)-C(34)	1.422(7)
Re(1)-C(2)	1.894(5)	O(5)-C(36)	1.410(8)
Re(1)-C(1)	1.915(5)	O(5)-C(35)	1.443(7)
Re(1)-N(1)	2.074(3)	O(6)-C(38)	1.408(7)
Re(1)-N(2)	2.085(4)	O(6)-C(37)	1.435(6)
Re(2)-C(20)	1.863(5)	O(7)-C(10)	1.428(7)
Re(2)-C(22)	1.897(5)	O(7)-C(39)	1.437(7)
Re(2)-C(21)	1.917(5)	O(8)-C(12)	1.419(6)
Re(2)-N(3)	2.079(3)	O(8)-C(11)	1.424(6)
Re(2)-N(4)	2.084(3)	O(9)-C(14)	1.416(7)
K(1)-O(8)	2.725(3)	O(9)-C(13)	1.420(6)
K(1)-O(3)	2.745(4)	O(30A)-C(19)	1.378(7)
K(1)-O(5)	2.773(4)	O(30A)-C(16A)	1.447(10)
K(1)-O(30A)	2.785(5)	O(30B)-C(17)	1.372(15)
K(1)-O(7)	2.801(4)	O(30B)-C(16B)	1.40(3)
K(1)-O(6)	2.807(4)	O(31)-C(20)	1.177(6)
K(1)-O(4)	2.816(4)	O(32)-C(21)	1.163(5)
K(1)-O(9)	2.857(4)	O(33)-C(22)	1.169(5)
K(1)-O(30B)	2.984(14)	O(34)-C(43)	1.410(6)
K(1)-C(16B)	3.53(3)	O(34)-C(54)	1.427(6)
K(2)-O(10)	2.720(4)	O(35)-C(45)	1.417(5)
K(2)-O(36)	2.722(3)	O(35)-C(44)	1.421(6)
K(2)-O(39)	2.751(3)	O(36)-C(47)	1.413(6)
K(2)-O(31)	2.775(4)	O(36)-C(46)	1.417(6)
K(2)-O(35)	2.813(3)	O(37)-C(49)	1.409(6)
K(2)-O(38)	2.822(3)	O(37)-C(48)	1.439(6)
K(2)-O(37)	2.837(3)	O(38)-C(50)	1.416(6)
K(2)-O(34)	2.861(3)	O(38)-C(51)	1.423(6)
O(3)-C(3)	1.166(6)	O(39)-C(52)	1.408(6)
O(1)-C(1)	1.167(5)	O(39)-C(53)	1.417(6)
O(2)-C(2)	1.166(6)	O(10)-C(55)	1.377(7)
O(4)-C(15)	1.420(8)	O(10)-C(58)	1.451(7)

Table 4.11 Cont.

N(1)-C(33)	1.385(5)	C(37)-H(17A)	0.9900
N(1)-C(9)	1.397(5)	C(37)-H(17B)	0.9900
N(2)-C(4)	1.382(6)	C(38)-C(39)	1.486(8)
N(2)-C(8)	1.394(6)	C(38)-H(18A)	0.9900
N(3)-C(28)	1.387(5)	C(38)-H(18B)	0.9900
N(3)-C(42)	1.389(5)	C(39)-H(19A)	0.9900
N(4)-C(23)	1.384(6)	C(39)-H(19B)	0.9900
N(4)-C(27)	1.388(5)	C(10)-C(11)	1.482(8)
C(4)-C(5)	1.346(7)	C(10)-H(20A)	0.9900
C(4)-H(4)	0.9500	C(10)-H(20B)	0.9900
C(5)-C(6)	1.415(7)	C(11)-H(21A)	0.9900
C(5)-H(5)	0.9500	C(11)-H(21B)	0.9900
C(6)-C(7)	1.350(7)	C(12)-C(13)	1.488(8)
C(6)-H(6)	0.9500	C(12)-H(22A)	0.9900
C(7)-C(8)	1.427(6)	C(12)-H(22B)	0.9900
C(7)-H(7)	0.9500	C(13)-H(23A)	0.9900
C(8)-C(9)	1.391(6)	C(13)-H(23B)	0.9900
C(9)-C(30)	1.408(6)	C(14)-C(15)	1.492(9)
C(30)-C(31)	1.355(6)	C(14)-H(24A)	0.9900
C(30)-H(10)	0.9500	C(14)-H(24B)	0.9900
C(31)-C(32)	1.414(6)	C(15)-H(25A)	0.9900
C(31)-H(11)	0.9500	C(15)-H(25B)	0.9900
C(32)-C(33)	1.351(6)	C(16A)-C(17)	1.555(10)
C(32)-H(12)	0.9500	C(16A)-H(26A)	0.9900
C(33)-H(13)	0.9500	C(16A)-H(26B)	0.9900
C(34)-C(35)	1.472(9)	C(16B)-C(19)	1.79(2)
C(34)-H(14A)	0.9900	C(16B)-H(26C)	0.9900
C(34)-H(14B)	0.9900	C(16B)-H(26D)	0.9900
C(35)-H(15A)	0.9900	C(17)-C(18)	1.527(8)
C(35)-H(15B)	0.9900	C(17)-H(27A)	0.9900
C(36)-C(37)	1.475(9)	C(17)-H(27B)	0.9900
C(36)-H(16A)	0.9900	C(17)-H(27C)	0.9(2)
C(36)-H(16B)	0.9900	C(17)-H(27D)	1.1(2)

Table 4.11 Cont.

C(18)-C(19)	1.491(7)	C(46)-H(46A)	0.9900
C(18)-H(27D)	1.2(2)	C(46)-H(46B)	0.9900
C(18)-H(28A)	0.9900	C(47)-C(48)	1.473(7)
C(18)-H(28B)	0.9900	C(47)-H(47A)	0.9900
C(19)-H(29A)	0.9900	C(47)-H(47B)	0.9900
C(19)-H(29B)	0.9900	C(48)-H(48A)	0.9900
C(19)-H(29C)	1.2(2)	C(48)-H(48B)	0.9900
C(19)-H(29D)	1.3(2)	C(49)-C(50)	1.491(7)
C(23)-C(24)	1.344(6)	C(49)-H(49A)	0.9900
C(23)-H(33)	0.9500	C(49)-H(49B)	0.9900
C(24)-C(25)	1.422(6)	C(50)-H(50A)	0.9900
C(24)-H(34)	0.9500	C(50)-H(50B)	0.9900
C(25)-C(26)	1.354(6)	C(51)-C(52)	1.479(7)
C(25)-H(35)	0.9500	C(51)-H(51A)	0.9900
C(26)-C(27)	1.406(6)	C(51)-H(51B)	0.9900
C(26)-H(36)	0.9500	C(52)-H(52A)	0.9900
C(27)-C(28)	1.413(6)	C(52)-H(52B)	0.9900
C(28)-C(29)	1.421(6)	C(53)-C(54)	1.477(7)
C(29)-C(40)	1.350(6)	C(53)-H(53A)	0.9900
C(29)-H(39)	0.9500	C(53)-H(53B)	0.9900
C(40)-C(41)	1.423(6)	C(54)-H(54A)	0.9900
C(40)-H(40)	0.9500	C(54)-H(54B)	0.9900
C(41)-C(42)	1.342(6)	C(55)-C(56)	1.481(9)
C(41)-H(41)	0.9500	C(55)-H(55A)	0.9900
C(42)-H(42)	0.9500	C(55)-H(55B)	0.9900
C(43)-C(44)	1.495(7)	C(56)-C(57A)	1.514(12)
C(43)-H(43A)	0.9900	C(56)-C(57B)	1.689(16)
C(43)-H(43B)	0.9900	C(56)-H(56C)	0.9900
C(44)-H(44A)	0.9900	C(56)-H(56D)	0.9900
C(44)-H(44B)	0.9900	C(56)-H(56A)	0.9900
C(45)-C(46)	1.502(7)	C(56)-H(56B)	0.9900
C(45)-H(45A)	0.9900	C(57A)-C(58)	1.544(13)
C(45)-H(45B)	0.9900	C(57A)-H(57A)	0.9900

Table 4.11 Cont.

C(57A)-H(57B)	0.9900	O(8)-K(1)-O(30A)	93.37(12)
C(57B)-C(58)	1.378(16)	O(3)-K(1)-O(30A)	164.16(17)
C(57B)-H(57C)	0.9900	O(5)-K(1)-O(30A)	84.99(13)
C(57B)-H(57D)	0.9900	O(8)-K(1)-O(7)	60.69(11)
C(57B)-H(58D)	1.02(11)	O(3)-K(1)-O(7)	92.48(14)
C(58)-H(58A)	0.9900	O(5)-K(1)-O(7)	120.68(13)
C(58)-H(58B)	0.9900	O(30A)-K(1)-O(7)	74.27(13)
C(58)-H(58C)	0.91(11)	O(8)-K(1)-O(6)	121.06(12)
C(58)-H(58D)	1.19(11)	O(3)-K(1)-O(6)	84.82(13)
		O(5)-K(1)-O(6)	60.80(13)
C(3)-Re(1)-C(2)	92.5(2)	O(30A)-K(1)-O(6)	81.23(13)
C(3)-Re(1)-C(1)	91.1(2)	O(7)-K(1)-O(6)	61.43(12)
C(2)-Re(1)-C(1)	85.78(19)	O(8)-K(1)-O(4)	118.26(13)
C(3)-Re(1)-N(1)	110.33(18)	O(3)-K(1)-O(4)	86.08(14)
C(2)-Re(1)-N(1)	156.5(2)	O(5)-K(1)-O(4)	60.42(13)
C(1)-Re(1)-N(1)	98.64(17)	O(30A)-K(1)-O(4)	107.29(13)
C(3)-Re(1)-N(2)	102.8(2)	O(7)-K(1)-O(4)	178.29(11)
C(2)-Re(1)-N(2)	95.23(18)	O(6)-K(1)-O(4)	119.30(13)
C(1)-Re(1)-N(2)	165.94(17)	O(8)-K(1)-O(9)	60.34(11)
N(1)-Re(1)-N(2)	75.04(14)	O(3)-K(1)-O(9)	94.82(13)
C(20)-Re(2)-C(22)	92.8(2)	O(5)-K(1)-O(9)	117.82(13)
C(20)-Re(2)-C(21)	91.0(2)	O(30A)-K(1)-O(9)	99.31(13)
C(22)-Re(2)-C(21)	88.41(19)	O(7)-K(1)-O(9)	120.05(11)
C(20)-Re(2)-N(3)	111.60(17)	O(6)-K(1)-O(9)	178.51(12)
C(22)-Re(2)-N(3)	154.84(17)	O(4)-K(1)-O(9)	59.22(12)
C(21)-Re(2)-N(3)	96.81(17)	O(8)-K(1)-O(30B)	72.0(3)
C(20)-Re(2)-N(4)	103.13(17)	O(3)-K(1)-O(30B)	158.1(3)
C(22)-Re(2)-N(4)	93.90(17)	O(5)-K(1)-O(30B)	105.7(3)
C(21)-Re(2)-N(4)	165.50(18)	O(30A)-K(1)-O(30B)	31.5(3)
N(3)-Re(2)-N(4)	75.27(14)	O(7)-K(1)-O(30B)	84.0(3)
O(8)-K(1)-O(3)	87.41(11)	O(6)-K(1)-O(30B)	111.9(3)
O(8)-K(1)-O(5)	177.34(12)	O(4)-K(1)-O(30B)	96.9(3)
O(3)-K(1)-O(5)	94.74(11)	O(9)-K(1)-O(30B)	68.8(3)

Table 4.11 Cont.

O(8)-K(1)-C(16B)	82.3(4)	O(31)-K(2)-O(34)	99.33(12)
O(3)-K(1)-C(16B)	163.1(4)	O(35)-K(2)-O(34)	59.89(10)
O(5)-K(1)-C(16B)	96.0(4)	O(38)-K(2)-O(34)	119.97(10)
O(30A)-K(1)-C(16B)	11.3(4)	O(37)-K(2)-O(34)	176.52(10)
O(7)-K(1)-C(16B)	70.8(4)	C(3)-O(3)-K(1)	130.2(3)
O(6)-K(1)-C(16B)	89.0(4)	C(15)-O(4)-C(34)	111.9(5)
O(4)-K(1)-C(16B)	110.6(4)	C(15)-O(4)-K(1)	117.2(3)
O(9)-K(1)-C(16B)	91.7(4)	C(34)-O(4)-K(1)	114.3(4)
O(30B)-K(1)-C(16B)	22.9(5)	C(36)-O(5)-C(35)	112.3(5)
O(10)-K(2)-O(36)	83.90(12)	C(36)-O(5)-K(1)	116.1(4)
O(10)-K(2)-O(39)	89.24(13)	C(35)-O(5)-K(1)	115.9(3)
O(36)-K(2)-O(39)	172.80(11)	C(38)-O(6)-C(37)	113.4(5)
O(10)-K(2)-O(31)	173.09(14)	C(38)-O(6)-K(1)	112.6(3)
O(36)-K(2)-O(31)	94.93(10)	C(37)-O(6)-K(1)	111.2(3)
O(39)-K(2)-O(31)	92.15(10)	C(10)-O(7)-C(39)	112.6(4)
O(10)-K(2)-O(35)	98.09(11)	C(10)-O(7)-K(1)	111.1(3)
O(36)-K(2)-O(35)	59.89(10)	C(39)-O(7)-K(1)	110.9(3)
O(39)-K(2)-O(35)	119.28(11)	C(12)-O(8)-C(11)	113.4(4)
O(31)-K(2)-O(35)	87.13(12)	C(12)-O(8)-K(1)	118.7(3)
O(10)-K(2)-O(38)	81.62(11)	C(11)-O(8)-K(1)	117.4(3)
O(36)-K(2)-O(38)	120.14(11)	C(14)-O(9)-C(13)	110.7(4)
O(39)-K(2)-O(38)	60.63(10)	C(14)-O(9)-K(1)	112.5(4)
O(31)-K(2)-O(38)	93.16(12)	C(13)-O(9)-K(1)	110.3(3)
O(35)-K(2)-O(38)	179.69(11)	C(19)-O(30A)-C(16A)	100.8(5)
O(10)-K(2)-O(37)	89.52(13)	C(19)-O(30A)-K(1)	119.9(4)
O(36)-K(2)-O(37)	61.46(10)	C(16A)-O(30A)-K(1)	111.2(5)
O(39)-K(2)-O(37)	120.82(11)	C(17)-O(30B)-C(16B)	100.1(14)
O(31)-K(2)-O(37)	83.96(11)	C(17)-O(30B)-K(1)	123.8(8)
O(35)-K(2)-O(37)	119.44(10)	C(16B)-O(30B)-K(1)	101.1(13)
O(38)-K(2)-O(37)	60.68(10)	C(20)-O(31)-K(2)	123.6(3)
O(10)-K(2)-O(34)	87.23(13)	C(43)-O(34)-C(54)	112.1(4)
O(36)-K(2)-O(34)	116.87(10)	C(43)-O(34)-K(2)	109.2(3)
O(39)-K(2)-O(34)	60.43(10)	C(54)-O(34)-K(2)	111.8(3)

Table 4.11 Cont.

C(45)-O(35)-C(44)	111.0(4)	C(5)-C(4)-N(2)	124.1(5)
C(45)-O(35)-K(2)	112.9(3)	C(5)-C(4)-H(4)	117.9
C(44)-O(35)-K(2)	117.3(3)	N(2)-C(4)-H(4)	117.9
C(47)-O(36)-C(46)	113.3(4)	C(4)-C(5)-C(6)	119.0(5)
C(47)-O(36)-K(2)	117.7(3)	C(4)-C(5)-H(5)	120.5
C(46)-O(36)-K(2)	120.3(3)	C(6)-C(5)-H(5)	120.5
C(49)-O(37)-C(48)	111.7(4)	C(7)-C(6)-C(5)	119.2(5)
C(49)-O(37)-K(2)	112.7(3)	C(7)-C(6)-H(6)	120.4
C(48)-O(37)-K(2)	107.2(3)	C(5)-C(6)-H(6)	120.4
C(50)-O(38)-C(51)	114.0(4)	C(6)-C(7)-C(8)	121.0(5)
C(50)-O(38)-K(2)	111.7(3)	C(6)-C(7)-H(7)	119.5
C(51)-O(38)-K(2)	110.1(3)	C(8)-C(7)-H(7)	119.5
C(52)-O(39)-C(53)	113.7(4)	C(9)-C(8)-N(2)	114.5(4)
C(52)-O(39)-K(2)	117.2(3)	C(9)-C(8)-C(7)	126.1(4)
C(53)-O(39)-K(2)	116.6(3)	N(2)-C(8)-C(7)	119.4(4)
C(55)-O(10)-C(58)	107.7(4)	C(8)-C(9)-N(1)	113.8(4)
C(55)-O(10)-K(2)	129.0(3)	C(8)-C(9)-C(30)	125.3(4)
C(58)-O(10)-K(2)	116.1(4)	N(1)-C(9)-C(30)	120.9(4)
C(33)-N(1)-C(9)	115.8(4)	C(31)-C(30)-C(9)	121.1(4)
C(33)-N(1)-Re(1)	125.7(3)	C(31)-C(30)-H(10)	119.4
C(9)-N(1)-Re(1)	118.4(3)	C(9)-C(30)-H(10)	119.4
C(4)-N(2)-C(8)	117.0(4)	C(30)-C(31)-C(32)	118.5(4)
C(4)-N(2)-Re(1)	125.2(3)	C(30)-C(31)-H(11)	120.7
C(8)-N(2)-Re(1)	117.7(3)	C(32)-C(31)-H(11)	120.7
C(28)-N(3)-C(42)	116.3(4)	C(33)-C(32)-C(31)	119.3(4)
C(28)-N(3)-Re(2)	117.9(3)	C(33)-C(32)-H(12)	120.3
C(42)-N(3)-Re(2)	125.7(3)	C(31)-C(32)-H(12)	120.3
C(23)-N(4)-C(27)	116.3(4)	C(32)-C(33)-N(1)	124.3(4)
C(23)-N(4)-Re(2)	125.3(3)	C(32)-C(33)-H(13)	117.8
C(27)-N(4)-Re(2)	118.3(3)	N(1)-C(33)-H(13)	117.8
O(3)-C(3)-Re(1)	179.5(5)	O(4)-C(34)-C(35)	110.1(5)
O(1)-C(1)-Re(1)	177.5(4)	O(4)-C(34)-H(14A)	109.6
O(2)-C(2)-Re(1)	178.1(5)	C(35)-C(34)-H(14A)	109.6

Table 4.11 Cont.

O(4)-C(34)-H(14B)	109.6	O(7)-C(10)-C(11)	108.3(5)
C(35)-C(34)-H(14B)	109.6	O(7)-C(10)-H(20A)	110.0
H(14A)-C(34)-H(14B)	108.2	C(11)-C(10)-H(20A)	110.0
O(5)-C(35)-C(34)	109.2(5)	O(7)-C(10)-H(20B)	110.0
O(5)-C(35)-H(15A)	109.8	C(11)-C(10)-H(20B)	110.0
C(34)-C(35)-H(15A)	109.8	H(20A)-C(10)-H(20B)	108.4
O(5)-C(35)-H(15B)	109.8	O(8)-C(11)-C(10)	107.7(4)
C(34)-C(35)-H(15B)	109.8	O(8)-C(11)-H(21A)	110.2
H(15A)-C(35)-H(15B)	108.3	C(10)-C(11)-H(21A)	110.2
O(5)-C(36)-C(37)	108.7(5)	O(8)-C(11)-H(21B)	110.2
O(5)-C(36)-H(16A)	109.9	C(10)-C(11)-H(21B)	110.2
C(37)-C(36)-H(16A)	109.9	H(21A)-C(11)-H(21B)	108.5
O(5)-C(36)-H(16B)	109.9	O(8)-C(12)-C(13)	107.4(4)
C(37)-C(36)-H(16B)	109.9	O(8)-C(12)-H(22A)	110.2
H(16A)-C(36)-H(16B)	108.3	C(13)-C(12)-H(22A)	110.2
O(6)-C(37)-C(36)	109.6(5)	O(8)-C(12)-H(22B)	110.2
O(6)-C(37)-H(17A)	109.7	C(13)-C(12)-H(22B)	110.2
C(36)-C(37)-H(17A)	109.7	H(22A)-C(12)-H(22B)	108.5
O(6)-C(37)-H(17B)	109.7	O(9)-C(13)-C(12)	110.1(4)
C(36)-C(37)-H(17B)	109.7	O(9)-C(13)-H(23A)	109.6
H(17A)-C(37)-H(17B)	108.2	C(12)-C(13)-H(23A)	109.6
O(6)-C(38)-C(39)	108.6(5)	O(9)-C(13)-H(23B)	109.6
O(6)-C(38)-H(18A)	110.0	C(12)-C(13)-H(23B)	109.6
C(39)-C(38)-H(18A)	110.0	H(23A)-C(13)-H(23B)	108.2
O(6)-C(38)-H(18B)	110.0	O(9)-C(14)-C(15)	108.9(5)
C(39)-C(38)-H(18B)	110.0	O(9)-C(14)-H(24A)	109.9
H(18A)-C(38)-H(18B)	108.3	C(15)-C(14)-H(24A)	109.9
O(7)-C(39)-C(38)	108.6(5)	O(9)-C(14)-H(24B)	109.9
O(7)-C(39)-H(19A)	110.0	C(15)-C(14)-H(24B)	109.9
C(38)-C(39)-H(19A)	110.0	H(24A)-C(14)-H(24B)	108.3
O(7)-C(39)-H(19B)	110.0	O(4)-C(15)-C(14)	107.6(5)
C(38)-C(39)-H(19B)	110.0	O(4)-C(15)-H(25A)	110.2
H(19A)-C(39)-H(19B)	108.3	C(14)-C(15)-H(25A)	110.2

Table 4.11 Cont.

O(4)-C(15)-H(25B)	110.2	H(27B)-C(17)-H(27C)	10.6
C(14)-C(15)-H(25B)	110.2	O(30B)-C(17)-H(27D)	81(10)
H(25A)-C(15)-H(25B)	108.5	C(18)-C(17)-H(27D)	53(10)
O(30A)-C(16A)-C(17)	102.8(6)	C(16A)-C(17)-H(27D)	100(10)
O(30A)-C(16A)-H(26A)	111.2	H(27A)-C(17)-H(27D)	62.5
C(17)-C(16A)-H(26A)	111.2	H(27B)-C(17)-H(27D)	147.5
O(30A)-C(16A)-H(26B)	111.2	H(27C)-C(17)-H(27D)	144(10)
C(17)-C(16A)-H(26B)	111.2	C(19)-C(18)-C(17)	104.0(5)
H(26A)-C(16A)-H(26B)	109.1	C(19)-C(18)-H(27D)	98(10)
O(30B)-C(16B)-C(19)	96.9(15)	C(17)-C(18)-H(27D)	47(10)
O(30B)-C(16B)-K(1)	56.0(11)	C(19)-C(18)-H(28A)	110.9
C(19)-C(16B)-K(1)	79.9(10)	C(17)-C(18)-H(28A)	110.9
O(30B)-C(16B)-H(26C)	112.4	H(27D)-C(18)-H(28A)	70.5
C(19)-C(16B)-H(26C)	112.4	C(19)-C(18)-H(28B)	110.9
K(1)-C(16B)-H(26C)	70.7	C(17)-C(18)-H(28B)	110.9
O(30B)-C(16B)-H(26D)	112.4	H(27D)-C(18)-H(28B)	148.3
C(19)-C(16B)-H(26D)	112.4	H(28A)-C(18)-H(28B)	109.0
K(1)-C(16B)-H(26D)	165.1	O(30A)-C(19)-C(18)	107.3(5)
H(26C)-C(16B)-H(26D)	109.9	O(30A)-C(19)-C(16B)	32.6(8)
O(30B)-C(17)-C(18)	108.4(7)	C(18)-C(19)-C(16B)	97.4(9)
O(30B)-C(17)-C(16A)	32.4(6)	O(30A)-C(19)-H(29A)	110.2
C(18)-C(17)-C(16A)	100.3(5)	C(18)-C(19)-H(29A)	110.3
O(30B)-C(17)-H(27A)	79.8	C(16B)-C(19)-H(29A)	140.9
C(18)-C(17)-H(27A)	111.7	O(30A)-C(19)-H(29B)	110.3
C(16A)-C(17)-H(27A)	111.7	C(18)-C(19)-H(29B)	110.3
O(30B)-C(17)-H(27B)	130.8	C(16B)-C(19)-H(29B)	85.8
C(18)-C(17)-H(27B)	111.7	H(29A)-C(19)-H(29B)	108.5
C(16A)-C(17)-H(27B)	111.7	O(30A)-C(19)-H(29C)	117(10)
H(27A)-C(17)-H(27B)	109.5	C(18)-C(19)-H(29C)	112(10)
O(30B)-C(17)-H(27C)	135(10)	C(16B)-C(19)-H(29C)	94(10)
C(18)-C(17)-H(27C)	102(10)	H(29A)-C(19)-H(29C)	100.2
C(16A)-C(17)-H(27C)	111(10)	H(29B)-C(19)-H(29C)	8.8
H(27A)-C(17)-H(27C)	118.2	O(30A)-C(19)-H(29D)	83(9)

Table 4.11 Cont.

C(18)-C(19)-H(29D)	131(9)	C(42)-C(41)-H(41)	120.3
C(16B)-C(19)-H(29D)	112(9)	C(40)-C(41)-H(41)	120.3
H(29A)-C(19)-H(29D)	29.4	C(41)-C(42)-N(3)	124.2(4)
H(29B)-C(19)-H(29D)	110.3	C(41)-C(42)-H(42)	117.9
H(29C)-C(19)-H(29D)	105(10)	N(3)-C(42)-H(42)	117.9
O(31)-C(20)-Re(2)	179.5(5)	O(34)-C(43)-C(44)	109.4(4)
O(32)-C(21)-Re(2)	179.3(4)	O(34)-C(43)-H(43A)	109.8
O(33)-C(22)-Re(2)	176.7(4)	C(44)-C(43)-H(43A)	109.8
C(24)-C(23)-N(4)	124.0(4)	O(34)-C(43)-H(43B)	109.8
C(24)-C(23)-H(33)	118.0	C(44)-C(43)-H(43B)	109.8
N(4)-C(23)-H(33)	118.0	H(43A)-C(43)-H(43B)	108.2
C(23)-C(24)-C(25)	119.6(4)	O(35)-C(44)-C(43)	108.6(4)
C(23)-C(24)-H(34)	120.2	O(35)-C(44)-H(44A)	110.0
C(25)-C(24)-H(34)	120.2	C(43)-C(44)-H(44A)	110.0
C(26)-C(25)-C(24)	118.1(4)	O(35)-C(44)-H(44B)	110.0
C(26)-C(25)-H(35)	121.0	C(43)-C(44)-H(44B)	110.0
C(24)-C(25)-H(35)	121.0	H(44A)-C(44)-H(44B)	108.3
C(25)-C(26)-C(27)	121.2(4)	O(35)-C(45)-C(46)	109.4(4)
C(25)-C(26)-H(36)	119.4	O(35)-C(45)-H(45A)	109.8
C(27)-C(26)-H(36)	119.4	C(46)-C(45)-H(45A)	109.8
N(4)-C(27)-C(26)	120.8(4)	O(35)-C(45)-H(45B)	109.8
N(4)-C(27)-C(28)	113.4(4)	C(46)-C(45)-H(45B)	109.8
C(26)-C(27)-C(28)	125.8(4)	H(45A)-C(45)-H(45B)	108.2
N(3)-C(28)-C(27)	114.6(4)	O(36)-C(46)-C(45)	107.9(4)
N(3)-C(28)-C(29)	120.6(4)	O(36)-C(46)-H(46A)	110.1
C(27)-C(28)-C(29)	124.8(4)	C(45)-C(46)-H(46A)	110.1
C(40)-C(29)-C(28)	121.1(4)	O(36)-C(46)-H(46B)	110.1
C(40)-C(29)-H(39)	119.4	C(45)-C(46)-H(46B)	110.1
C(28)-C(29)-H(39)	119.4	H(46A)-C(46)-H(46B)	108.4
C(29)-C(40)-C(41)	118.4(4)	O(36)-C(47)-C(48)	108.9(4)
C(29)-C(40)-H(40)	120.8	O(36)-C(47)-H(47A)	109.9
C(41)-C(40)-H(40)	120.8	C(48)-C(47)-H(47A)	109.9
C(42)-C(41)-C(40)	119.4(4)	O(36)-C(47)-H(47B)	109.9

Table 4.11 Cont.

C(48)-C(47)-H(47B)	109.9	O(39)-C(53)-H(53A)	110.0
H(47A)-C(47)-H(47B)	108.3	C(54)-C(53)-H(53A)	110.0
O(37)-C(48)-C(47)	110.0(4)	O(39)-C(53)-H(53B)	110.0
O(37)-C(48)-H(48A)	109.7	C(54)-C(53)-H(53B)	110.0
C(47)-C(48)-H(48A)	109.7	H(53A)-C(53)-H(53B)	108.4
O(37)-C(48)-H(48B)	109.7	O(34)-C(54)-C(53)	110.4(4)
C(47)-C(48)-H(48B)	109.7	O(34)-C(54)-H(54A)	109.6
H(48A)-C(48)-H(48B)	108.2	C(53)-C(54)-H(54A)	109.6
O(37)-C(49)-C(50)	109.1(4)	O(34)-C(54)-H(54B)	109.6
O(37)-C(49)-H(49A)	109.9	C(53)-C(54)-H(54B)	109.6
C(50)-C(49)-H(49A)	109.9	H(54A)-C(54)-H(54B)	108.1
O(37)-C(49)-H(49B)	109.9	O(10)-C(55)-C(56)	105.8(5)
C(50)-C(49)-H(49B)	109.9	O(10)-C(55)-H(55A)	110.6
H(49A)-C(49)-H(49B)	108.3	C(56)-C(55)-H(55A)	110.6
O(38)-C(50)-C(49)	108.5(4)	O(10)-C(55)-H(55B)	110.6
O(38)-C(50)-H(50A)	110.0	C(56)-C(55)-H(55B)	110.6
C(49)-C(50)-H(50A)	110.0	H(55A)-C(55)-H(55B)	108.7
O(38)-C(50)-H(50B)	110.0	C(55)-C(56)-C(57A)	107.5(6)
C(49)-C(50)-H(50B)	110.0	C(55)-C(56)-C(57B)	89.3(7)
H(50A)-C(50)-H(50B)	108.4	C(57A)-C(56)-C(57B)	31.8(6)
O(38)-C(51)-C(52)	109.3(4)	C(55)-C(56)-H(56C)	110.2
O(38)-C(51)-H(51A)	109.8	C(57A)-C(56)-H(56C)	110.2
C(52)-C(51)-H(51A)	109.8	C(57B)-C(56)-H(56C)	93.6
O(38)-C(51)-H(51B)	109.8	C(55)-C(56)-H(56D)	110.2
C(52)-C(51)-H(51B)	109.8	C(57A)-C(56)-H(56D)	110.2
H(51A)-C(51)-H(51B)	108.3	C(57B)-C(56)-H(56D)	142.0
O(39)-C(52)-C(51)	108.7(4)	H(56C)-C(56)-H(56D)	108.5
O(39)-C(52)-H(52A)	109.9	C(55)-C(56)-H(56A)	113.8
C(51)-C(52)-H(52A)	109.9	C(57A)-C(56)-H(56A)	124.8
O(39)-C(52)-H(52B)	109.9	C(57B)-C(56)-H(56A)	113.8
C(51)-C(52)-H(52B)	109.9	H(56C)-C(56)-H(56A)	20.9
H(52A)-C(52)-H(52B)	108.3	H(56D)-C(56)-H(56A)	88.5
O(39)-C(53)-C(54)	108.6(4)	C(55)-C(56)-H(56B)	113.8

Table 4.11 Cont.

C(57A)-C(56)-H(56B)	82.4	C(57B)-C(58)-O(10)	105.3(7)
C(57B)-C(56)-H(56B)	113.8	C(57B)-C(58)-C(57A)	35.1(7)
H(56C)-C(56)-H(56B)	127.5	O(10)-C(58)-C(57A)	105.0(6)
H(56D)-C(56)-H(56B)	28.8	C(57B)-C(58)-H(58A)	110.7
H(56A)-C(56)-H(56B)	111.0	O(10)-C(58)-H(58A)	110.7
C(56)-C(57A)-C(58)	102.1(7)	C(57A)-C(58)-H(58A)	137.2
C(56)-C(57A)-H(57A)	111.4	C(57B)-C(58)-H(58B)	110.7
C(58)-C(57A)-H(57A)	111.4	O(10)-C(58)-H(58B)	110.7
C(56)-C(57A)-H(57B)	111.4	C(57A)-C(58)-H(58B)	78.6
C(58)-C(57A)-H(57B)	111.4	H(58A)-C(58)-H(58B)	108.8
H(57A)-C(57A)-H(57B)	109.2	C(57B)-C(58)-H(58C)	133(7)
C(58)-C(57B)-C(56)	101.1(9)	O(10)-C(58)-H(58C)	120(7)
C(58)-C(57B)-H(57C)	111.6	C(57A)-C(58)-H(58C)	115(7)
C(56)-C(57B)-H(57C)	111.6	H(58A)-C(58)-H(58C)	65.1
C(58)-C(57B)-H(57D)	111.6	H(58B)-C(58)-H(58C)	44.2
C(56)-C(57B)-H(57D)	111.6	C(57B)-C(58)-H(58D)	46(5)
H(57C)-C(57B)-H(57D)	109.4	O(10)-C(58)-H(58D)	103(5)
C(58)-C(57B)-H(58D)	57(6)	C(57A)-C(58)-H(58D)	81(5)
C(56)-C(57B)-H(58D)	127(6)	H(58A)-C(58)-H(58D)	69.3
H(57C)-C(57B)-H(58D)	121.7	H(58B)-C(58)-H(58D)	144.4
H(57D)-C(57B)-H(58D)	54.8	H(58C)-C(58)-H(58D)	125(9)

Table 4.12 Crystal data and structure refinement for $[Re(bpy)(CO)_3(THF)][PF_6]$

Identification code	eb_110912_0ma	
Empirical formula	C17 H16 F6 N2 O4 P Re	
Formula weight	643.49	
Temperature	100(2) K	
Wavelength	0.71073 Å	
Crystal system	Monoclinic	
Space group	C2/c	
Unit cell dimensions	a = 19.7428(11) Å	α= 90°.
	b = 9.7824(4) Å	β= 93.428(2)°.
	c = 20.5661(10) Å	γ = 90°.
Volume	3964.9(3) $Å^3$	
Z	8	
Density (calculated)	2.156 Mg/m^3	
Absorption coefficient	6.294 mm^{-1}	
F(000)	2464	
Crystal size	0.20 x 0.20 x 0.05 mm^3	
Theta range for data collection	1.98 to 25.43°.	
Index ranges	-23<=h<=23, -11<=k<=10, -24<=l<=24	
Reflections collected	16937	
Independent reflections	3658 [R(int) = 0.0246]	
Completeness to theta = 25.00°	99.7 %	
Absorption correction	Semi-empirical from equivalents	
Max. and min. transmission	0.7437 and 0.3658	
Refinement method	Full-matrix least-squares on F^2	
Data / restraints / parameters	3658 / 0 / 280	
Goodness-of-fit on F^2	1.218	
Final R indices [I>2sigma(I)]	R1 = 0.0188, wR2 = 0.0508	
R indices (all data)	R1 = 0.0216, wR2 = 0.0688	
Largest diff. peak and hole	1.671 and -0.959 $e.Å^{-3}$	

Table 4.13 Bond lengths [Å] and angles [°] for $[Re(bpy)(CO)_3(THF)][PF_6]$

C(1)-O(1)	1.159(5)	C(15)-H(15A)	0.9900
C(1)-Re(1)	1.895(5)	C(15)-H(15B)	0.9900
C(2)-O(2)	1.157(5)	C(16)-C(17)	1.507(7)
C(2)-Re(1)	1.916(4)	C(16)-H(16A)	0.9900
C(3)-O(3)	1.143(5)	C(16)-H(16B)	0.9900
C(3)-Re(1)	1.943(5)	C(17)-O(4)	1.464(5)
C(4)-N(1)	1.338(6)	C(17)-H(17A)	0.9900
C(4)-C(5)	1.380(6)	C(17)-H(17B)	0.9900
C(4)-H(4)	0.9500	N(1)-Re(1)	2.172(3)
C(5)-C(6)	1.383(6)	N(2)-Re(1)	2.159(3)
C(5)-H(5)	0.9500	O(4)-Re(1)	2.213(3)
C(6)-C(7)	1.395(6)	F(1)-P(1)	1.599(3)
C(6)-H(6)	0.9500	F(2)-P(1)	1.589(3)
C(7)-C(8)	1.380(6)	F(3)-P(1)	1.575(3)
C(7)-H(7)	0.9500	F(4)-P(1)	1.576(3)
C(8)-N(1)	1.355(5)	F(5)-P(1)	1.608(3)
C(8)-C(9)	1.475(6)	F(6)-P(1)	1.597(3)
C(9)-N(2)	1.359(5)		
C(9)-C(10)	1.388(6)	O(1)-C(1)-Re(1)	178.1(4)
C(10)-C(11)	1.377(6)	O(2)-C(2)-Re(1)	177.0(4)
C(10)-H(10)	0.9500	O(3)-C(3)-Re(1)	177.4(4)
C(11)-C(12)	1.390(6)	N(1)-C(4)-C(5)	122.1(4)
C(11)-H(11)	0.9500	N(1)-C(4)-H(4)	119.0
C(12)-C(13)	1.377(6)	C(5)-C(4)-H(4)	119.0
C(12)-H(12)	0.9500	C(4)-C(5)-C(6)	119.2(4)
C(13)-N(2)	1.352(5)	C(4)-C(5)-H(5)	120.4
C(13)-H(13)	0.9500	C(6)-C(5)-H(5)	120.4
C(14)-O(4)	1.460(5)	C(5)-C(6)-C(7)	119.1(4)
C(14)-C(15)	1.517(6)	C(5)-C(6)-H(6)	120.5
C(14)-H(14A)	0.9900	C(7)-C(6)-H(6)	120.5
C(14)-H(14B)	0.9900	C(8)-C(7)-C(6)	118.7(4)
C(15)-C(16)	1.509(7)	C(8)-C(7)-H(7)	120.7

Table 4.13 Cont.

C(6)-C(7)-H(7)	120.7	C(15)-C(16)-H(16A)	111.1
N(1)-C(8)-C(7)	121.9(4)	C(17)-C(16)-H(16B)	111.1
N(1)-C(8)-C(9)	115.3(3)	C(15)-C(16)-H(16B)	111.1
C(7)-C(8)-C(9)	122.9(4)	H(16A)-C(16)-H(16B)	109.1
N(2)-C(9)-C(10)	121.2(4)	O(4)-C(17)-C(16)	103.1(4)
N(2)-C(9)-C(8)	115.4(4)	O(4)-C(17)-H(17A)	111.1
C(10)-C(9)-C(8)	123.3(4)	C(16)-C(17)-H(17A)	111.1
C(11)-C(10)-C(9)	119.3(4)	O(4)-C(17)-H(17B)	111.1
C(11)-C(10)-H(10)	120.3	C(16)-C(17)-H(17B)	111.1
C(9)-C(10)-H(10)	120.3	H(17A)-C(17)-H(17B)	109.1
C(10)-C(11)-C(12)	119.8(4)	C(4)-N(1)-C(8)	119.1(4)
C(10)-C(11)-H(11)	120.1	C(4)-N(1)-Re(1)	123.8(3)
C(12)-C(11)-H(11)	120.1	C(8)-N(1)-Re(1)	116.9(3)
C(13)-C(12)-C(11)	118.4(4)	C(13)-N(2)-C(9)	118.8(4)
C(13)-C(12)-H(12)	120.8	C(13)-N(2)-Re(1)	123.8(3)
C(11)-C(12)-H(12)	120.8	C(9)-N(2)-Re(1)	117.1(3)
N(2)-C(13)-C(12)	122.5(4)	C(14)-O(4)-C(17)	108.8(3)
N(2)-C(13)-H(13)	118.7	C(14)-O(4)-Re(1)	120.2(2)
C(12)-C(13)-H(13)	118.7	C(17)-O(4)-Re(1)	129.7(3)
O(4)-C(14)-C(15)	106.3(3)	F(3)-P(1)-F(4)	93.0(2)
O(4)-C(14)-H(14A)	110.5	F(3)-P(1)-F(2)	89.1(2)
C(15)-C(14)-H(14A)	110.5	F(4)-P(1)-F(2)	177.8(2)
O(4)-C(14)-H(14B)	110.5	F(3)-P(1)-F(6)	89.77(17)
C(15)-C(14)-H(14B)	110.5	F(4)-P(1)-F(6)	90.19(18)
H(14A)-C(14)-H(14B)	108.7	F(2)-P(1)-F(6)	89.17(17)
C(16)-C(15)-C(14)	103.9(4)	F(3)-P(1)-F(1)	90.41(17)
C(16)-C(15)-H(15A)	111.0	F(4)-P(1)-F(1)	90.21(19)
C(14)-C(15)-H(15A)	111.0	F(2)-P(1)-F(1)	90.42(17)
C(16)-C(15)-H(15B)	111.0	F(6)-P(1)-F(1)	179.55(18)
C(14)-C(15)-H(15B)	111.0	F(3)-P(1)-F(5)	177.6(2)
H(15A)-C(15)-H(15B)	109.0	F(4)-P(1)-F(5)	89.3(2)
C(17)-C(16)-C(15)	103.3(4)	F(2)-P(1)-F(5)	88.5(2)
C(17)-C(16)-H(16A)	111.1	F(6)-P(1)-F(5)	89.87(17)

Table 4.13 Cont.

F(1)-P(1)-F(5)	89.93(17)	C(2)-Re(1)-N(1)	173.20(15)
C(1)-Re(1)-C(2)	87.74(17)	C(3)-Re(1)-N(1)	98.94(15)
C(1)-Re(1)-C(3)	90.39(17)	N(2)-Re(1)-N(1)	75.08(13)
C(2)-Re(1)-C(3)	87.84(17)	C(1)-Re(1)-O(4)	176.77(13)
C(1)-Re(1)-N(2)	95.44(15)	C(2)-Re(1)-O(4)	93.81(14)
C(2)-Re(1)-N(2)	98.20(15)	C(3)-Re(1)-O(4)	92.50(15)
C(3)-Re(1)-N(2)	171.75(15)	N(2)-Re(1)-O(4)	81.54(11)
C(1)-Re(1)-N(1)	91.79(15)	N(1)-Re(1)-O(4)	86.33(11

Chapter 5

FTIR and XRD characterization of M(bipy-R)$(CO)_3^-$ anions: electronic and structural properties of compounds relevant to the electrocatalytic reduction of CO_2

5.1 Introduction

One key aspect of catalyst optimization deals with selectivity of the catalyst towards the desired substrates. The reduction of CO_2 to useful products is inherently proton-dependent.[1] This is true not only for the production of carbohydrates by natural photosynthesis, but also for the synthetic production of other value-added products from the reduction of CO_2. The protons required are susceptible to competitive, direct

reduction to H_2, a process that occurs at a more positive (i.e., more favorable) thermodynamic potential. A functional artificial photosynthetic system therefore requires a catalyst that is kinetically *selective* for CO_2 reduction over H^+ reduction.

Recently, our group has explored complexes of the type $Re(bipy\text{-}R)(CO)_3(L)$ (where bipy-R = 4,4'-disubstituted-2,2'-bipyridine and L = an anionic ligand or a neutral ligand with $^-$OTf as the counter ion) and reported that $Re(bipy\text{-}tBu)(CO)_3Cl$ (**3**) is a pre-catalyst for the electrochemical reduction of CO_2 to CO at high turnover frequency (>200 s^{-1}) compared with the previous reports on $Re(bipy)(CO)_3Cl$ (**1**).[2-4] Complex (**3**) has one of the highest turnover frequencies reported for the reduction of CO_2 to CO, and exhibits nearly 100% Faradaic efficiency with very high turnover numbers (less than 5% degradation over a period of more than 24 hours). We have also successfully coupled the catalyst to a semiconductor electrode, p-type silicon (p-Si), which enables us to provide part of the thermodynamic energy for catalysis using illumination with light in the solar spectrum.[5]

In recent studies we have shown that is possible to isolate and structurally characterize the five-coordinate anion $Re(bipy)(CO)_3^-$.[6] With a small change in the catalyst ligand having such a profound effect on the rate of catalysis, we sought to investigate a series of compounds in their chemically reduced states to elucidate the structural and electronic properties. By studying these reduced compounds by FTIR and XRD we can attempt to correlate structure, electronics and function. By synthesizing a series of complexes with different electronics and sterics at the 4,4'

position of 2,2'-bipyridine we could then use a strong reductant (KC_8) to access the catalytically relevant active species.

Using the Hammett parameter as a gauge of the donating and withdrawing properties of various substituents we chose five different bipyridines (R = CF_3, H, CH_3, *t*Bu, OMe) varied at the 4,4' position that offered different steric and electronic properties. The σ parameter, defined as the change in pKa of benzoic acid vs. the substituted benzoic acid (E5.1), gives us the relative donation ability of substituents para to the pyridyl nitrogen. With these five ligands we can vary the electronics from withdrawing (CF_3, σ_p = 0.54) to donating (CH_3, σ_p = -0.170; *t*Bu, σ_p = -0.197; OMe, σ_p = -0.268) and compare ligands with similar steric properties (CF_3, CH_3).[7, 8]

$$\sigma = pKa(C_6H_5COOH) - pKa(X\text{-}C_6H_4COOH) \qquad \text{E5.1}$$

5.2 Results and discussion

5.2.1 Synthesis and Infrared Spectroscopy

While most of the ligands were commercially available, the 4,4'-trifluoromethyl-2,2'-bipyridine had to be synthesized. This was accomplished from the symmetric Ulmann coupling of two 2-bromo-4-trifluoromethyl pyridines in modest yield (52%). Once all ligands were in hand, metalation was accomplished through previously reported means.[2]

It has long been postulated that the doubly-reduced $[Re(bipy\text{-}R)(CO)_3]^{-1}$ anions are the species that actively bind CO_2, rendering them the most immediately relevant intermediate in studies of CO_2/H^+ selectivity.[9, 10] We recently observed that solutions of this species could be generated by reduction of the starting halide material

with 2.1 equivalents of KC_8, and that by careful handling, they could be maintained and characterized by a variety of techniques.[6] The three facial carbonyl groups on the rhenium are a strong reporter of the electronics at the metal center. The IR frequencies of the starting halide complexes (**1-5**) and KC_8 reduced products (**1a-5a**) are shown in Table 5.1.

The IR stretching frequencies of complexes **1-5** follow the donating ability of the substituted bipyridine, with the most donating (R = OMe, **4**) shifting the high energy band 3 cm^{-1} lower in energy, while the least donating (R = CF_3, **5**) shifts 4 cm^{-1} higher in energy compared to the 2,2'-bipyridine complex, (R = H, **1**). Reduction with KC_8 shows a shift of the high energy band from 2020 cm^{-1} to 1945 cm^{-1} for complex (**1**), suggesting significant back donation to the carbonyls. These ν(CO) stretching frequencies are in good agreement with the frequencies reported in previous spectroelectrochemical studies.[9, 11]

Table 5.1 IR stretching frequencies for compounds **1-5** and **1a-5a**

Compound	ν(CO), X = Cl, **1-5**	ν(CO), X = K(18-crown-6), **1a-5a**
$Re(bpy)(CO)_3X$ (**1, 1a**)	2020, 1917, 1893 cm^{-1}	1945, 1839 cm^{-1}
$Re(bpy\text{-}CH_3)(CO)_3X$ (**2, 2a**)	2018, 1916, 1891 cm^{-1}	1941, 1835 cm^{-1}
$Re(bpy\text{-}tBu)(CO)_3X$ (**3, 3a**)	2018, 1915, 1891 cm^{-1}	1940, 1835 cm^{-1}
$Re(bpy\text{-}OMe)(CO)_3X$ (**4, 4a**)	2017, 1911, 1888 cm^{-1}	1940, 1834 cm^{-1}
Re(bpy-CF3)$(CO)_3X$ (**5, 5a**)	2024, 1926, 1902 cm^{-1}	1966, 1860 cm^{-1}

As with the starting halides, the stretching frequencies of the reduced products follow the donating ability of the bipyridine. Surprisingly, the stretching frequencies of the reduced complexes of **2-4** all show similar stretching frequencies, with variations of only 1 cm^{-1}, they were close enough that the resolution and data spacing of the instrument (1 cm^{-1} resolution, 0.482 cm^{-1} data spacing) had to be increased to differentiate between them. Although these three compounds have similar stretches and thus presumably similar electronics, there is a significant difference in catalytic properties. With our previous success isolating and structurally characterizing the anions $[Re(tripbipy)(CO)_3][K(THF)_2]\cdot THF$ and $[Re(bipy)(CO)_3][K(18\text{-crown-}6)(THF)]$ (**1a**) we sought to see if there was a structural explanation for the significant differences observed in the catalytic rates.[6]

5.2.2 Crystallography of rhenium anions

With stable solutions of the $[Re(bipy\text{-}R)(CO)_3]^{-1}$ species in hand, the source of CO_2 selectivity and activity could be investigated through structural studies. Single crystals suitable for X-ray diffraction were grown from the vapor diffusion of pentane into a THF solution of the anion containing 18-crown-6 as a stabilizing agent. Similar to what was seen in the reduced complex (**1a**) (Figure 4.3); reduction of complex (**2**) results in the formation of a rhenium center that is coordinated by three facial carbonyls and the chelating bipyridine. The potassium cation is encapsulated by the crown ether and is weakly associated with one axial carbonyl (K1 – O1, 2.7504(16)) and one equatorial carbonyl from an adjacent molecule in the unit cell (K1 – O2', 2.7342(16)).

Complex (**2a**) adopts a distorted trigonal bipyriamidal (τ_5 = 0.11) geometry shown in Figure 5.1. The τ_5 method proposed by Verschoor,[12] allows for the quantitative determination of trigonal distortion. The value is determined by E5.2, where β and α are the two greatest angles (β > α) around a five-coordinate center. For a complex in C_{4v} symmetry (square pyramid) it results in a value of 0, where a five-coordinate complex in C_{3v} symmetry (trigonal bipyramid) gives a value of 1. A table of τ_5 values for reduced complexes (**1a-4a**) can be found in Table 5.2.

$$\tau_5 = (\beta - \alpha)/60 \qquad \text{(E5.2)}$$

After reduction, complex (**3a**) is distorted towards a trigonal bipyramid (τ_5 = 0.46) geometry in the solid state. The Re center is coordinated by three facial

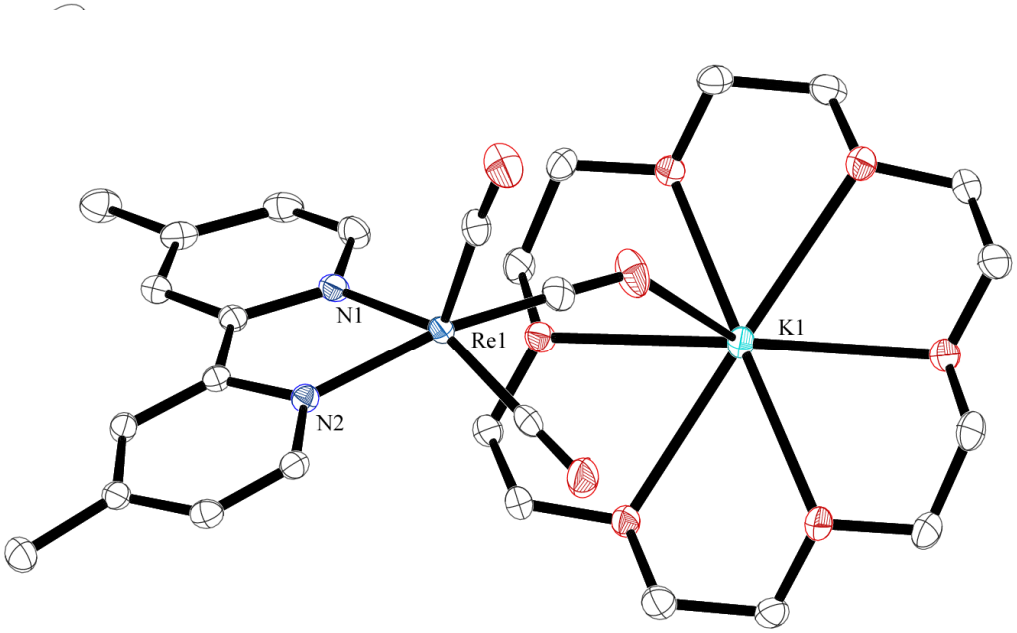

Figure 5.1 Molecular structure of the $[Re(6,6'\text{-DMB})(CO)_3]^{-1}$ anion. Hydrogen atoms are omitted for clarity and ellipsoids are shown at 50% probability.

carbonyl ligands and a chelating bipyridine (Figure 5.2). A table of bond lengths and angles can be found in the appendix. The potassium cation is encapsulated by the crown ether and has one bound THF molecule. It is also associated with the axial carbonyl (O3–K1, 2.945(7) Å). The Re–N distance contracts and the bite angle of the bipyridine increases slightly compared with the unreduced starting material (**3**) (Figure 5.8, appendix). This behavior is indicative of improved orbital overlap between the ligand and metal center in the anion. A useful marker for the occupancy of the bipyridine π* orbital is the bridging 2,2' carbon distance.[11] Table 5.2 gives the bridging bond lengths for compounds (**1a**-**4a**).

For complex (**4a**) there are two independent molecules in the unit cell, with one of the molecules possessing slight whole molecule disorder (~6% shifted 1.03 Å).

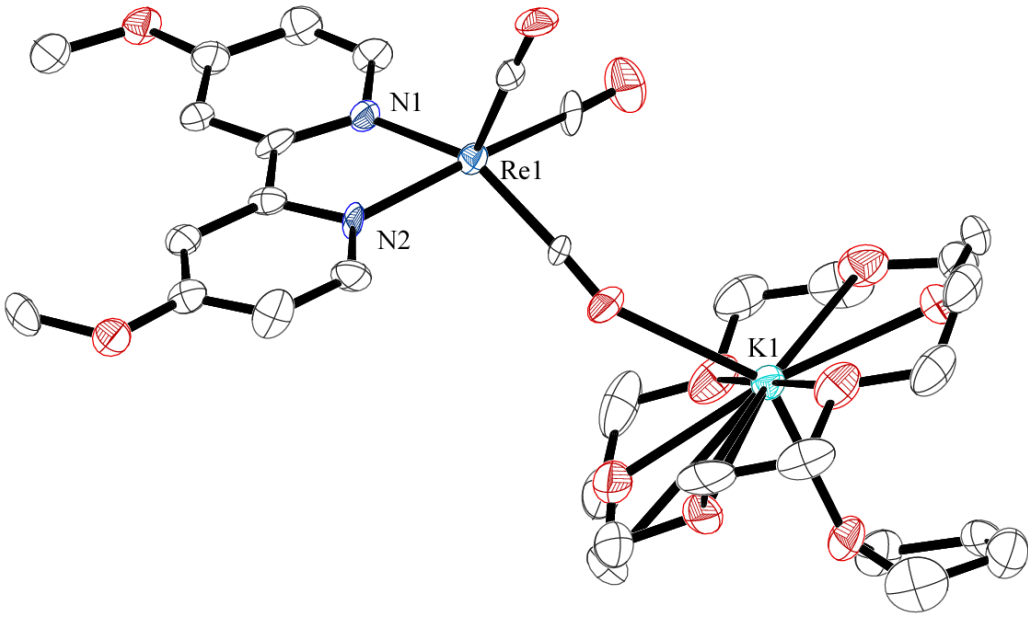

Figure 5.3 Molecular structure of one of the $[Re(bpy\text{-}OMe)(CO)_3]^{-1}$ anions in the unit cell, Z' = 2. Hydrogen atoms are omitted for clarity and ellipsoids are shown at 50% probability.

Within the unit cell, one of the independent molecules has a τ_5 = 0.33, while the other molecule has a τ_5 = 0.18. Again, the potassium cation is encapsulated by the crown ether and has one bound THF molecule and associated with an equatorial carbonyl (K1 – O3, 3.043(12); K2 – O7, 2.844(9)).

Unfortunately attempts to grow crystals of (**5a**) have been unsuccessful. From the change of color during crystallization we believe that the complex is slowly decomposing at room temperature. This could be due to a loss of fluoride, but this was not further investigated. If solutions of (**5a**) were left in the freezer, the compound was stable for extended periods of time (weeks), and if left at room temperature it would lose its characteristic color within 24 hours. Attempts have been made to crystalize the complex at lower temperatures, but they have been unsuccessful to date.

With the XRD structures of the four anions (**1a-4a**) we can begin to look for

Table 5.2 τ_5 parameter and selected bond lengths for compounds (**1a-4a**)

Compound	τ_5	bipy 2,2' distance (Å)	Re – N (Å)[b]
$Re(bpy)(CO)_3^-$ (**1a**)	0.18, 0.16[a]	1.391(6), 1.413(6)[a]	2.081(5)
$Re(6,6'\text{-dmb})(CO)_3^-$ (**2a**)	0.11	1.394(3)	2.094(5)
$Re(bpy\text{-}tBu)(CO)_3^-$ (**3a**)	0.46	1.370(15)	2.09(3)
$Re(bpy\text{-}OMe)(CO)_3^-$ (**4a**)	0.33, 0.18[a]	1.388(13), 1.405(14)[a]	2.10(2)

[a]Two independent molecules in the unit cell, Z' = 2. [b]Average of distances found in the asymmetric unit.

structural parameters that track with catalyst activity. While the IR spectra showed similar stretches, indicating similar electronics at the metal center, we can look at several structural parameters such as coordination geometry and charge on the bipyridine using the bridging carbon distance. In previous electrochemical studies the rate of electrocatalysis has been reported as (**4**) << (**1**) < (**2**) < (**3**).[2] While the catalysis seems to follow donation ability of the bipyridine (pKa) the notable exception is complex (**4**). One explanation for this exception is σ vs. π donation. Complex (**2**) and (**3**) both contain groups at the 4,4' position that are primarily σ donors, whereas with the OMe groups, they contain a significant amount of O → N (py) π-donation. This effect has been described in Ir pincer dehydrogenation catalysts.[13, 14] Another possible explanation is the stabilization of the ligand-based radical through the extended π–conjugation, similar to that seen with the extended conjugation of 1,6,7,12,13,18-Hexaazatrinaphthylene (HATN) ligands.[15] It should also be noted that the bridging 2,2' distance is closer to that of the isolated $bipy^{2-}$ structure reported earlier,[11] but is most likely actually $bipy^{1-}$ (Chapter 6).

5.2.3 DFT of rhenium anions

To obtain a better understanding of the electronic structure of these reduced states, we employed DFT calculations using ADF 2007.1. The calculated HOMO of (**3**) is a hybrid involving both the ligand and the metal center, containing substantial π* character (Figure 5.4, *xyz* coordinates in appendix). This is consistent with the bond length alternation observed in the bipyridine rings of the Re anion crystal structure. The bond alternation in the bipy is similar to what is seen in crystal structures of

reduced 2,2'-bipyridine[11] and suggests significant electron density on the ligand. An example input file as well as the tables of geometry optimized coordinates for complexes (**1a-5a**) can be found in the appendix.

Table 5.3 contains selected geometric parameters from the gas-phase calculations of the anions (**1a-5a**) using ADF 2007.1. Input geometries were taken from crystal structures when available, and the input geometry of (**5a**) was modified from (**3a**). As with the structural parameters from the XRD studies, there does not seem to be a strong correlation between any of the selected parameters and the observed electrocatalytic rates. In hindsight, this is not completely unexpected due to such similar ν(CO) stretching frequencies. One possible explanation for the differences in rates of electrocatalysis is that the rate limiting step is not the reaction of the anion with CO_2, but the protonation of the CO_2 bound species. However, in recent stopped-flow FTIR studies it has been reported that (**3a**) reacts with CO_2 *ca*. 10 times faster than complex (**1a**).[16]

ADF 2007.1.

Table 5.3 τ_5 parameters and selected bond lengths from ADF 2007.1

Compound	τ_5	bipy 2,2' distance	Re – N (Å)
$Re(bpy)(CO)_3^-$ (**1a**)	0.15	1.409 Å	2.107, 2.128
$Re(bpy\text{-}CH_3)(CO)_3^-$ (**2a**)	0.11	1.404 Å	2.107, 2.116
$Re(bpy\text{-}tBu)(CO)_3^-$ (**3a**)	0.42	1.406 Å	2.104, 2.135
$Re(bpy\text{-}OMe)(CO)_3^-$ (**4a**)	0.35	1.395 Å	2.112, 2.139
$Re(bpy\text{-}CF_3)(CO)_3^-$ (**5a**)	0.44	1.413 Å	2.093, 2.131

The geometry of the HOMO of the reduced complexes diffuses the directional basicity of the Re anion, and thus, other factors such as π interactions become important. We expect that the mixed character of the HOMO ($bipy^-$ + Re^0) relative to a doubly-occupied d_z^2 "lone-pair," is sufficient to cause CO_2 binding to be more favorable than H^+ binding. Similarly, a HOMO that is delocalized over bipy (π*) and Re *d*-orbitals disfavors direct protonation of the Re d_z^2 orbital to produce a hydride.

The nature of the binding of CO_2 to the anion can also be better understood through DFT. The geometry-optimized electronic structure of a Re(bipy-*t*Bu)$(CO)_3(CO_2)$K complex was calculated. The structure did not converge without the addition of a cation (H, Li, Na, K) to support the highly electronegative oxygen atoms. We observed that the d_z^2 orbital can form a σ bond to the carbon atom of CO_2 (HOMO) and the interaction with CO_2 can be further stabilized by a π interaction of the metal d_{xz} and d_{yz} orbitals with *p* orbitals on the CO_2 oxygen atoms (HOMO-4) (Figure 5.5, *xyz* coordinates in Table 5.22). This stabilizing interaction is clearly not available for the interaction with H^+. This interaction is somewhat similar to that calculated by Fujita and co-workers in the $[Co(macrocycle)(CO_2)(CH_3CN)]^+$ binding, but the Re complex forms an extended bonding interaction with the CO_2 oxygen atoms rather than just with the carbon center as in the Co example.[17]

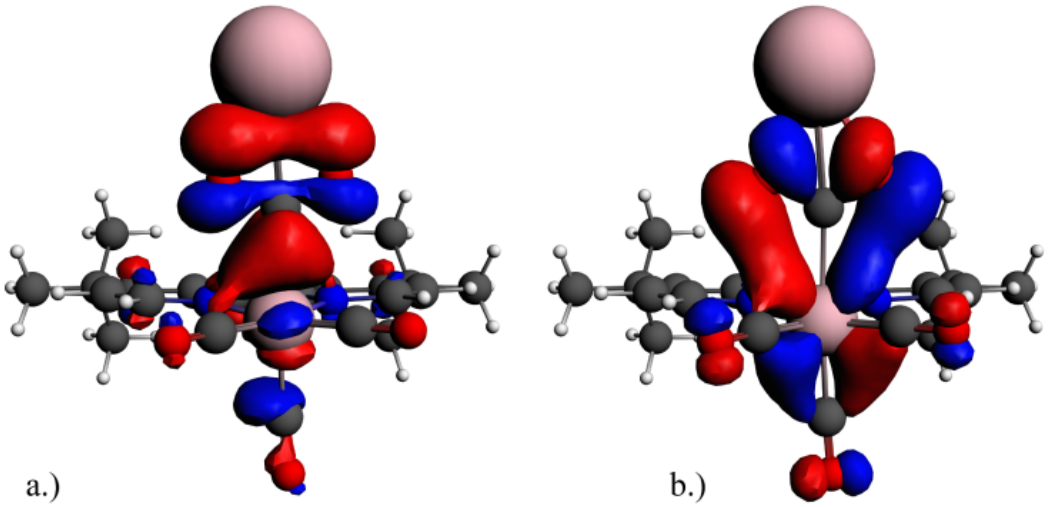

Figure 5.5 Calculated orbitals of Re(bipy-tBu)$(CO)_3(CO_2)$K using ADF 2007.1 showing a.) the d_z^2 orbital that forms a σ bond to CO_2 and b.) the π interactions with CO_2.

5.2.4 Re(bipy-CF_3)$(CO)_3$Cl

When reducing complex (**5**) with KC_8, if the reaction is filtered/quenched early, formation of the singly reduced [Re(bipy-CF_3)$(CO)_3$Cl][K(18-crown-6)] (**5b**) complex can be seen. Interestingly, the reduction does not result in the loss of the halide, but instead results in the formation of the complex with a reduced ligand (Figure 5.6). FTIR of this complex in THF shows three distinct bands at 2001, 1891, and 1973 cm^{-1} which correspond well with previous reports of Re(bipy-R)$(CO)_3Cl^-$ (R = *t*Bu, H) complexes previously only seen in IR-SEC studies.[2, 9] The bridging 2,2' carbon distance of 1.433(6) Å agrees with reported values for a reduced bipyridine,[11]

-crown-6)].
ı at 50%

and is longer than is seen in complexes (**1a-4a**). In comparison the bond distance of 1.471(7) Å for the unreduced complex (**5**) (Figure 5.10, appendix) is slightly shorter than the reported distance of neutral bipyridine, 1.490(3) Å.

The formation of this complex highlights the importance of the electronic overlap between the ligand and metal center. With complex (**1**) the one electron reduction results in the loss of chloride and subsequent dimer formation.[6] With the electron withdrawing trifluoromethyl groups we have altered the electronics enough that the ligand does not have the proper overlap to perform the ligand to metal charge transfer that results in loss of chloride as seen with complexes (**1, 3**). We are currently investigating the effects of abstracting the halide on the IR and electrochemistry.

5.2.5 Mn(bipy-tBu)$(CO)_3$Cl

With the recent report that Mn(bipy)$(CO)_3$Br and Mn(dmb)$(CO)_3$Br are electrocatalysts for the reduction of CO_2 to CO with added Brönsted acids,[18] we sought to investigate the electrochemical and structural properties of the Mn 4,4'-di-*tert*-butyl substituted bipyridine complex. The synthesis of this compond is similar to those of the Re complexes, where 4,4'-di-*tert*-butylbipyridine is refluxed in Et_2O with $Mn(CO)_5$Br to form Mn(bipy-tBu)$(CO)_3$Br (**6**).

The starting bromide material (**6**), can also be reduced with KC_8 to form the five-coordinate active species [Mn(bipy-*t*Bu)$(CO)_3$][K(18-crown-6)(THF)] (**6a**) (Figure 5.12, appendix). As with the Re complexes, the anion loses the axial halide and adopts a distorted trigonal bipyrimidal geometry. There are two independent molecules in the unit cell, Z' = 2, with one of the molecules possesing rotational disorder of the carbonyls. The potassium counterion is encapsulated by the crown ether, and the axial sites are occupied by a THF solvent molecule and a carbonyl from the anion.

The geometry around the manganese center is quite similar to its rhenium analog and a structural overlay can be seen in Figure 5.7. While the bridging 2,2' carbon distance is nearly indistiguishable between the Mn and Re complexes, there is a significant difference after reduction with KC_8. A table of τ_5 values and selected bond lengths can be found in Table 5.4. . The 2,2' carbon distance in (**6a**) is 1.41 Å, whereas the distance in the analagous Re complex is shorter at 1.37 Å. The distance

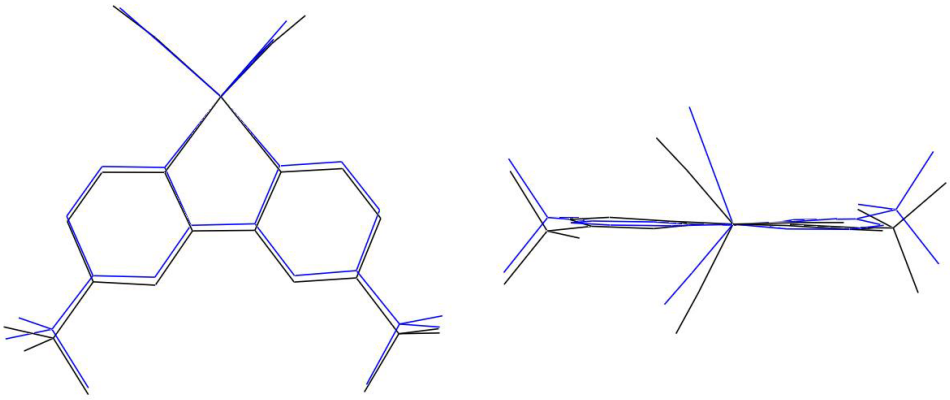

Figure 5.7 Structural overlay of Mn(bipy-*t*Bu)$(CO)_3^-$ (**6a,** blue) and Re(bipy-tBu)$(CO)_3^-$ (**3a**, black).

Table 5.4 τ_5 parameter and selected bond lengths for compounds (**3, 3a, 6, 6a**)

Compound	τ_5	bipy 2,2' distance (Å)	Re – N (Å)
Mn(bipy-tBu)$(CO)_3$Br (**6**)	-	1.480(3), 1.477(3)[a]	2.024(2)[b]
Mn(bipy-tBu)$(CO)_3^-$ (**6a**)	0.46(8)[b]	1.414(9), 1.406(10)[a]	1.982(10)[b]
Re(bpy-tBu)$(CO)_3$Cl (**3**)	-	1.487(5), 1.475(5)[a]	2.173(6)[b]
Re(bpy-tBu)$(CO)_3^-$ (**3a**)	0.46	1.370(15)	2.09(3)

[a]Two independent molecules in the unit cell, Z' = 2. [b]Average of distances found in the asymmetric unit.

for (**6a**) is shorter than those reported for Cr^{III} tris bipyridines with reduced ligands, suggesting there is a significant amount of charge on the ligand. This distance however is not as short as that reported for $(bipy)^{2-}$.[19] In order for us to correctly and definitivly assign the oxidation state of the metal center, we will need to use X-Ray absorption near edge structure (XANES). XANES studies (Chapter 6) are currently underway with the series of rhenium complexes and may be extended to the manganese complexes at a later date.

In previous electrochemical studies of this complex it was shown that the voltamograms do not change under an atmosphere of CO_2. It is not until a proton source is added that the compex is able to catalytically activate carbon dioxide.[20] With this knowledge we believe that we may be sucsessful in isolating a metal carboxalate, and are currently investigating the reaction of (**6a**) with CO_2.

5.3 Conclusions

We have been able to synthesize and characterize several anionic rhenium complexes relevant to the electrochemical reduction of carbon dioxide. We were able to crystalize several of these compounds, including Re(bipy-*t*Bu)$(CO)_3^-$, which has been proposed as the active species that binds CO_2. From the structural data we cannot come to a conclusion on the origin of the differences in electrocatalytic rates. However with this structural data, combined with DFT studies of the reduced complex, we can gain a better understanding of the origins of selectivity for these types of complexes. From the crystal structures and DFT, we can ascertain that the HOMO is mixed metal-ligand in character. It is this mixed metal-ligand character that makes these complexes incredibly selective for the reduction of carbon dioxide in the presence of H^+.

Acknowledgment. Financial support was provided by DARPA (Surface Catalysis for Energy Program). We thank Prof. Arnold Rheingold and Dr. Curtis Moore at the UCSD Crystallography Facility. This research was supported at the University of California, San Diego by the DARPA Surface Catalysis for Energy Program and by the Air Force Office of Scientific Research through the MURI program under AFOSR Award No. FA9550-10-1-0572. The authors would like to thank Dr. John Goeltz for his thorough editing of the manuscript, and Prof. Joshua Figueroa for his assistance with computations.

5.4 Experimental

General considerations. Complexes (**1-4**) and KC_8 were synthesized by previously reported methods.[2, 21] 18-crown-6 was recrystallized from acetonitrile, tetrabutylammonium hexafluorophosphate (TBAH) was recrystallized twice from methanol, and both were dried under vacuum. All other chemicals were purchased from commercial sources and used as received. THF, CH_3CN, and pentane were sparged with argon and dried over basic alumina with a custom dry solvent system. THF and pentane were then stored over activated molecular sieves. All elemental analyses were performed by Midwest MicroLab, LLC (Indianapolis, IN) for C, H and N. Infrared spectra were collected on a Thermo Scientific Nicolet 6700. NMR spectra were collected on either a Jeol 500 MHz Spectrometer or a Varian 400 MHz Spectrometer and analyzed using Jeol Delta software.

Synthesis of 4,4'-trifluoromethyl-2,2'-bipyridine. 1.2 g (5.31 mmol) of 2-bromo-4-trifluromethyl pyridine was placed in a round bottom flask with 7.14 g of activated copper bronze. The reaction flask was then flushed with N_2 and a reflux condenser was affixed. The reaction was then heated to 190° C for 16 hours. The reaction was then cooled to room temperature and the ligand extracted with acetone and chloroform (~100 mL). The organic fraction was then extracted with 1.2 N HCl. Once the aq. fraction turned blue, the organic fraction was extracted then evaporated to afford a yellow oil. The ligand was then purified by vacuum sublimation. ^{1}H NMR (500 MHz, CD_2Cl_2, 20 °C): δ 7.61 (d, 2H, J = 5 Hz), δ 8.74 (s, 2H), δ 8.89 (d, 2H, *J* = 5 Hz), ^{19}F(470 MHz, CD_2Cl_2, 20 °C) δ -65.1 (s, 6F).

Reductions of Re(bipy-R)$(CO)_3$Cl with KC_8. 1–10 mM solutions of Re(bipy-*R*)$(CO)_3$Cl were prepared in THF in an inert atmosphere and cooled to –35 °C. Either 18-crown-6 (2.5 eq. for X-ray and FTIR) or tetrabutylammonium hexafluorophosphate (0.1 M for stopped-flow) were added as stabilizing agents. 2.1 equivalents of KC_8 were added to the cooled solution and allowed to warm to room temperature over a period of 30 minutes. The solution was then filtered, affording a deep purple solution of the anion. The solution was concentrated from 20 mL to approximately 3 mL and 15 mL of pentane was added. That solution was stored in the freezer for two hours. The solution was then decanted and the purple solid was dried under vacuum. X-ray quality crystals were grown by the vapor diffusion of pentane into a THF solution of the complex. A typical yield of 66% was observed. All solutions were spectroscopically pure by FTIR (THF). (**3a**) ν(CO) 1940 cm^{-1} and 1835 cm^{-1}. ^{1}H NMR (500 MHz, TFH-d_8, 20 °C): δ 1.21 (s, 18H), δ 3.54 (s(br), 24H), δ 3.59 (d, 2H, *J* = 6 Hz), δ 7.13 (s, 2H), δ 8.86 (d, 2H, *J* = 7 Hz). Anal. Calcd, $C_{33}H_{48}KN_2O_9Re$: C, 47.07; H, 5.75; N, 3.33. Found: C, 47.02; H, 5.72; N, 3.35.

Synthesis of [Re(4,4'-trifluoromethyl-2,2'-bipyridine)$(CO)_3$Cl][K(18-crown-6)]. 25 mg of Re(4,4'-trifluoromethyl-2,2'-bipyridine)$(CO)_3$Cl (0.042 mmol) and 23 mg of 18-crown-6 ether (0.088 mmol) were dissolved in ~10 mL of THF and cooled to -35°C. 12 mg of KC_8 (0.088 mmol) was then added to the solutions and shaken briefly. After 15 minutes the deep purple solution was filtered to remove any unreacted KC_8 and was spectroscopically pure by FTIR (THF) ν(CO) 2001, 1891, and 1973 cm^{-1}.

Synthesis of Mn(4,4'-di-*tert*-butyl-2,2'-bipyridine)(CO)$_3$Br. $Mn(CO)_5Br$ (500 mg, 1.82 mmol) was added to an argon-sparged Schlenk flask with 50 ml Et_2O. 4,4'-di-*tert*-butyl-2,2'-bipyridine (494 mg, 1.84 mmol) was added to the mixture and the reaction was brought to reflux. The mixture quickly turned from colorless to orange after reflux began and product began crashing out of solution after 30-40 minutes. The reaction mixture was removed from heat after one hour and submerged in a –80 °C acetone/dry ice bath. After 30 minutes in the cold bath, the reaction mixture was removed and the yellow solid was filtered and dried under vacuum at 90 °C overnight. The yield of Mn(bipy-*t*Bu)$(CO)_3Br$ was 601 mg (67%). ^{1}H NMR ($CDCl_3$): δ 1.43 (br, 18 H, *t*Bu), δ 7.50 (br, 2 H, 5 and 5' H's), δ 8.03 (br, 2 H, 6 and 6' H's), δ 9.13 (br, 2 H, 3 and 3' H's). IR (CH_3CN) ν(CO): 2028 cm^{-1}, 1933 cm^{-1}, 1923 cm^{-1}. Anal. Calcd for **1**, $C_{21}H_{24}BrMnN_2O_3$: C, 51.76; H, 4.96; N, 5.75. Found: C, 51.80; H, 4.95; N, 5.69.

Synthesis of [Mn(4,4'-di-*tert*-butyl-2,2'-bipyridine)(CO)$_3$][K(18-crown-6)]. 50 mg of Mn(bipy-*t*Bu)$(CO)_3Br$ (0.102 mmol) and 57 mg of 18-crown-6 (0.216 mmol) were disolved in THF under an inert atmosphere and then cooled to –35 °C. 2.1 equivalents of KC_8 (29 mg, 216 mmol) were added to the cooled solution and allowed to warm to room temperature over a period of 30 minutes. The solution was then filtered, affording a deep purple solution of the anion. The solution was concentrated from 20 mL to approximately 3 mL and 15 mL of pentane was added. That solution was stored in the freezer for two hours. The solution was then decanted and the purple solid was dried under vacuum to yield 62 mg. (0.087 mmol, 86% yield). X-ray quality crystals

were grown by the vapor diffusion of pentane into a THF solution of the complex. All solutions were spectroscopically pure by FTIR (THF). (**3a**) ν(CO) 1907 and 1807 cm^{-1}. Anal. Calcd, $C_{33}H_{48}KMnN_2O_9$: C, 55.76; H, 6.81; N, 3.94. Found: C, 53.40; H, 6.99; N, 3.40.

X-ray structure determination. The single crystal X-ray diffraction studies were carried out on a Bruker Kappa APEX-II CCD diffractometer equipped with Mo Kα radiation (λ = 0.71073 Å) or a Bruker Kappa APEX CCD diffractometer equipped with Cu Kα radiation (λ = 1.54184 Å). The crystals were mounted on a Cryoloop with Paratone oil and data was collected under a nitrogen gas stream at 100(2) K using ω and ϕ scans. Data were integrated using the Bruker SAINT software program and scaled using the SADABS software program. Solution by direct methods (SHELXS) produced a complete phasing model consistent with the proposed structure. All nonhydrogen atoms were refined anisotropically by full-matrix least-squares (SHELXL-97).[22] All hydrogen atoms were placed using a riding model. Their positions were constrained relative to their parent atom using the appropriate HFIX command in SHELXL-97. Crystallographic data are summarized in the appendix.

Computational methods. The DFT calculations were performed with the Amsterdam Density Functional (ADF) program suite [23, 24], version 2007.1 using the triple-ζ Slater-type orbital basis set. Zero-order regular approximation (ZORA) [25, 26] was included for relativistic effects in conjunction with the local density approximation of Vosko et al. (VWN) [27]. Generalized gradient approximations for electron exchange and correlation were used as described by Becke[28] and Perdew.[29, 30] Molecular orbitals and

final geometries were visualized with ADF-GUI. The final structure obtained for $[Re(bipy\text{-}tBu)(CO)_3]^{-1}$ is very similar to the structure obtained by X-ray crystallography. Both are five-coordinate and both are distorted between square pyramidal and trigonal bipyramidal. The τ_5 value for the DFT calculated structure, however, is only 0.13, while the τ_5 for the structure obtained by x-ray crystallography is 0.46. This indicates that the DFT optimized structure is closer to a square pyramid. The barrier for rotation in these five-coordinate species is low, and crystal structure packing features could account for the difference in geometry. The *xyz* coordinates obtained from DFT calculations can be found in the appendix.

Electrochemistry. All electrochemical experiments were performed using a BASi Epsilon potentiostat and an air-tight one compartment electrochemical cell. Either glassy carbon (BASi 1 mm diameter) or p-Si were used as the working electrode, a Pt wire was used as the counter, and an Ag wire separated from the solution by a Vycor tip was used as a pseudo reference (Ferrocene added as an additional reference). All electrochemical experiments were performed in acetonitrile with 0.1 M tetrabutylammonium hexafluorophosphate (TBAH) as the supporting electrolyte except where otherwise noted, and were purged with either argon or CO_2 before CVs were taken. Re concentrations started at 1 mM in all cases and decreased with addition of Brönsted acid. CO_2 experiments were performed at gas saturation (~ 0.28 M).

Note: Some of the material for this chapter comes directly from a manuscript entitled “Kinetic and structural studies, origins of selectivity, and interfacial charge transfer in the artificial photosynthesis of CO” by Jonathan M, Smieja, Eric E. Benson, Bhupendra Kumar, Kyle A. Grice, Candace S. Seu, Alexander J.M. Miller, James M. Mayer, and Clifford P. Kubiak, which has been published in *Proceedings of the National Academy of Sciences*, **2012**, *In Press.*

5.5 References

1. Benson EE, Kubiak CP, Sathrum AJ, & Smieja JM (2009) Electrocatalytic and homogeneous approaches to conversion of CO_2 to liquid fuels. *Chem. Soc. Rev.* 38(1):89-99.

2. Smieja JM & Kubiak CP (2010) Re(bipy-tBu)$(CO)_3$Cl−improved Catalytic Activity for Reduction of Carbon Dioxide: IR-Spectroelectrochemical and Mechanistic Studies. *Inorg. Chem.* 49(20):9283-9289.

3. Hawecker J, Lehn JM, & Ziessel R (1984) Electrocatalytic Reduction of Carbon-Dioxide Mediated by Re(bipy)$(CO)_3$Cl (Bipy=2,2'-Bipyridine). *J. Chem. Soc.-Chem. Commun.* (6):328-330.

4. Hawecker J, Lehn JM, & Ziessel R (1986) Photochemical and Electrochemical Reduction of Carbon-Dioxide to Carbon-Monoxide Mediated by (2,2'-Bipyridine)Tricarbonylchlororhenium(I) and Related Complexes as Homogeneous Catalysts. *Helv. Chim. Acta* 69(8):1990-2012.

5. Kumar B, Smieja JM, & Kubiak CP (2010) Photoreduction of CO_2 on p-type Silicon Using Re(bipy-Bu ')$(CO)_3$Cl: Photovoltages Exceeding 600 mV for the Selective Reduction of CO_2 to CO. *J. Phys. Chem. C* 114(33):14220-14223.

6. Benson EE & Kubiak CP (2012) Structural investigations into the deactivation pathway of the CO_2 reduction electrocatalyst Re(bipy)$(CO)_3$Cl. *Chem. Commun.*:Submitted.

7. McDaniel DH & Brown HC (1958) An Extended Table of Hammett Substitutent Constants Based on the Ionization of Substituted Benzoic Acids. *The Journal of Organic Chemistry* 23(3):420-427.

8. Hammett LP (1937) The Effect of Structure upon the Reactions of Organic Compounds. Benzene Derivatives. *J. Am. Chem. Soc.* 59(1):96-103.

9. Johnson FPA, George MW, Hartl F, & Turner JJ (1996) Electrocatalytic Reduction of CO_2 Using the Complexes [Re(bpy)$(CO)_3$L]n (n = +1, L = $P(OEt)_3$, CH_3CN; n = 0, L = Cl-, Otf-; bpy = 2,2‘-Bipyridine; Otf- = CF_3SO_3) as Catalyst Precursors: Infrared Spectroelectrochemical Investigation. *Organometallics* 15(15):3374-3387.

10. Stor GJ, Hartl F, van Outersterp JWM, & Stufkens DJ (1995) Spectroelectrochemical (IR, UV/Vis) Determination of the Reduction Pathways for a Series of $[Re(CO)_3(.alpha.\text{-diimine})L']^{0/+}$ (L' = Halide, OTf-, THF, MeCN, n-PrCN, PPh_3, $P(OMe)_3$) Complexes. *Organometallics* 14(3):1115-1131.

11. Gore-Randall E, Irwin M, Denning MS, & Goicoechea JM (2009) Synthesis and Characterization of Alkali-Metal Salts of 2,2′- and 2,4′-Bipyridyl Radicals and Dianions. *Inorg. Chem.* 48(17):8304-8316.

12. Addison AW, Rao TN, Reedijk J, van Rijn J, & Verschoor GC (1984) Synthesis, structure, and spectroscopic properties of copper(II) compounds containing nitrogen-sulphur donor ligands; the crystal and molecular structure of aqua[1,7-bis(N-methylbenzimidazol-2'-yl)-2,6-dithiaheptane]copper(II) perchlorate. *J. Chem. Soc. Dalton* (7):1349-1356.

13. Zhu K, Achord PD, Zhang X, Krogh-Jespersen K, & Goldman AS (2004) Highly Effective Pincer-Ligated Iridium Catalysts for Alkane Dehydrogenation. DFT Calculations of Relevant Thermodynamic, Kinetic, and Spectroscopic Properties. *J. Am. Chem. Soc.* 126(40):13044-13053.

14. Göttker-Schnetmann I, White PS, & Brookhart M (2004) Synthesis and Properties of Iridium Bis(phosphinite) Pincer Complexes (p-XPCP)IrH_2, (p-XPCP)Ir(CO), (p-XPCP)Ir(H)(aryl), and {(p-XPCP)Ir}$_2${μ-N_2} and Their Relevance in Alkane Transfer Dehydrogenation. *Organometallics* 23(8):1766-1776.

15. Roy S & Kubiak CP (2010) Tricarbonylrhenium(i) complexes of highly symmetric hexaazatrinaphthylene ligands (HATN): structural, electrochemical and spectroscopic properties. *Dalton T.* 39(45):10937-10943.

16. Smieja JM (2012) Electrocatalytic reduction of carbon dioxide to carbon monoxide by rhenium and manganese polypyridyl catalysts. Ph.D. (University of California San Diego, La Jolla, CA).

17. Schneider J, Jia H, Muckerman JT, & Fujita E (2012) Thermodynamics and kinetics of CO_2, CO, and H^+ binding to the metal centre of CO_2 reduction catalysts. *Chem. Soc. Rev.* 41(6).

18. Bourrez M, Molton F, Chardon-Noblat S, & Deronzier A (2011) [Mn(bipyridyl)$(CO)_3$Br]: An Abundant Metal Carbonyl Complex as Efficient Electrocatalyst for CO_2 Reduction. *Angew. Chem. Int. Edit.* 50(42):9903-9906.

19. Bock H, Lehn J-M, Pauls J, Holl S, & Krenzel V (1999) Sodium Salts of the Bipyridine Dianion: Polymer $[(bpy)_2{-}\{Na^+(dme)\}_2]^{\infty}$, Cluster $[(Na_8O)^{6+}Na{+}_6(bpy)_6^{2-}(tmeda)_6]$, and Monomer $[(bpy)^{2-}\{Na{+}(pmdta)\}_2]$. *Angew. Chem. Int. Edit.* 38(7):952-955.

20. Smieja JM, *et al.* (2012) Kinetic and structural studies, origins of selectivity, and interfacial charge transfer in the artificial photosynthesis of CO. *P. Nat. Acad. Sci. USA*:Accepted.

21. Schwindt MA, Lejon T, & Hegedus LS (1990) Improved synthesis of (aminocarbene)chromium(0) complexes with use of C8K-generated Cr(CO)52-. Multivariant optimization of an organometallic reaction. *Organometallics* 9(10):2814-2819.

22. Sheldrick G (2008) A short history of SHELX. *Acta Crystall. A* 64(1):112-122.

23. te Velde G, *et al.* (2001) Chemistry with ADF. *Journal of Computational Chemistry* 22(9):931-967.

24. Fonseca Guerra C, Snijders JG, te Velde G, & Baerends EJ (1998) Towards an order-N DFT method. *Theoretical Chemistry Accounts: Theory, Computation, and Modeling (Theoretica Chimica Acta)* 99(6):391-403.

25. van Lenthe E, Snijders JG, & Baerends EJ (1996) The zero-order regular approximation for relativistic effects: The effect of spin--orbit coupling in closed shell molecules. *The Journal of Chemical Physics* 105(15):6505-6516.

26. van Lenthe E, Baerends EJ, & Snijders JG (1993) Relativistic regular two-component Hamiltonians. *The Journal of Chemical Physics* 99(6):4597-4610.

27. Vosko SH, Wilk L, & Nusair M (1980) Accurate spin-dependent electron liquid correlation energies for local spin density calculations: a critical analysis. *Canadian Journal of Physics* 58(8):1200-1211.

28. Becke AD (1988) Density-functional exchange-energy approximation with correct asymptotic behavior. *Physical Review A* 38(6):3098-3100.

29. Perdew JP (1986) Erratum: Density-functional approximation for the correlation energy of the inhomogeneous electron gas. *Physical Review B* 34(10):7406-7406.

30. Perdew JP (1986) Density-functional approximation for the correlation energy of the inhomogeneous electron gas. *Physical Review B* 33(12):8822-8824.

5.6 Appendix

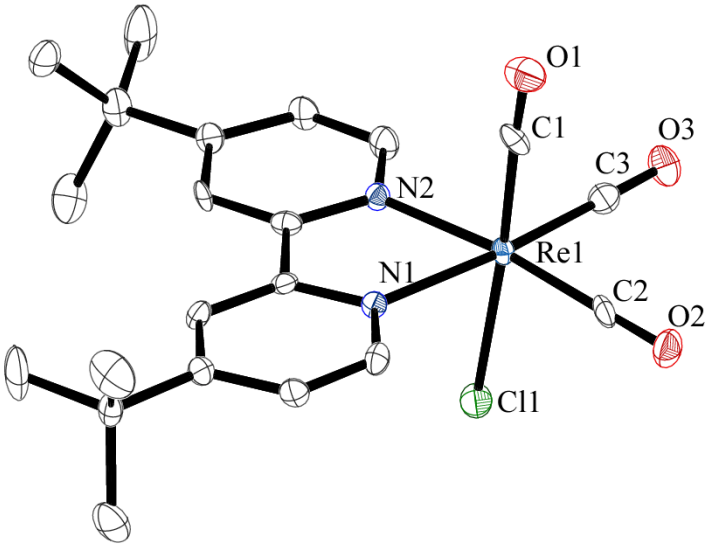

Figure 5.8 Molecular structure of one of the molecules of Re(bipy-tBu)$(CO)_3$Cl in the asymmetric unit, Z' = 2. Hydrogen atoms are omitted for clarity and ellipsoids are shown at 50% probability.

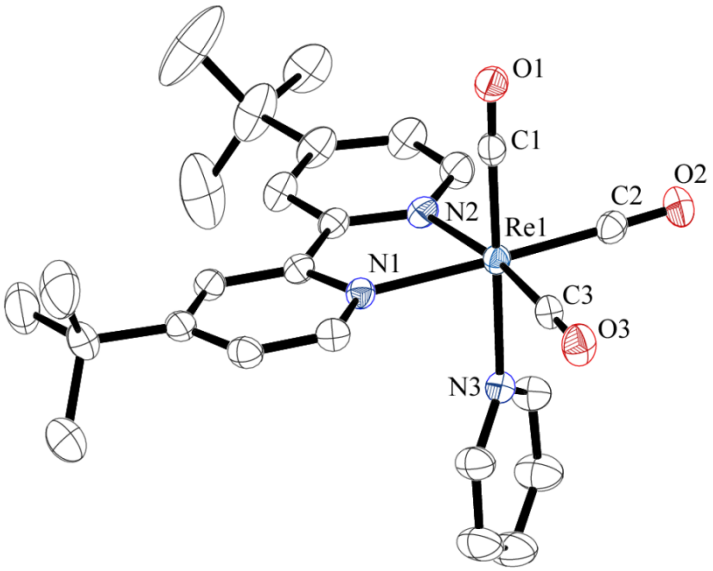

Figure 5.9 Molecular structure of Re(bipy-tBu)$(CO)_3$(py)(CF_3SO_3). Hydrogen atoms and a disordered triflate are omitted for clarity. Ellipsoids are shown at 50% probability.

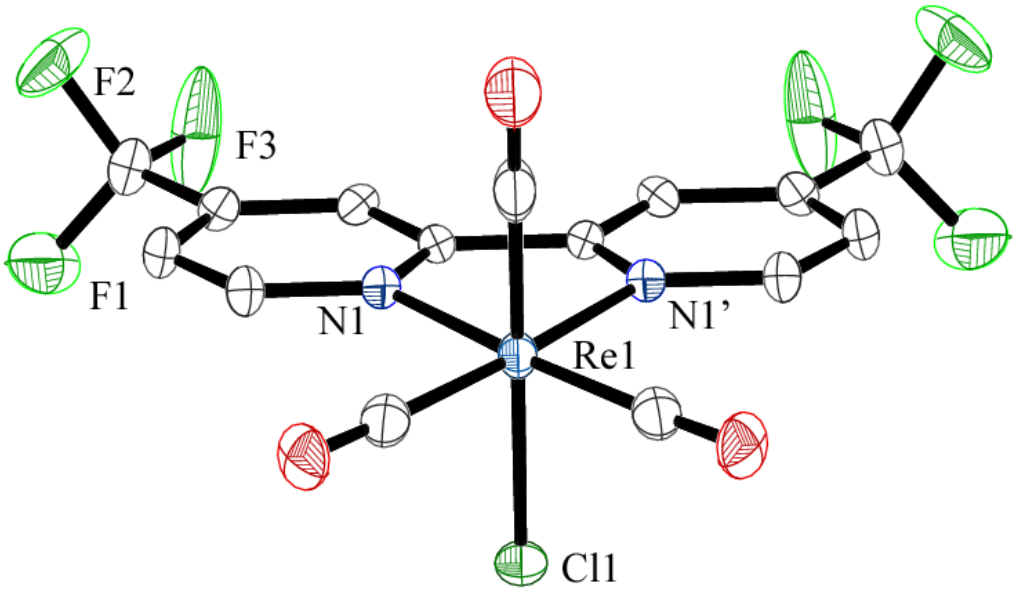

Figure 5.10 Molecular structure of Re(bipy-CF_3)$(CO)_3$Cl (**5**). Hydrogen atoms omitted for clarity and ellipsoids are shown at 50% probability.

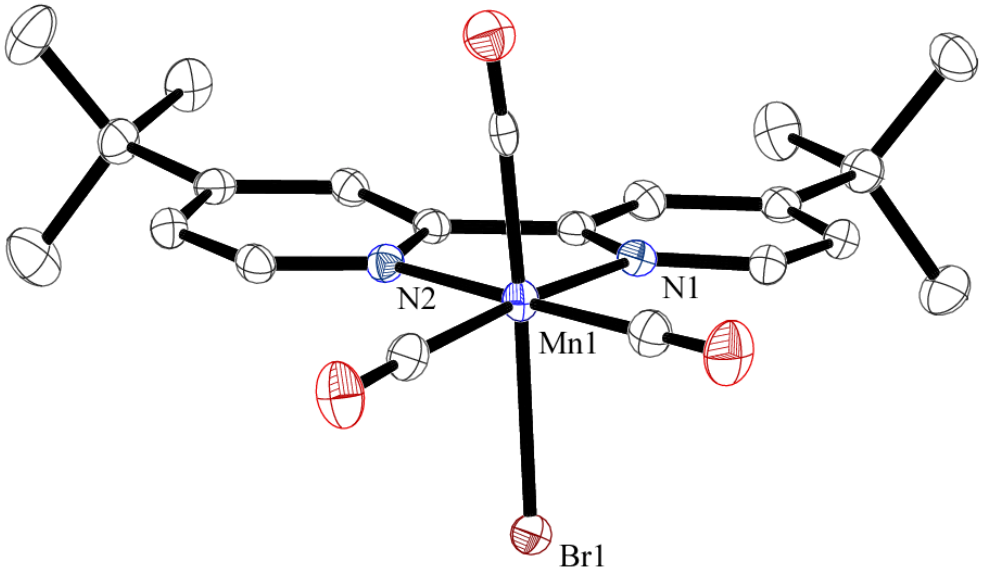

Figure 5.11 Molecular structure of one of the molecules of Mn(bipy-tBu)$(CO)_3$Br in the asymmetric unit, Z' = 2. Hydrogen atoms omitted for clarity and ellipsoids are shown at 50% probability.

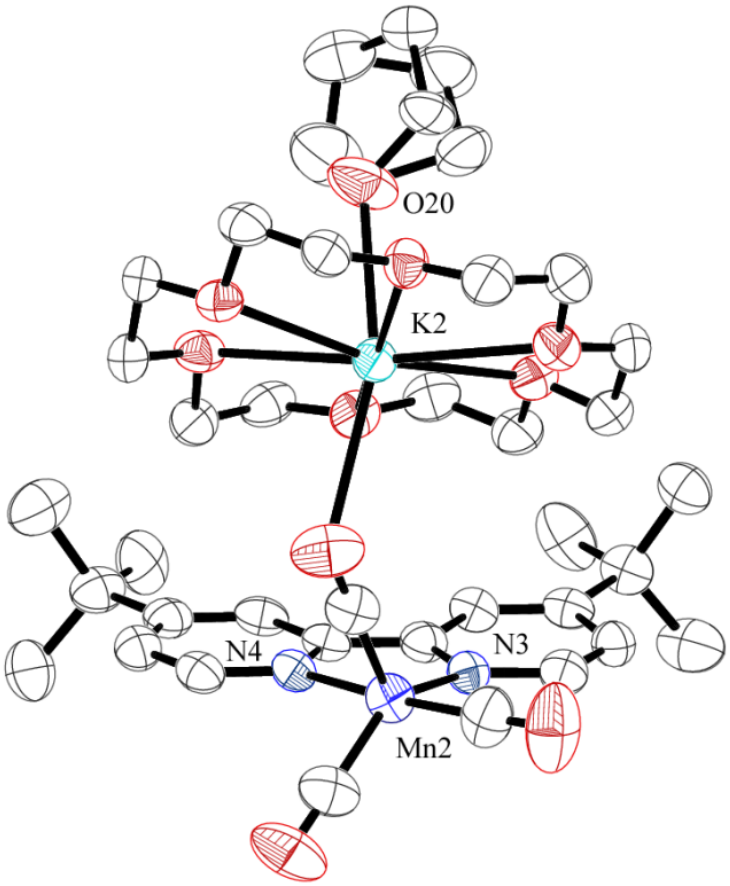

Figure 5.12 Molecular structure of one of the $[Mn(bpy\text{-}tBu)(CO)_3]^{-1}$ anions in the unit cell, Z' = 2. Hydrogen atoms are omitted for clarity and ellipsoids are shown at 50% probability.

Table 5.5 Selected bond lengths and angles for Re(bipy-*t*Bu)$(CO)_3$Cl, [Re(bipy-*t*Bu)$(CO)_3]^{-1}$ and Re(bipy-*t*Bu)$(CO)_3$(py)(OTf).

	Re(bipy-*t*Bu)$(CO)_3$Cl	Re(bipy-*t*Bu)$(CO)_3^-$	Re(bipy-*t*Bu)$(CO)_3$(py)(OTf)
Re - N1	2.174(3)	2.070(7)	2.165(2)
Re - N2	2.178(3)	2.115(7)	2.167(2)
Re - C1	1.909(4)	1.903(11)	1.922(3)
Re - C2	1.909(4)	1.919(8)	1.922(3)
Re - C3	1.914(4)	1.926(11)	1.927(3)
C1 - O1	1.148(5)	1.145(15)	1.153(3)
C2 - O2	1.172(5)	1.144(12)	1.151(3)
C3 - O3	1.161(5)	1.166(13)	1.151(3)
N1 - Re1 - N2	74.36(11)	75.1(3)	74.93(8)
N1 - Re1 - C1	92.73(14)	127.2(5)	94.2(1)
N1 - Re1 - C2	100.45(14)	142.4(3)	171.2(1)
N1 - Re1 - C3	171.97(14)	95.3(4)	97.9(1)
N2 - Re1 - C1	96.05(14)	97.3(4)	95.1(1)
N2 - Re1 - C2	173.67(14)	95.1(3)	96.6(1)
N2 - Re1 - C3	97.72(14)	170.0(4)	172.2(1)
N1 - C4	1.337(5)	1.372(14)	1.349(3)
C4 - C5	1.379(5)	1.324(15)	1.373(4)
C5 - C6	1.396(5)	1.442(13)	1.397(4)
C6 - C7	1.393(5)	1.364(14)	1.389(4)
C7 - C8	1.385(5)	1.439(14)	1.390(4)
C8 - N1	1.360(5)	1.422(12)	1.355(4)
C8 - C9	1.487(5)	1.373(15)	1.476(3)
C9 - N2	1.361(5)	1.402(12)	1.360(3)
C9 - C10	1.386(5)	1.424(13)	1.387(4)
C10 - C11	1.404(5)	1.370(16)	1.401(3)
C11 - C12	1.385(5)	1.407(16)	1.380(4)
C12 - C13	1.378(5)	1.375(14)	1.379(4)
C13 - N2	1.345(5)	1.346(13)	1.343(3)
Re1 - N3	N/A	N/A	2.209(2)
N2 - Re1 - N3	N/A	N/A	85.23(8)
N3 - Re1 - C1	N/A	N/A	179.0(1)
N3 - Re1 - C2	N/A	N/A	91.9(1)
N3 - Re1 - C3	N/A	N/A	91.2(1)

Table 5.6 Crystal data and structure refinement for Re(tBu-bipy)$(CO)_3$Cl

Identification code	eb_111110mo_0m	
Empirical formula	C21 H24 Cl N2 O3 Re	
Formula weight	574.07	
Temperature	100(2) K	
Wavelength	0.71073 Å	
Crystal system	Monoclinic	
Space group	P2(1)/n	
Unit cell dimensions	a = 15.9538(6) Å	α= 90°.
	b = 12.8056(5) Å	β= 104.2910(10)°.
	c = 22.6304(10) Å	γ = 90°.
Volume	4480.3(3) $Å^3$	
Z	8	
Density (calculated)	1.702 Mg/m^3	
Absorption coefficient	5.566 mm^{-1}	
F(000)	2240	
Crystal size	0.10 x 0.07 x 0.04 mm^3	
Theta range for data collection	1.79 to 25.44°.	
Index ranges	-19<=h<=17, -13<=k<=15, -27<=l<=27	
Reflections collected	28704	
Independent reflections	8253 [R(int) = 0.0415]	
Completeness to theta = 25.00°	100.0 %	
Absorption correction	Semi-empirical from equivalents	
Max. and min. transmission	0.8080 and 0.6060	
Refinement method	Full-matrix least-squares on F^2	
Data / restraints / parameters	8253 / 0 / 527	
Goodness-of-fit on F^2	1.144	
Final R indices [I>2sigma(I)]	R1 = 0.0239, wR2 = 0.0551	
R indices (all data)	R1 = 0.0283, wR2 = 0.0564	
Largest diff. peak and hole	0.957 and -1.105 $e.Å^{-3}$	

Table 5.7 Bond lengths [Å] and angles [°] for Re(tBu-bipy)$(CO)_3$Cl.

Re(1)-C(1)	1.909(4)	C(6)-C(7)	1.393(5)
Re(1)-C(2)	1.909(4)	C(6)-C(14)	1.521(5)
Re(1)-C(3)	1.914(4)	C(7)-C(8)	1.385(5)
Re(1)-N(1)	2.174(3)	C(7)-H(7)	0.9500
Re(1)-N(2)	2.178(3)	C(8)-C(9)	1.487(5)
Re(1)-Cl(1)	2.4626(10)	C(9)-C(10)	1.386(5)
Re(2)-C(22B)	1.82(4)	C(10)-C(11)	1.404(5)
Re(2)-C(22A)	1.892(6)	C(10)-H(10)	0.9500
Re(2)-C(24)	1.925(4)	C(11)-C(12)	1.385(5)
Re(2)-C(23)	1.938(4)	C(11)-C(18)	1.535(5)
Re(2)-N(4)	2.164(3)	C(12)-C(13)	1.378(5)
Re(2)-N(3)	2.175(3)	C(12)-H(12)	0.9500
Re(2)-Cl(2B)	2.453(11)	C(13)-H(13)	0.9500
Re(2)-Cl(2A)	2.4749(14)	C(14)-C(17)	1.532(6)
O(1)-C(1)	1.148(5)	C(14)-C(16)	1.533(6)
O(2)-C(2)	1.172(5)	C(14)-C(15)	1.536(6)
O(3)-C(3)	1.161(5)	C(15)-H(15A)	0.9800
O(4A)-C(22A)	1.174(8)	C(15)-H(15B)	0.9800
O(4B)-C(22B)	1.14(5)	C(15)-H(15C)	0.9800
O(5)-C(23)	1.145(4)	C(16)-H(16A)	0.9800
O(6)-C(24)	1.157(4)	C(16)-H(16B)	0.9800
N(1)-C(4)	1.337(5)	C(16)-H(16C)	0.9800
N(1)-C(8)	1.360(5)	C(17)-H(17A)	0.9800
N(2)-C(13)	1.345(5)	C(17)-H(17B)	0.9800
N(2)-C(9)	1.361(5)	C(17)-H(17C)	0.9800
N(3)-C(25)	1.343(5)	C(18)-C(21)	1.531(6)
N(3)-C(29)	1.360(5)	C(18)-C(19)	1.531(6)
N(4)-C(34)	1.340(5)	C(18)-C(20)	1.539(6)
N(4)-C(30)	1.361(5)	C(19)-H(19A)	0.9800
C(4)-C(5)	1.379(5)	C(19)-H(19B)	0.9800
C(4)-H(4)	0.9500	C(19)-H(19C)	0.9800
C(5)-C(6)	1.396(5)	C(20)-H(20A)	0.9800
C(5)-H(5)	0.9500	C(20)-H(20B)	0.9800

Table 5.7 Cont.

C(20)-H(20C)	0.9800	C(38)-H(38C)	0.9800
C(21)-H(21A)	0.9800	C(39)-C(41)	1.529(5)
C(21)-H(21B)	0.9800	C(39)-C(40)	1.532(6)
C(21)-H(21C)	0.9800	C(39)-C(42)	1.535(5)
C(25)-C(26)	1.381(5)	C(40)-H(40A)	0.9800
C(25)-H(25)	0.9500	C(40)-H(40B)	0.9800
C(26)-C(27)	1.388(5)	C(40)-H(40C)	0.9800
C(26)-H(26)	0.9500	C(41)-H(41A)	0.9800
C(27)-C(28)	1.404(5)	C(41)-H(41B)	0.9800
C(27)-C(35)	1.515(5)	C(41)-H(41C)	0.9800
C(28)-C(29)	1.396(5)	C(42)-H(42A)	0.9800
C(28)-H(28)	0.9500	C(42)-H(42B)	0.9800
C(29)-C(30)	1.475(5)	C(42)-H(42C)	0.9800
C(30)-C(31)	1.388(5)		
C(31)-C(32)	1.404(5)	C(1)-Re(1)-C(2)	87.74(17)
C(31)-H(31)	0.9500	C(1)-Re(1)-C(3)	89.37(17)
C(32)-C(33)	1.388(5)	C(2)-Re(1)-C(3)	87.37(17)
C(32)-C(39)	1.528(5)	C(1)-Re(1)-N(1)	92.73(14)
C(33)-C(34)	1.377(5)	C(2)-Re(1)-N(1)	100.45(14)
C(33)-H(33)	0.9500	C(3)-Re(1)-N(1)	171.97(14)
C(34)-H(34)	0.9500	C(1)-Re(1)-N(2)	96.05(15)
C(35)-C(36)	1.532(5)	C(2)-Re(1)-N(2)	173.67(14)
C(35)-C(37)	1.536(6)	C(3)-Re(1)-N(2)	97.72(14)
C(35)-C(38)	1.547(6)	N(1)-Re(1)-N(2)	74.36(11)
C(36)-H(36A)	0.9800	C(1)-Re(1)-Cl(1)	174.82(12)
C(36)-H(36B)	0.9800	C(2)-Re(1)-Cl(1)	92.40(12)
C(36)-H(36C)	0.9800	C(3)-Re(1)-Cl(1)	95.80(13)
C(37)-H(37A)	0.9800	N(1)-Re(1)-Cl(1)	82.15(9)
C(37)-H(37B)	0.9800	N(2)-Re(1)-Cl(1)	83.36(9)
C(37)-H(37C)	0.9800	C(22B)-Re(2)-C(22A)	173.3(11)
C(38)-H(38A)	0.9800	C(22B)-Re(2)-C(24)	87.0(11)
C(38)-H(38B)	0.9800	C(22A)-Re(2)-C(24)	88.0(2)

Table 5.7 Cont.

C(22B)-Re(2)-C(23)	86.6(11)	C(25)-N(3)-Re(2)	125.1(3)
C(22A)-Re(2)-C(23)	88.9(2)	C(29)-N(3)-Re(2)	116.5(3)
C(24)-Re(2)-C(23)	91.33(16)	C(34)-N(4)-C(30)	117.6(3)
C(22B)-Re(2)-N(4)	90.8(11)	C(34)-N(4)-Re(2)	124.7(3)
C(22A)-Re(2)-N(4)	94.3(2)	C(30)-N(4)-Re(2)	117.6(2)
C(24)-Re(2)-N(4)	96.52(14)	O(1)-C(1)-Re(1)	177.0(4)
C(23)-Re(2)-N(4)	171.62(14)	O(2)-C(2)-Re(1)	179.2(4)
C(22B)-Re(2)-N(3)	87.5(11)	O(3)-C(3)-Re(1)	179.3(4)
C(22A)-Re(2)-N(3)	98.1(2)	N(1)-C(4)-C(5)	123.2(4)
C(24)-Re(2)-N(3)	169.30(14)	N(1)-C(4)-H(4)	118.4
C(23)-Re(2)-N(3)	97.52(14)	C(5)-C(4)-H(4)	118.4
N(4)-Re(2)-N(3)	74.37(12)	C(4)-C(5)-C(6)	120.5(4)
C(22B)-Re(2)-Cl(2B)	171.5(11)	C(4)-C(5)-H(5)	119.7
C(22A)-Re(2)-Cl(2B)	13.0(3)	C(6)-C(5)-H(5)	119.7
C(24)-Re(2)-Cl(2B)	100.9(3)	C(7)-C(6)-C(5)	116.0(4)
C(23)-Re(2)-Cl(2B)	90.2(2)	C(7)-C(6)-C(14)	124.2(3)
N(4)-Re(2)-Cl(2B)	91.2(2)	C(5)-C(6)-C(14)	119.8(3)
N(3)-Re(2)-Cl(2B)	85.1(3)	C(8)-C(7)-C(6)	121.0(3)
C(22B)-Re(2)-Cl(2A)	9.2(11)	C(8)-C(7)-H(7)	119.5
C(22A)-Re(2)-Cl(2A)	176.42(18)	C(6)-C(7)-H(7)	119.5
C(24)-Re(2)-Cl(2A)	91.43(12)	N(1)-C(8)-C(7)	121.8(3)
C(23)-Re(2)-Cl(2A)	94.62(12)	N(1)-C(8)-C(9)	114.5(3)
N(4)-Re(2)-Cl(2A)	82.29(9)	C(7)-C(8)-C(9)	123.6(3)
N(3)-Re(2)-Cl(2A)	81.91(9)	N(2)-C(9)-C(10)	121.1(3)
Cl(2B)-Re(2)-Cl(2A)	166.7(3)	N(2)-C(9)-C(8)	115.1(3)
C(4)-N(1)-C(8)	117.4(3)	C(10)-C(9)-C(8)	123.8(4)
C(4)-N(1)-Re(1)	124.3(3)	C(9)-C(10)-C(11)	121.2(4)
C(8)-N(1)-Re(1)	118.2(2)	C(9)-C(10)-H(10)	119.4
C(13)-N(2)-C(9)	117.8(3)	C(11)-C(10)-H(10)	119.4
C(13)-N(2)-Re(1)	124.4(3)	C(12)-C(11)-C(10)	116.4(3)
C(9)-N(2)-Re(1)	117.7(2)	C(12)-C(11)-C(18)	123.1(4)
C(25)-N(3)-C(29)	117.7(3)	C(10)-C(11)-C(18)	120.5(3)

Table 5.7 Cont.

C(13)-C(12)-C(11)	120.2(4)	C(19)-C(18)-C(11)	108.9(3)
C(13)-C(12)-H(12)	119.9	C(21)-C(18)-C(20)	107.9(4)
C(11)-C(12)-H(12)	119.9	C(19)-C(18)-C(20)	109.4(3)
N(2)-C(13)-C(12)	123.3(4)	C(11)-C(18)-C(20)	109.6(3)
N(2)-C(13)-H(13)	118.3	C(18)-C(19)-H(19A)	109.5
C(12)-C(13)-H(13)	118.3	C(18)-C(19)-H(19B)	109.5
C(6)-C(14)-C(17)	111.1(3)	H(19A)-C(19)-H(19B)	109.5
C(6)-C(14)-C(16)	108.9(3)	C(18)-C(19)-H(19C)	109.5
C(17)-C(14)-C(16)	109.4(4)	H(19A)-C(19)-H(19C)	109.5
C(6)-C(14)-C(15)	109.2(3)	H(19B)-C(19)-H(19C)	109.5
C(17)-C(14)-C(15)	108.6(4)	C(18)-C(20)-H(20A)	109.5
C(16)-C(14)-C(15)	109.6(4)	C(18)-C(20)-H(20B)	109.5
C(14)-C(15)-H(15A)	109.5	H(20A)-C(20)-H(20B)	109.5
C(14)-C(15)-H(15B)	109.5	C(18)-C(20)-H(20C)	109.5
H(15A)-C(15)-H(15B)	109.5	H(20A)-C(20)-H(20C)	109.5
C(14)-C(15)-H(15C)	109.5	H(20B)-C(20)-H(20C)	109.5
H(15A)-C(15)-H(15C)	109.5	C(18)-C(21)-H(21A)	109.5
H(15B)-C(15)-H(15C)	109.5	C(18)-C(21)-H(21B)	109.5
C(14)-C(16)-H(16A)	109.5	H(21A)-C(21)-H(21B)	109.5
C(14)-C(16)-H(16B)	109.5	C(18)-C(21)-H(21C)	109.5
H(16A)-C(16)-H(16B)	109.5	H(21A)-C(21)-H(21C)	109.5
C(14)-C(16)-H(16C)	109.5	H(21B)-C(21)-H(21C)	109.5
H(16A)-C(16)-H(16C)	109.5	O(4A)-C(22A)-Re(2)	177.9(6)
H(16B)-C(16)-H(16C)	109.5	O(4B)-C(22B)-Re(2)	174(3)
C(14)-C(17)-H(17A)	109.5	O(5)-C(23)-Re(2)	178.2(3)
C(14)-C(17)-H(17B)	109.5	O(6)-C(24)-Re(2)	175.7(3)
H(17A)-C(17)-H(17B)	109.5	N(3)-C(25)-C(26)	123.9(4)
C(14)-C(17)-H(17C)	109.5	N(3)-C(25)-H(25)	118.1
H(17A)-C(17)-H(17C)	109.5	C(26)-C(25)-H(25)	118.1
H(17B)-C(17)-H(17C)	109.5	C(25)-C(26)-C(27)	120.1(4)
C(21)-C(18)-C(19)	109.6(4)	C(25)-C(26)-H(26)	119.9
C(21)-C(18)-C(11)	111.4(4)	C(27)-C(26)-H(26)	119.9

Table 5.7 Cont.

C(26)-C(27)-C(28)	115.9(4)	H(36A)-C(36)-H(36B)	109.5
C(26)-C(27)-C(35)	123.3(4)	C(35)-C(36)-H(36C)	109.5
C(28)-C(27)-C(35)	120.8(4)	H(36A)-C(36)-H(36C)	109.5
C(29)-C(28)-C(27)	121.7(4)	H(36B)-C(36)-H(36C)	109.5
C(29)-C(28)-H(28)	119.1	C(35)-C(37)-H(37A)	109.5
C(27)-C(28)-H(28)	119.1	C(35)-C(37)-H(37B)	109.5
N(3)-C(29)-C(28)	120.7(4)	H(37A)-C(37)-H(37B)	109.5
N(3)-C(29)-C(30)	115.3(3)	C(35)-C(37)-H(37C)	109.5
C(28)-C(29)-C(30)	124.0(3)	H(37A)-C(37)-H(37C)	109.5
N(4)-C(30)-C(31)	121.5(3)	H(37B)-C(37)-H(37C)	109.5
N(4)-C(30)-C(29)	114.5(3)	C(35)-C(38)-H(38A)	109.5
C(31)-C(30)-C(29)	124.0(3)	C(35)-C(38)-H(38B)	109.5
C(30)-C(31)-C(32)	121.0(4)	H(38A)-C(38)-H(38B)	109.5
C(30)-C(31)-H(31)	119.5	C(35)-C(38)-H(38C)	109.5
C(32)-C(31)-H(31)	119.5	H(38A)-C(38)-H(38C)	109.5
C(33)-C(32)-C(31)	115.9(4)	H(38B)-C(38)-H(38C)	109.5
C(33)-C(32)-C(39)	123.1(3)	C(32)-C(39)-C(41)	108.4(3)
C(31)-C(32)-C(39)	121.0(3)	C(32)-C(39)-C(40)	109.4(3)
C(34)-C(33)-C(32)	120.8(4)	C(41)-C(39)-C(40)	109.9(3)
C(34)-C(33)-H(33)	119.6	C(32)-C(39)-C(42)	111.3(3)
C(32)-C(33)-H(33)	119.6	C(41)-C(39)-C(42)	109.5(3)
N(4)-C(34)-C(33)	123.2(4)	C(40)-C(39)-C(42)	108.3(3)
N(4)-C(34)-H(34)	118.4	C(39)-C(40)-H(40A)	109.5
C(33)-C(34)-H(34)	118.4	C(39)-C(40)-H(40B)	109.5
C(27)-C(35)-C(36)	111.8(3)	H(40A)-C(40)-H(40B)	109.5
C(27)-C(35)-C(37)	108.9(3)	C(39)-C(40)-H(40C)	109.5
C(36)-C(35)-C(37)	108.9(4)	H(40A)-C(40)-H(40C)	109.5
C(27)-C(35)-C(38)	110.0(3)	H(40B)-C(40)-H(40C)	109.5
C(36)-C(35)-C(38)	107.4(3)	C(39)-C(41)-H(41A)	109.5
C(37)-C(35)-C(38)	109.8(4)	C(39)-C(41)-H(41B)	109.5
C(35)-C(36)-H(36A)	109.5	H(41A)-C(41)-H(41B)	109.5
C(35)-C(36)-H(36B)	109.5	C(39)-C(41)-H(41C)	109.5

Table 5.7 Cont.

H(41A)-C(41)-H(41C)	109.5	H(42A)-C(42)-H(42B)	109.5
H(41B)-C(41)-H(41C)	109.5	C(39)-C(42)-H(42C)	109.5
C(39)-C(42)-H(42A)	109.5	H(42A)-C(42)-H(42C)	109.5
C(39)-C(42)-H(42B)	109.5	H(42B)-C(42)-H(42C)	109.

Table 5.8 Crystal data and structure refinement for Re(tBu-bipy)$(CO)_3$(py)(CF_3SO_3).

Identification code	eb_110615b_0m	
Empirical formula	C27 H29 F3 N3 O6 Re S	
Formula weight	766.79	
Temperature	100(2) K	
Wavelength	0.71073 Å	
Crystal system	Monoclinic	
Space group	P2(1)/n	
Unit cell dimensions	a = 12.1032(4) Å	α= 90°.
	b = 10.2197(4) Å	β= 96.5900(10)°.
	c = 25.5513(9) Å	γ = 90°.
Volume	3139.6(2) $Å^3$	
Z	4	
Density (calculated)	1.622 Mg/m^3	
Absorption coefficient	3.997 mm^{-1}	
F(000)	1512	
Crystal size	0.20 x 0.10 x 0.05 mm^3	
Theta range for data collection	1.60 to 25.35°.	
Index ranges	-14<=h<=14, -12<=k<=12, -30<=l<=30	
Reflections collected	50114	
Independent reflections	5757 [R(int) = 0.0316]	
Completeness to theta = 25.00°	100.0 %	
Absorption correction	Semi-empirical from equivalents	
Max. and min. transmission	0.8252 and 0.5020	
Refinement method	Full-matrix least-squares on F^2	
Data / restraints / parameters	5757 / 0 / 304	
Goodness-of-fit on F^2	1.069	
Final R indices [I>2sigma(I)]	R1 = 0.0191, wR2 = 0.0453	
R indices (all data)	R1 = 0.0202, wR2 = 0.0459	
Largest diff. peak and hole	0.777 and -0.424 e.$Å^{-3}$	

Table 5.9 Bond lengths [Å] and angles [°] for Re(tBu-bipy)$(CO)_3$(py)(CF_3SO_3).

Re(1)-C(1)	1.922(3)	C(14)-C(15)	1.532(4)
Re(1)-C(2)	1.923(3)	C(14)-C(17)	1.549(5)
Re(1)-C(3)	1.927(3)	C(15)-H(15A)	0.9800
Re(1)-N(1)	2.164(2)	C(15)-H(15B)	0.9800
Re(1)-N(2)	2.167(2)	C(15)-H(15C)	0.9800
Re(1)-N(3)	2.209(2)	C(16)-H(16A)	0.9800
O(1)-C(1)	1.153(3)	C(16)-H(16B)	0.9800
O(2)-C(2)	1.150(3)	C(16)-H(16C)	0.9800
O(3)-C(3)	1.151(3)	C(17)-H(17A)	0.9800
N(1)-C(4)	1.349(3)	C(17)-H(17B)	0.9800
N(1)-C(8)	1.355(3)	C(17)-H(17C)	0.9800
N(2)-C(13)	1.343(3)	C(18)-C(19)	1.524(5)
N(2)-C(9)	1.360(3)	C(18)-C(20)	1.528(5)
N(3)-C(22)	1.340(4)	C(18)-C(21)	1.548(6)
N(3)-C(26)	1.348(3)	C(19)-H(19A)	0.9800
C(4)-C(5)	1.374(4)	C(19)-H(19B)	0.9800
C(4)-H(4)	0.9500	C(19)-H(19C)	0.9800
C(5)-C(6)	1.397(4)	C(20)-H(20A)	0.9800
C(5)-H(5)	0.9500	C(20)-H(20B)	0.9800
C(6)-C(7)	1.389(4)	C(20)-H(20C)	0.9800
C(6)-C(14)	1.527(4)	C(21)-H(21A)	0.9800
C(7)-C(8)	1.389(4)	C(21)-H(21B)	0.9800
C(7)-H(7)	0.9500	C(21)-H(21C)	0.9800
C(8)-C(9)	1.477(4)	C(22)-C(23)	1.376(4)
C(9)-C(10)	1.387(4)	C(22)-H(22)	0.9500
C(10)-C(11)	1.401(4)	C(23)-C(24)	1.377(4)
C(10)-H(10)	0.9500	C(23)-H(23)	0.9500
C(11)-C(12)	1.380(4)	C(24)-C(25)	1.368(5)
C(11)-C(18)	1.537(4)	C(24)-H(24)	0.9500
C(12)-C(13)	1.379(4)	C(25)-C(26)	1.371(4)
C(12)-H(12)	0.9500	C(25)-H(25)	0.9500
C(13)-H(13)	0.9500	C(26)-H(26)	0.9500
C(14)-C(16)	1.508(5)		

Table 5.9 Cont.

C(1)-Re(1)-C(2)	89.04(11)	C(6)-C(5)-H(5)	119.9
C(1)-Re(1)-C(3)	88.34(11)	C(7)-C(6)-C(5)	116.9(2)
C(2)-Re(1)-C(3)	90.42(11)	C(7)-C(6)-C(14)	122.7(3)
C(1)-Re(1)-N(1)	94.25(9)	C(5)-C(6)-C(14)	120.3(3)
C(2)-Re(1)-N(1)	171.16(9)	C(8)-C(7)-C(6)	120.5(3)
C(3)-Re(1)-N(1)	97.87(10)	C(8)-C(7)-H(7)	119.7
C(1)-Re(1)-N(2)	95.10(9)	C(6)-C(7)-H(7)	119.7
C(2)-Re(1)-N(2)	96.61(10)	N(1)-C(8)-C(7)	121.6(2)
C(3)-Re(1)-N(2)	172.21(10)	N(1)-C(8)-C(9)	115.3(2)
N(1)-Re(1)-N(2)	74.94(8)	C(7)-C(8)-C(9)	123.0(2)
C(1)-Re(1)-N(3)	179.00(9)	N(2)-C(9)-C(10)	121.3(2)
C(2)-Re(1)-N(3)	91.85(10)	N(2)-C(9)-C(8)	115.2(2)
C(3)-Re(1)-N(3)	91.21(10)	C(10)-C(9)-C(8)	123.5(2)
N(1)-Re(1)-N(3)	84.93(8)	C(9)-C(10)-C(11)	121.2(3)
N(2)-Re(1)-N(3)	85.24(8)	C(9)-C(10)-H(10)	119.4
C(4)-N(1)-C(8)	118.0(2)	C(11)-C(10)-H(10)	119.4
C(4)-N(1)-Re(1)	124.59(18)	C(12)-C(11)-C(10)	116.3(3)
C(8)-N(1)-Re(1)	117.35(17)	C(12)-C(11)-C(18)	124.1(3)
C(13)-N(2)-C(9)	117.4(2)	C(10)-C(11)-C(18)	119.7(3)
C(13)-N(2)-Re(1)	125.42(19)	C(13)-C(12)-C(11)	120.3(3)
C(9)-N(2)-Re(1)	117.15(17)	C(13)-C(12)-H(12)	119.8
C(22)-N(3)-C(26)	116.8(2)	C(11)-C(12)-H(12)	119.8
C(22)-N(3)-Re(1)	121.52(18)	N(2)-C(13)-C(12)	123.5(3)
C(26)-N(3)-Re(1)	121.65(18)	N(2)-C(13)-H(13)	118.2
O(1)-C(1)-Re(1)	177.6(2)	C(12)-C(13)-H(13)	118.2
O(2)-C(2)-Re(1)	177.0(2)	C(16)-C(14)-C(6)	108.5(3)
O(3)-C(3)-Re(1)	178.5(2)	C(16)-C(14)-C(15)	111.2(3)
N(1)-C(4)-C(5)	122.7(3)	C(6)-C(14)-C(15)	109.3(3)
N(1)-C(4)-H(4)	118.7	C(16)-C(14)-C(17)	107.9(3)
C(5)-C(4)-H(4)	118.7	C(6)-C(14)-C(17)	112.2(3)
C(4)-C(5)-C(6)	120.2(3)	C(15)-C(14)-C(17)	107.7(3)
C(4)-C(5)-H(5)	119.9	C(14)-C(15)-H(15A)	109.5

Table 5.9 Cont.

C(14)-C(15)-H(15B)	109.5	H(19B)-C(19)-H(19C)	109.5
H(15A)-C(15)-H(15B)	109.5	C(18)-C(20)-H(20A)	109.5
C(14)-C(15)-H(15C)	109.5	C(18)-C(20)-H(20B)	109.5
H(15A)-C(15)-H(15C)	109.5	H(20A)-C(20)-H(20B)	109.5
H(15B)-C(15)-H(15C)	109.5	C(18)-C(20)-H(20C)	109.5
C(14)-C(16)-H(16A)	109.5	H(20A)-C(20)-H(20C)	109.5
C(14)-C(16)-H(16B)	109.5	H(20B)-C(20)-H(20C)	109.5
H(16A)-C(16)-H(16B)	109.5	C(18)-C(21)-H(21A)	109.5
C(14)-C(16)-H(16C)	109.5	C(18)-C(21)-H(21B)	109.5
H(16A)-C(16)-H(16C)	109.5	H(21A)-C(21)-H(21B)	109.5
H(16B)-C(16)-H(16C)	109.5	C(18)-C(21)-H(21C)	109.5
C(14)-C(17)-H(17A)	109.5	H(21A)-C(21)-H(21C)	109.5
C(14)-C(17)-H(17B)	109.5	H(21B)-C(21)-H(21C)	109.5
H(17A)-C(17)-H(17B)	109.5	N(3)-C(22)-C(23)	123.3(3)
C(14)-C(17)-H(17C)	109.5	N(3)-C(22)-H(22)	118.3
H(17A)-C(17)-H(17C)	109.5	C(23)-C(22)-H(22)	118.3
H(17B)-C(17)-H(17C)	109.5	C(22)-C(23)-C(24)	118.9(3)
C(19)-C(18)-C(20)	110.1(3)	C(22)-C(23)-H(23)	120.6
C(19)-C(18)-C(11)	108.3(3)	C(24)-C(23)-H(23)	120.6
C(20)-C(18)-C(11)	111.4(3)	C(25)-C(24)-C(23)	118.6(3)
C(19)-C(18)-C(21)	109.5(4)	C(25)-C(24)-H(24)	120.7
C(20)-C(18)-C(21)	109.0(3)	C(23)-C(24)-H(24)	120.7
C(11)-C(18)-C(21)	108.5(3)	C(24)-C(25)-C(26)	119.6(3)
C(18)-C(19)-H(19A)	109.5	C(24)-C(25)-H(25)	120.2
C(18)-C(19)-H(19B)	109.5	C(26)-C(25)-H(25)	120.2
H(19A)-C(19)-H(19B)	109.5	N(3)-C(26)-C(25)	122.9(3)
C(18)-C(19)-H(19C)	109.5	N(3)-C(26)-H(26)	118.6
H(19A)-C(19)-H(19C)	109.5	C(25)-C(26)-H(26)	118.6

Table 5.10 Crystal data and structure refinement for[Re(dmb)$(CO)_3$] [K(18-crown-6)]

Identification code	eb_111109_0m	
Empirical formula	C27 H36 K N2 O9 Re	
Formula weight	757.88	
Temperature	100(2) K	
Wavelength	0.71073 Å	
Crystal system	Monoclinic	
Space group	P2(1)/n	
Unit cell dimensions	a = 9.5487(6) Å	α= 90°.
	b = 21.2714(13) Å	β= 100.452(2)°.
	c = 15.0618(10) Å	γ = 90°.
Volume	3008.5(3) $Å^3$	
Z	4	
Density (calculated)	1.673 Mg/m^3	
Absorption coefficient	4.230 mm^{-1}	
F(000)	1512	
Crystal size	0.10 x 0.10 x 0.05 mm^3	
Theta range for data collection	1.68 to 25.38°.	
Index ranges	-11<=h<=11, -25<=k<=24, -18<=l<=18	
Reflections collected	29026	
Independent reflections	5525 [R(int) = 0.0312]	
Completeness to theta = 25.00°	100.0 %	
Absorption correction	Semi-empirical from equivalents	
Max. and min. transmission	0.8163 and 0.6771	
Refinement method	Full-matrix least-squares on F^2	
Data / restraints / parameters	5525 / 0 / 363	
Goodness-of-fit on F^2	1.045	
Final R indices [I>2sigma(I)]	R1 = 0.0146, wR2 = 0.0341	
R indices (all data)	R1 = 0.0170, wR2 = 0.0352	
Largest diff. peak and hole	0.536 and -0.528 $e.Å^{-3}$	

Table 5.11 Bond lengths [Å] and angles [°] for [Re(dmb)$(CO)_3$][K(18-crown-6)]

Re(1)-C(1)	1.880(2)	C(8)-C(7)	1.424(3)
Re(1)-C(3)	1.907(2)	O(1)-C(1)	1.170(2)
Re(1)-C(2)	1.907(2)	O(1)-K(1)#2	2.7504(16)
Re(1)-N(2)	2.0899(17)	C(13)-C(12)	1.347(3)
Re(1)-N(1)	2.0979(17)	C(13)-H(13)	0.9500
K(1)-O(3)	2.7342(16)	C(12)-C(11)	1.432(3)
K(1)-O(1)#1	2.7504(16)	C(12)-H(12)	0.9500
K(1)-O(9)	2.7514(14)	C(11)-C(10)	1.358(3)
K(1)-O(6)	2.7650(14)	C(11)-C(15)	1.505(3)
K(1)-O(8)	2.7992(14)	C(15)-H(15A)	0.9800
K(1)-O(4)	2.8215(14)	C(15)-H(15B)	0.9800
K(1)-O(5)	2.8306(15)	C(15)-H(15C)	0.9800
K(1)-O(7)	2.8659(14)	C(10)-C(9)	1.436(3)
K(1)-C(1)#1	3.463(2)	C(10)-H(10)	0.9500
N(2)-C(13)	1.386(3)	C(4)-C(5)	1.353(3)
N(2)-C(9)	1.397(3)	C(4)-H(4)	0.9500
N(1)-C(4)	1.378(3)	C(5)-C(6)	1.433(3)
N(1)-C(8)	1.408(2)	C(5)-H(5)	0.9500
O(3)-C(3)	1.174(3)	C(6)-C(7)	1.358(3)
O(9)-C(26)	1.426(2)	C(6)-C(14)	1.506(3)
O(9)-C(25)	1.428(2)	C(14)-H(14A)	0.9800
O(4)-C(27)	1.423(2)	C(14)-H(14B)	0.9800
O(4)-C(16)	1.428(2)	C(14)-H(14C)	0.9800
O(5)-C(18)	1.421(3)	C(7)-H(7)	0.9500
O(5)-C(17)	1.430(2)	C(26)-C(27)	1.498(3)
O(6)-C(19)	1.421(3)	C(26)-H(26A)	0.9900
O(6)-C(20)	1.425(3)	C(26)-H(26B)	0.9900
O(7)-C(21)	1.424(2)	C(27)-H(27A)	0.9900
O(7)-C(22)	1.429(2)	C(27)-H(27B)	0.9900
O(8)-C(23)	1.424(2)	C(16)-C(17)	1.495(3)
O(8)-C(24)	1.428(2)	C(16)-H(16A)	0.9900
O(2)-C(2)	1.165(3)	C(16)-H(16B)	0.9900
C(8)-C(9)	1.394(3)	C(17)-H(17A)	0.9900

Table 5.11 Cont.

C(17)-H(17B)	0.9900	N(2)-Re(1)-N(1)	74.96(6)
C(18)-C(19)	1.501(3)	O(3)-K(1)-O(1)#1	155.04(5)
C(18)-H(18A)	0.9900	O(3)-K(1)-O(9)	73.53(4)
C(18)-H(18B)	0.9900	O(1)#1-K(1)-O(9)	94.24(5)
C(19)-H(19A)	0.9900	O(3)-K(1)-O(6)	109.90(5)
C(19)-H(19B)	0.9900	O(1)#1-K(1)-O(6)	82.96(5)
C(20)-C(21)	1.496(3)	O(9)-K(1)-O(6)	176.42(5)
C(20)-H(20A)	0.9900	O(3)-K(1)-O(8)	90.11(5)
C(20)-H(20B)	0.9900	O(1)#1-K(1)-O(8)	102.75(5)
C(21)-H(21A)	0.9900	O(9)-K(1)-O(8)	60.16(4)
C(21)-H(21B)	0.9900	O(6)-K(1)-O(8)	118.21(4)
C(22)-C(23)	1.496(3)	O(3)-K(1)-O(4)	87.45(5)
C(22)-H(22A)	0.9900	O(1)#1-K(1)-O(4)	67.61(4)
C(22)-H(22B)	0.9900	O(9)-K(1)-O(4)	61.36(4)
C(23)-H(23A)	0.9900	O(6)-K(1)-O(4)	119.19(4)
C(23)-H(23B)	0.9900	O(8)-K(1)-O(4)	119.53(4)
C(24)-C(25)	1.502(3)	O(3)-K(1)-O(5)	91.36(5)
C(24)-H(24A)	0.9900	O(1)#1-K(1)-O(5)	76.03(4)
C(24)-H(24B)	0.9900	O(9)-K(1)-O(5)	120.68(4)
C(25)-H(25A)	0.9900	O(6)-K(1)-O(5)	60.87(4)
C(25)-H(25B)	0.9900	O(8)-K(1)-O(5)	178.48(4)
C(1)-K(1)#2	3.463(2)	O(4)-K(1)-O(5)	60.94(4)
		O(3)-K(1)-O(7)	97.46(5)
C(1)-Re(1)-C(3)	88.52(8)	O(1)#1-K(1)-O(7)	107.49(5)
C(1)-Re(1)-C(2)	89.12(9)	O(9)-K(1)-O(7)	118.95(4)
C(3)-Re(1)-C(2)	86.37(9)	O(6)-K(1)-O(7)	60.14(4)
C(1)-Re(1)-N(2)	115.25(8)	O(8)-K(1)-O(7)	59.61(4)
C(3)-Re(1)-N(2)	96.23(8)	O(4)-K(1)-O(7)	174.97(4)
C(2)-Re(1)-N(2)	155.50(8)	O(5)-K(1)-O(7)	119.77(4)
C(1)-Re(1)-N(1)	109.15(8)	O(3)-K(1)-C(1)#1	156.67(5)
C(3)-Re(1)-N(1)	162.23(7)	O(1)#1-K(1)-C(1)#1	17.30(5)
C(2)-Re(1)-N(1)	95.45(8)	O(9)-K(1)-C(1)#1	84.48(5)

Table 5.11 Cont.

O(6)-K(1)-C(1)#1	92.26(5)	N(1)-C(8)-C(7)	120.11(18)
O(8)-K(1)-C(1)#1	85.50(5)	C(1)-O(1)-K(1)#2	118.36(14)
O(4)-K(1)-C(1)#1	74.98(4)	C(12)-C(13)-N(2)	124.2(2)
O(5)-K(1)-C(1)#1	93.29(5)	C(12)-C(13)-H(13)	117.9
O(7)-K(1)-C(1)#1	99.99(5)	N(2)-C(13)-H(13)	117.9
C(13)-N(2)-C(9)	116.11(17)	C(13)-C(12)-C(11)	120.9(2)
C(13)-N(2)-Re(1)	125.56(14)	C(13)-C(12)-H(12)	119.6
C(9)-N(2)-Re(1)	118.32(13)	C(11)-C(12)-H(12)	119.6
C(4)-N(1)-C(8)	116.08(16)	C(10)-C(11)-C(12)	116.50(19)
C(4)-N(1)-Re(1)	125.92(13)	C(10)-C(11)-C(15)	123.3(2)
C(8)-N(1)-Re(1)	117.95(13)	C(12)-C(11)-C(15)	120.22(19)
C(3)-O(3)-K(1)	139.23(14)	C(11)-C(15)-H(15A)	109.5
C(26)-O(9)-C(25)	112.12(15)	C(11)-C(15)-H(15B)	109.5
C(26)-O(9)-K(1)	114.28(11)	H(15A)-C(15)-H(15B)	109.5
C(25)-O(9)-K(1)	118.56(11)	C(11)-C(15)-H(15C)	109.5
C(27)-O(4)-C(16)	111.49(15)	H(15A)-C(15)-H(15C)	109.5
C(27)-O(4)-K(1)	112.39(11)	H(15B)-C(15)-H(15C)	109.5
C(16)-O(4)-K(1)	110.53(11)	C(11)-C(10)-C(9)	122.13(19)
C(18)-O(5)-C(17)	112.32(17)	C(11)-C(10)-H(10)	118.9
C(18)-O(5)-K(1)	111.69(11)	C(9)-C(10)-H(10)	118.9
C(17)-O(5)-K(1)	113.53(11)	C(8)-C(9)-N(2)	114.59(17)
C(19)-O(6)-C(20)	112.31(17)	C(8)-C(9)-C(10)	125.19(18)
C(19)-O(6)-K(1)	115.86(12)	N(2)-C(9)-C(10)	120.17(18)
C(20)-O(6)-K(1)	115.78(12)	C(5)-C(4)-N(1)	124.65(18)
C(21)-O(7)-C(22)	111.35(15)	C(5)-C(4)-H(4)	117.7
C(21)-O(7)-K(1)	113.41(12)	N(1)-C(4)-H(4)	117.7
C(22)-O(7)-K(1)	111.64(11)	C(4)-C(5)-C(6)	119.84(19)
C(23)-O(8)-C(24)	112.11(15)	C(4)-C(5)-H(5)	120.1
C(23)-O(8)-K(1)	117.60(11)	C(6)-C(5)-H(5)	120.1
C(24)-O(8)-K(1)	112.90(11)	C(7)-C(6)-C(5)	117.19(18)
C(9)-C(8)-N(1)	114.00(17)	C(7)-C(6)-C(14)	122.84(19)
C(9)-C(8)-C(7)	125.61(18)	C(5)-C(6)-C(14)	119.90(18)

Table 5.11 Cont.

C(6)-C(14)-H(14A)	109.5	C(16)-C(17)-H(17B)	109.9
C(6)-C(14)-H(14B)	109.5	H(17A)-C(17)-H(17B)	108.3
H(14A)-C(14)-H(14B)	109.5	O(5)-C(18)-C(19)	108.5(2)
C(6)-C(14)-H(14C)	109.5	O(5)-C(18)-H(18A)	110.0
H(14A)-C(14)-H(14C)	109.5	C(19)-C(18)-H(18A)	110.0
H(14B)-C(14)-H(14C)	109.5	O(5)-C(18)-H(18B)	110.0
C(6)-C(7)-C(8)	122.08(18)	C(19)-C(18)-H(18B)	110.0
C(6)-C(7)-H(7)	119.0	H(18A)-C(18)-H(18B)	108.4
C(8)-C(7)-H(7)	119.0	O(6)-C(19)-C(18)	109.24(19)
O(3)-C(3)-Re(1)	177.98(19)	O(6)-C(19)-H(19A)	109.8
O(9)-C(26)-C(27)	108.70(16)	C(18)-C(19)-H(19A)	109.8
O(9)-C(26)-H(26A)	109.9	O(6)-C(19)-H(19B)	109.8
C(27)-C(26)-H(26A)	110.0	C(18)-C(19)-H(19B)	109.8
O(9)-C(26)-H(26B)	110.0	H(19A)-C(19)-H(19B)	108.3
C(27)-C(26)-H(26B)	109.9	O(6)-C(20)-C(21)	108.88(18)
H(26A)-C(26)-H(26B)	108.3	O(6)-C(20)-H(20A)	109.9
O(4)-C(27)-C(26)	109.09(16)	C(21)-C(20)-H(20A)	109.9
O(4)-C(27)-H(27A)	109.9	O(6)-C(20)-H(20B)	109.9
C(26)-C(27)-H(27A)	109.9	C(21)-C(20)-H(20B)	109.9
O(4)-C(27)-H(27B)	109.9	H(20A)-C(20)-H(20B)	108.3
C(26)-C(27)-H(27B)	109.9	O(7)-C(21)-C(20)	108.67(17)
H(27A)-C(27)-H(27B)	108.3	O(7)-C(21)-H(21A)	110.0
O(4)-C(16)-C(17)	108.06(16)	C(20)-C(21)-H(21A)	110.0
O(4)-C(16)-H(16A)	110.1	O(7)-C(21)-H(21B)	110.0
C(17)-C(16)-H(16A)	110.1	C(20)-C(21)-H(21B)	110.0
O(4)-C(16)-H(16B)	110.1	H(21A)-C(21)-H(21B)	108.3
C(17)-C(16)-H(16B)	110.1	O(7)-C(22)-C(23)	108.50(16)
H(16A)-C(16)-H(16B)	108.4	O(7)-C(22)-H(22A)	110.0
O(5)-C(17)-C(16)	108.72(17)	C(23)-C(22)-H(22A)	110.0
O(5)-C(17)-H(17A)	109.9	O(7)-C(22)-H(22B)	110.0
C(16)-C(17)-H(17A)	109.9	C(23)-C(22)-H(22B)	110.0
O(5)-C(17)-H(17B)	109.9	H(22A)-C(22)-H(22B)	108.4

Table 5.11 Cont.

O(8)-C(23)-C(22)	108.21(17)	H(24A)-C(24)-H(24B)	108.4
O(8)-C(23)-H(23A)	110.1	O(9)-C(25)-C(24)	108.51(16)
C(22)-C(23)-H(23A)	110.1	O(9)-C(25)-H(25A)	110.0
O(8)-C(23)-H(23B)	110.1	C(24)-C(25)-H(25A)	110.0
C(22)-C(23)-H(23B)	110.1	O(9)-C(25)-H(25B)	110.0
H(23A)-C(23)-H(23B)	108.4	C(24)-C(25)-H(25B)	110.0
O(8)-C(24)-C(25)	108.17(17)	H(25A)-C(25)-H(25B)	108.4
O(8)-C(24)-H(24A)	110.1	O(1)-C(1)-Re(1)	176.52(18)
C(25)-C(24)-H(24A)	110.1	O(1)-C(1)-K(1)#2	44.35(11)
O(8)-C(24)-H(24B)	110.1	Re(1)-C(1)-K(1)#2	136.95(9)
C(25)-C(24)-H(24B)	110.1	O(2)-C(2)-Re(1)	178.2(2

Symmetry transformations used to generate equivalent atoms:

#1 x-1,y,z #2 x+1,y,z

Table 5.12 Crystal data and structure refinement for [Re(tBu-bipy)$(CO)_3$] [K(18-crown-6)(THF)]

Identification code	cc	
Empirical formula	C37 H56 K N2 O10 Re	
Formula weight	914.14	
Temperature	100(2) K	
Wavelength	1.54184 Å	
Crystal system	Monoclinic	
Space group	Cc	
Unit cell dimensions	a = 20.856(2) Å	α= 90°.
	b = 10.2525(8) Å	β= 112.170(11)°.
	c = 20.295(2) Å	γ = 90°.
Volume	4018.9(6) $Å^3$	
Z	4	
Density (calculated)	1.511 Mg/m^3	
Absorption coefficient	7.300 mm^{-1}	
F(000)	1864	
Crystal size	0.10 x 0.10 x 0.01 mm^3	
Theta range for data collection	4.58 to 68.43°.	
Index ranges	-24<=h<=23, -11<=k<=12, -24<=l<=23	
Reflections collected	15825	
Independent reflections	5770 [R(int) = 0.0501]	
Completeness to theta = 60.00°	99.0 %	
Absorption correction	Semi-empirical from equivalents	
Max. and min. transmission	0.9306 and 0.5289	
Refinement method	Full-matrix least-squares on F^2	
Data / restraints / parameters	5770 / 2 / 454	
Goodness-of-fit on F^2	1.035	
Final R indices [I>2sigma(I)]	R1 = 0.0495, wR2 = 0.1241	
R indices (all data)	R1 = 0.0535, wR2 = 0.1278	
Absolute structure parameter	-0.056(15)	
Largest diff. peak and hole	2.875 and -1.004 $e.Å^{-3}$	

Table 5.13 Bond lengths [Å] and angles [°] for [Re(tBu-bipy)$(CO)_3$] [K(18-crown-6)(THF)].

Re(1)-C(1)	1.902(12)	N(1)-C(4)	1.373(14)
Re(1)-C(2)	1.922(9)	N(1)-C(8)	1.419(12)
Re(1)-C(3)	1.927(11)	N(2)-C(13)	1.348(13)
Re(1)-N(1)	2.070(7)	N(2)-C(9)	1.401(12)
Re(1)-N(2)	2.115(7)	C(4)-C(5)	1.323(15)
K(1)-O(5)	2.761(8)	C(4)-H(4)	0.9500
K(1)-O(10)	2.773(9)	C(5)-C(6)	1.442(13)
K(1)-O(6)	2.774(8)	C(5)-H(5)	0.9500
K(1)-O(8)	2.779(8)	C(6)-C(7)	1.362(14)
K(1)-O(4)	2.806(7)	C(6)-C(14)	1.517(13)
K(1)-O(7)	2.836(9)	C(7)-C(8)	1.444(14)
K(1)-O(9)	2.868(8)	C(7)-H(7)	0.9500
K(1)-O(3)	2.945(7)	C(8)-C(9)	1.370(15)
K(1)-C(24)	3.513(11)	C(9)-C(10)	1.424(13)
K(1)-C(35)	3.537(14)	C(10)-C(11)	1.368(16)
O(1)-C(1)	1.147(15)	C(10)-H(10)	0.9500
O(2)-C(2)	1.146(12)	C(11)-C(12)	1.408(16)
O(3)-C(3)	1.164(12)	C(11)-C(18)	1.539(15)
O(4)-C(34)	1.373(16)	C(12)-C(13)	1.375(14)
O(4)-C(22)	1.426(14)	C(12)-H(12)	0.9500
O(5)-C(23)	1.404(14)	C(13)-H(13)	0.9500
O(5)-C(24)	1.407(15)	C(14)-C(17)	1.518(14)
O(6)-C(25)	1.412(14)	C(14)-C(15)	1.530(18)
O(6)-C(27)	1.425(14)	C(14)-C(16)	1.539(19)
O(7)-C(28)	1.393(17)	C(15)-H(15A)	0.9800
O(7)-C(29)	1.411(15)	C(15)-H(15B)	0.9800
O(8)-C(31)	1.423(14)	C(15)-H(15C)	0.9800
O(8)-C(30)	1.431(12)	C(16)-H(16A)	0.9800
O(9)-C(33)	1.412(15)	C(16)-H(16B)	0.9800
O(9)-C(32)	1.416(14)	C(16)-H(16C)	0.9800
O(10)-C(35)	1.407(18)	C(17)-H(17A)	0.9800
O(10)-C(38)	1.422(19)	C(17)-H(17B)	0.9800

Table 5.13 Cont.

C(17)-H(17C)	0.9800	C(31)-C(32)	1.492(16)
C(18)-C(19)	1.482(17)	C(31)-H(31A)	0.9900
C(18)-C(20)	1.521(18)	C(31)-H(31B)	0.9900
C(18)-C(21)	1.544(16)	C(32)-H(32A)	0.9900
C(19)-H(19A)	0.9800	C(32)-H(32B)	0.9900
C(19)-H(19B)	0.9800	C(33)-C(34)	1.541(19)
C(19)-H(19C)	0.9800	C(33)-H(33A)	0.9900
C(20)-H(20A)	0.9800	C(33)-H(33B)	0.9900
C(20)-H(20B)	0.9800	C(34)-H(34A)	0.9900
C(20)-H(20C)	0.9800	C(34)-H(34B)	0.9900
C(21)-H(21A)	0.9800	C(35)-C(36)	1.55(2)
C(21)-H(21B)	0.9800	C(35)-H(35A)	0.9900
C(21)-H(21C)	0.9800	C(35)-H(35B)	0.9900
C(22)-C(23)	1.46(2)	C(36)-C(37)	1.52(3)
C(22)-H(22A)	0.9900	C(36)-H(36A)	0.9900
C(22)-H(22B)	0.9900	C(36)-H(36B)	0.9900
C(23)-H(23A)	0.9900	C(37)-C(38)	1.47(2)
C(23)-H(23B)	0.9900	C(37)-H(37A)	0.9900
C(24)-C(25)	1.501(16)	C(37)-H(37B)	0.9900
C(24)-H(24A)	0.9900	C(38)-H(38A)	0.9900
C(24)-H(24B)	0.9900	C(38)-H(38B)	0.9900
C(25)-H(25A)	0.9900		
C(25)-H(25B)	0.9900	C(1)-Re(1)-C(2)	89.7(5)
C(27)-C(28)	1.51(2)	C(1)-Re(1)-C(3)	90.8(5)
C(27)-H(27A)	0.9900	C(2)-Re(1)-C(3)	90.8(4)
C(27)-H(27B)	0.9900	C(1)-Re(1)-N(1)	127.2(5)
C(28)-H(28A)	0.9900	C(2)-Re(1)-N(1)	142.4(4)
C(28)-H(28B)	0.9900	C(3)-Re(1)-N(1)	95.3(4)
C(29)-C(30)	1.477(18)	C(1)-Re(1)-N(2)	97.3(4)
C(29)-H(29A)	0.9900	C(2)-Re(1)-N(2)	95.2(4)
C(29)-H(29B)	0.9900	C(3)-Re(1)-N(2)	169.9(4)
C(30)-H(30A)	0.9900	N(1)-Re(1)-N(2)	75.1(3)
C(30)-H(30B)	0.9900	O(5)-K(1)-O(10)	78.9(3)

Table 5.13 Cont.

O(5)-K(1)-O(6)	61.0(2)	O(7)-K(1)-C(24)	102.1(3)
O(10)-K(1)-O(6)	94.5(3)	O(9)-K(1)-C(24)	140.5(3)
O(5)-K(1)-O(8)	174.0(2)	O(3)-K(1)-C(24)	64.4(2)
O(10)-K(1)-O(8)	95.2(3)	O(5)-K(1)-C(35)	100.0(3)
O(6)-K(1)-O(8)	118.9(2)	O(10)-K(1)-C(35)	21.7(3)
O(5)-K(1)-O(4)	61.1(2)	O(6)-K(1)-C(35)	100.1(3)
O(10)-K(1)-O(4)	79.0(3)	O(8)-K(1)-C(35)	74.0(3)
O(6)-K(1)-O(4)	121.9(2)	O(4)-K(1)-C(35)	93.8(3)
O(8)-K(1)-O(4)	119.2(2)	O(7)-K(1)-C(35)	72.9(3)
O(5)-K(1)-O(7)	117.7(3)	O(9)-K(1)-C(35)	72.7(3)
O(10)-K(1)-O(7)	87.6(3)	O(3)-K(1)-C(35)	174.0(3)
O(6)-K(1)-O(7)	60.0(3)	C(24)-K(1)-C(35)	111.5(3)
O(8)-K(1)-O(7)	60.4(3)	C(3)-O(3)-K(1)	155.4(7)
O(4)-K(1)-O(7)	166.5(2)	C(34)-O(4)-C(22)	111.4(9)
O(5)-K(1)-O(9)	120.2(2)	C(34)-O(4)-K(1)	113.7(7)
O(10)-K(1)-O(9)	79.0(3)	C(22)-O(4)-K(1)	111.0(7)
O(6)-K(1)-O(9)	172.7(2)	C(23)-O(5)-C(24)	114.5(9)
O(8)-K(1)-O(9)	59.1(2)	C(23)-O(5)-K(1)	114.2(7)
O(4)-K(1)-O(9)	60.4(2)	C(24)-O(5)-K(1)	110.6(6)
O(7)-K(1)-O(9)	116.0(3)	C(25)-O(6)-C(27)	112.1(9)
O(5)-K(1)-O(3)	74.6(2)	C(25)-O(6)-K(1)	117.1(7)
O(10)-K(1)-O(3)	152.3(3)	C(27)-O(6)-K(1)	118.5(8)
O(6)-K(1)-O(3)	79.9(2)	C(28)-O(7)-C(29)	112.1(9)
O(8)-K(1)-O(3)	111.4(2)	C(28)-O(7)-K(1)	114.9(7)
O(4)-K(1)-O(3)	81.2(2)	C(29)-O(7)-K(1)	112.0(7)
O(7)-K(1)-O(3)	111.8(2)	C(31)-O(8)-C(30)	113.0(8)
O(9)-K(1)-O(3)	107.4(2)	C(31)-O(8)-K(1)	120.0(6)
O(5)-K(1)-C(24)	22.0(3)	C(30)-O(8)-K(1)	117.2(6)
O(10)-K(1)-C(24)	93.2(3)	C(33)-O(9)-C(32)	114.0(9)
O(6)-K(1)-C(24)	42.3(3)	C(33)-O(9)-K(1)	112.0(7)
O(8)-K(1)-C(24)	160.1(3)	C(32)-O(9)-K(1)	109.4(6)
O(4)-K(1)-C(24)	80.1(3)	C(35)-O(10)-C(38)	108.7(11)

Table 5.13 Cont.

C(35)-O(10)-K(1)	111.4(7)	C(10)-C(11)-C(12)	116.0(10)
C(38)-O(10)-K(1)	114.3(10)	C(10)-C(11)-C(18)	123.5(10)
C(4)-N(1)-C(8)	115.5(8)	C(12)-C(11)-C(18)	120.6(10)
C(4)-N(1)-Re(1)	126.3(6)	C(13)-C(12)-C(11)	120.2(10)
C(8)-N(1)-Re(1)	118.2(7)	C(13)-C(12)-H(12)	119.9
C(13)-N(2)-C(9)	117.4(7)	C(11)-C(12)-H(12)	119.9
C(13)-N(2)-Re(1)	125.4(5)	N(2)-C(13)-C(12)	124.4(8)
C(9)-N(2)-Re(1)	117.2(6)	N(2)-C(13)-H(13)	117.8
O(1)-C(1)-Re(1)	177.4(11)	C(12)-C(13)-H(13)	117.8
O(2)-C(2)-Re(1)	174.8(9)	C(6)-C(14)-C(17)	113.1(9)
O(3)-C(3)-Re(1)	175.0(9)	C(6)-C(14)-C(15)	109.6(9)
C(5)-C(4)-N(1)	125.0(9)	C(17)-C(14)-C(15)	107.2(10)
C(5)-C(4)-H(4)	117.5	C(6)-C(14)-C(16)	108.6(9)
N(1)-C(4)-H(4)	117.5	C(17)-C(14)-C(16)	108.3(11)
C(4)-C(5)-C(6)	121.6(9)	C(15)-C(14)-C(16)	110.1(12)
C(4)-C(5)-H(5)	119.2	C(14)-C(15)-H(15A)	109.5
C(6)-C(5)-H(5)	119.2	C(14)-C(15)-H(15B)	109.5
C(7)-C(6)-C(5)	116.2(9)	H(15A)-C(15)-H(15B)	109.5
C(7)-C(6)-C(14)	122.3(8)	C(14)-C(15)-H(15C)	109.5
C(5)-C(6)-C(14)	121.5(9)	H(15A)-C(15)-H(15C)	109.5
C(6)-C(7)-C(8)	121.3(8)	H(15B)-C(15)-H(15C)	109.5
C(6)-C(7)-H(7)	119.4	C(14)-C(16)-H(16A)	109.5
C(8)-C(7)-H(7)	119.4	C(14)-C(16)-H(16B)	109.5
C(9)-C(8)-N(1)	114.6(9)	H(16A)-C(16)-H(16B)	109.5
C(9)-C(8)-C(7)	125.1(9)	C(14)-C(16)-H(16C)	109.5
N(1)-C(8)-C(7)	120.3(9)	H(16A)-C(16)-H(16C)	109.5
C(8)-C(9)-N(2)	114.8(8)	H(16B)-C(16)-H(16C)	109.5
C(8)-C(9)-C(10)	126.8(9)	C(14)-C(17)-H(17A)	109.5
N(2)-C(9)-C(10)	118.4(9)	C(14)-C(17)-H(17B)	109.5
C(11)-C(10)-C(9)	123.5(9)	H(17A)-C(17)-H(17B)	109.5
C(11)-C(10)-H(10)	118.3	C(14)-C(17)-H(17C)	109.5
C(9)-C(10)-H(10)	118.3	H(17A)-C(17)-H(17C)	109.5

Table 5.13 Cont.

H(17B)-C(17)-H(17C)	109.5	O(5)-C(23)-H(23A)	109.9
C(19)-C(18)-C(20)	109.7(11)	C(22)-C(23)-H(23A)	109.9
C(19)-C(18)-C(11)	112.2(9)	O(5)-C(23)-H(23B)	109.9
C(20)-C(18)-C(11)	109.8(9)	C(22)-C(23)-H(23B)	109.9
C(19)-C(18)-C(21)	108.8(10)	H(23A)-C(23)-H(23B)	108.3
C(20)-C(18)-C(21)	109.3(9)	O(5)-C(24)-C(25)	109.9(9)
C(11)-C(18)-C(21)	107.0(9)	O(5)-C(24)-K(1)	47.4(5)
C(18)-C(19)-H(19A)	109.5	C(25)-C(24)-K(1)	82.7(7)
C(18)-C(19)-H(19B)	109.5	O(5)-C(24)-H(24A)	109.7
H(19A)-C(19)-H(19B)	109.5	C(25)-C(24)-H(24A)	109.7
C(18)-C(19)-H(19C)	109.5	K(1)-C(24)-H(24A)	157.0
H(19A)-C(19)-H(19C)	109.5	O(5)-C(24)-H(24B)	109.7
H(19B)-C(19)-H(19C)	109.5	C(25)-C(24)-H(24B)	109.7
C(18)-C(20)-H(20A)	109.5	K(1)-C(24)-H(24B)	84.3
C(18)-C(20)-H(20B)	109.5	H(24A)-C(24)-H(24B)	108.2
H(20A)-C(20)-H(20B)	109.5	O(6)-C(25)-C(24)	108.9(9)
C(18)-C(20)-H(20C)	109.5	O(6)-C(25)-H(25A)	109.9
H(20A)-C(20)-H(20C)	109.5	C(24)-C(25)-H(25A)	109.9
H(20B)-C(20)-H(20C)	109.5	O(6)-C(25)-H(25B)	109.9
C(18)-C(21)-H(21A)	109.5	C(24)-C(25)-H(25B)	109.9
C(18)-C(21)-H(21B)	109.5	H(25A)-C(25)-H(25B)	108.3
H(21A)-C(21)-H(21B)	109.5	O(6)-C(27)-C(28)	108.7(10)
C(18)-C(21)-H(21C)	109.5	O(6)-C(27)-H(27A)	109.9
H(21A)-C(21)-H(21C)	109.5	C(28)-C(27)-H(27A)	109.9
H(21B)-C(21)-H(21C)	109.5	O(6)-C(27)-H(27B)	109.9
O(4)-C(22)-C(23)	109.5(10)	C(28)-C(27)-H(27B)	109.9
O(4)-C(22)-H(22A)	109.8	H(27A)-C(27)-H(27B)	108.3
C(23)-C(22)-H(22A)	109.8	O(7)-C(28)-C(27)	112.1(11)
O(4)-C(22)-H(22B)	109.8	O(7)-C(28)-H(28A)	109.2
C(23)-C(22)-H(22B)	109.8	C(27)-C(28)-H(28A)	109.2
H(22A)-C(22)-H(22B)	108.2	O(7)-C(28)-H(28B)	109.2
O(5)-C(23)-C(22)	109.1(11)	C(27)-C(28)-H(28B)	109.2

Table 5.13 Cont.

H(28A)-C(28)-H(28B)	107.9	O(4)-C(34)-H(34A)	110.1
O(7)-C(29)-C(30)	111.5(10)	C(33)-C(34)-H(34A)	110.1
O(7)-C(29)-H(29A)	109.3	O(4)-C(34)-H(34B)	110.1
C(30)-C(29)-H(29A)	109.3	C(33)-C(34)-H(34B)	110.1
O(7)-C(29)-H(29B)	109.3	H(34A)-C(34)-H(34B)	108.4
C(30)-C(29)-H(29B)	109.3	O(10)-C(35)-C(36)	105.8(12)
H(29A)-C(29)-H(29B)	108.0	O(10)-C(35)-K(1)	46.9(6)
O(8)-C(30)-C(29)	108.6(9)	C(36)-C(35)-K(1)	110.4(10)
O(8)-C(30)-H(30A)	110.0	O(10)-C(35)-H(35A)	110.6
C(29)-C(30)-H(30A)	110.0	C(36)-C(35)-H(35A)	110.6
O(8)-C(30)-H(30B)	110.0	K(1)-C(35)-H(35A)	65.4
C(29)-C(30)-H(30B)	110.0	O(10)-C(35)-H(35B)	110.6
H(30A)-C(30)-H(30B)	108.4	C(36)-C(35)-H(35B)	110.6
O(8)-C(31)-C(32)	108.9(9)	K(1)-C(35)-H(35B)	137.7
O(8)-C(31)-H(31A)	109.9	H(35A)-C(35)-H(35B)	108.7
C(32)-C(31)-H(31A)	109.9	C(37)-C(36)-C(35)	101.8(15)
O(8)-C(31)-H(31B)	109.9	C(37)-C(36)-H(36A)	111.4
C(32)-C(31)-H(31B)	109.9	C(35)-C(36)-H(36A)	111.4
H(31A)-C(31)-H(31B)	108.3	C(37)-C(36)-H(36B)	111.4
O(9)-C(32)-C(31)	108.7(9)	C(35)-C(36)-H(36B)	111.4
O(9)-C(32)-H(32A)	109.9	H(36A)-C(36)-H(36B)	109.3
C(31)-C(32)-H(32A)	109.9	C(38)-C(37)-C(36)	104.2(14)
O(9)-C(32)-H(32B)	109.9	C(38)-C(37)-H(37A)	110.9
C(31)-C(32)-H(32B)	109.9	C(36)-C(37)-H(37A)	110.9
H(32A)-C(32)-H(32B)	108.3	C(38)-C(37)-H(37B)	110.9
O(9)-C(33)-C(34)	108.4(10)	C(36)-C(37)-H(37B)	110.9
O(9)-C(33)-H(33A)	110.0	H(37A)-C(37)-H(37B)	108.9
C(34)-C(33)-H(33A)	110.0	O(10)-C(38)-C(37)	109.9(14)
O(9)-C(33)-H(33B)	110.0	O(10)-C(38)-H(38A)	109.7
C(34)-C(33)-H(33B)	110.0	C(37)-C(38)-H(38A)	109.7
H(33A)-C(33)-H(33B)	108.4	O(10)-C(38)-H(38B)	109.7
O(4)-C(34)-C(33)	107.9(9)	C(37)-C(38)-H(38B)	109.7

Table 5.13 Cont.

H(38A)-C(38)-H(38B)	108.2

Table 5.14 Crystal data and structure refinement for [Re(bipy-OMe)$(CO)_3$] [K(18-crown-6)(THF)]

Identification code	cc	
Empirical formula	C31 H44 K N2 O12 Re	
Formula weight	861.98	
Temperature	100(2) K	
Wavelength	1.54184 Å	
Crystal system	Monoclinic	
Space group	Cc	
Unit cell dimensions	a = 20.6969(10) Å	α= 90°.
	b = 17.4004(9) Å	β= 93.936(3)°.
	c = 19.7862(10) Å	γ = 90°.
Volume	7108.9(6) $Å^3$	
Z	8	
Density (calculated)	1.611 Mg/m^3	
Absorption coefficient	8.261 mm^{-1}	
F(000)	3472	
Crystal size	0.02 x 0.01 x 0.01 mm^3	
Theta range for data collection	3.32 to 69.73°.	
Index ranges	-24<=h<=24, -21<=k<=21, -24<=l<=24	
Reflections collected	9984	
Independent reflections	9984 [R(int) = 0.0000]	
Completeness to theta = 60.00°	97.6 %	
Absorption correction	Semi-empirical from equivalents	
Max. and min. transmission	0.9219 and 0.8522	
Refinement method	Full-matrix least-squares on F^2	
Data / restraints / parameters	9984 / 2 / 856	
Goodness-of-fit on F^2	1.092	
Final R indices [I>2sigma(I)]	R1 = 0.0517, wR2 = 0.1302	
R indices (all data)	R1 = 0.0537, wR2 = 0.1329	
Absolute structure parameter	0.041(13)	
Largest diff. peak and hole	3.000 and -1.253 $e.Å^{-3}$	

Table 5.15 Bond lengths [Å] and angles [°] for [Re(bipy-OMe)$(CO)_3$] [K(18-crown-6)(THF)]

Re(1)-C(1)	1.915(12)	O(7)-C(17)	1.166(19)
Re(1)-C(3)	1.962(11)	O(7)-K(2)#1	3.043(12)
Re(1)-C(2)	1.965(11)	N(2)-C(9)	1.390(14)
Re(1)-N(2)	2.073(9)	N(2)-C(13)	1.417(13)
Re(1)-N(1)	2.104(8)	O(21)-C(52)	1.412(14)
Re(2)-C(17)	1.878(17)	O(21)-C(53)	1.429(15)
Re(2)-C(16)	1.909(10)	O(21)-K(2)	2.824(8)
Re(2)-C(18)	1.931(16)	N(3)-C(19)	1.368(15)
Re(2)-N(3)	2.098(9)	N(3)-C(23)	1.398(13)
Re(2)-N(4)	2.121(9)	O(24)-C(59)	1.395(16)
N(1)-C(4)	1.374(14)	O(24)-C(62)	1.412(17)
N(1)-C(8)	1.400(15)	O(24)-K(2)	2.700(10)
O(10)-C(26)	1.387(15)	O(16)-C(40)	1.399(17)
O(10)-C(30)	1.445(16)	O(16)-C(41)	1.421(17)
N(4)-C(24)	1.366(14)	O(16)-K(1)	2.788(9)
N(4)-C(28)	1.370(15)	O(23)-C(57)	1.410(15)
O(6)-C(16)	1.132(15)	O(23)-C(56)	1.421(16)
O(9)-C(21)	1.382(16)	O(23)-K(2)	2.848(9)
O(9)-C(29)	1.436(17)	O(22)-C(54)	1.416(15)
O(2)-C(2)	1.114(15)	O(22)-C(55)	1.427(15)
O(3)-C(3)	1.095(15)	O(22)-K(2)	2.810(10)
O(3)-K(1)	2.844(9)	O(8)-C(18)	1.149(18)
O(12)-C(32)	1.35(2)	O(17)-C(46)	1.421(18)
O(12)-C(33)	1.405(17)	O(17)-C(43)	1.48(2)
O(12)-K(1)	2.778(9)	O(17)-K(1)	2.691(10)
O(19)-C(48)	1.417(15)	O(11)-C(42)	1.400(17)
O(19)-C(49)	1.423(14)	O(11)-C(31)	1.401(17)
O(19)-K(2)	2.781(9)	O(11)-K(1)	2.835(9)
O(20)-C(51)	1.422(13)	C(21)-C(22)	1.358(15)
O(20)-C(50)	1.429(14)	C(21)-C(20)	1.450(16)
O(20)-K(2)	2.797(8)	O(4)-C(6)	1.367(14)
C(1)-O(1)	1.133(15)	O(4)-C(14)	1.448(15)

Table 5.15 Cont.

O(5)-C(11)	1.389(14)	C(50)-C(49)	1.489(17)
O(5)-C(15)	1.411(15)	C(50)-H(50A)	0.9900
O(18)-C(58)	1.420(15)	C(50)-H(50B)	0.9900
O(18)-C(47)	1.446(14)	C(40)-C(39)	1.51(3)
O(18)-K(2)	2.868(8)	C(40)-H(40A)	0.9900
C(4)-C(5)	1.361(17)	C(40)-H(40B)	0.9900
C(4)-H(4)	0.9500	C(10)-C(9)	1.427(15)
O(14)-C(37)	1.406(19)	C(10)-H(10)	0.9500
O(14)-C(36)	1.41(2)	C(59)-C(60)	1.513(18)
O(14)-K(1)	2.782(10)	C(59)-H(59A)	0.9900
C(30)-H(30A)	0.9800	C(59)-H(59B)	0.9900
C(30)-H(30B)	0.9800	C(9)-C(8)	1.388(13)
C(30)-H(30C)	0.9800	C(8)-C(7)	1.450(15)
C(29)-H(29A)	0.9800	C(58)-C(57)	1.478(18)
C(29)-H(29B)	0.9800	C(58)-H(58A)	0.9900
C(29)-H(29C)	0.9800	C(58)-H(58B)	0.9900
O(15)-C(39)	1.40(2)	C(39)-K(1)	3.515(14)
O(15)-C(38)	1.44(2)	C(39)-H(39A)	0.9900
O(15)-K(1)	2.769(10)	C(39)-H(39B)	0.9900
C(26)-C(25)	1.372(16)	C(22)-C(23)	1.451(14)
C(26)-C(27)	1.430(16)	C(22)-H(22)	0.9500
C(52)-C(51)	1.487(17)	C(23)-C(24)	1.405(14)
C(52)-K(2)	3.498(11)	C(32)-C(31)	1.52(2)
C(52)-H(52A)	0.9900	C(32)-H(32A)	0.9900
C(52)-H(52B)	0.9900	C(32)-H(32B)	0.9900
C(19)-C(20)	1.360(18)	C(12)-C(13)	1.347(17)
C(19)-H(19)	0.9500	C(12)-H(12)	0.9500
C(11)-C(10)	1.366(16)	C(27)-C(28)	1.352(16)
C(11)-C(12)	1.436(17)	C(27)-H(27)	0.9500
C(44)-C(45)	1.50(2)	C(6)-C(7)	1.373(16)
C(44)-C(43)	1.54(2)	C(6)-C(5)	1.400(16)
C(44)-H(44A)	0.9900	C(20)-H(20)	0.9500
C(44)-H(44B)	0.9900	C(13)-H(13)	0.9500

Table 5.15 Cont.

C(57)-H(57A)	0.9900	C(62)-H(62A)	0.9900
C(57)-H(57B)	0.9900	C(62)-H(62B)	0.9900
C(7)-H(7)	0.9500	C(60)-H(60A)	0.9900
C(24)-C(25)	1.458(14)	C(60)-H(60B)	0.9900
C(54)-C(53)	1.516(19)	C(45)-C(46)	1.51(2)
C(54)-H(54A)	0.9900	C(45)-H(45A)	0.9900
C(54)-H(54B)	0.9900	C(45)-H(45B)	0.9900
C(48)-C(47)	1.471(18)	C(33)-C(34)	1.48(2)
C(48)-H(48A)	0.9900	C(33)-H(33A)	0.9900
C(48)-H(48B)	0.9900	C(33)-H(33B)	0.9900
C(5)-H(5)	0.9500	C(31)-H(31A)	0.9900
K(2)-O(7)#2	3.043(12)	C(31)-H(31B)	0.9900
K(2)-C(62)	3.433(15)	C(38)-C(37)	1.48(3)
C(47)-H(47A)	0.9900	C(38)-H(38A)	0.9900
C(47)-H(47B)	0.9900	C(38)-H(38B)	0.9900
C(51)-H(51A)	0.9900	C(42)-C(41)	1.50(2)
C(51)-H(51B)	0.9900	C(42)-H(42A)	0.9900
C(55)-C(56)	1.49(2)	C(42)-H(42B)	0.9900
C(55)-H(55A)	0.9900	C(43)-H(43A)	0.9900
C(55)-H(55B)	0.9900	C(43)-H(43B)	0.9900
C(49)-H(49A)	0.9900	C(36)-C(35)	1.47(2)
C(49)-H(49B)	0.9900	C(36)-H(36A)	0.9900
C(53)-H(53A)	0.9900	C(36)-H(36B)	0.9900
C(53)-H(53B)	0.9900	C(46)-H(46A)	0.9900
C(56)-H(56A)	0.9900	C(46)-H(46B)	0.9900
C(56)-H(56B)	0.9900	C(41)-H(41A)	0.9900
K(1)-O(13)	2.872(10)	C(41)-H(41B)	0.9900
K(1)-C(41)	3.527(12)	C(37)-H(37A)	0.9900
C(61)-C(62)	1.52(2)	C(37)-H(37B)	0.9900
C(61)-C(60)	1.546(17)	O(13)-C(35)	1.396(18)
C(61)-H(61A)	0.9900	O(13)-C(34)	1.397(17)
C(61)-H(61B)	0.9900	C(34)-H(34A)	0.9900

Table 5.15 Cont.

C(34)-H(34B)	0.9900	C(4)-N(1)-C(8)	116.7(9)
C(35)-H(35A)	0.9900	C(4)-N(1)-Re(1)	124.7(7)
C(35)-H(35B)	0.9900	C(8)-N(1)-Re(1)	118.6(6)
C(25)-H(25)	0.9500	C(26)-O(10)-C(30)	116.8(9)
C(28)-H(28)	0.9500	C(24)-N(4)-C(28)	117.1(9)
C(14)-H(14A)	0.9800	C(24)-N(4)-Re(2)	118.1(7)
C(14)-H(14B)	0.9800	C(28)-N(4)-Re(2)	124.8(8)
C(14)-H(14C)	0.9800	C(21)-O(9)-C(29)	116.5(9)
C(15)-H(15A)	0.9800	C(3)-O(3)-K(1)	131.0(9)
C(15)-H(15B)	0.9800	C(32)-O(12)-C(33)	109.9(12)
C(15)-H(15C)	0.9800	C(32)-O(12)-K(1)	120.9(10)
		C(33)-O(12)-K(1)	119.9(9)
C(1)-Re(1)-C(3)	88.9(5)	C(48)-O(19)-C(49)	114.2(10)
C(1)-Re(1)-C(2)	91.0(5)	C(48)-O(19)-K(2)	119.3(7)
C(3)-Re(1)-C(2)	89.2(5)	C(49)-O(19)-K(2)	117.1(6)
C(1)-Re(1)-N(2)	116.5(4)	C(51)-O(20)-C(50)	112.4(8)
C(3)-Re(1)-N(2)	154.0(4)	C(51)-O(20)-K(2)	115.3(6)
C(2)-Re(1)-N(2)	95.2(5)	C(50)-O(20)-K(2)	110.3(6)
C(1)-Re(1)-N(1)	103.5(4)	O(1)-C(1)-Re(1)	174.8(9)
C(3)-Re(1)-N(1)	95.8(4)	O(6)-C(16)-Re(2)	179.3(13)
C(2)-Re(1)-N(1)	164.7(5)	C(17)-O(7)-K(2)#1	117.3(10)
N(2)-Re(1)-N(1)	74.2(3)	C(9)-N(2)-C(13)	115.0(9)
C(17)-Re(2)-C(16)	92.8(6)	C(9)-N(2)-Re(1)	119.4(7)
C(17)-Re(2)-C(18)	89.4(6)	C(13)-N(2)-Re(1)	125.5(7)
C(16)-Re(2)-C(18)	90.1(6)	C(52)-O(21)-C(53)	114.0(9)
C(17)-Re(2)-N(3)	145.0(4)	C(52)-O(21)-K(2)	106.5(6)
C(16)-Re(2)-N(3)	122.1(5)	C(53)-O(21)-K(2)	111.4(7)
C(18)-Re(2)-N(3)	92.5(5)	C(19)-N(3)-C(23)	117.6(9)
C(17)-Re(2)-N(4)	97.0(4)	C(19)-N(3)-Re(2)	125.2(8)
C(16)-Re(2)-N(4)	102.1(5)	C(23)-N(3)-Re(2)	117.2(7)
C(18)-Re(2)-N(4)	165.8(5)	C(59)-O(24)-C(62)	104.1(10)
N(3)-Re(2)-N(4)	75.0(4)	C(59)-O(24)-K(2)	138.9(8)

Table 5.15 Cont.

C(62)-O(24)-K(2)	109.2(9)	C(36)-O(14)-K(1)	113.1(8)
C(40)-O(16)-C(41)	111.5(12)	O(7)-C(17)-Re(2)	177.0(13)
C(40)-O(16)-K(1)	112.5(9)	C(39)-O(15)-C(38)	114.3(13)
C(41)-O(16)-K(1)	109.5(7)	C(39)-O(15)-K(1)	110.7(8)
C(57)-O(23)-C(56)	112.5(9)	C(38)-O(15)-K(1)	113.9(9)
C(57)-O(23)-K(2)	110.5(7)	C(25)-C(26)-O(10)	125.0(11)
C(56)-O(23)-K(2)	112.4(7)	C(25)-C(26)-C(27)	119.3(10)
C(54)-O(22)-C(55)	112.3(11)	O(10)-C(26)-C(27)	115.7(9)
C(54)-O(22)-K(2)	115.5(7)	O(21)-C(52)-C(51)	108.2(9)
C(55)-O(22)-K(2)	116.0(7)	O(21)-C(52)-K(2)	50.7(5)
C(46)-O(17)-C(43)	104.4(10)	C(51)-C(52)-K(2)	83.4(6)
C(46)-O(17)-K(1)	125.8(8)	O(21)-C(52)-H(52A)	110.1
C(43)-O(17)-K(1)	117.7(9)	C(51)-C(52)-H(52A)	110.1
C(42)-O(11)-C(31)	113.6(11)	K(2)-C(52)-H(52A)	78.8
C(42)-O(11)-K(1)	115.3(8)	O(21)-C(52)-H(52B)	110.1
C(31)-O(11)-K(1)	114.1(8)	C(51)-C(52)-H(52B)	110.1
C(22)-C(21)-O(9)	126.6(11)	K(2)-C(52)-H(52B)	160.3
C(22)-C(21)-C(20)	119.3(11)	H(52A)-C(52)-H(52B)	108.4
O(9)-C(21)-C(20)	114.2(10)	C(20)-C(19)-N(3)	124.2(11)
C(6)-O(4)-C(14)	116.4(8)	C(20)-C(19)-H(19)	117.9
C(11)-O(5)-C(15)	116.8(8)	N(3)-C(19)-H(19)	117.9
O(2)-C(2)-Re(1)	178.0(13)	C(10)-C(11)-O(5)	125.6(10)
C(58)-O(18)-C(47)	111.8(9)	C(10)-C(11)-C(12)	120.1(11)
C(58)-O(18)-K(2)	116.8(7)	O(5)-C(11)-C(12)	114.2(9)
C(47)-O(18)-K(2)	117.7(7)	C(45)-C(44)-C(43)	105.3(13)
O(3)-C(3)-Re(1)	176.4(11)	C(45)-C(44)-H(44A)	110.7
O(8)-C(18)-Re(2)	177.5(13)	C(43)-C(44)-H(44A)	110.7
C(5)-C(4)-N(1)	124.3(11)	C(45)-C(44)-H(44B)	110.7
C(5)-C(4)-H(4)	117.8	C(43)-C(44)-H(44B)	110.7
N(1)-C(4)-H(4)	117.8	H(44A)-C(44)-H(44B)	108.8
C(37)-O(14)-C(36)	115.7(12)	O(20)-C(50)-C(49)	108.8(10)
C(37)-O(14)-K(1)	112.0(9)	O(20)-C(50)-H(50A)	109.9

Table 5.15 Cont.

C(49)-C(50)-H(50A)	109.9	O(15)-C(39)-K(1)	47.5(6)
O(20)-C(50)-H(50B)	109.9	C(40)-C(39)-K(1)	79.6(8)
C(49)-C(50)-H(50B)	109.9	O(15)-C(39)-H(39A)	109.6
H(50A)-C(50)-H(50B)	108.3	C(40)-C(39)-H(39A)	109.6
O(16)-C(40)-C(39)	109.8(13)	K(1)-C(39)-H(39A)	87.7
O(16)-C(40)-H(40A)	109.7	O(15)-C(39)-H(39B)	109.6
C(39)-C(40)-H(40A)	109.7	C(40)-C(39)-H(39B)	109.6
O(16)-C(40)-H(40B)	109.7	K(1)-C(39)-H(39B)	156.6
C(39)-C(40)-H(40B)	109.7	H(39A)-C(39)-H(39B)	108.2
H(40A)-C(40)-H(40B)	108.2	C(21)-C(22)-C(23)	119.6(10)
C(11)-C(10)-C(9)	119.2(10)	C(21)-C(22)-H(22)	120.2
C(11)-C(10)-H(10)	120.4	C(23)-C(22)-H(22)	120.2
C(9)-C(10)-H(10)	120.4	N(3)-C(23)-C(24)	115.2(9)
O(24)-C(59)-C(60)	107.1(10)	N(3)-C(23)-C(22)	120.5(9)
O(24)-C(59)-H(59A)	110.3	C(24)-C(23)-C(22)	124.3(9)
C(60)-C(59)-H(59A)	110.3	O(12)-C(32)-C(31)	108.6(12)
O(24)-C(59)-H(59B)	110.3	O(12)-C(32)-H(32A)	110.0
C(60)-C(59)-H(59B)	110.3	C(31)-C(32)-H(32A)	110.0
H(59A)-C(59)-H(59B)	108.6	O(12)-C(32)-H(32B)	110.0
C(8)-C(9)-N(2)	114.5(10)	C(31)-C(32)-H(32B)	110.0
C(8)-C(9)-C(10)	123.0(10)	H(32A)-C(32)-H(32B)	108.4
N(2)-C(9)-C(10)	122.5(9)	C(13)-C(12)-C(11)	118.2(10)
C(9)-C(8)-N(1)	113.3(9)	C(13)-C(12)-H(12)	120.9
C(9)-C(8)-C(7)	126.3(11)	C(11)-C(12)-H(12)	120.9
N(1)-C(8)-C(7)	120.4(9)	C(28)-C(27)-C(26)	119.2(9)
O(18)-C(58)-C(57)	108.4(11)	C(28)-C(27)-H(27)	120.4
O(18)-C(58)-H(58A)	110.0	C(26)-C(27)-H(27)	120.4
C(57)-C(58)-H(58A)	110.0	O(4)-C(6)-C(7)	123.8(10)
O(18)-C(58)-H(58B)	110.0	O(4)-C(6)-C(5)	116.9(10)
C(57)-C(58)-H(58B)	110.0	C(7)-C(6)-C(5)	119.3(10)
H(58A)-C(58)-H(58B)	108.4	C(19)-C(20)-C(21)	118.7(10)
O(15)-C(39)-C(40)	110.1(13)	C(19)-C(20)-H(20)	120.6

Table 5.15 Cont.

C(21)-C(20)-H(20)	120.6	O(24)-K(2)-O(20)	75.6(3)
C(12)-C(13)-N(2)	125.0(10)	O(19)-K(2)-O(20)	60.5(2)
C(12)-C(13)-H(13)	117.5	O(24)-K(2)-O(22)	90.1(3)
N(2)-C(13)-H(13)	117.5	O(19)-K(2)-O(22)	162.3(3)
O(23)-C(57)-C(58)	109.6(10)	O(20)-K(2)-O(22)	121.6(2)
O(23)-C(57)-H(57A)	109.7	O(24)-K(2)-O(21)	74.0(3)
C(58)-C(57)-H(57A)	109.7	O(19)-K(2)-O(21)	117.8(3)
O(23)-C(57)-H(57B)	109.7	O(20)-K(2)-O(21)	60.8(2)
C(58)-C(57)-H(57B)	109.7	O(22)-K(2)-O(21)	60.8(2)
H(57A)-C(57)-H(57B)	108.2	O(24)-K(2)-O(23)	90.3(3)
C(6)-C(7)-C(8)	119.5(10)	O(19)-K(2)-O(23)	112.9(3)
C(6)-C(7)-H(7)	120.3	O(20)-K(2)-O(23)	165.6(3)
C(8)-C(7)-H(7)	120.3	O(22)-K(2)-O(23)	60.2(2)
N(4)-C(24)-C(23)	114.5(9)	O(21)-K(2)-O(23)	118.6(3)
N(4)-C(24)-C(25)	121.9(9)	O(24)-K(2)-O(18)	95.0(3)
C(23)-C(24)-C(25)	123.5(9)	O(19)-K(2)-O(18)	58.6(2)
O(22)-C(54)-C(53)	108.1(10)	O(20)-K(2)-O(18)	118.5(3)
O(22)-C(54)-H(54A)	110.1	O(22)-K(2)-O(18)	119.0(3)
C(53)-C(54)-H(54A)	110.1	O(21)-K(2)-O(18)	169.0(3)
O(22)-C(54)-H(54B)	110.1	O(23)-K(2)-O(18)	59.0(3)
C(53)-C(54)-H(54B)	110.1	O(24)-K(2)-O(7)#2	147.1(3)
H(54A)-C(54)-H(54B)	108.4	O(19)-K(2)-O(7)#2	116.4(3)
O(19)-C(48)-C(47)	111.3(12)	O(20)-K(2)-O(7)#2	82.5(3)
O(19)-C(48)-H(48A)	109.4	O(22)-K(2)-O(7)#2	80.8(3)
C(47)-C(48)-H(48A)	109.4	O(21)-K(2)-O(7)#2	74.0(3)
O(19)-C(48)-H(48B)	109.4	O(23)-K(2)-O(7)#2	111.6(3)
C(47)-C(48)-H(48B)	109.4	O(18)-K(2)-O(7)#2	117.1(3)
H(48A)-C(48)-H(48B)	108.0	O(24)-K(2)-C(62)	22.9(3)
C(4)-C(5)-C(6)	119.8(10)	O(19)-K(2)-C(62)	66.0(3)
C(4)-C(5)-H(5)	120.1	O(20)-K(2)-C(62)	91.0(3)
C(6)-C(5)-H(5)	120.1	O(22)-K(2)-C(62)	96.3(3)
O(24)-K(2)-O(19)	73.2(3)	O(21)-K(2)-C(62)	96.2(3)

Table 5.15 Cont.

O(23)-K(2)-C(62)	74.7(3)	C(50)-C(49)-H(49A)	110.0
O(18)-K(2)-C(62)	72.8(3)	O(19)-C(49)-H(49B)	110.0
O(7)#2-K(2)-C(62)	170.0(3)	C(50)-C(49)-H(49B)	110.0
O(24)-K(2)-C(52)	84.0(3)	H(49A)-C(49)-H(49B)	108.4
O(19)-K(2)-C(52)	102.9(3)	O(21)-C(53)-C(54)	109.0(9)
O(20)-K(2)-C(52)	42.5(3)	O(21)-C(53)-H(53A)	109.9
O(22)-K(2)-C(52)	80.4(3)	C(54)-C(53)-H(53A)	109.9
O(21)-K(2)-C(52)	22.8(3)	O(21)-C(53)-H(53B)	109.9
O(23)-K(2)-C(52)	140.3(3)	C(54)-C(53)-H(53B)	109.9
O(18)-K(2)-C(52)	160.6(3)	H(53A)-C(53)-H(53B)	108.3
O(7)#2-K(2)-C(52)	63.4(3)	O(23)-C(56)-C(55)	110.3(10)
C(62)-K(2)-C(52)	106.7(3)	O(23)-C(56)-H(56A)	109.6
O(18)-C(47)-C(48)	110.1(10)	C(55)-C(56)-H(56A)	109.6
O(18)-C(47)-H(47A)	109.6	O(23)-C(56)-H(56B)	109.6
C(48)-C(47)-H(47A)	109.6	C(55)-C(56)-H(56B)	109.6
O(18)-C(47)-H(47B)	109.6	H(56A)-C(56)-H(56B)	108.1
C(48)-C(47)-H(47B)	109.6	O(17)-K(1)-O(15)	79.3(3)
H(47A)-C(47)-H(47B)	108.2	O(17)-K(1)-O(12)	92.8(3)
O(20)-C(51)-C(52)	109.3(8)	O(15)-K(1)-O(12)	172.0(3)
O(20)-C(51)-H(51A)	109.8	O(17)-K(1)-O(14)	78.5(3)
C(52)-C(51)-H(51A)	109.8	O(15)-K(1)-O(14)	61.8(3)
O(20)-C(51)-H(51B)	109.8	O(12)-K(1)-O(14)	117.3(3)
C(52)-C(51)-H(51B)	109.8	O(17)-K(1)-O(16)	78.1(3)
H(51A)-C(51)-H(51B)	108.3	O(15)-K(1)-O(16)	62.4(3)
O(22)-C(55)-C(56)	109.0(10)	O(12)-K(1)-O(16)	115.7(3)
O(22)-C(55)-H(55A)	109.9	O(14)-K(1)-O(16)	122.4(3)
C(56)-C(55)-H(55A)	109.9	O(17)-K(1)-O(11)	99.3(3)
O(22)-C(55)-H(55B)	109.9	O(15)-K(1)-O(11)	121.5(3)
C(56)-C(55)-H(55B)	109.9	O(12)-K(1)-O(11)	58.9(3)
H(55A)-C(55)-H(55B)	108.3	O(14)-K(1)-O(11)	175.8(3)
O(19)-C(49)-C(50)	108.3(9)	O(16)-K(1)-O(11)	60.2(3)
O(19)-C(49)-H(49A)	110.0	O(17)-K(1)-O(3)	144.9(3)

Table 5.15 Cont.

O(15)-K(1)-O(3)	68.9(3)	C(62)-C(61)-H(61B)	111.5
O(12)-K(1)-O(3)	118.6(3)	C(60)-C(61)-H(61B)	111.5
O(14)-K(1)-O(3)	98.3(3)	H(61A)-C(61)-H(61B)	109.3
O(16)-K(1)-O(3)	74.3(3)	O(24)-C(62)-C(61)	105.5(11)
O(11)-K(1)-O(3)	85.6(3)	O(24)-C(62)-K(2)	48.0(7)
O(17)-K(1)-O(13)	93.8(3)	C(61)-C(62)-K(2)	116.2(9)
O(15)-K(1)-O(13)	121.8(3)	O(24)-C(62)-H(62A)	110.6
O(12)-K(1)-O(13)	58.7(3)	C(61)-C(62)-H(62A)	110.6
O(14)-K(1)-O(13)	60.2(3)	K(2)-C(62)-H(62A)	63.1
O(16)-K(1)-O(13)	170.3(3)	O(24)-C(62)-H(62B)	110.6
O(11)-K(1)-O(13)	116.6(3)	C(61)-C(62)-H(62B)	110.6
O(3)-K(1)-O(13)	115.1(3)	K(2)-C(62)-H(62B)	132.2
O(17)-K(1)-C(39)	69.5(4)	H(62A)-C(62)-H(62B)	108.8
O(15)-K(1)-C(39)	21.9(4)	C(59)-C(60)-C(61)	103.5(10)
O(12)-K(1)-C(39)	153.0(4)	C(59)-C(60)-H(60A)	111.1
O(14)-K(1)-C(39)	79.9(4)	C(61)-C(60)-H(60A)	111.1
O(16)-K(1)-C(39)	42.5(4)	C(59)-C(60)-H(60B)	111.1
O(11)-K(1)-C(39)	102.7(4)	C(61)-C(60)-H(60B)	111.1
O(3)-K(1)-C(39)	75.5(3)	H(60A)-C(60)-H(60B)	109.0
O(13)-K(1)-C(39)	139.4(4)	C(44)-C(45)-C(46)	104.6(11)
O(17)-K(1)-C(41)	94.9(3)	C(44)-C(45)-H(45A)	110.8
O(15)-K(1)-C(41)	79.8(4)	C(46)-C(45)-H(45A)	110.8
O(12)-K(1)-C(41)	100.6(4)	C(44)-C(45)-H(45B)	110.8
O(14)-K(1)-C(41)	141.6(4)	C(46)-C(45)-H(45B)	110.8
O(16)-K(1)-C(41)	22.3(3)	H(45A)-C(45)-H(45B)	108.9
O(11)-K(1)-C(41)	41.8(3)	O(12)-C(33)-C(34)	108.2(11)
O(3)-K(1)-C(41)	65.8(3)	O(12)-C(33)-H(33A)	110.1
O(13)-K(1)-C(41)	157.9(4)	C(34)-C(33)-H(33A)	110.1
C(39)-K(1)-C(41)	62.6(4)	O(12)-C(33)-H(33B)	110.1
C(62)-C(61)-C(60)	101.6(10)	C(34)-C(33)-H(33B)	110.1
C(62)-C(61)-H(61A)	111.5	H(33A)-C(33)-H(33B)	108.4
C(60)-C(61)-H(61A)	111.5	O(11)-C(31)-C(32)	111.4(11)

Table 5.15 Cont.

O(11)-C(31)-H(31A)	109.4	O(17)-C(46)-H(46B)	110.6
C(32)-C(31)-H(31A)	109.4	C(45)-C(46)-H(46B)	110.6
O(11)-C(31)-H(31B)	109.4	H(46A)-C(46)-H(46B)	108.8
C(32)-C(31)-H(31B)	109.4	O(16)-C(41)-C(42)	107.7(11)
H(31A)-C(31)-H(31B)	108.0	O(16)-C(41)-K(1)	48.2(5)
O(15)-C(38)-C(37)	109.9(13)	C(42)-C(41)-K(1)	83.0(7)
O(15)-C(38)-H(38A)	109.7	O(16)-C(41)-H(41A)	110.2
C(37)-C(38)-H(38A)	109.7	C(42)-C(41)-H(41A)	110.2
O(15)-C(38)-H(38B)	109.7	K(1)-C(41)-H(41A)	158.2
C(37)-C(38)-H(38B)	109.7	O(16)-C(41)-H(41B)	110.2
H(38A)-C(38)-H(38B)	108.2	C(42)-C(41)-H(41B)	110.2
O(11)-C(42)-C(41)	109.0(11)	K(1)-C(41)-H(41B)	81.6
O(11)-C(42)-H(42A)	109.9	H(41A)-C(41)-H(41B)	108.5
C(41)-C(42)-H(42A)	109.9	O(14)-C(37)-C(38)	110.6(12)
O(11)-C(42)-H(42B)	109.9	O(14)-C(37)-H(37A)	109.5
C(41)-C(42)-H(42B)	109.9	C(38)-C(37)-H(37A)	109.5
H(42A)-C(42)-H(42B)	108.3	O(14)-C(37)-H(37B)	109.5
O(17)-C(43)-C(44)	101.1(11)	C(38)-C(37)-H(37B)	109.5
O(17)-C(43)-H(43A)	111.5	H(37A)-C(37)-H(37B)	108.1
C(44)-C(43)-H(43A)	111.5	C(35)-O(13)-C(34)	113.9(12)
O(17)-C(43)-H(43B)	111.5	C(35)-O(13)-K(1)	113.1(8)
C(44)-C(43)-H(43B)	111.5	C(34)-O(13)-K(1)	112.2(7)
H(43A)-C(43)-H(43B)	109.4	O(13)-C(34)-C(33)	110.2(11)
O(14)-C(36)-C(35)	109.9(11)	O(13)-C(34)-H(34A)	109.6
O(14)-C(36)-H(36A)	109.7	C(33)-C(34)-H(34A)	109.6
C(35)-C(36)-H(36A)	109.7	O(13)-C(34)-H(34B)	109.6
O(14)-C(36)-H(36B)	109.7	C(33)-C(34)-H(34B)	109.6
C(35)-C(36)-H(36B)	109.7	H(34A)-C(34)-H(34B)	108.1
H(36A)-C(36)-H(36B)	108.2	O(13)-C(35)-C(36)	110.2(12)
O(17)-C(46)-C(45)	105.5(11)	O(13)-C(35)-H(35A)	109.6
O(17)-C(46)-H(46A)	110.6	C(36)-C(35)-H(35A)	109.6
C(45)-C(46)-H(46A)	110.6	O(13)-C(35)-H(35B)	109.6

Table 5.15 Cont.

C(36)-C(35)-H(35B)	109.6	C(24)-C(25)-H(25)	121.0
H(35A)-C(35)-H(35B)	108.1	C(27)-C(28)-N(4)	124.4(11)
C(26)-C(25)-C(24)	118.0(10)	C(27)-C(28)-H(28)	117.8
C(26)-C(25)-H(25)	121.0	N(4)-C(28)-H(28)	117.8

Symmetry transformations used to generate equivalent atoms:

#1 x,-y-1,z+1/2 #2 x,-y-1,z-1/2

Table 5.16 Example input file for ADF 2007.1 for $Re(bipy)(CO)_3^-$

```
$ADFBIN/adf -n8 \
TITLE Bipy Anion
MAXMEMORYUSAGE 23000
RELATIVISTIC ZORA
UNRESTRICTED
CHARGE -1 0
SCF
DIIS
END
XC
 LDA VWN
 GGA Becke Perdew
END
SYMMETRY NOSYM
ATOMS
Re    13.4609   17.5774    3.7471
O    16.4404   18.1103    3.9397
O    13.9140   15.4275    1.5875
O    13.5729   15.2370    5.7157
N    12.5450   19.0365    2.5928
N    12.6663   18.9307    5.1196
C    15.2962   17.8988    3.8631
C    13.7389   16.2634    2.3828
C    13.5541   16.1297    4.9648
C    12.6935   18.7807    6.4941
H    13.0349   17.9675    6.8466
C    12.2658   19.7149    7.3645
H    12.2933   19.5523    8.2993
C    11.7728   20.9437    6.8650
H    11.4956   21.6286    7.4611
C    11.7036   21.1298    5.5288
H    11.3798   21.9557    5.1886
C    12.1116   20.1089    4.6216
C    12.0237   20.1613    3.2348
C    11.4685   21.2238    2.4962
H    11.1148   21.9773    2.9544
C    11.4287   21.1913    1.1416
H    11.0634   21.9159    0.6482
C    11.9447   20.0528    0.4796
H    11.9224   19.9986   -0.4689
C    12.4694   19.0427    1.2090
H    12.8094   18.2892    0.7432
END
GEOMETRY
 GO
END
BASIS
 type TZ2P
END
END INPUT
```

Table 5.17 Geometry optimized *xyz* coordinates for $[Re(bipy)(CO)_3]^-$ from ADF

Atom	X	Y	Z
Re	13.47469	17.57199	3.746709
O	16.51662	18.00957	3.929424
O	13.88504	15.44476	1.509608
O	13.56352	15.21905	5.778273
N	12.55176	19.05766	2.570975
N	12.66103	18.94675	5.151909
C	15.35167	17.83459	3.862036
C	13.72752	16.26509	2.342013
C	13.55114	16.1124	5.008633
C	12.71562	18.81532	6.517439
H	13.16415	17.89199	6.869393
C	12.25795	19.75729	7.399586
H	12.33635	19.57066	8.470645
C	11.69244	20.97029	6.892416
H	11.33417	21.74555	7.569906
C	11.61679	21.13308	5.53124
H	11.19743	22.04439	5.115227
C	12.08248	20.12981	4.640857
C	12.01465	20.18724	3.235158
C	11.44509	21.25164	2.485329
H	11.04412	22.10982	3.026072
C	11.38348	21.21463	1.114241
H	10.94069	22.03014	0.551331
C	11.91862	20.0664	0.450543
H	11.89746	19.97516	-0.63516
C	12.47268	19.05834	1.193501
H	12.8943	18.17568	0.715498

Table 5.18 Geometry optimized *xyz* coordinates for $[Re(dmb)(CO)_3]^-$ from ADF

Atom	X	Y	Z
Re	2.339501	4.608821	5.11787
N	1.805883	6.477139	4.30351
N	3.433946	6.022996	6.248902
O	-0.00273	3.0155	3.857272
O	2.389311	2.397474	7.287377
C	3.330158	7.381882	5.877689
O	4.273198	2.910554	3.44191
C	0.865737	6.687978	3.318837
H	0.379419	5.786953	2.947143
C	0.535828	7.915502	2.815014
H	-0.2318	7.982692	2.040961
C	1.205084	9.095198	3.294292
C	0.847949	10.45366	2.749944
H	-0.17468	10.75345	3.043411
H	0.874971	10.47123	1.646583
H	1.539237	11.22692	3.116654
C	2.150875	8.911809	4.273244
H	2.689217	9.776654	4.667948
C	2.452766	7.629383	4.809608
C	4.21358	5.742689	7.344468
H	4.294287	4.685015	7.59211
C	4.850306	6.687623	8.103018
H	5.43555	6.368334	8.96763
C	4.744734	8.077247	7.753387
C	5.387287	9.134379	8.612944
H	5.247746	10.1379	8.185265
H	6.470624	8.964204	8.737033
H	4.952003	9.140821	9.628638
C	4.001481	8.380338	6.638589
H	3.895477	9.423874	6.332624
C	0.885468	3.633273	4.327261
C	3.544832	3.588634	4.077624
C	2.388015	3.239559	6.461

Table 5.19 Geometry optimized *xyz* coordinates for $[Re(bipy\text{-}tBu)(CO)_3]^-$ from ADF

Atom	X	Y	Z
Re1	0.536714	1.381065	-0.833598
C1	1.13192	3.214844	-0.768546
C2	-1.093185	1.912348	-1.64912
C3	1.37484	1.178334	-2.555934
C4	0.401052	-1.676506	-1.46259
H4	0.524419	-1.306904	-2.477681
C5	0.271962	-3.019266	-1.222763
H5	0.303856	-3.694769	-2.074695
C6	0.098872	-3.50264	0.11749
C7	0.077756	-2.539753	1.105094
H7	-0.051004	-2.834852	2.147055
C8	0.22211	-1.156056	0.833505
C9	0.238145	-0.130762	1.798988
C10	0.117953	-0.32202	3.197314
H10	-0.015705	-1.344652	3.551552
C11	0.167304	0.715712	4.104612
C12	0.347367	2.025323	3.541019
H12	0.399406	2.913565	4.167289
C13	0.454233	2.190824	2.186593
H13	0.581222	3.183538	1.762001
C14	-0.044013	-4.995009	0.456281
C15	-0.032561	-5.871241	-0.809085
H15a	-0.85427	-5.606527	-1.488719
H15b	0.912093	-5.767909	-1.36051
H15c	-0.147772	-6.930275	-0.533054
C16	1.127316	-5.443314	1.361034
H16a	1.14728	-4.866999	2.295266
H16b	1.035774	-6.511398	1.618364
H16c	2.090208	-5.288419	0.854475
C17	-1.374341	-5.244274	1.202986
H17a	-1.427189	-4.657602	2.129144
H17b	-2.230273	-4.955092	0.5775
H17c	-1.479156	-6.309208	1.46693
C18	0.04751	0.459715	5.615171
C19	1.228821	-0.415173	6.096603
H19a	1.154162	-0.612541	7.178887
H19b	1.244004	-1.380296	5.573281
H19c	2.187151	0.084946	5.89937
C20	-1.275507	-0.277341	5.925667
H20a	-2.138519	0.325585	5.610274
H20b	-1.330205	-1.237441	5.396129

Table 5.19 Cont.

H20c	-1.365918	-0.478618	7.005784
C21	0.065813	1.770884	6.421235
H21a	-0.035667	1.551812	7.494927
H21b	1.007829	2.317721	6.277283
H21c	-0.76077	2.43383	6.130744
N1	0.387006	-0.706788	-0.492001
N2	0.411623	1.167047	1.266153
O1	1.511642	4.329432	-0.70028
O2	-2.098259	2.253439	-2.164843
O3	1.901737	1.006333	-3.596916

Table 5.20 Geometry optimized *xyz* coordinates for $[Re(bipy\text{-}OMe)(CO)_3]^-$ from ADF

Atom	X	Y	Z
Re	-7.57036	-4.29157	-15.1053
O	-6.94674	-8.16373	-20.1
N	-7.3544	-5.62011	-16.7679
O	-10.3498	-5.04314	-14.0122
O	-6.85593	-0.61143	-20.2181
C	-9.28143	-4.77351	-14.435
O	-6.10985	-6.09794	-13.0515
N	-7.32394	-3.04617	-16.7934
O	-7.42199	-1.90374	-13.1256
C	-7.0047	-1.4906	-19.1566
C	-7.4867	-2.82792	-13.8561
C	-6.80476	-7.61571	-21.4013
H	-6.71709	-8.46667	-22.0863
H	-7.68172	-7.00777	-21.6818
H	-5.90095	-6.98741	-21.4789
C	-6.68392	-5.42231	-13.8293
C	-6.75149	-1.19753	-21.5049
H	-6.63519	-0.36931	-22.2129
H	-5.87651	-1.86628	-21.5756
H	-7.65689	-1.7745	-21.7604
C	-7.07739	-7.25381	-19.0641
C	-7.28132	-1.66889	-16.7697
H	-7.38523	-1.2207	-15.7848
C	-7.04593	-2.85529	-19.2455
H	-6.96167	-3.35915	-20.2049
C	-7.19909	-3.65525	-18.0671
C	-7.21717	-7.82728	-17.7616
H	-7.2149	-8.90704	-17.6317
C	-7.12654	-0.87523	-17.8681
H	-7.09938	0.208423	-17.7727
C	-7.21516	-5.05008	-18.047
C	-7.08104	-5.89108	-19.2002
H	-6.97716	-5.42219	-20.1747
C	-7.3502	-6.98503	-16.6895
H	-7.46181	-7.38622	-15.6847

Table 5.21 Geometry optimized *xyz* coordinates for $[Re(bipy\text{-}CF_3)(CO)_3]^-$ from ADF

Atom	X	Y	Z
Re	14.87166	3.059365	0.108437
O	13.6384	1.222523	-2.03438
O	12.04059	4.099482	0.802251
O	14.80985	0.79413	2.233892
N	16.90187	3.465372	0.416919
N	15.29909	4.712282	-1.16625
C	14.10645	1.908414	-1.20153
C	13.10728	3.664295	0.565001
C	14.79488	1.651055	1.428894
C	17.74416	2.770129	1.273458
H	17.27571	1.950383	1.812547
C	19.06186	3.055916	1.461485
H	19.64779	2.457234	2.1569
C	19.65136	4.157317	0.748703
C	18.85563	4.852202	-0.13814
H	19.27093	5.690172	-0.69466
C	17.50163	4.5168	-0.32324
C	16.62128	5.177649	-1.20947
C	16.98716	6.205806	-2.10567
H	18.02729	6.52064	-2.1571
C	16.05028	6.796007	-2.92505
C	14.68969	6.355462	-2.83884
H	13.90871	6.802234	-3.45105
C	14.38466	5.341172	-1.97334
H	13.36653	4.966409	-1.89257
C	21.07434	4.500661	0.95836
F	21.41923	4.561993	2.292789
F	21.9527	3.569286	0.426513
F	21.43115	5.702126	0.410999
C	16.41748	7.855715	-3.89894
F	17.74994	8.149164	-3.90784
F	16.08915	7.524108	-5.19622
F	15.762	9.048456	-3.67125

Table 5.22 Geometry optimized *xyz* coordinates for [Re(bipy-*t*Bu)$(CO)_3(CO_2)$(K)] from ADF

Atom	X	Y	Z
Re1	-0.770017	0.812243	-0.525125
C1	-0.215189	0.393285	1.305915
C2	-0.760067	-1.071318	-0.961721
C3	1.068274	0.93293	-1.096108
C4	-3.750073	-0.027131	0.037431
H4	-3.382341	-0.970276	-0.356338
C5	-5.041344	0.088645	0.525417
H5	-5.675972	-0.794397	0.508073
C6	-5.50508	1.314911	1.035163
C7	-4.605151	2.380633	0.965222
H7	-4.906157	3.364895	1.318921
C8	-3.313391	2.218027	0.454889
C9	-2.340146	3.297151	0.337055
C10	-2.596415	4.622215	0.70273
H10	-3.568995	4.865816	1.125458
C11	-1.637769	5.625482	0.545193
C12	-0.421466	5.220989	-0.037713
H12	0.38055	5.931232	-0.225499
C13	-0.210384	3.896331	-0.381947
H13	0.723443	3.575634	-0.833593
C14	-6.903421	1.504609	1.641305
C15	-7.694845	2.540761	0.811281
H15a	-7.819239	2.203244	-0.227077
H15b	-8.693925	2.687828	1.2477
H15c	-7.189135	3.515676	0.793259
C16	-6.768266	2.02001	3.092941
H16a	-6.210101	1.306492	3.714579
H16b	-6.245488	2.984864	3.13489
H16c	-7.764434	2.159045	3.538304
C17	-7.697362	0.187437	1.665234
H17a	-8.682575	0.358586	2.120625
H17b	-7.86277	-0.207397	0.653392
H17c	-7.184896	-0.583076	2.25736
C18	-1.92514	7.064964	0.994337
C19	-3.136897	7.624505	0.214803
H19a	-2.937677	7.643878	-0.865677
H19b	-4.039743	7.021684	0.382778
H19c	-3.353154	8.651874	0.543379
C20	-2.252162	7.074979	2.505815
H20a	-1.411699	6.681817	3.093974
H20b	-2.456506	8.102751	2.840335

Table 5.22 Cont.

H20c	-3.137453	6.465832	2.733121
C21	-0.720246	7.99031	0.752647
H21a	-0.960317	9.004652	1.099154
H21b	0.168297	7.651582	1.302513
H21c	-0.463563	8.054242	-0.313574
C22	-1.408784	1.129889	-2.690726
N1	-2.866848	0.995755	0.025125
N2	-1.126782	2.920552	-0.180207
O1	0.110322	0.088974	2.385489
O2	-0.782213	-2.213096	-1.204893
O3	2.189237	1.030124	-1.411852
O4	-2.347448	0.430007	-3.189785
O5	-0.785641	2.04654	-3.322452
K1	-2.489982	2.037527	-5.149897

Table 5.23 Crystal data and structure refinement for $Re(bipy\text{-}CF_3)(CO)_3Cl \cdot ACN$

Identification code	eb_111214_0m	
Empirical formula	C17 H9 Cl F6 N3 O3 Re	
Formula weight	638.92	
Temperature	90(2) K	
Wavelength	0.71073 Å	
Crystal system	Orthorhombic	
Space group	Pnma	
Unit cell dimensions	a = 7.5968(4) Å	α= 90°.
	b = 14.9635(7) Å	β= 90°.
	c = 17.0710(10) Å	γ = 90°.
Volume	1940.54(18) $Å^3$	
Z	4	
Density (calculated)	2.187 Mg/m^3	
Absorption coefficient	6.482 mm^{-1}	
F(000)	1208	
Crystal size	0.50 x 0.15 x 0.10 mm^3	
Theta range for data collection	1.81 to 25.53°.	
Index ranges	-9<=h<=9, -18<=k<=16, -20<=l<=20	
Reflections collected	13272	
Independent reflections	1866 [R(int) = 0.0275]	
Completeness to theta = 25.00°	100.0 %	
Absorption correction	Semi-empirical from equivalents	
Max. and min. transmission	0.5634 and 0.1400	
Refinement method	Full-matrix least-squares on F^2	
Data / restraints / parameters	1866 / 0 / 152	
Goodness-of-fit on F^2	1.149	
Final R indices [I>2sigma(I)]	R1 = 0.0212, wR2 = 0.0488	
R indices (all data)	R1 = 0.0264, wR2 = 0.0513	
Largest diff. peak and hole	0.726 and -0.994 $e.Å^{-3}$	

Table 5.24 Bond lengths [Å] and angles [°] for Re(bipy-CF_3)$(CO)_3$Cl·ACN

Re(1)-C(1)	1.904(7)	C(2)#1-Re(1)-N(1)	98.00(16)
Re(1)-C(2)	1.915(5)	C(1)-Re(1)-N(1)#1	95.1(2)
Re(1)-C(2)#1	1.915(5)	C(2)-Re(1)-N(1)#1	98.00(16)
Re(1)-N(1)	2.164(3)	C(2)#1-Re(1)-N(1)#1	172.53(16)
Re(1)-N(1)#1	2.164(3)	N(1)-Re(1)-N(1)#1	74.74(17)
Re(1)-Cl(1)	2.4621(13)	C(1)-Re(1)-Cl(1)	177.4(3)
F(1)-C(8)	1.322(5)	C(2)-Re(1)-Cl(1)	94.65(12)
F(2)-C(8)	1.320(5)	C(2)#1-Re(1)-Cl(1)	94.65(12)
F(3)-C(8)	1.307(5)	N(1)-Re(1)-Cl(1)	82.82(9)
O(1)-C(1)	1.151(8)	N(1)#1-Re(1)-Cl(1)	82.82(9)
O(2)-C(2)	1.151(5)	C(3)-N(1)-C(7)	118.9(3)
N(1)-C(3)	1.351(5)	C(3)-N(1)-Re(1)	123.9(3)
N(1)-C(7)	1.353(5)	C(7)-N(1)-Re(1)	117.2(2)
N(1S)-C(1S)	1.135(15)	O(1)-C(1)-Re(1)	177.8(8)
C(1S)-C(2S)	1.492(18)	N(1S)-C(1S)-C(2S)	175.2(15)
C(2S)-H(2SA)	0.9800	O(2)-C(2)-Re(1)	178.0(4)
C(2S)-H(2SB)	0.9800	C(1S)-C(2S)-H(2SA)	109.5
C(2S)-H(2SC)	0.9800	C(1S)-C(2S)-H(2SB)	109.5
C(3)-C(4)	1.374(6)	C(1S)-C(2S)-H(2SC)	109.5
C(3)-H(3)	0.9500	N(1)-C(3)-C(4)	122.2(4)
C(4)-C(5)	1.383(6)	N(1)-C(3)-H(3)	118.9
C(4)-H(4)	0.9500	C(4)-C(3)-H(3)	118.9
C(5)-C(6)	1.386(6)	C(3)-C(4)-C(5)	118.7(4)
C(5)-C(8)	1.499(6)	C(3)-C(4)-H(4)	120.7
C(6)-C(7)	1.384(5)	C(5)-C(4)-H(4)	120.7
C(6)-H(6)	0.9500	C(4)-C(5)-C(6)	119.8(4)
C(7)-C(7)#1	1.471(7)	C(4)-C(5)-C(8)	119.6(4)
		C(6)-C(5)-C(8)	120.6(4)
C(1)-Re(1)-C(2)	87.2(2)	C(7)-C(6)-C(5)	118.7(4)
C(1)-Re(1)-C(2)#1	87.2(2)	C(7)-C(6)-H(6)	120.7
C(2)-Re(1)-C(2)#1	89.2(3)	C(5)-C(6)-H(6)	120.7
C(1)-Re(1)-N(1)	95.1(2)	N(1)-C(7)-C(6)	121.7(3)
C(2)-Re(1)-N(1)	172.53(15)	N(1)-C(7)-C(7)#1	115.3(2)

Table 5.24 Cont.

C(6)-C(7)-C(7)#1	123.0(2)	F(3)-C(8)-C(5)	113.5(4)
F(3)-C(8)-F(2)	106.3(4)	F(2)-C(8)-C(5)	112.0(4)
F(3)-C(8)-F(1)	107.1(4)	F(1)-C(8)-C(5)	112.3(4
F(2)-C(8)-F(1)	105.1(3)		

Symmetry transformations used to generate equivalent atoms:

#1 x,-y+3/2,z

Table 5.25 Crystal data and structure refinement for [Re(bipy-CF_3)$(CO)_3$Cl] [K(18-crown-6)]

Identification code	eb_111105_0ma	
Empirical formula	C29 H34 Cl F6 K N2 O9.50 Re	
Formula weight	937.33	
Temperature	100(2) K	
Wavelength	0.71073 Å	
Crystal system	Monoclinic	
Space group	C2/c	
Unit cell dimensions	a = 21.9399(18) Å	α= 90°.
	b = 17.4453(18) Å	β= 117.080(2)°.
	c = 20.978(2) Å	γ = 90°.
Volume	7148.9(12) $Å^3$	
Z	8	
Density (calculated)	1.742 Mg/m^3	
Absorption coefficient	3.675 mm^{-1}	
F(000)	3704	
Crystal size	0.10 x 0.05 x 0.05 mm^3	
Theta range for data collection	1.56 to 25.40°.	
Index ranges	-26<=h<=26, -21<=k<=21, -25<=l<=24	
Reflections collected	44785	
Independent reflections	6558 [R(int) = 0.0541]	
Completeness to theta = 25.00°	100.0 %	
Absorption correction	Semi-empirical from equivalents	
Max. and min. transmission	0.8376 and 0.7101	
Refinement method	Full-matrix least-squares on F^2	
Data / restraints / parameters	6558 / 0 / 481	
Goodness-of-fit on F^2	1.043	
Final R indices [I>2sigma(I)]	R1 = 0.0330, wR2 = 0.0673	
R indices (all data)	R1 = 0.0471, wR2 = 0.0744	
Largest diff. peak and hole	1.602 and -0.830 e.$Å^{-3}$	

Table 5.26 Bond lengths [Å] and angles [°] for [Re(bipy-CF_3)$(CO)_3$Cl] [K(18-crown-6)]

Re(1)-C(1A)	1.898(13)	O(1A)-K(1)#2	2.657(11)
Re(1)-C(1B)	1.90(3)	O(1B)-C(1B)	1.22(4)
Re(1)-C(2)	1.914(5)	O(1S)-C(1S)#3	1.460(8)
Re(1)-C(3)	1.916(5)	O(1S)-C(1S)	1.460(8)
Re(1)-N(1)	2.149(4)	O(2)-C(2)	1.159(6)
Re(1)-N(2)	2.150(4)	O(3)-C(3)	1.154(6)
Re(1)-Cl(1B)	2.443(9)	O(4)-C(27)	1.412(6)
Re(1)-Cl(1A)	2.481(3)	O(4)-C(16)	1.425(6)
K(1)-O(1A)#1	2.657(11)	O(5)-C(18)	1.408(7)
K(1)-O(8)	2.761(4)	O(5)-C(17)	1.418(7)
K(1)-O(6)	2.769(4)	O(6)-C(19)	1.413(7)
K(1)-O(4)	2.810(4)	O(6)-C(20)	1.422(7)
K(1)-O(7)	2.835(4)	O(7)-C(21)	1.419(7)
K(1)-O(9)	2.836(4)	O(7)-C(22)	1.425(7)
K(1)-O(5)	2.841(4)	O(8)-C(23)	1.408(7)
K(1)-O(1B)	2.877(17)	O(8)-C(24)	1.435(6)
K(1)-Cl(1A)	3.106(3)	O(9)-C(25)	1.418(6)
K(1)-Cl(1B)#1	3.373(12)	O(9)-C(26)	1.421(6)
Cl(1B)-K(1)#2	3.373(12)	N(1)-C(4)	1.357(6)
F(1)-C(14)	1.341(6)	N(1)-C(8)	1.381(6)
F(2)-C(14)	1.324(6)	N(2)-C(13)	1.350(6)
F(4B)-C(15)	1.402(14)	N(2)-C(9)	1.387(6)
F(6B)-C(15)	1.367(10)	C(1S)-C(2S)	1.449(8)
F(5)-C(14)	1.339(6)	C(1S)-H(1SA)	0.9900
F(5B)-C(15)	1.300(9)	C(1S)-H(1SB)	0.9900
F(6C)-C(15)	1.302(15)	C(2S)-C(2S)#3	1.486(12)
F(5A)-C(15)	1.341(15)	C(2S)-H(2SA)	0.9900
F(5C)-C(15)	1.552(18)	C(2S)-H(2SB)	0.9900
F(6A)-C(15)	1.509(19)	C(4)-C(5)	1.366(7)
F(4A)-C(15)	1.26(2)	C(4)-H(4)	0.9500
F(4C)-C(15)	1.23(3)	C(5)-C(6)	1.403(6)
O(1A)-C(1A)	1.167(19)	C(5)-H(5)	0.9500

Table 5.26 Cont.

C(6)-C(7)	1.373(6)	C(24)-C(25)	1.490(8)
C(6)-C(14)	1.486(7)	C(24)-H(24A)	0.9900
C(7)-C(8)	1.411(7)	C(24)-H(24B)	0.9900
C(7)-H(7)	0.9500	C(25)-H(25A)	0.9900
C(8)-C(9)	1.433(6)	C(25)-H(25B)	0.9900
C(9)-C(10)	1.404(6)	C(26)-C(27)	1.483(8)
C(10)-C(11)	1.368(7)	C(26)-H(26A)	0.9900
C(10)-H(10)	0.9500	C(26)-H(26B)	0.9900
C(11)-C(12)	1.416(7)	C(27)-H(27A)	0.9900
C(11)-C(15)	1.489(7)	C(27)-H(27B)	0.9900
C(12)-C(13)	1.363(7)		
C(12)-H(12)	0.9500	C(1A)-Re(1)-C(1B)	172.3(9)
C(13)-H(13)	0.9500	C(1A)-Re(1)-C(2)	89.4(4)
C(16)-C(17)	1.487(8)	C(1B)-Re(1)-C(2)	83.6(8)
C(16)-H(16A)	0.9900	C(1A)-Re(1)-C(3)	87.7(4)
C(16)-H(16B)	0.9900	C(1B)-Re(1)-C(3)	89.0(8)
C(17)-H(17A)	0.9900	C(2)-Re(1)-C(3)	87.9(2)
C(17)-H(17B)	0.9900	C(1A)-Re(1)-N(1)	91.8(4)
C(18)-C(19)	1.489(9)	C(1B)-Re(1)-N(1)	95.4(9)
C(18)-H(18A)	0.9900	C(2)-Re(1)-N(1)	175.97(17)
C(18)-H(18B)	0.9900	C(3)-Re(1)-N(1)	95.97(17)
C(19)-H(19A)	0.9900	C(1A)-Re(1)-N(2)	94.3(4)
C(19)-H(19B)	0.9900	C(1B)-Re(1)-N(2)	90.0(8)
C(20)-C(21)	1.488(9)	C(2)-Re(1)-N(2)	100.49(18)
C(20)-H(20A)	0.9900	C(3)-Re(1)-N(2)	171.37(17)
C(20)-H(20B)	0.9900	N(1)-Re(1)-N(2)	75.59(14)
C(21)-H(21A)	0.9900	C(1A)-Re(1)-Cl(1B)	7.9(6)
C(21)-H(21B)	0.9900	C(1B)-Re(1)-Cl(1B)	172.8(7)
C(22)-C(23)	1.494(9)	C(2)-Re(1)-Cl(1B)	90.9(3)
C(22)-H(22A)	0.9900	C(3)-Re(1)-Cl(1B)	95.5(3)
C(22)-H(22B)	0.9900	N(1)-Re(1)-Cl(1B)	89.7(2)
C(23)-H(23A)	0.9900	N(2)-Re(1)-Cl(1B)	86.4(3)
C(23)-H(23B)	0.9900	C(1A)-Re(1)-Cl(1A)	176.5(4)

Table 5.26 Cont.

C(1B)-Re(1)-Cl(1A)	10.9(9)	O(5)-K(1)-O(1B)	126.3(4)
C(2)-Re(1)-Cl(1A)	94.12(18)	O(1A)#1-K(1)-Cl(1A)	163.78(18)
C(3)-Re(1)-Cl(1A)	92.25(16)	O(8)-K(1)-Cl(1A)	73.11(9)
N(1)-Re(1)-Cl(1A)	84.72(14)	O(6)-K(1)-Cl(1A)	94.83(11)
N(2)-Re(1)-Cl(1A)	85.25(12)	O(4)-K(1)-Cl(1A)	106.92(11)
Cl(1B)-Re(1)-Cl(1A)	170.9(3)	O(7)-K(1)-Cl(1A)	85.82(10)
O(1A)#1-K(1)-O(8)	90.67(18)	O(9)-K(1)-Cl(1A)	90.74(11)
O(1A)#1-K(1)-O(6)	93.19(18)	O(5)-K(1)-Cl(1A)	123.07(10)
O(8)-K(1)-O(6)	120.89(13)	O(1B)-K(1)-Cl(1A)	15.5(5)
O(1A)#1-K(1)-O(4)	81.35(17)	O(1A)#1-K(1)-Cl(1B)#1	1.4(3)
O(8)-K(1)-O(4)	120.36(12)	O(8)-K(1)-Cl(1B)#1	90.37(18)
O(6)-K(1)-O(4)	118.52(12)	O(6)-K(1)-Cl(1B)#1	94.56(18)
O(1A)#1-K(1)-O(7)	85.86(17)	O(4)-K(1)-Cl(1B)#1	80.28(17)
O(8)-K(1)-O(7)	60.88(12)	O(7)-K(1)-Cl(1B)#1	86.94(17)
O(6)-K(1)-O(7)	60.65(12)	O(9)-K(1)-Cl(1B)#1	79.97(18)
O(4)-K(1)-O(7)	167.13(12)	O(5)-K(1)-Cl(1B)#1	73.47(18)
O(1A)#1-K(1)-O(9)	81.35(18)	O(1B)-K(1)-Cl(1B)#1	154.6(5)
O(8)-K(1)-O(9)	60.63(11)	Cl(1A)-K(1)-Cl(1B)#1	163.45(18)
O(6)-K(1)-O(9)	174.42(12)	Re(1)-Cl(1A)-K(1)	137.37(9)
O(4)-K(1)-O(9)	59.74(11)	Re(1)-Cl(1B)-K(1)#2	140.8(4)
O(7)-K(1)-O(9)	119.68(12)	C(1A)-O(1A)-K(1)#2	146.7(7)
O(1A)#1-K(1)-O(5)	73.12(18)	C(1B)-O(1B)-K(1)	119.1(16)
O(8)-K(1)-O(5)	163.70(12)	C(1S)#3-O(1S)-C(1S)	108.1(8)
O(6)-K(1)-O(5)	59.98(12)	C(27)-O(4)-C(16)	112.3(4)
O(4)-K(1)-O(5)	59.94(11)	C(27)-O(4)-K(1)	116.8(3)
O(7)-K(1)-O(5)	114.84(12)	C(16)-O(4)-K(1)	114.0(3)
O(9)-K(1)-O(5)	116.87(12)	C(18)-O(5)-C(17)	112.0(5)
O(1A)#1-K(1)-O(1B)	154.0(5)	C(18)-O(5)-K(1)	110.9(3)
O(8)-K(1)-O(1B)	68.6(4)	C(17)-O(5)-K(1)	114.1(3)
O(6)-K(1)-O(1B)	84.8(4)	C(19)-O(6)-C(20)	112.1(5)
O(4)-K(1)-O(1B)	122.3(5)	C(19)-O(6)-K(1)	117.9(3)
O(7)-K(1)-O(1B)	70.6(5)	C(20)-O(6)-K(1)	117.5(3)
O(9)-K(1)-O(1B)	100.6(4)	C(21)-O(7)-C(22)	112.8(5)

Table 5.26 Cont.

C(21)-O(7)-K(1)	108.2(3)	C(4)-C(5)-C(6)	118.1(4)
C(22)-O(7)-K(1)	111.6(3)	C(4)-C(5)-H(5)	120.9
C(23)-O(8)-C(24)	113.9(4)	C(6)-C(5)-H(5)	120.9
C(23)-O(8)-K(1)	115.7(3)	C(7)-C(6)-C(5)	119.7(5)
C(24)-O(8)-K(1)	117.2(3)	C(7)-C(6)-C(14)	120.4(4)
C(25)-O(9)-C(26)	112.9(4)	C(5)-C(6)-C(14)	119.9(4)
C(25)-O(9)-K(1)	108.9(3)	C(6)-C(7)-C(8)	119.9(4)
C(26)-O(9)-K(1)	109.6(3)	C(6)-C(7)-H(7)	120.0
C(4)-N(1)-C(8)	118.2(4)	C(8)-C(7)-H(7)	120.0
C(4)-N(1)-Re(1)	125.1(3)	N(1)-C(8)-C(7)	120.0(4)
C(8)-N(1)-Re(1)	116.7(3)	N(1)-C(8)-C(9)	115.4(4)
C(13)-N(2)-C(9)	117.5(4)	C(7)-C(8)-C(9)	124.6(4)
C(13)-N(2)-Re(1)	126.3(3)	N(2)-C(9)-C(10)	120.9(4)
C(9)-N(2)-Re(1)	116.1(3)	N(2)-C(9)-C(8)	116.0(4)
O(1A)-C(1A)-Re(1)	178.9(11)	C(10)-C(9)-C(8)	123.1(4)
O(1B)-C(1B)-Re(1)	178(2)	C(11)-C(10)-C(9)	119.8(5)
C(2S)-C(1S)-O(1S)	105.9(6)	C(11)-C(10)-H(10)	120.1
C(2S)-C(1S)-H(1SA)	110.6	C(9)-C(10)-H(10)	120.1
O(1S)-C(1S)-H(1SA)	110.6	C(10)-C(11)-C(12)	119.3(5)
C(2S)-C(1S)-H(1SB)	110.6	C(10)-C(11)-C(15)	120.5(5)
O(1S)-C(1S)-H(1SB)	110.6	C(12)-C(11)-C(15)	120.1(5)
H(1SA)-C(1S)-H(1SB)	108.7	C(13)-C(12)-C(11)	118.2(5)
O(2)-C(2)-Re(1)	178.8(4)	C(13)-C(12)-H(12)	120.9
C(1S)-C(2S)-C(2S)#3	104.8(4)	C(11)-C(12)-H(12)	120.9
C(1S)-C(2S)-H(2SA)	110.8	N(2)-C(13)-C(12)	124.2(5)
C(2S)#3-C(2S)-H(2SA)	110.8	N(2)-C(13)-H(13)	117.9
C(1S)-C(2S)-H(2SB)	110.8	C(12)-C(13)-H(13)	117.9
C(2S)#3-C(2S)-H(2SB)	110.8	F(2)-C(14)-F(5)	106.9(4)
H(2SA)-C(2S)-H(2SB)	108.9	F(2)-C(14)-F(1)	106.1(4)
O(3)-C(3)-Re(1)	178.0(5)	F(5)-C(14)-F(1)	104.0(4)
N(1)-C(4)-C(5)	123.9(4)	F(2)-C(14)-C(6)	114.4(4)
N(1)-C(4)-H(4)	118.1	F(5)-C(14)-C(6)	111.9(4)
C(5)-C(4)-H(4)	118.1	F(1)-C(14)-C(6)	112.7(4)

Table 5.26 Cont.

F(4C)-C(15)-F(4A)	27.8(14)	F(6B)-C(15)-F(6A)	24.2(5)
F(4C)-C(15)-F(5B)	109.5(14)	F(4B)-C(15)-F(6A)	83.7(10)
F(4A)-C(15)-F(5B)	86.8(9)	C(11)-C(15)-F(6A)	107.4(7)
F(4C)-C(15)-F(6C)	116.2(12)	F(4C)-C(15)-F(5C)	93.2(14)
F(4A)-C(15)-F(6C)	126.2(13)	F(4A)-C(15)-F(5C)	66.1(11)
F(5B)-C(15)-F(6C)	74.0(9)	F(5B)-C(15)-F(5C)	28.9(5)
F(4C)-C(15)-F(5A)	125.5(13)	F(6C)-C(15)-F(5C)	102.6(11)
F(4A)-C(15)-F(5A)	114.9(11)	F(5A)-C(15)-F(5C)	66.6(10)
F(5B)-C(15)-F(5A)	37.7(8)	F(6B)-C(15)-F(5C)	135.1(7)
F(6C)-C(15)-F(5A)	37.3(9)	F(4B)-C(15)-F(5C)	84.3(9)
F(4C)-C(15)-F(6B)	86.5(10)	C(11)-C(15)-F(5C)	105.9(7)
F(4A)-C(15)-F(6B)	109.8(14)	F(6A)-C(15)-F(5C)	146.6(8)
F(5B)-C(15)-F(6B)	110.5(6)	O(4)-C(16)-C(17)	107.7(5)
F(6C)-C(15)-F(6B)	41.0(9)	O(4)-C(16)-H(16A)	110.2
F(5A)-C(15)-F(6B)	77.3(9)	C(17)-C(16)-H(16A)	110.2
F(4C)-C(15)-F(4B)	18.0(11)	O(4)-C(16)-H(16B)	110.2
F(4A)-C(15)-F(4B)	20.2(10)	C(17)-C(16)-H(16B)	110.2
F(5B)-C(15)-F(4B)	106.9(8)	H(16A)-C(16)-H(16B)	108.5
F(6C)-C(15)-F(4B)	133.5(10)	O(5)-C(17)-C(16)	109.5(5)
F(5A)-C(15)-F(4B)	133.7(9)	O(5)-C(17)-H(17A)	109.8
F(6B)-C(15)-F(4B)	103.8(9)	C(16)-C(17)-H(17A)	109.8
F(4C)-C(15)-C(11)	120.3(12)	O(5)-C(17)-H(17B)	109.8
F(4A)-C(15)-C(11)	120.1(11)	C(16)-C(17)-H(17B)	109.8
F(5B)-C(15)-C(11)	114.1(6)	H(17A)-C(17)-H(17B)	108.2
F(6C)-C(15)-C(11)	113.6(7)	O(5)-C(18)-C(19)	109.3(5)
F(5A)-C(15)-C(11)	113.9(7)	O(5)-C(18)-H(18A)	109.8
F(6B)-C(15)-C(11)	112.8(5)	C(19)-C(18)-H(18A)	109.8
F(4B)-C(15)-C(11)	108.1(6)	O(5)-C(18)-H(18B)	109.8
F(4C)-C(15)-F(6A)	68.2(12)	C(19)-C(18)-H(18B)	109.8
F(4A)-C(15)-F(6A)	95.1(14)	H(18A)-C(18)-H(18B)	108.3
F(5B)-C(15)-F(6A)	130.5(7)	O(6)-C(19)-C(18)	108.9(5)
F(6C)-C(15)-F(6A)	65.2(10)	O(6)-C(19)-H(19A)	109.9
F(5A)-C(15)-F(6A)	100.9(11)	C(18)-C(19)-H(19A)	109.9

Table 5.26 Cont.

O(6)-C(19)-H(19B)	109.9	H(23A)-C(23)-H(23B)	108.4
C(18)-C(19)-H(19B)	109.9	O(8)-C(24)-C(25)	107.9(4)
H(19A)-C(19)-H(19B)	108.3	O(8)-C(24)-H(24A)	110.1
O(6)-C(20)-C(21)	109.7(5)	C(25)-C(24)-H(24A)	110.1
O(6)-C(20)-H(20A)	109.7	O(8)-C(24)-H(24B)	110.1
C(21)-C(20)-H(20A)	109.7	C(25)-C(24)-H(24B)	110.1
O(6)-C(20)-H(20B)	109.7	H(24A)-C(24)-H(24B)	108.4
C(21)-C(20)-H(20B)	109.7	O(9)-C(25)-C(24)	108.7(5)
H(20A)-C(20)-H(20B)	108.2	O(9)-C(25)-H(25A)	109.9
O(7)-C(21)-C(20)	109.3(5)	C(24)-C(25)-H(25A)	109.9
O(7)-C(21)-H(21A)	109.8	O(9)-C(25)-H(25B)	109.9
C(20)-C(21)-H(21A)	109.8	C(24)-C(25)-H(25B)	109.9
O(7)-C(21)-H(21B)	109.8	H(25A)-C(25)-H(25B)	108.3
C(20)-C(21)-H(21B)	109.8	O(9)-C(26)-C(27)	108.0(5)
H(21A)-C(21)-H(21B)	108.3	O(9)-C(26)-H(26A)	110.1
O(7)-C(22)-C(23)	110.1(5)	C(27)-C(26)-H(26A)	110.1
O(7)-C(22)-H(22A)	109.6	O(9)-C(26)-H(26B)	110.1
C(23)-C(22)-H(22A)	109.6	C(27)-C(26)-H(26B)	110.1
O(7)-C(22)-H(22B)	109.6	H(26A)-C(26)-H(26B)	108.4
C(23)-C(22)-H(22B)	109.6	O(4)-C(27)-C(26)	109.2(5)
H(22A)-C(22)-H(22B)	108.2	O(4)-C(27)-H(27A)	109.8
O(8)-C(23)-C(22)	108.1(5)	C(26)-C(27)-H(27A)	109.8
O(8)-C(23)-H(23A)	110.1	O(4)-C(27)-H(27B)	109.8
C(22)-C(23)-H(23A)	110.1	C(26)-C(27)-H(27B)	109.8
O(8)-C(23)-H(23B)	110.1	H(27A)-C(27)-H(27B)	108.3
C(22)-C(23)-H(23B)	110.1		

Symmetry transformations used to generate equivalent atoms:

#1 x,-y,z+1/2 #2 x,-y,z-1/2 #3 -x+1,y,-z+3/2

Table 5.27 Crystal data and structure refinement for Mn(bipy-*t*Bu)$(CO)_3$Br

Identification code	eb_111026mo_0m
Empirical formula	C21 H24 Br Mn N2 O3
Formula weight	487.27

Temperature	100(2) K	
Wavelength	0.71073 Å	
Crystal system	Monoclinic	
Space group	P2(1)/n	
Unit cell dimensions	a = 13.5528(5) Å	α= 90°.
	b = 17.1546(6) Å	β= 96.8790(10)°.
	c = 19.1899(6) Å	γ = 90°.
Volume	4429.4(3) $Å^3$	
Z	8	
Density (calculated)	1.461 Mg/m^3	
Absorption coefficient	2.423 mm^{-1}	
F(000)	1984	
Crystal size	0.10 x 0.05 x 0.05 mm^3	
Theta range for data collection	2.11 to 31.78°.	
Index ranges	-19<=h<=19, -25<=k<=23, -22<=l<=28	
Reflections collected	45311	
Independent reflections	13529 [R(int) = 0.0384]	
Completeness to theta = 25.00°	99.9 %	
Absorption correction	Semi-empirical from equivalents	
Max. and min. transmission	0.8885 and 0.7937	
Refinement method	Full-matrix least-squares on F^2	
Data / restraints / parameters	13529 / 0 / 517	
Goodness-of-fit on F^2	1.079	
Final R indices [I>2sigma(I)]	R1 = 0.0407, wR2 = 0.1031	
R indices (all data)	R1 = 0.0617, wR2 = 0.1103	
Largest diff. peak and hole	0.866 and -0.716 $e.Å^{-3}$	

Table 5.28 Bond lengths [Å] and angles [°] for Mn(bipy-*t*Bu)$(CO)_3$Br

Br(1)-Mn(1)	2.5101(5)	C(7)-H(7)	0.9500
Br(2)-Mn(2)	2.5234(5)	C(8)-C(9)	1.480(3)
Mn(1)-C(3)	1.806(3)	C(9)-C(10)	1.388(3)
Mn(1)-C(2)	1.813(3)	C(10)-C(11)	1.394(3)
Mn(1)-C(1)	1.848(3)	C(10)-H(10)	0.9500
Mn(1)-N(2)	2.040(2)	C(11)-C(12)	1.395(3)
Mn(1)-N(1)	2.045(2)	C(11)-C(18)	1.526(3)
Mn(2)-C(23)	1.810(3)	C(12)-C(13)	1.378(4)
Mn(2)-C(24)	1.815(3)	C(12)-H(12)	0.9500
Mn(2)-C(22)	1.848(3)	C(13)-H(13)	0.9500
Mn(2)-N(4)	2.038(2)	C(14)-C(17)	1.530(4)
Mn(2)-N(3)	2.046(2)	C(14)-C(16)	1.534(4)
O(1)-C(1)	1.091(3)	C(14)-C(15)	1.536(4)
O(2)-C(2)	1.144(3)	C(15)-H(15A)	0.9800
O(3)-C(3)	1.141(3)	C(15)-H(15B)	0.9800
O(4)-C(22)	1.082(3)	C(15)-H(15C)	0.9800
O(5)-C(23)	1.147(3)	C(16)-H(16A)	0.9800
O(6)-C(24)	1.145(3)	C(16)-H(16B)	0.9800
N(1)-C(4)	1.344(3)	C(16)-H(16C)	0.9800
N(1)-C(8)	1.349(3)	C(17)-H(17A)	0.9800
N(2)-C(13)	1.343(3)	C(17)-H(17B)	0.9800
N(2)-C(9)	1.357(3)	C(17)-H(17C)	0.9800
N(3)-C(25)	1.344(3)	C(18)-C(19)	1.533(4)
N(3)-C(29)	1.351(3)	C(18)-C(21)	1.536(4)
N(4)-C(34)	1.342(3)	C(18)-C(20)	1.536(4)
N(4)-C(30)	1.349(3)	C(19)-H(19A)	0.9800
C(4)-C(5)	1.386(3)	C(19)-H(19B)	0.9800
C(4)-H(4)	0.9500	C(19)-H(19C)	0.9800
C(5)-C(6)	1.397(4)	C(20)-H(20A)	0.9800
C(5)-H(5)	0.9500	C(20)-H(20B)	0.9800
C(6)-C(7)	1.394(3)	C(20)-H(20C)	0.9800
C(6)-C(14)	1.531(3)	C(21)-H(21A)	0.9800
C(7)-C(8)	1.397(3)	C(21)-H(21B)	0.9800

Table 5.28 Cont.

C(21)-H(21C)	0.9800	C(40)-H(40A)	0.9800
C(25)-C(26)	1.386(3)	C(40)-H(40B)	0.9800
C(25)-H(25)	0.9500	C(40)-H(40C)	0.9800
C(26)-C(27)	1.397(3)	C(41)-H(41A)	0.9800
C(26)-H(26)	0.9500	C(41)-H(41B)	0.9800
C(27)-C(28)	1.397(3)	C(41)-H(41C)	0.9800
C(27)-C(35)	1.531(3)	C(42)-H(42A)	0.9800
C(28)-C(29)	1.398(3)	C(42)-H(42B)	0.9800
C(28)-H(28)	0.9500	C(42)-H(42C)	0.9800
C(29)-C(30)	1.477(3)		
C(30)-C(31)	1.392(3)	C(3)-Mn(1)-C(2)	87.44(12)
C(31)-C(32)	1.399(3)	C(3)-Mn(1)-C(1)	90.02(11)
C(31)-H(31)	0.9500	C(2)-Mn(1)-C(1)	90.84(11)
C(32)-C(33)	1.397(3)	C(3)-Mn(1)-N(2)	96.98(10)
C(32)-C(39)	1.520(3)	C(2)-Mn(1)-N(2)	175.37(10)
C(33)-C(34)	1.381(3)	C(1)-Mn(1)-N(2)	90.54(9)
C(33)-H(33)	0.9500	C(3)-Mn(1)-N(1)	171.40(10)
C(34)-H(34)	0.9500	C(2)-Mn(1)-N(1)	97.01(10)
C(35)-C(37)	1.524(4)	C(1)-Mn(1)-N(1)	97.24(9)
C(35)-C(38)	1.526(4)	N(2)-Mn(1)-N(1)	78.42(8)
C(35)-C(36)	1.545(4)	C(3)-Mn(1)-Br(1)	85.66(9)
C(36)-H(36A)	0.9800	C(2)-Mn(1)-Br(1)	88.90(9)
C(36)-H(36B)	0.9800	C(1)-Mn(1)-Br(1)	175.68(7)
C(36)-H(36C)	0.9800	N(2)-Mn(1)-Br(1)	90.06(6)
C(37)-H(37A)	0.9800	N(1)-Mn(1)-Br(1)	87.07(6)
C(37)-H(37B)	0.9800	C(23)-Mn(2)-C(24)	87.04(12)
C(37)-H(37C)	0.9800	C(23)-Mn(2)-C(22)	86.32(13)
C(38)-H(38A)	0.9800	C(24)-Mn(2)-C(22)	93.69(11)
C(38)-H(38B)	0.9800	C(23)-Mn(2)-N(4)	177.60(11)
C(38)-H(38C)	0.9800	C(24)-Mn(2)-N(4)	95.28(10)
C(39)-C(42)	1.537(4)	C(22)-Mn(2)-N(4)	92.94(9)
C(39)-C(40)	1.538(4)	C(23)-Mn(2)-N(3)	99.33(10)
C(39)-C(41)	1.539(4)	C(24)-Mn(2)-N(3)	168.49(11)

Table 5.28 Cont.

C(22)-Mn(2)-N(3)	96.27(9)	C(8)-C(7)-H(7)	119.7
N(4)-Mn(2)-N(3)	78.48(8)	N(1)-C(8)-C(7)	122.0(2)
C(23)-Mn(2)-Br(2)	91.66(11)	N(1)-C(8)-C(9)	114.3(2)
C(24)-Mn(2)-Br(2)	85.01(9)	C(7)-C(8)-C(9)	123.7(2)
C(22)-Mn(2)-Br(2)	177.65(7)	N(2)-C(9)-C(10)	122.1(2)
N(4)-Mn(2)-Br(2)	89.14(6)	N(2)-C(9)-C(8)	113.7(2)
N(3)-Mn(2)-Br(2)	85.23(6)	C(10)-C(9)-C(8)	124.2(2)
C(4)-N(1)-C(8)	117.7(2)	C(9)-C(10)-C(11)	120.6(2)
C(4)-N(1)-Mn(1)	125.56(17)	C(9)-C(10)-H(10)	119.7
C(8)-N(1)-Mn(1)	116.65(16)	C(11)-C(10)-H(10)	119.7
C(13)-N(2)-C(9)	117.4(2)	C(10)-C(11)-C(12)	116.4(2)
C(13)-N(2)-Mn(1)	125.70(17)	C(10)-C(11)-C(18)	123.7(2)
C(9)-N(2)-Mn(1)	116.76(16)	C(12)-C(11)-C(18)	119.9(2)
C(25)-N(3)-C(29)	117.3(2)	C(13)-C(12)-C(11)	120.3(2)
C(25)-N(3)-Mn(2)	125.80(17)	C(13)-C(12)-H(12)	119.9
C(29)-N(3)-Mn(2)	116.01(16)	C(11)-C(12)-H(12)	119.9
C(34)-N(4)-C(30)	117.6(2)	N(2)-C(13)-C(12)	123.2(2)
C(34)-N(4)-Mn(2)	125.71(17)	N(2)-C(13)-H(13)	118.4
C(30)-N(4)-Mn(2)	116.70(16)	C(12)-C(13)-H(13)	118.4
O(1)-C(1)-Mn(1)	175.7(2)	C(17)-C(14)-C(6)	112.0(2)
O(2)-C(2)-Mn(1)	177.3(2)	C(17)-C(14)-C(16)	108.8(2)
O(3)-C(3)-Mn(1)	177.5(2)	C(6)-C(14)-C(16)	108.8(2)
N(1)-C(4)-C(5)	123.1(2)	C(17)-C(14)-C(15)	109.3(2)
N(1)-C(4)-H(4)	118.4	C(6)-C(14)-C(15)	108.8(2)
C(5)-C(4)-H(4)	118.4	C(16)-C(14)-C(15)	109.1(2)
C(4)-C(5)-C(6)	120.2(2)	C(14)-C(15)-H(15A)	109.5
C(4)-C(5)-H(5)	119.9	C(14)-C(15)-H(15B)	109.5
C(6)-C(5)-H(5)	119.9	H(15A)-C(15)-H(15B)	109.5
C(7)-C(6)-C(5)	116.4(2)	C(14)-C(15)-H(15C)	109.5
C(7)-C(6)-C(14)	123.5(2)	H(15A)-C(15)-H(15C)	109.5
C(5)-C(6)-C(14)	120.1(2)	H(15B)-C(15)-H(15C)	109.5
C(6)-C(7)-C(8)	120.6(2)	C(14)-C(16)-H(16A)	109.5
C(6)-C(7)-H(7)	119.7	C(14)-C(16)-H(16B)	109.5

Table 5.28 Cont.

H(16A)-C(16)-H(16B)	109.5	H(21B)-C(21)-H(21C)	109.5
C(14)-C(16)-H(16C)	109.5	O(4)-C(22)-Mn(2)	176.2(2)
H(16A)-C(16)-H(16C)	109.5	O(5)-C(23)-Mn(2)	173.0(3)
H(16B)-C(16)-H(16C)	109.5	O(6)-C(24)-Mn(2)	176.9(3)
C(14)-C(17)-H(17A)	109.5	N(3)-C(25)-C(26)	123.1(2)
C(14)-C(17)-H(17B)	109.5	N(3)-C(25)-H(25)	118.4
H(17A)-C(17)-H(17B)	109.5	C(26)-C(25)-H(25)	118.4
C(14)-C(17)-H(17C)	109.5	C(25)-C(26)-C(27)	120.4(2)
H(17A)-C(17)-H(17C)	109.5	C(25)-C(26)-H(26)	119.8
H(17B)-C(17)-H(17C)	109.5	C(27)-C(26)-H(26)	119.8
C(11)-C(18)-C(19)	111.8(2)	C(26)-C(27)-C(28)	116.3(2)
C(11)-C(18)-C(21)	109.5(2)	C(26)-C(27)-C(35)	120.9(2)
C(19)-C(18)-C(21)	109.0(2)	C(28)-C(27)-C(35)	122.8(2)
C(11)-C(18)-C(20)	108.7(2)	C(27)-C(28)-C(29)	120.3(2)
C(19)-C(18)-C(20)	108.6(2)	C(27)-C(28)-H(28)	119.8
C(21)-C(18)-C(20)	109.2(2)	C(29)-C(28)-H(28)	119.8
C(18)-C(19)-H(19A)	109.5	N(3)-C(29)-C(28)	122.5(2)
C(18)-C(19)-H(19B)	109.5	N(3)-C(29)-C(30)	114.2(2)
H(19A)-C(19)-H(19B)	109.5	C(28)-C(29)-C(30)	123.3(2)
C(18)-C(19)-H(19C)	109.5	N(4)-C(30)-C(31)	122.1(2)
H(19A)-C(19)-H(19C)	109.5	N(4)-C(30)-C(29)	114.0(2)
H(19B)-C(19)-H(19C)	109.5	C(31)-C(30)-C(29)	123.9(2)
C(18)-C(20)-H(20A)	109.5	C(30)-C(31)-C(32)	120.7(2)
C(18)-C(20)-H(20B)	109.5	C(30)-C(31)-H(31)	119.7
H(20A)-C(20)-H(20B)	109.5	C(32)-C(31)-H(31)	119.7
C(18)-C(20)-H(20C)	109.5	C(33)-C(32)-C(31)	116.0(2)
H(20A)-C(20)-H(20C)	109.5	C(33)-C(32)-C(39)	120.3(2)
H(20B)-C(20)-H(20C)	109.5	C(31)-C(32)-C(39)	123.7(2)
C(18)-C(21)-H(21A)	109.5	C(34)-C(33)-C(32)	120.4(2)
C(18)-C(21)-H(21B)	109.5	C(34)-C(33)-H(33)	119.8
H(21A)-C(21)-H(21B)	109.5	C(32)-C(33)-H(33)	119.8
C(18)-C(21)-H(21C)	109.5	N(4)-C(34)-C(33)	123.2(2)
H(21A)-C(21)-H(21C)	109.5	N(4)-C(34)-H(34)	118.4

Table 5.28 Cont.

C(33)-C(34)-H(34)	118.4	C(32)-C(39)-C(42)	110.7(2)
C(37)-C(35)-C(38)	109.7(3)	C(32)-C(39)-C(40)	111.4(2)
C(37)-C(35)-C(27)	112.0(2)	C(42)-C(39)-C(40)	108.6(2)
C(38)-C(35)-C(27)	108.6(2)	C(32)-C(39)-C(41)	108.1(2)
C(37)-C(35)-C(36)	108.1(2)	C(42)-C(39)-C(41)	108.5(2)
C(38)-C(35)-C(36)	109.0(2)	C(40)-C(39)-C(41)	109.5(2)
C(27)-C(35)-C(36)	109.5(2)	C(39)-C(40)-H(40A)	109.5
C(35)-C(36)-H(36A)	109.5	C(39)-C(40)-H(40B)	109.5
C(35)-C(36)-H(36B)	109.5	H(40A)-C(40)-H(40B)	109.5
H(36A)-C(36)-H(36B)	109.5	C(39)-C(40)-H(40C)	109.5
C(35)-C(36)-H(36C)	109.5	H(40A)-C(40)-H(40C)	109.5
H(36A)-C(36)-H(36C)	109.5	H(40B)-C(40)-H(40C)	109.5
H(36B)-C(36)-H(36C)	109.5	C(39)-C(41)-H(41A)	109.5
C(35)-C(37)-H(37A)	109.5	C(39)-C(41)-H(41B)	109.5
C(35)-C(37)-H(37B)	109.5	H(41A)-C(41)-H(41B)	109.5
H(37A)-C(37)-H(37B)	109.5	C(39)-C(41)-H(41C)	109.5
C(35)-C(37)-H(37C)	109.5	H(41A)-C(41)-H(41C)	109.5
H(37A)-C(37)-H(37C)	109.5	H(41B)-C(41)-H(41C)	109.5
H(37B)-C(37)-H(37C)	109.5	C(39)-C(42)-H(42A)	109.5
C(35)-C(38)-H(38A)	109.5	C(39)-C(42)-H(42B)	109.5
C(35)-C(38)-H(38B)	109.5	H(42A)-C(42)-H(42B)	109.5
H(38A)-C(38)-H(38B)	109.5	C(39)-C(42)-H(42C)	109.5
C(35)-C(38)-H(38C)	109.5	H(42A)-C(42)-H(42C)	109.5
H(38A)-C(38)-H(38C)	109.5	H(42B)-C(42)-H(42C)	109.5
H(38B)-C(38)-H(38C)	109.5		

Table 5.29 Crystal data and structure refinement for [Mn(bipy-tBu)$(CO)_3$] [K(18-crown-6)]

Identification code	eb_111019_0m	
Empirical formula	C74 H112 K2 Mn2 N4 O20	
Formula weight	1565.76	
Temperature	100(2) K	
Wavelength	1.54178 Å	
Crystal system	Monoclinic	
Space group	P2(1)/n	
Unit cell dimensions	a = 18.2559(4) Å	α= 90°.
	b = 18.4759(4) Å	β= 98.5560(10)°.
	c = 24.2973(5) Å	γ = 90°.
Volume	8104.1(3) $Å^3$	
Z	4	
Density (calculated)	1.283 Mg/m^3	
Absorption coefficient	4.023 mm^{-1}	
F(000)	3328	
Crystal size	0.10 x 0.10 x 0.01 mm^3	
Theta range for data collection	2.83 to 50.00°.	
Index ranges	-13<=h<=18, -18<=k<=18, -24<=l<=24	
Reflections collected	28572	
Independent reflections	8004 [R(int) = 0.0488]	
Completeness to theta = 50.00°	96.1 %	
Absorption correction	Semi-empirical from equivalents	
Max. and min. transmission	0.9609 and 0.6891	
Refinement method	Full-matrix least-squares on F^2	
Data / restraints / parameters	8004 / 0 / 957	
Goodness-of-fit on F^2	1.026	
Final R indices [I>2sigma(I)]	R1 = 0.0733, wR2 = 0.1941	
R indices (all data)	R1 = 0.1060, wR2 = 0.2255	
Largest diff. peak and hole	1.401 and -0.301 e.$Å^{-3}$	

Table 5.30 Bond lengths [Å] and angles [°] for [Mn(bipy-tBu)$(CO)_3$] [K(18-crown-6)]

Mn(1)-C(3A)	1.66(3)	O(2B)-C(2B)	1.16(3)
Mn(1)-C(1)	1.746(8)	O(3A)-C(3A)	1.22(3)
Mn(1)-C(2A)	1.796(13)	O(3B)-C(3B)	1.21(7)
Mn(1)-C(2B)	1.85(3)	O(4)-C(22)	1.168(9)
Mn(1)-N(2)	1.970(6)	O(5)-C(23)	1.183(9)
Mn(1)-C(3B)	1.98(6)	O(6)-C(24)	1.188(10)
Mn(1)-N(1)	1.987(6)	O(7)-C(44)	1.412(8)
Mn(2)-C(24)	1.765(9)	O(7)-C(45)	1.427(8)
Mn(2)-C(22)	1.773(9)	O(8)-C(47)	1.417(8)
Mn(2)-C(23)	1.785(8)	O(8)-C(46)	1.426(8)
Mn(2)-N(3)	1.980(5)	O(9)-C(49)	1.411(8)
Mn(2)-N(4)	1.992(5)	O(9)-C(48)	1.437(8)
K(1)-O(13)	2.698(6)	O(10)-C(51)	1.425(8)
K(1)-O(8)	2.742(5)	O(10)-C(50)	1.426(8)
K(1)-O(11)	2.785(5)	O(11)-C(53)	1.416(8)
K(1)-O(9)	2.791(5)	O(11)-C(52)	1.441(9)
K(1)-O(12)	2.814(5)	O(12)-C(43)	1.399(8)
K(1)-O(7)	2.836(5)	O(12)-C(54)	1.429(8)
K(1)-O(10)	2.895(5)	O(13)-C(55B)	1.31(2)
K(1)-O(2A)	3.012(9)	O(13)-C(58B)	1.380(14)
K(1)-C(55A)	3.52(6)	O(13)-C(55A)	1.40(6)
K(1)-C(55B)	3.53(2)	O(13)-C(58A)	1.65(5)
K(2)-O(20)	2.709(6)	O(14)-C(60)	1.413(8)
K(2)-O(15)	2.739(5)	O(14)-C(61)	1.432(8)
K(2)-O(18)	2.798(5)	O(15)-C(63)	1.420(8)
K(2)-O(16)	2.817(5)	O(15)-C(62)	1.421(9)
K(2)-O(14)	2.820(5)	O(16)-C(64)	1.424(8)
K(2)-O(17)	2.843(5)	O(16)-C(65)	1.433(8)
K(2)-O(5)	2.846(6)	O(17)-C(67)	1.426(8)
K(2)-O(19)	2.871(5)	O(17)-C(66)	1.433(8)
O(1)-C(1)	1.203(9)	O(18)-C(69)	1.405(8)
O(2A)-C(2A)	1.168(13)	O(18)-C(68)	1.428(8)

Table 5.30 Cont.

O(19)-C(59)	1.408(8)	C(15)-H(15A)	0.9800
O(19)-C(70)	1.417(8)	C(15)-H(15B)	0.9800
O(20)-C(71)	1.369(11)	C(15)-H(15C)	0.9800
O(20)-C(74A)	1.438(13)	C(16)-H(16A)	0.9800
O(20)-C(74B)	1.62(4)	C(16)-H(16B)	0.9800
N(1)-C(4)	1.350(9)	C(16)-H(16C)	0.9800
N(1)-C(8)	1.372(9)	C(17)-H(17A)	0.9800
N(2)-C(13)	1.366(9)	C(17)-H(17B)	0.9800
N(2)-C(9)	1.389(8)	C(17)-H(17C)	0.9800
N(3)-C(25)	1.376(9)	C(18)-C(21)	1.529(10)
N(3)-C(29)	1.395(9)	C(18)-C(19)	1.530(12)
N(4)-C(34)	1.360(8)	C(18)-C(20)	1.548(12)
N(4)-C(30)	1.385(9)	C(19)-H(19A)	0.9800
C(4)-C(5)	1.350(10)	C(19)-H(19B)	0.9800
C(4)-H(4)	0.9500	C(19)-H(19C)	0.9800
C(5)-C(6)	1.405(10)	C(20)-H(20A)	0.9800
C(5)-H(5)	0.9500	C(20)-H(20B)	0.9800
C(6)-C(7)	1.360(10)	C(20)-H(20C)	0.9800
C(6)-C(14)	1.526(10)	C(21)-H(21A)	0.9800
C(7)-C(8)	1.413(9)	C(21)-H(21B)	0.9800
C(7)-H(7)	0.9500	C(21)-H(21C)	0.9800
C(8)-C(9)	1.414(9)	C(25)-C(26)	1.351(10)
C(9)-C(10)	1.427(10)	C(25)-H(25)	0.9500
C(10)-C(11)	1.346(10)	C(26)-C(27)	1.437(10)
C(10)-H(10)	0.9500	C(26)-H(26)	0.9500
C(11)-C(12)	1.443(10)	C(27)-C(28)	1.361(9)
C(11)-C(18)	1.519(10)	C(27)-C(35)	1.514(10)
C(12)-C(13)	1.367(10)	C(28)-C(29)	1.403(10)
C(12)-H(12)	0.9500	C(28)-H(28)	0.9500
C(13)-H(13)	0.9500	C(29)-C(30)	1.406(10)
C(14)-C(15)	1.515(10)	C(30)-C(31)	1.430(10)
C(14)-C(17)	1.536(11)	C(31)-C(32)	1.363(10)
C(14)-C(16)	1.544(10)	C(31)-H(31)	0.9500

Table 5.30 Cont.

C(32)-C(33)	1.428(10)	C(44)-H(44B)	0.9900
C(32)-C(39)	1.507(10)	C(45)-C(46)	1.482(10)
C(33)-C(34)	1.349(10)	C(45)-H(45A)	0.9900
C(33)-H(33)	0.9500	C(45)-H(45B)	0.9900
C(34)-H(34)	0.9500	C(46)-H(46A)	0.9900
C(35)-C(38)	1.518(11)	C(46)-H(46B)	0.9900
C(35)-C(36)	1.519(10)	C(47)-C(48)	1.509(9)
C(35)-C(37)	1.527(10)	C(47)-H(47A)	0.9900
C(36)-H(36A)	0.9800	C(47)-H(47B)	0.9900
C(36)-H(36B)	0.9800	C(48)-H(48A)	0.9900
C(36)-H(36C)	0.9800	C(48)-H(48B)	0.9900
C(37)-H(37A)	0.9800	C(49)-C(50)	1.507(9)
C(37)-H(37B)	0.9800	C(49)-H(49A)	0.9900
C(37)-H(37C)	0.9800	C(49)-H(49B)	0.9900
C(38)-H(38A)	0.9800	C(50)-H(50A)	0.9900
C(38)-H(38B)	0.9800	C(50)-H(50B)	0.9900
C(38)-H(38C)	0.9800	C(51)-C(52)	1.504(10)
C(39)-C(40)	1.512(11)	C(51)-H(51A)	0.9900
C(39)-C(41)	1.542(10)	C(51)-H(51B)	0.9900
C(39)-C(42)	1.552(10)	C(52)-H(52A)	0.9900
C(40)-H(40A)	0.9800	C(52)-H(52B)	0.9900
C(40)-H(40B)	0.9800	C(53)-C(54)	1.495(10)
C(40)-H(40C)	0.9800	C(53)-H(53A)	0.9900
C(41)-H(41A)	0.9800	C(53)-H(53B)	0.9900
C(41)-H(41B)	0.9800	C(54)-H(54A)	0.9900
C(41)-H(41C)	0.9800	C(54)-H(54B)	0.9900
C(42)-H(42A)	0.9800	C(55A)-C(56A)	1.81(7)
C(42)-H(42B)	0.9800	C(55A)-H(55A)	0.9900
C(42)-H(42C)	0.9800	C(55A)-H(55B)	0.9900
C(43)-C(44)	1.493(10)	C(55B)-C(56B)	1.51(2)
C(43)-H(43A)	0.9900	C(55B)-C(58A)	1.96(5)
C(43)-H(43B)	0.9900	C(55B)-H(55C)	0.9900
C(44)-H(44A)	0.9900	C(55B)-H(55D)	0.9900

Table 5.30 Cont.

C(56A)-C(57)	1.21(5)	C(65)-H(65A)	0.9900
C(56A)-H(56A)	0.9900	C(65)-H(65B)	0.9900
C(56A)-H(56B)	0.9900	C(66)-H(66A)	0.9900
C(56B)-C(57)	1.546(17)	C(66)-H(66B)	0.9900
C(56B)-C(58A)	2.00(5)	C(67)-C(68)	1.500(10)
C(56B)-H(56C)	0.9900	C(67)-H(67A)	0.9900
C(56B)-H(56D)	0.9900	C(67)-H(67B)	0.9900
C(57)-C(58B)	1.402(16)	C(68)-H(68A)	0.9900
C(57)-C(58A)	1.43(5)	C(68)-H(68B)	0.9900
C(57)-H(57C)	0.9900	C(69)-C(70)	1.493(10)
C(57)-H(57D)	0.9900	C(69)-H(69A)	0.9900
C(57)-H(57A)	0.9900	C(69)-H(69B)	0.9900
C(57)-H(57B)	0.9900	C(70)-H(70A)	0.9900
C(58A)-H(58A)	0.9900	C(70)-H(70B)	0.9900
C(58A)-H(58B)	0.9900	C(71)-C(72)	1.438(13)
C(58B)-H(58C)	0.9900	C(71)-H(71A)	0.9900
C(58B)-H(58D)	0.9900	C(71)-H(71B)	0.9900
C(59)-C(60)	1.486(10)	C(72)-C(73A)	1.446(14)
C(59)-H(59A)	0.9900	C(72)-C(73B)	1.52(3)
C(59)-H(59B)	0.9900	C(72)-H(72C)	0.9900
C(60)-H(60A)	0.9900	C(72)-H(72D)	0.9900
C(60)-H(60B)	0.9900	C(72)-H(72A)	0.9900
C(61)-C(62)	1.489(10)	C(72)-H(72B)	0.9900
C(61)-H(61A)	0.9900	C(73A)-C(74A)	1.529(16)
C(61)-H(61B)	0.9900	C(73A)-H(73A)	0.9900
C(62)-H(62A)	0.9900	C(73A)-H(73B)	0.9900
C(62)-H(62B)	0.9900	C(73B)-C(74B)	1.56(4)
C(63)-C(64)	1.486(10)	C(73B)-H(73C)	0.9900
C(63)-H(63A)	0.9900	C(73B)-H(73D)	0.9900
C(63)-H(63B)	0.9900	C(74A)-H(74A)	0.9900
C(64)-H(64A)	0.9900	C(74A)-H(74B)	0.9900
C(64)-H(64B)	0.9900	C(74B)-H(74C)	0.9900
C(65)-C(66)	1.498(9)	C(74B)-H(74D)	0.9900

Table 5.30 Cont.

		O(13)-K(1)-O(11)	80.81(17)
C(3A)-Mn(1)-C(1)	86.0(8)	O(8)-K(1)-O(11)	168.43(15)
C(3A)-Mn(1)-C(2A)	104.2(15)	O(13)-K(1)-O(9)	76.61(17)
C(1)-Mn(1)-C(2A)	89.2(5)	O(8)-K(1)-O(9)	60.57(13)
C(3A)-Mn(1)-C(2B)	66.8(18)	O(11)-K(1)-O(9)	118.50(15)
C(1)-Mn(1)-C(2B)	95.0(9)	O(13)-K(1)-O(12)	97.13(18)
C(2A)-Mn(1)-C(2B)	38.4(10)	O(8)-K(1)-O(12)	120.13(14)
C(3A)-Mn(1)-N(2)	143.3(14)	O(11)-K(1)-O(12)	59.38(14)
C(1)-Mn(1)-N(2)	94.9(3)	O(9)-K(1)-O(12)	173.73(15)
C(2A)-Mn(1)-N(2)	112.5(6)	O(13)-K(1)-O(7)	86.3(2)
C(2B)-Mn(1)-N(2)	149.0(12)	O(8)-K(1)-O(7)	60.09(13)
C(3A)-Mn(1)-C(3B)	17.5(16)	O(11)-K(1)-O(7)	116.16(15)
C(1)-Mn(1)-C(3B)	88.3(17)	O(9)-K(1)-O(7)	118.42(14)
C(2A)-Mn(1)-C(3B)	122(2)	O(12)-K(1)-O(7)	60.80(14)
C(2B)-Mn(1)-C(3B)	84(2)	O(13)-K(1)-O(10)	81.30(19)
N(2)-Mn(1)-C(3B)	125.8(19)	O(8)-K(1)-O(10)	120.87(14)
C(3A)-Mn(1)-N(1)	95.5(8)	O(11)-K(1)-O(10)	60.10(13)
C(1)-Mn(1)-N(1)	171.3(3)	O(9)-K(1)-O(10)	60.36(13)
C(2A)-Mn(1)-N(1)	98.7(5)	O(12)-K(1)-O(10)	118.86(14)
C(2B)-Mn(1)-N(1)	93.5(9)	O(7)-K(1)-O(10)	167.48(15)
N(2)-Mn(1)-N(1)	78.8(2)	O(13)-K(1)-O(2A)	160.5(2)
C(3B)-Mn(1)-N(1)	90.7(16)	O(8)-K(1)-O(2A)	75.80(18)
C(24)-Mn(2)-C(22)	91.3(4)	O(11)-K(1)-O(2A)	114.73(18)
C(24)-Mn(2)-C(23)	88.9(4)	O(9)-K(1)-O(2A)	103.7(2)
C(22)-Mn(2)-C(23)	97.2(4)	O(12)-K(1)-O(2A)	82.3(2)
C(24)-Mn(2)-N(3)	93.0(3)	O(7)-K(1)-O(2A)	76.4(2)
C(22)-Mn(2)-N(3)	139.7(3)	O(10)-K(1)-O(2A)	116.2(2)
C(23)-Mn(2)-N(3)	122.9(3)	O(13)-K(1)-C(55A)	21.3(11)
C(24)-Mn(2)-N(4)	171.7(3)	O(8)-K(1)-C(55A)	90.1(9)
C(22)-Mn(2)-N(4)	95.8(3)	O(11)-K(1)-C(55A)	78.4(9)
C(23)-Mn(2)-N(4)	94.6(3)	O(9)-K(1)-C(55A)	96.1(10)
N(3)-Mn(2)-N(4)	78.8(2)	O(12)-K(1)-C(55A)	77.7(10)
O(13)-K(1)-O(8)	87.91(17)	O(7)-K(1)-C(55A)	69.2(11)

Table 5.30 Cont.

O(10)-K(1)-C(55A)	98.3(11)	O(15)-K(2)-O(19)	119.96(15)
O(2A)-K(1)-C(55A)	145.4(12)	O(18)-K(2)-O(19)	58.30(13)
O(13)-K(1)-C(55B)	19.0(3)	O(16)-K(2)-O(19)	172.98(14)
O(8)-K(1)-C(55B)	98.6(3)	O(14)-K(2)-O(19)	59.84(14)
O(11)-K(1)-C(55B)	69.8(3)	O(17)-K(2)-O(19)	118.51(14)
O(9)-K(1)-C(55B)	95.6(3)	O(5)-K(2)-O(19)	104.05(16)
O(12)-K(1)-C(55B)	78.2(3)	C(2A)-O(2A)-K(1)	127.6(10)
O(7)-K(1)-C(55B)	78.4(4)	C(23)-O(5)-K(2)	122.9(5)
O(10)-K(1)-C(55B)	89.3(4)	C(44)-O(7)-C(45)	112.4(5)
O(2A)-K(1)-C(55B)	153.4(4)	C(44)-O(7)-K(1)	109.6(4)
C(55A)-K(1)-C(55B)	10.1(12)	C(45)-O(7)-K(1)	113.4(4)
O(20)-K(2)-O(15)	86.82(18)	C(47)-O(8)-C(46)	112.7(5)
O(20)-K(2)-O(18)	79.81(17)	C(47)-O(8)-K(1)	118.3(4)
O(15)-K(2)-O(18)	165.96(15)	C(46)-O(8)-K(1)	117.2(4)
O(20)-K(2)-O(16)	75.77(16)	C(49)-O(9)-C(48)	113.2(5)
O(15)-K(2)-O(16)	59.90(14)	C(49)-O(9)-K(1)	113.4(4)
O(18)-K(2)-O(16)	119.87(14)	C(48)-O(9)-K(1)	109.6(4)
O(20)-K(2)-O(14)	86.76(19)	C(51)-O(10)-C(50)	111.7(5)
O(15)-K(2)-O(14)	60.66(14)	C(51)-O(10)-K(1)	110.4(4)
O(18)-K(2)-O(14)	113.83(14)	C(50)-O(10)-K(1)	110.4(4)
O(16)-K(2)-O(14)	118.51(15)	C(53)-O(11)-C(52)	112.4(5)
O(20)-K(2)-O(17)	81.12(19)	C(53)-O(11)-K(1)	117.3(4)
O(15)-K(2)-O(17)	121.27(14)	C(52)-O(11)-K(1)	116.8(4)
O(18)-K(2)-O(17)	61.04(13)	C(43)-O(12)-C(54)	112.0(5)
O(16)-K(2)-O(17)	61.40(13)	C(43)-O(12)-K(1)	114.8(4)
O(14)-K(2)-O(17)	167.49(14)	C(54)-O(12)-K(1)	116.3(4)
O(20)-K(2)-O(5)	158.20(18)	C(55B)-O(13)-C(58B)	110.7(11)
O(15)-K(2)-O(5)	78.54(15)	C(55B)-O(13)-C(55A)	26(3)
O(18)-K(2)-O(5)	115.49(15)	C(58B)-O(13)-C(55A)	99(2)
O(16)-K(2)-O(5)	82.90(16)	C(55B)-O(13)-C(58A)	82.1(18)
O(14)-K(2)-O(5)	99.74(16)	C(58B)-O(13)-C(58A)	44.0(16)
O(17)-K(2)-O(5)	92.69(16)	C(55A)-O(13)-C(58A)	61(3)
O(20)-K(2)-O(19)	97.22(16)	C(55B)-O(13)-K(1)	118.9(10)

Table 5.30 Cont.

C(58B)-O(13)-K(1)	124.2(7)	C(25)-N(3)-C(29)	114.7(6)
C(55A)-O(13)-K(1)	114(3)	C(25)-N(3)-Mn(2)	127.6(5)
C(58A)-O(13)-K(1)	119.7(17)	C(29)-N(3)-Mn(2)	117.4(5)
C(60)-O(14)-C(61)	111.6(5)	C(34)-N(4)-C(30)	117.3(6)
C(60)-O(14)-K(2)	110.8(4)	C(34)-N(4)-Mn(2)	126.4(5)
C(61)-O(14)-K(2)	112.8(4)	C(30)-N(4)-Mn(2)	116.2(5)
C(63)-O(15)-C(62)	113.4(6)	O(1)-C(1)-Mn(1)	178.2(8)
C(63)-O(15)-K(2)	119.5(4)	O(2A)-C(2A)-Mn(1)	178.6(11)
C(62)-O(15)-K(2)	116.5(4)	O(2B)-C(2B)-Mn(1)	173(3)
C(64)-O(16)-C(65)	113.4(5)	O(3A)-C(3A)-Mn(1)	175(2)
C(64)-O(16)-K(2)	109.1(4)	O(3B)-C(3B)-Mn(1)	173(5)
C(65)-O(16)-K(2)	109.5(4)	C(5)-C(4)-N(1)	125.2(7)
C(67)-O(17)-C(66)	111.9(5)	C(5)-C(4)-H(4)	117.4
C(67)-O(17)-K(2)	110.1(4)	N(1)-C(4)-H(4)	117.4
C(66)-O(17)-K(2)	111.3(4)	C(4)-C(5)-C(6)	120.3(7)
C(69)-O(18)-C(68)	113.1(5)	C(4)-C(5)-H(5)	119.8
C(69)-O(18)-K(2)	119.2(4)	C(6)-C(5)-H(5)	119.8
C(68)-O(18)-K(2)	114.5(4)	C(7)-C(6)-C(5)	115.3(6)
C(59)-O(19)-C(70)	112.9(5)	C(7)-C(6)-C(14)	124.5(7)
C(59)-O(19)-K(2)	114.9(4)	C(5)-C(6)-C(14)	120.1(7)
C(70)-O(19)-K(2)	116.3(4)	C(6)-C(7)-C(8)	123.2(7)
C(71)-O(20)-C(74A)	107.3(8)	C(6)-C(7)-H(7)	118.4
C(71)-O(20)-C(74B)	86.8(16)	C(8)-C(7)-H(7)	118.4
C(74A)-O(20)-C(74B)	48.0(13)	N(1)-C(8)-C(7)	119.8(6)
C(71)-O(20)-K(2)	126.7(6)	N(1)-C(8)-C(9)	113.6(6)
C(74A)-O(20)-K(2)	121.5(6)	C(7)-C(8)-C(9)	126.5(7)
C(74B)-O(20)-K(2)	109.5(10)	N(2)-C(9)-C(8)	113.3(6)
C(4)-N(1)-C(8)	116.1(6)	N(2)-C(9)-C(10)	121.1(6)
C(4)-N(1)-Mn(1)	126.6(5)	C(8)-C(9)-C(10)	125.6(6)
C(8)-N(1)-Mn(1)	117.1(5)	C(11)-C(10)-C(9)	122.9(7)
C(13)-N(2)-C(9)	115.3(6)	C(11)-C(10)-H(10)	118.6
C(13)-N(2)-Mn(1)	127.5(5)	C(9)-C(10)-H(10)	118.6
C(9)-N(2)-Mn(1)	117.1(4)	C(10)-C(11)-C(12)	115.6(7)

Table 5.30 Cont.

C(10)-C(11)-C(18)	125.1(7)	C(11)-C(18)-C(19)	111.9(7)
C(12)-C(11)-C(18)	119.3(7)	C(21)-C(18)-C(19)	107.8(7)
C(13)-C(12)-C(11)	120.2(7)	C(11)-C(18)-C(20)	109.6(7)
C(13)-C(12)-H(12)	119.9	C(21)-C(18)-C(20)	107.9(7)
C(11)-C(12)-H(12)	119.9	C(19)-C(18)-C(20)	109.6(8)
N(2)-C(13)-C(12)	124.9(7)	C(18)-C(19)-H(19A)	109.5
N(2)-C(13)-H(13)	117.6	C(18)-C(19)-H(19B)	109.5
C(12)-C(13)-H(13)	117.6	H(19A)-C(19)-H(19B)	109.5
C(15)-C(14)-C(6)	110.1(6)	C(18)-C(19)-H(19C)	109.5
C(15)-C(14)-C(17)	108.6(7)	H(19A)-C(19)-H(19C)	109.5
C(6)-C(14)-C(17)	112.5(7)	H(19B)-C(19)-H(19C)	109.5
C(15)-C(14)-C(16)	108.6(7)	C(18)-C(20)-H(20A)	109.5
C(6)-C(14)-C(16)	109.8(6)	C(18)-C(20)-H(20B)	109.5
C(17)-C(14)-C(16)	107.1(6)	H(20A)-C(20)-H(20B)	109.5
C(14)-C(15)-H(15A)	109.5	C(18)-C(20)-H(20C)	109.5
C(14)-C(15)-H(15B)	109.5	H(20A)-C(20)-H(20C)	109.5
H(15A)-C(15)-H(15B)	109.5	H(20B)-C(20)-H(20C)	109.5
C(14)-C(15)-H(15C)	109.5	C(18)-C(21)-H(21A)	109.5
H(15A)-C(15)-H(15C)	109.5	C(18)-C(21)-H(21B)	109.5
H(15B)-C(15)-H(15C)	109.5	H(21A)-C(21)-H(21B)	109.5
C(14)-C(16)-H(16A)	109.5	C(18)-C(21)-H(21C)	109.5
C(14)-C(16)-H(16B)	109.5	H(21A)-C(21)-H(21C)	109.5
H(16A)-C(16)-H(16B)	109.5	H(21B)-C(21)-H(21C)	109.5
C(14)-C(16)-H(16C)	109.5	O(4)-C(22)-Mn(2)	179.0(8)
H(16A)-C(16)-H(16C)	109.5	O(5)-C(23)-Mn(2)	179.2(7)
H(16B)-C(16)-H(16C)	109.5	O(6)-C(24)-Mn(2)	178.6(9)
C(14)-C(17)-H(17A)	109.5	C(26)-C(25)-N(3)	124.8(7)
C(14)-C(17)-H(17B)	109.5	C(26)-C(25)-H(25)	117.6
H(17A)-C(17)-H(17B)	109.5	N(3)-C(25)-H(25)	117.6
C(14)-C(17)-H(17C)	109.5	C(25)-C(26)-C(27)	121.2(7)
H(17A)-C(17)-H(17C)	109.5	C(25)-C(26)-H(26)	119.4
H(17B)-C(17)-H(17C)	109.5	C(27)-C(26)-H(26)	119.4
C(11)-C(18)-C(21)	109.9(6)	C(28)-C(27)-C(26)	114.4(6)

Table 5.30 Cont.

C(28)-C(27)-C(35)	126.1(7)	H(36A)-C(36)-H(36C)	109.5
C(26)-C(27)-C(35)	119.5(7)	H(36B)-C(36)-H(36C)	109.5
C(27)-C(28)-C(29)	123.6(7)	C(35)-C(37)-H(37A)	109.5
C(27)-C(28)-H(28)	118.2	C(35)-C(37)-H(37B)	109.5
C(29)-C(28)-H(28)	118.2	H(37A)-C(37)-H(37B)	109.5
N(3)-C(29)-C(28)	121.3(7)	C(35)-C(37)-H(37C)	109.5
N(3)-C(29)-C(30)	112.5(6)	H(37A)-C(37)-H(37C)	109.5
C(28)-C(29)-C(30)	126.1(7)	H(37B)-C(37)-H(37C)	109.5
N(4)-C(30)-C(29)	114.8(6)	C(35)-C(38)-H(38A)	109.5
N(4)-C(30)-C(31)	119.5(6)	C(35)-C(38)-H(38B)	109.5
C(29)-C(30)-C(31)	125.7(7)	H(38A)-C(38)-H(38B)	109.5
C(32)-C(31)-C(30)	122.5(7)	C(35)-C(38)-H(38C)	109.5
C(32)-C(31)-H(31)	118.8	H(38A)-C(38)-H(38C)	109.5
C(30)-C(31)-H(31)	118.8	H(38B)-C(38)-H(38C)	109.5
C(31)-C(32)-C(33)	115.8(7)	C(32)-C(39)-C(40)	112.6(7)
C(31)-C(32)-C(39)	124.0(7)	C(32)-C(39)-C(41)	110.3(6)
C(33)-C(32)-C(39)	120.2(7)	C(40)-C(39)-C(41)	107.5(6)
C(34)-C(33)-C(32)	120.8(7)	C(32)-C(39)-C(42)	109.4(6)
C(34)-C(33)-H(33)	119.6	C(40)-C(39)-C(42)	109.2(7)
C(32)-C(33)-H(33)	119.6	C(41)-C(39)-C(42)	107.7(7)
C(33)-C(34)-N(4)	124.1(7)	C(39)-C(40)-H(40A)	109.5
C(33)-C(34)-H(34)	118.0	C(39)-C(40)-H(40B)	109.5
N(4)-C(34)-H(34)	118.0	H(40A)-C(40)-H(40B)	109.5
C(27)-C(35)-C(38)	111.3(6)	C(39)-C(40)-H(40C)	109.5
C(27)-C(35)-C(36)	110.3(6)	H(40A)-C(40)-H(40C)	109.5
C(38)-C(35)-C(36)	108.3(7)	H(40B)-C(40)-H(40C)	109.5
C(27)-C(35)-C(37)	110.0(6)	C(39)-C(41)-H(41A)	109.5
C(38)-C(35)-C(37)	107.4(7)	C(39)-C(41)-H(41B)	109.5
C(36)-C(35)-C(37)	109.6(7)	H(41A)-C(41)-H(41B)	109.5
C(35)-C(36)-H(36A)	109.5	C(39)-C(41)-H(41C)	109.5
C(35)-C(36)-H(36B)	109.5	H(41A)-C(41)-H(41C)	109.5
H(36A)-C(36)-H(36B)	109.5	H(41B)-C(41)-H(41C)	109.5
C(35)-C(36)-H(36C)	109.5	C(39)-C(42)-H(42A)	109.5

Table 5.30 Cont.

C(39)-C(42)-H(42B)	109.5	C(48)-C(47)-H(47B)	110.2
H(42A)-C(42)-H(42B)	109.5	H(47A)-C(47)-H(47B)	108.5
C(39)-C(42)-H(42C)	109.5	O(9)-C(48)-C(47)	107.0(5)
H(42A)-C(42)-H(42C)	109.5	O(9)-C(48)-H(48A)	110.3
H(42B)-C(42)-H(42C)	109.5	C(47)-C(48)-H(48A)	110.3
O(12)-C(43)-C(44)	110.5(6)	O(9)-C(48)-H(48B)	110.3
O(12)-C(43)-H(43A)	109.5	C(47)-C(48)-H(48B)	110.3
C(44)-C(43)-H(43A)	109.5	H(48A)-C(48)-H(48B)	108.6
O(12)-C(43)-H(43B)	109.5	O(9)-C(49)-C(50)	107.3(5)
C(44)-C(43)-H(43B)	109.5	O(9)-C(49)-H(49A)	110.3
H(43A)-C(43)-H(43B)	108.1	C(50)-C(49)-H(49A)	110.3
O(7)-C(44)-C(43)	108.9(6)	O(9)-C(49)-H(49B)	110.3
O(7)-C(44)-H(44A)	109.9	C(50)-C(49)-H(49B)	110.3
C(43)-C(44)-H(44A)	109.9	H(49A)-C(49)-H(49B)	108.5
O(7)-C(44)-H(44B)	109.9	O(10)-C(50)-C(49)	107.5(6)
C(43)-C(44)-H(44B)	109.9	O(10)-C(50)-H(50A)	110.2
H(44A)-C(44)-H(44B)	108.3	C(49)-C(50)-H(50A)	110.2
O(7)-C(45)-C(46)	108.7(6)	O(10)-C(50)-H(50B)	110.2
O(7)-C(45)-H(45A)	109.9	C(49)-C(50)-H(50B)	110.2
C(46)-C(45)-H(45A)	109.9	H(50A)-C(50)-H(50B)	108.5
O(7)-C(45)-H(45B)	109.9	O(10)-C(51)-C(52)	108.3(6)
C(46)-C(45)-H(45B)	109.9	O(10)-C(51)-H(51A)	110.0
H(45A)-C(45)-H(45B)	108.3	C(52)-C(51)-H(51A)	110.0
O(8)-C(46)-C(45)	108.7(6)	O(10)-C(51)-H(51B)	110.0
O(8)-C(46)-H(46A)	109.9	C(52)-C(51)-H(51B)	110.0
C(45)-C(46)-H(46A)	109.9	H(51A)-C(51)-H(51B)	108.4
O(8)-C(46)-H(46B)	109.9	O(11)-C(52)-C(51)	107.9(6)
C(45)-C(46)-H(46B)	109.9	O(11)-C(52)-H(52A)	110.1
H(46A)-C(46)-H(46B)	108.3	C(51)-C(52)-H(52A)	110.1
O(8)-C(47)-C(48)	107.7(6)	O(11)-C(52)-H(52B)	110.1
O(8)-C(47)-H(47A)	110.2	C(51)-C(52)-H(52B)	110.1
C(48)-C(47)-H(47A)	110.2	H(52A)-C(52)-H(52B)	108.4
O(8)-C(47)-H(47B)	110.2	O(11)-C(53)-C(54)	107.9(6)

Table 5.30 Cont.

O(11)-C(53)-H(53A)	110.1	C(58A)-C(55B)-H(55D)	162.8
C(54)-C(53)-H(53A)	110.1	K(1)-C(55B)-H(55D)	93.7
O(11)-C(53)-H(53B)	110.1	H(55C)-C(55B)-H(55D)	108.4
C(54)-C(53)-H(53B)	110.1	C(57)-C(56A)-C(55A)	95(3)
H(53A)-C(53)-H(53B)	108.4	C(57)-C(56A)-H(56A)	112.7
O(12)-C(54)-C(53)	109.6(6)	C(55A)-C(56A)-H(56A)	112.7
O(12)-C(54)-H(54A)	109.7	C(57)-C(56A)-H(56B)	112.7
C(53)-C(54)-H(54A)	109.7	C(55A)-C(56A)-H(56B)	112.7
O(12)-C(54)-H(54B)	109.7	H(56A)-C(56A)-H(56B)	110.2
C(53)-C(54)-H(54B)	109.7	C(55B)-C(56B)-C(57)	103.7(11)
H(54A)-C(54)-H(54B)	108.2	C(55B)-C(56B)-C(58A)	66.4(14)
O(13)-C(55A)-C(56A)	106(4)	C(57)-C(56B)-C(58A)	45.4(13)
O(13)-C(55A)-K(1)	44(2)	C(55B)-C(56B)-H(56C)	111.0
C(56A)-C(55A)-K(1)	143(3)	C(57)-C(56B)-H(56C)	111.0
O(13)-C(55A)-H(55A)	110.4	C(58A)-C(56B)-H(56C)	100.7
C(56A)-C(55A)-H(55A)	110.4	C(55B)-C(56B)-H(56D)	111.0
K(1)-C(55A)-H(55A)	72.6	C(57)-C(56B)-H(56D)	111.0
O(13)-C(55A)-H(55B)	110.4	C(58A)-C(56B)-H(56D)	148.2
C(56A)-C(55A)-H(55B)	110.4	H(56C)-C(56B)-H(56D)	109.0
K(1)-C(55A)-H(55B)	102.7	C(56A)-C(57)-C(58B)	116(2)
H(55A)-C(55A)-H(55B)	108.6	C(56A)-C(57)-C(58A)	74(3)
O(13)-C(55B)-C(56B)	108.0(14)	C(58B)-C(57)-C(58A)	48.4(19)
O(13)-C(55B)-C(58A)	56.4(15)	C(56A)-C(57)-C(56B)	39(3)
C(56B)-C(55B)-C(58A)	68.8(15)	C(58B)-C(57)-C(56B)	102.2(10)
O(13)-C(55B)-K(1)	42.0(8)	C(58A)-C(57)-C(56B)	84(2)
C(56B)-C(55B)-K(1)	148.3(11)	C(56A)-C(57)-H(57C)	152.9
C(58A)-C(55B)-K(1)	82.2(14)	C(58B)-C(57)-H(57C)	66.2
O(13)-C(55B)-H(55C)	110.1	C(58A)-C(57)-H(57C)	114.6
C(56B)-C(55B)-H(55C)	110.1	C(56B)-C(57)-H(57C)	114.6
C(58A)-C(55B)-H(55C)	87.4	C(56A)-C(57)-H(57D)	84.9
K(1)-C(55B)-H(55C)	80.1	C(58B)-C(57)-H(57D)	138.2
O(13)-C(55B)-H(55D)	110.1	C(58A)-C(57)-H(57D)	114.6
C(56B)-C(55B)-H(55D)	110.1	C(56B)-C(57)-H(57D)	114.6

Table 5.30 Cont.

H(57C)-C(57)-H(57D)	111.7	C(57)-C(58B)-H(58D)	108.9
C(56A)-C(57)-H(57A)	108.3	H(58C)-C(58B)-H(58D)	107.7
C(58B)-C(57)-H(57A)	108.3	O(19)-C(59)-C(60)	110.6(6)
C(58A)-C(57)-H(57A)	101.6	O(19)-C(59)-H(59A)	109.5
C(56B)-C(57)-H(57A)	143.9	C(60)-C(59)-H(59A)	109.5
H(57C)-C(57)-H(57A)	95.4	O(19)-C(59)-H(59B)	109.5
H(57D)-C(57)-H(57A)	30.7	C(60)-C(59)-H(59B)	109.5
C(56A)-C(57)-H(57B)	108.3	H(59A)-C(59)-H(59B)	108.1
C(58B)-C(57)-H(57B)	108.3	O(14)-C(60)-C(59)	109.0(6)
C(58A)-C(57)-H(57B)	148.1	O(14)-C(60)-H(60A)	109.9
C(56B)-C(57)-H(57B)	80.1	C(59)-C(60)-H(60A)	109.9
H(57C)-C(57)-H(57B)	50.3	O(14)-C(60)-H(60B)	109.9
H(57D)-C(57)-H(57B)	97.3	C(59)-C(60)-H(60B)	109.9
H(57A)-C(57)-H(57B)	107.4	H(60A)-C(60)-H(60B)	108.3
C(57)-C(58A)-O(13)	98(3)	O(14)-C(61)-C(62)	108.9(6)
C(57)-C(58A)-C(55B)	89(3)	O(14)-C(61)-H(61A)	109.9
O(13)-C(58A)-C(55B)	41.5(12)	C(62)-C(61)-H(61A)	109.9
C(57)-C(58A)-C(56B)	50.3(16)	O(14)-C(61)-H(61B)	109.9
O(13)-C(58A)-C(56B)	77(2)	C(62)-C(61)-H(61B)	109.9
C(55B)-C(58A)-C(56B)	44.8(13)	H(61A)-C(61)-H(61B)	108.3
C(57)-C(58A)-H(58A)	112.2	O(15)-C(62)-C(61)	108.3(6)
O(13)-C(58A)-H(58A)	112.2	O(15)-C(62)-H(62A)	110.0
C(55B)-C(58A)-H(58A)	78.7	C(61)-C(62)-H(62A)	110.0
C(56B)-C(58A)-H(58A)	78.6	O(15)-C(62)-H(62B)	110.0
C(57)-C(58A)-H(58B)	112.2	C(61)-C(62)-H(62B)	110.0
O(13)-C(58A)-H(58B)	112.2	H(62A)-C(62)-H(62B)	108.4
C(55B)-C(58A)-H(58B)	150.4	O(15)-C(63)-C(64)	107.9(6)
C(56B)-C(58A)-H(58B)	162.2	O(15)-C(63)-H(63A)	110.1
H(58A)-C(58A)-H(58B)	109.8	C(64)-C(63)-H(63A)	110.1
O(13)-C(58B)-C(57)	113.3(11)	O(15)-C(63)-H(63B)	110.1
O(13)-C(58B)-H(58C)	108.9	C(64)-C(63)-H(63B)	110.1
C(57)-C(58B)-H(58C)	108.9	H(63A)-C(63)-H(63B)	108.4
O(13)-C(58B)-H(58D)	108.9	O(16)-C(64)-C(63)	108.3(6)

Table 5.30 Cont.

Table 5.30 Cont.

O(16)-C(64)-H(64A)	110.0	C(70)-C(69)-H(69A)	110.0
C(63)-C(64)-H(64A)	110.0	O(18)-C(69)-H(69B)	110.0
O(16)-C(64)-H(64B)	110.0	C(70)-C(69)-H(69B)	110.0
C(63)-C(64)-H(64B)	110.0	H(69A)-C(69)-H(69B)	108.4
H(64A)-C(64)-H(64B)	108.4	O(19)-C(70)-C(69)	110.0(6)
O(16)-C(65)-C(66)	107.0(6)	O(19)-C(70)-H(70A)	109.7
O(16)-C(65)-H(65A)	110.3	C(69)-C(70)-H(70A)	109.7
C(66)-C(65)-H(65A)	110.3	O(19)-C(70)-H(70B)	109.7
O(16)-C(65)-H(65B)	110.3	C(69)-C(70)-H(70B)	109.7
C(66)-C(65)-H(65B)	110.3	H(70A)-C(70)-H(70B)	108.2
H(65A)-C(65)-H(65B)	108.6	O(20)-C(71)-C(72)	111.8(9)
O(17)-C(66)-C(65)	108.0(5)	O(20)-C(71)-H(71A)	109.3
O(17)-C(66)-H(66A)	110.1	C(72)-C(71)-H(71A)	109.3
C(65)-C(66)-H(66A)	110.1	O(20)-C(71)-H(71B)	109.3
O(17)-C(66)-H(66B)	110.1	C(72)-C(71)-H(71B)	109.3
C(65)-C(66)-H(66B)	110.1	H(71A)-C(71)-H(71B)	107.9
H(66A)-C(66)-H(66B)	108.4	C(71)-C(72)-C(73A)	106.0(9)
O(17)-C(67)-C(68)	108.2(6)	C(71)-C(72)-C(73B)	89.9(13)
O(17)-C(67)-H(67A)	110.1	C(73A)-C(72)-C(73B)	56.7(15)
C(68)-C(67)-H(67A)	110.1	C(71)-C(72)-H(72C)	110.5
O(17)-C(67)-H(67B)	110.1	C(73A)-C(72)-H(72C)	110.5
C(68)-C(67)-H(67B)	110.1	C(73B)-C(72)-H(72C)	159.0
H(67A)-C(67)-H(67B)	108.4	C(71)-C(72)-H(72D)	110.5
O(18)-C(68)-C(67)	108.9(6)	C(73A)-C(72)-H(72D)	110.5
O(18)-C(68)-H(68A)	109.9	C(73B)-C(72)-H(72D)	66.4
C(67)-C(68)-H(68A)	109.9	H(72C)-C(72)-H(72D)	108.7
O(18)-C(68)-H(68B)	109.9	C(71)-C(72)-H(72A)	113.7
C(67)-C(68)-H(68B)	109.9	C(73A)-C(72)-H(72A)	57.3
H(68A)-C(68)-H(68B)	108.3	C(73B)-C(72)-H(72A)	113.7
O(18)-C(69)-C(70)	108.6(6)	H(72C)-C(72)-H(72A)	54.4
O(18)-C(69)-H(69A)	110.0	H(72D)-C(72)-H(72A)	135.8

C(71)-C(72)-H(72B)	113.7	C(72)-C(73B)-H(73D)	111.5
C(73A)-C(72)-H(72B)	139.4	C(74B)-C(73B)-H(73D)	111.5
C(73B)-C(72)-H(72B)	113.7	H(73C)-C(73B)-H(73D)	109.3
H(72C)-C(72)-H(72B)	63.5	O(20)-C(74A)-C(73A)	106.4(9)
H(72D)-C(72)-H(72B)	47.4	O(20)-C(74A)-H(74A)	110.4
H(72A)-C(72)-H(72B)	110.9	C(73A)-C(74A)-H(74A)	110.4
C(72)-C(73A)-C(74A)	105.5(9)	O(20)-C(74A)-H(74B)	110.4
C(72)-C(73A)-H(73A)	110.6	C(73A)-C(74A)-H(74B)	110.4
C(74A)-C(73A)-H(73A)	110.6	H(74A)-C(74A)-H(74B)	108.6
C(72)-C(73A)-H(73B)	110.6	C(73B)-C(74B)-O(20)	106.1(19)
C(74A)-C(73A)-H(73B)	110.6	C(73B)-C(74B)-H(74C)	110.5
H(73A)-C(73A)-H(73B)	108.8	O(20)-C(74B)-H(74C)	110.5
C(72)-C(73B)-C(74B)	101(2)	C(73B)-C(74B)-H(74D)	110.5
C(72)-C(73B)-H(73C)	111.5	O(20)-C(74B)-H(74D)	110.5
C(74B)-C(73B)-H(73C)	111.5	H(74C)-C(74B)-H(74D)	108.7

Chapter 6

EXAFS and XANES of rhenium compounds relevant to the electrochemical reduction of CO2

6.1 Introduction

Research in the field of catalytic reduction of carbon dioxide to liquid fuels has grown rapidly in the recent decades. Carbon dioxide is a stable molecule produced on the gigaton scale from many industrial processes as well as fossil fuel combustion. Returning CO_2 to a useful state by activation/reduction is a scientifically challenging problem and requires a catalyst that operates efficiently over long periods of time.[1] Although there is a wealth of information on transformations of CO_2, we do not yet have an efficient catalyst that can reduce CO_2 to liquid fuels on an industrial scale. Of the systems that are able to electrocatalytically activate CO_2, the $Re(bpy)(CO)_3Cl$ family of compounds (where bpy is 2,2'-bipyridine) is one of the most robust and well

characterized systems.[2-6] This system is able to convert CO_2 into carbon monoxide (CO) with high rates and efficiencies. This catalyst, however, suffers from large overpotentials, presumably arising from the necessity to access the highly reduced, formally Re(-1) state. Despite all that is known about this family of complexes, there is a lack of information on the catalyst in its reduced (active) state and its subsequent interaction with CO_2.

We have recently reported the solid state structures of both $Re(bpy)(CO)_3^-$ and $Re(bpy\text{-}tBu)(CO)_3^-$, which have long been proposed as the active state of the catalyst.[2, 3] These complexes have a five-coordinate, unsaturated Re center with one site available for CO_2 binding. In the X-Ray diffraction studies the bipyridine ligand exhibits bond alternation, and a short C_{py}–C_{py} bond distance (1.370(15) Å), suggesting that there is significant electron density on the ligand. This data is consistent with a $Re(0)(bipy)^-$ rather than a Re(-1) state. It is this redox activity, or non-innocence of the ligand, that allows for the two electron reduction of CO_2. The redox activity of bipyridines,[7, 8] as well as other ligands has been extensively studied.[9-11]

In our previous reports the $Re(bpy\text{-}t\text{Bu})(CO)_3^-$ anion reacts ~35 times faster with CO_2 than H^+.[3] This is attributed to the ability of bipyridine to act as a non-innocent ligand, which not only stores charge, but prevents the formation of a doubly-occupied d_z^2 orbital that can readily form a metal hydride. Knowledge gained about the nature of the electronic state of the anion and the ability of non-innocent ligands to store charge, may allow us to extend this work to the six-electron, six-proton reduction

of carbon dioxide to methanol, which requires less energy than the two-electron, two-proton reduction to CO.

Herein we report the X-Ray Absorption Near Edge Structure (XANES) and Extended X-Ray Absorption Fine Structure (EXAFS) on samples of the starting halide materials ($Re(bpy)(CO)_3Cl$ (**1**), $Re(bpy\text{-}tBu)(CO)_3Cl$ (**2**)), the one-electron reduced dimer $[Re(bpy)(CO)_3]_2$ (**3**), and the two-electron reduced anions $[Re(bpy)(CO)_3][K(18\text{-crown-}6)]$ (**4**), and $Re(bpy\text{-}tBu)(CO)_3][K(18\text{-crown-}6)]$ (**5**). XANES[12, 13] at the Re L_3 edge probes the unoccupied density of Re 5*d* states via dipole-allowed $2s \rightarrow 5d$ transitions giving rise to a strong "white line" absorption (Figure 6.1). Significant changes in the white line intensity are observed when the amount of unoccupied states with Re *5d* character are decreased, such as a formal

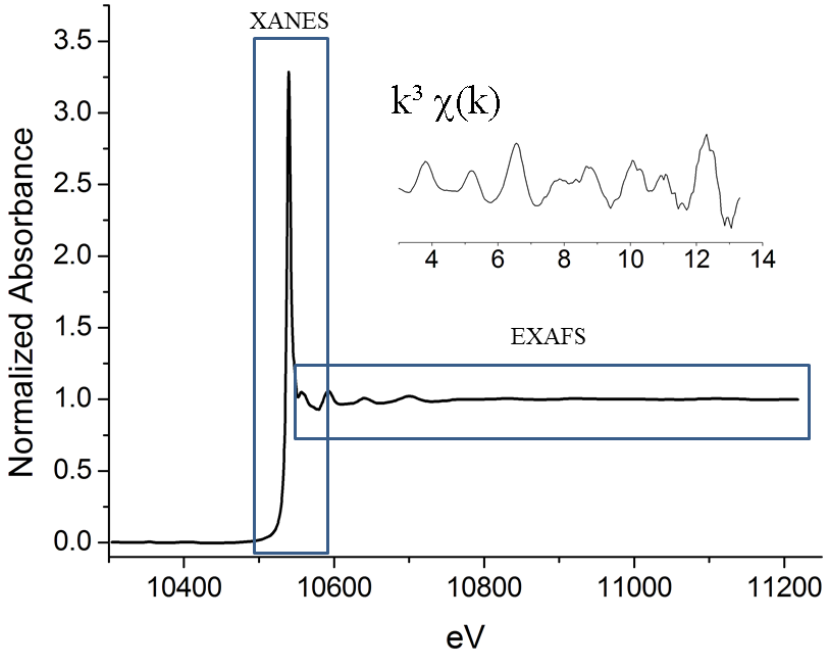

Figure 6.1 Normalized X-Ray absorption spectra for $Re(bipy)(CO)_3Cl$ showing the XANES and EXAFS regions. The k^3 weighted $\chi(k)$ spectrum is shown in the inset.

change in oxidation state. EXAFS allows us to study the local coordination environment around the central absorbing atom. The photoelectron produced from the core excitation is backscattered from atoms surrounding the absorber atom within distances up to ~8 Å and, due to its wave nature, interferes with the outgoing photoelectron wave (Figure 6.2). This results in an oscillatory fine structure of the absorption coefficient that can be observed over an energy range of 30 up to ~1000 eV above the absorption threshold which can be described by equation 6.1.[14, 15]

$$\chi(k) = \sum_R S_0^2 N_R \frac{|f(k)|}{kR^2} \sin(2kR + 2\delta_c + \Phi) e^{-2R/\lambda(k)} e^{-2\sigma^2 k^2} \qquad \text{E6.1}$$

Where R is the interatomic distance, S_0^2 is the amplitude reduction factor, N_R is the coordination number, $f(k)$ is the backscattering amplitude, δ_c is the partial-wave phase shift of the final state, $\lambda(k)$ is the energy-dependent mean free path, and σ is the temperature dependent fluctuation in bond length. By simulation and subsequent fitting of the scattering paths we can obtain bond lengths as well as coordination numbers (Figure 6.3).

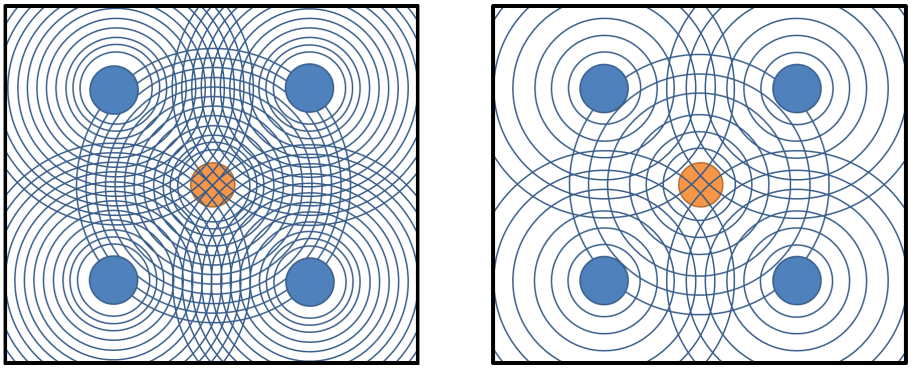

Figure 6.2 Illustration showing constructive interference of the backscattered photoelectron with the outgoing photoelectron wave (left) as well as the deconstructive interference (right).

6.2 Results and discussion

Compounds were prepared according to literature procedures.[2, 3, 6] 10 mM solutions in THF were prepared under an inert atmosphere and quickly transferred to a Dewar of liquid nitrogen before being transferred to a He cryostat. X-Ray absorption spectra (XAS) were collected at SSRL beam line 4-1 at the Re L_3 edge for compounds (**1**-**5**). The SIXPack[16] software suite was used for background subtraction, spline fitting and least-square fitting of the Fourier-transformed EXAFS signal. Backscattering phase and amplitude functions required for fitting of spectra were obtained from FEFF 6.[17]

XANES of the well-characterized Re(1) chloride complexes (**1**) and (**2**) show a strong white line spectra arising from empty *5d* states. The intensity of the white line

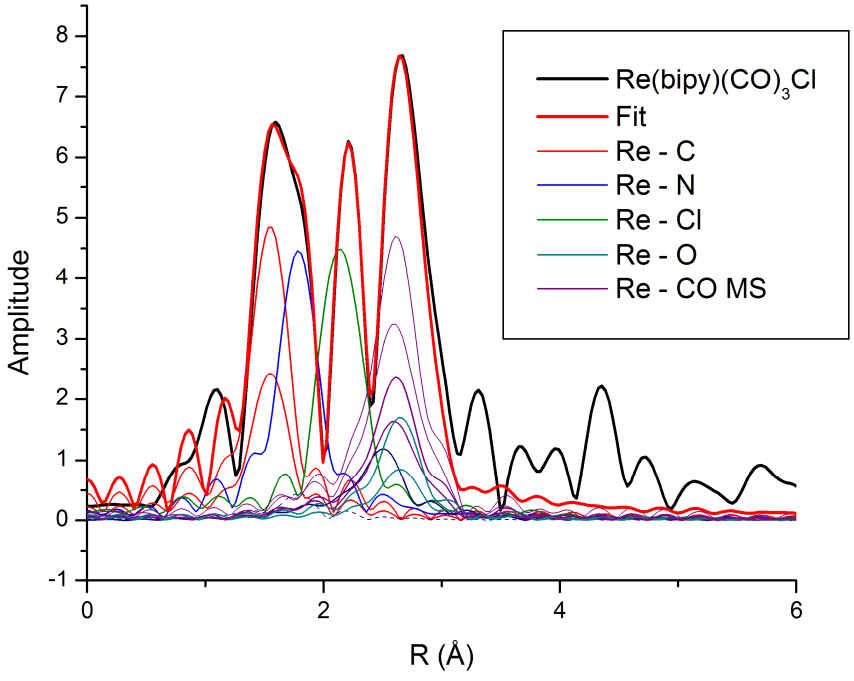

Figure 6.3 Fourier transformed EXAFS data, fit and individual scattering paths for $Re(bipy)(CO)_3Cl$ (MS = multiple scattering)

is stronger than expected when compared to rhenium metal and the intensity is similar to some rhenium oxides.[18, 19] This is attributed to the π-bonding from the metal *d* orbitals to the carbonyl and bipyridine ligands, thus increasing the total amount of unoccupied states with partial Re *5d* character.

Reduction of complexes (**1**) and (**2**) in THF with KC_8 in the presence of 18-crown-6 results in the loss of the axial halide and the formation of the five-coordinate catalytically relevant species, (**4**) and (**5**). The XANES spectra of these complexes show a decrease in the white line height and a broadening of the white line when compared to the unreduced compounds (Figure 6.4, **Table 6.3**). When the XANES

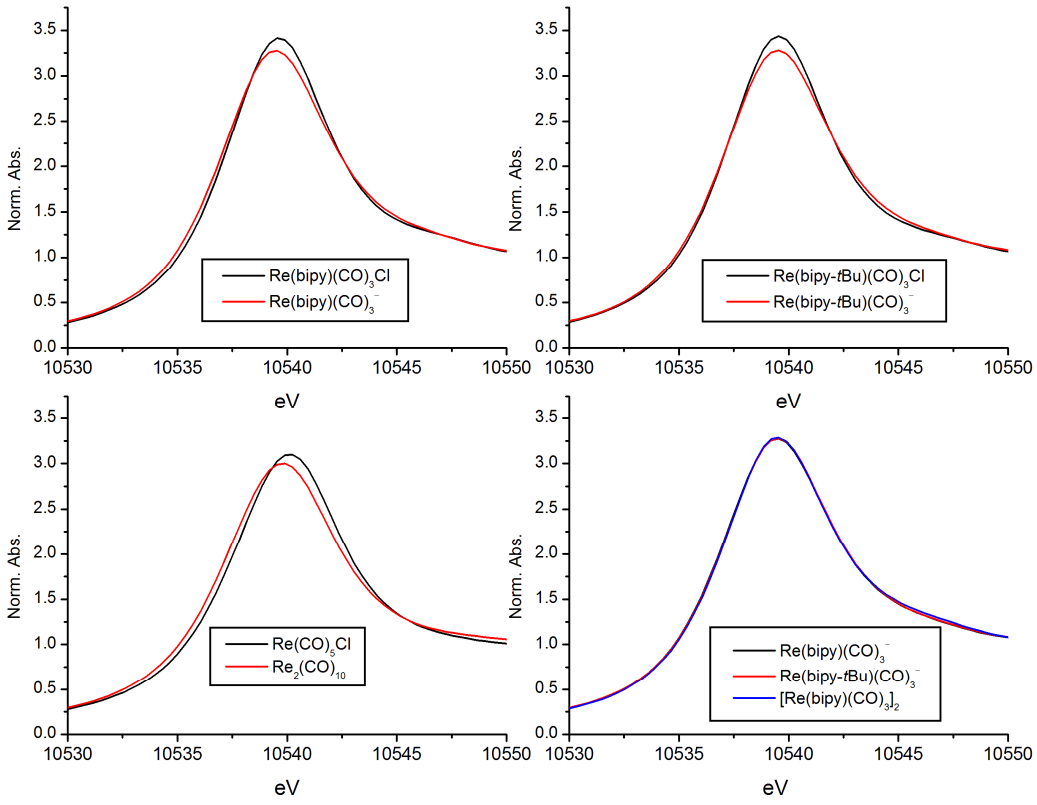

Figure 6.4 Comparison of the white line spectra from XANES for complexes **1**-**5** and the reference compounds $Re(CO)_5Cl$ and $Re_2(CO)_{10}$

spectra of the anions (**4**) and (**5**) are compared to the formally Re(0) dimer (**3**) we do not see a change in the white line height or width, indicating that the electronic state of the central rhenium atom is similar to that of the Re(0) dimer (Figure 6.4, bottom right). When comparing the difference spectra between (**3**) and the anions (**4**) and (**5**) the minimal differences are attributed to the change in coordination geometry around the rhenium center (**Figure 6.7**, appendix).

When compared to the standards $Re(CO)_5Cl$ and $Re_2(CO)_{10}$, a similar decrease in the white line intensity and broadening of the white line is observed, again suggesting that the electronics around the metal centers (**4**) and (**5**) are similar to that

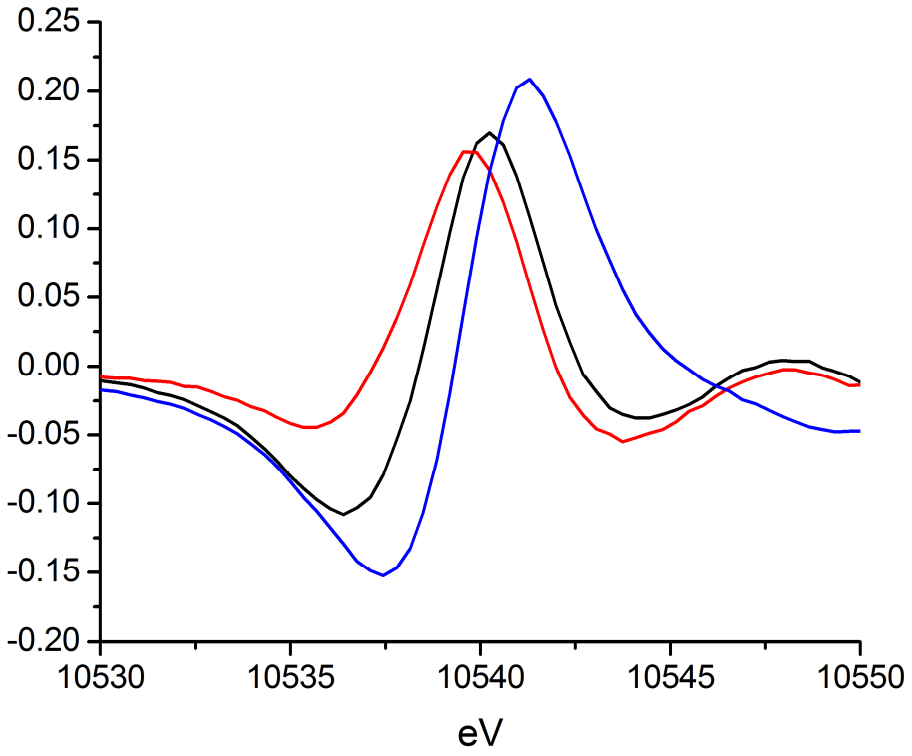

Figure 6.5 Difference in XANES spectra for the unreduced complexes (**1**) and (**2**) and the reduced complexes (**4**) and (**5**). $Re(bipy)(CO)_3$ is shown in black, while the $Re(bipy\text{-}tBu)(CO)_3$ is shown in red. For reference, the difference in XANES for $Re(CO)_5Cl$ and $Re_2(CO)_{10}$ is shown in blue.

of a formal Re(0) center and the electronics around the meter center of (**1**) and (**2**) are formally Re(+1). Difference spectra between unreduced and reduced states can be found in Figure 6.5. The larger difference in the standards $Re(CO)_5Cl$ and $Re_2(CO)_{10}$ is attributed to the ability of the bipyridine ligand to store additional charge.

To obtain a greater understanding of the structure of the complexes in solution, EXAFS data was collected at the Re L_3 edge of complexes (**1-5**) in frozen THF. Fluorescence data was collected for compounds (**1-5**) out to a k of 13. Unfortunately, the solubility of the dimer (**3**) was too low to collect reliable data within the available beam time. During least-squares fitting, the Debye-Waller factors were fixed at values consistent with other experiments,[20-22] while the coordination number and bond distances were allowed to refine. The fitting parameters for complexes (**1**), (**2**), (**4**), and (**5**) can be found in the appendix.

The bond lengths and coordination around the metal center obtained from the frozen solution EXAFS are in good agreement with the X-Ray diffraction (XRD)

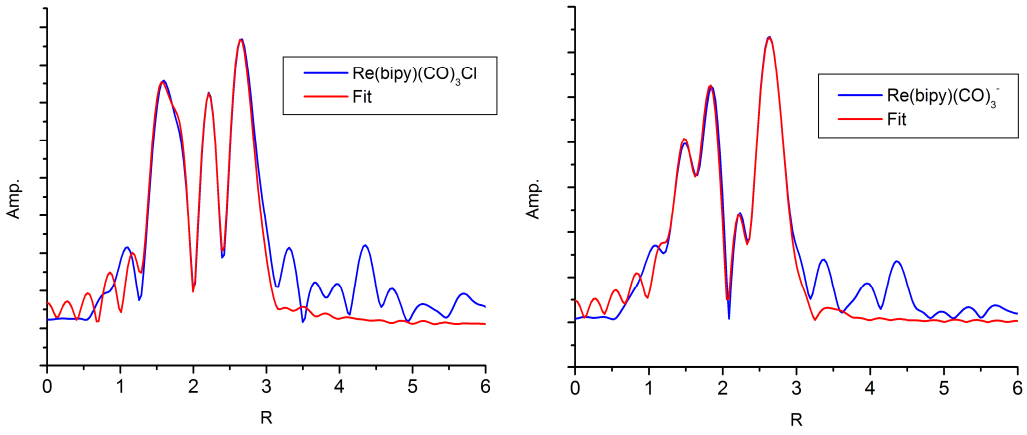

Figure 6.6 Fourier transformed EXAFS data and fit for complexes (**1**) and (**4**)

structures previously reported,[3, 23] as well as the structures obtained through DFT.[24] A table of atoms and bond lengths can be found in Table 6.1 for the starting halides and Table 6.2 for the anions. For the fitting of the anions the same scattering paths as the starting chloride complexes were kept, except for the single scattering path for Re – Cl. This can be seen as a significant decrease in the peak in the Fourier transformed EXAFS data at R = 2.21 (Figure 6.6).

From the solution structure we can determine the local coordination environment around the active Re center. From the EXAFS data we can conclude that the anions remain 5-coordinate in solution with no detectable coordination of solvent and no dimer formation.

Table 6.1 Coordination numbers (CN) and bond distances (Å) for compounds (**1**) and (**2**)

	Re(bipy)$(CO)_3$Cl (**1**)		Re(bipy-*t*Bu)$(CO)_3$Cl (**2**)	
	EXAFS	XRD[a,b]	EXAFS	XRD[a,c]
CN	5.85(36)	6	6.01(37)	6
Re – C	1.926(5)	1.930	1.921(5)	1.911
Re – N	2.179(8)	2.175	2.177(10)	2.176
Re – Cl	2.499(39)	2.460	2.493(6)	2.463

[a]Averages of values found in the unit cell. [b]Values taken from Alberto *et al.*[23]
[c]Values taken from Kubiak *et al.*[3]

Table 6.2 Coordination numbers (CN) and bond distances (Å) for compounds (**4**) and (**5**)

	[Re(bipy)(CO)$_3$] [K(18-crown-6)]		[Re(bipy-*t*Bu)(CO)$_3$] [K(18-crown-6)]	
	EXAFS	XRD[a]	EXAFS	XRD[a]
CN	5.05(33)	5	5.17(36)	5
Re – C	1.909(8)	1.892	1.908(9)	1.917
Re – N	2.139(6)	2.082	2.141(6)	2.093

[a]Averages of values found in the unit cell, values taken from Kubiak *et al.*[2,3]

6.3 Conclusions

The application of XANES and EXAFS has allowed us to study the electronic structure as well as the local coordination environment around catalytically relevant Re complexes, including the reactive anions. The anions Re(bpy)(CO)$_3^-$ and Re(bpy-*t*Bu)(CO)$_3^-$ both appear to possess formally Re(0) metal centers with reduced bipyridine ligands. The anions are 5-coordinate in solution, with no coordination of solvent or dimer formation, consistent with the XRD structures obtained in previous experiments.

Acknowledgement: This research was partly carried out at the Stanford Synchrotron Radiation Lightsource, a National User Facility operated by Stanford University on behalf of the U.S. Department of Energy, Office of Basic Energy Sciences. This

material is based upon work supported by the Air Force Office of Scientific Research through the MURI program under AFOSR Award No. FA9550-10-1-0572.

6.4 Experimental

Complexes (**1-5**) and were synthesized by previously reported methods.[2, 3] All other chemicals were purchased from commercial sources and used as received. THF was sparged with argon and dried over basic alumina with a custom dry solvent system. The Re L_3 edge (~10.5 keV) EXAFS and XANES measurements were carried out at the Stanford Synchrotron Radiation Lightsource (SSRL) on beamline 4-1 equipped with a Si (220) monochronomator. Samples were prepared under an inert atmosphere in a nitrogen filled glovebox. 10 mM solutions of the complexes were injected into a custom cell for use in a He cryostat. For $Re(CO)_5Cl$ and $Re_2(CO)_{10}$ the samples were diluted in boron nitride and pressed into the sample holder. The cell and sample holder were removed from the box and immediately submerged in liquid nitrogen for transfer to the beam station. The sample was then transferred to a liquid He cryostat where the temperature was maintained at 50(5) K. EXAFS and XANES measurements were both carried out in transmission as well as fluorescence mode.

Note: The material in this chapter is unpublished work and much of it was performed in collaboration with Dr. Daniel Friebel, Matthew Sampson, Dr. Jonathan Smieja, Dr. Kyle Grice and Prof. Anders Nilsson

6.5 References

1. Benson EE, Kubiak CP, Sathrum AJ, & Smieja JM (2009) Electrocatalytic and homogeneous approaches to conversion of CO_2 to liquid fuels. *Chem. Soc. Rev.* 38(1):89-99.

2. Benson EE & Kubiak CP (2012) Structural investigations into the deactivation pathway of the CO_2 reduction electrocatalyst $Re(bipy)(CO)_3Cl$. *Chem. Commun.*:Submitted.

3. Smieja JM, *et al.* (2012) Kinetic and structural studies, origins of selectivity, and interfacial charge transfer in the artificial photosynthesis of CO. *P. Nat. Acad. Sci. USA*:Accepted.

4. Savéant J-M (2008) Molecular Catalysis of Electrochemical Reactions. Mechanistic Aspects. *Chem. Rev.* 108(7):2348-2378.

5. Morris AJ, Meyer GJ, & Fujita E (2009) Molecular Approaches to the Photocatalytic Reduction of Carbon Dioxide for Solar Fuels. *Accounts Chem. Res.* 42(12):1983-1994.

6. Smieja JM & Kubiak CP (2010) $Re(bipy\text{-}tBu)(CO)_3Cl$−improved Catalytic Activity for Reduction of Carbon Dioxide: IR-Spectroelectrochemical and Mechanistic Studies. *Inorg. Chem.* 49(20):9283-9289.

7. Scarborough CC, Sproules S, Weyhermüller T, DeBeer S, & Wieghardt K (2011) Electronic and Molecular Structures of the Members of the Electron Transfer Series $[Cr(tbpy)_3]^n$ (n = 3+, 2+, 1+, 0): An X-ray Absorption Spectroscopic and Density Functional Theoretical Study. *Inorg. Chem.* 50(24):12446-12462.

8. Gore-Randall E, Irwin M, Denning MS, & Goicoechea JM (2009) Synthesis and Characterization of Alkali-Metal Salts of 2,2′- and 2,4′-Bipyridyl Radicals and Dianions. *Inorg. Chem.* 48(17):8304-8316.

9. Kaim W (2012) The Shrinking World of Innocent Ligands: Conventionaland Non-Conventional Redox-Active Ligands. *Eur. J. Inorg. Chem.* 2012(3):343-348.

10. de Bruin B, Bill E, Bothe E, Weyhermüller T, & Wieghardt K (2000) Molecular and Electronic Structures of Bis(pyridine-2,6-diimine)metal Complexes $[ML_2](PF6)_n$ (n = 0, 1, 2, 3; M = Mn, Fe, Co, Ni, Cu, Zn)†. *Inorg. Chem.* 39(13):2936-2947.

11. Spikes GH, Milsmann C, Bill E, Weyhermu□ller T, & Wieghardt K (2008) One- and Two-Electron Reduced 1,2-Diketone Ligands in $[ZnII(L\bullet)_2(Et_2O)]$,

[$Co^{II}(L^{\bullet})_2(Et_2O)$], and $Na_2(Et_2O)_4[Co^{II}(LRed)_2]$. *Inorg. Chem.* 47(24):11745-11754.

12. Hall MD, Foran GJ, Zhang M, Beale PJ, & Hambley TW (2003) XANES Determination of the Platinum Oxidation State Distribution in Cancer Cells Treated with Platinum(IV) Anticancer Agents. *J. Am. Chem. Soc.* 125(25):7524-7525.

13. Bauer M, Muller S, Kickelbick G, & Bertagnolli H (2007) The structures of the precursor Hf((OBu)-Bu-n)(4) and its modification in solution: EXAFS-investigation in combination with XANES- and IR-spectroscopy. (Translated from English) *New J. Chem.* 31(11):1950-1959 (in English).

14. Rehr JJ & Albers RC (2000) Theoretical approaches to x-ray absorption fine structure. *Reviews of Modern Physics* 72(3):621-654.

15. Sayers DE, Stern EA, & Lytle FW (1971) New Technique for Investigating Noncrystalline Structures: Fourier Analysis of the Extended X-Ray—Absorption Fine Structure. *Phys. Rev. Lett.* 27(18):1204-1207.

16. Webb SM (2005) SIXpack: a graphical user interface for XAS analysis using IFEFFIT. *Phys. Scr.* T115:1011-1014.

17. Rehr JJ, Albers RC, & Zabinsky SI (1992) High-order multiple-scattering calculations of x-ray-absorption fine structure. *Phys. Rev. Lett.* 69(23):3397-3400.

18. Fröba M, Lochte K, & Metz W (1996) XANES studies on rhenium L absorption edges of Re_2O_7 graphite intercalation compounds and of other rhenium-oxygen compounds. *Journal of Physics and Chemistry of Solids* 57(5):635-641.

19. Tougerti A, *et al.* (2012) XANES study of rhenium oxide compounds at the L_1 and L_3 absorption edges. *Physical Review B* 85(12):125136.

20. Vila FD, Rehr JJ, Rossner HH, & Krappe HJ (2007) Theoretical x-ray absorption Debye-Waller factors. *Physical Review B* 76(1):014301.

21. Sapelkin AV & Bayliss SC (2002) Distance dependence of mean-square relative displacements in EXAFS. *Physical Review B* 65(17):172104.

22. Dalba G & Fornasini P (1997) EXAFS Debye-Waller Factor and Thermal Vibrations of Crystals. *Journal of Synchrotron Radiation* 4(4):243-255.

23. Kurz P, Probst B, Spingler B, & Alberto R (2006) Ligand Variations in [ReX(diimine)$(CO)_3$] Complexes: Effects on Photocatalytic CO_2 Reduction. *Eur. J. Inorg. Chem.* 2006(15):2966-2974.

24. Fujita E & Muckerman JT (2004) Why Is Re−Re Bond Formation/Cleavage in [Re(bpy)$(CO)_3]_2$ Different from That in $[Re(CO)_5]_2$? Experimental and Theoretical Studies on the Dimers and Fragments. *Inorg. Chem.* 43(24):7636-7647.

6.6 Appendix

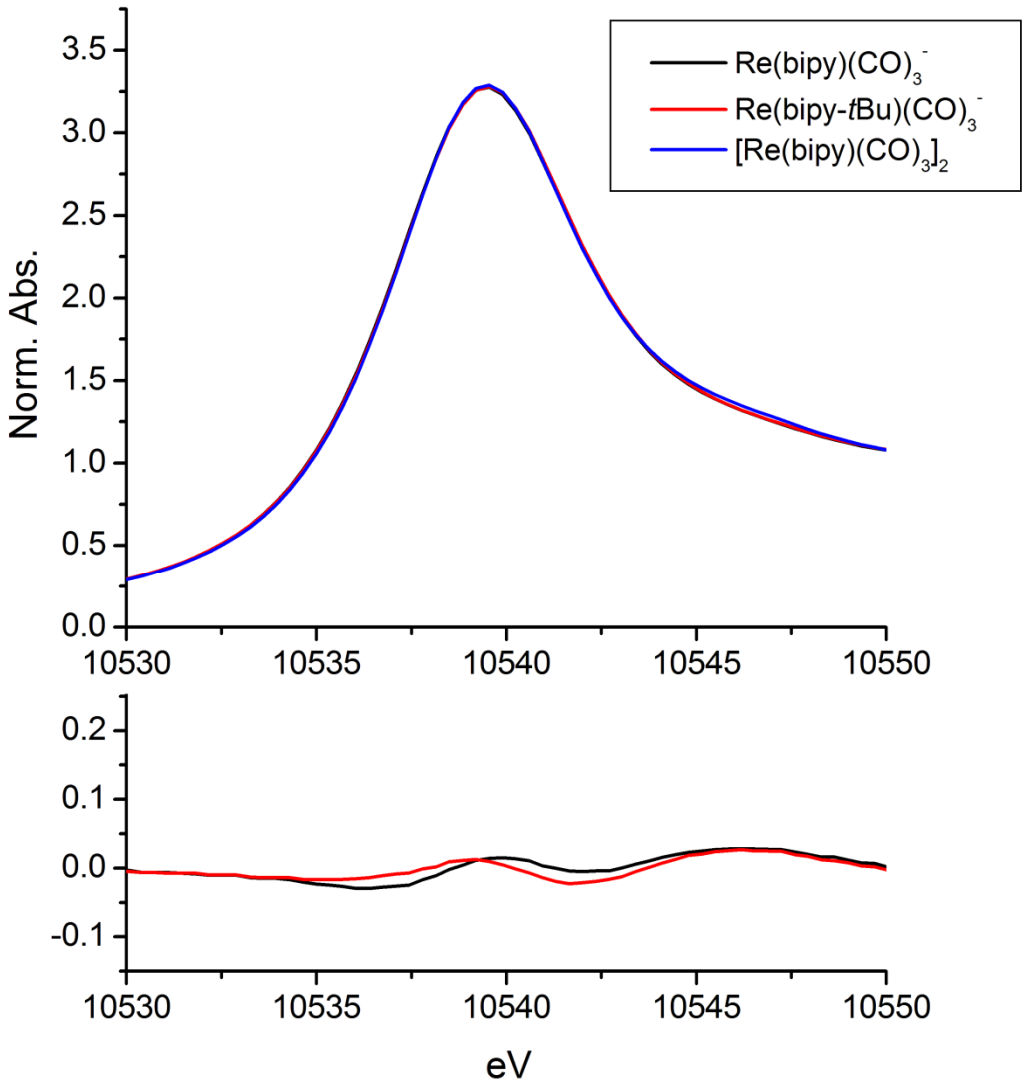

Figure 6.7 Normalized XANES spectra of compounds (**3**), (**4**) and (**5**) and the difference spectra

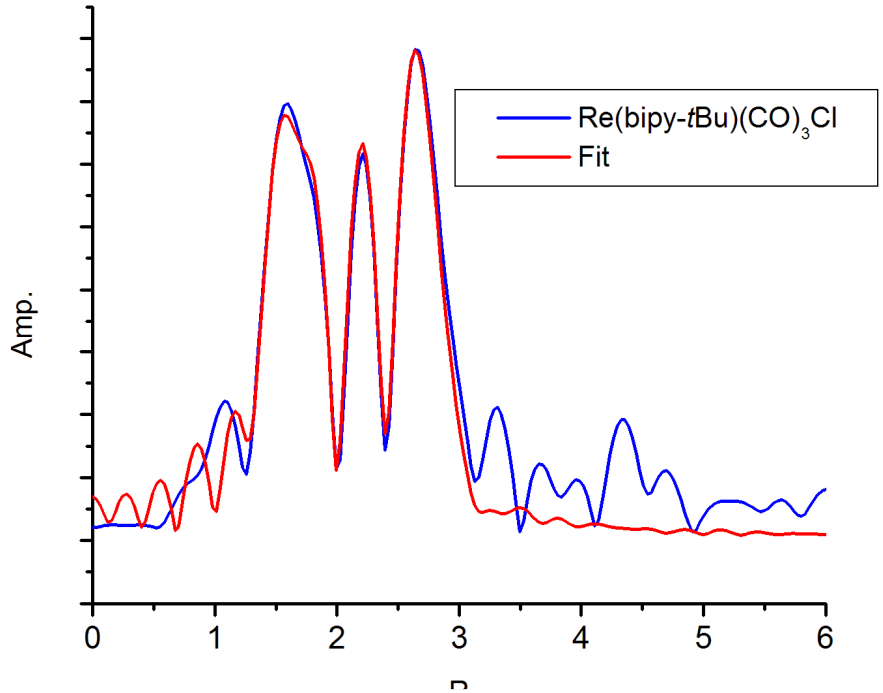

Figure 6.8 Fourier transformed EXAFS data and fit for complexes (**2**)

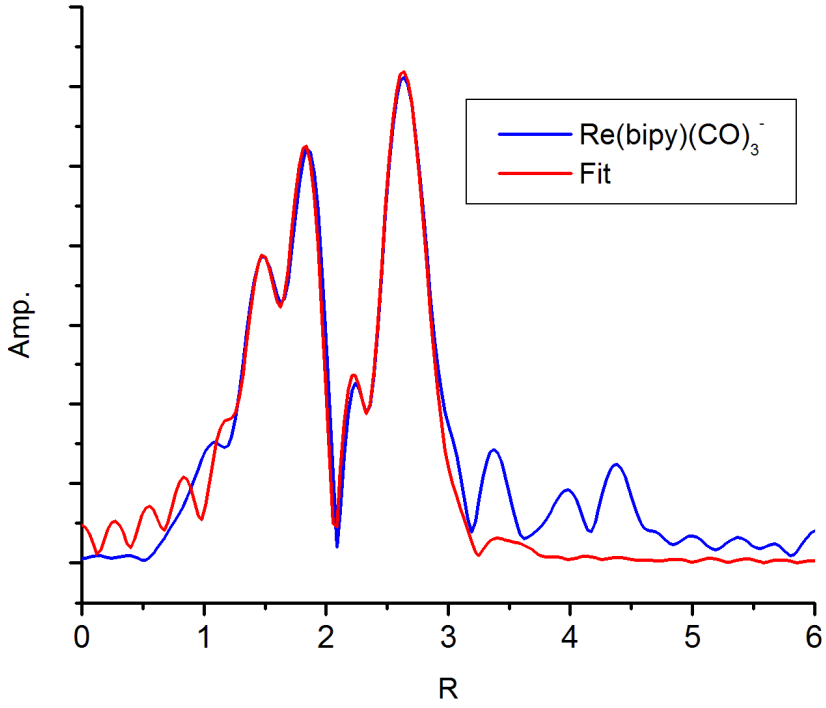

Figure 6.9 Fourier transformed EXAFS data and fit for complexes (**2**)

Table 6.3 XANES white line intensities and widths for complexes **1**-**5** and the reference compounds $Re(CO)_5Cl$ and $Re_2(CO)_{10}$

	Height (a.u.)	FWHM (eV)
$Re(bipy)(CO)_3Cl$ (**1**)	3.41	6.98
$Re(bipy\text{-}tBu)(CO)_3Cl$ (**2**)	3.44	6.98
$[Re(bipy)(CO)_3]_2$ (**3**)	3.29	7.62
$Re(bipy)(CO)_3^-$ (**4**)	3.28	7.64
$Re(bipy\text{-}tBu)(CO)_3^-$ (**5**)	3.28	7.63
$Re(CO)_5Cl$	3.10	7.29
$Re_2(CO)_{10}$	3.00	7.71

Table 6.4 EXAFS fitting parameters for compounds **1**, **2**, **4**, and **5**

	$Re(bipy)(CO)_3Cl$ (**1**)	Re(bipy-*t*Bu)(CO)3Cl (**2**)	$[Re(bipy)(CO)_3]$ [K(18-crown-6)] (**4**)	[Re(bipy-*t*Bu)$(CO)_3$] [K(18-crown-6)] (**5**)
S_0^2	0.98	0.98	0.98	0.98
e_0	13.50(87)	13.26(85)	10.81(1.14)	10.38(1.16)
CN	5.85(36)	6.01(37)	5.50(33)	5.17(36)
Re – C	1.926(5)	1.921(5)	1.909(8)	1.908(9)
σ^2	0.0019	0.0019	0.004	0.0045
Re – N	2.179(8)	2.177(10)	2.139(6)	2.141.(6)
σ^2	0.0015	0.0015	0.0012	0.0012
Re – Cl	2.499(39)	2.493(6)		
σ^2	0.001	0.001		

Chapter 7

Second coordination sphere effects on the model system $Re(bipy)(CO)_3Cl$

7.1 Introduction

The reduction of carbon dioxide to value added products is inherently a proton dependent process. From E7.1-E7.5 we can see that each of the half reactions requires the addition of protons to complete the chemical transformation (pH 7 in aqueous solution versus NHE, 25 °C, 1 atmosphere gas pressure, and 1 M for the other solutes). As more protons are consumed in the reduction of carbon dioxide the lower the potential required for the reaction. As we go from a 2 e^-, 2 H^+ process (HCO_2H) to a 6 e^-, 6 H^+ process (MeOH) the thermodynamic potential required drops by 230 mV. With respect to CO_2 reduction to liquid fuels or fuel precursors such as CO/H_2

(synthesis gas), proton-coupled multi-electron steps are generally more favorable than single electron reductions, as thermodynamically more stable molecules are produced.[1]

$$CO_2 + 2H^+ + 2e^- \rightarrow CO + H_2O \qquad E° = -0.53\ V \qquad (E7.1)$$

$$CO_2 + 2H^+ + 2e^- \rightarrow HCO_2H \qquad E° = -0.61\ V \qquad (E7.2)$$

$$CO_2 + 4H^+ + 4e^- \rightarrow HCHO + H_2O \qquad E° = -0.48\ V \qquad (E7.3)$$

$$CO_2 + 6H^+ + 6e^- \rightarrow CH_3OH + H_2O \qquad E° = -0.38\ V \qquad (E7.4)$$

$$CO_2 + 8H^+ + 8e^- \rightarrow CH_4 + 2H_2O \qquad E° = -0.24\ V \qquad (E7.5)$$

Of all of the synthetic systems reported for the electrochemical reduction of carbon dioxide[1, 2] none are as efficient and selective as the systems found in nature. The class of enzymes that catalyzes the oxidation of carbon monoxide (and the reverse reaction) are designated as carbon monoxide dehydrogenases (CODH's). They are the only catalysts that are kinetically and thermodynamically optimized to equilibrate CO_2 and CO at room temperature. Anaerobic CODHs can operate at very high turnover rates (31,000 s^{-1}), but it is also remarkable that the aerobic CODHs can selectively reduce CO_2 in the presence of oxygen (107 s^{-1}).[3-5] Recent crystallographic studies

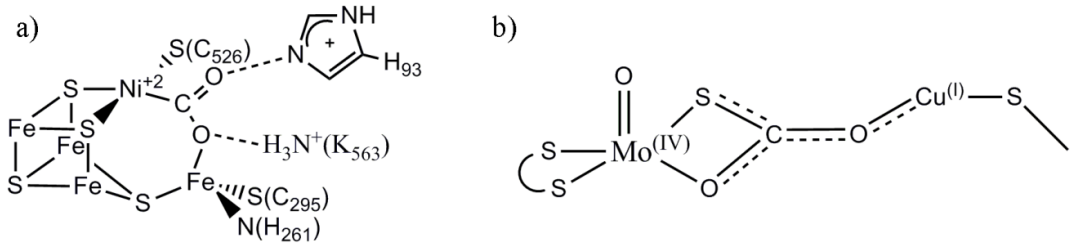

Figure 7.1 a) Isolated structure of the CO_2 bound active site of anaerobic CODH and b) proposed structure of the CO_2 bound species from inhibition studies of aerobic CODH using n-butyl isocyanide.

have shown that an extensive array of hydrogen bonding groups near the active site of these catalysts stabilize any partial negative charge on the oxygen atoms of CO_2 (Figure 7.1).

Proton coupled electron transfer (PCET) is frequently discussed as a key concept in mechanisms for water splitting and biological processes[6-8] and has been recently gaining traction within the carbon dioxide community. Savéant originally reported that Fe(0) porphyrins would catalyze the reduction of CO_2 with the addition of weak Brönsted acids.[9] While initial studies of the Re(bipy)$(CO)_3$Cl were originally done in 10% water in DMF,[10] it was later reported that the addition of Brönsted acids would increase the rate of catalysis drastically.[11] Further work by our group then showed that the addition of Brönsted acids not only increases the rate of electrocatalysis with Re(bipy-*t*Bu)$(CO)_3$Cl, but that there is a primary kinetic isotope effect, suggesting that the rate limiting step involves the transfer of a proton.[12] In a similar system, Ni(II)(cyclam) is selective for CO production from CO_2 in H_2O,[13, 14] but is not electrocatalytic in organic solvents without the addition of a proton source (H_2O).[15]

Originally studied for the electrochemical reduction of protons to molecular hydrogen, the $Ni(P_2N_2)^{2+}$ complexes are the closest synthetic models for artificial hydrogenases.[16-19] These complexes are one of the few synthetic electrocatalysts that can catalyse both the oxidation of hydrogen and the reduction of protons. It has recently been extended to the oxidation of formate to CO_2.[20, 21] These complexes owe much of their catalytic properties to the pendant amines in the second coordination

sphere. It is these bifunctional ligands that allow for the stabilization of intermediates and proton management within the catalytic cycle. With this as a guide we sought out to investigate the role of the second coordination sphere in the reduction of CO_2 to CO using the model system $Re(bpy)(CO)_3Cl$.

7.2 Results and discussion

7.2.1 Synthesis

We initially chose several targets with the goal of being able to adjust both the functional group near the active site (**1-4**), but also the distance to the metal center (**5-8**) (Scheme 7.1). Our initial screening was to vary the carbon linker length using one or two carbon chains. The functional groups initially chosen were alcohols, primary, secondary, and tertiary amines. While we were primarily focused on amines, similar

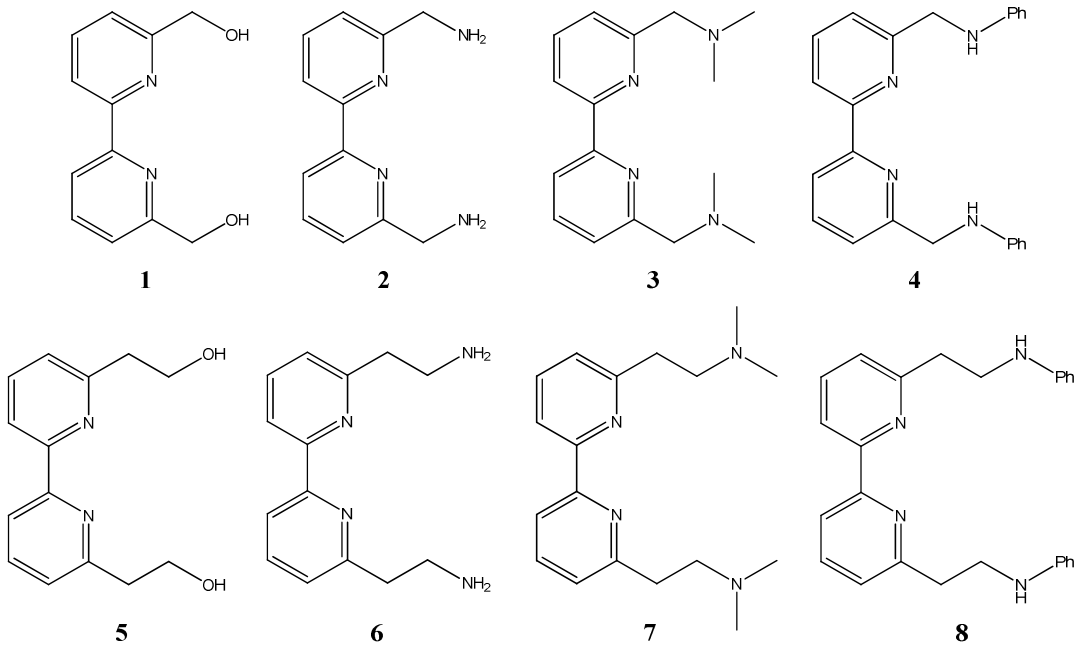

Scheme 7.1 Proposed ligands incorporating different acid/base groups and linker lengths

to the Dubois systems, the alcohol (**1**) was synthesized as it was a valuable synthetic precursor for other desired ligands. Once the initial synthesis had been developed we could then extend the synthesis to other amines to systematically vary the pKa of the pendant nitrogen.

Our initial synthetic target was the 6,6'-hydroxymethyl-2,2'-bipyridine, as it was easily synthesized as well as a precursor to several of the other compounds of interest. Oxidation of the commercially available 6,6'-dimethyl substituted bipyridine with CrO_3 and H_2SO_4 led to the formation of the carboxylic acid in high yields (90%). Esterification and subsequent reduction with sodium borohydride gave us the hydroxymethyl substituted bipyrine in modest yields (50%) (Scheme 7.2). Metalation was then accomplished by refluxing the ligand with $Re(CO)_5Cl$ in toluene for an hour to yield $Re(bipy\text{-}6,6'\text{-}CH_2OH)(CO)_3Cl$ (**1a**) with isolated yields in excess of 80%.

Synthesis of (**4**) was accomplished by the reaction of the ethyl carboxylic ester

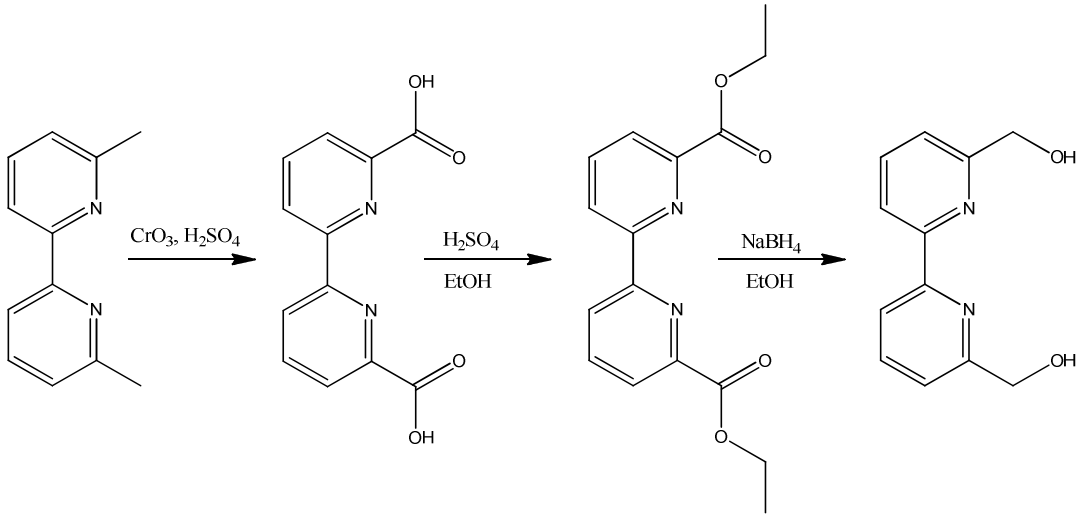

Scheme 7.2 Synthetic route for 6,6'-hydroxymethyl-2,2'-bipyridine

from the previous synthesis using a procedure analogous to that of Dias *et al.* for the conversion of esters to functionalized amides.[22] Reduction of this amide using lithium aluminum hydride and subsequent workup gave (**4**) in low isolated yields. Metalation of this ligand was attempted on the NMR scale (~5mg) but due to several binding geometries of the ligand and the possibility of multiple metals coordinating, no clean formation of the product was detected by NMR. This has also been seen by other members in our group for the attempted coordination of (**2**) to $Re(CO)_5Cl$.[23]

We have currently shifted our focus to compounds (**5-8**) as the 5-membered ring formed by the coordination of the bipyridine will likely be more favorable than the formation of the 6-membered ring by coordination of one of the pendant groups. Hopefully this will allow us to selectively coordinate the bipyridine while not coordinating the pendant base.

7.2.2 FTIR and X-Ray crystallography

The three *fac.* carbonyls on the complexes can be used as an accurate gauge of electron density at the metal due to modulation of their IR stretching frequencies by π back-bonding. Using this, we can compare the change in electronics around the

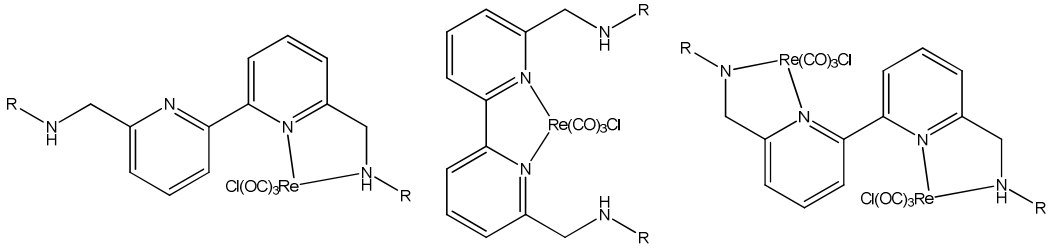

Figure 7.2 Possible coordination geometries of $Re(CO)_5Cl$ to ligands (**2-4**)

rhenium center from the known 4,4'-dimethyl-bipyridine complex compared to the substitution at the 6,6' position. $Re(6,6'\text{-dmb})(CO)_3Cl$ (6,6'-dmb = 6,6'-dimethyl-2,2'-bipyridine) (**9**) has three ν(CO) stretches at 2020, 1916, and 1892 cm^{-1}, which are slightly higher (~1 cm^{-1}) in energy than seen with the 4,4'-substitution. $Re(bipy\text{-}CH_2OH)(CO)_3Cl$ (bipy-CH_2OH = 6,6'-dihydroxymethyl-2,2'-bipyridine) (**1a**) has ν(CO) stretches at 2020, 1914, and 1895 cm^{-1}. While the high energy band is the same as (**9**), the splitting of the low energy bands is lower, possibly due to proximity of the hydroxymethyl groups to the equatorial carbonyls.

X-Ray quality crystals of (**1a**) were grown from the cooling of a warm saturated solution of the complex in ACN over a period of 15 minutes. The complex is an octahedral rhenium center with three facial carbonyls, a chelating bipyridine, and

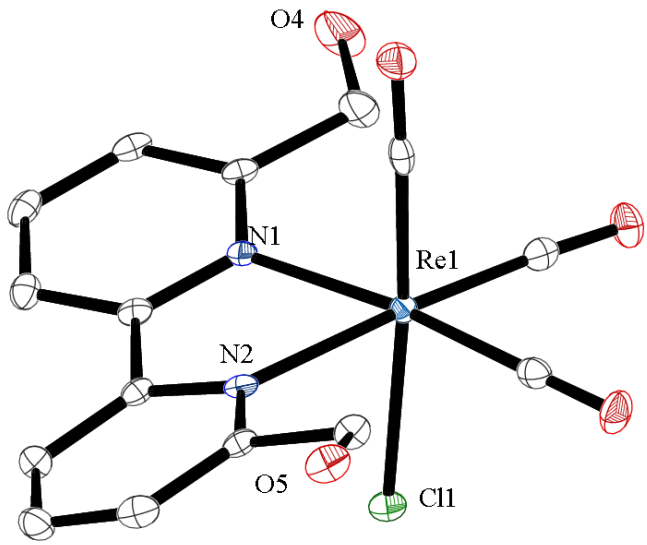

Figure 7.3 Molecular structure of (bipy-6,6'-CH_2OH)$(CO)_3Cl$. Hydrogen atoms and solvent of crystallization (ACN) omitted for clarity, ellipsoids are set at 50% probability

an axial chlorine. While the coordination environment around the metal center is unremarkable, there is a significant distortion of the bipyridine ligand. The bipyridine plane has twisted down towards the chloride (~20°), presumably from an electrostatic repulsion between the 6,6'-hydroxymethyl groups and the equatorial carbonyls (C2 – C15, 2.915 Å) (Figure 7.7, appendix).

X-Ray quality crystals of the control complex Re(6,6'-dmb)$(CO)_3$Cl (**9**) were grown from the vapor diffusion of Et_2O into a solution of the complex in acetonitrile. Within the unit cell there are three independent molecules (Z' = 3). Complex (**9**) also exists as an octahedral rhenium center with three facial carbonyls and a chelating bipyridine, with the sixth site occupied by a chorine atom. As with the 6,6'-

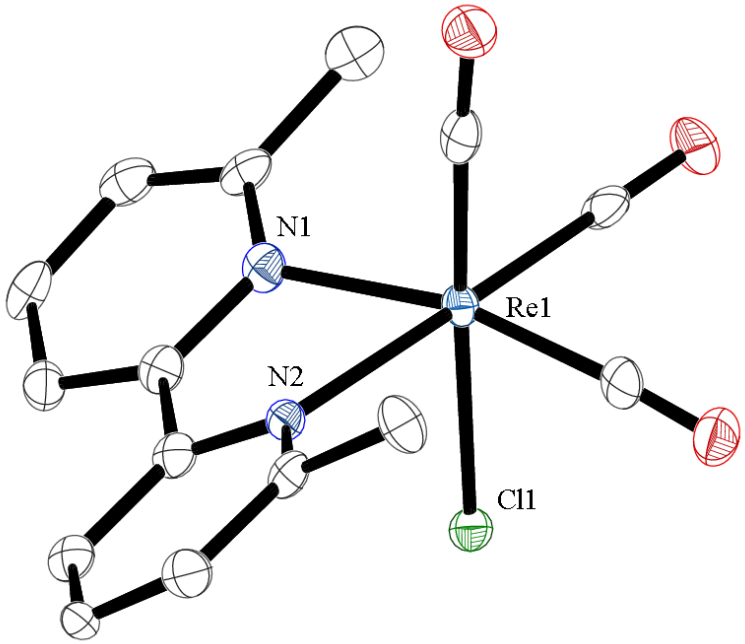

Figure 7.4 Molecular structure of one of the Re(6,6'-dmb)$(CO)_3$Cl molecules in the unit cell, Z' = 3. Hydrogen atoms omitted for clarity, and ellipsoids are set at 50% probability

dihydroxymethyl substituted bipyridine, there is a significant distortion of the bipyridine away from forming a square plane between the bipyridine and equatorial carbonyls. The largest distortion in the asymmetric unit is near 33° and is striking when compared to $Re(bipy)(CO)_3Cl$, as the chelating ligand and equatorial carbonyls form a plane with a RMSD of 0.052 Å.[24]

7.2.3 Electrochemistry

Electrochemistry of (**1a**) in acetonitrile shows three distinct reductions (Figure 7.8, appendix). The first reduction at -1.74 V is reversible and attributed to a ligand-based reduction. The second reduction at -2.12 V is irreversible and metal-based. The third quasi-reversible reduction at -2.33 V is attributed to a second ligand-based reduction (all potentials are referenced to Fc/Fc^+). The electrochemistry of this complex matches well with previously reported similar complexes.[25]

Upon saturation of the solution with CO_2 we see an increase in the current at the second reduction that we attribute to the electrocatalytic reduction of CO_2 to CO.

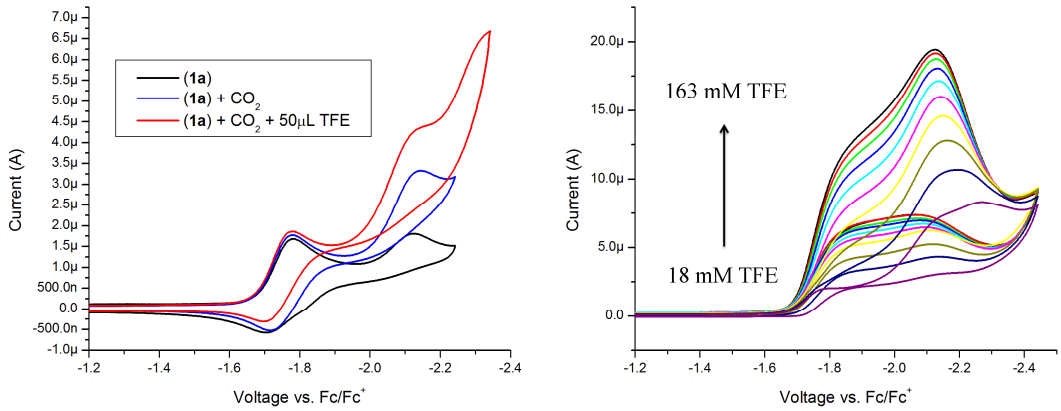

Figure 7.5 Cyclic voltammetry of 0.7mM $Re(bipy\text{-}CH_2OH)(CO)_3Cl$ with addition of carbon dioxide (left) and CO_2 saturated solutions with added TFE (right)

The peak current at the second reduction potential increases, giving an I_c/I_p of 1.8, where the I_c is the peak current under catalytic conditions and I_p is the peak current with no substrate.[11] Addition of a Brönstead acid such as 2,2,2-trifluoroethanol (TFE) increases the catalytic current until it reaches a maximum I_c/I_p of 10.8 with a total volume of 2mL of TFE added (163 mM).

As an electrochemical control, as well as a gauge on the steric effects of having substituents at the 6,6' position of 2,2'-bipyridine we compared the electrochemistry of (**9**) to that of complex (**1a**). Electrochemistry of (**9**) shows two reductions; the first one is ligand-based and the second one is attributed to a metal-based reduction (-1.81 V and -2.19 V vs. Fc/Fc^+ respectively). Upon saturation of the solution with CO_2 the current at the second reduction increases due to catalytic reduction of CO_2 to CO. The I_c/I_p for the reduction of CO2 to CO is 3.5, suggesting that this is in fact a better catalyst than (**1a**), however, when compared to the 4,4'-substituted dimethyl substituted bipyridine it does not appear to operate as efficiently.[11, 25] The catalytic

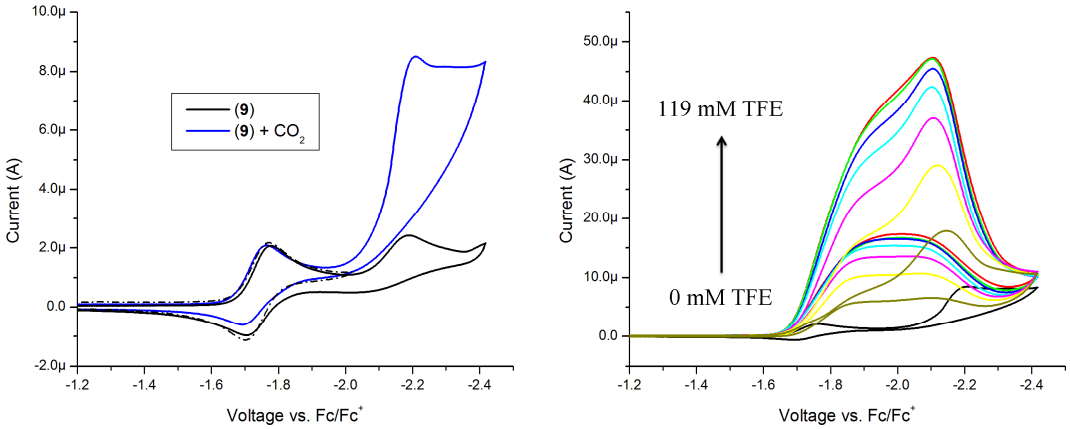

Figure 7.6 Cyclic voltammetry of 0.7mM Re(6,6'-dmb)$(CO)_3$Cl with addition of carbon dioxide (left) and CO_2 saturated solutions with added TFE (right)

peak plateaus with the addition of 1.4 mL of TFE at a corresponding I_c/I_p of 19.4, much higher than that of complex (**1a**). When comparing the addition of Brönstead acids to both complexes it is interesting to note the ratio of I_c/I_p is increased by the same amount for each complex, suggesting that the hydroxymethyl groups at the 6,6' position do not have any effect on the proton-coupled reduction of CO_2.

7.3 Conclusions and future work

We report the synthesis of two bipyridines, 6,6'-dihydroxymethyl-2,2'-bipyridine (**1**) and N,N'-([2,2'-bipyridine]-6,6'-diylbis(methylene))dianiline (**4**) and the coordination complexes Re(**1**)$(CO)_3$Cl (**1a**) and Re(6,6'-dmb)$(CO)_3$Cl (**9**). Adding substituents at the 6,6' position of 2,2'-bipyridine does not alter the electronics significantly when compared to substituents at the 4,4' position, as seen from the ν(CO) stretches. From the crystal structure we can see a steric effect of adding substituents at the 6,6' position, resulting in distortions in the coordination of the ligand to the metal.

From the electrochemistry we see a reduced rate of catalysis for the electrochemical reduction of CO_2 to CO, again presumably from the steric bulk near the metal center. While the addition of Brönsted acids does increase the catalytic rate for both complexes, the addition of the hydroxyl group does not show added benefit when compared to the methyl substitution. The addition of acid increases the relative rate of each catalyst equally, thus the addition of the alcohol has no positive net effect.

While these complexes are still catalysts, the next round of development may want to focus on placement of functional groups away from the 6,6' position (Scheme 7.3). It may be worth investigating hangman/pacman type ligand frameworks where the group is attached off the back, similar to those developed by Chang and Nocera.[26-29] This would be synthetically challenging, but has an interesting architecture that does not have any substituents close to the equatorial carbonyls, but hangs them from the back of the bipyridine. Another possible framework is the addition of P_2N_2 type ligands replacing a carbonyl and halide. The simple replacement of the bipyridine with a P_2N_2 ligand will presumably not be an electrocatalyst for the reduction of CO_2, due to the need of this class of complexes to have an electro-active bipyridine as an electron reservoir. However, addition of the chelating phosphine to make an Re(I) mixed ligand framework, similar to Sullivan *et al.*,[30] may allow for cooperative interaction between the pendant amine and bound CO_2.

While this has the possibility to increase catalytic rates, one problem still

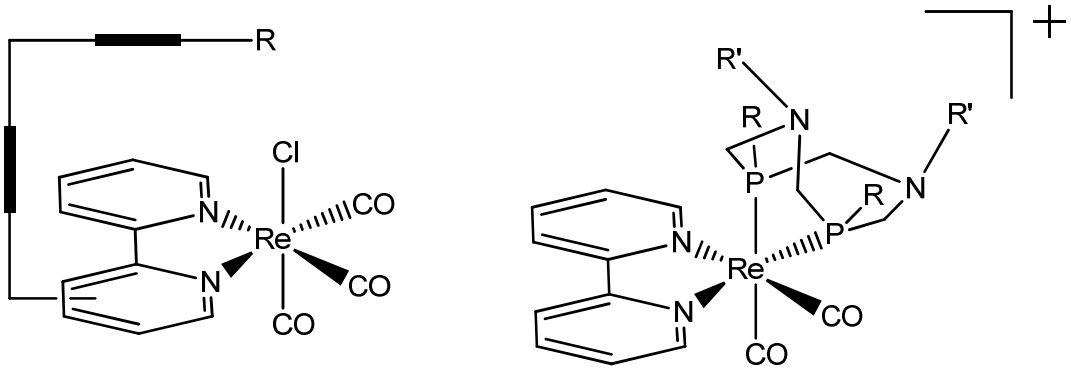

Scheme 7.3 Proposed complexes for the addition of pendant amines to the model system $Re(bipy)(CO)_3Cl$

remains, and that is that of the large overpotential (~1 V) for the reduction of CO_2 to CO. The catalytic reaction requires accessing the Re(0) state, which in these systems requires voltages near -2 V vs. Fc/Fc^+. It may be beneficial to focus work on a system that does not operate at these very negative potentials, such as the Ni(cyclam) system. This system has much lower overpotentials, arising from only having to access the Ni(I) state, but suffers from slow kinetics.[15] Ni(cyclam) may benefit more from the addition of proton relays than the rhenium system, which already operates at some of the fastest known catalytic rates for the electrocatalytic reduction of CO_2.

7.4 Experimental

General considerations. 6,6'-dicarboxylic acid-2,2'-bipyridine was synthesized according to literature procedures.[31] TBAH was recrystallized twice from methanol, and dried under vacuum. All other chemicals were purchased from commercial sources and used as received. CH_3CN, THF, Et_2O and Toluene were all sparged with argon and dried over basic alumina with a custom dry solvent system. Infrared spectra were collected on a Thermo Scientific Nicolet 6700. NMR spectra were collected on either a Jeol 500 MHz Spectrometer or a Varian 400 MHz Spectrometer and analyzed using Jeol Delta software.

Synthesis of diethyl [2,2'-bipyridine]-6,6'-dicarboxylate. 0.5 g (2.05 mmol) of 6,6'-dicarboxylic acid-2,2'-bipyridine was placed in a flask with 50ml EtOH. 7mL of concentrated H_2SO_4 was added dropwise. The reaction was then refluxed for three hours. After cooling, the product was extracted into $CHCl_3$ (3 x20 mL), dried with $NaSO_4$, and evaporated to dryness resulting in 0.58 g (1.93mmol, 94%) of diethyl

[2,2'-bipyridine]-6,6'-dicarboxylate. ^{1}H NMR (400 MHz, $CDCl_3$, 20 °C): δ 1.47 (t, 6H, J = 7 Hz), δ 4.50 (q, 4H, J = 7 Hz), δ 7.99 (t, 2H, *J* = 7 Hz), δ 8.15 (dd, 2H, *J* = 8,1 Hz), δ 8.77 (dd, 2H, *J* = 8,1 Hz).

Synthesis of 6,6'-dihydroxymethyl-2,2'-bipyridine. 0.5 g (1.66 mmol) of diethyl [2,2'-bipyridine]-6,6'-dicarboxylate was placed in a flask with 25 mL of EtOH. An excess of $NaBH_4$ (~1 g) was added to the solution and stirred overnight. The product was then extracted into $CHCl_3$ (3 x20 mL), dried with $NaSO_4$, and evaporated to dryness resulting in 0.208 g (0.963 mmol, 58%). ^{1}H NMR (400 MHz, $CDCl_3$, 20 °C): δ 4.00 (t, 2H, *J* = 5 Hz), δ 4.84 (d, 4H, *J* = 4 Hz), δ 7.27 (d, 2H, *J* = 8 Hz), δ 7.84 (t, 2H, *J* = 8 Hz), δ 8.35 (d, 2H, *J* = 8 Hz).

Synthesis of N^6,$N^{6'}$-diphenyl-[2,2'-bipyridine]-6,6'-dicarboxamide. 93 mg (1.0 mmol) of analine was dissolved in 10 mL of Et_2O in a schlenk flask and was sparged with argon for 15 minutes then cooled to -78°C. 0.5 mL of 1.6 M *n*Bu-Li was then added dropwise affording a brown solution. The solution was allowed to warm to 0°C for 10 minutes then cooled back down to -78°C. 100 mg of diethyl [2,2'-bipyridine]-6,6'-dicarboxylate (0.33 mmol) in 10 mL Et_2O was added dropwise. The solution was then allowed to warm to room temperature and quenched with 5 mL of H_2O. The product was then extracted into CH_2Cl_2 (3 x 20 mL) dried over $NaSO_4$ and evaporated to dryness resulting in 63 mg (0.16 mmol, 48% yield) of a white powder. ^{1}H NMR (500 MHz, $CDCl_3$, 20 °C): δ 7.20 (t, 2H, *J* = 7 Hz), δ 7.44 (t, 4H, *J* = 8 Hz), δ 7.83 (d, 4H, *J* = 8 Hz) δ 8.16 (t, 2H, *J* = 8 Hz) δ 8.43 (d, 2H, *J* = 7 Hz) δ 8.64 (d, 2H, *J* = 8 Hz).

Synthesis of N,N'-([2,2'-bipyridine]-6,6'-diylbis(methylene))dianiline (4). 0.063 g (0.16 mmol) of N^6,$N^{6'}$-diphenyl-[2,2'-bipyridine]-6,6'-dicarboxamide was dissolved in 5 mL of Et_2O under an inert atmosphere. Approximately 0.5 grams (xs) of $LiAlH_4$ was added and the solution and was stirred under nitrogen for 2 hours. The reaction was then diluted with 10 mL of Et_2O and cooled to 0°C. 0.5 mL of H_2O was added slowly to quench the reaction. Then 0.5 mL of 15% aq. sodium hydroxide, followed by an additional 1.5 mL of H_2O. The solution was then allowed to reach room temperature where it was dried with MgSO4, filtered and evaporated to dryness to yield 35 mg (0.096 mmol, 60% yield) of a white powder. ^{1}H NMR (400 MHz, CD_2Cl_2, 20 °C): δ 4.54 (s, 4H), δ 6.72 (m, 6H), δ 7.19 (t, 4H, *J* = 7 Hz) δ 7.36 (d, 2H, *J* = 8 Hz) δ 7.80 (t, 2H, *J* = 8 Hz) δ 8.34 (d, 2H, *J* = 8 Hz) N-H proton was not observed due to exchange with residual solvent H_2O.

Synthesis of Re(bipy-CH_2OH)$(CO)_3$Cl (1a). 83.5 mg of (**1**) (0.386 mmol) and 140 mg of $Re(CO)_5Cl$ (0.386 mmol) were dissolved in 20 mL of toluene and refluxed for 1 hour. After cooling the product was filtered off to yield 164 mg of (**1a**) (0.313 mmol, 81% yield). ν(CO)(THF): 2020, 1914, 1895 cm^{-1}, ^{1}H NMR (500 MHz, CD_3CN, 20 °C): δ 4.07 (t, 2H, *J* = 6 Hz), δ 5.10 (dd, 4H, *J* = 59, 6 Hz), δ 7.95 (d, 2H, *J* = 8 Hz), δ 8.17 (t, 2H, *J* = 8 Hz), δ 8.30 (d, 2H, *J* = 8 Hz).

Synthesis of Re(6,6'-dmb)$(CO)_3$Cl (9). 100 mg of 6,6'-dimethyl-2,2'-bipyridine (0.543 mmol) and 196 mg of $Re(CO)_5Cl$ (0.543 mmol) were dissolved in 20 mL of toluene and refluxed for 1 hour. After cooling the product was filtered off to yield 237 mg of (**9**) (0.483 mmol, 89% yield) ν(CO)(THF): 2020, 1916, 1892 cm^{-1} ^{1}H NMR

(500 MHz, CD_3CN, 20 °C): δ 3.05 (s, 6H), δ 7.58 (d, 2H, *J* = 8 Hz), δ 8.02 (t, 2H, *J* = 8 Hz), δ 8.19 (d, 2H, *J* = 8 Hz).

X-ray structure determination. The single crystal X-ray diffraction studies were carried out on either a Bruker Kappa APEX-II CCD diffractometer or Bruker Platform APEX CCD diffractometer, and both instruments were equipped with Mo Kα radiation (λ = 0.71073 Å). The crystals were mounted on a Cryoloop with Paratone oil, and data was collected under a nitrogen gas stream at 100(2) K using ω and ϕ scans. Data was integrated using the Bruker SAINT software program and scaled using the SADABS software program. Solution by direct methods (SHELXS) produced a complete phasing model consistent with the proposed structure. All nonhydrogen atoms were refined anisotropically by full-matrix least-squares methods (SHELXL-97).[32] All hydrogen atoms were placed using a riding model. Their positions were constrained relative to their parent atom using the appropriate HFIX command in SHELXL-97. Crystallographic data are summarized in the appendix.

Electrochemistry. All electrochemical experiments were performed using a BASi Epsilon potentiostat and an air-tight one compartment electrochemical cell. Glassy carbon (BASi 1 mm diameter) was used as the working electrode, a Pt wire was used as the counter, and an Ag wire separated from the solution by a Vycor tip was used as a pseudo reference (Ferrocene added as an additional reference). All electrochemical experiments were performed in acetonitrile with 0.1 M tetrabutylammonium hexafluorophosphate (TBAH) as the supporting electrolyte except where otherwise noted, and were purged with either argon or CO_2 before CVs were taken. Re

concentrations started at stated concentrations and decreased with addition of Brönsted acid. CO_2 experiments were performed at gas saturation (~ 0.28 M).

Note: The material in this chapter is unpublished work and was performed in collaboration with Frank Mariskal.

7.5 References

1. Benson EE, Kubiak CP, Sathrum AJ, & Smieja JM (2009) Electrocatalytic and homogeneous approaches to conversion of CO_2 to liquid fuels. *Chem. Soc. Rev.* 38(1):89-99.

2. Savéant J-M (2008) Molecular Catalysis of Electrochemical Reactions. Mechanistic Aspects. *Chem. Rev.* 108(7):2348-2378.

3. Dobbek H, Gremer L, Kiefersauer R, Huber R, & Meyer O (2002) Catalysis at a dinuclear [CuSMo(==O)OH] cluster in a CO dehydrogenase resolved at 1.1-angstrom resolution. *P. Nat. Acad. Sci. USA* 99(25):15971-15976.

4. Jeoung JH & Dobbek H (2007) Carbon dioxide activation at the Ni,Fe-cluster of anaerobic carbon monoxide dehydrogenase. *Science* 318:1461-1464.

5. Dobbek H, Gremer L, Meyer O, & Huber R (1999) Crystal structure and mechanism of CO dehydrogenase, a molybdo iron-sulfur flavoprotein containing S-selanylcysteine. *P. Nat. Acad. Sci. USA* 96(16):8884-8889.

6. Hammes-Schiffer S & Soudackov AV (2008) Proton-Coupled Electron Transfer in Solution, Proteins, and Electrochemistry. *J. Phys. Chem. B* 112(45):14108-14123.

7. Hammes-Schiffer S (2009) Theory of Proton-Coupled Electron Transfer in Energy Conversion Processes. *Accounts Chem. Res.* 42(12):1881-1889.

8. Huynh MHV & Meyer TJ (2007) Proton-Coupled Electron Transfer. *Chem. Rev.* 107(11):5004-5064.

9. Bhugun I, Lexa D, & Saveant JM (1996) Catalysis of the electrochemical reduction of carbon dioxide by iron(O) porphyrins: Synergystic effect of weak Bronsted acids. *J. Am. Chem. Soc.* 118(7):1769-1776.

10. Hawecker J, Lehn JM, & Ziessel R (1984) Electrocatalytic Reduction of Carbon-Dioxide Mediated by $Re(bipy)(CO)_3Cl$ (Bipy=2,2'-Bipyridine). *J. Chem. Soc.-Chem. Commun.* (6):328-330.

11. Wong K-Y, Chung W-H, & Lau C-P (1998) The effect of weak Brönsted acids on the electrocatalytic reduction of carbon dioxide by a rhenium tricarbonyl bipyridyl complex. *J. Electroanal. Chem.* 453(1-2):161-169.

12. Smieja JM, *et al.* (2012) Kinetic and structural studies, origins of selectivity, and interfacial charge transfer in the artificial photosynthesis of CO. *P. Nat. Acad. Sci. USA*:Accepted.

13. Beley M, Collin JP, Ruppert R, & Sauvage JP (1986) Electrocatalytic Reduction of Co2 by Ni Cyclam2+ in Water - Study of the Factors Affecting the Efficiency and the Selectivity of the Process. *J. Am. Chem. Soc.* 108(24):7461-7467.

14. Beley M, Collin JP, Ruppert R, & Sauvage JP (1984) Nickel(Ii) Cyclam - an Extremely Selective Electrocatalyst for Reduction of CO_2 in Water. *J. Chem. Soc.-Chem. Commun.* (19):1315-1316.

15. Froehlich JD & Kubiak CP (2012) Homogeneous CO_2 Reduction by Ni(cyclam) at a Glassy Carbon Electrode. *Inorg. Chem.* 51(7):3932-3934.

16. DuBois DL & Bullock RM (2011) Molecular Electrocatalysts for the Oxidation of Hydrogen and the Production of Hydrogen – The Role of Pendant Amines as Proton Relays. *Eur. J. Inorg. Chem.* 2011(7):1017-1027.

17. Rakowski Dubois M & Dubois DL (2009) Development of Molecular Electrocatalysts for CO_2 Reduction and H_2 Production/Oxidation. *Accounts Chem. Res.* 42(12):1974-1982.

18. DuBois MR & DuBois DL (2008) The role of pendant bases in molecular catalysts for H2 oxidation and production. *Comptes Rendus Chimie* 11(8):805-817.

19. Wilson AD, *et al.* (2005) Hydrogen Oxidation and Production Using Nickel-Based Molecular Catalysts with Positioned Proton Relays. *J. Am. Chem. Soc.* 128(1):358-366.

20. Seu CS, Appel AM, Doud MD, DuBois DL, & Kubiak CP (2012) Formate oxidation via β-deprotonation in $[Ni(PR_2NR'_2)_2(CH_3CN)]^{2+}$ complexes. *Energy & Eviron. Sci.*

21. Galan BR, *et al.* (2011) Electrocatalytic Oxidation of Formate by $[Ni(PR_2NR'_2)_2(CH_3CN)]^{2+}$ Complexes. *J. Am. Chem. Soc.* 133(32):12767-12779.

22. Rivière-Baudet M, Morère A, & Dias M (1992) A simple general method for conversion of functionalized esters to functionalized amides. *Tetrahedron Letters* 33(43):6453-6456.

23. Grice KA (2012) Unpublished results. (University of California San Diego).

24. Kurz P, Probst B, Spingler B, & Alberto R (2006) Ligand Variations in $[ReX(diimine)(CO)_3]$ Complexes: Effects on Photocatalytic CO_2 Reduction. *Eur. J. Inorg. Chem.* 2006(15):2966-2974.

25. Smieja JM & Kubiak CP (2010) Re(bipy-tBu)$(CO)_3$Cl−improved Catalytic Activity for Reduction of Carbon Dioxide: IR-Spectroelectrochemical and Mechanistic Studies. *Inorg. Chem.* 49(20):9283-9289.

26. McGuire Jr R, *et al.* (2010) Oxygen reduction reactivity of cobalt(ii) hangman porphyrins. *Chemical Science* 1(3):411-414.

27. Rosenthal J & Nocera DG (2007) Role of Proton-Coupled Electron Transfer in O–O Bond Activation. *Accounts Chem. Res.* 40(7):543-553.

28. Chang CJ, Deng Y, Heyduk AF, Chang CK, & Nocera DG (2000) Xanthene-Bridged Cofacial Bisporphyrins. *Inorg. Chem.* 39(5):959-966.

29. Chang CJ, *et al.* (2000) Electrocatalytic four-electron reduction of oxygen to water by a highly flexible cofacial cobalt bisporphyrin. *Chem. Commun.* (15):1355-1356.

30. Smithback JL, Helms JB, Schutte E, Woessner SM, & Sullivan BP (2006) Preparative Routes to Luminescent Mixed-Ligand Rhenium(I) Dicarbonyl Complexes. *Inorg. Chem.* 45(5):2163-2174.

31. Alyapyshev MY, *et al.* (2008) New systems based on 2,2’-dipyridyl-6,6’-dicarboxylic acid diamides for Am–Eu separation. *Mendeleev Communications* 18(6):336-337.

32. Sheldrick G (2008) A short history of SHELX. *Acta Crystallographica Section A* 64(1):112-122.

7.6 Appendix

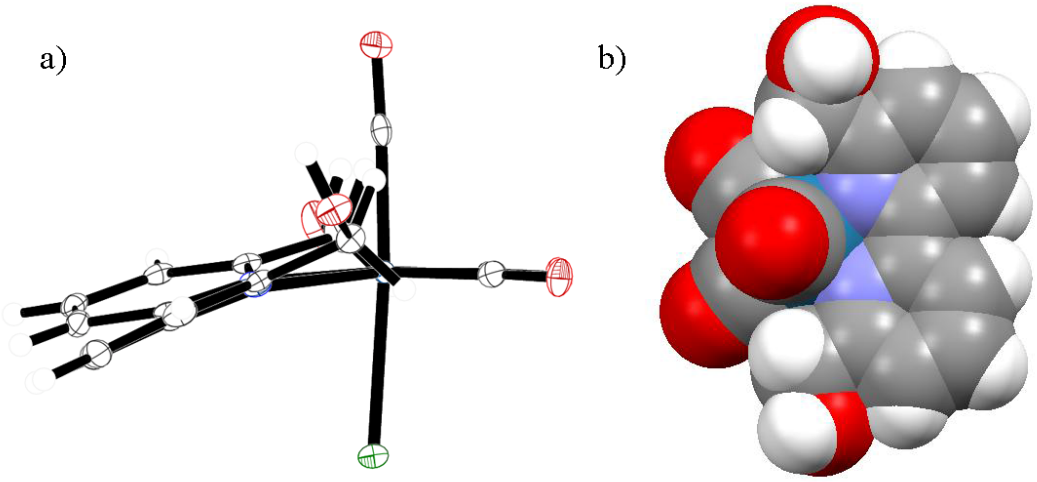

Figure 7.7 Molecular structure of (**1a**) a) showing the distortion of the bipyridine and b) the spacefill model of complex (**1a**)

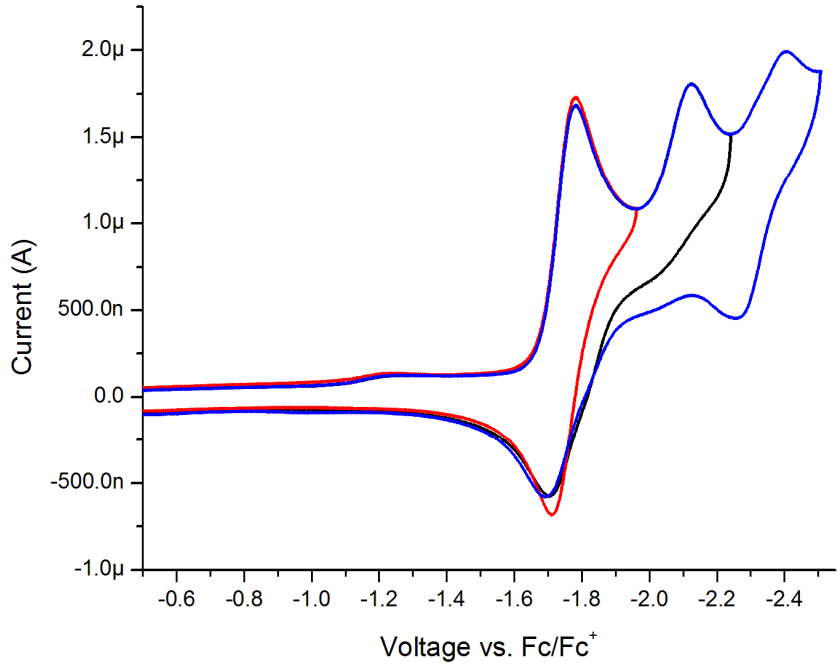

Figure 7.8 Cyclic voltammetry of 0.7mM Re(bipy-CH_2OH)$(CO)_3Cl$ in ACN at 100mV/s using a glassy carbon working electrode, Pt counter, and silver wire reference with Fc as an internal standard**.**

Table 7.1 Crystal data and structure refinement for $Re(6,6'\text{-dmb})(CO)_3Cl$

Identification code	twin4	
Empirical formula	C15 H12 Cl1 N2 O3 Re1	
Formula weight	489.93	
Temperature	100(2) K	
Wavelength	0.71073 Å	
Crystal system	Triclinic	
Space group	P-1	
Unit cell dimensions	a = 7.7306(6) Å	α= 107.4040(10)°.
	b = 17.2712(14) Å	β= 89.9610(10)°.
	c = 17.9778(14) Å	γ = 100.6640(10)°.
Volume	2247.1(3) $Å^3$	
Z	6	
Density (calculated)	2.172 Mg/m^3	
Absorption coefficient	8.303 mm^{-1}	
F(000)	1392	
Crystal size	0.20 x 0.20 x 0.05 mm^3	
Theta range for data collection	1.19 to 25.43°.	
Index ranges	-9<=h<=9, -20<=k<=19, 0<=l<=21	
Reflections collected	8305	
Independent reflections	8305 [R(int) = 0.0000]	
Completeness to theta = 25.00°	100.0 %	
Absorption correction	Semi-empirical from equivalents	
Max. and min. transmission	0.6816 and 0.2875	
Refinement method	Full-matrix least-squares on F^2	
Data / restraints / parameters	8305 / 0 / 584	
Goodness-of-fit on F^2	1.083	
Final R indices [I>2sigma(I)]	R1 = 0.0301, wR2 = 0.0780	
R indices (all data)	R1 = 0.0338, wR2 = 0.0796	
Largest diff. peak and hole	1.422 and -1.944 $e.Å^{-3}$	

Table 7.2 Bond lengths [Å] and angles [°] for Re(6,6'-dmb)$(CO)_3$Cl.

C(1)-O(1)	1.146(9)	C(16)-O(4)	1.170(10)
C(1)-Re(1)	1.935(8)	C(16)-Re(2)	1.896(9)
C(2)-O(2)	1.156(9)	C(17)-O(5)	1.166(10)
C(2)-Re(1)	1.921(7)	C(17)-Re(2)	1.904(8)
C(3)-O(3)	1.154(9)	C(18)-O(6)	1.096(9)
C(3)-Re(1)	1.910(8)	C(18)-Re(2)	1.955(8)
C(4)-N(1)	1.362(9)	C(19)-N(4)	1.365(9)
C(4)-C(5)	1.378(11)	C(19)-C(20)	1.385(11)
C(4)-C(14)	1.503(10)	C(19)-C(30)	1.500(11)
C(5)-C(6)	1.364(11)	C(20)-C(21)	1.364(11)
C(5)-H(5)	0.9500	C(20)-H(20)	0.9500
C(6)-C(7)	1.390(10)	C(21)-C(22)	1.386(10)
C(6)-H(6)	0.9500	C(21)-H(21)	0.9500
C(7)-C(8)	1.386(10)	C(22)-C(23)	1.402(10)
C(7)-H(7)	0.9500	C(22)-H(22)	0.9500
C(8)-N(1)	1.352(9)	C(23)-N(4)	1.360(9)
C(8)-C(9)	1.485(10)	C(23)-C(24)	1.475(10)
C(9)-N(2)	1.352(10)	C(24)-N(3)	1.348(10)
C(9)-C(10)	1.405(10)	C(24)-C(25)	1.405(10)
C(10)-C(11)	1.382(10)	C(25)-C(26)	1.369(11)
C(10)-H(10)	0.9500	C(25)-H(25)	0.9500
C(11)-C(12)	1.395(11)	C(26)-C(27)	1.373(12)
C(11)-H(11)	0.9500	C(26)-H(26)	0.9500
C(12)-C(13)	1.381(9)	C(27)-C(28)	1.408(11)
C(12)-H(12)	0.9500	C(27)-H(27)	0.9500
C(13)-N(2)	1.361(9)	C(28)-N(3)	1.359(9)
C(13)-C(15)	1.493(10)	C(28)-C(29)	1.481(11)
C(14)-H(14A)	0.9800	C(29)-H(29A)	0.9800
C(14)-H(14B)	0.9800	C(29)-H(29B)	0.9800
C(14)-H(14C)	0.9800	C(29)-H(29C)	0.9800
C(15)-H(15A)	0.9800	C(30)-H(30A)	0.9800
C(15)-H(15B)	0.9800	C(30)-H(30B)	0.9800
C(15)-H(15C)	0.9800	C(30)-H(30C)	0.9800

Table 7.2 Cont.

C(31)-O(7)	1.167(9)	C(45)-H(0AC)	0.9800
C(31)-Re(3)	1.906(8)	N(1)-Re(1)	2.207(6)
C(32)-O(8)	1.158(10)	N(2)-Re(1)	2.202(5)
C(32)-Re(3)	1.910(8)	N(3)-Re(2)	2.200(6)
C(33)-O(9)	1.152(10)	N(4)-Re(2)	2.220(6)
C(33)-Re(3)	1.914(9)	N(5)-Re(3)	2.209(5)
C(34)-N(6)	1.356(9)	N(6)-Re(3)	2.194(6)
C(34)-C(35)	1.400(11)	Cl(1)-Re(1)	2.4871(18)
C(34)-C(45)	1.498(10)	Cl(2)-Re(2)	2.4663(19)
C(35)-C(36)	1.375(11)	Cl(3)-Re(3)	2.4744(19)
C(35)-H(35)	0.9500		
C(36)-C(37)	1.390(10)	O(1)-C(1)-Re(1)	175.5(7)
C(36)-H(36)	0.9500	O(2)-C(2)-Re(1)	176.9(7)
C(37)-C(38)	1.387(10)	O(3)-C(3)-Re(1)	176.1(6)
C(37)-H(37)	0.9500	N(1)-C(4)-C(5)	120.5(7)
C(38)-N(6)	1.375(9)	N(1)-C(4)-C(14)	119.3(7)
C(38)-C(39)	1.477(9)	C(5)-C(4)-C(14)	120.2(6)
C(39)-N(5)	1.352(10)	C(6)-C(5)-C(4)	121.5(7)
C(39)-C(40)	1.390(9)	C(6)-C(5)-H(5)	119.2
C(40)-C(41)	1.386(10)	C(4)-C(5)-H(5)	119.2
C(40)-H(40)	0.9500	C(5)-C(6)-C(7)	118.3(8)
C(41)-C(42)	1.374(11)	C(5)-C(6)-H(6)	120.9
C(41)-H(41)	0.9500	C(7)-C(6)-H(6)	120.9
C(42)-C(43)	1.400(10)	C(8)-C(7)-C(6)	118.6(7)
C(42)-H(42)	0.9500	C(8)-C(7)-H(7)	120.7
C(43)-N(5)	1.356(9)	C(6)-C(7)-H(7)	120.7
C(43)-C(44)	1.500(11)	N(1)-C(8)-C(7)	122.7(7)
C(44)-H(44A)	0.9800	N(1)-C(8)-C(9)	115.6(6)
C(44)-H(44B)	0.9800	C(7)-C(8)-C(9)	121.4(7)
C(44)-H(44C)	0.9800	N(2)-C(9)-C(10)	121.5(6)
C(45)-H(0AA)	0.9800	N(2)-C(9)-C(8)	116.0(6)
C(45)-H(0AB)	0.9800	C(10)-C(9)-C(8)	122.2(7)

Table 7.2 Cont.

C(11)-C(10)-C(9)	119.2(7)	C(19)-C(20)-H(20)	119.3
C(11)-C(10)-H(10)	120.4	C(20)-C(21)-C(22)	118.3(7)
C(9)-C(10)-H(10)	120.4	C(20)-C(21)-H(21)	120.9
C(10)-C(11)-C(12)	118.8(6)	C(22)-C(21)-H(21)	120.9
C(10)-C(11)-H(11)	120.6	C(21)-C(22)-C(23)	119.9(7)
C(12)-C(11)-H(11)	120.6	C(21)-C(22)-H(22)	120.1
C(13)-C(12)-C(11)	119.7(7)	C(23)-C(22)-H(22)	120.1
C(13)-C(12)-H(12)	120.1	N(4)-C(23)-C(22)	120.8(6)
C(11)-C(12)-H(12)	120.1	N(4)-C(23)-C(24)	117.0(6)
N(2)-C(13)-C(12)	121.5(6)	C(22)-C(23)-C(24)	122.1(7)
N(2)-C(13)-C(15)	119.3(6)	N(3)-C(24)-C(25)	122.0(7)
C(12)-C(13)-C(15)	119.2(6)	N(3)-C(24)-C(23)	116.3(6)
C(4)-C(14)-H(14A)	109.5	C(25)-C(24)-C(23)	121.6(7)
C(4)-C(14)-H(14B)	109.5	C(26)-C(25)-C(24)	119.1(8)
H(14A)-C(14)-H(14B)	109.5	C(26)-C(25)-H(25)	120.5
C(4)-C(14)-H(14C)	109.5	C(24)-C(25)-H(25)	120.5
H(14A)-C(14)-H(14C)	109.5	C(25)-C(26)-C(27)	118.9(7)
H(14B)-C(14)-H(14C)	109.5	C(25)-C(26)-H(26)	120.6
C(13)-C(15)-H(15A)	109.5	C(27)-C(26)-H(26)	120.6
C(13)-C(15)-H(15B)	109.5	C(26)-C(27)-C(28)	120.7(7)
H(15A)-C(15)-H(15B)	109.5	C(26)-C(27)-H(27)	119.7
C(13)-C(15)-H(15C)	109.5	C(28)-C(27)-H(27)	119.7
H(15A)-C(15)-H(15C)	109.5	N(3)-C(28)-C(27)	119.9(7)
H(15B)-C(15)-H(15C)	109.5	N(3)-C(28)-C(29)	119.3(7)
O(4)-C(16)-Re(2)	174.4(7)	C(27)-C(28)-C(29)	120.7(7)
O(5)-C(17)-Re(2)	174.7(7)	C(28)-C(29)-H(29A)	109.5
O(6)-C(18)-Re(2)	175.7(7)	C(28)-C(29)-H(29B)	109.5
N(4)-C(19)-C(20)	120.4(7)	H(29A)-C(29)-H(29B)	109.5
N(4)-C(19)-C(30)	119.7(7)	C(28)-C(29)-H(29C)	109.5
C(20)-C(19)-C(30)	119.9(6)	H(29A)-C(29)-H(29C)	109.5
C(21)-C(20)-C(19)	121.4(7)	H(29B)-C(29)-H(29C)	109.5
C(21)-C(20)-H(20)	119.3	C(19)-C(30)-H(30A)	109.5

Table 7.2 Cont.

C(19)-C(30)-H(30B)	109.5	C(41)-C(42)-C(43)	120.0(7)
H(30A)-C(30)-H(30B)	109.5	C(41)-C(42)-H(42)	120.0
C(19)-C(30)-H(30C)	109.5	C(43)-C(42)-H(42)	120.0
H(30A)-C(30)-H(30C)	109.5	N(5)-C(43)-C(42)	120.7(7)
H(30B)-C(30)-H(30C)	109.5	N(5)-C(43)-C(44)	120.5(6)
O(7)-C(31)-Re(3)	173.2(7)	C(42)-C(43)-C(44)	118.8(7)
O(8)-C(32)-Re(3)	175.1(6)	C(43)-C(44)-H(44A)	109.5
O(9)-C(33)-Re(3)	175.8(7)	C(43)-C(44)-H(44B)	109.5
N(6)-C(34)-C(35)	121.6(7)	H(44A)-C(44)-H(44B)	109.5
N(6)-C(34)-C(45)	119.1(7)	C(43)-C(44)-H(44C)	109.5
C(35)-C(34)-C(45)	119.3(7)	H(44A)-C(44)-H(44C)	109.5
C(36)-C(35)-C(34)	119.9(7)	H(44B)-C(44)-H(44C)	109.5
C(36)-C(35)-H(35)	120.1	C(34)-C(45)-H(0AA)	109.5
C(34)-C(35)-H(35)	120.1	C(34)-C(45)-H(0AB)	109.5
C(35)-C(36)-C(37)	119.0(8)	H(0AA)-C(45)-H(0AB)	109.5
C(35)-C(36)-H(36)	120.5	C(34)-C(45)-H(0AC)	109.5
C(37)-C(36)-H(36)	120.5	H(0AA)-C(45)-H(0AC)	109.5
C(38)-C(37)-C(36)	119.4(7)	H(0AB)-C(45)-H(0AC)	109.5
C(38)-C(37)-H(37)	120.3	C(8)-N(1)-C(4)	118.1(7)
C(36)-C(37)-H(37)	120.3	C(8)-N(1)-Re(1)	113.1(5)
N(6)-C(38)-C(37)	121.8(6)	C(4)-N(1)-Re(1)	127.7(5)
N(6)-C(38)-C(39)	115.9(6)	C(9)-N(2)-C(13)	118.9(6)
C(37)-C(38)-C(39)	121.9(6)	C(9)-N(2)-Re(1)	112.8(4)
N(5)-C(39)-C(40)	122.0(6)	C(13)-N(2)-Re(1)	127.4(5)
N(5)-C(39)-C(38)	117.2(6)	C(24)-N(3)-C(28)	119.0(7)
C(40)-C(39)-C(38)	120.6(7)	C(24)-N(3)-Re(2)	113.8(5)
C(41)-C(40)-C(39)	119.0(7)	C(28)-N(3)-Re(2)	126.2(5)
C(41)-C(40)-H(40)	120.5	C(23)-N(4)-C(19)	119.2(6)
C(39)-C(40)-H(40)	120.5	C(23)-N(4)-Re(2)	113.1(4)
C(42)-C(41)-C(40)	119.1(7)	C(19)-N(4)-Re(2)	127.5(5)
C(42)-C(41)-H(41)	120.5	C(39)-N(5)-C(43)	119.1(6)
C(40)-C(41)-H(41)	120.5	C(39)-N(5)-Re(3)	112.6(4)

Table 7.2 Cont.

C(43)-N(5)-Re(3)	127.4(5)	C(16)-Re(2)-N(4)	171.0(3)
C(34)-N(6)-C(38)	118.2(6)	C(17)-Re(2)-N(4)	100.9(3)
C(34)-N(6)-Re(3)	128.3(5)	C(18)-Re(2)-N(4)	92.9(3)
C(38)-N(6)-Re(3)	113.1(4)	N(3)-Re(2)-N(4)	75.0(2)
C(3)-Re(1)-C(2)	85.0(3)	C(16)-Re(2)-Cl(2)	87.8(2)
C(3)-Re(1)-C(1)	90.6(3)	C(17)-Re(2)-Cl(2)	94.7(2)
C(2)-Re(1)-C(1)	84.8(3)	C(18)-Re(2)-Cl(2)	177.6(2)
C(3)-Re(1)-N(2)	97.3(3)	N(3)-Re(2)-Cl(2)	83.28(16)
C(2)-Re(1)-N(2)	176.0(3)	N(4)-Re(2)-Cl(2)	85.01(16)
C(1)-Re(1)-N(2)	98.3(3)	C(31)-Re(3)-C(32)	81.6(3)
C(3)-Re(1)-N(1)	100.5(3)	C(31)-Re(3)-C(33)	88.5(3)
C(2)-Re(1)-N(1)	102.1(3)	C(32)-Re(3)-C(33)	90.4(4)
C(1)-Re(1)-N(1)	167.4(3)	C(31)-Re(3)-N(6)	101.1(3)
N(2)-Re(1)-N(1)	74.4(2)	C(32)-Re(3)-N(6)	174.3(3)
C(3)-Re(1)-Cl(1)	177.3(2)	C(33)-Re(3)-N(6)	94.7(3)
C(2)-Re(1)-Cl(1)	94.1(2)	C(31)-Re(3)-N(5)	173.0(3)
C(1)-Re(1)-Cl(1)	86.8(2)	C(32)-Re(3)-N(5)	101.3(3)
N(2)-Re(1)-Cl(1)	83.70(15)	C(33)-Re(3)-N(5)	97.8(3)
N(1)-Re(1)-Cl(1)	82.24(16)	N(6)-Re(3)-N(5)	75.5(2)
C(16)-Re(2)-C(17)	85.1(3)	C(31)-Re(3)-Cl(3)	90.7(2)
C(16)-Re(2)-C(18)	94.2(3)	C(32)-Re(3)-Cl(3)	90.7(3)
C(17)-Re(2)-C(18)	86.6(3)	C(33)-Re(3)-Cl(3)	178.5(3)
C(16)-Re(2)-N(3)	98.8(3)	N(6)-Re(3)-Cl(3)	84.23(16)
C(17)-Re(2)-N(3)	175.5(3)	N(5)-Re(3)-Cl(3)	82.93(15)
C(18)-Re(2)-N(3)	95.2(3)		

Table 7.3 Crystal data and structure refinement for Re(bipy-$CH_3OH)(CO)_3Cl\cdot ACN$

Identification code	new	
Empirical formula	C17 H15 Cl N3 O5 Re	
Formula weight	562.97	
Temperature	100(2) K	
Wavelength	0.71073 Å	
Crystal system	Triclinic	
Space group	P-1	
Unit cell dimensions	a = 7.0241(5) Å	α= 76.999(3)°.
	b = 10.8167(8) Å	β= 81.051(3)°.
	c = 12.5125(9) Å	γ = 76.370(3)°.
Volume	894.92(11) $Å^3$	
Z	2	
Density (calculated)	2.089 Mg/m^3	
Absorption coefficient	6.974 mm^{-1}	
F(000)	540	
Crystal size	0.303 x 0.161 x 0.144 mm^3	
Theta range for data collection	1.68 to 25.60°.	
Index ranges	-8<=h<=8, -13<=k<=13, -15<=l<=14	
Reflections collected	11926	
Independent reflections	3338 [R(int) = 0.0225]	
Completeness to theta = 25.00°	99.7 %	
Absorption correction	Numerical	
Max. and min. transmission	0.4333 and 0.2264	
Refinement method	Full-matrix least-squares on F^2	
Data / restraints / parameters	3338 / 0 / 247	
Goodness-of-fit on F^2	1.078	
Final R indices [I>2sigma(I)]	R1 = 0.0139, wR2 = 0.0303	
R indices (all data)	R1 = 0.0153, wR2 = 0.0316	
Largest diff. peak and hole	0.437 and -0.498 e.$Å^{-3}$	

Table 7.4 Bond lengths [Å] and angles [°] for $Re(bipy\text{-}CH_3OH)(CO)_3Cl\cdot ACN$.

C(1)-O(1)	1.146(3)	C(14)-H(14A)	0.9900
C(1)-Re(1)	1.925(3)	C(14)-H(14B)	0.9900
C(1S)-N(1S)	1.130(4)	C(15)-O(4)	1.423(3)
C(1S)-C(2S)	1.461(4)	C(15)-H(15A)	0.9900
C(2)-O(2)	1.151(3)	C(15)-H(15B)	0.9900
C(2)-Re(1)	1.915(3)	N(1)-Re(1)	2.215(2)
C(2S)-H(2SA)	0.9800	N(2)-Re(1)	2.209(2)
C(2S)-H(2SB)	0.9800	O(3)-H(3)	0.8400
C(2S)-H(2SC)	0.9800	O(4)-H(4)	0.8400
C(3)-0(3)	1.148(3)	Re(1)-Cl(1)	2.4744(7)
C(3)-Re(1)	1.903(3)		
C(4)-N(1)	1.354(3)	O(1)-C(1)-Re(1)	176.0(2)
C(4)-C(5)	1.387(4)	N(1S)-C(1S)-C(2S)	179.1(4)
C(4)-C(14)	1.505(4)	O(2)-C(2)-Re(1)	177.2(2)
C(5)-C(6)	1.374(4)	C(1S)-C(2S)-H(2SA)	109.5
C(5)-H(5)	0.9500	C(1S)-C(2S)-H(2SB)	109.5
C(6)-C(7)	1.379(4)	H(2SA)-C(2S)-H(2SB)	109.5
C(6)-H(6)	0.9500	C(1S)-C(2S)-H(2SC)	109.5
C(7)-C(8)	1.388(4)	H(2SA)-C(2S)-H(2SC)	109.5
C(7)-H(7)	0.9500	H(2SB)-C(2S)-H(2SC)	109.5
C(8)-N(1)	1.359(3)	0(3)-C(3)-Re(1)	177.2(2)
C(8)-C(9)	1.476(4)	N(1)-C(4)-C(5)	121.8(2)
C(9)-N(2)	1.360(3)	N(1)-C(4)-C(14)	118.6(2)
C(9)-C(10)	1.381(4)	C(5)-C(4)-C(14)	119.6(2)
C(10)-C(11)	1.377(4)	C(6)-C(5)-C(4)	119.8(3)
C(10)-H(10)	0.9500	C(6)-C(5)-H(5)	120.1
C(11)-C(12)	1.378(4)	C(4)-C(5)-H(5)	120.1
C(11)-H(11)	0.9500	C(5)-C(6)-C(7)	119.0(3)
C(12)-C(13)	1.383(4)	C(5)-C(6)-H(6)	120.5
C(12)-H(12)	0.9500	C(7)-C(6)-H(6)	120.5
C(13)-N(2)	1.356(3)	C(6)-C(7)-C(8)	119.4(3)
C(13)-C(15)	1.508(4)	C(6)-C(7)-H(7)	120.3
C(14)-O(3)	1.413(3)	C(8)-C(7)-H(7)	120.3

Table 7.4 Cont.

N(1)-C(8)-C(7)	121.9(2)	O(4)-C(15)-H(15B)	109.0
N(1)-C(8)-C(9)	117.0(2)	C(13)-C(15)-H(15B)	109.0
C(7)-C(8)-C(9)	120.9(2)	H(15A)-C(15)-H(15B)	107.8
N(2)-C(9)-C(10)	121.9(2)	C(4)-N(1)-C(8)	118.1(2)
N(2)-C(9)-C(8)	116.5(2)	C(4)-N(1)-Re(1)	127.88(17)
C(10)-C(9)-C(8)	121.4(2)	C(8)-N(1)-Re(1)	114.01(17)
C(11)-C(10)-C(9)	119.3(3)	C(13)-N(2)-C(9)	118.3(2)
C(11)-C(10)-H(10)	120.3	C(13)-N(2)-Re(1)	127.42(17)
C(9)-C(10)-H(10)	120.3	C(9)-N(2)-Re(1)	113.48(16)
C(10)-C(11)-C(12)	118.9(3)	C(14)-O(3)-H(3)	109.5
C(10)-C(11)-H(11)	120.5	C(15)-O(4)-H(4)	109.5
C(12)-C(11)-H(11)	120.5	C(3)-Re(1)-C(2)	92.50(11)
C(11)-C(12)-C(13)	120.0(3)	C(3)-Re(1)-C(1)	90.77(11)
C(11)-C(12)-H(12)	120.0	C(2)-Re(1)-C(1)	82.14(11)
C(13)-C(12)-H(12)	120.0	C(3)-Re(1)-N(2)	94.96(9)
N(2)-C(13)-C(12)	121.3(2)	C(2)-Re(1)-N(2)	100.05(9)
N(2)-C(13)-C(15)	118.5(2)	C(1)-Re(1)-N(2)	173.75(9)
C(12)-C(13)-C(15)	120.2(2)	C(3)-Re(1)-N(1)	91.65(9)
O(3)-C(14)-C(4)	110.3(2)	C(2)-Re(1)-N(1)	174.13(10)
O(3)-C(14)-H(14A)	109.6	C(1)-Re(1)-N(1)	101.96(9)
C(4)-C(14)-H(14A)	109.6	N(2)-Re(1)-N(1)	75.44(8)
O(3)-C(14)-H(14B)	109.6	C(3)-Re(1)-Cl(1)	175.25(8)
C(4)-C(14)-H(14B)	109.6	C(2)-Re(1)-Cl(1)	91.74(8)
H(14A)-C(14)-H(14B)	108.1	C(1)-Re(1)-Cl(1)	91.93(8)
O(4)-C(15)-C(13)	112.9(2)	N(2)-Re(1)-Cl(1)	82.19(6)
O(4)-C(15)-H(15A)	109.0	N(1)-Re(1)-Cl(1)	83.97(6)
C(13)-C(15)-H(15A)	109.0		